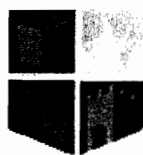


**A functional genomics approach: Characterisation
of two Non-ribosomal peptide synthetase genes, and
investigation of an adaptive response towards
alkylating DNA damage in *Aspergillus fumigatus***

Karen O'Hanlon BSc



NUI MAYNOOTH

Ollscoil na hÉireann Má Nuad

This thesis is submitted to the

National University of Ireland

for the degree of

Doctor of Philosophy

October 2010

Supervisor:

Professor Sean Doyle,

Biotechnology,

National University of Ireland Maynooth,

Co. Kildare

Head of Department:

Professor Kay Ohlendieck

Table of Contents

Declaration of Authorship	x
Acknowledgements	xi
Presentations	xii
Abbreviations	xiv
Summary	xviii
1.1. General characteristics of <i>Aspergillus fumigatus</i> .	1
1.2. Pathobiology of <i>A. fumigatus</i> .	3
1.3. Anti-fungal strategies currently in place for the treatment of IA.	6
1.4. <i>A. fumigatus</i> : toxins and virulence factors.	10
1.5. <i>A. fumigatus</i> genetics and genome information.	15
1.6. Secondary metabolites and clustering of biosynthetic genes.	18
1.7. Regulation of secondary metabolism gene clusters by the global secondary metabolite regulator LaeA.	20
1.8. Association of secondary metabolism with development.	21
1.9. Non-ribosomal peptide synthesis (NRPS)	24
1.9.1. NRPS – An overview	24
1.9.2. Structural arrangements and domain architecture of NRP synthetases.	28
1.9.3. 4'phosphopantetheinyl transferases and requirement for NRP Synthetase activation to holoenzyme.	32
1.9.4. NRPS – Mechanisms of Non-ribosomal Peptide Synthesis.	34
1.10. NRPS in <i>A. fumigatus</i> .	39
1.11. Genetic manipulations available for characterisation of genes within <i>A. fumigatus</i> .	41
1.11.1. Transformation systems.	41
1.11.2. Preparation of transforming DNA for targeted gene deletions.	42
1.11.3. Selection markers used for <i>A. fumigatus</i> genetic manipulation.	46
1.11.4. The use of non-homologous end joining (NHEJ)-deficient strains to increase targeted integrations.	49
1.12. The oxidative stress response in <i>A. fumigatus</i> .	52
1.13. Use of the <i>Galleria mellonella</i> insect model to study <i>A. fumigatus</i> virulence.	55
1.14 Rationale and objectives of this thesis.	57

2.1. Materials	59
2.1.1 Microbiological Medias and Reagents	59
2.1.1.1 <i>Aspergillus</i> Trace Elements	59
2.1.1.2 <i>Aspergillus</i> Salt Solution	59
2.1.1.3 100x Ammonium Tartrate	59
2.1.1.4 20 mM L-Glutamine	59
2.1.1.5 Malt Extract Agar	60
2.1.1.6 <i>Aspergillus</i> Minimal Media (AMM) Agar	60
2.1.1.7 <i>Aspergillus</i> Minimal Media (AMM)	60
2.1.1.8 Yeast Glucose (YG) Media	60
2.1.1.9 Sabourard- Dextrose Media	61
2.1.1.10 RPMI Media	61
2.1.1.11 Czapek's Broth	61
2.1.1.12 Czapek's Agar	61
2.1.1.13 MEM Media supplemented with 5 % (w/v) Foetal Calf Serum (FCS)	61
2.1.1.14 <i>Aspergillus</i> Transformation Regeneration Media	62
2.1.1.15 <i>Aspergillus</i> Transformation Soft Agar	62
2.1.1.16 Phosphate Buffered Saline (PBS)	62
2.1.1.17 Phosphate Buffer Saline/ 0.1 % (w/v) Tween-20 (PBST) NaCl (0.9 % w/v)	63
2.1.1.18 Luria-Bertani (LB) Agar	63
2.1.1.19 Luria-Bertani (LB) Broth	63
2.1.1.20 80 % (w/v) Glycerol	63
2.1.1.21 40 % (w/v) Glycerol	63
2.1.1.22 YPD broth	64
2.1.1.23 YPD Agar	64
2.1.1.24 Dropout Mix	64
2.1.1.25 Synthetic Complete Media (SC)	64
2.1.1.26 Synthetic Complete Agar (SC)	64
2.1.1.27 Antibiotics and Plate Assay Supplements	65
2.1.2 Molecular Biological Reagents	69
2.1.2.1 Agarose Gel Electrophoresis Reagents	69
2.1.2.1.1 50 X Tris-Acetate (TAE)	69
2.1.2.1.2 1 X Tris-Acetate (TAE)	69
2.1.2.1.3 Ethidium Bromide Solution	69
2.1.2.1.4 SYBR® Safe DNA Gel Stain	69
2.1.2.1.5 1 % (w/v) Agarose Gel	69
2.1.2.2 DNA Reagents	70
2.1.2.2.1 100 % (v/v) Ethanol (ice-cold)	70
2.1.2.2.2 70 % (v/v) Ethanol (ice-cold)	70
2.1.2.2.3 3 M Na-acetate	70
2.1.3 <i>Aspergillus</i> Transformation Buffers	74
2.1.3.1 Lysis Buffer	74
2.1.3.2 Mycelial lysing solution	74
2.1.3.3 0.7 M KCl	74
2.1.3.4 L6 Buffer	74
2.1.3.5 L7 Buffer	75
2.1.4 Southern and Northern Blotting Reagents	75

2.1.4.1 Southern Transfer Buffer.....	75
2.1.4.2 20 X SSC Buffer.....	75
2.1.4.3 10 X SSC Buffer.....	75
2.1.4.4 2 X SSC Buffer.....	75
2.1.4.5 10 % (w/v) Sodium Dodecyl Sulphate (SDS).....	76
2.1.4.6 0.1 % (w/v) SDS / 1 X SSC buffer.....	76
2.1.5 Digoxigenin (DIG) Detection Buffers.....	76
2.1.5.1 Membrane Pre-Hybridisation Buffer.....	76
2.1.5.2 DIG Buffer 1.....	76
2.1.5.3 Antibody Blocking Buffer.....	76
2.1.5.4 DIG Buffer 3.....	77
2.1.5.5 DIG Wash Buffer.....	77
2.1.5.6 Anti-DIG FaB Fragments.....	77
2.1.5.7 CSPD chemiluminescent substrate.....	77
2.1.5.8 DIG-labelled deoxynucleotide Triphosphates (dNTP's).....	77
2.1.6 Blot Development Solutions.....	78
2.1.6.1 Developing Solution.....	78
2.1.6.2 Fixing Solution.....	78
2.1.7 RNA Reagents.....	78
2.1.7.1 RNA Glassware.....	78
2.1.7.2 10 X Formaldehyde Agarose (FA) Gel Buffer.....	78
2.1.7.3 1 X Formaldehyde Agarose (FA) Running Buffer.....	78
2.1.8 Reverse-Phase High Performance Liquid Chromatography (RP-HPLC) Solvents.....	79
2.1.8.1 RP-HPLC Running Solvents.....	79
2.1.8.1.1 Solvent A.....	79
2.1.8.1.2 Solvent B.....	79
2.1.8.2 RP-HPLC Sample Preparation Reagents/Extraction Mixtures.....	79
2.1.8.2.1 Acetonitrile/H ₂ O Extraction Mixture.....	79
2.1.8.2.2 Ethyl Acetate: Dichloromethane: Methanol Extraction Mixture.....	79
2.1.9 <i>E. coli</i> Competent Cell Buffers.....	80
2.1.9.1 RF 1.....	80
2.1.9.2 RF 2.....	80
2.1.10 Yeast Transformation Buffers.....	80
2.1.10.1 50 % (w/v) Polyethylene Glycol (PEG).....	80
2.1.10.2 1 M Lithium Acetate.....	80
2.1.10.3 100 mM Lithium Acetate.....	81
2.1.10.4 Carrier DNA for transformation.....	81
2.2 Methods.....	82
2.2.1 Microbiological Methods – Strain Storage and Growth.....	82
2.2.1.1 <i>A. fumigatus</i> growth, maintenance and storage.....	82
2.2.1.2 <i>E. coli</i> growth, maintenance and storage.....	83
2.2.1.3 Yeast growth, maintenance and storage.....	84
2.2.2 Molecular Biological Methods.....	87
2.2.2.1 Isolation of Genomic DNA from <i>A. fumigatus</i>	87

2.2.2.2 Precipitation of <i>A. fumigatus</i> genomic DNA.....	88
2.2.2.3 Polymerase Chain Reaction (PCR)	88
2.2.2.4 DNA Gel Electrophoresis.....	90
2.2.2.4.1 Preparation of Agarose Gel	90
2.2.2.4.2 Loading and Running Samples.....	91
2.2.2.5 DNA Gel Extraction	91
2.2.2.6 Restriction Enzyme Digests.....	92
2.2.2.7 Ligation of DNA Fragments.....	93
2.2.3 Generation of <i>Aspergillus fumigatus</i> mutant strains.....	94
2.2.3.1 Generation of <i>A. fumigatus</i> gene disruption constructs.....	94
2.2.3.2 <i>A. fumigatus</i> Protoplast Production and Transformation	97
2.2.3.2.1 <i>A. fumigatus</i> Protoplast Formation	97
2.2.3.2.2. <i>A. fumigatus</i> protoplast transformation	98
2.2.3.2.3. Plating of <i>A. fumigatus</i> transformed protoplasts and selection with either phleomycin or pyrithiamine.....	98
2.2.3.3 Isolation of <i>A. fumigatus</i> transformants following transformation.....	99
2.2.3.4 Single Spore Isolation of <i>A. fumigatus</i> transformants	100
2.2.4 Southern Blotting.....	100
2.2.4.1 Southern Blotting – Nucleic Acid Transfer.....	100
2.2.4.2 Disassembly of Southern Blots Following Nucleic Acid Transfer	101
2.2.5 Digoxigenin (DIG) - Detection of Hybridised DNA fragments on Southern blot	101
2.2.5.1 Generation of DIG-labelled DNA probes.....	101
2.2.5.2 Prehybridisation of Nylon Membrane Following UV Cross-linking	103
2.2.5.3 Addition of DIG-labelled probe to Southern blots.....	103
2.2.5.4 DIG Detection.....	103
2.2.5.5 Developing of DIG-detected Southern Blots.....	104
2.2.6 RNA analysis.....	105
2.2.6.1 RNA Extraction	105
2.2.6.2 RNA Gel Electrophoresis	106
2.2.6.3 DNase Treatment of RNA	107
2.2.6.4 cDNA Synthesis	107
2.2.6.5 Semi-quantitative RT-PCR.....	108
2.2.6.6 Real-Time PCR	109
2.2.7 Comparative metabolite analysis by Reverse Phase High Performance Liquid Chromatography (RP-HPLC).....	110
2.2.7.1 Culture Supernatant Preparation for RP-HPLC analysis.....	110
2.2.7.2 Organic Extraction of culture SN for RP-HPLC analysis.....	111
2.2.7.3 Preparation of <i>A. fumigatus</i> Conidial Extracts for Analysis by RP-HPLC	111
2.2.7.4 Preparation of <i>Aspergillus fumigatus</i> plug extracts from agar plates.....	112
2.2.7.5 RP-HPLC Procedure	113
2.2.8 <i>A. fumigatus</i> Plate Assays.....	113
2.2.9 <i>A. fumigatus</i> growth curves.	113
2.2.10 <i>A. fumigatus</i> germination assay	114
2.2.11 Murine Virulence Testing.....	115

2.2.12 <i>Galleria mellonella</i> Virulence Testing.....	115
2.2.13 Murine Cell Signalling in Response to <i>Aspergillus fumigatus</i>	116
2.2.13.1 Cultivation and Maintenance of Murine Bone Marrow Derived Macrophages (BMMØS).....	116
2.2.13.2 Subculturing or Passaging of BMMØS.....	116
2.2.13.3 Fungal stimulation of BMMØS.....	117
2.2.13.4 Cytokine Determination in Murine Cells by ELISA.....	118
2.2.14 Preparation of Chemically Competent <i>E. coli</i> cells.....	118
2.2.15 Minute Transformation of Chemically Competent <i>E. coli</i> cells.....	119
2.2.16 Colony PCR.....	119
2.2.17 Small Scale Plasmid Purification.....	120
2.2.18 DNA Sequencing.....	120
2.2.19 Cloning of <i>Afmpt</i> and <i>Afagt</i> into pC210 plasmid for transformation into <i>S. cerevisiae</i>	121
2.2.20 Yeast Cell Transformation.....	121
2.2.21 Yeast Dot Growth Assays.....	123
3.1 Introduction.....	124
3.1.1 The non-ribosomal peptide synthetase gene, <i>pes3</i>	124
3.1.2 Structure of the <i>Aspergillus fumigatus</i> cell wall.....	125
3.1.3 The innate immune response towards <i>Aspergillus fumigatus</i>	133
3.1.3.1 The cells of the innate immune system.....	133
3.1.3.2 The antimicrobial activity of respiratory cells.....	137
3.1.3.3 Pattern recognition systems.....	140
3.1.3.4 Chemical Immune Effectors.....	147
3.1.4 Model systems for studying <i>A. fumigatus</i> virulence.....	149
3.2 Aims and Objectives.....	153
3.3 Results.....	154
3.3.1 Genetic manipulation of <i>pes3</i> gene within <i>A. fumigatus</i>	154
3.3.2 Generation of <i>pes3</i> disruption constructs.....	154
3.3.3 Isolation of an <i>A. fumigatus pes3</i> mutant strain ($\Delta pes3$).....	155
3.3.4 Generation of <i>pes3</i> replacement constructs and isolation of a <i>pes3</i> complemented strain ($\Delta pes3::PES3$).....	158
3.3.5 Expression analysis of <i>pes3</i> in <i>A. fumigatus</i>	164
3.3.5.1 Disruption of <i>pes3</i> leads to abolition of <i>pes3</i> expression in <i>A. fumigatus</i>	164
3.3.5.2 Restoration of <i>pes3</i> expression in $\Delta pes3::PES3$	166
3.3.6 Restoration of <i>pes3</i> locus in <i>pes3</i> complemented strain confirmed by restriction mapping.....	168

3.3.7. Comparative metabolite analysis reveals no difference in metabolite profile between <i>A. fumigatus</i> wild-type and $\Delta pes3$	170
3.3.8 Phenotypic Characterisation of the <i>A. fumigatus</i> $\Delta pes3$ mutant.....	179
3.3.9 <i>A. fumigatus</i> $\Delta pes3$ exhibits increased sensitivity to the anti-fungal Voriconazole.....	183
3.3.10 <i>A. fumigatus</i> $\Delta pes3$ grows and undergoes conidial germination at a rate comparable to wild-type.....	191
3.3.11. <i>A. fumigatus</i> $\Delta pes3$ is more virulent than wild-type <i>A. fumigatus</i>	194
3.3.11.1 Deletion of <i>A. fumigatus pes3</i> leads to increased virulence in the <i>Galleria mellonella</i> model of infection.....	194
3.3.11.2 Deletion of <i>A. fumigatus pes3</i> leads to increased virulence in a Murine Hydrocortisone Acetate (HCA) Immunocompromised model of Invasive Aspergillosis (IA).	197
3.3.11.3 The deletion of <i>pes3</i> within <i>A. fumigatus</i> does not affect virulence in a murine neutropenic model of Invasive Aspergillosis (IA).	204
3.3.12 <i>A. fumigatus</i> $\Delta pes3$ is immunologically silenced compare to wild-type.....	210
3.4 Discussion.....	221
4.1 Introduction.	238
4.1.1. <i>pesL</i> in the genome of <i>A. fumigatus</i>	238
4.1.2. Secondary metabolite production in <i>A. fumigatus</i>	242
4.1.2.1. The fumiquinazolines.	242
4.1.2.2. The fumitremorgins.	245
4.1.2.3. The ergot alkaloids.	248
4.2 Aims and Objectives.....	252
4.3. Results.	253
4.3.1. Generation of <i>pesL</i> disruption constructs.	253
4.3.2. Isolation of an <i>A. fumigatus pesL</i> mutant strain ($\Delta pesL$).....	256
4.3.3. Expression analysis of <i>pesL</i> in <i>A. fumigatus</i>	259
4.3.3.1. Disruption of <i>pesL</i> leads to abolition of <i>pesL</i> expression in <i>A. fumigatus</i>	259
4.3.3.2. <i>pesL</i> is expressed under a range of conditions in <i>A. fumigatus</i>	262
4.3.3.3. The 5 genes in the putative <i>pesL</i> cluster are expressed in the <i>A. fumigatus</i> $\Delta akuB$ strain.	265
4.3.4. Phenotypic characterisation of <i>A. fumigatus</i> $\Delta pesL$	267
4.3.4.1. <i>pesL</i> protects <i>A. fumigatus</i> against oxidative stress caused by hydrogen peroxide.....	269
4.3.4.2. <i>pesL</i> protects <i>A. fumigatus</i> against voriconazole toxicity.	275
4.3.5. <i>pesL</i> contributes to <i>A. fumigatus</i> virulence in an insect model of infection.....	280
4.3.6. Comparative metabolite profiling reveals that <i>pesL</i> encodes a peptide(s) that is up-regulated during oxidative stress caused by hydrogen peroxide.	282
4.3.7. PesL is essential for Fumigaclavine C biosynthesis in <i>A. fumigatus</i>	288

4.3.8. <i>PesL</i> is not essential for fumiquinazoline production in <i>A. fumigatus</i>	293
4.4. Discussion.....	296
5.1. Introduction.....	317
5.2. Aims and Objectives.....	329
5.3. Results.....	330
5.3.1. Identification of candidate genes for an adaptive response to alkylation damage in <i>A. fumigatus</i>	330
5.3.2. Confirmation of an adaptive response towards alkylating agents in <i>Aspergillus fumigatus</i>	335
5.3.3. Deletion of <i>Afmpt</i> and <i>Afagt</i> from the genome of <i>A. fumigatus</i>	340
5.3.3.1. Generation of AFUA_5G06350 and AFUA_2G02090 bipartite disruption constructs.....	340
5.3.3.2. Identification of <i>A. fumigatus</i> AFUA_5G06350 and AFUA_2G02090 mutant strains.....	344
5.3.3.2.1. Identification of <i>A. fumigatus</i> AFUA_5G06350 mutant strain (termed $\Delta Afmpt$).....	344
5.3.3.2.2. Identification of <i>A. fumigatus</i> AFUA_2G02090 mutant strain (termed $\Delta Afagt$).....	348
5.3.4. <i>A. fumigatus</i> $\Delta Afmpt$ and $\Delta Afagt$ are impaired in the response to alkylating DNA damage.....	351
5.3.5. <i>A. fumigatus</i> <i>mpt</i> is essential for the induction of <i>A. fumigatus</i> <i>agt</i> in response to alkylating DNA damage.....	359
5.3.6. Cloning of AFUA_5G06350 and AFUA_2G02090 into PC210 vector for expression in <i>Saccharomyces cerevisiae</i>	362
5.3.7. Transformation of pC-AFUA_5G06350 and pC-AFUA_2G02090 into <i>S. cerevisiae</i>	365
5.3.8. <i>Aspergillus fumigatus</i> <i>Afmpt</i> and <i>Afagt</i> are capable of complementing an <i>MGT1</i> deletion in <i>Saccharomyces cerevisiae</i>	367
5.4. Discussion.....	369

Declaration of Authorship

This thesis has not previously been submitted in whole or in part to this or any other University for any other degree. This thesis is the sole work of the author, with the exception of the generation of the *A. fumigatus* $\Delta pes3$ mutant which was generated by Dr. Deirdre Stack Chapter 3), the HPLC-MS analysis which was carried in collaboration with Professor Thomas Larsen (Danish Technical University), and the murine virulence testing of the *A. fumigatus* $\Delta pes3$ mutant which was carried out by Timothy Cairns (Imperial College London).

Karen O'Hanlon B.Sc.

Acknowledgements

I would first and foremost like to thank my supervisor Professor Sean Doyle for all the support, advice, encouragement and ideas I have received throughout this PhD. I couldn't have asked for a better PhD supervisor. I would also like to thank Dr. Gary Jones (NUIM), for developing the ideas leading to Chapter 5 of this thesis, and for guidance on the same. I would also like to thank all members of the Biotechnology Lab (past and present); in particular Dr. Deirdre Stack, who generated the *pes3* mutant used in this study, and Drs. Stephen Carberry and Luke O'Shaughnessy for general advice and many interesting scientific discussions! I would also like to extend a sincere thanks to Dr. Markus Schrettl whose expertise and training at the start of this work is greatly appreciated.

Many thanks to collaborators who have contributed to the development of certain aspects of this work; Professor Thomas Larsen (Danish Technical University, Denmark), Dr. Elaine Bignell (Imperial College London), and Dr. Sinéad Miggin, Cell Signalling Laboratory, NUI Maynooth. I would like to sincerely thank Ircset and the Department of Biology, NUI Maynooth, for funding this PhD.

I would especially like to thank my all my colleagues at NUI Maynooth, many of whom are also very close friends; in alphabetical order to avoid any misunderstandings!! - Ciara, Cindy, Gráinne, Jennifer, John, Natasha, Rebecca, Sarah and especially to Carol, Karen and Lorna, who have always been there for all the highest and lowest moments (there were many of each!) of this PhD, including some fun conference trips ☺. I'll really miss the craic, and it would not have been half as enjoyable without you all. Many thanks also to the Biology Department staff, in particular Michelle Finnegan, and also Jean, Loretta and Terry in the Biology Office.

I would also like to thank my closest and oldest friends at home for being patient with me while I turned into a hermit the past few months; especially to Deirdre and my sister Lisa for constantly listening to my rants – you don't know how much that helped! And also, Jacqueline, where would I have been without you on the last day putting together all of those thesis pages!! – thank you ☺.

Massive thanks to Cindy and Dave for making me feel so at home the last 6 months – it made things so much easier ☺.

I would like to thank my parents and family for all the encouragement I have received throughout all my college years.

Finally, I would like to thank my boyfriend Emil, for all your patience and support, and always managing to make me smile ☺. This thesis is dedicated to you.

Presentations

Oral Presentations

Characterisation of *pesL*, a non-ribosomal peptide synthetase gene from the opportunistic pathogen *Aspergillus fumigatus*. The Irish Biochemical Society Annual Meeting, Conway Institute, University College Dublin, 13th November 2009.

Differential Roles for *Aspergillus fumigatus* non-ribosomal peptides in protection against oxidative stress and virulence in the *Galleria mellonella* insect model. The Irish Fungal Meeting, Conway Institute, University College Dublin, 25th June 2009.

Differential Roles for *Aspergillus fumigatus* non-ribosomal peptides in protection against oxidative stress and virulence in the *Galleria mellonella* insect model. Royal Academy of Medicine in Ireland Annual Meeting, NUI Maynooth, 18th June 2009. *Awarded Donegal Medal for Best Talk at this Meeting.*

Differential Roles for *Aspergillus fumigatus* non-ribosomal peptides in protection against oxidative stress and virulence in the *Galleria mellonella* insect model. Presentation at NUI Maynooth, Departmental Seminar, 6th June 2009.

Investigating the role of *PesL*, a non-ribosomal peptide synthetase from the opportunistic pathogen *Aspergillus fumigatus*. Presentation at NUI Maynooth Departmental Seminar, June 2008.

Poster Presentations

Non-Ribosomal Peptides play an Important Role in the Virulence of the Opportunistic Pathogen *Aspergillus fumigatus*. Poster Presentation at the 7th Asperfest Meeting, and the 10th European Fungal Genetics Conferences, 28th March – 1st April 2010, NH Conference Centre, Leeuwenhorst, The Netherlands.

Non-Ribosomal Peptides play an Important Role in the Virulence of the Opportunistic Pathogen *Aspergillus fumigatus*. Poster Presentation at the 4th ‘Advances against Aspergillosis’ Meeting, February 2010, Rome, Italy.

Functional characterisation of a non-ribosomal peptide synthetase from the opportunistic pathogen *Aspergillus fumigatus*. Poster Presentation at Ircset Symposium – Innovation Fuelling the Smart Economy. The RDS, Dublin. 25th September 2009.

Functional characterisation of a non-ribosomal peptide synthetase from the opportunistic pathogen *Aspergillus fumigatus*. Poster Presentation at The 25th International Fungal Genetics Conference, Asilomar, Pacific Grove, California, U.S.A, March 2009.

Functional characterisation of a non-ribosomal peptide synthetase from the opportunistic pathogen *Aspergillus fumigatus*. The Irish Fungal Meeting, National University of Ireland, Galway. June 2008.

Abbreviations

aa	Amino acid
ABPA	Allergic bronchopulmonary aspergillosis
ACP	Acyl Carrier Protein
ACV	δ -(L- α -aminoadipoyl)-L-cysteinyl-D-valine
Ala	Alanine
AMP	Adenosine monophosphate
ATCC	American Type Culture Collection
ATP	Adenosine triphosphate
BLAST	Basic Local Alignment Search Tool
bp	Base Pairs
BPS	Bathophenanthrolinedisulfonate
CADRE	Cadre Aspergillus Data Repository
CoA	Coenzyme A
dH ₂ O	Distilled Water
DMSO	Dimethyl Sulfoxide
DNA	Deoxyribonucleic Acid
EA	Ergot Alkaloids
EM	Elongation Module
EMS	Ethyl Methanesulfonate
ETP	Epipolythiodioxopiperazine
FCS	Foetal Calf Serum
FTMs	Fumitremorgins
G-CSF	Granulocyte colony-stimulating factor

GST	Glutathione s-transferase
H ₂ O ₂	Hydrogen Peroxide
IA	Invasive Aspergillosis
IFN	Interferon
Ig	Immunoglobulin
IL	Interleukin
IM	Initiation Module
kb	Kilobase
LB	Luria Bertani
LPS	Lipopolysaccharide
Lys	Lysine
mb	Megabase
MMS	Methyl Methanesulfonate
MNNG	N-methyl-N'-nitro-N-nitrosoguanidine
NADPH	Nicotinamide Adenine Dinucleotide Phosphate
NCBI	National Centre for Biotechnology Information
NET	Nuclear Extracellular Trap
NHEJ	Non-homologous End Joining
nm	Nanometers
NRP	Non-ribosomal peptide
NRPS	Non-ribosomal Peptide Synthesis
nt	Nucleotide
ORF	Open Reading Frame
PAMP	Pathogen Associated Molecular Pattern
PBS	Phosphate Buffered Saline

PBST	Phosphate Buffered Saline-Tween
PCP	Peptidyl Carrier Protein
PCR	Polymerase Chain Reaction
Pes	Peptide Synthetase
Phe	Phenylalanine
PK	Polyketide
PMN	Polymorphonuclear neutrophil
Ppant	Phosphopantetheine Group
PPTase	4'-Phosphopantetheine Transferase
PRR	Pattern Recognition Receptor
<i>ptrA</i>	Pyriothiamine resistance cassette
RNA	Ribonucleic Acid
RNI	Reactive Nitrogen Intermediates
ROS	Reactive Oxygen Species
RP-HPLC	Reverse-Phase High Performance Liquid Chromatography
RT	Reverse Transcriptase
SAM	S-adenosyl methionine
SC	Synthetic Complete
SDS	Sodium Dodecyl Sulphate
SM	Secondary Metabolites
SOD	Superoxide Dismutase
ST	Sterigmatocystin
TE	Thioesterase
Th	T-helper
TIGR	The Institute of Genomic Research

TLR	Toll-like Receptor
tRNA	transfer RNA
UV	Ultra Violet
v/v	Volume per volume
Val	Valine
w/v	Weight per volume
X-gal	1,5-bromo-4-chloro-3-indolyl- β -DNA-galactosidase
YG	Yeast Glucose

Summary

Aspergillus fumigatus is a serious opportunistic human pathogen. Availability of the complete genome sequence of *A. fumigatus* allows the identification and subsequent characterisation of genes which may encode virulence factors, or novel drug targets. Non-ribosomal peptide (NRP) synthetases have been implicated in virulence of *A. fumigatus* and other fungi. The work presented here reports opposing roles for two previously uncharacterised NRP synthetases with respect to *A. fumigatus* virulence. The NRP synthetase Pes3 appears to encode a structural peptide necessary for fungal recognition by the innate immune system; deletion of *pes3* resulted in hypervirulence in both insect ($p < 0.001$) and murine ($p = 0.02$) models of invasive aspergillosis, and increased susceptibility to voriconazole ($p < 0.001$). The NRP synthetase PesL was found to be essential for fumigaclavine C biosynthesis and deletion of *pesL* resulted in complete loss of fumigaclavine C accompanied by severely reduced virulence ($p < 0.001$), increased sensitivity of $\Delta pesL$ to H_2O_2 (> 1 mM) ($p = 0.05$), and increased sensitivity to the anti-fungal voriconazole (> 0.25 $\mu\text{g/ml}$) ($p < 0.01$) compared to wild-type.

An adaptive response to alkylating agents (e.g. N-methyl-N'-nitro-N-nitrosoguanidine (MNNG)) was identified in *A. fumigatus*. *Afmpt* is a transcriptional regulator for this response, and exposure to MNNG causes up-regulation of *Afmpt* and *Afagt*, an alkylguaninetransferase. *Afmpt* and *Afagt* functions were confirmed through targeted gene deletion, phenotypic and expression analyses, and yeast complementation studies. Identification of this response, which has no mammalian equivalent, makes this pathway an attractive anti-fungal drug target worthy of further investigation.

Overall, this work further highlights the importance that NRPS plays in this serious human pathogen, and uncovered some interesting features such as possible secondary metabolite cluster cross-talk and NRP synthetase redundancy, themes which are beginning to emerge in the literature.

1.1. General characteristics of *Aspergillus fumigatus*.

The genus *Aspergillus* was described as early as 1729 by Micheli and comprises approximately 200 species found worldwide (Tomee & van der Werf, 2001). About 20 species are associated with disease, including *A. fumigatus*, *A. flavus*, *A. niger*, *A. terreus*, *A. nidulans* and *A. oryzae* (Tomee & van der Werf, 2001). However, *A. fumigatus* is the most pathogenic of these species, and is responsible for approximately 90 % of all invasive aspergillosis infections (Dagenais & Keller, 2009).

A. fumigatus is a ubiquitous saprophytic filamentous fungus that plays an important role in the recycling of carbon and nitrogen in the environment (Latge, 2001). Its primary habitat is soil or decaying vegetation, and it produces small hydrophobic conidia (spores) which are airborne, and can survive a vast range of environmental conditions (Dagenais & Keller, 2009). In the laboratory, *A. fumigatus* can grow rapidly on minimal agar plates containing a carbon source (e.g. glucose), a nitrogen source (e.g. ammonium tartrate), and trace elements (Brakhage & Langfelder, 2002). *A. fumigatus* is a thermotolerant fungus, and can grow at temperatures as high as 55 °C, with survival maintained at 70 °C (Latge, 1999). Although *A. fumigatus* is not the most abundant fungus in the world, it is one of the most ubiquitous fungus with airborne conidia (Mullins *et al.*, 1984).

The fungus has a simple life cycle, which is shown in Figure 1.1. *A. fumigatus* is characterised by green powdery conidia, which are produced asexually in chains from conidiophores (Latge, 1999). Until recently, it was thought that no sexual stage was present in *A. fumigatus* (Latge, 1999). However, genome sequencing revealed several genes associated with mating processes and sexual development (Galagan *et al.*, 2005). Recently, a fully functioning sexual cycle was discovered in *A. fumigatus* (O'Gorman *et al.*, 2009).

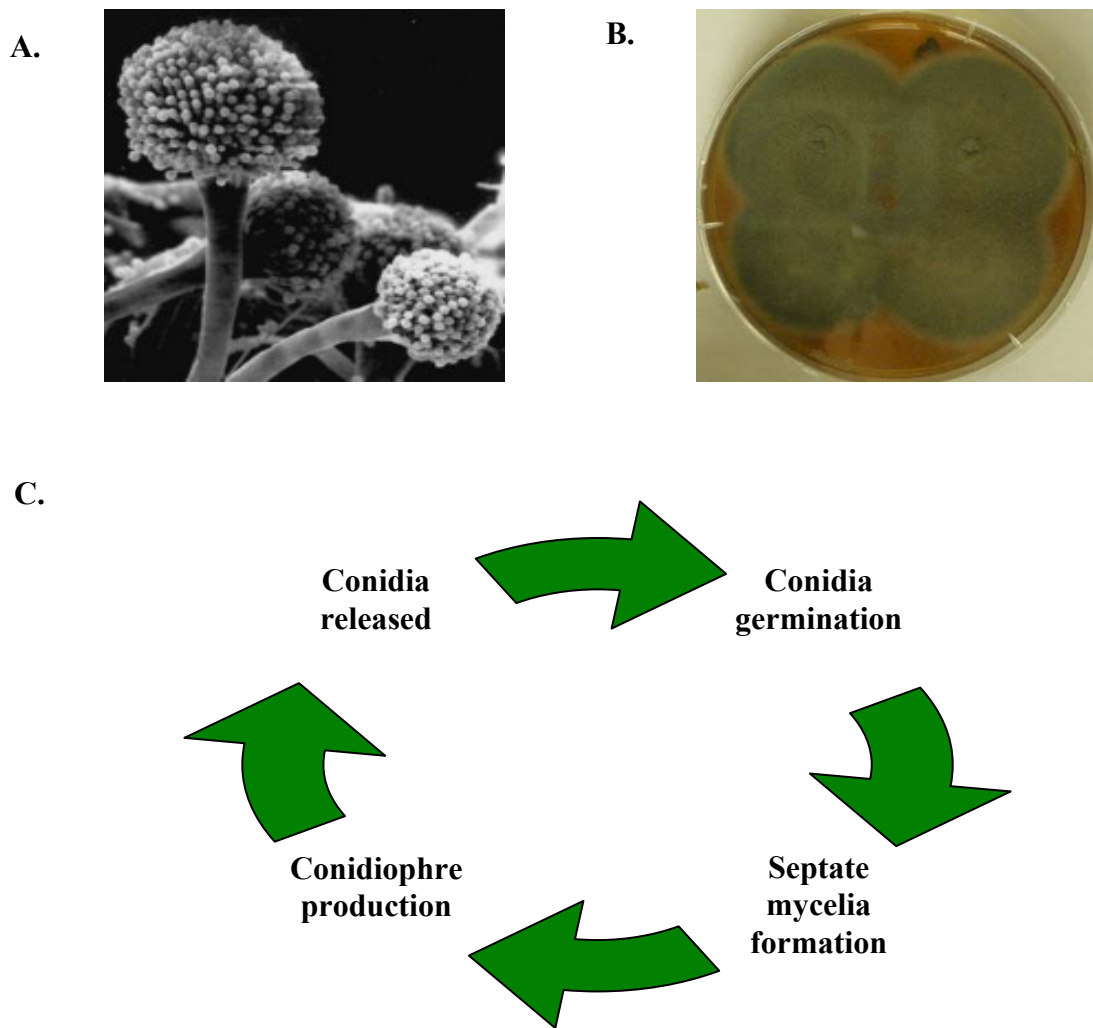


Figure 1.1. Life cycle of *A. fumigatus*. **A.** Scanning electron microscopy of *A. fumigatus* conidiophores which burst to release thousands of asexual conidia (Image from Hannover Medical School). **B.** *A. fumigatus* Af293 colonies growing on Malt Extract agar (Section 2.1.1.5) (photographed at NUIM). **C.** Conidia are released from conidiophores, and they germinate to form septate mycelia. Mycelia then produce conidiophores that release conidia and the cycle continues (Latge, 2001).

1.2. Pathobiology of *A. fumigatus*.

Aspergillus fumigatus is an opportunistic pathogen which can cause a range of human illnesses depending on the immune status of the host (Dagenais & Keller, 2009; Latge, 1999), and is responsible for about 4 % of all hospital-based deaths in Europe (Brookman & Denning, 2000). Although once thought to be relatively harmless, the status of *A. fumigatus* has changed over the last three decades, with an increasing number of immunosuppressed patients and an increase in the severity of immunosuppressive therapies (Latge, 2001). Conidia of *A. fumigatus* are inhaled on a daily basis, and it has been suggested that approximately 2000 spores are lodged in the terminal airways every day (Philippe *et al.*, 2003). The conidia are small enough (2-3 μm in diameter) to easily reach the lung alveoli (Latge, 1999). For most patients therefore, disease occurs in the lung, although systemic infection to any body organ occurs in the most severely immunocompromised individuals (Latge, 1999). Pulmonary disease caused by *A. fumigatus* can be categorised according to the location of infection in the respiratory tract and the extent of mycelial invasion, which are influenced by host immune status (Latge, 1999). The innate immune system represents a tightly regulated defence system which is constitutively active, and is involved in the recognition and elimination of pathogenic microbes (Balloy and Chignard, 2009). In immunocompetent individuals, *A. fumigatus* conidial inhalation is relatively harmless, and conidia that enter terminal airways are phagocytosed and killed by alveolar macrophages (Philippe *et al.*, 2003). The innate immune response to *A. fumigatus* will be discussed in more detail in Chapter 3.

A. fumigatus infections may be classed into three main categories; 1) allergic bronchopulmonary aspergillosis (ABPA), 2) aspergilloma (fungal ball) and 3) invasive aspergillosis (IA) (Daly & Kavanagh, 2001; Thompson & Patterson, 2008; Tomee & van der Werf, 2001). ABPA is a hypersensitivity to conidia of *A. fumigatus*. It is a potentially

fatal, non-infectious disease, causing extensive inflammation of the respiratory system (Banerjee *et al.*, 1997; Cramer, 2002). It mainly occurs in cystic fibrosis (CF) and asthma patients and it is estimated that approximately 25 % of CF sufferers and 10 % of asthmatics have ABPA (Daly & Kavanagh, 2001). Allergens implicated in ABPA are identified on an ongoing basis, such as the recently described Asp f 34, a novel cell wall major allergen (Glaser *et al.*, 2009) and more recently described novel allergens from proteomic analysis of secreted hyphal proteins and cytosolic allergens produced by *A. fumigatus* conidia (Singh *et al.*, 2010a; Singh *et al.*, 2010b). Treatment for ABPA usually involves reducing the hypersensitivity reaction to the fungus, and the use of corticosteroids such as prednisone has proven effective (Daly & Kavanagh, 2001; Elliott & Taylor, 1997). ABPA can be distinguished from other *A. fumigatus* infections by the elevated presence of IgE in serum (Moss, 2002), and therefore, constant monitoring of IgE is critical during corticosteroid therapy for ABPA (Daly & Kavanagh, 2001; Moss, 2002).

Aspergilloma or fungus ball typically grows in existing lung cavities, caused by carcinoma, emphysema, or a past incidence of TB (Thompson & Patterson, 2008). The aspergilloma consists of living and dead fungal elements, and can remain quiescent for many months, or even years, growing in size without invading pulmonary tissue (Daly & Kavanagh, 2001). Aspergilloma was the classical form of aspergillosis in the 1950's and occurs today in approximately 15 % of patients with pre-existing lung cavities (Latge, 1999). Haemoptysis is a common symptom of aspergilloma and may be massive and sometimes fatal (Latge, 1999). Treatment of aspergilloma is usually directed towards preventing life-threatening haemoptysis, and can result in surgical removal of the fungal ball (Kaestel *et al.*, 1999; Tomee & van der Werf, 2001), or local anti-fungal therapy (Tomee & van der Werf, 2001). As surgical removal carries a risk of mortality due to pre-existing lung conditions in aspergilloma patients, it should only be offered in cases of extreme

haemoptysis (Stevens *et al.*, 2000). When surgical treatment cannot be offered, long-term anti-fungal treatment with itraconazole alone or in combination with amphotericin B has been found to stabilise patient health or improve symptoms (Denning *et al.*, 2003).

Invasive aspergillosis (IA) is the most common form of invasive disease caused by *A. fumigatus* (Thompson & Patterson, 2008). It is the most devastating *A. fumigatus*-related disease, targeting severely immunocompromised patients (Dagenais & Keller, 2009). Patient cohorts most at risk of developing life-threatening IA are those with haematological malignancies such as leukaemia, solid-organ and hematopoietic stem cell transplant recipients, those undergoing prolonged corticosteroid therapy for the treatment of graft-versus-host disease, patients with genetic immunodeficiencies such as chronic granulomatous disease (CGD), and those infected with HIV (Marr *et al.*, 2002; Mikulska *et al.*, 2009; Pagano *et al.*, 2001; Post *et al.*, 2007; Wiederhold & Lewis, 2003). Mortality rates associated with *A. fumigatus* infections are high, ranging between 40 – 80 % depending on patient immune status, the site of infection and the anti-fungal regimen administered (Lin *et al.*, 2001). Prolonged neutropenia is defined as the most dominant risk factor for IA, and is often caused by cytotoxic therapies such as corticosteroid treatments used for transplant recipients or patients with haematological diseases (Dagenais & Keller, 2009). Cyclophosphamide interrupts cell replication, and leads to a depletion of white blood cells including neutrophils, and IA in neutropenic patients is characterised by extensive blood clotting and haemorrhage from rapid and uncontrolled hyphal growth (Chiang *et al.*, 2008; Stergiopoulou *et al.*, 2007). Without neutrophil infiltration, the inflammatory response is low, and dissemination to other body organs results through the blood (Dagenais & Keller, 2009). IA is extremely difficult to treat and is often diagnosed relatively late (Denning & Hope, 2010). Treatment usually involves administration of anti-

fungal therapy from the polyene, azole, and echinocandin classes of drugs (Denning & Hope, 2010). A selection of these will be described in the next section.

1.3. Anti-fungal strategies currently in place for the treatment of IA.

Many anti-fungal agents target the cell wall, since it is unique to the fungal pathogen (Beauvais & Latge, 2001). The fungal cell wall will be described in detail in Chapter 3. Currently, four classes of drugs are available for the treatment of invasive fungal infections: the polyenes, azoles, echinocandins and the nucleoside analogues (Das *et al.*, 2009). Ergosterol is the principal sterol in the fungal cell membrane, and its absence in mammalian cell membranes has been the basis of polyene and triazole anti-fungal drug development for a long time (Beauvais & Latge, 2001). The polyenes bind membrane sterols through van der Waals forces to membrane sterols, and have much greater affinity for ergosterol than cholesterol, leading to the production of pores, increasing the permeability of the membrane (Brajtburg & Bolard, 1996). Amphotericin B is a polyene anti-fungal, and targets ergosterol in the fungal cell membrane. Amphotericin B forms channel structures or pores in the cell membrane, leading to the release of cellular components, mainly potassium ions, eventually leading to cell death (Baginski & Czub, 2009). Amphotericin B deoxycholate, and more recently, liposomal formulations of amphotericin B (commercially available as AmBisome) is the anti-fungal of choice for most invasive fungal infections (Dupont, 2002; Moen *et al.*, 2009).

Voriconazole (available commercially as Vfend) is a synthetic derivative of the triazole class of anti-fungal drugs. Drugs in this class block various components of sterol biosynthesis, thereby disrupting the fungal cell membrane and halting fungal growth. Specifically, voriconazole inhibits the cytochrome P450 (CYP)-dependent enzyme, 14- α -sterol demethylase, inhibiting the conversion of lanosterol to ergosterol, and

interrupting cell membrane synthesis at this point (Scott & Simpson, 2007). This leads to a lack of ergosterol in the cell membrane, resulting in membrane leakage (Baginski & Czub, 2009). Voriconazole is useful in the treatment of medically important fungi which cause infections in immunocompromised patients, especially those suffering from IA, where it has been shown to improve the overall survival of patients (Donnelly & De Pauw, 2004; Herbrecht *et al.*, 2002).

Caspofungin was the first drug approved in a novel class of anti-fungal agents, the echinocandins, which are glucan synthase inhibitors. Drugs in this class are fungal-specific, interfering with fungal cell wall biosynthesis by blocking the activity of 1, 3- β -D-glucan synthase, which is a crucial enzyme for cell wall synthesis (Sucher *et al.*, 2009). This subsequently inhibits the biosynthesis of 1,3- β -D-glucan, an important fungal cell wall component (Lamaris *et al.*, 2008). Caspofungin has shown efficacy against a wide range of fungal species, including *Aspergillus* species (Keating & Jarvis, 2001).

Nucleoside analogues have recently been explored as novel antimicrobial agents, whereby these analogues interfere with transcription and DNA replication, essential processes for microbial survival. Analogues were produced; which were closely related to the naturally occurring nucleoside, S-adenosylhomocysteine (SAH), which is important for biological transmethylation reactions. Some of these analogues showed anti-fungal activity *in vitro* towards *A. fumigatus* and other important human pathogens (Srivastava *et al.*, 2007).

Aside from the use of anti-fungal drugs for the treatment of invasive fungal infections, by inhibiting fungal growth directly, another avenue which is now being explored is the possibility of immunomodulation, whereby anti-fungal treatment has the ability to boost the host immune system. Voriconazole has been shown to inhibit fungal growth, either alone or in combination with phagocytes, and has been shown to enhance the

inhibition of hyphal growth by neutrophils *in vitro* (Vora *et al.*, 1998). Recently, it was found that in combination with voriconazole, *A. fumigatus* hyphae induce a higher level of gene expression in the human THP-1 monocytic cell line than hyphae alone, potentially increasing host resistance to the fungus, supporting the hypothesis that voriconazole has immunomodulatory effects (Simitopoulou *et al.*, 2008). Caspofungin also has the ability to enhance immune responses; polymorphonuclear neutrophil (PMN) killing of *A. fumigatus* hyphae was increased following caspofungin exposure and this is likely due to increased β -glucan unmasking on the fungal cell wall, and also coincided with induced expression of the innate immune receptor Dectin-1 by PMNs (Lamaris *et al.*, 2008).

Currently, there are a range of avenues being explored for the discovery and development of new anti-fungals. One possibility being explored is the inhibition of fungal natural product and secondary metabolite biosynthesis (Cisar & Tan, 2008). Briefly, this notion involves inhibiting pathways, or components of pathways involved in the production of fungal-specific molecules which are important for growth and expressed during virulence, for example the iron-chelating siderophores, which are essential for *A. fumigatus* virulence (Schrettl *et al.*, 2004). This idea has already led to the development of a screening method to identify compounds which inhibit siderophore biosynthesis in *A. fumigatus* (Pinto & Moore, 2009). Heat-shock protein 90 (Hsp90), has been found to enable the acquisition and maintenance of drug resistance in fungal species (Cowen & Lindquist, 2005; Cowen *et al.*, 2006). Hsp90 inhibition has been examined for its potential as an anti-fungal therapy, and these studies showed that drug-mediated inhibition of Hsp90 blocked the development of azole resistance, and counteracted resistance in laboratory strains of *C. albicans*. Using two host systems; larvae of the greater wax-moth *Galleria mellonella* challenged with *A. fumigatus*, or a murine model of systemic candidosis, the combination of caspofungin or fluconazole (an azole) with Hsp90 inhibitors significantly increased the

activity of these drugs against *A. fumigatus* and *C. albicans* respectively (Cowen *et al.*, 2009).

Despite major advances in anti-fungal therapy development, many important challenges remain in this area. Much of the difficulty in treating IA stems from late diagnosis when significant tissue damage has already occurred, and a lack of effective biomarkers to monitor success of anti-fungal treatment over time (Denning & Hope, 2010). Also, the frequent appearance of resistance to anti-fungal drugs in pathogen populations is a significant problem (Cowen *et al.*, 2009; Loeffler & Stevens, 2003). Anti-fungal drug resistance usually involves over-expression of plasma membrane efflux pumps, which actively transport the drug out of the cell, and this has been the subject of many recent reviews (Cannon *et al.*, 2009; Chamilos & Kontoyiannis, 2005). Transcriptional regulation of efflux transporters is already under-going many avenues of investigation in order to circumvent this major problem (Monk & Goffeau, 2008). It is suggested that improvements in diagnostics, development of strategies with faster maximal anti-fungal activities; including new dosing strategies and therapeutic drug monitoring, and development of new orally bioavailable, broad spectrum anti-*Aspergillus* compounds with a low potential for development of drug resistance are all needed in order to confront the major challenges associated with current anti-fungal therapy (Denning & Hope, 2010). Furthermore, despite the fact that the fungal cell wall has proven to be an effective drug target, and with one third of *A. fumigatus* genes thought to be involved in cell wall synthesis and structural organisation, only one class of available anti-fungal drugs actually target the cell wall, the echinocandins (Aimanianda & Latge, 2010). More work is needed in this area, especially since strains resistant to the azole class of anti-fungals have been isolated among patients receiving long-term anti-fungal therapy (Aimanianda & Latge, 2010; Larsen *et al.*, 2005).

1.4. *A. fumigatus*: toxins and virulence factors.

In order to invade host tissue, *A. fumigatus* must be able to adhere to and penetrate respiratory epithelium, and kill phagocytic cells that defend the host by engulfing *A. fumigatus* conidia (Latge, 1999). A plethora of literature is available reporting putative virulence factors of *A. fumigatus*, and this topic has been reviewed in detail (Ben-Ami *et al.*, 2010; Rementeria *et al.*, 2005; Tomee & Kauffman, 2000). It is beyond the scope of this work to discuss every proposed virulence factor here, so an overview will be given of the most significant ones.

A. fumigatus produces a repertoire of adhesins, pigments and enzymes which are regarded as putative virulence factors (Latge, 1999; Rementeria *et al.*, 2005). These factors are summarised in Table 1.1. *A. fumigatus* also possesses several characteristics which allow it to evade attack from the immune system, and several important findings have been made in this area. A hydrophobic ‘rodlet layer’ comprised of hydrophobic RodA protein is covalently linked to the cell wall, covering *A. fumigatus* conidia and preventing their recognition by the immune system (Aimanianda *et al.*, 2009). Recently, a secreted protease Alp1, was identified in *A. fumigatus*, which degrades human complement proteins C3, C4, and C5, helping the fungus to evade the hosts complement attack (Behnsen *et al.*, 2010).

Table 1.1. Adhesins, pigments and enzymes regarded as putative *A. fumigatus* virulence factors. Adapted from Latge, (1999).

Category of virulence factor	Role <i>in vivo</i>	Molecule	Reference (s)
Adhesins	Aid the interactions of host proteins (e.g. fibrinogen, complement, Igs, and surfactant proteins) and cells with <i>A. fumigatus</i>	Complement receptor (54-58 kDa)	Sturtevant & Latge (1992)
		Laminarin Receptor (72 kDa)	Tronchin <i>et al.</i> (2002)
		Hydrophobins (RodA and RodB proteins (14, 16 kDa)	Thau <i>et al.</i> (1994)
Pigments	Inhibition of conidial phagocytosis by macrophages	Dihydroxynaphthalene-melanin	Tsai <i>et al.</i> (1999) Brakhage & Liebmann (2005)
Enzymes	Epithelial damage	Phospholipase(s)	Birch <i>et al.</i> (1996, 2004)
	Antioxidants during phagocytosis	Catalases	Calera <i>et al.</i> (1997) Paris <i>et al.</i> (2003)
		Superoxide dismutases (SODs)	Holdom <i>et al.</i> (1996), Paris <i>et al.</i> (2003b)
	Promotion of lung colonisation and/or degradation of humoral factors	Serine protease (33 kDa) Aspartic protease (38 kDa) Aspartic protease (CtsD) Metalloprotease (40 kDa) Dipeptidylpeptidases (88, 94 kDa)	Behnsen <i>et al.</i> (2010) Reichard (1998) Vickers <i>et al.</i> (2007) Monod <i>et al.</i> (1993) Beauvais <i>et al.</i> (1997)

Many toxic molecules and secondary metabolites produced by *A. fumigatus* have been implicated in virulence. Secondary metabolites will be discussed in more detail in a subsequent section. Of all the secondary metabolites reported to be virulence factors, the one which has attracted the most attention is gliotoxin, an epipolythiodioxopiperazine (ETP) molecule, characterised by a highly reactive disulphide bridge (Gardiner *et al.*, 2005). Gliotoxin exhibits immunosuppressive properties and was found to slow ciliary beat frequency in association with damage to human respiratory epithelial tissue *in vitro* (Amitani *et al.*, 1995). Gliotoxin also blocks T-cell and B-cell activation and the generation of cytotoxic cells *in vitro*, and has been detected in infected animals and humans at concentrations sufficient to cause these effects *in vitro* (Latge, 1999). Gliotoxin also inhibits the activation of the NADPH oxidase complex in polymorphonuclear lymphocytes (Tsunawaki *et al.*, 2004). Despite these important findings, there appears to be discrepancy regarding the importance of gliotoxin as a virulence factor, and this appears to be attributed to differences in the type of murine infection model used, including the route of inoculation and the type of immunosuppression employed (reviewed in Kwon-Chung & Sugui, 2009).

Besides gliotoxin, other toxins produced by *A. fumigatus*; fumagillin and helvolic acid, also hinder ciliary beating of epithelial tissue, but at concentrations much higher than those reported for gliotoxin (Amitani *et al.*, 1995). Helvolic acid (also known as fumigacin) belongs to a small family of natural steroid antibiotics known as the fusidane (Rementeria *et al.*, 2005). At high concentrations, helvolic acid can hinder the oxidative burst of macrophages and also cause a complete ciliostasis and rupture of epithelial cells *in vitro* (Amitani *et al.*, 1995; Mitchell *et al.*, 1997). Fumagillin is an anti-tumour antibiotic which had received attention due to its potent inhibition of angiogenesis (Ingber *et al.*, 1990). Fumagillin has recently been shown to reduce the local immune response to *A. fumigatus* and other microbes by inhibiting several neutrophil functions, including NADPH oxidase

complex assembly and reduced phagocytosis of conidia (Fallon *et al.*, 2010). The role of helvolic acid and fumagillin and the concentrations at which they occur *in vivo* is unclear, and remains to be characterised, but due to the activities described above, a role in pathogenesis can be speculated (Latge, 1999).

Other secondary metabolites produced by *A. fumigatus*, including the fumitremorgins and the ergot alkaloids, which will be discussed later, are likely to contribute to pathogenicity due to their toxic properties, although characterisation of these metabolites as virulence factors demonstrated by *in vivo* studies has not been forthcoming.

The ribotoxins are a family of ribosome inhibitory proteins which have activity against the highly conserved 28S ribosomal RNA (Kao & Davies, 1995; Kao & Davies, 1999). *A. fumigatus* produces several of these molecules, one of which, Asp f1, is a principal allergen, and is one of the immuno-dominant antigens in patients suffering from IA (Rementeria *et al.*, 2005). Asp f1, also known as restrictocin or mitogillin, is found in the urine of IA infected patients, and is believed to be a virulence factor for IA (Arruda *et al.*, 1992; Madan *et al.*, 2004). Its presence in infected patients and detailed characterisation of its structure has been used as a strategy for the diagnosis of *A. fumigatus*, with opposing views on its usefulness (Weig *et al.*, 2001; Woo *et al.*, 2001). Recent studies investigating the interaction of Aspfl with immature dendritic cells (iDCs), demonstrated that Aspfl was able to induce apoptosis, and trigger cytokine expression in iDCs, possibly representing a new immunomodulatory mechanism, resulting in the impairment of iDC's, and the immune evasion of *A. fumigatus* (Ok *et al.*, 2009).

Finally, non-ribosomal peptide synthesis (NRPS), which will be discussed in detail later, may also be a virulence strategy for *A. fumigatus*. Lactoferrin is produced by cells of the immune system during microbial infection and it binds iron, depriving the pathogen of iron (Zarembek *et al.*, 2007). To cope with this, *A. fumigatus* produces siderophores, via

NRPS, which are low molecular weight, ferric iron-specific chelators produced by many organisms under conditions of iron starvation (Haas, 2003; Leong and Winkelmann, 1998). Siderophore-mediated iron uptake was found to be essential for virulence in a murine model of IA (Schrettl *et al.*, 2004). Furthermore, gliotoxin, implicated in *A. fumigatus* virulence, as described above, is also produced via NRPS (Balibar & Walsh, 2006; Cramer *et al.*, 2006a; Gardiner & Howlett, 2005). Moreover, deletion of an NRP synthetase gene, *pes1*, in *A. fumigatus*, lead to a reduction in virulence in the *G. mellonella* insect model system of virulence (Reeves *et al.*, 2006). Further investigations into NRP synthetases in *A. fumigatus*, of which the majority remain uncharacterised, might provide further support for NRPS as an important strategy for *A. fumigatus* virulence.

Overall, since *A. fumigatus* is an opportunistic pathogen which usually only causes disease in the immunocompromised population, study of component virulence factors can be difficult. The higher mortality rate associated with *A. fumigatus* infections compared to other *Aspergillus* species, is likely due to a combination of factors, including the immune status of the host, the virulence factors of *A. fumigatus*, allied to delays in diagnosis, which allow the fungus to thrive in the host tissue making anti-fungal treatment challenging (Araujo & Rodrigues, 2004; Rementeria *et al.*, 2005). It is likely that basic characteristics associated with the fungus contribute to virulence; the conidia are small enough to spread through the entire respiratory tract, growth of mycelia at temperatures of 37 °C and higher is rapid, and the fungus does not have specific nutrition requirements (Latge, 2001). *A. fumigatus* virulence is suggested to be polygenic, since a true virulence factor, unique and indispensable for the growth of the fungus does not appear to exist (Latge, 2001; Rementeria *et al.*, 2005). Genome-wide transcriptional and/or proteomic analyses of *A. fumigatus* during infection may reveal global regulators involved in virulence (Latge,

2001), and significant progress in this area has already been achieved with the availability of the full genome sequence for *A. fumigatus* (Nierman *et al.*, 2005).

1.5. *A. fumigatus* genetics and genome information.

The complete sequence of the *A. fumigatus* genome was published in 2005, and the sequenced strain was *A. fumigatus* Af293 (Nierman *et al.*, 2005). This sequencing project revealed that the genome is 29.4 Mb in size, comprising 8 chromosomes, on which 9,926 predicted genes are present (Nierman *et al.*, 2005). The main features of the genome are presented in Table 1.2.

The Central *Aspergillus* Data Repository (CADRE), was built prior to completion of the genome sequence in order to manage the complete annotated genome sequence of *A. fumigatus*, to take part in secondary annotation of genes, and to facilitate future comparative studies with other *Aspergillus* genomes as they became available (Mabey *et al.*, 2004). Currently, the full genome sequence of 8 *Aspergillus* species is available on the CADRE database, including a clinical isolate of *A. fumigatus* (A1163), the closely related species *Neosartorya fisheri* and *A. clavatus* (Fedorova *et al.*, 2008), the model fungus *A. nidulans* (Galagan *et al.*, 2005), *A. oryzae* (Machida *et al.*, 2005), the industrially relevant *A. niger* (Pel *et al.*, 2007), *A. terreus* (Broad Institute, USA), and *A. flavus* (North Carolina University and J. Craig Venter Institute, USA). Each gene is given a unique CADRE identifier, and is classified as known, putative, or unknown (Mabey *et al.*, 2004). CADRE provides *in silico* transcripts, translated protein sequences, protein molecular weight calculations, and other useful information regarding genes of interest (Mabey *et al.*, 2004).

Availability of the full genome sequence has been a landmark towards advancing *A. fumigatus* research. It has provided a platform for a range of genome-wide transcriptional analyses to be performed, in order to gain a better understanding of the fungus and the

transcriptional responses to particular environments. Amongst these are the response to heat shock (Albrecht *et al.*, 2010; Do *et al.*, 2009; Nierman *et al.*, 2005), the transcriptional profile upon exposure to the anti-fungal voriconazole (Ferreira *et al.*, 2006b), analysis of the genes expressed upon exit of spores from dormancy (Lamarre *et al.*, 2008) and the transcriptional response of *A. fumigatus* upon exposure to human neutrophils (Sugui *et al.*, 2008).

Comparison of the *A. fumigatus* A1163 genome sequence to the Af293 sequence revealed that a large translocation had taken place between chromosomes 1 and 6 of Af293 and a genomic region of A1163 (Fedorova *et al.*, 2008). Most translocation events involving *A. fumigatus* chromosomes are reported to have taken place within 300 kb of the telomeres (Fedorova *et al.*, 2008). Approximately 500 *A. fumigatus*-specific genes were found, having no homologues in *A. niger* or *A. nidulans*, and approximately one third of these showed sequence similarity to fungal gene products (Nierman *et al.*, 2005). Many of the *A. fumigatus*-specific genes appear to be involved in secondary metabolite production, for example the developmentally-regulated pigment biosynthetic cluster (Nierman *et al.*, 2005). Secondary metabolites will be discussed in the following sections.

Table 1.2. The key features of the *A. fumigatus* genome Modified from Nierman *et al.* (2005).

Genome	Value
Nuclear genome	
Size (Mb)	29.4 Mb
G + C content (%)	49.9 %
Number of predicted genes	9,926
Mean gene length (bp)	1.431
% of genes coding	50.1 %
Genes of unknown function	3,288
% of genes containing introns	77 %
RNA	
tRNA number	179
5S rRNA number	33
Mitochondrial genome	
Size (bp)	31,892
G + C content (%)	25.4 %
Number of predicted genes	16
% of genes coding	44.1 %
tRNA number	33

1.6. Secondary metabolites and clustering of biosynthetic genes.

Fungal secondary metabolites (SM) constitute a diverse suite of small molecules that are not deemed essential for normal growth and development (Fox & Howlett, 2008). They may interchangeably be referred to as natural products. Secondary metabolites are considered to be the chemical arsenal necessary for adaptation to ecological niches (Calvo *et al.*, 2002). Secondary metabolites have received intense interest due to their biotechnological and therapeutic applications. Compounds such as the penicillin antibiotics G and V, the anti-hypercholesteremic drug lovastatin, the immunosuppressant cyclosporin, and all derivatives are fungal secondary metabolites (Berth-Jones, 2005; Demain & Elander, 1999; Misiak & Hoffmeister, 2007). Mycotoxins on the other hand are harmful SM that are mainly produced by fungi of the genera *Fusarium*, *Aspergillus* and *Penicillium* (Reverberi *et al.*, 2010). Classes of fungal secondary metabolites include the polyketides (the aflatoxins and fumonisins), non-ribosomal peptides (gliotoxin, siderophores and sirodesmin) and terpenes and indole terpenes (Fox & Howlett, 2008). The first dedicated step in the biosynthesis of a secondary metabolite is usually catalysed by one of five enzymes, referred to as a 'backbone enzyme' (Khaldi *et al.*, 2010). These enzymes include the non-ribosomal peptide (NRP) synthetases, polyketide synthetases (PKSs), hybrid NRP-PKS enzymes, prenyltransferases (DMATS) and terpene cyclases (Khaldi *et al.*, 2010). Genes for the biosynthesis of secondary metabolites are usually clustered (Keller & Hohn, 1997), aiding identification from completed fungal genome sequences. Intermediate products formed by these backbone enzymes can usually be modified by 'decorating' enzymes, and the final product transported out of the fungal cell by a specific transporter, and the genes for these enzymes can also be found within the specific cluster (Khaldi *et al.*, 2010). Secondary metabolite gene clusters often contain a transcription factor that specifically regulates expression of the genes within the cluster, for example, the GliZ

transcriptional regulator of the gliotoxin biosynthetic cluster (Bok *et al.*, 2006). Other gene clusters do not have transcription factors, such as the ergot alkaloid and lolitrem clusters in the endophytes *Neophytodium lolli* and *Epichloe festucae* (Fleetwood *et al.*, 2007; Young *et al.*, 2005; Young *et al.*, 2006). In fact, the level of gene expression is much higher *in plantae* than under standard laboratory culturing conditions for some of these endophyte clusters, suggesting that they are regulated by plant signalling pathways (Young *et al.*, 2006).

Sequencing of the genome revealed that *A. fumigatus* possesses 26 SM gene clusters, containing polyketide synthase (PKS), non-ribosomal peptide (NRP) synthetases and/or dimethylallyl tryptophan (DMAT) synthase genes (Nierman *et al.*, 2005). Thirteen of these clusters have orthologues in *A. oryzae* and/or *A. nidulans*, and 10 of those orthologous clusters are missing many of the genes present in the *A. fumigatus* clusters (Nierman *et al.*, 2005). It has since been suggested that there are only 22 SM gene clusters within *A. fumigatus* (Perrin *et al.*, 2007). Although found throughout the genome, SM clusters location appears to be biased towards the telomeres (Nierman *et al.*, 2005). The observation that translocations occur in the genome of *A. fumigatus*, particularly at telomeric regions, highlights the fact that the genomes are still evolving, and the bias of secondary metabolite clusters for telomeric locations might make them more susceptible to reorganisation, aiding their structural diversity (Fedorova *et al.*, 2008).

Examples of characterised biosynthetic secondary metabolite gene clusters in *A. fumigatus* are those directing the biosynthesis of gliotoxin (Gardiner & Howlett, 2005), the fumitremogin family of secondary metabolites (Grundmann & Li, 2005), the ergot alkaloids (Coyle & Panaccione, 2005; Unsold & Li, 2005) and the siderophores (Reiber *et al.*, 2005).

1.7. Regulation of secondary metabolism gene clusters by the global secondary metabolite regulator LaeA.

Sterigmatocystin (ST) is one of the most toxic secondary metabolites known, and is produced by a gene cluster in *A. nidulans* (Brown *et al.*, 1996). In a mutagenesis study, 23 *A. nidulans* mutants impaired in ST production were isolated (Butchko *et al.*, 1999). A gene was identified, *laeA*, which could restore one of these mutants (Bok & Keller, 2004). *laeA* encodes a nuclear protein, with a conserved S-adenosyl methionine (SAM) binding site, characteristic of nuclear methyltransferases (Bok & Keller, 2004). LaeA was found to transcriptionally regulate the sterigmatocystin, penicillin and pigment biosynthetic clusters in *A. nidulans*; gliotoxin and mycelial pigments in *A. fumigatus*, and the lovastatin gene cluster in *A. terreus* (Bok & Keller, 2004). LaeA is thought to regulate the expression of secondary metabolite gene clusters by acting at a chromatin remodelling level, an activity which has been observed for other nuclear transferases (Bok & Keller, 2004). LaeA is highly conserved amongst pathogenic filamentous fungi but absent in *S. cerevisiae*, which does not produce secondary metabolites (Bok & Keller, 2004).

Subsequent studies showed that deletion of *laeA* resulted in reduced virulence in a murine model of IA, associated with a loss of gliotoxin production, increased conidial susceptibility to phagocytosis by macrophages, and decreased ability of hyphae to kill neutrophils (Bok *et al.*, 2005). Conidial surfaces of the *laeA* mutant were altered in comparison to wild-type, with loss of the characteristic protrusions normally observed on conidia. These findings implied that LaeA regulates the expression of certain genes involved in conidial biosynthesis (Bok *et al.*, 2005). This also provides support for a link between secondary metabolism and fungal development (Calvo *et al.*, 2002). Recently, it was found that the reduced virulence observed in the *laeA* mutant was associated with a perturbation of the hydrophobic layer on the surface of the conidia, and decreased

hydrophobicity of the $\Delta laeA$ conidia most likely leads to increased phagocytic uptake (Dagenais *et al.*, 2010). A transcriptional profiling study of an *A. fumigatus laeA* mutant identified 13 SM gene clusters that were under the transcriptional regulation of LaeA (Bok & Keller, 2004; Perrin *et al.*, 2007).

1.8. Association of secondary metabolism with development.

Secondary metabolites are often associated with sporulation and developmental processes (reviewed in (Calvo *et al.*, 2002). BrlA is a C₂H₂ zinc finger transcription factor that is essential for sporulation in *A. nidulans* (Adams *et al.*, 1988; Boylan *et al.*, 1987). *brlA* is expressed in response to sporulation signals in both *A. nidulans* and *A. fumigatus*, and BrlA regulates the expression of two other genes *wetA* and *abaA*, which together comprise the central regulatory pathway for sporulation (Boylan *et al.*, 1987; Mirabito *et al.*, 1989). StuA is another transcription factor also required for regulation of sporulation in *A. nidulans* (Aguirre, 1993; Busby *et al.*, 1996; Miller *et al.*, 1991). Deletion of *A. nidulans stuA* interferes with the localisation of BrlA and AbaA, and results in deformed conidiophores (Clutterbuck, 1969; Miller *et al.*, 1992). A similar phenotype was observed in an *A. fumigatus stuA* mutant (Sheppard *et al.*, 2005). The expression of genes involved in ergot alkaloid biosynthesis in *A. fumigatus* is dependant on BrlA, with ergot alkaloids accounting for 1 % of total conidial weight (Coyle *et al.*, 2007). Gliotoxin production is dependant on StuA both *in vitro* and *in vivo* (Gravelat *et al.*, 2008). A further analysis of the transcriptional program regulated by BrlA and StuA indicated that 6 secondary metabolite gene clusters are dependant on StuA, including the ergot alkaloid, fumitremorgin, gliotoxin, pseurotin A, and two unknown clusters (Twumasi-Boateng *et al.*, 2009). Only the ergot alkaloid cluster was found to be dependant on BrlA (Twumasi-Boateng *et al.*, 2009). Recent phylogenetic analyses revealed a correlation between the presence of secondary

metabolite biosynthetic pathways and filamentous growth among the fungi (Khaldi *et al.*, 2010).

Secondary metabolism and development in *A. nidulans* are also regulated in response to external cues such as light (Bayram *et al.*, 2008). There is genetic evidence for an association between sporulation, secondary metabolite production and light, but until recently, the underlying molecular mechanisms were unknown (Busch *et al.*, 2003; Kato *et al.*, 2003; Kim *et al.*, 2002). A possible candidate protein was velvet (VeA), whose expression and function is coordinated with sexual reproduction and light (Kim *et al.*, 2002; Stinnett *et al.*, 2007). VeA was found to negatively regulate asexual sporulation and antibiotic biosynthesis (Mooney & Yager, 1990; Sprote & Brakhage, 2007). Recently, a study was undertaken to identify proteins that interact with *A. nidulans* VeA, and an interaction complex was identified, comprising VeA, velvet-like protein B (VelB), the global SM regulator LaeA, and an importin KapA, and these proteins were found to interact with VeA in the dark (Bayram *et al.*, 2008). VeA expression was negligible in the light (Bayram *et al.*, 2008). The authors proposed a model for this complex set of interactions, referred to as the VelB/VeA/LaeA (velvet) complex. In the dark, the velvet complex interaction controls and possibly supports the epigenetic activity of LaeA, leading to the up-regulation of SM gene cluster expression (Bayram *et al.*, 2008). The authors suggest that this complex regulates the level of SM production by modulating the epigenetic control of chromatin remodelling by the LaeA methyltransferase (Bayram *et al.*, 2008). The *velvet* complex is represented schematically in Figure 1.2.

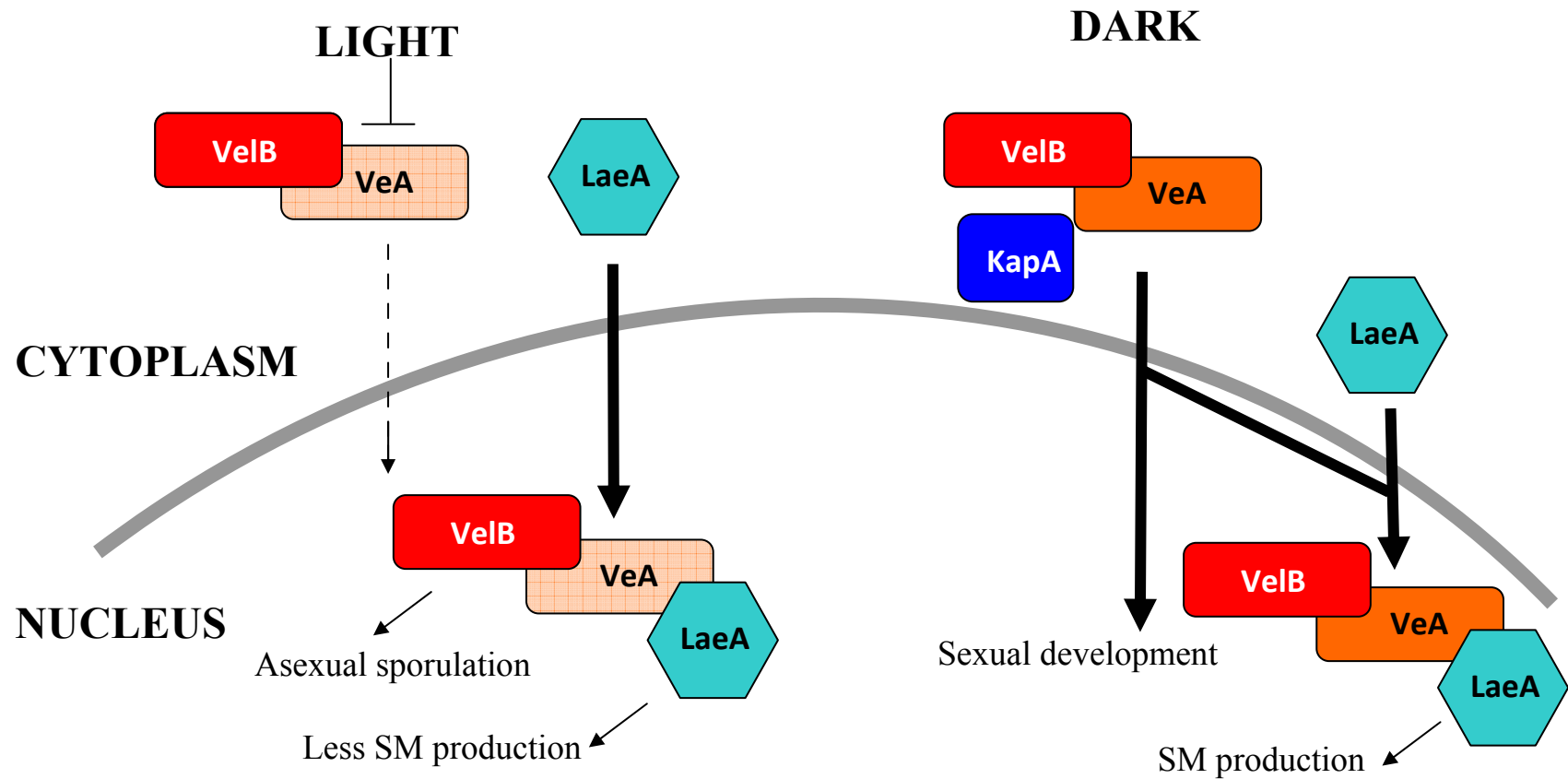


Figure 1.2. Proposed model for the action of the VelB/VeA/LaeA complex in the regulation of SM production. Re-drawn from Bayram *et al.* (2008). In the light, VeA is mostly abundant in the cytoplasm (light orange), while VelB is present in the nucleus and supports asexual sporulation, and LaeA is poorly active, resulting in a low level of SM production. In the dark, KapA imports VeA into the nucleus (dark orange) where it interacts with LaeA and VeB to form the *velvet* complex, resulting in sexual sporulation and an increase in SM production (Bayram *et al.*, 2008).

1.9. Non-ribosomal peptide synthesis (NRPS)

1.9.1. NRPS – An overview

NRPS is a key mechanism which is responsible for the biosynthesis of a large number of bioactive metabolites in bacterial and fungal species (Mootz *et al.*, 2002b; Reiber *et al.*, 2005; Stack *et al.*, 2007). As the name indicates, NRPS produces peptides independently of the ribosome, and this process was first identified by Lipmann and colleagues while investigating the biosynthesis of the antibiotics gramicidin S and tyrocidin in the bacterium *Bacillus. brevis* (Lipmann, 1971; Lipmann *et al.*, 1971). NRPS has gained significant attention as it represents a reservoir of current and new natural product medicines, and it has the potential for antimicrobial drug development by the targeting of NRP synthetases which are essential for survival of pathogens in the human host (Doyle, 2009; Schrettl *et al.*, 2004).

Products of NRP synthetases include pharmaceutically important products such as the immunosuppressant cyclosporine **1** and the antibiotic penicillin G **2** (Cramer *et al.*, 2006b; Doyle, 2009), HC-toxin **3** and AM-toxin in phytopathogenic fungi (Turgeon *et al.*, 2008), anti-tumour agents (actinomycin **4**, bleomycin) (Turgeon *et al.*, 2008), the iron-chelating siderophores fusarane C and ferricrocin **5** (Eisendle *et al.*, 2003; Schrettl *et al.*, 2004), the toxic metabolites gliotoxin **6** and sirodesmin from *A. fumigatus* and *L. maculans*, respectively (Fox & Howlett, 2008), and the fumitremorgin family of secondary metabolites in *A. fumigatus* (Maiya *et al.*, 2006). Various non-ribosomally produced peptides are shown in Figure 1.3.

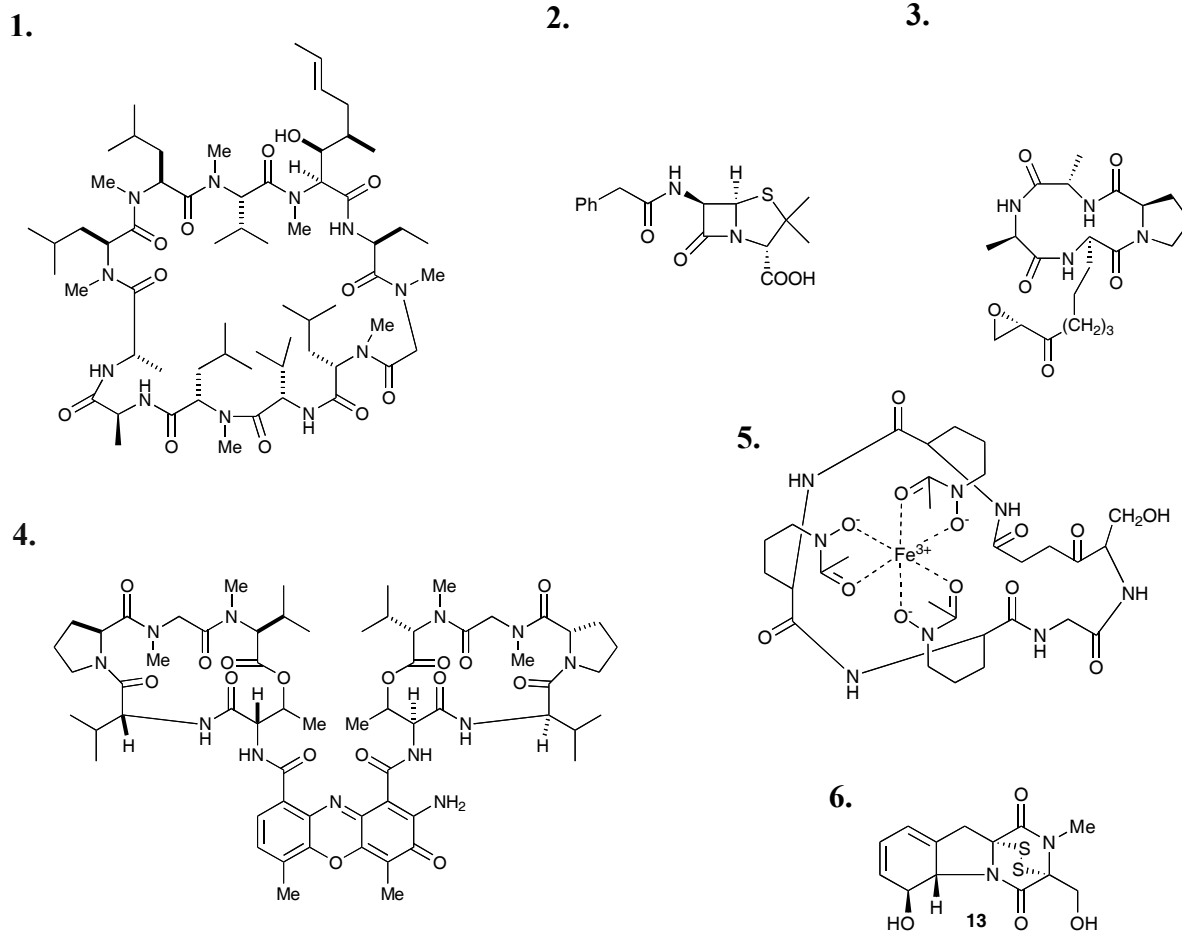


Figure 1.3. Non-ribosomally synthesised peptides of bacterial or fungal origin.

1. The immunosuppressant cyclosporin 2. Penicillin G, one of the β -lactam antibiotics is synthesised by the tri-modular ACV synthetase. This enzyme had been found in fungi of the genera *Penicillium*, *Streptomyces*, *Acremonium* and *Aspergillus* (Doyle, 2009; Martin, 2000), 3. HC-toxin produced by *Cochliobolus carbonum*, implicated in plant pathogenesis, 4. The anti-tumour agent actinomycin C1 is produced in *Streptomyces* spp. by a three gene cluster of NRP synthetases (vonDohren *et al.*, 1997), 5. The intracellular siderophore, ferricrocin, produced in *A. fumigatus*, by a three module NRP synthetase, SidC (Schrettl *et al.*, 2007), 6. Gliotoxin, is part-synthesised by a di-modular NRP synthetase, GliP, in *A. fumigatus* (Balibar & Walsh, 2006; Cramer *et al.*, 2006a).

An overview of NRPS is presented in Figure 1.4. NRP synthetases are produced as inactive apo-enzymes. The synthesis of a non-ribosomal peptide requires NRP synthetase activation, which is mediated by the activity of a 4'phosphopantetheinyl transferase (4'-PPTase) (Neville *et al.*, 2005). Conversion of apo-NRP synthetase to holo-NRP synthetase is performed post-translationally by the addition of a phosphopantetheine group (Ppant) from Coenzyme A (CoA) to a specific residue on the NRP synthetase by 4'PPTase. The activated holo-NRP synthetase then generates the NRP product by incorporating amino acid substrates into a peptide chain (Stack *et al.*, 2007). NRP synthetases may be mono- or multi-modular, with each module responsible for the incorporation of an individual amino acid into the growing peptide (Stack *et al.*, 2007). The generated peptide chain can then undergo further modifications before being released from the NRP synthetase as the final NRP product.

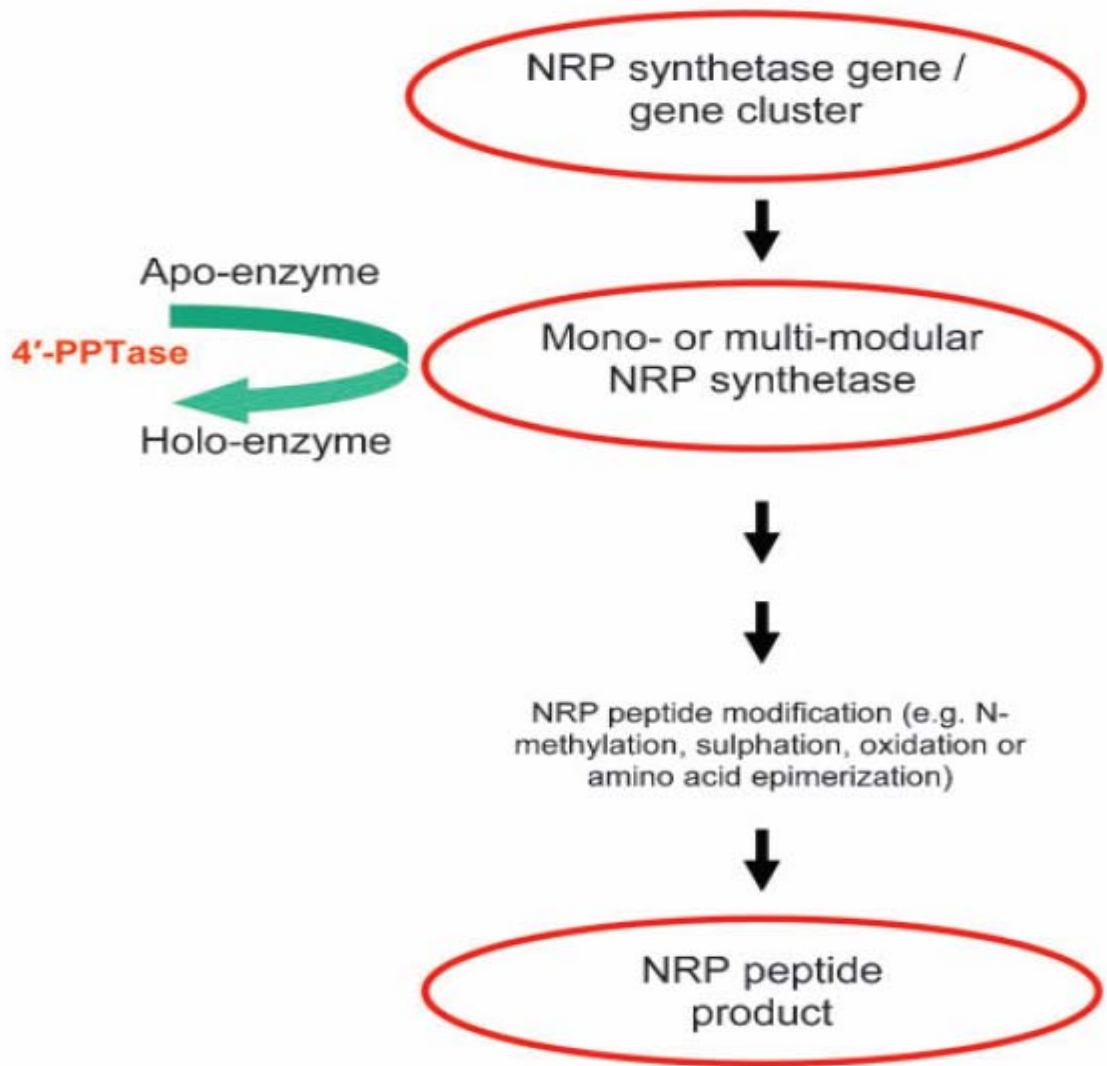


Figure 1.4. Schematic overview of the process of, and enzymatic functions involved in, NRP synthesis (Stack *et al.*, 2007). Key: 4'-PPTase, 4'phosphopantetheinyl transferase; NRP synthetase, non-ribosomal peptide synthetase; NRP, non-ribosomal peptide.

1.9.2. Structural arrangements and domain architecture of NRP synthetases.

Non-ribosomal peptide synthetase genes, which are generally present in multi-gene clusters as described earlier, encode NRP synthetases, which can be up to 2.3 MDa molecular mass (Stack *et al.*, 2007). NRP synthetases are organised into sets of catalytic units known as modules, whereby the minimal module is comprised of three discrete domains; namely adenylation (A), thiolation (T) (or peptidyl carrier protein (PCP)), and condensation (C) domains (Grunewald & Marahiel, 2006; Stack *et al.*, 2007). Each module is responsible for the recognition, via the A domain, and incorporation of a single amino acid into the cognate peptide product (Stack *et al.*, 2007). Amino acids are selected from a large repertoire of substrates, as mentioned previously, which leads to the high level of structural diversity observed in NRPs (Grunewald & Marahiel, 2006; Stack *et al.*, 2007).

NRP synthetase modules can also contain additional domains for the epimerisation (L- to D- conversion), cyclization or methylation of the amino acid substrates (Tiburzi *et al.*, 2007). The final module of an NRP synthetase usually contains a thioesterase domain (TE), which functions in the release of the final peptide product. However, to date, very few TE domains have been found in fungal NRP synthetases (Cramer *et al.*, 2006b). In fungal NRP synthetases, the TE domain is often replaced by a specialised C domain, which is believed to catalyse cyclization and release of the NRP (Cramer *et al.*, 2006b; Keating *et al.*, 2001).

The organisation and order of NRP synthetase modules usually corresponds to the amino acid sequence of the peptide product, a feature known as the co-linearity rule (Grunewald & Marahiel, 2006; Lautru & Challis, 2004; Tiburzi *et al.*, 2007). The basic organisation of a typical NRP synthetase comprises an initiation module, followed by a variable number of elongation modules, which are required for the propagation of the growing peptide, and finally, a termination module, where if present, a TE domain

catalyses peptide release (Strieker *et al.*, 2010). The arrangement of *A. fumigatus* Pes3 (Cramer *et al.*, 2006b; Stack *et al.*, 2009), a multi-modular NRP synthetase, which is of major interest in this work, is detailed in Figure 1.5.

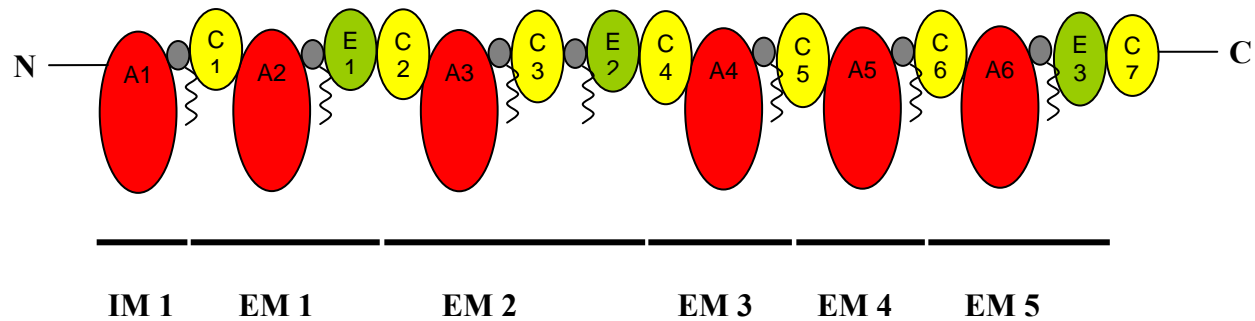


Figure 1.5. Diagrammatic representation of the domain architecture of *A. fumigatus* Pes3, comprising six adenylation domains (A1-A6), seven thiolation domains (in grey), seven condensation domains (C1-C7), and three epimerisation domains (E1-E3). The black helices extending from the thiolation domains represent Ppant groups which are post-translationally added, thereby converting Pes3 to a holo-enzyme. An initiation module consists of an N-terminal adenylation and thiolation domain (Cramer *et al.*, 2006b), and each elongation module minimally consists of a condensation, an adenylation and a thiolation domain. The final C domain may function in release of the peptide from the NRP synthetase (Cramer *et al.*, 2006b; Keating *et al.*, 2001). Initiation modules (IM) and elongation modules (EM) are shown. Adapted from (Cramer *et al.*, 2006b; Stack *et al.*, 2007; Stack *et al.*, 2009).

NRP synthetases can broadly be grouped into three categories; (A) linear, (B) iterative and (C) non-linear (Mootz *et al.*, 2002b). Linear NRP synthetases have the classical domain architecture of C-A-T, with each module used once during peptide synthesis, to incorporate an individual amino acid into the growing peptide, thus following the co-linearity rule (Grunewald & Marahiel, 2006; Mootz *et al.*, 2002b). Known linear NRP synthetases include those which produce surfactin, cyclosporin, and ACV, the precursor to the penicillin antibiotics (Mootz *et al.*, 2002b). Iterative NRP synthetases use modules more than once in the synthesis of one single peptide product, a strategy that leads to a peptide chain consisting of repeated smaller sequences (Mootz *et al.*, 2002b). Iterative NRP synthetases include those which biosynthesise siderophores (Mootz *et al.*, 2002b; Reiber *et al.*, 2005; Stack *et al.*, 2007). Non-linear NRP synthetases deviate from the standard C-A-T modular arrangement, and it is thought that they represent a large part of the NRP synthetase repertoire in nature (Mootz *et al.*, 2002b). Non-linear NRP synthetases are complex and require detailed biochemical studies in order to understand the functions of each module and the peptide produced, as it is impossible to accurately predict the peptide sequence due to the unusual domain organisation (Mootz *et al.*, 2002b). Examples of non-linear NRP synthetases include those which are responsible for bleomycin, vibriobactin or mycobactin biosynthesis (Mootz *et al.*, 2002b).

1.9.3. 4'phosphopantetheinyl transferases and requirement for NRP Synthetase activation to holoenzyme.

NRP synthetases are produced in an inactive apo-form and require post-translational modification in order to yield the active holo-form (Lambalot *et al.*, 1996). Activation of an NRP synthetase from an inactive apo-form to an active holo-form is mediated by a 4'phosphopantetheinyl transferase (4'-PPTase), in a magnesium-dependant reaction (Lambalot *et al.*, 1996; Walsh *et al.*, 1997). PPTases also catalyse the transfer of phosphopantetheine (Ppant) groups from CoA to the carrier or thiolation domain of enzymes involved in polyketide and fatty acid biosynthesis (Mootz *et al.*, 2002a). The Ppant group is transferred to a conserved serine within the thiolation domain of an apo-NRP synthetase yielding an activated holo-NRP synthetase (Stack *et al.*, 2007). The Ppant groups serve to anchor activated amino acid substrates during NRPS, and allow their movement between active sites within the NRP synthetase (Grunewald & Marahiel, 2006). In *A. nidulans*, a 4'-PPTase (*npgA*) was found to be essential for penicillin biosynthesis (Keszenman-Pereyra *et al.*, 2003). An *A. fumigatus* 4'-PPTase was characterised and shown to post-translationally activate modules of recombinant *A. fumigatus* NRP synthetase, Pes1 and Pes3 (Neville *et al.*, 2005; Stack *et al.*, 2009). A diagrammatic representation of 4'-PPTase activity is shown in Figure 1.6.

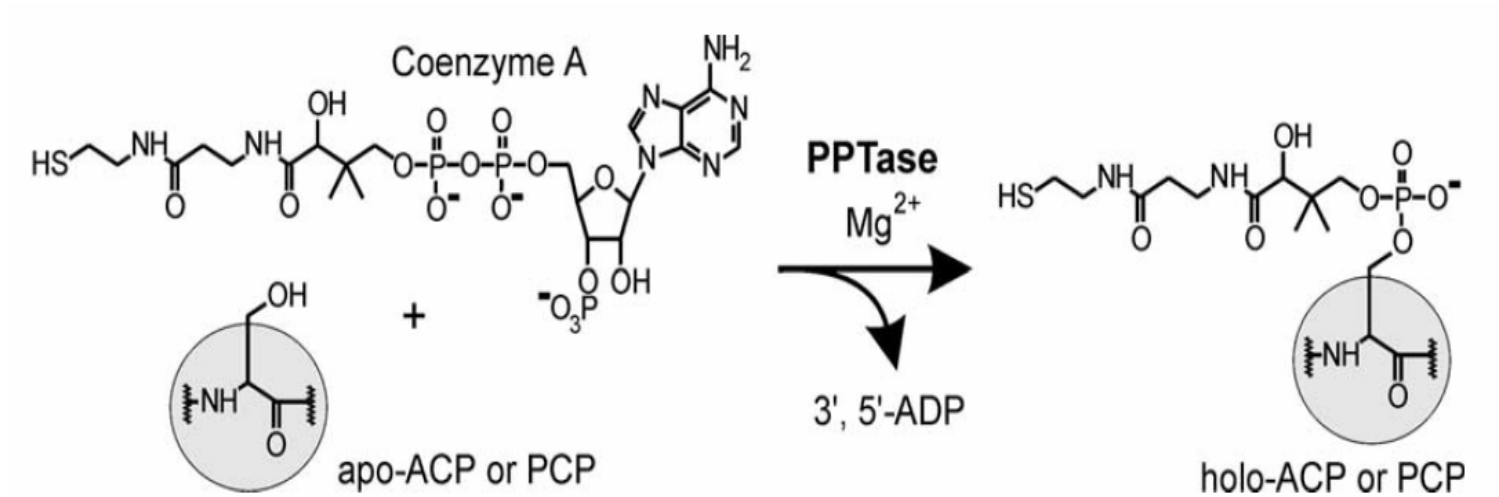


Figure 1.6. Reaction catalysed by PPTases to convert apo- to holo- NRP synthetase. PPTases catalyse the activation of an apo-enzyme to a holo-enzyme by the transfer of a Ppant group from CoA onto the side chain hydroxyl group of a conserved serine residue in the thiolation/ peptidyl carrier domain of an NRP synthetase. The –SH of the Ppant group acts as a nucleophile for acylation by the adenylation domain specific substrate (Lambalot *et al.*, 1996; Mootz *et al.*, 2002a).

1.9.4. NRPS – Mechanisms of Non-ribosomal Peptide Synthesis.

Amino acid selection and activation for ribosomal protein synthesis is mediated by the activity of tRNA synthetases, whereby amino acyladenylate is converted into amino acyl-tRNA (Stachelhaus & Marahiel, 1995). NRP synthetases biosynthesise peptides similarly; the adenylation domain of the NRP synthetase selects and activates a specific amino acid. However, there are striking differences between ribosomal and NRP synthesis. Firstly, non-ribosomal peptides contain not only the 20 common proteinogenic L-amino acids, but many other different building blocks, including D-amino acids, N-terminally attached fatty acids, methylated, hydroxylated and acetylated amino acids, as well as various phosphorylated and glycosylated residues (Grunewald & Marahiel, 2006; Tiburzi *et al.*, 2007). A common feature of NRPs is heterocyclization of the peptide backbone, which poses structural constraints on the peptide necessary for ensuring specific interaction with the correct molecular target (Kohli & Walsh, 2003; Tiburzi *et al.*, 2007). Furthermore, ribosomal protein synthesis involves strict proof-reading mechanisms to ensure that the correct amino acid is incorporated during peptide synthesis, whereas NRPS shows less strict substrate selection and incorporation (Stachelhaus *et al.*, 1999).

The specific mechanisms underlying the biosynthesis of peptides by modular enzymes such as NRP synthetases has been widely studied and has seen significant breakthroughs over the last 30 years (Meier & Burkart, 2009). As mentioned earlier, the A domain controls the first step of NRPS, which is the selection of an amino acid substrate and activation to an amino acyl adenylate (Schwarzer & Marahiel, 2001). The A domain is about 550 amino acids in length and contains a non-linear 8-13 aa ‘signature motif’ which is believed to govern the substrate specificity of the particular A domain (Grunewald & Marahiel, 2006; Stack *et al.*, 2007).

The first A domain to be crystallised was the phenylalanine activating module (PheA) of gramicidin synthetase 1 (GrsA), responsible for antibiotic biosynthesis in *Bacillus brevis* (Conti *et al.*, 1997). PheA was crystallised with bound substrate and ATP and this led to the identification of a 10 amino acid active site, revealing the basis for substrate recognition and activation (Conti *et al.*, 1997; Schwarzer & Marahiel, 2001).

The second dedicated step of NRPS is the transfer of the activated substrate from the A domain to the T or PCP domain of the NRP synthetase. T domains are approximately 80-100 amino acids in length, and are located downstream of A domains. The T domain covalently binds the amino acyl adenylate as thioester to the terminal thiol of the Ppant group, and the group can now act as a 'swinging arm' to reach various catalytic centres of the NRP synthetase (e.g. for condensation of modification at other domains) (Schwarzer & Marahiel, 2001). The C domain is usually the third domain present in a minimal NRP module, and this represents the condensation unit, catalysing peptide bond formation between amino acid adenylates on two adjacent thiolation domains (Marahiel *et al.*, 1997). Finally, the completed peptide can be released from the enzyme by the activity of a thioesterase (TE) domain (Grunewald & Marahiel, 2006; Mootz *et al.*, 2002b; Stack *et al.*, 2007), or in the case of fungal NRP synthetases, peptide release is more likely to be catalysed by a specialised C domain (Cramer *et al.*, 2006b; Keating *et al.*, 2001). A simplified mechanism for NRPS is shown in Figure 1.7.

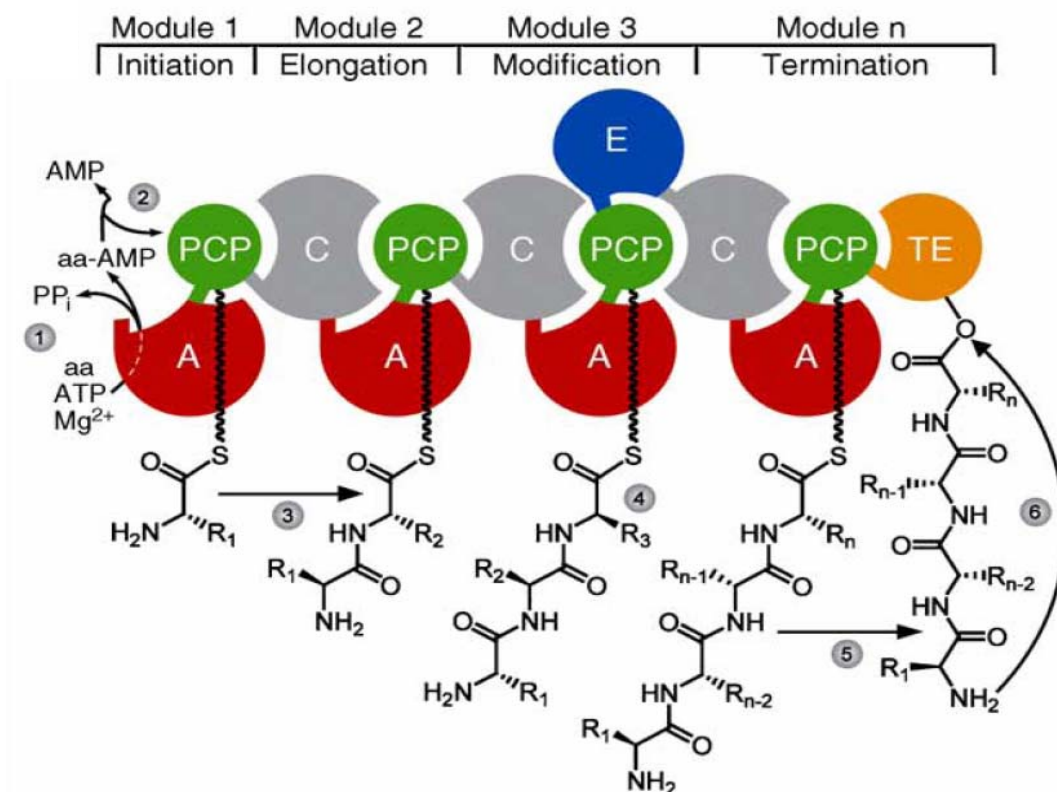


Figure 1.7. A simplified illustration of the process of NRPS. 1. The substrate amino acid is activated as amino-acyl AMP by the adenylation domain. 2. The amino acid is transferred onto the T/PCP domain, which has been post-translationally modified by the addition of a Ppant group (indicated by a black helix). 3. Condensation or peptide bond formation between thiolation bound amino acid intermediates on adjacent T/PCP domains. 4. Possible amino acid modifications which may occur; E domains can mediate L- to D-amino acid conversion. 5. Trans-esterification of the complete peptide from the terminal T/PCP domain onto the TE domain (Note this may be a specialised terminal C domain in fungal NRP synthetases). 6. Peptide is released from TE domain by either hydrolysis or macrocyclization. Strieker *et al.* (2010).

Since the crystallisation of GrsA, and the identification of substrate specificity conferring residues in NRP synthetase A domains, subsequent comparisons between GrsA and corresponding moieties in other A domains have led to the successful substrate prediction of bacterial NRP synthetase A domains, and therefore might allow prediction of NRP products (Stachelhaus *et al.*, 1999). These selectivity motifs, also known as core domains appear to be highly conserved and are shown in Table 1.3 (Schwarzer *et al.*, 2003).

Table 1.3. Core motifs governing substrate specificity of NRP synthetase A domains Schwarzer *et al.* (2003).

NRP synthetase adenylation domain core motifs	
A1	L(TS)YxEL
A2	LGAGxAYL(VL)P(LI)D
A3	LAYxxYTSG(ST)TGxPKG
A4	FDxS
A5	NxYGPTE
A6	GELxJGX(VL)ARGYL
A7	Y(RK)TGDL
A8	GRxPxQVKIRGxRIELGEIE
A9	LPxYM(IV)P
A10	NGK(VL)DR

Despite significant progress in elucidating the NRPS specificity conferring ‘code’, initial studies focused on bacterial A domain specificity, and don’t appear to be predictive of fungal A domain specificity (Bushley *et al.*, 2008; Stack *et al.*, 2007). Fungal A domain specificity therefore remains to be elucidated, with only a handful of specific substrates identified to date, detailed in Table 1.4 Doyle, (2009).

Table 1.4. A domain specificity of fungal NRP or PK/NRP synthetases Doyle, (2009).

Enzyme type	Final product	A domain	Species	Reference
NRP synthetases				
SidD	TAFC	A1 (n5-cis-anhydromevalonyl-N5-hydroxy-L-ornithine	<i>A. fumigatus</i>	Schrettl <i>et al.</i> (2007)
SidC	FC	N5-acetyl-N5-hydroxy-L-ornithine, Ser, Gly	<i>A. fumigatus</i>	Schrettl <i>et al.</i> (2007)
GliP	Gliotoxin	A1 (L-Phe), A2 (L-Ser)	<i>A. fumigatus</i>	Balibar and Walsh (2006)
Hybrid polyketide/NRP synthetases				
FUSS	Fusarin C	A1 (homoserine)	<i>Fusarium moniliforme</i>	Rees <i>et al.</i> (2007)
TENS	2-pyridone tenellin	L-Tyr	<i>Beauveria bassiana</i>	Eley <i>et al.</i> (2007)
PsoA	pseurotin A	L-Phe	<i>A. fumigatus</i>	Maiya <i>et al.</i> (2007)
TdiA	terriquinone A	Arylic acid	<i>A. nidulans</i>	Bok <i>et al.</i> (2006b)
CheA	Cytochalasan	L-Trp	<i>Penicillium expansum</i>	Schumann and Hertweck (2007)

1.10. NRPS in *A. fumigatus*.

Sequencing and analysis of the *A. fumigatus* genome revealed the presence of 14 NRP synthetase encoding genes (Cramer *et al.*, 2006b; Nierman *et al.*, 2005). Domain architecture of NRP synthetases were predicted using *in silico* methods. Table 1.5 gives an overview of the NRP synthetases within *A. fumigatus*, their predicted organisation, and known NRP products are included. None of the *A. fumigatus* NRP synthetases contain a TE domain, while 10 of the 14 NRP synthetases end in a unique C domain, which may function in the release of the NRP, similar to a finding made for *C. heterostrophus* NRP synthetases (Cramer *et al.*, 2006b; Lee *et al.*, 2005).

Peptides produced by a small number of these NRP synthetases have been elucidated to date, mainly through targeted gene deletion studies. A combined bioinformatic and gene deletion approach led to the identification of an NRP synthetase, GliP, which is essential in the early biosynthesis of gliotoxin in *A. fumigatus* (Cramer *et al.*, 2006a; Gardiner & Howlett, 2005). Heterologous expression and gene deletion strategies were used to confirm that the NRP synthetase FtmA makes the diketopiperazine scaffold brevianamide F, which is the precursor to the fumitremorgin family of secondary metabolites produced by *A. fumigatus* (Maiya *et al.*, 2006). Two NRP synthetases, encoded by the genes *sidD* and *sidC* in *A. fumigatus* have been found to be essential for the biosynthesis of siderophores (Reiber *et al.*, 2005; Schrettl *et al.*, 2007). A multi-modular NRP synthetase, *pesI* was found to important for virulence and protection against oxidative stress, although no corresponding peptide was identified in that study (Reeves *et al.*, 2006). The lack of information relating the remaining NRP synthetases to peptide products presents a functional genomics challenge that can now be addressed with the available genome sequence. This challenge is addressed by much of the work described in this thesis.

Table 1.5. NRP synthetase genes in *A. fumigatus*, with predicted domain organisation (Cramer *et al.*, 2006b; Stack *et al.*, 2007).

Gene	Domain Architecture	CADRE I.D.	NRP product
<i>pes1 (NRPS1)</i>	ATECACACATECTCT	AFUA_1G10380	
<i>sidC (NRPS2)</i>	ATCATCATCTCTC	AFUA_1G17200	Ferrichrome
<i>sidE (NRPS3)</i>	ATCATC	AFUA_3G03350	
<i>sidD (NRPS4)</i>	ATCATC	AFUA_3G03420	TAFC
<i>pesF (NRPS5)</i>	ATCATCT	AFUA_3G12920	
<i>pesG (NRPS6)</i>	ATC	AFUA_3G13730	
<i>pesH (NRPS7)</i>	ACATC	AFUA_3G15270	
<i>pes3/I (NRPS8)</i>	ATCATECATCETCATCATCATEC	AFUA_5G12730	
<i>pesJ (NRPS9)</i>	C*ATC	AFUA_6G09610	
<i>gliK (NRPS10)</i>	ATCATCT	AFUA_6G09660	Gliotoxin
<i>pesL (NRPS11)</i>	ATC	AFUA_6G12050	
<i>pesM (NRPS12)</i>	ATCATCEATC(TE)	AFUA_6G12080	
<i>pesN (NRPS13)</i> (<i>ftmA</i>)	ACATC	AFUA_9G00170	FTMs
<i>pesO (NRPS14)</i>	PKSNNCAT(DH)	AFUA_8G00540	

Key: A, adenlyation domain; T, thiolation domain; C, condensation domain; E, epimerisation domain TE, thioesterase domain; DH, putative dehydrogenase domain; C*, partial condensation domain; PKS, polyketide synthetase; N, incomplete domain; FTMs, fumitremorgin family of secondary metabolites.

1.11. Genetic manipulations available for characterisation of genes within *A. fumigatus*.

The availability of the complete *A. fumigatus* genome sequence has provided the necessary information to facilitate characterisation of gene function by genetic manipulation (Xue *et al.*, 2004). To investigate gene function, genetic manipulation systems which are capable of specifically targeting genes of interest for deletion or disruption, leading to the creation of isogenic mutant strains, are essential, whereby mutant strains differ from their parental strain by only one gene, the gene of interest. A range of transformation systems exist for the genetic manipulation of fungi, and there have been some major developments in the strategies used to prepare gene deletion substrates in recent years. Several other advancements, including the generation of non-homologous end joining (NHEJ) - deficient strains have greatly improved the success rate of targeted gene disruptions in *A. fumigatus* and other fungi (Ferreira *et al.*, 2006a; Krappmann *et al.*, 2006; Ninomiya *et al.*, 2004b), and these topics will be discussed in the following sections.

1.11.1. Transformation systems.

A range of transformation systems exist for *A. fumigatus* and other filamentous fungi, including protoplast transformation, electroporation of germinating conidia, and *Agrobacterium tumefaciens*-mediated transformation (ATMT) (Brakhage & Langfelder, 2002; Meyer, 2008; Michielse *et al.*, 2005b). Protoplast transformation involves the enzymatic removal of the fungal cell wall of recently germinated spores before transforming DNA is taken up by the cells through heat shocking or by the addition of polyethylene glycol (PEG) and calcium chloride (Brookman & Denning, 2000; Meyer, 2008). Electroporation (EP) involves the reversible permeabilisation of the membrane with electrical impulses which mediates DNA uptake (Meyer, 2008; Ruiz-Diez, 2002). EP has

been successful for transforming a range of *Aspergilli* and is relatively quick compared to protoplast transformation in *A. niger* (Ozeki *et al.*, 1994). In *A. fumigatus*, transformation efficiencies have been reported to be up to 10-fold higher following electroporation compared to protoplast transformation, with the limitation that the percentage of ectopic integrations into non-desired genomic sites is also significantly high (Brakhage & Langfelder, 2002). The principle behind ATMT is that *A. tumefaciens* possesses two vectors, one in which the transforming DNA is cloned into, and another one (Ti), which is important for DNA transfer during the infection of the fungus with *A. tumefaciens* (Meyer, 2008; Michielse *et al.*, 2005b). ATMT was successfully used to transform *A. niger* (de Groot *et al.*, 1998). Despite reports of its usefulness in various *Aspergillus* species, including the industrially relevant *A. awamori* (Michielse *et al.*, 2005a), and its reported use as a tool for transformation, random insertional mutagenesis and targeted gene disruption in *A. fumigatus* (Sugui *et al.*, 2005), there have still only been a few reports of ATMT being used to genetically modify *A. fumigatus*.

The most frequently used method of transformation appears to be protoplast-mediated transformation, and this was the method used for the functional characterisation of the genes involved in the gliotoxin and siderophore biosynthetic pathways of *A. fumigatus* (Balibar & Walsh, 2006; Cramer *et al.*, 2006a; Gardiner *et al.*, 2004; Schrettl *et al.*, 2004; Schrettl *et al.*, 2007). Therefore, it is a powerful technique for the delineation of biosynthetic pathways, and secondary metabolite gene clusters, that have been identified through genome sequencing, but as of yet remain uncharacterised.

1.11.2. Preparation of transforming DNA for targeted gene deletions.

Strategies currently available for fungal gene deletion involve various methods for preparing the transforming DNA (constructs), including the use of plasmid integrations

(Kubodera *et al.*, 2002), single linear constructs (Kuwayama *et al.*, 2002), the Double-joint method (Yu *et al.*, 2004) and the bipartite method (Nielsen *et al.*, 2006). *A. fumigatus* gene deletion strategies require the use of a non- *A. fumigatus* selection marker, and in the case of previously mutated strains, a selection marker which has not been previously used. Targeted gene replacements can be achieved by homologous recombination (HR), whereby the selection marker replaces the gene of interest with the aid of homologous recombination sequences (HRS) that flank the selection marker (Brakhage & Langfelder, 2002). Despite the presence of HRS, ectopic integrations of transforming DNA can still occur, and the efficiency of HR was found to correlate with the size of the homologous fragment (Bird & Bradshaw, 1997). Recombination between the homologous flanking regions leads to replacement of the targeted gene by the selection marker, and there is no risk of reversion since the gene is entirely deleted (Brakhage & Langfelder, 2002). The HRSs must be identical to the sequence in the genome and are usually amplified by PCR to create a suitable gene replacement construct. Flanking regions of approximately 1.0 kb result in a reasonably high transformation efficiency (Brakhage & Langfelder, 2002) (Figure 1.8).

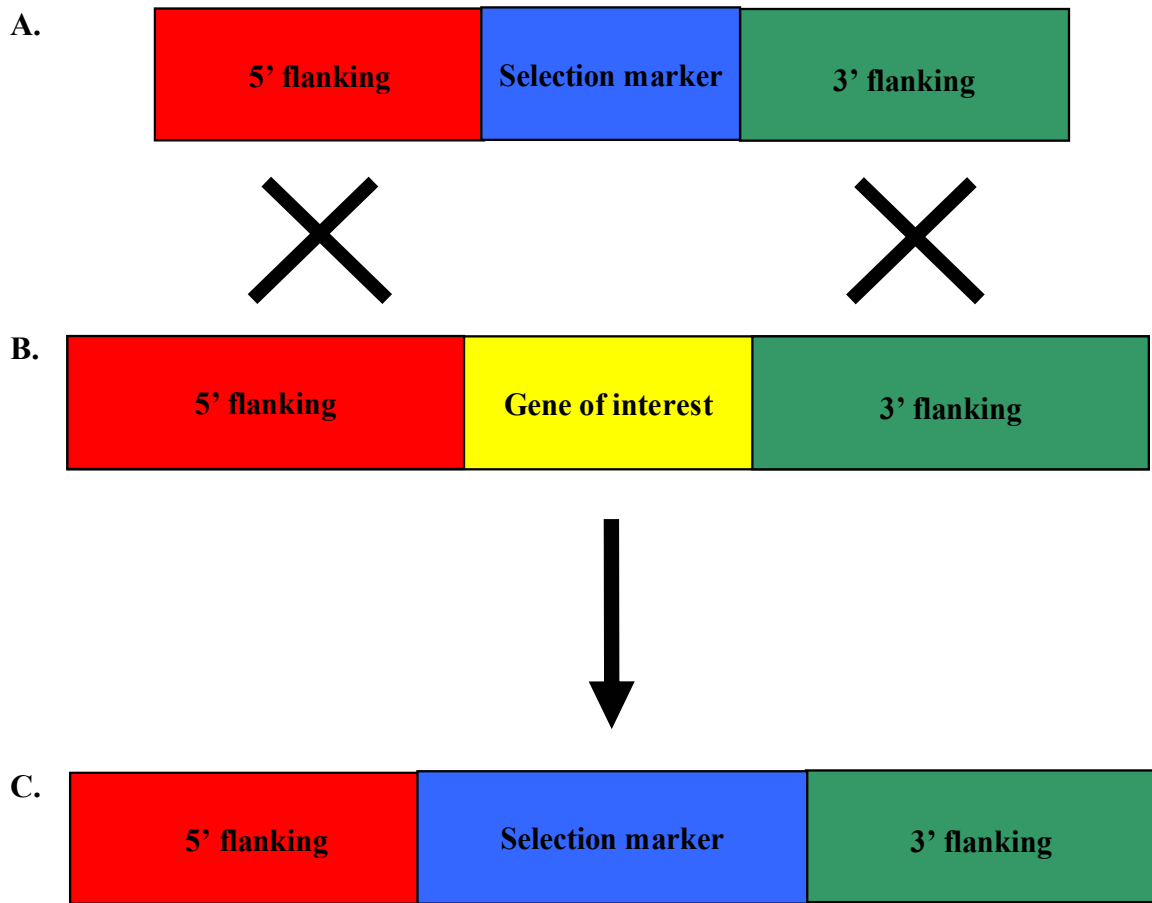


Figure 1.8. Schematic representation of targeted gene replacement by homologous recombination (HR).

The flanking regions of the gene of interest are fused to a selection marker (A), and these serve as the HRSs that recombine with the flanking regions on the chromosomal DNA (B), resulting in replacement of the gene of interest with the selection marker (C). Adapted from Brakhage and Langfelder, 2002.

Following the availability of many complete fungal genome sequences, technologies were developed to rapidly create gene disruption constructs using various PCR based approaches (Kuwayama *et al.*, 2002; Yang *et al.*, 2004; Yu *et al.*, 2004). Earlier approaches tended to involve several *E. coli* cloning steps which was both tedious and time-consuming (Nielsen *et al.*, 2006). Kuwayama *et al.* (2002) described a two-step PCR-based protocol for generating suitable constructs for gene deletion, whereby regions 5' and 3' to the gene of interest are PCR amplified, a selection marker is amplified, and all three are fused together to create a linear construct. A second PCR reaction is then performed to generate sufficient amounts of the entire construct which is transformed into the recipient (Kuwayama *et al.*, 2002). The main advantage reported for this technique was the freedom to generate flanking regions of any length which could then be fused to the ends of the selection marker (Kuwayama *et al.*, 2002).

A similar approach, known as the Double-joint PCR method was described to generate gene replacement constructs for use in filamentous fungi, and this was successful in the targeted deletion of 31 genes from *A. fumigatus*, *A. nidulans*, and *Fusarium graminearum* (Yu *et al.*, 2004). The final replacement construct consisted of a linear DNA fragment containing a centrally located selection marker fused to 0.5-3.0 kb upstream and downstream regions flanking the gene of interest (Yu *et al.*, 2004). The use of flanking regions with a length of 2-3 kb yielded the highest rate of homologous recombination (approx. 20 % of cases) resulting in replacement of the desired gene (Yu *et al.*, 2004). Of major importance when generating PCR-based gene deletion constructs is the use of high-fidelity polymerases for amplification of all components, due to the high gene density in the fungal genome (approx. 1 gene per 3 kb), and the possible risk that an erroneous base in the flanking region might interrupt an adjacent gene (Yu *et al.*, 2004). The double-joint

approach was subsequently used to disrupt the NRP synthetase gene, *pes1*, in *A. fumigatus* (Reeves *et al.*, 2006).

More recently, a new PCR-based strategy was described for use in *A. nidulans*, known as the bipartite strategy (Nielsen *et al.*, 2006). The bipartite method involves the generation of two overlapping constructs, each containing either the 5' or 3' flanking region of the gene of interest, fused to partial overlapping fragments of a selection marker and is based on an earlier method described for use in *S. cerevisiae* (Erdeniz *et al.*, 1997). The principle behind the bipartite strategy is that the two overlapping constructs recombine *in vivo*, reconstituting the selection marker, and this increases the frequency of targeted disruptions, presumably by channelling the entire DNA construct into the homologous recombination mode of DNA recombination (Nielsen *et al.*, 2006). As stated above, bipartite deletion constructs yield greater success than continuous constructs, with at least double the rate of targeted integrations associated with the bipartite construct compared to the continuous construct for the same gene locus (Nielsen *et al.*, 2006). The bipartite strategy resembles a split-marker strategy which was earlier proposed for use in filamentous fungi (Catlett *et al.*, 2002). The bipartite strategy has now been widely used for the generation of targeted gene deletions in *A. fumigatus* (Al-Bader *et al.*, 2010; Ejzykowicz *et al.*, 2009; Ejzykowicz *et al.*, 2010; Schrettl *et al.*, 2010).

1.11.3. Selection markers used for *A. fumigatus* genetic manipulation.

A. fumigatus and other fungi are naturally sensitive to certain antibiotics such as phleomycin/bleomycin and hygromycin (Brakhage & Langfelder, 2002). Bacterial genes conferring resistance to these antibiotics can be used as dominant selection markers for the transformation of *A. fumigatus* (Brakhage & Langfelder, 2002). Such genes have been found and in order to ensure their expression in fungi, they are usually engineered into

cassettes where they are placed under the transcriptional control of a fungal promoter and a suitable terminator sequence (Brakhage & Langfelder, 2002).

One particular cassette, which is widely used, comprises the hygromycin resistance gene, *hph*, encoding the hygromycin B phosphotransferase protein, under the control of the constitutive glyceraldehyde-3-phosphate dehydrogenase promoter and the *trpC* terminator from *A. nidulans*. The *hph* gene has now been used to generate large numbers of transformants in *A. fumigatus* (Coyle *et al.*, 2010; Ejzykowicz *et al.*, 2009; Fleck & Brock, 2010; Hissen *et al.*, 2005; Kim *et al.*, 2009; Krappmann *et al.*, 2004; Lessing *et al.*, 2007; Schrettl *et al.*, 2007). The *ble* gene, which confers resistance to phleomycin is also used for the transformation of *A. fumigatus* (Ejzykowicz *et al.*, 2009; Krappmann *et al.*, 2004; Lessing *et al.*, 2007; Levdansky *et al.*, 2010; Maubon *et al.*, 2006).

Auxotrophic or nutritional markers are an alternative to the selectable markers described above (Brakhage & Langfelder, 2002). The *pyrG* gene represents the most common auxotrophic marker used for *A. fumigatus*. *pyrG* encodes orotidine-5'-monophosphate decarboxylase which is critical for uracil biosynthesis (Brakhage & Langfelder, 2002). *pyrG* mutants exhibit uracil auxotrophy, and can be identified by their ability to grow on medium containing 5-fluoro-orotic acid (FOA), because FOA is converted to the toxic intermediate 5-fluoro-UMP by uracil prototrophs (Boeke *et al.*, 1984; Boeke *et al.*, 1987). Because of this, the *pyrG* gene can then be used as a selection marker to replace target genes of interest, thus restoring uracil prototrophy. *pyrG* homologs have been identified in a number of other *Aspergilli*, including *A. nidulans* (*pyrG*) (Oakley *et al.*, 1987), *A. niger* (*pyrG*) (Wilson *et al.*, 1988) and *A. flavus* (Chang *et al.*, 2010) and this strategy was pioneered for *A. fumigatus* by complementing uracil auxotrophy with the *A. niger pyrG* gene (dEnfert, 1996). *pyrG*-based gene deletion constructs, often referred to as *pyrG*-blaster, usually comprise a *pyrG* gene flanked with direct repeats of a bacterial

transposon sequence, flanked by sequence homologous to the target locus (dEnfert, 1996). Recombination between the two direct repeats, leading to *pyrG* excision, can be selected for in the presence of FOA following transformation, meaning that the *pyrG* cassette can be re-used to disrupt another gene, in the same strain if required, making it an attractive selective marker (dEnfert, 1996).

A pyrithiamine (PT) resistance gene was cloned from a PT-resistant *A. oryzae* mutant, and was used as a positive selection marker to transform *A. nidulans* and wild-type *A. oryzae* strains (Kubodera *et al.*, 2000). PT is a potent antagonist of thiamine, and inhibits the activity of thiamine pyrophosphokinase (TPK), which is essential enzyme in catalysing the transfer of pyrophosphate group from ATP to thiamine to form the coenzyme thiamine pyrophosphate (TPP), which is an essential co-factor in many metabolic reactions (Baker *et al.*, 2001). The product of the pyrithiamine resistance gene (*ptrA*) provides resistance to the otherwise lethal effects of PT and allows normal growth of the fungus (Kubodera *et al.*, 2000). It was observed that a single integration of a plasmid vector harbouring *ptrA* into the genome could confer PT resistance, rendering it useful as a dominant selectable marker in PT sensitive fungi (Kubodera *et al.*, 2000). Later, two plasmid vectors containing *ptrA* were constructed, and were used as selection markers for the transformation of other filamentous fungi including *A. fumigatus* (Kubodera *et al.*, 2002).

The *ptrA* gene is now widely used as a selection marker in a range of different experimental situations. It has been used for mutant complementation in *A. fumigatus*, where a plasmid (pSK275) containing *ptrA* was co-transformed with transforming DNA to restore a previously disrupted gene (Schrettl *et al.*, 2007), complementation of disrupted genes using *ptrA* fused to the target gene as a linear construct (Bergmann *et al.*, 2009), deletion of genes using a linearised vector containing *ptrA* as a selection marker (Valiante *et al.*, 2009), and more recently, gene deletion using *ptrA* as a selection marker in a linear

construct comprising target flanking regions for HR (Fleck & Brock, 2010), and gene deletion using *ptrA* as the selection marker in combination with the bipartite strategy (Nielsen *et al.*, 2006; Schrettl *et al.*, 2010).

1.11.4. The use of non-homologous end joining (NHEJ)-deficient strains to increase targeted integrations.

In order to produce stable genetic manipulations in *A. fumigatus*, the transforming DNA must be integrated at a chromosomal locus (Brakhage & Langfelder, 2002). Targeting and replacing genes in filamentous fungi, usually with antibiotic resistance cassettes, is facilitated by the cellular machinery that carries out recombination and repair of DNA (Krappmann *et al.*, 2006). Double-strand DNA breaks (DSBs) are the underlying principle for genetic modification by recombination of chromosomal DNA with transforming DNA in yeast and filamentous fungi (Paques & Haber, 1999).

In eukaryotic cells, two principle recombination pathways have been identified for the repair of DSBs; homologous recombination (HR) and DNA repair by non-homologous end joining (NHEJ) (Haarmann *et al.*, 2008). HR involves the targeted integration of exogenous DNA at homologous regions by virtue of homologous sequence, and this occurs at low frequencies of 10-30 % in filamentous fungi such as *A. fumigatus* and *A. niger* compared to *S. cerevisiae*, meaning that many transformants need to be screened to find the correct one, making transformation of fungi tedious and time-consuming (Carvalho *et al.*, 2010; Meyer, 2008). The NHEJ pathway involves direct ligation of DNA strands irrespective of the presence of sequence homology, thereby leading to ectopic integrations of transforming DNA into the genome, hampering the isolation of a targeted gene disruption. The NHEJ pathway is present in all eukaryotes and competes with the HR pathway (Critchlow & Jackson, 1998; Shrivastav *et al.*, 2008).

The NHEJ pathway is facilitated by the activation of the Ku heterodimer, also known as the Ku70/Ku80-protein complex, and the DNA ligase IV-Xrcc4 complex (Dudasova *et al.*, 2004; Krogh & Symington, 2004). The Ku70/Ku80 heterodimer forms a three protein complex with a catalytic subunit DNA-PKcs. The Ku heterodimer directs the catalytic subunit to DNA ends and stabilizes its binding to DNA where it becomes activated (Spagnolo *et al.*, 2006). The HR pathway is mediated by the Rad52 group of proteins. According to the gate-keeper model, both pathways compete with each other, so that when Rad52 binds DNA, HR results, whereas when Ku binds DNA, the DNA becomes integrated by NHEJ and can enter the genomic DNA ectopically (Meyer, 2008). It appears that higher eukaryotic organisms, including filamentous fungi, preferentially use NHEJ to repair DSBs (Haarmann *et al.*, 2008). HR and NHEJ are not the only pathways of DNA repair that exist in eukaryotic organisms; in fact not much attention has been given to the processes of DNA repair in *A. fumigatus*. Investigation into an adaptive response towards alkylating DNA damage in *A. fumigatus* is described in Chapter 5 of this thesis.

A huge advance was made in the generation of targeted gene deletions in the model ascomycete fungus *Neurospora crassa* by disruption of the NHEJ pathway (Ninomiya *et al.*, 2004a). Deletion of the *ku70* and *ku80* genes in *N. crassa*, *mus-51* and *mus-52*, respectively, led to transformants which exhibited 100 % targeted integration of transforming DNA, compared to 10-30 % targeted integration in the wild-type background, when flanking regions of 2 kb were used to generate transformation constructs (Ninomiya *et al.*, 2004a). Since this breakthrough, the use of NHEJ-deficient strains has been extended to facilitate gene disruption in a range of filamentous fungi, including *A. fumigatus* (Ferreira *et al.*, 2006a; Krappmann *et al.*, 2006). A NHEJ-deficient strain was employed to characterise an NRP synthetase gene in the *Claviceps purpurea* ergot alkaloid (EA) biosynthetic cluster, a cluster which is widespread throughout fungi, including *A.*

fumigatus, and this led to significant advances in the understanding of EA biosynthesis (Haarmann *et al.*, 2008).

One concern that exists about the use of NHEJ-deficient strains is that complementation of resulting mutants may be difficult, as this usually involves reintroducing the deleted gene ectopically into the genome in order to restore mutant phenotypes, and the rate of ectopic integrations is significantly reduced in NHEJ-deficient strains (Carvalho *et al.*, 2010). To circumvent any issues that may occur with the use of NHEJ-deficient strains, Nielsen *et al.* (2008) have developed a method whereby components of the NHEJ machinery (Ku70 and Ku80) can be transiently disrupted in order to facilitate deletion of gene(s) of interest, and then NHEJ can be restored by a simple selection scheme. In combination with the bipartite strategy described above (Nielsen *et al.*, 2006), this strategy resulted in rates of homologous integration of above 95 % compared to less than 2 % in wild-type strains of *A. nidulans* (Nielsen *et al.*, 2008). This strategy was adapted to create a transiently disrupted *A. niger* strain where the Ku70 NHEJ component was firstly disrupted and then replaced after genes of interest had been disrupted in the NHEJ-deficient state (Carvalho *et al.*, 2010).

Despite the obvious advantages to using NHEJ-deficient and transiently disrupted NHEJ-deficient strains, there has not yet been a report of transient NHEJ-disruption usage in *A. fumigatus*. In contrast, the majority of gene deletions currently emerging in the literature are based on the bipartite method alone, and this has been successfully used to generate targeted gene deletions in a number of strains, including the fully-genome sequenced strain Af293 (Ejzykiewicz *et al.*, 2010; Sheppard *et al.*, 2005), and in other strains such as ATCC 46645 and ATCC 26933 (Schrettl *et al.*, 2010). The design of a gene deletion construct for *A. fumigatus* employing the bipartite strategy will be dealt with in Chapter 2.

1.12. The oxidative stress response in *A. fumigatus*.

Oxidative stress is a shift in the normal balance of oxidants and antioxidants in favour of oxidant species, leading to an accumulation of reactive oxygen species (ROS) and cell damage (Sies, 1991). Cells can respond to oxidative stress by producing antioxidant molecules such as ascorbic acid, carotene and reduced glutathione, and by activating specific anti-oxidant enzymes (Reverberi *et al.*, 2010). Chemicals which generate reactive oxygen species are routinely used to induce antioxidant defence systems in organisms of interest, in order to study defence systems against oxidative stress (Gutteridge & Halliwell, 2000). Among the routinely used oxidising agents are hydrogen peroxide (H_2O_2), menadione and diamide. H_2O_2 causes oxidative stress by increasing intracellular peroxide levels (O_2^{2-}), and this leads to direct oxidation of sulphur-containing amino acids and production of OH^\cdot radicals (Pocsi *et al.*, 2005). H_2O_2 is also known to cause DNA damage in cells, as a downstream effect of oxidative stress (Klaunig *et al.*, 2010). Menadione causes a redox cycle, leading to the generation of superoxide anions (O_2^\cdot), inactivating 4Fe-4S cluster-containing proteins (Pocsi *et al.*, 2005). Detoxification of menadione catalyzed by glutathione-s-transferases (GSTs) may also affect the intracellular glutathione pool (Pocsi *et al.*, 2004). Diamide is a thiol-oxidising chemical resulting in fast oxidation of glutathione (GSH) to oxidised glutathione (GSSG) resulting in GSH/GSSH redox imbalance in the cell (Pocsi *et al.*, 2005).

The production of ROS by alveolar macrophages has been reported to play an important role in the innate immune response towards *A. fumigatus* (Paris *et al.*, 2003b; Schaffner *et al.*, 1982). Amongst the *A. fumigatus* cellular defences to oxidative stress are antioxidant enzymes including superoxide dismutase (SOD), thioredoxin, glutathione reductase, catalase (CAT) and glutathione peroxidase (GPX) (Chauhan *et al.*, 2006). SOD converts one harmful ROS, superoxide, into another, H_2O_2 , thus shunting the superoxide in

the direction of ROS, and away from the formation of harmful reactive nitrogen intermediates (RNI) such as peroxyxynitrite (Missall *et al.*, 2004). SOD activity is beneficial to the cell, since many defence systems exist to counteract peroxides, but few are present to deal with RNI (Missall *et al.*, 2004).

Catalases are metalloenzymes, found in all aerobic organisms, and mediate the conversion of H₂O₂ to water and oxygen (Missall *et al.*, 2004). *A. fumigatus* possesses three catalases which are produced during IA, one conidial catalase, CatA, and two mycelial catalases; Cat1 and Cat2 (Paris *et al.*, 2003b). CatA protects *A. fumigatus* spores against the effects of H₂O₂ *in vitro*, but does not protect against the ROS released from macrophages, indicating that H₂O₂ may not be the most important ROS involved in the killing of *A. fumigatus* conidia by macrophages (Paris *et al.*, 2003b). Deletion of both mycelial catalases led to slightly increased sensitivity to H₂O₂ compared to wild-type, and reduced fungal development *in vivo*, whereas individual deletions had no effect on either protection against H₂O₂ or virulence (Paris *et al.*, 2003b). *A. fumigatus* possesses several SOD enzymes, as well as GSTs and peroxidases, and glutaredoxin and thioredoxin systems (Chauhan *et al.*, 2006; Holdom *et al.*, 2000).

Melanins are multi-functional polymers that can reduce oxidants, and are implicated in the virulence of many human pathogenic fungi (Missall *et al.*, 2004). Melanin is an important conidial pigment of *A. fumigatus* which protects the fungus from reactive oxygen and chlorine species as well as from oxidative killing by macrophages, conferring virulence to the organism (Langfelder *et al.*, 1998). Trehalose, a carbohydrate, which serves as reserve energy supply and a stress metabolite, has the ability to scavenge free radicals which accumulate during oxidative stress (Al-Bader *et al.*, 2010; Singer & Lindquist, 1998). Recently, basal levels of trehalose were found to be important in protecting *A. fumigatus* against oxidative stress *in vitro* (Al-Bader *et al.*, 2010).

An important finding was made when the *A. fumigatus* AfYAP1 transcriptional regulator was identified as the major regulator of enzymes in the defence against ROS through a proteomic analysis of *A. fumigatus* exposed to H₂O₂ (Lessing *et al.*, 2007). An AfYAP1 deletion strain ($\Delta Afyap1$) confirmed these findings (Lessing *et al.*, 2007). Proteomic analysis of *A. fumigatus* $\Delta Afyap1$ revealed that catalases, peroxiredoxins, cytochrome C peroxidase, and a putative thioredoxin peroxidase AspF3 were the specific antioxidant enzymes that were regulated by AfYAP1 (Lessing *et al.*, 2007). Other protein families were also up-regulated upon exposure to H₂O₂ including heat shock proteins, protein translation machinery, enzymes involved in glycolysis and the Krebs's cycle (Lessing *et al.*, 2007). In that study, AfYAP1 was found to be dispensable for pathogenicity in a murine model for IA (Lessing *et al.*, 2007).

The oxidative stress response was of interest for this work since several NRP synthetases characterised to date have been important for protection against oxidative stress (Eisendle *et al.*, 2006; Lee *et al.*, 2005; Reeves *et al.*, 2006; Schrettl *et al.*, 2007). Furthermore, there appears to be a link between fungal secondary metabolite production and oxidative stress (Reverberi *et al.*, 2010). It has been shown that some secondary metabolites are produced during fungal developmental and metabolic transitions, coinciding with an accumulation of ROS (Reverberi *et al.*, 2010). Conidial germination to hyphae occurs with a burst of ROS and this coincides with the onset of mycotoxin biosynthesis in *Aspergillus parasiticus* (Reverberi *et al.*, 2010). Oxidative stress and aflatoxin biosynthesis are closely related events (Fanelli *et al.*, 2004). Links between secondary metabolite production have also been inferred in *A. flavus* (Mahoney *et al.*, 2010), and *Fusarium graminearum* (Ponts *et al.*, 2006; Ponts *et al.*, 2007).

1.13. Use of the *Galleria mellonella* insect model to study *A. fumigatus* virulence.

The last decade has seen an increase in the number of non-vertebrate models used to study microbial virulence. The use of insects as hosts has received major attention, and derives from the high degree of similarity between the innate immune system of insects and mammals (Muller *et al.*, 2008; Vilmos & Kurucz, 1998). The use of insect models carries many advantages, including ease of handling and infection, reduction in the need for mammalian suffering, and insects are inexpensive to purchase and store (Cotter *et al.*, 2000; Kavanagh & Fallon, 2010). Furthermore, use of such a system allows the screening of large number of pathogenic isolates at any given time, allowing comparisons of virulence between different fungal strains and species (Cotter *et al.*, 2000) and also allowing the screening of mutants to identify ones which may be defective in virulence (Kavanagh & Reeves, 2004). Larvae of *G. mellonella* (the wax moth) have been used for the development of a robust insect model for the *in vivo* pathogenicity testing of yeasts (Cotter *et al.*, 2000). Previously, *G. mellonella* were used to examine virulence associated with LPS-deficient mutants of *Pseudomonas aeruginosa*, and are now used to investigate the molecular basis of pathogenicity in a wide range of important pathogens, for example, *Listeria monocytogenes* (Joyce & Gahan, 2010), and *Enterococcus faecalis* (Hanin *et al.*, 2010). Results from experiments using *G. mellonella* can usually be obtained within 72 hr of infection, further allowing the screening of large numbers of isolates in a relatively short period of time (Cotter *et al.*, 2000). The immune system of insects including *G. mellonella* comprises structural and passive barriers to protect against microbes, and cellular and humoral responses mediate the immune response (Cotter *et al.*, 2000). Haemocytes, analogous to mammalian phagocytes are found within the haemolymph of the insect (Dunphy & Thurston, 1990). Six different types of haemocytes have been identified and these have found to be important in defending the insect against bacteria and unicellular

fungi (Walters & Ratcliffe, 1983). Some of these haemocytes are involved in phagocytosis, encapsulation and nodule formation (Matha & Mracek, 1984). Humoral factors in insect immunity include lysozyme, lectins and the pro-phenoloxidase cascade (Dunphy & Thurston, 1990). The phenoloxidase (PO) pathway is catalysed by phenoloxidase (PO), which becomes activated in the presence of microbial components, such as *A. fumigatus* β -1,3 glucans, lipopolysaccharide (LPS), and peptidoglycan, ensuring its activation upon pathogen presence (Cerenius & Soderhall, 2004). Activated PO mediates melanisation around the damaged tissue or invading microbe, which may retard microbial growth, and during melanisation, many reactive and toxic quinone intermediates are produced (Cerenius & Soderhall, 2004). The insect humoral response also includes the production of a range of antimicrobial peptides which are released from a range of organs and cells (Bulet *et al.*, 1999; Leclerc & Reichhart, 2004) into the haemolymph where they can diffuse to the infected site and attack bacterial and fungal cell wall components (Ratcliffe, 1985). Furthermore, *G. mellonella* possesses proteins orthologous to the components of the NADPH oxidase complex in human neutrophils, and these are responsible for superoxide production in the haemocytes indicating that the haemocytes kill conidia of *A. fumigatus* in a similar manner to human neutrophils (Bergin *et al.*, 2005).

The use of the *Galleria* model to investigate the pathogenicity and virulence of *A. fumigatus* has been well documented to date (Kavanagh & Fallon, 2010). A correlation between the production of gliotoxin and the virulence of different isolates of *A. fumigatus* was observed in a *G. mellonella* infection model (Reeves *et al.*, 2004). This model was also able to imply a role for the non-ribosomal peptide synthetase *Pes1* in the virulence of *A. fumigatus*, as larvae infected with a *Pes1* deletion mutant exhibited reduced mortality compared to wild-type (Reeves *et al.*, 2006). Recently, the robustness of the *G. mellonella*

model was reported with strong correlations between *G. mellonella* and murine virulence studies using a previously characterised set of *A. fumigatus* mutants (Slater *et al.*, 2010).

1.14 Rationale and objectives of this thesis.

A. fumigatus is a serious human pathogen whose complete genome sequence has recently become available, revealing the presence of at least 22 SM biosynthetic clusters, for which the majority of products are unknown (Nierman *et al.*, 2005). The virulence of this organism in part relies on secondary metabolite production since the finding that a LaeA mutant, crippled in secondary metabolite production, exhibited reduced virulence in a murine model of IA (Bok *et al.*, 2005). Fourteen NRP synthetase genes have been found in the *A. fumigatus* genome, however, specific data relating these NRP synthetases to their downstream peptide has not been forthcoming (Stack *et al.*, 2007). Further studies, including the analysis of NRPS mutants, are therefore required to link specific metabolites with their corresponding NRP synthetase, and to address the role of individual secondary metabolites in the pathogenesis of *A. fumigatus* (Cramer *et al.*, 2006b). Several strategies may be used to identify the products of NRP synthetases, and gene deletion studies have proved to be successful for the *A. fumigatus* NRP synthetases characterised to date.

However, these studies, described earlier, only account for 5 of the 14 NRP synthetases found within the *A. fumigatus* genome (Cramer *et al.*, 2006b; Nierman *et al.*, 2005), and underpins the functional genomics challenge in the elucidation of the peptide products of the remaining NRP synthetases.

Therefore, the overall work objectives presented in this thesis are as follows:

- 1) Elucidation of the function of two distinct NRP synthetases, encoded by the genes *pes3* and *pesL* in *A. fumigatus*, using a targeted gene deletion approach, followed by phenotypic analysis.
- 2) Identification of NRP products of PesL and Pes3 by comparative metabolite profiling between wild-type and mutant strains.
- 3) Taking advantage of the gene deletion technology, an adaptive response pathway for the repair of alkylating DNA damage was investigated in *A. fumigatus*. This topic will be discussed entirely in Volume 2 of this thesis.

2.1. Materials

All chemicals were purchased from Sigma-Aldrich Chemical Co. Ltd. (U.K.), unless otherwise stated.

2.1.1 Microbiological Medias and Reagents

2.1.1.1 *Aspergillus* Trace Elements

$\text{Na}_2\text{B}_4\text{O}_7 \cdot 7\text{H}_2\text{O}$ (0.04 g), $\text{CuSO}_4 \cdot (5\text{H}_2\text{O})$, $\text{FeSO}_4 \cdot 7\text{H}_2\text{O}$ (1.2 g), MnSO_4 (0.7 g), $\text{Na}_2\text{MoO}_4 \cdot 2\text{H}_2\text{O}$ (0.8 g) and $\text{ZnSO}_4 \cdot 7\text{H}_2\text{O}$ (10 g) were added to 800 ml dH_2O and dissolved. The solution was made up to 1 L with dH_2O and subsequently autoclaved. The solution was aliquoted (50 ml) and stored at -20°C .

2.1.1.2 *Aspergillus* Salt Solution

KCl (26 g), $\text{MgSO}_4 \cdot 7\text{H}_2\text{O}$ (26 g), KH_2PO_4 (76 g) and *Aspergillus* Trace Elements (50 ml) (Section 2.1.1.1) were added to 800 ml dH_2O and dissolved. The solution was made up to 1 L with dH_2O and autoclaved. The solution was stored at room temperature.

2.1.1.3 100x Ammonium Tartrate

Ammonium tartrate (92 g) was dissolved in 1 L dH_2O and autoclaved. The solution was stored at room temperature.

2.1.1.4 20 mM L-Glutamine

A 200 mM L-Glutamine stock was purchased from Sigma-Aldrich and stored at -20°C . L- Glutamine was used as a Nitrogen source at a final concentration of 20 mM.

2.1.1.5 Malt Extract Agar

Malt extract agar (30 g) (Difco, Maryland, USA) was added to 600 ml dH₂O, and dissolved. The solution was autoclaved, and allowed to cool to ~50 °C. Agar (25 ml) was then poured into 90 mm petri dishes, under sterile conditions. The plates were allowed to set and were stored at 4 °C.

2.1.1.6 *Aspergillus* Minimal Media (AMM) Agar

Ammonium tartrate (100 X, 10 ml) (Section 2.1.1.3), *Aspergillus* salt solution (20 ml) (Section 2.1.1.2) and glucose (10 g) were added to 800 ml dH₂O and dissolved. The pH of the solution was adjusted to pH 6.8 and made up to 1 L with dH₂O prior to the addition of agar (18 g) (Scharlau Chemie S.A., Barcelona, Spain). The solution was mixed and autoclaved and allowed to cool to ~50 °C before being poured into 90 mm petri dishes, under sterile conditions. The plates were allowed to set and were stored at 4 °C.

2.1.1.7 *Aspergillus* Minimal Media (AMM)

Ammonium tartrate (100 X, 10 ml), *Aspergillus* salt solution (20 ml) and glucose (10 g) were added to 800 ml dH₂O and dissolved. The pH of the solution was adjusted to pH 6.8 and made up to 1 L with dH₂O. The solution was autoclaved and stored at 4 °C.

2.1.1.8 Yeast Glucose (YG) Media

Yeast extract (5 g) (Oxoid Ltd., Basinstoke, Hampshire, England) and glucose (20 g) were added to 800 ml dH₂O and dissolved. The solution was made to 1 L with dH₂O, autoclaved and stored at 4 °C.

2.1.1.9 Sabourard- Dextrose Media

Sabourard-Dextrose media (30 g) (Oxoid Ltd., Basinstoke, Hampshire, England) was added to 1 L dH₂O, and dissolved. The solution was autoclaved and stored at 4 °C.

2.1.1.10 RPMI Media

RPMI media (Gibco®, Invitrogen Life Sciences, California, USA) was supplemented with L- Glutamine (final concentration 20 mM) (Section 2.1.1.4.) and stored at 4 °C.

2.1.1.11 Czapek's Broth

Czapek-Dox powder (30 g) (Difco, Maryland, USA) was added to 1 L dH₂O, and dissolved. The solution was autoclaved and stored at 4 °C.

2.1.1.12 Czapek's Agar

Czapek-Dox powder (30 g) (Difco, Maryland, USA) was added to 1 L of dH₂O, and dissolved prior to the addition of agar (18 g) (Scharlau Chemie S.A., Barcelona, Spain). The solution was mixed and autoclaved and allowed to cool to ~50 °C before being poured into 90 mm petri dishes, under sterile conditions. The plates were allowed to set and were stored at 4 °C.

2.1.1.13 MEM Media supplemented with 5 % (w/v) Foetal Calf Serum (FCS)

Minimal Essential Media (MEM) (Gibco®, Invitrogen Life Sciences, California, USA) was supplemented with FCS as required to a final concentration of 5 % (v/v), and stored at 4 °C.

2.1.1.14 *Aspergillus* Transformation Regeneration Media

Ammonium tartrate (100 X, 10 ml) (Section 2.1.1.3), *Aspergillus* salt solution (20 ml) (Section 2.1.1.2), glucose (10 g) and sucrose (342 g) were added to 800 ml dH₂O and dissolved. The pH of the solution was adjusted to pH 6.8 and made up to 1 L with dH₂O prior to the addition of agar (18 g) (Scharlau Chemie S.A., Barcelona, Spain). The solution was mixed and autoclaved and allowed to cool to ~50 °C. The mixture was supplemented with desired drug for selection before being poured (25 ml) into 90 mm petri dishes, under sterile conditions. The plates were allowed to set and were stored at 4 °C.

2.1.1.15 *Aspergillus* Transformation Soft Agar

Ammonium tartrate (100 X, 10 ml), *Aspergillus* salt solution (20 ml), glucose (10 g) and sucrose (342 g) were added to 800 ml dH₂O and dissolved. The pH of the solution was adjusted to pH 6.8 and made up to 1 L with dH₂O prior to the addition of agar (7 g) (Scharlau Chemie S.A., Barcelona, Spain). The solution was mixed and autoclaved and allowed to cool to ~50 °C before being poured (25 ml) into 90 mm petri dishes, under sterile conditions. The plates were allowed to set and stored at 4 °C.

2.1.1.16 Phosphate Buffered Saline (PBS)

One PBS tablet was added to 200 ml of dH₂O, and dissolved by stirring. The solution was autoclaved and stored at room temperature.

2.1.1.17 Phosphate Buffer Saline/ 0.1 % (w/v) Tween-20 (PBST) NaCl (0.9 % w/v)

Tween-20 (0.1 ml) was added to 1 L PBS (Section 2.1.1.16). NaCl (9 g) was added and the solution was dissolved. The solution was autoclaved and stored at room temperature.

2.1.1.18 Luria-Bertani (LB) Agar

LB agar (40 g) (Difco, Maryland, USA) was added to 1 L dH₂O, and dissolved by stirring. The solution was autoclaved and allowed to cool to ~50 °C before being poured (25 ml) into 90 mm petri dishes, under sterile conditions. The plates were allowed to set and were stored at 4 °C.

2.1.1.19 Luria-Bertani (LB) Broth

LB broth (25 g) (Difco, Maryland, USA) was added to 1 L dH₂O, and dissolved by stirring. The solution was autoclaved and stored at 4 °C.

2.1.1.20 80 % (w/v) Glycerol

Glycerol (80 ml) was added to 20 ml dH₂O. The solution was autoclaved, and stored at 4 °C.

2.1.1.21 40 % (w/v) Glycerol

Glycerol (40 ml) was added to 60 ml dH₂O. The solution was autoclaved, and stored at 4 °C.

2.1.1.22 YPD broth

BactoYeast™ Extract (10 g) BactoPeptone™ (20 g), and BactoDextrose™ (20 g) (Becton and Dickinson, France) were dissolved in 500 ml dH₂O. The volume was brought to 1 L with dH₂O. The mixture was subsequently autoclaved and stored at room temperature.

2.1.1.23 YPD Agar

A solution was prepared as for YPD broth (Section 2.1.1.22), and 20 g of Bacto agar (Difco) was added. The solution was autoclaved and allowed to cool to ~50 °C before being poured (25 ml) into 90 mm petri dishes, under sterile conditions. The plates were allowed to set and were stored at 4 °C.

2.1.1.24 Dropout Mix

The drop-out mix used contained all of the ingredients listed in Table 2.1.

2.1.1.25 Synthetic Complete Media (SC)

SC media was prepared by dissolving the following ingredients in 1 L dH₂O: 6.7 g of Bacto-yeast nitrogen base without amino acids™ (Becton and Dickinson, France), 20 g glucose and 2 g Dropout mix (Section 2.1.1.24). The solution was autoclaved and stored at room temperature.

2.1.1.26 Synthetic Complete Agar (SC)

SC agar was prepared as for SC media (Section 2.1.1.25) and 20 g of agar was added. The solution was autoclaved and allowed to cool to ~50 °C before being poured (25

ml) into 90 mm petri dishes, under sterile conditions. The plates were allowed to set and were stored at 4 °C.

2.1.1.27 Antibiotics and Plate Assay Supplements

Antibiotics and Plate Assay Supplements were prepared as stock solutions in water, methanol, ethanol or dimethyl sulfoxide (DMSO) and filter sterilised. All were stored at -20 °C. All antibiotics were supplied by Sigma-Aldrich. Further details are provided in Table 2.2.

Table 2.1. Components used to prepare Dropout Mix (Section 2.1.1.24).

Component added	Amount added (g)	Component added	Amount added (g)	Component added	Amount added (g)
Adenine	0.5	Lysine	2.0	Glycine	2.0
Alanine	2.0	Methionine	2.0	Histidine	2.0
Arginine	2.0	<i>para</i> -Aminobenzoic acid	2.0	Inositol	2.0
Asparagine	2.0	Phenylalanine	2.0	Isoleucine	2.0
Aspartic Acid	2.0	Proline	2.0	Tyrosine	2.0
Cysteine	2.0	Serine	2.0	Uracil	2.0
Glutamine	2.0	Threonine	2.0	Valine	2.0
Glutamic Acid	2.0	Tryptophan	2.0		

Table 2.2. Additives and antibiotics used in this study (Section 2.1.1.27).

Condition Tested	Reagent added	Concentrations Tested	Stock Concentration
Sensitivity to Oxidative Stress	H ₂ O ₂	1 mM, 2 mM, 3 mM	1 M stock prepared in H ₂ O
	Diamide	100 µM, 200 µM, 400 µM, 1 mM, 2 mM	1 M Diamide prepared in Methanol
	Menadione	5 µM, 10 µM, 15 µM etc. up to 40 µM	10 mM Menadione prepared in Methanol
Sensitivity to Anti-fungals	Voriconazole	0.25 µg/ml, 0.5 µg/ml, 0.75 µg/ml, 1.0 µg/ml	0.5 mg/ml stock prepared in H ₂ O
	Caspofungin	0.2 µg/ml, 0.5 µg/ml, 1.0 µg/ml	350 µg/ml stock prepared in H ₂ O
	Amphotericin B	0.125 µg/ml, 0.25 µg/ml, 0.5 µg/ml, 1.0 µg/ml	250 µg/ml stock purchased commercially
Cell Wall Stress	Calcofluor White	100 µg/ml, 200 µg/ml	100 mg/ml stock prepared in H ₂ O
	Congo Red	5 µg/ml, 10 µg/ml, 15 µg/ml	50 mg/ml stock prepared in H ₂ O
	SDS	0.01 %, 0.02 % (w/v)	10 % (w/v) stock prepared in H ₂ O
	Caffeine	2 mM, 5 mM	0.5 M stock prepared in DMSO
Heavy Metal Stress	Cobalt Chloride	0.1 mM, 0.5 mM, 1 mM	0.5 M stock prepared in H ₂ O
Various Iron Conditions	Iron Sulphate (FeSO ₄)	10 µM, 1.5 mM, 200 µM BPS	5 mM / 72 mM stock prepared in H ₂ O
	BPS		
Gliotoxin Sensitivity	Gliotoxin from	5 µg/ml, 10 µg/ml, 20 µg/ml	1 mg/ml stock prepared in Methanol

Condition Tested	Reagent added	Concentrations Tested	Stock Concentration
	<i>Gliocladium</i>		
	<i>fimbriatum</i>		
Phleomycin Sensitivity	Phleomycin from	2 µg/ml, 5 µg/ml, 10 µ/ml	25 mg/ml stock prepared in H ₂ O
	<i>Streptomyces</i>		
	<i>verticillus</i>		
Alkylating DNA damage	N-Methyl-N'-Nitro-Nitrosoguanidine (MNNG)	0.5 µg/ml, 1.0 µg/ml, 2.0 µg/ml, 4 µg/ml	2 mg/ml stock in Methanol
	Ethyl methanesulfonate (EMS)	0.02 %, 0.04 %, 0.08 % (w/v)	200 mg/ml stock purchased commercially
	Methyl methanesulfonate (MMS)	0.01 %, 0.02 %, 0.04 %	200 mg/ml stock purchased commercially
Pyriithiamine Resistance	Pyriithiamine Hydrochloride	0.1 µg/ml	0.1 mg/ml in H ₂ O
Phleomycin Resistance	Phleomycin	40 µg/ml	25 mg/ml in H ₂ O
Ampicillin resistance in <i>E. coli</i>	Ampicillin	0.1 mg/ml	0.1 g/ml in H ₂ O

2.1.2 Molecular Biological Reagents

2.1.2.1 Agarose Gel Electrophoresis Reagents

2.1.2.1.1 50 X Tris-Acetate (TAE)

Trizma Base (242 g) was added to 57.1 ml glacial acetic acid and 100 ml of 0.5 M EDTA, pH 8.0. The volume was adjusted to 1 L with dH₂O, and the solution was stored at room temperature. This solution was diluted to a 1 X concentration in dH₂O before use.

2.1.2.1.2 1 X Tris-Acetate (TAE)

50 X Tris-Acetate (Section 2.1.2.1.1) (40 ml) was added to 960 ml of dH₂O and the solution was stirred and stored at room temperature.

2.1.2.1.3 Ethidium Bromide Solution

Ethidium Bromide (0.1 mg) was added to 100 ml PBS (Section 2.1.1.16). The solution was stored at room temperature.

2.1.2.1.4 SYBR® Safe DNA Gel Stain

A 10,000 X concentrate solution of SYBR® Safe was diluted into 1 % (w/v) agarose gel (Section 2.1.2.1.3) at a 1 X concentration.

2.1.2.1.5 1 % (w/v) Agarose Gel

Agarose powder (1 g) was dissolved into 100 ml 1 X TAE (Section 2.1.2.1.2). This mixture was heated in a microwave oven until the agarose had dissolved and the mixture was molten. The solution was then air-cooled until hand-hot and was then poured into a gel casting tray. Immediately, either 3 µl Ethidium Bromide solution (Section 2.1.2.1.3), or 10

μ l SYBR® SAFE DNA Gel Stain (Section 2.1.2.1.4) was added. Combs were then placed on top to create wells for sample loading. The gel was left to set for at least 30 minutes.

2.1.2.2 DNA Reagents

2.1.2.2.1 100 % (v/v) Ethanol (ice-cold)

Molecular Biology Grade Ethanol (100 % (v/v)) was poured into a sterile 50 ml falcon tube and stored at -20 °C.

2.1.2.2.2 70 % (v/v) Ethanol (ice-cold)

Molecular Biology Grade Ethanol (35 ml) was added to 15 ml of Molecular Biology Grade H₂O in a sterile 50 ml falcon tube and the solution was stored at -20 °C.

2.1.2.2.3 3 M Na-acetate

Sodium acetate (12.3 g) was dissolved in 50 ml Molecular Grade H₂O in a sterile 50 ml tube. The solution was pH adjusted to pH 5.2 and stored at room temperature.

Table 2.3. Primers used in this study. Primers named according to the gene of interest, e.g. *Afpes3-x* used for *pes3* disruption construct, while *AfpesL-x* used for *pesL* disruption construct. AFUA_5G06350 -x and AFUA_2G02090-x used for *Afmpt* and *Afagt* disruption constructs respectively.

Primer Name	F/R	Sequence 5'-3'	Used in PCR reaction
o <i>Afpes3</i> -1	F	gaggcggaacgttgaa	PCR 1 / 1 st Round PCR
o <i>Afpes3</i> -4	R	cagtgctatgttcgccac	<i>pes3</i> 5' DIG- probe
o <i>Afpes3</i> -3	F	ttgagatgcggtactcg	
o <i>Afpes3</i> -2	R	aagctgcgctcaacctc	PCR 2 / 1 st Round PCR
o <i>Afpes3</i> -5	F	ggaaccgatcactcaagac	PCR 3 / 2 nd Round PCR
o <i>PtrA2</i>	R	catcgtgaccagtggtag	<i>ptrA</i> DIG probe
o <i>PtrA1</i>	F	gaggacctggacaagtac	<i>ptrA</i> DIG probe
o <i>Afpes3</i> -6	R	cgacgtagatgagcgatc	PCR 4 / 2 nd Round PCR
o <i>Afpes3</i> -5	F	ggaaccgatcactcaagac	
<i>Afpes3</i> Comp1	R	ccagagatcggctaagtgtca	<i>pes3</i> -left
<i>Afpes3</i> Comp2	F	cggagggtttattagacgcctg	
o <i>Afpes3</i> -6	R	cgacgtagatgagcgatc	<i>pes3</i> -right
<i>pes3</i> RT-F	F	ctctggcactcctccaagtc	
<i>pes3</i> RT-R	R	agcaatctatcccacggatg	<i>pes3</i> RT-PCR
o <i>Afpes3</i> -5	F	ggaaccgatcactcaagac	
o <i>Afpes3</i> -6	R	cgacgtagatgagcgatc	3.7kb <i>pes3</i> replacement construct

Primer Name	F/R	Sequence 5'-3'	Used in PCR reaction
<i>calm</i> F	F	ccgagtacaaggaagctttctc	<i>calm</i> RT-PCR
<i>calm</i> R	R	gaatcatctcgtcgattcgtcgtctcagt	
<i>oAfpesL-1</i>	F	gtctatcagcacacccttaccg	PCR 1
<i>oAfpesL-4</i>	R	aatctgcaggacaacgcagcatcaagg	
<i>oAfpesL-3</i>	F	cctgttgcctcgacattcc	PCR 2
<i>oAfpesL-2</i>	R	aactccgcttcacagacc	<i>pesL</i> 3' DIG- probe
<i>oAfpesL-5</i>	F	gattctgccttggatgcg	
<i>oPtrA2</i>	R	catcgtgaccagtggtag	PCR 3
<i>oPtrA1</i>	F	gaggacctggacaagtac	
<i>oAfpesL-6</i>	R	tcaggtccttctcacac	PCR 4
<i>pesLRT-F</i>	F	gggccgctatataccacaga	
<i>pesLRT-R</i>	R	aagaggagtgccaccaacac	<i>pesL</i> RT-PCR
AFUA_6G12040 RT-F	F	tctatgccacggttggtgta	AFUA_6G12040 RT-PCR
AFUA_6G12040 RT-R	R	attgcccgaatcgacattat	
AFUA_6G12060 RT-F	F	gtgtctttgcgtttcccaat	AFUA_6G12060 RT-PCR
AFUA_6G12060 RT-R	R	atgtgtcctccaccgataa	
AFUA_6G12070 RT-F	F	tcatgggggtccaatgaagat	AFUA_6G12070 RT-PCR
AFUA_6G12070 RT-R	R	tggtgcacatctgttctctg	
AFUA_6G12070 RT-F	F	tcatgggggtccaatgaagat	AFUA_6G12070 RT-PCR
AFUA_6G12070 RT-R	R	tggtgcacatctgttctctg	

Primer Name	F/R	Sequence 5'-3'	Used in PCR reaction
AFUA_5G06350 -1	F	gagggcaagaccagaatcaa	PCR 1
AFUA_5G06350 -2	R	ggacaattgtaaccagga	5' DIG probe
AFUA_5G06350 -3	F	gctaagcttctgccttcaacct	PCR 2
AFUA_5G06350 -4	R	cctcttggcaggattgtctc	
AFUA_5G06350 -5	F	gtaccgacaagcctctgctc	PCR 3, 5' DIG probe
AFUA_5G06350 -6	R	ggatgacaagcggagtgtgat	PCR 4
AFUA_5G06350 -RT-F	F	tctatgacacgccctcacag	AFUA_5G06350 RT-PCR
AFUA_5G06350 -RT-R	R	atctaaaccgccaagaggt	
AFUA5G06350 PC210 F	F	gggtttcatatgcatgtggctgatgattca	Cloning AFUA_5G06350 into
AFUA5G06350 PC210 -R	R	gcacatgcatgcctattgtacttcgtctgg	pPC210
AFUA_2G02090-1	F	tacaccgaaggactgggtct	PCR 1 , 5' DIG probe
AFUA_2G02090-2	R	gctcccccggtcttctgcaagtattgg	
AFUA_2G02090-3	F	gaggggtaccgaatgatctgg	PCR 2
AFUA_2G02090-4	R	tggggcctattacctctcaa	
AFUA_2G02090-5	F	caggagtaccgcaccaagat	PCR 3
AFUA_2G02090-6	R	tcttcgctgagatggagctt	PCR 4
AFUA_2G02090-RT-F	F	catcccaccctaaccctta	AFUA_2G02090 RT-PCR
AFUA_2G02090-RT-R	R	agccgcttctcaacctgata	
AFUA_2G02090 PC210 F	F	gggtttcatatgagaaccaagcagtcccca	Cloning AFUA_2G02090 into
AFUA_2G02090 PC210 R	R	gcacatgcatgcctacttccactccca	pPC210

2.1.3 *Aspergillus* Transformation Buffers

2.1.3.1 Lysis Buffer

A 50 mM KH_2PO_4 solution was prepared by dissolving 1.70 g KH_2PO_4 in 500 ml dH_2O (Buffer L1). A 50 mM K_2HPO_4 was prepared by dissolving 0.87 g K_2HPO_4 in 200 ml dH_2O (Buffer L2). A 0.8 M solution of KCl was prepared by dissolving 26.1 g of KCl in 350 ml Buffer L1. This solution was pH adjusted to pH 5.8 using Buffer L1 and Buffer L2. The solution was brought to a final volume of 500 ml with dH_2O . This solution was autoclaved and stored at room temperature.

2.1.3.2 Mycelial lysing solution

An enzyme preparation was purchased from Sigma-Aldrich (Lytic Enzymes from *Trichoderma harzianum* Cat. No. L1412) which contains β -glucanase, cellulase, protease, and chitinase activities. Lytic Enzymes (0.9 g) were dissolved in 30 ml of Lysis Buffer (2.1.3.1). This solution was stirred and filtered through a 0.45 μm filter.

2.1.3.3 0.7 M KCl

KCl (26.1 g) was dissolved into 500 ml dH_2O . This solution was autoclaved and stored at room temperature.

2.1.3.4 L6 Buffer

A solution of 1 M sorbitol, 10 mM Tris-HCl and 10 mM CaCl_2 was prepared by dissolving 72.88 g sorbitol, 0.484 g Tris-HCl and 0.876 g $\text{CaCl}_2 \cdot 6\text{H}_2\text{O}$ into 300 ml dH_2O . This solution was adjusted to pH 7.5. The solution was then brought to a final volume of 400 ml with dH_2O . The solution was then autoclaved and stored at room temperature.

2.1.3.5 L7 Buffer

PEG 6000 (60 g) was dissolved in 40 ml dH₂O. To this, 0.157 g Tris-HCl was added and dissolved (final concentration 10 mM Tris-HCl). The solution was adjusted to pH 7.5. The solution was then autoclaved and stored at room temperature.

2.1.4 Southern and Northern Blotting Reagents

2.1.4.1 Southern Transfer Buffer

A 0.4 M NaOH / 0.6 M NaCl solution was prepared by dissolving 16 g NaOH pellets and 35.06 g NaCl in 1 L dH₂O. The solution was prepared freshly prior to each Southern blot procedure.

2.1.4.2 20 X SSC Buffer

NaCl (175.3 g) and 88.2 g sodium citrate was dissolved into 800 ml dH₂O. The solution was pH adjusted to pH 7.0 and the final volume was brought to 1 L with dH₂O. The solution was autoclaved and stored at room temperature.

2.1.4.3 10 X SSC Buffer

20 X SSC Buffer (Section 2.1.4.2) (500 ml) was added to 500 ml dH₂O and stirred. The solution was stored at room temperature.

2.1.4.4 2 X SSC Buffer

20 X SSC Buffer (Section 2.1.4.2) (100 ml) was added to 900 ml dH₂O and stirred. The solution was stored at room temperature.

2.1.4.5 10 % (w/v) Sodium Dodecyl Sulphate (SDS)

SDS (100 g) was dissolved into 1 L dH₂O. The solution was stored at room temperature.

2.1.4.6 0.1 % (w/v) SDS / 1 X SSC buffer

20 X SSC (Section 2.1.4.2) (50 ml) and 10 ml of 10 % (w/v) SDS (Section 2.1.4.5) were dissolved in 1 L dH₂O. The solution was prepared freshly prior to each use and stored at room temperature.

2.1.5 Digoxigenin (DIG) Detection Buffers

2.1.5.1 Membrane Pre-Hybridisation Buffer

SDS (35 g), 250 ml Formamide (deionised), 100 ml 10% (w/v) Blocking reagent (Roche), 5 ml 10% (w/v) Laurylosarcosine were dissolved in 500 ml dH₂O. The solution was stirred well and autoclaved. The solution was stored at 4 °C.

2.1.5.2 DIG Buffer 1

Maleic acid (1.161 g) and NaCl (0.876 g) were dissolved in 80 ml dH₂O. The solution was pH adjusted to pH 7.5 and the final volume was brought to 100 ml with dH₂O. The solution was filter sterilized and stored at room temperature for a maximum of one month.

2.1.5.3 Antibody Blocking Buffer

Blocking reagent (0.4 g) (Roche) was dissolved at 50 °C into 40 ml DIG Buffer 1 (Section 2.1.5.2). The solution was prepared freshly before each use.

2.1.5.4 DIG Buffer 3

Tris-HCl (1.57 g), 0.58 g NaCl and 1.01 g MgCl₂·6H₂O were dissolved into 80 ml dH₂O. The solution was pH adjusted to pH 9.5 and the final volume was brought to 100 ml with dH₂O. The solution was filter sterilized and stored at room temperature for a maximum of one month.

2.1.5.5 DIG Wash Buffer

Tween-20 (0.15 g) was dissolved into 50 ml DIG Buffer 1 (Section 2.1.5.2). This solution was prepared in a 50 ml falcon tube and stored at room temperature.

2.1.5.6 Anti-DIG FaB Fragments

Anti-DIG FaB Fragments (1 µl) (Roche) was added to 10 ml Antibody Blocking Buffer (Section 2.1.5.3). This solution was prepared freshly in a 50 ml falcon tube prior to each use.

2.1.5.7 CSPD chemiluminescent substrate

CSPD (50 µl) (Roche) was added to 4.95 ml DIG Buffer 3 (Section 2.1.5.4). This solution was prepared freshly in a 50 ml falcon tube prior to each use.

2.1.5.8 DIG-labelled deoxynucleotide Triphosphates (dNTP's)

Pre-mixed DIG-labelled dNTP's were purchased from Roche and used according to supplier recommendations for the generation of DIG-labelled probes for Southern blot detection.

2.1.6 Blot Development Solutions

2.1.6.1 Developing Solution

Developing solution (200 ml) (Kodak) was added to 400 ml dH₂O in a Duran bottle covered in tin foil and stirred. The solution was stored at room temperature in the dark.

2.1.6.2 Fixing Solution

Fixing solution (150 ml) (Kodak) was added to 450 ml dH₂O in a Duran bottle covered in tin foil and stirred. The solution was stored at room temperature in the dark.

2.1.7 RNA Reagents

2.1.7.1 RNA Glassware

All glassware required for RNA reagent preparation and RNA extraction was autoclaved twice before use.

2.1.7.2 10 X Formaldehyde Agarose (FA) Gel Buffer

MOPS (41.9 g) (0.2 M), sodium acetate (6.8 g) (82mM) and 0.5 M EDTA pH 8.0 (20 ml) were dissolved in 800 ml double autoclaved dH₂O. The pH of the solution was adjusted to pH 7.0 and the final volume was adjusted to 1 L with double autoclaved dH₂O. The solution was then autoclaved and stored at room temperature.

2.1.7.3 1 X Formaldehyde Agarose (FA) Running Buffer

FA gel buffer (10 X, 100 ml), 37 % (v/v) (12.3 M) formaldehyde (20 ml) and double autoclaved dH₂O were added to an autoclaved 1 L Duran bottle (Section 2.1.10.2). The solution was stirred and stored at room temperature.

2.1.8 Reverse-Phase High Performance Liquid Chromatography (RP-HPLC) Solvents

2.1.8.1 RP-HPLC Running Solvents

2.1.8.1.1 Solvent A

Trifluoroacetic acid (TCA) (1 ml) was added to 999 ml of HPLC grade water to yield a solution 0.1 % (v/v) of TCA and water. The solution was prepared freshly before each use.

2.1.8.1.2 Solvent B

Trifluoroacetic acid (1 ml) (TCA) was added to 999 ml of HPLC grade acetonitrile to yield a solution of 0.1 % (v/v) of TCA and acetonitrile. The solution was prepared freshly before each use.

2.1.8.2 RP-HPLC Sample Preparation Reagents/Extraction Mixtures

2.1.8.2.1 Acetonitrile/H₂O Extraction Mixture

A 25 % (v/v) acetonitrile extraction reagent was prepared. HPLC grade acetonitrile (25 ml) was added to 75 ml HPLC grade water and mixed. The solution was prepared freshly before use.

2.1.8.2.2 Ethyl Acetate: Dichloromethane: Methanol Extraction Mixture

A 3:2:1 dilution of ethyl acetate: dichloromethane: methanol was prepared using HPLC grade solvents as follows: 30 ml of ethyl acetate, 20 ml dichloromethane and 10 ml methanol were placed in a Duran bottle and mixed. This reagent was prepared freshly before each use or was stored at 4 °C for 1 week.

2.1.9 *E. coli* Competent Cell Buffers

2.1.9.1 RF 1

Potassium acetate (1.47 g), 0.75 g of calcium chloride ($\text{CaCl}_2 \cdot 2\text{H}_2\text{O}$), and 75 g of glycerol were dissolved sequentially in 450 ml dH_2O . The pH was adjusted to 5.92 and then the following components were added: 6 g of rubidium chloride (RbCl) and 4.95 g of manganese chloride ($\text{MnCl}_2 \cdot 4\text{H}_2\text{O}$). The volume was adjusted to 500 ml with dH_2O , and the solution was filter sterilized and stored at 4 °C.

2.1.9.2 RF 2

Rubidium chloride (0.6 g), 5.5 g of calcium chloride ($\text{CaCl}_2 \cdot 2\text{H}_2\text{O}$), 1.05 g of 3-(N-Morpholinopropanesulfonic acid (MOPS), and 75 g of glycerol were sequentially dissolved in 450 ml dH_2O . The pH of the solution was adjusted to 6.8. The volume was brought to 500 ml with dH_2O , and the solution was filter sterilized and stored at room temperature.

2.1.10 Yeast Transformation Buffers

2.1.10.1 50 % (w/v) Polyethylene Glycol (PEG)

PEG (50 g) was dissolved in 100 ml dH_2O . The solution was autoclaved and stored at 4 °C.

2.1.10.2 1 M Lithium Acetate

Lithium acetate (6.59 g) was dissolved in 100 ml dH_2O . The solution was autoclaved and stored at room temperature.

2.1.10.3 100 mM Lithium Acetate

Lithium acetate (0.659 g) was dissolved in 100 ml dH₂O. The solution was autoclaved and stored at room temperature.

2.1.10.4 Carrier DNA for transformation

Salmon sperm carrier DNA (Sigma) was used at a concentration of 2mg/ml in dH₂O in all yeast transformations.

2.2 Methods

2.2.1 Microbiological Methods – Strain Storage and Growth

Fungal strains used in this study are listed in Table 2.4. Yeast strains used in the study are listed in Table 2.5. *E. coli* DH5 α was used throughout this study for plasmid propagation.

2.2.1.1 *A. fumigatus* growth, maintenance and storage

A. fumigatus strains were stored on either Malt extract agar (Section 2.1.1.5) or on AMM (*Aspergillus* minimal media) agar (Section 2.1.1.6). To culture fungal strains on agar, a loop of spores from a spore solution was spread around a culture plate and plates were incubated at 37 °C in a static incubator in the dark for 5-7 days. Once grown, conidia were harvested from plates for immediate use. Freshly grown spores were harvested from plates by adding 10 ml sterile PBST (Section 2.1.1.17) to the conidiating culture and rubbing the surface with the side of a sterile Pasteur pipette to dislodge the spores. The spore suspension was then collected with the sterile Pasteur pipette and placed in a sterile 50 ml tube. Spores were either used immediately or were stored at 4 °C. *A. fumigatus* conidial suspensions (usually at a density of $\times 10^7$ spores/ml) were used to inoculate liquid media cultures for relevant experiments. The cultures were incubated for a defined time point, with shaking at 200 rpm. Subsequently, overnight cultures were harvested by filtering the mycelia through sterile miracloth. Sterile water was used to wash media from the mycelia, and the mycelia were then scraped from the miracloth using a sterile spatula and were either used immediately or wrapped in two layers of tin foil. The wrapped mycelia were then placed into a container of liquid nitrogen and rapidly frozen. At this point, mycelia were frozen at -70 °C until required. For long term storage of fungal strains, aliquots of the conidial suspensions in PBST (800 μ l) (Section 2.1.1.17) were added to 200

μl of sterile 80 % (v/v) glycerol (Section 2.1.1.20) in sterile 1.5 ml tubes. Tubes were vortexed and rapid-frozen in liquid nitrogen before transferring to – 80 °C.

2.2.1.2 *E. coli* growth, maintenance and storage

E. coli strains were grown on LB agar (Section 2.1.1.18) overnight at 37 °C or in LB broth (Section 2.1.1.19) at 37 °C, shaking at 200 rpm. Where appropriate, media was supplemented with suitable antibiotics. Bacterial strains were stored at 4 °C for short term storage. For long term storage, 500 μl of freshly grown liquid culture of the desired strain (with plasmid(s) where appropriate), were mixed with an equal volume of 40 % (v/v) glycerol (Section 2.1.1.21) in a screw cap 1.5 ml eppendorf tube. Tubes were rapid-frozen in liquid nitrogen before transferring to – 80 °C. To regenerate bacterial strains, tubes were removed from – 80 °C and placed on ice. A cooled sterile loop was scraped across the surface of the frozen culture and streaked onto a LB agar plate with appropriate antibiotics. Tubes were then re-frozen in liquid nitrogen and returned to – 80 °C. Fresh glycerol stocks were prepared as required to avoid loss of viability from numerous freeze-thaw cycles.

2.2.1.3 Yeast growth, maintenance and storage

Saccharomyces cerevisiae strains were grown on YPD agar plates (Section 2.1.1.23) at 30 °C in a static incubator in the dark for 2 days. For liquid cultures, yeast strains were grown in YPD broth (Section 2.1.1.22) at 30 °C shaking with 200 rpm. Where yeast strains contained plasmids, such strains were grown in SC media (Section 2.1.1.25) or on SC agar (Section 2.1.1.26) lacking an appropriate amino acid to ensure plasmid maintenance. Yeast strains were stored at 4 °C for short term storage. For long term storage, 500 µl of freshly grown liquid culture of the desired strain (with plasmid(s) where appropriate), were mixed with an equal volume of 40 % (v/v) glycerol (Section 2.1.1.21) in a screw cap 1.5 ml eppendorf tube. Tubes were rapid-frozen in liquid nitrogen before transferring to – 80 °C. To regenerate yeast strains, tubes were removed from – 80 °C and placed on ice. A cooled sterile loop was scraped across the surface of the frozen culture and streaked onto an SC agar plate lacking appropriate amino acids. Tubes were then re-frozen in liquid nitrogen and returned to – 80 °C. Fresh glycerol stocks were prepared as required to avoid loss of viability from numerous freeze-thaw cycles.

Table 2.4. List of fungal strains used in this study.

Strain used	Genotype	Reference
<i>Aspergillus fumigatus</i> ATCC 46645	Wild-type	ATCC collection
<i>Aspergillus fumigatus</i> Af293	Wild-type fully genome-sequenced strain	Nierman <i>et al.</i> , (2005)
<i>Aspergillus fumigatus</i> CEA17	\DeltaakuB (NHEJ-deficient strain)	da Silva Ferreira <i>et al.</i> , 2006
<i>Aspergillus fumigatus</i> $\Delta pesL$	$\Delta pesL::ptrA$ in the $akuB^{\Delta KU80}$ background.	This study
<i>Aspergillus fumigatus</i> $\Delta pes3$	$\Delta pes3::ptrA$ in the ATCC 46645 background.	Dr. Deirdre Stack, NUI Maynooth
<i>Aspergillus fumigatus</i> $\Delta pes3::PES3$	$\Delta pes3^{ATCC\ 46645}::pes3$ -phleomycin ($pes3$ disruption restored)	This study
<i>Aspergillus fumigatus</i> $\Delta Afmpt$	$\Delta Afmpt::ptrA$ in the Af293 background	This study
<i>Aspergillus fumigatus</i> $\Delta Afagt$	$\Delta Afagt::ptrA$ in the Af293 background	This study

Table 2.5. List of yeast strains used in this study

Strain Used	Genotype	Source
<i>S. cerevisiae</i> BY4741	(Mat a; his3D1; leu2D0; met15D0; ura3D0; YDL200c::kanMX4) YDL200 = <i>A. fumigatus</i> AFUA_5G06350 homologue, and is deleted in this <i>S. cerevisiae</i> strain	European <i>Saccharomyces cerevisiae</i> archive for functional analysis. (Euroscarf)
<i>S. cerevisiae</i> SC + <i>Afmpt</i>	<i>S. cerevisiae</i> Δ <i>MGT1</i> bearing a plasmid-borne copy of <i>A. fumigatus</i> AFUA_5G06350 (<i>Afmpt</i>)	This study
<i>S. cerevisiae</i> SC + <i>Afagt</i>	<i>S. cerevisiae</i> Δ <i>MGT1</i> bearing a plasmid-borne copy of <i>A. fumigatus</i> AFUA_2G02090 (<i>Afagt</i>)	This study

2.2.2 Molecular Biological Methods

2.2.2.1 Isolation of Genomic DNA from *A. fumigatus*

A. fumigatus conidial suspensions were used to inoculate 100 ml Sabourard liquid (Section 2.1.1.9) cultures. The cultures were incubated overnight at 37 °C shaking at 200 rpm. Subsequently, overnight cultures were harvested by filtering the mycelia through sterile miracloth. Sterile water was used to wash media from the mycelia, and the mycelia were then removed from the miracloth using a sterile spatula and wrapped in two layers of tin foil. The wrapped mycelia were then placed into a container of liquid nitrogen and rapidly frozen. At this point, mycelia were either frozen at -70 °C until required or DNA isolation was carried out on the day. For DNA isolation, the ZR Fungal/Bacterial DNA Kit™ (Zymo Research U.S.A.) was used with reagents and columns supplied with the kit and following the manufacturer's instructions. All buffer constituents (Lysis Solution, Fungal/Bacterial DNA Binding Buffer, DNA Pre-Wash Buffer and Fungal/Bacterial DNA Wash Buffer) are described in the ZR Fungal/Bacterial DNA kit manual supplied with the kit. Briefly, the frozen mycelia were crushed to a powdery consistency with a pestle and 100 mg of this was added to a ZR BashingBead™ Lysis Tube. Lysis Solution (750 µl) was added to the tube. The tubes were vortexed at high speed for ten min to disrupt the mycelial cell walls. The ZR BashingBead™ Lysis Tube was centrifuged in a microcentrifuge at 10,000 x g for 1 min. Subsequently, 400 µl of the supernatant was added to a Zymo-Spin™ IV Spin Filter in a collection tube and this was centrifuged at 7,000 x g for 1 min. After this centrifugation step, 1,200 µl of Fungal/Bacterial DNA Binding Buffer was added to the filtrate in the collection tube and mixed. Subsequently, 800 µl of this mixture was added to a Zymo-Spin™ IIC Column in a new collection tube and this was centrifuged at 10,000 x g for 1 min. The flow-through was discarded and this step was repeated with the remaining 800 µl that was left from the DNA binding step. DNA Pre-Wash Buffer (200 µl) was added

to the Zymo-Spin™ IIC Column in a new collection tube and this was centrifuged at 10,000 x g for 1 min. The flow-through was discarded and 500 µl of Fungal/Bacterial DNA Wash Buffer was added to the Zymo-Spin™ IIC Column and then centrifuged at 10,000 x g for 1 min. Following these wash steps, the Zymo-Spin™ IIC Column was transferred to a sterile 1.5 ml microcentrifuge tube. Sterile water (100 µl) was added to the centre of the column in order to elute the DNA. The DNA was eluted by centrifuging at 10,000 x g for 1 min and collected in the 1.5 ml microcentrifuge tube.

2.2.2.2 Precipitation of *A. fumigatus* genomic DNA

Sterile water was added to genomic DNA in a 1.5 ml microcentrifuge tube until the final volume in the tube was 100 µl. Sodium acetate (10 µl) (Section 2.1.2.2.3) and 250 µl of ice-cold ethanol (100 % (v/v)) was added and samples were mixed by inversion. Samples were incubated for at least an hour at – 20 °C. Subsequently, samples were centrifuged at 13,000 x g for 10 min at 4 °C. The supernatants were discarded and 70 % ethanol (v/v) (100 µl) (Section 2.1.2.2.2) was added to the tube. The samples were handled carefully at this point so as not to disturb the DNA pellet. Subsequently, the samples were centrifuged at 13,000 x g for 10 min at 4 °C. The supernatant was discarded and a quick spin on the microcentrifuge was performed (10,000 x g, 15 sec). Residual ethanol remaining in the tube was removed by pipetting, taking care not to disturb the pellet. The pellet was air-dried and resuspended in 16 µl sterile water.

2.2.2.3 Polymerase Chain Reaction (PCR)

Polymerase chain reaction (PCR) was used to amplify fragments of DNA for cloning, to test *E. coli* for recombinant plasmids, for generation of *A. fumigatus* gene disruption constructs, and for the generation of DIG-labelled DNA probes for use in

Southern blot analysis. PCR for the generation of gene disruption constructs and the generation of DIG-labelled DNA probes was performed using the Expand Long Range Template system (Roche). All other PCR was carried out using *AccuTaq* LA polymerase (Sigma) where the DNA amplified was to be used for cloning. For testing *E. coli* for recombinant plasmids, a *Taq* polymerase (Sigma-Aldrich) was used. The general reaction constituents for each polymerase used was as follows:

Expand Long Range Template system

10x reaction buffer	5 μ l
dNTP mix (20 μ M)	5 μ l
Primer 1 (100 pmol/ μ l)	2 μ l
Primer 2 (100 pmol/ μ l)	2 μ l
DNA Template	Up to 500 ng
Sterile Water	to a total of 50 μ l

AccuTaq LA polymerase

10X reaction buffer	2 μ l
dNTP mix (10 μ M)	2 μ l
Primer 1 (100 pmol/ μ l)	1 μ l
Primer 2 (100 pmol/ μ l)	1 μ l
DMSO	0.8 μ l
DNA template	10-100 ng
Sterile water	to a total of 20 μ l

Taq polymerase

10X reaction buffer	2 μ l
dNTP mix (10 μ M)	2 μ l
Primer 1 (100 pmol/ μ l)	1 μ l
Primer 2 (100 pmol/ μ l)	1 μ l
DNA template	10-100 ng
Sterile water	to a total of 20 μ l

The following reaction cycle was used unless otherwise stated:

95 °C (denaturing)	5 min		
95 °C (denaturing)	1 min	}	X 30-40 cycles
55 °C (annealing)	1 min 30 sec		
72 °C (extending)	1 min		
72 °C (extending)	10 min		

Annealing temperatures were estimated as *ca.* 4 °C below the lowest melting temperature (T_m) of the primer pair used. Extension times used were *ca.* 1 min/kb of DNA target to be amplified. When *AccuTaq* was used, extension temperature was reduced to 68 °C as per supplier recommendations. Reactions were carried out using an Eppendorf PCR machine or a G-Storm Thermal Cycler (Mason Technologies)

2.2.2.4 DNA Gel Electrophoresis

2.2.2.4.1 Preparation of Agarose Gel

Agarose gel electrophoresis was used to visualise PCR products, restriction digest reactions, to separate DNA for Southern analysis, to separate differently sized DNA fragments prior to purification and for estimation of DNA yield. Agarose gels were cast and

run using Bio-Rad electrophoresis equipment. Agarose gels of between 0.7 % -2 % (w/v) in 1X TAE (Section 2.1.2.1.2) buffer were used, although for most applications, a 1 % (w/v) gel strength was suitable. Powdered agarose was added to the appropriate volume of 1X TAE buffer in a 200 ml flask with a loose stopper. This was then gently heated in a microwave oven, with frequent mixing, until the agarose had dissolved. While allowing the gel to cool, a mould was prepared by sealing the ends of a gel tray with masking tape, and inserting a gel comb. After allowing the gel to cool to 40-50 °C, 5 µg/ml ethidium bromide (Section 2.1.2.1.3) or Sybr-Green (1 µl/10 ml) (Section 2.1.2.1.4) was added and mixed by swirling. The molten gel was then poured into the prepared mould, and was allowed to set on a level surface. Once set, the gel comb and masking tape were removed gently, and the gel tray placed into the gel tank, with the wells nearer the negative (black) electrode. 1X TAE buffer was then poured into the gel tank to fully submerge the gel.

2.2.2.4.2 Loading and Running Samples

In order to apply DNA samples to the wells in the agarose gel, samples were first mixed with 6X loading dye (Promega). DNA fragment size was estimated by running molecular weight markers alongside the unknown samples. Three different molecular weight markers were used throughout this study; marker VII and marker VII (DIG-labelled) (Roche) and 50 bp DNA ladder (Sigma-Aldrich). Gels were electrophoresed at 50-100 volts for 30-60 min.

2.2.2.5 DNA Gel Extraction

DNA gel extraction was carried out using the QIA quick gel extraction Kit (Qiagen, U.K.) using reagents and columns supplied with the kit and following the manufacturer's instructions. All buffer constituents (PE buffer) are described in the Qia quick spin

handbook supplied with the kit. DNA fragments were excised from the agarose gel using a sterile blade and the gel piece placed in a sterile pre-weighed microfuge tube and weighed. For every 1 volume of gel, 3 volumes of Buffer QG were added. Samples were incubated for 10 min at 50 °C in a heating block, vortexing the samples every 2 min. When the gel had fully dissolved, the solution was transferred to the QIA quick spin column placed in a 2 ml collection tube. The samples were centrifuged at 12,000 x g for 1 min and the flow-through removed. Buffer PE (750 µl) was applied to the column and centrifuged at 12,000 x g for 1 min and the flow-through once again removed. A further centrifugation step was carried out at 12,000 x g for 1 min to remove any residual ethanol from the column and the column was placed in a sterile 1.5 ml microfuge tube. To elute DNA, 30 µl of sterile water was added to the centre of the column membrane and the column was allowed to stand for 2 min. A final centrifugation step (12,000 x g for 1 min) was carried out and DNA collected in the microfuge tube was analysed by agarose gel electrophoresis.

2.2.2.6 Restriction Enzyme Digests

Restriction enzymes, 10 X reaction buffers, and bovine serum albumin (BSA) were obtained from either Promega or New England Biolabs. Reactions were carried out according to the manufacturer's instructions, but a typical reaction was performed as follows:

DNA	1-5 µg
Enzyme 1	1 µl
Enzyme 2	1 µl
10 x buffer	2.5/5 µl
10 x BSA	2.5/5 µl
Sterile water	to a total of 25/50 µl

The total reaction was always > 10 X the volume of enzyme used in order to prevent high glycerol concentrations, which could cause non-specific digestion (star activity). Reactions were typically carried out at 37 °C for 3 hr, although some enzymes require different incubation temperatures, as per the manufacturer's instructions. Digestion reactions were visualised by agarose gel electrophoresis.

2.2.2.7 Ligation of DNA Fragments

Ligation of DNA fragments was required for the generation of gene disruption constructs and for the cloning of *A. fumigatus* genes into vectors suitable for expression in *S. cerevisiae* yeast strains. DNA was digested (Section 2.2.2.6) to produce compatible fragments. These fragments were then separated by DNA gel electrophoresis (Section 2.2.2.4) and the DNA isolated from the gel (Section 2.2.2.5). Ligation of DNA fragments was carried out using the Ligafast™ Rapid DNA Ligation System (Promega) which employs T4 DNA ligase. Ligations were carried out according to manufacturer's instructions. Restriction digests either produce a DNA fragment with an overhang of single-stranded DNA at either end of the double-stranded section, known as cohesive ends, or blunt ended molecules, which have no such overhangs. Creation of recombinant molecules for cloning genes into plasmid vectors usually involved the ligation of a smaller fragment to a larger fragment (backbone). For cohesive ended ligation, the preferred molecular ratio of was 3 insert to 1 backbone. This was estimated from the size of the DNA fragments, according to the following formula:

$$\frac{(\text{ng of vector}) * (\text{kb size of insert})}{\text{kb size of}} * \frac{3}{1} = \text{ng of insert}$$

Ligations were assembled in a sterile 0.5 ml using 50-200 ng of vector DNA, T4 DNA ligase (1 μ l), and 2X Rapid Ligation Buffer. For ligations where inserts were ligated to vectors, a control ligation was also carried out whereby the insert DNA was omitted from the reaction. For the generation of linear DNA constructs for gene disruptions, a 1:1 ratio of each molecule was used and this was estimated again based on the size of the DNA fragments, according to the formula described above. Ligation reactions containing cohesive-ended molecules were usually incubated for 10 min- 1 hr at 20 °C, while for linear constructs for gene disruption cassettes, and ligations containing blunt-ended molecules, reactions were usually incubated overnight at 20 °C. All ligation reactions were carried out in a thermal cycler to ensure constant temperature.

2.2.3 Generation of *Aspergillus fumigatus* mutant strains

2.2.3.1 Generation of *A. fumigatus* gene disruption constructs

A bipartite gene disruption strategy was employed for the generation of all *A. fumigatus* mutant strains used in this study. The use of the bipartite method allows the generation of gene replacement substrates by PCR and a ligation step, thereby abrogating the need for time-consuming bacterial sub-cloning steps (Nielsen *et al.*, 2006). More specifically, this strategy involves the generation of two overlapping constructs, each containing partial fragments of a selection marker gene which are ligated to 5' and 3' flanking regions of the specific gene of interest (GOI). In this study, the pyrithiamine (PT) resistance gene (*ptrA*) gene from *Aspergillus oryzae* (Kubodera *et al.*, 2000; 2002) was used as the selection marker. *ptrA* was present on a plasmid vector pSK275 (a kind gift from Professor Sven Krappmann), and was released by digestion with appropriate restriction enzymes (Section 2.2.2.6). Respective GOI fragments were amplified from *A. fumigatus* genomic DNA by PCR (Section 2.2.2.3). Usually about 1-1.2 kb of 5' and 3'

flanking regions were amplified in these PCR reactions. The resulting products of these PCR reactions were digested with the same enzymes as *ptrA* to make the ends compatible for ligation (Section 2.2.2.7). Ligation products were used as the DNA template for a second round of PCR reactions, this time using primers that would amplify the majority of the flanking region, while only amplifying a portion of *ptrA*. A schematic representation of the bipartite gene deletion strategy is shown in Figure 2.1.

PCR reactions for Round 1 and Round 2 PCR were performed using the Expand Long Range Template PCR System (Roche). In all cases, PCR products were extracted from 1 % (w/v) agarose gels and purified using a Qiagen gel extraction kit (Section 2.2.2.5). PCR products were resolved on 1% (w/v) agarose gels (Section 2.2.2.4). Successful transformation of both of these constructs, referred to as PCR 3 and PCR 4 into protoplasts of the recipient strain can lead to the growth of PT-resistant colonies when transformants are grown on selective media, due to the reconstitution of the selection marker by homologous recombination between the two overlapping constructs. This often results in the replacement of the desired gene region with *ptrA*, and a single homologous integration of *ptrA* can be confirmed by Southern blot analysis.

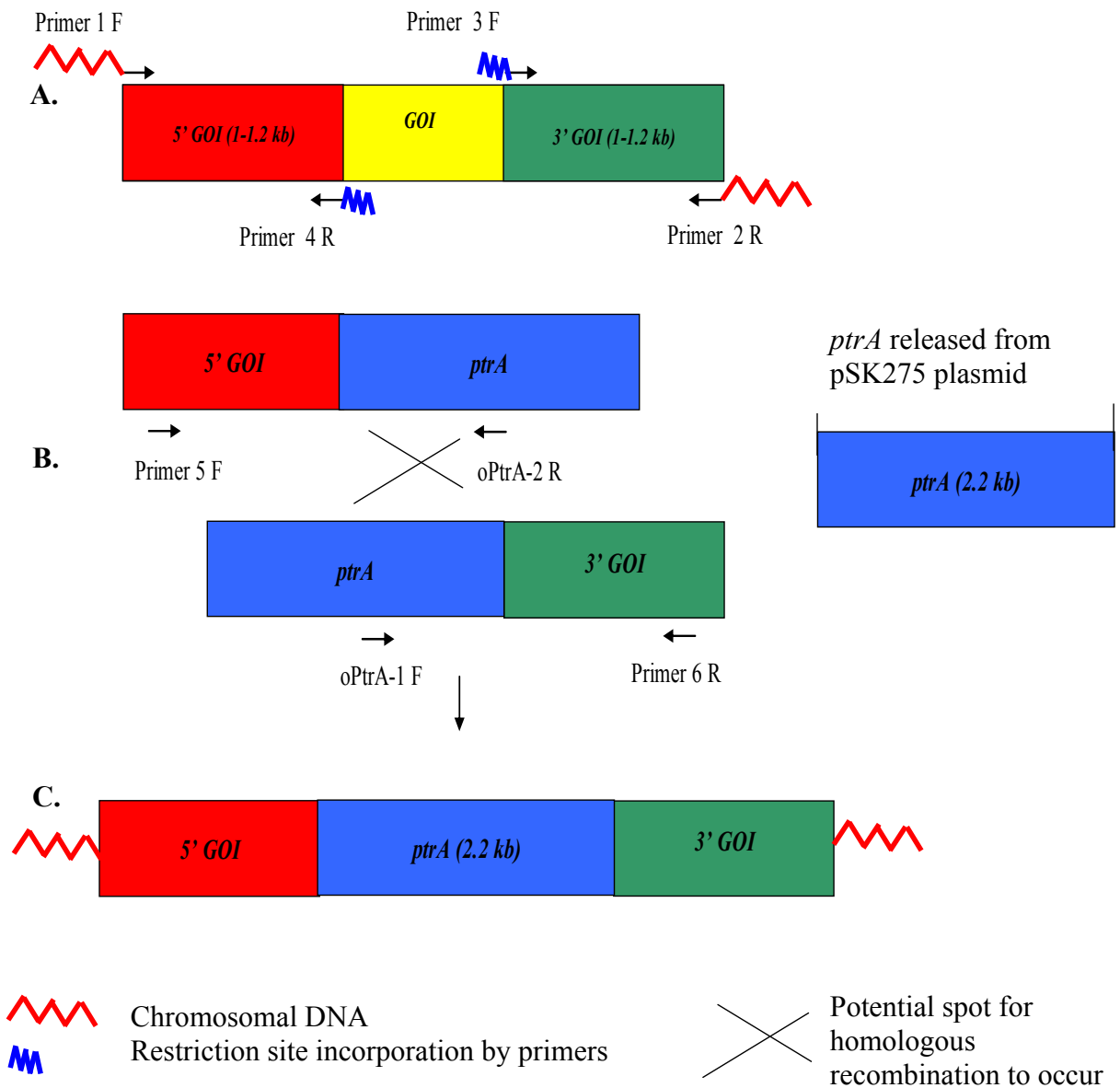


Figure 2.1. The bipartite strategy used to disrupt *A. fumigatus* genes in this study, using *ptrA* as a selection marker. Using this strategy, approximately 1-1.2 kb of 5' and 3' flanking regions are amplified by PCR (A), with suitable restriction sites engineered for ligation to *ptrA* (B) (Kubodera *et al.*, 2000; Kubodera *et al.*, 2002). C. Another round of PCR generates two overlapping constructs which only contain approx. two thirds of the selection marker due to the use of nested primers. Primers indicated by black arrows. Adapted from the original method of Nielsen *et al.* (2006).

2.2.3.2 *A. fumigatus* Protoplast Production and Transformation

2.2.3.2.1 *A. fumigatus* Protoplast Formation

AMM cultures (200 ml) of *A. fumigatus* were incubated overnight at 37 ° C, and the mycelia were harvested by filtering through sterile miracloth. Sterile water was used to wash media from the mycelia, and subsequently 1.5 g of mycelia was placed into a sterile 50 ml tube. For each transformation, protoplasting of 1.5 g mycelia was performed in duplicate. Mycelial lysing solution (Section 2.1.3.2) (15 ml) was added to each tube, and the mycelia were lysed by incubating the tubes at 30 °C at 200 rpm. After 10 min incubation, the tubes were removed and a 1000 µl pipette tip with a 200 µl pipette tip on top were used to pipette the mixture up and down continuously for 10 min in order to break up clumps of mycelia. Subsequently, the tubes were incubated at 30 °C at 200 rpm shaking for a further 2 hr and 40 min. The samples were then placed on ice for 5 min to terminate the lysing reaction. The samples were then centrifuged at 900 x g for 18 min in order to pellet cellular debris. The brake was left off the centrifuge for all of the protoplasting centrifuge steps so as not to disrupt the protoplasts. The supernatant was then filtered through sterile miracloth into a fresh 50 ml tube, and the volume was brought to 40 ml with 0.7 M KCL (Section 2.1.3.3). The protoplast solutions were centrifuged at 3,300 x g for 18 min, and the supernatant was immediately removed, being careful not to disturb the pellet. The pellets were resuspended in 10 ml of 0.7 M KCL, and were then centrifuged at 3,300 x g for 12 min. Again, the supernatant was removed and the tubes were left upside down on sterile tissue paper for 1 min. The pellet was then resuspended by gently pipetting and swirling in 70 µl of L6 Buffer (Section 2.1.3.4). The samples were given a quick spin at 600 x g to gather all the contents at the bottom of the tube. Duplicate samples were combined and the protoplasts were kept on ice for no longer than 20 min before use. Protoplasts (5 µl) were checked for integrity using a light microscope.

2.2.3.2.2. *A. fumigatus* protoplast transformation

For each transformation, usually 10 µg of transforming DNA was used. The DNA was placed in a 50 ml tube and the volume was brought to 50 µl with Buffer L6 (Section 2.1.3.4). An *A. fumigatus* protoplast suspension (150 µl) (Section 2.2.3.2.1), was added to the DNA and the tube was swirled gently to mix. A negative control was prepared by adding 15 µl of the same protoplast preparation to 185 µl of Buffer L6 in a 50 ml tube, and the tube was swirled gently to mix. Buffer L7 (50 µl) (Section 2.1.3.5) was added to the tubes, and they were shaken gently to mix. Tubes were incubated on ice for 20 min. Buffer L7 (1 ml) was added to the tubes and they were left standing at room temperature for 5 min. Buffer L6 (5 ml) was then added to the mixtures. The transformed protoplasts were now ready to be plated.

2.2.3.2.3. Plating of *A. fumigatus* transformed protoplasts and selection with either phleomycin or pyrithiamine

Aspergillus Transformation Regeneration Media (Section 2.1.1.14) was prepared freshly on the morning of transformation, and final concentrations of either pyrithiamine (0.1 µg/ml) or phleomycin (40 µg/ml) were added to the agar prior to pouring (Table 2.2). These plates were stored at room temperature while the transformation was underway. For each transformation, six plates containing the selective agent were prepared, and two were prepared only containing regeneration media, and these were used to set up protoplast viability plates. For plating the negative control, 1.25 ml of the negative control protoplasts were added to a fresh 50 ml tube, and this was brought up to a final volume of 6 ml with *Aspergillus* Transformation Soft Agar (Section 2.1.1.15) and poured onto a plate containing a selection agent. For the protoplast viability plates, two protoplasts concentrations were prepared in fresh 50 ml tubes. Transformed protoplasts (12.5 µl or 1.25 µl) was added into these tubes, and the final volume of each was brought to 6 ml with soft agar before pouring onto plates lacking a selection agent. Finally, the

transformed protoplasts were topped up to 30 ml with soft agar, and 6 ml was poured onto each of 5 transformation plates containing the desired selection agent. Plates were incubated at room temperature overnight. The following day, plates were overlaid with 6 ml of fresh soft agar, and pyrithiamine or phleomycin was added to this accordingly (Table 2.2). Once agar had set, the plates were incubated at 37 °C for about 5-7 days until colonies began to become visible. The appearance of colonies on the protoplast viability plates after approx. 2 days indicated that the protoplasts had been sustained during the preparation procedure and were capable of regeneration.

2.2.3.3 Isolation of *A. fumigatus* transformants following transformation

Potential *Aspergillus* transformants were initially identified by resistance to either pyrithiamine or phleomycin supplied in the agar plates following transformation. There were usually between 10-40 colonies from each transformation experiment. Spores of these colonies (usually 10 were isolated at any time) were picked aseptically from transformation plates, using a sterile 1000 µl pipette tip and were subcultured onto fresh selective agar plates and incubated at 37 °C. This subculturing step was performed in order to verify resistance. Once sporulated, which was usually two days after inoculation, agar plugs of these colonies were picked aseptically, using an inverted 1000 µl pipette tip, and transferred to sterile 1.5 ml tubes. Colony plugs were then resuspended in 1 ml PBST (Section 2.2.1.17) and were vortexed to dislodge conidia from agar plugs. Conidial suspensions (500 µl) were used to inoculate 50 ml of Sabourard liquid (Section 2.1.1.9) and cultures were incubated at 37 °C shaking with 200 rpm for 16 hr. These cultures were prepared to facilitate genomic DNA isolation (Section 2.2.2.1) from the transformants for further analysis by Southern blotting (Section 2.2.4).

2.2.3.4 Single Spore Isolation of *A. fumigatus* transformants

Following Southern blot analysis of transformants that were picked from a transformation plate, colonies which yielded a hybridisation pattern indicating the desired mutation were subjected to single spore isolation, in order to gain colonies of nuclear homogeneity. To do this, conidial suspensions from each transformant picked from the agar plates were diluted 10,000 fold in PBST (Section 2.2.1.17) and 100 µl of these suspensions were spread onto individual selective agar plates. These plates were incubated at 37 °C until individual colonies became visible. These colonies were then isolated as described earlier (Section 2.2.3.3) and were subjected to a second round of Southern blot analysis (Section 2.2.4).

2.2.4 Southern Blotting

2.2.4.1 Southern Blotting – Nucleic Acid Transfer

Southern blotting analysis was performed to detect gene fragments at desired loci in *A. fumigatus* genomic DNA (gDNA) in order to identify transformants that had undergone either gene deletion or gene replacement. gDNA was isolated (Section 2.2.2.1) from relevant transformants, and was restriction digested with a suitable restriction enzyme. The enzyme choice depended on the sequence of the region of interest in the genome. An enzyme was used which would cut the region in a wild-type gDNA and a corresponding mutant gDNA differentially. Restriction digests were carried out as described (Section 2.2.2.6) and the digestion reactions were resolved on 0.7 % (w/v) agarose gels (Section 2.2.2.4). Once the gels had completed running, the gel was placed into a UV cross-linking machine and was pulsed with 800 µJ. This creates nicks in the DNA which aids transfer onto a nylon membrane. Following this, a Southern blotting tower was set up. Southern transfer buffer (I L) (Section 2.1.4.1) was poured into a large Biorad gel tank, and two sheets of Whatman filter paper (about 12 inches L x 4 inches H) were dipped into the transfer buffer and then laid across the top of the tank. On top of this the gel

containing the restricted DNA was placed (load side down), and a piece of H⁺ Nylon Membrane (Amersham) was placed directly on top of the gel in one single movement. On top of these, three more pieces of Whatman filter paper were placed, and finally three packets of pocket-size tissues were removed from their packaging and placed on top for absorbance of the transfer buffer as it moved up through the layers. For Southern blotting, the gels used were exactly the same size as a pocket-size tissue, and the Whatman filter pieces and nylon membrane were cut to exactly this size. A glass plate was placed across the top of the assembly, and a Duran bottle containing about 400 ml of water was used as a weight. Southern blotting was carried out overnight at room temperature.

2.2.4.2 Disassembly of Southern Blots Following Nucleic Acid Transfer

Following Southern blotting overnight, the stacks of tissue paper and Whatman filter paper was carefully removed from the gel and the nylon membrane to which the DNA had been transferred. The nylon membranes were washed for 2 X 5 min with gentle rocking in 0.1 % (w/v) SDS / 1 X SSC buffer (Section 2.1.4.6). Following this, the blots were placed onto clean tissue paper and the excess water was allowed to air-dry for 1 min. Subsequently, the membranes were placed into a UV cross-linking machine and were pulsed with 1200 μ J in order to cross-link the DNA onto the membrane and prevent it from being washed away during subsequent steps.

2.2.5 Digoxigenin (DIG) - Detection of Hybridised DNA fragments on Southern blot

2.2.5.1 Generation of DIG-labelled DNA probes

DIG-labelled DNA probes were generated by PCR (Section 2.2.2.3) using specific primers (Table 2.3). In order to DIG-label the PCR product, DIG-labelled dNTP's (Section 2.1.5.8) were employed. PCR products were resolved on a 1 % (w/v) agarose gel (Section

2.2.2.4) and excised from the gel (Section 2.2.2.5). DNA was denatured by heating at 100 °C for 8 min in a heated block, and was immediately placed on ice. DNA was quantified using a Nanodrop spectrophotometer and 400 ng DNA was added to membrane pre-hybridisation buffer (5 ml) (Section 2.1.5.1) that had been preheated to 65 °C in a water bath for at least 30 min. This probe solution was stored at – 20 °C, and was heated to 65 °C in a water bath for at least 30 min before each use.

2.2.5.2 Prehybridisation of Nylon Membrane Following UV Cross-linking

Immediately after UV cross-linking, the blots were placed into a clean glass hybridisation tube which had been pre-heated to 42 °C in a hybridisation oven. Immediately, 10-20 ml of membrane pre-hybridisation buffer (Section 2.1.5.1), which had been pre-heated at 65 °C was poured down the side of the hybridisation tube, and the tubes were incubated at 42 °C rotating for 4-5 hr in a hybridisation oven, in order to block the blots.

2.2.5.3 Addition of DIG-labelled probe to Southern blots

Following the prehybridisation of blots (Section 2.2.5.2), the membrane pre-hybridisation buffer was removed from the hybridisation tubes. The specific DIG-labelled probe solution (containing approx 400 ng probe DNA) was poured into the hybridisation tube, careful not to pour directly on the blot, and the tubes were incubated at 42 °C rotating overnight in a hybridisation oven, in order to allow the probe to hybridise homologous regions on the membrane.

2.2.5.4 DIG Detection

The DIG-labelled probe solution was poured from the hybridisation tube and stored in a clean 50 ml tube at – 20 °C. The blots were removed from the hybridisation tube and were washed for 2 X 5 min with gentle rocking in 0.1 % (w/v) SDS / 1 X SSC buffer (Section 2.1.4.6). Subsequently, the blots were placed back into clean hybridisation tubes which were pre-heated at 65 °C. The tubes were filled about half-way with 0.1 % (w/v) SDS / 1 X SSC buffer and the tubes were placed into a hybridisation oven for 15 min rotating at 65 °C. These steps were repeated and each time, the tubes were placed upside down on clean tissue paper between each wash step to drain excess liquid from the blots.

Draining of blots on clean tissue was employed throughout the entire DIG Detection procedure. Blots were next washed with DIG Wash Buffer (10 ml) (Section 2.1.5.5) for 5 min rotating at 25 °C. Subsequently, the blots were blocked with Antibody Blocking Buffer (10 ml) (Section 2.1.5.3) for 30 min rotating at 25 °C. The Antibody Blocking Buffer was poured off and the Anti-DIG Fab Fragments - alkaline phosphatase (10 ml) (Section 2.1.5.6) were added to the blots and were left rotating at 25 °C for 30 min. Subsequently, the blots were washed with DIG Wash Buffer (10 ml) for 10 min at 25 °C. This step was repeated. DIG Buffer 3 (5 ml) (Section 2.1.5.4) was then added to the blots and the blots were left for 5 min rotating at 25 °C. The DIG Buffer 3 was poured off and the CSPD chemiluminescent substrate (5 ml) (Section 2.1.5.7) was then added to the blots and the blots were left for a further 5 min rotating at 25 °C. When this 5 min was complete, the CSPD was poured off the blots and stored in a fresh 50 ml tube covered in tin-foil at 4 °C to be re-used within a week. The blots were carefully removed from the hybridisation tube, and were placed on clean tissue paper to dry for 1 min. The blots were then carefully wrapped in cling film and incubated at 37 °C for 15 min, as this increases the intensity of the signal emitted by the processing of the CSPD by the Anti-DIG Fab-alkaline phosphatase conjugate.

2.2.5.5 Developing of DIG-detected Southern Blots

Following DIG detection, (Section 2.2.5), blots were placed into a Kodak film cassette and exposed to a Kodak film in the dark. The blots were usually exposed for 1 hr, and 3 hr if necessary. After the required time, blots were developed using the Kodak developing solution (Section 2.1.6.1), rinsed in water, and fixed using the Kodak fixing solution (Section 2.1.6.2).

2.2.6 RNA analysis

2.2.6.1 RNA Extraction

For RNA extraction, the QIAGEN RNeasy plant mini kit was used following manufacturer's instructions. All buffers (RLC, RWI, and RPE) and columns were supplied with the kit and details of buffer constituents are outlined in the Qiagen RNeasy plant mini kit Handbook. *Aspergillus fumigatus* mycelia (100 or 200 ml cultures) were harvested aseptically by filtering through sterile miracloth. Mycelia were washed with sterile water. Following this, the mycelia were placed in a mortar. For rapid freezing liquid nitrogen was poured onto the mycelia. A pestle was then used to crush the mycelia into a very fine powdery consistency. Crushed mycelia (100 mg) were placed in a sterile 1.5 ml eppendorf tube containing 450 μ l RLC (containing β -Mercaptoethanol) and the tube was vortexed vigorously. Samples were then incubated for 3 min at 56 °C in a water bath to help further disrupt the mycelia. Subsequently, the lysate was added to a QIAshredder spin column placed in a 2 ml collection tube and the sample was centrifuged at 13,000 x g for 2 min. The filtrate was then transferred to a fresh eppendorf tube for subsequent steps. Ethanol (100 % (v/v)) (250 μ l) was added to the filtrate and the sample was mixed immediately by pipetting. The samples were then transferred to an RNeasy spin column placed in a 2 ml collection tube and centrifuged at 10,000 x g for 15 sec. The flow-through was discarded. Buffer RWI (700 μ l) was added to the RNeasy spin column and the sample was centrifuged at 10,000 x g for 2 min to wash the spin column membrane. The flow-through was discarded. Buffer RPE (500 μ l) was added to the RNeasy spin column and the samples were centrifuged at 10,000 x g for 15 sec to wash the spin column membrane. The flow-through was discarded. Buffer RPE (500 μ l) was added to the RNeasy spin column, and the sample was centrifuged at 10,000 x g for 2 min to wash the spin column membrane once again. To remove residual RPE, the RNeasy spin column was placed in a new 2 ml

collection tube, and the sample was centrifuged at 13,000 x g for 2 min. Subsequently, the RNA was eluted into a new 1.5 ml eppendorf tube. Sterile water (50 µl) was placed on the centre of the column, and the column was allowed to stand for 1 min. The column was centrifuged at 10,000 x g for 1 min. To increase RNA concentration, the eluent was removed from the eppendorf tube by pipetting and eluted a second time through the RNeasy spin column by centrifuging at 10,000 x g for 1 min. RNA was stored at – 20 °C for up to 6 months until required.

2.2.6.2 RNA Gel Electrophoresis

Agarose gels (1.2 % (w/v)) were prepared by adding agarose (1.2 g) to double autoclaved water (80 ml). The agarose was melted in a microwave, and was allowed to cool to 65 °C. Formaldehyde Agarose (FA) gel buffer (10 X) (10 ml) (Section 2.1.7.2) was subsequently added in a fume hood, and the final volume was adjusted to 100 ml with double autoclaved water. Subsequently, the gel was poured into a gel casting tray and allowed to set. The gel was then placed in an electrophoresis rig and submerged in 1 X Formaldehyde Agarose running buffer (Section 2.1.7.3). The gel was allowed to equilibrate in this buffer for 10 min prior to use. RNA samples were prepared for loading at the desired concentration of RNA in a 4 µl volume added to the following components: 10 X FA Buffer (2.5 µl), Formaldehyde (37 %; 4 µl), Formamide (12 µl) and Ethidium Bromide (1 mg/ml; 1 µl). The mixtures were incubated at 65 °C for 15 min and allowed to chill on ice. Samples were loaded onto the gel and electrophoresed at 100 V for 60 min. Formaldehyde Agarose gels were visualised using an AlphaTech DigiDoc still video system (Alpha Technologies).

2.2.6.3 DNase Treatment of RNA

DNase treatment of RNA was performed using a DNase kit purchased from Sigma-Aldrich. *A. fumigatus* RNA (0.5 µg) was brought to an 8 µl volume with molecular grade water in a microfuge tube, 1 µl of 10 X reaction buffer and 1 µl of DNase were added to the microfuge tube, and the mixture was incubated at room temperature for 15 min. Stop solution (supplied with DNase kit) (1 µl) was added to the solution, which was incubated at 70 °C for 10 min. The samples were chilled on ice, and were stored long-term at - 70 °C.

2.2.6.4 cDNA Synthesis

cDNA synthesis was performed using either the Superscript® First-Strand Synthesis System for RT-PCR (Invitrogen), or the Transcriptor First Strand cDNA Synthesis Kit (Roche Applied Science) for Real-Time PCR experiments. In both cases, all buffers and reagents were supplied with the kit, and cDNA was prepared according to suppliers instructions. Using the Superscript® cDNA synthesis kit, DNase-treated RNA (8 µl), 10 mM DNTP mix (1 µl), Oligo (dT) (1 µl), were added to a microfuge tube. Tubes were incubated at 65 °C for 5 min, and placed on ice for 1 min. A master mix of 10 X RT buffer (2 µl), 25 mM MgCl₂ (4 µl), 0.1 M DTT (2 µl) and RNase OUT recombinant RNase Inhibitor (1 µl), and Superscript III Reverse Transcriptase (1 µl) per sample, was prepared. This master mix (10 µl) was added to each RNA sample and mixed gently by pipetting. The samples were then incubated at 50 °C for 50 min. Reactions were terminated by incubating samples at 85 °C for 5 min. RNase H (1 µl) was then added to each sample to remove any remaining RNA, and the samples were incubated at 37 °C for 20 min. The samples were then chilled on ice for immediate use or stored at – 20 °C.

Using the Transcriptor First Strand Synthesis kit, DNase-treated RNA was added to a microfuge tube, and Anchored-oligo(dT)₁₈ Primer (1 µl) was added. The volume was

brought to 13 μ l with RNase-free water (Sigma-Aldrich). The template-primer mixture was denatured by an initial incubation at 65 °C for 10 min, and the samples were subsequently cooled on ice. To the samples, the remaining components required for cDNA synthesis were added as a master mix containing the following: 5 X Transcriptor Reverse Transcriptase Reaction Buffer (4 μ l), Protector RNase Inhibitor (0.5 μ l), Deoxyribonucleotide Mix (10 mM each) (2 μ l) and Transcriptor Reverse Transcriptase (0.5 μ l), bringing the final volume of the samples to 20 μ l. The samples were carefully mixed by pipetting, and incubated for 60 min at 55 °C. Samples were then incubated at 85 °C for 5 min to inactivate the reverse transcriptase. The reactions were chilled on ice for immediate use or stored at – 20 °C.

2.2.6.5 Semi-quantitative RT-PCR

PCR was carried out on the cDNA samples as described in Section 2.2.2.3 with the *A. fumigatus calmodulin (calm)* gene (AFUA_4G10050) serving as a house-keeping control in RT-PCR experiments (Burns *et al.*, 2005). The primers *calm F* - ccgagtacaaggaagctttctc and *calm R* - gaatcatctctgctgattcgtctctcagt were used for *calm* RT-PCR. These primers span an intronic region in the *calm* coding region, so *calm* amplicons generated from genomic DNA (gDNA) and cDNA will be of different sizes (617 bp and 314 bp respectively). This feature is used to confirm the absence of contaminating gDNA in cDNA preparations. Due to the large size of some of the genes investigated in this study (specifically *pesL* and *pes3*), primers were designed within 1 kb of the poly A+ tail. RT-PCR amplicons were resolved by gel electrophoresis (Section 2.2.2.4) using a 2 % (w/v) agarose gel. Visualisation of PCR products was performed using an AlphaTech DigiDoc still video system (Alpha Technologies). All RT-PCR primers are listed in Table 2.3.

2.2.6.6 Real-Time PCR

Aspergillus fumigatus strains (Table 2.4) were cultured in the desired media for the defined time point. Usually RPMI (Section 2.1.1.10), AMM (Section 2.1.1.7) or Czapek's (Section 2.1.1.11) cultures (200 ml) were incubated for 24, 48 or 72 hr at 37 °C with 200 rpm, and mycelia were harvested aseptically through miracloth. Total RNA was isolated (Section 2.1.6.1), DNase treated (Section 2.1.6.2) and reverse transcribed (Section 2.1.6.4). cDNA was subsequently assayed for endogenous *calmodulin* (*calm*) expression and the gene(s) of interest, using the LightCycler[®] 480 Sybr Green 1 Master Mix (Roche) and also using the LightCycler[®] 480 Real-Time PCR System. PCR reactions were carried out in 96-well plates in a reaction volume of 20 µl containing 5 µl of template DNA. Relative Quantification analysis was performed to investigate differences in gene expression over different growth conditions, time periods, and within different *A. fumigatus* strains, by using the Relative Quantification module on the LightCycler[®] 480 Real-Time PCR System. This module calculates the differences in levels of gene expression between different samples, and this is most accurate when standard curves are prepared for all gene(s) to be assayed, so that PCR quality can be taken into consideration. Also, standard curves were used as a check to confirm optimal PCR conditions. Standard curves were prepared for *calm* and each gene of interest to be assayed by generating 5 orders of 10-fold serial dilutions of cDNA in molecular grade water, and performing between 3 and 5 replicate PCR reactions on these dilutions with specific primer pairs. Cycling conditions for all Real-Time PCR reactions were calculated using the recommendations from Roche and 40 cycles of PCR were performed.

The extension time for PCR amplification was calculated as the number of base pairs expected in the product / 25 = extension time (sec).

The standard curves were calculated automatically using the Absolute Quantification Module on the LightCycler® 480 Real-Time PCR System, and PCR efficiency was given as a value between 0 and 2, with 2 being the highest quality of PCR. Where standard curves had a PCR efficiency of 1.8 or more, with an error value of less than 0.2, the standard curve was saved onto the LightCycler® 480 Real-Time PCR System, and the cycling conditions were used for subsequent Real-time PCR analysis by Relative Quantification. For this, usually a 1/10 dilution of cDNA from each sample was used as a template for PCR and each PCR reaction was set up and performed in triplicate. Relative gene expression levels for all genes in comparison to *calm* were calculated automatically by the $2^{-(\Delta\Delta C(T))}$ method (Livak & Schmittgen, 2001), using the LightCycler® system software, and results were given as a bar chart, and a table containing the relative ratio of *calm* gene expression: target gene expression. Negative controls containing 5 µl of molecular grade water were performed in triplicate on each 96-well plate, and T_m Calling Analysis was performed after each PCR reaction to check that only one PCR product was present in each well following the PCR run. A proportion of PCR reactions were also analysed by Agarose Gel Electrophoresis and PCR products were resolved on a 2 % (w/v) agarose gel.

2.2.7 Comparative metabolite analysis by Reverse Phase High Performance Liquid Chromatography (RP-HPLC)

2.2.7.1 Culture Supernatant Preparation for RP-HPLC analysis

Aspergillus fumigatus was grown in liquid culture (200 ml) for the desired incubation period. Mycelia were harvested, and the culture supernatant (SN) was collected into 50 ml tubes. SN was stored at – 20 °C until required for analysis. Preparation of SN for analysis involved thawing the frozen material at room temperature, and transferring 1

ml of the material to an eppendorf tube. Subsequently, the samples were centrifuged at 13,000 x rpm for 15 min in order to pellet any particulate material that may have been present in the culture SN. The SN was removed and placed into glass vials for immediate analysis by RP- HPLC.

2.2.7.2 Organic Extraction of culture SN for RP-HPLC analysis

Aspergillus fumigatus was grown in liquid culture (200 ml) for the desired incubation period. Mycelia were harvested, and the culture supernatant (SN) was collected into 50 ml tubes. SN (20 ml) was then transferred to a new 50 ml tube and mixed with an equal volume of HPLC grade chloroform (20 ml). The solution was placed on a daisy wheel and was left rotating to mix at 4 °C overnight. Following overnight mixing, the samples were centrifuged at 5,000 x rpm for 5 min to allow the organic and non-organic layer to separate. The organic (lower) layer was removed with a Pasteur pipette and placed into a new 50 ml tube. A 1 ml aliquot of this was placed into an eppendorf tube and centrifuged at 13,000 x rpm for 15 min to pellet any particulate material that was present in the organic extract. The organic material was then transferred into glass vials and was left in a fume hood overnight to allow the chloroform to evaporate. The remaining pellet was dissolved in either 20 µl or 100 µl of HPLC grade methanol for immediate analysis by RP-HPLC.

2.2.7.3 Preparation of *A. fumigatus* Conidial Extracts for Analysis by RP-HPLC

A. fumigatus conidia were harvested from 6 day old AMM plates using 10 ml sterile deionised water and a Pasteur pipette. Subsequently, the spore suspensions were filtered through sterile miracloth to remove any mycelial material. Supernatant was removed but retained at -20° C for later analysis of any polar material. The conidial pellet was

resuspended in 250-500 μ l HPLC Grade Methanol, mixed by vortexing and transferred to new eppendorf tubes. Sonication was performed in a sonicator bath for 5 min. Finally, conidial suspensions were centrifuged at 13,000 x rpm for 10 min and the supernatant was removed for immediate RP-HPLC analysis or was stored at -20°C until required. This method was adapted from an earlier method (Moon *et al.*, 2008).

2.2.7.4 Preparation of *Aspergillus fumigatus* plug extracts from agar plates

Plug extracts from *A. fumigatus* were prepared according to the methods used by Smedsgaard (1997). Plugs ($n = 6$) were removed from agar plates beginning at the centre of the colony and extending outwards, so that all regions of the colony could be sampled. Plugs were taken using a stainless steel hollow cylinder with a 6 mm diameter. Plugs were transferred to a 2 ml eppendorf tube and 1 ml of extraction buffer was added to the tube. These plugs were then organically extracted using 1 ml of an extraction mixture (Section 2.1.8.2). The extraction mixture was either a mix of acetonitrile and H₂O (extraction mixture 1) (Section 2.1.8.2.1), or a mix of ethyl acetate, dichloromethane and methanol (extraction mixture 2) (Section 2.1.8.2.2), so that a range of metabolites, with different polarities, could be analysed respectively. Tubes were sonicated in a sonication bath for 1 hr. After sonication, supernatant was removed from the tubes and transferred to a fresh 2 ml eppendorf tube. A further 1 ml of extraction mixture was added to the remaining plugs and these plugs were sonicated again for a further 1 hr in order to re-extract the samples. Supernatant which was removed from the plugs following sonication was placed in a fume hood overnight in order to evaporate the solvent. Extracted material was then resuspended in 400 μ l and stored at -20 °C for RP-HPLC analysis.

2.2.7.5 RP-HPLC Procedure

Solvent A (Section 2.1.8.1.1) and Solvent B (Section 2.1.8.1.2.) were used for all RP-HPLC. Chromatography, using a C₁₈ column (Agilent Zorbax Eclipse XDB-C18; 5 mm particle size; 4.6 x 15 mm) was carried out using an Agilent Series 1200 HPLC system equipped with a diode array and fluorescence detector. Gradient HPLC conditions (0 -100 % Solvent B over 25 min) were employed for culture supernatants, organically extracted culture supernatants and conidial extract injections followed by absorbance detection (220 and 280 nm). Specimen injection volume was either 20 µl or 100 µl, in all cases, at a solvent flow rate of 1 ml /min. LC-MS analysis of *A. fumigatus* plug extracts was performed by Professor Thomas Larsen at the Danish Technical University.

2.2.8 *A. fumigatus* Plate Assays

A. fumigatus wild-type and mutant strains (Table 2.4) were grown on either AMM agar or MEA agar plates for one week at 37 °C. Conidia were harvested aseptically in PBST (Section 2.1.1.17) and filtered through sterile miracloth. Conidia were serially diluted 100-fold and 10000-fold in PBST and 5 µl of each dilution was used to spot test plates. Plates were incubated at 37 °C unless otherwise stated and growth was monitored periodically by measuring the radial span of fungal colonies. Plate assays were performed independently three times, and radial growths (cm) of colonies were tested for significant differences by means of a two-way Anova. Strains were tested for growth in a variety of conditions and these are summarized in Table 2.2.

2.2.9 *A. fumigatus* growth curves.

Growth curves were performed following a procedure adapted from Reeves *et al.* (2004). Conidia were harvested from 5 day-old MEA plates and used to inoculate AMM

cultures (1×10^7 conidia/100 ml media). Cultures were incubated for 24, 48, 72 or 96 hours at 37 °C with 200 rpm and mycelial biomass was collected through sterile miracloth. Mycelia was washed in sterile water and dried in a freeze dryer to remove excess liquid. Dry weights were recorded and plotted against incubation period. Growth curves were performed in triplicate and a t-test test was used to assess if there was any significant difference between the growth rates of the fungal strains.

2.2.10 *A. fumigatus* germination assay

A. fumigatus conidia of each strain to be assayed were harvested from 5 day old MEA agar plates and 1×10^7 /ml were inoculated into 10 ml of AMM liquid media (Section 2.1.1.7) in a 50 ml conical flask. The cultures were incubated at 37 °C with 200 rpm for at least 3 hr. To quantify the rate of germination, 500 µl of each primary culture was transferred into a 2 ml screw cap tube containing a 0.2 ml scoop of 0.1 mm glass beads (to break up clumps of germinating conidia), and the tubes were vortexed for about 10 sec. Cultures were immediately returned to the incubator once the samples had been taken. Following vortexing of samples, 10 µl of each sample was placed on a haemocytometer and conidia and germlings were counted up to 100 in total. The number of germinated conidia was expressed as a percentage of the total number of conidia counted at each time point. Swollen conidia were not counted as having been germinated. Each sample was counted in duplicate. Once germination had begun (around 3-4 hr from the time of inoculation), samples were removed every hour and germination was recorded. The assay was continued until germination rates became constant for all strains being tested.

2.2.11 Murine Virulence Testing

Murine virulence testing was carried out by a collaborating group at the Imperial College London under the direction of Dr. Elaine Bignell. Outbred male mice (strain CD1, 20 to 28 g; Charles Rivers Breeders) were used for animal experiments. Immunosuppression was carried out by subcutaneous injection of 112 mg/kg hydrocortisone acetate and intraperitoneal injection of 150 mg/kg cyclophosphamide following a sequential protocol as described (Bergmann *et al.*, 2009, and references therein). Bacterial infections were prevented by adding 1 g/liter tetracycline and 64 mg/liter ciprofloxacin to the drinking water. Inocula of 1×10^4 conidiospores in 40 μ l of saline were prepared by harvesting spores from 5-day-old slants of solid medium followed by filtration through Miracloth (Calbiochem) and washing with saline. Mice were anesthetized by inhalation of isoflurane and infected by intranasal instillation. The weights of infected mice were monitored for 5 days twice daily before animals were culled to isolate their lungs. In order to assess fungal burdens as a quantitative virulence criterion, qPCRs were performed on equivalent amounts (100 ng) of genomic DNA that had been extracted from equal amounts (250 mg) of homogenized lung tissue using several references for genomic DNA concentration and the oligonucleotides qPCRf and qPCRr to amplify the 18S rRNA locus from the *A. fumigatus* genome (Bergmann *et al.*, 2009).

2.2.12 *Galleria mellonella* Virulence Testing

G. mellonella virulence testing was carried out according to Reeves *et al.* (2004). Briefly, sixth instar larvae of *G. mellonella* (Lepidoptera: Pyralidae, the Greater Wax Moth) (Mealworm Company, Sheffield, England) were stored in wood shavings in the dark at 15 °C. Only larvae weighing between 0.2 and 0.4 g were used during this study. Conidial suspensions from *A. fumigatus* were prepared in sterile PBS (Section 2.1.1.16). Larvae

were injected ($n = 10$) with a fungal load of 1×10^7 conidia per 20 μ l inoculum. Injections were made with sterile syringes into the last left proleg. Injections of 20 μ l sterile PBS served as a control. Conidial suspensions were isolated from 3 independent cultures and 2 sets of injections were carried out for each replicate. Injected larvae were placed in sterile petri dishes and incubated in the dark at 30 °C in a stationary incubator. Mortality rates were determined over a 72 hr period. Larval death was assessed by the lack of movement of larvae in response to stimulation together with discolouration of the cuticle.

2.2.13 Murine Cell Signalling in Response to *Aspergillus fumigatus*

2.2.13.1 Cultivation and Maintenance of Murine Bone Marrow Derived Macrophages (BMMØS)

Murine BMMØs were cultured in Dulbecco's Modified Eagle Medium (Gibco) supplemented with foetal calf serum (10 % (v/v)), pen-strep (1 % (v/v)) and 0.5 ml gentamicin solution (Sigma-Aldrich). Cells were cultured in a T175 flask at 37 °C static with 5 % CO₂. Murine BMMØs are adherent cells and can be seen to adhere to the base of a tissue flask when healthy. Cells were inspected daily by placing the flask under the lens of a light microscope to ensure that they were adhering to the base of the flask. All culture media and reagents used for cell culture were pre-warmed to 37 °C for at least 40 min in a water bath prior to use. Culture media was changed by aspirating the media from the cells with a sterile pipette, and pipetting fresh media onto the cells. Culture media was usually changed every two days.

2.2.13.2 Subculturing or Passaging of BMMØS

When cells had become at least 80-90 % confluent and were covering the base of the flask, they were subcultured by removing them from the T175 flask and using a

proportion of them to start the next passage. This was carried out every 3-4 days depending on the level of confluency observed upon microscopic inspection. As the cells are adherent, it was necessary to remove them from the culture flask using trypsin. Culture media was aspirated from the cells with a sterile pipette, and Dulbecco's Phosphate Buffered Saline (PBS) (10 ml) was added to the flask by pipetting to wash the cells and remove any serum from the culture media which would inhibit the trypsin. PBS was removed by pipetting after the washing step. Subsequently, Trypsin-EDTA solution (Sigma-Aldrich) (1 x) (approximately 5 ml) was added to the flask by pipetting. This was swirled gently in order to cover the base of the flask, and the flask was replaced into the incubator at 37 °C static for a maximum of 10 min. After 10 min, the flask was removed from the incubator and tapped on a hard surface to dislodge cells that were loosely attached to the flask. At this point, cells were suspended in the Trypsin-EDTA solution. Fresh culture media (10 ml) was added to the cells, and the mixture was pipetted up and down several times to ensure homogeneity. In order to split in a 1:7 ratio at each passage, 10 ml of the cell suspension was removed, and 25 ml of fresh culture media was added to the flask before being returned to the incubator.

2.2.13.3 Fungal stimulation of BMMØS

For stimulation with *Aspergillus fumigatus*, BMMØs were washed in PBS and subsequently removed from flasks by trypsinisation as described (Section 2.2.13.2). Cells were counted twice using a haemocytometer and seeded onto 24-well plates containing Opti-MEM® at a cell density of 1×10^6 cells per well, and were left to adhere to 24-well plates overnight. *A. fumigatus* conidia (5×10^6) or germlings (5×10^6) were added to each well of BMMØs, and cells were stimulated for 18 hr at 37 °C with 5 % CO₂. Supernatants were subsequently collected for cytokine determination by ELISA. In order to achieve germling

formation, *A. fumigatus* strains were germinated for either 6 or 9 hr at 37 °C in AMM media (10 ml) at 1×10^7 conidia/ml. Preparatory experiments indicated that between 90-100 % of conidia had formed dichotomous germ tubes following 9 hours incubation. BMMØs were also exposed to filter sterilized culture supernatant (500 µl) from *A. fumigatus* strains. For experiments where dead conidia or germlings were assayed, killing was achieved by heat-inactivating fungal samples at 100 °C for 30 min in an autoclave. The efficiency of heat-killing was verified by plating serial dilutions of conidia or germlings on Malt extract agar. Aliquots of filter sterilized *Aspergillus* culture supernatant were inoculated onto Malt Extract agar and this confirmed that the supernatant was completely cell-free.

2.2.13.4 Cytokine Determination in Murine Cells by ELISA

Commercially available ELISA kits for TNF- α , IL-6, IL-10 and RANTES (Peprotech UK) were used according to manufacturer's instructions.

2.2.14 Preparation of Chemically Competent *E. coli* cells

LB broth (10 ml) (Section 2.1.1.19) was inoculated with an *E. coli* DH5 α colony and this was incubated overnight at 37 °C with 200 rpm. This culture was used to inoculate 1 L of LB broth and this was incubated for 2 hr at 37 °C with 200 rpm. Following this, the culture was split into 4 fresh tubes and the tubes were left on ice for 10 min. The cells were then subsequently centrifuged at 5,000 x g for 10 min at 4 °C. The supernatant was completely removed by decanting and pipetting. Each pellet was resuspended by pipetting and swirling in 10 ml of cold RF 1 buffer (Section 2.1.9.1). The tubes were then kept on ice for 30 min. The cells were subsequently centrifuged at 5,000 x g for 10 min at 4 °C and once again the supernatant was completely removed. Each pellet was resuspended in 3.2 ml

of cold RF 2 buffer (Section 2.1.9.2) and the tubes were kept on ice for 15 min. The cells were then aliquoted (100 μ l) into sterile, pre-cooled microcentrifuge tubes and stored at -80°C .

2.2.15 Minute Transformation of Chemically Competent *E. coli* cells

Competent *E. coli* cells (Section 2.2.14) were removed from -80°C storage and were thawed on ice for no more than 5 min. The DNA to be transformed (usually 2-5 μ l of a plasmid preparation (Section 2.2.17) or 5-10 μ l of a ligation reaction (section 2.2.2.7)) was added to the cells whilst on ice and mixed by gentle pipetting. The mixture was left on ice for 5 min. Subsequently, transformed cells were spread onto desired selection plates (usually LB agar with ampicillin added (Section 2.1.1.18, Table 2.2)).

2.2.16 Colony PCR

Bacterial and yeast colonies yielded by transformation could be directly screened for presence of the desired plasmid by PCR. Using aseptic techniques, a colony suspension was prepared. To this end, an isolated colony was removed using a sterile tip and resuspended in 10 μ l sterile water in a sterile 0.2 ml microfuge tube. Simultaneously, each colony was also restreaked onto a fresh reference plate. A PCR Mastermix containing all components necessary for PCR was prepared and aliquoted into an appropriate number of 0.2 ml microfuge tubes. The colony suspension (1 μ l) was used as a template for the PCR reactions. Genomic DNA and no template controls were included and PCR was carried out as described in Section 2.2.2.3.

2.2.17 Small Scale Plasmid Purification

Plasmid purification was carried out according to the Qiagen plasmid purification manual using the QIA prep Miniprep kit. All buffers (PI, P2, N3 and PE) and columns were supplied with the kit and details of buffer constituents are outlined in the Qiagen plasmid purification handbook. An isolated *E. coli* colony was picked aseptically and used to inoculate LB broth (5 ml) containing 100 µg/ml of ampicillin in a sterile 50 ml tube. The culture was grown overnight at 37 °C shaking at 200 rpm, and the cells harvested by centrifugation at 2,500 x g for 5 min. The supernatant was removed and the cells were resuspended in ice cold Buffer PI (250 µl). Buffer P2 (250 µl), and Buffer N3 (350 µl) were then added and the tubes inverted 5 times prior to centrifugation at 13,000 x g for 10 min. The supernatant was removed, applied to the Qiaprep spin column and centrifuged at 13,000 x g for 1 min. The flow-through was discarded and the column was washed with Buffer PE (750 µl) and centrifuged at 13,000 x g for 1 min. Once again the flow-through was discarded and the column was centrifuged at 13,000 x g for 1 min to remove residual ethanol. The column was then allowed to stand for 1 min before the DNA was eluted by the addition of 30 µl of sterile water to the centre of the column followed by a final centrifugation at 13,000 x g for 1 min. The purified plasmid was subsequently analysed by DNA gel electrophoresis (Section 2.2.2.4).

2.2.18 DNA Sequencing

DNA sequencing of recombinant clones was performed by Agowa Sequencing using the pre-paid barcode sequencing service.

2.2.19 Cloning of *Afmpt* and *Afagt* into pC210 plasmid for transformation into *S. cerevisiae*

The coding regions of AFUA_5G06350 and AFUA_2G02090 were amplified by PCR using primers AFUA_5G06350 PC210 F and AFUA_5G06350 PC210 R or AFUA_2G02090 PC210 F and AFUA_2G02090 PC210 R respectively (Primers listed in Table 2.3). These primers pairs were designed to incorporate 5' *NdeI* and 3' *SphI* restriction sites onto both *A. fumigatus* genes for subsequent directional cloning into the pC210 vector (Schwimmer & Masison, 2002). The PCR products (2 µg) and pC210 (5 µg) were doubly digested with *NdeI* and *SphI* and further purified from 1% (w/v) agarose gels (Section 2.2.2.5). Purified digested vector and insert (either AFUA_5G06350 or AFUA_2G02090) were quantified and ligations were set up (Section 2.2.2.7). Ligations were incubated overnight at 16 °C in a thermal cycler and the products of these ligations were transformed into *E. coli* DH5α (Section 2.2.15). Several bacterial colonies were subjected to colony PCR analysis (Section 2.2.16), using the same primers that were used for cloning, to check for presence of the insert. Plasmids were isolated from a selection of the colonies and diagnostic restriction digests was performed to check the orientation of the cloned inserts.

2.2.20 Yeast Cell Transformation

Plasmids were transformed into yeast using a Lithium Acetate/DMSO/Polyethylene Glycol Method (PEG). The yeast strain used in this study exhibits leucine auxotrophy. Therefore this strain can only grow either when cultured in a growth medium supplemented with leucine, or when a functioning copy of the *LEU2* gene has been transformed into the cells. This characteristic was the basis of the selection for transformed yeast cells, as there is a *LEU2* gene on transforming plasmids. Approximately 1 µg of plasmid was transformed into competent yeast cells and transformed cells were selected on media lacking leucine.

For transformation, a single colony of the recipient strain was inoculated into 5 ml of YPD broth (2.1.1.22) and incubated overnight at 30 °C shaking at 200 rpm. The overnight culture was counted using a haemocytometer and 50 ml of YPD broth was inoculated using the overnight culture at a cell density of 5×10^6 cells/ml. This culture was allowed to grow at 30 °C shaking at 200 rpm until it reached $1-2 \times 10^7$ cells/ml (usually 3-4 hr). When the cells had reached the required density, they were centrifuged at $2,500 \times g$ for 5 min. The supernatant was removed and the cell pellet was resuspended in 1 ml of 100 mM lithium acetate (Section 2.1.10.3) and this mixture was transferred to a fresh 1.5 ml eppendorf tube. This tube was centrifuged at $13,000 \times g$ for 10 sec to pellet the cells once again. The supernatant was then removed and the cells were resuspended in 500 μ l 100 mM lithium acetate. For each transformation performed, 50 μ l of this cell suspension was transferred to a fresh 1.5 ml eppendorf tube and the tubes were centrifuged at $13,000 \times g$ for 10 sec. Several components for the transformation were then added in the following order: 50 % (w/v) PEG (240 μ l), 1 M lithium acetate (36 μ l), carrier DNA (25 μ l) and 50 μ l of DNA/ sterile water mix (Section 2.1.10). In all cases, 1 μ g of plasmid DNA was used per transformation and this was prepared in a sterile eppendorf and sterile water was added up to a final volume of 50 μ l. The transformation reactions were then mixed by pipetting gently. Transformation reactions were then incubated for at 30 °C for 30 min in a water bath. Following this, the cells were heat-shocked by placing the transformation reactions into a pre-heated water bath at 42 °C for 25 min. Subsequently, the reactions were centrifuged at $7,000 \times g$ for 15 sec. The cell pellets were resuspended in 150 μ l of sterile water and were then spread out onto transformation plates (SC lacking leucine) (Section 2.1.1.24, 2.1.1.25) using a sterile disposable microbiological spreader.

2.2.21 Yeast Dot Growth Assays

Liquid cultures (5 ml) of relevant yeast strains were grown overnight in SC media (Section 2.1.1.26) lacking leucine in order to maintain relevant plasmids. These overnight cultures were used to inoculate fresh cultures the following day at an OD_{600} of 0.15 into 5 ml of fresh SC media. These cultures were subsequently grown for approximately 4 hours until the cell density had reached 3×10^6 cells/ ml. At this time, cells were harvested by centrifugation at 2,500 rpm for 5 min, and the cell pellets were resuspended in fresh SC media at a concentration of 5×10^6 cells/ ml. A 96-well plate was prepared as follows: 80 μ l of YPD (Section 2.1.1.22) was added to each of the wells in columns 2-12, rows A-H. Cells of the relevant strains (100 μ l) were added to the wells in column 1. Using a multi-channel pipette, a 10-fold serial dilution of the cells was created by pipetting 20 μ l from column 1 into column 2, mixing the cells by pipetting, and then pipetting 20 μ l from column 2 into column 3 etc. This was repeated until cells were added into the wells in column 6, so that the 96-well plate then contained 6 orders of dilution. Using a pin replicator, 5 μ l of the diluted culture was spotted onto YPD agar plates (Section 2.1.1.23) supplemented with increasing concentrations of MNNG (Table 2.2). Growth differences were recorded following incubation of the plates for 2–3 days at 30°C.

3.1 Introduction.

3.1.1 The non-ribosomal peptide synthetase gene, *pes3*.

The *pes3* open reading frame represents the largest gene within the *A. fumigatus* genome. *pes3* (CADRE locus identifier: AFUA_5G12730) (Mabey *et al.*, 2004), is found on Chromosome 5 and spans 25,548 bp in length. *pes3* is predicted to encode a protein of 8,515 amino acid residues with a predicted molecular mass of approximately 940 kDa. There are no annotated introns in the *pes3* gene. Blast searching of *pes3* using blastn at NCBI revealed no sequence homologues in any organism for which the full genome sequence is available, making it difficult to predict a peptide produced by Pes3 by comparison with other producing organisms (Cramer *et al.*, 2006b; Stack *et al.*, 2007). *pes3* is annotated to encode a multi-modular NRP synthetase, consisting of one initiation module and five elongation modules. The order of modules in Pes3 is ATCATECATCETCATCATCATEC (Cramer *et al.*, 2006b). Based on this number of modules, Pes3 would be predicted to encode a peptide with 6 amino acids, if each adenylation domain exhibited unique amino acid specificity. However, the non-linear arrangement of domains and modules within Pes3 (the domain arrangement of a typical elongation module is CAT), may suggest repetitive or non-linear use of these modules (Cramer *et al.*, 2006b). This possibility makes it difficult to predict the number of amino acid moieties in the downstream non-ribosomal peptide (NRP).

Pes3 was chosen as an interesting NRP synthetase to study for several reasons. Firstly, it represents the largest gene in *A. fumigatus* (Dr. David Fitzpatrick, NUI Maynooth – personal communication) and its expression is detected under various conditions (Cramer *et al.*, 2006b) indicating that it may be performing an important function in *A. fumigatus*. Interestingly, *pes3* displayed a unique pattern of gene expression in comparison to all other *A. fumigatus* NRP synthetase encoding genes, during a Real-Time PCR analysis, whereby *pes3* transcripts were most abundant in

ungerminated spores, in contrast to all other NRP synthetases examined (Cramer *et al.*, 2006b). Secondly, availability of the complete genome sequence of this important human pathogen (Nierman *et al.*, 2005) poses a functional genomics challenge in elucidating the role of genes for which no literature currently exists. Furthermore, the overall deficit of information relating NRP synthetase genes to peptides and their function in filamentous fungi, including *A. fumigatus*, makes NRP synthetase genes worthy of further investigation. *pes3* was the subject of a previous PhD project (Dr. Deirdre Stack), who disrupted *pes3* in the genome of *A. fumigatus* before the commencement of this work.

As mentioned previously, genes controlling secondary metabolite production are generally organised into clusters in the genome, many of which are specific to certain species (Keller & Hohn, 1997; Nierman *et al.*, 2005). LaeA has been identified as the master transcriptional regulator of SM biosynthetic clusters in *A. fumigatus* (Bok & Keller, 2004). Interestingly, *pes3* was not found to be under the transcriptional control of LaeA, suggesting that it might not be involved in SM production. The high level of expression in ungerminated spores (Cramer *et al.*, 2006b) hints that *pes3* may be involved in germination or cell wall structure in *A. fumigatus*. For this reason, cell wall structure will be discussed in detail in this chapter. Furthermore, mechanisms for innate immune recognition of, and the immune response to, *A. fumigatus* will be discussed, since this is largely dependant on cell wall structure. Lastly, virulence models currently in use for the investigation of *A. fumigatus* virulence will be described in detail.

3.1.2 Structure of the *Aspergillus fumigatus* cell wall.

The fungal cell wall is an important protective structure for the fungus, acting as a barrier in contact with harsh environments (Latge, 2007). Fungi will die if the cell wall is weakened or removed, unless they are osmotically stabilised (Latge, 2007). The

cell wall also bears an aggressive function, as it is a reservoir of toxic and hydrolytic molecules, which are used by the fungus to invade ecological niches (Latge, 2007). Despite the essential role of the fungal cell wall, the biosynthesis and accurate structure of the cell wall of most fungal species is not fully understood, and this is particularly obvious amongst filamentous fungi (Latge & Calderone, 2002; Lesage & Bussey, 2006). The cell wall can be organised into two distinct layers; an inner and an outer layer, whose composition varies between fungal species and growth stage of the fungus. A schematic representation of the *A. fumigatus* cell wall is shown in Figure 3.1 (Latge, 2010). Fibrillar polysaccharides are close to the plasma membrane, while amorphous polysaccharides are located throughout the cell wall but mostly facing outwards (Latge, 2010). This distinction between the two layers is purely theoretical since it is impossible to analyse the cell wall without prior enzymatic or chemical treatment, thereby altering the arrangement of the layers (Latge, 2010).

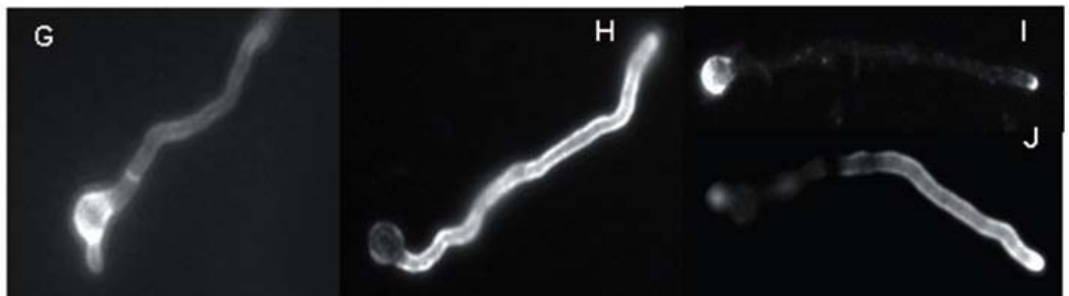
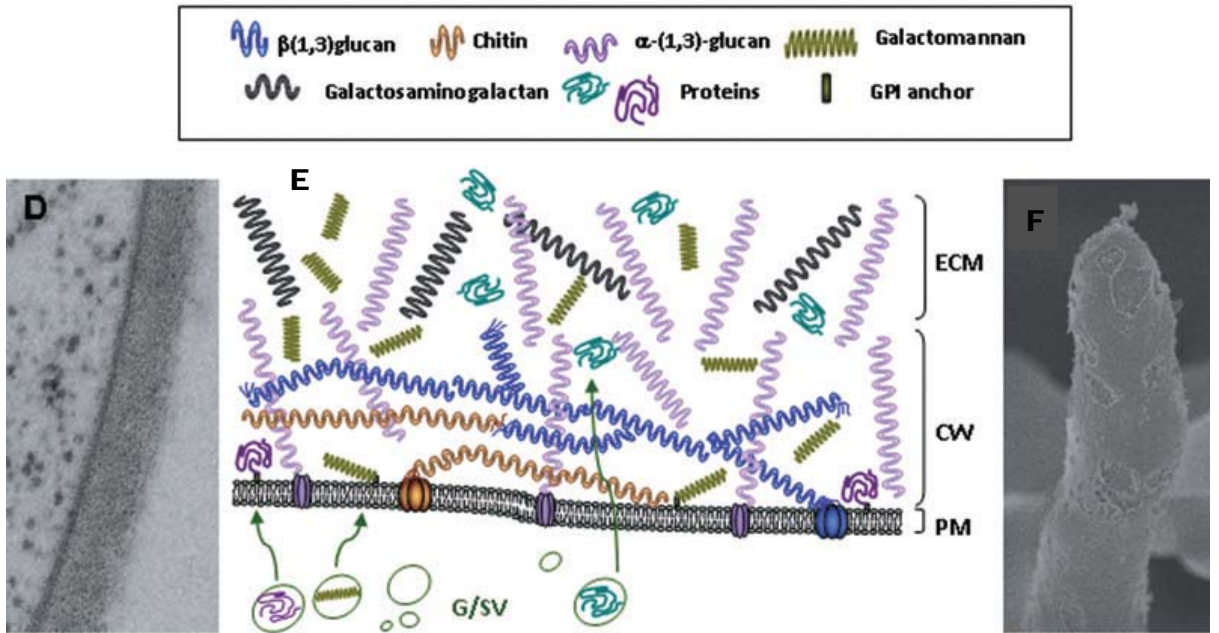
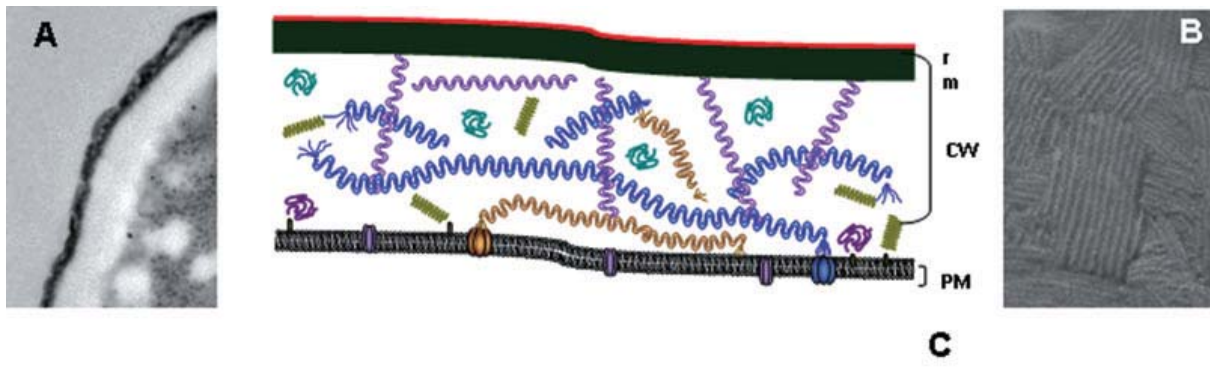


Figure 3.1. The structure of the *A. fumigatus* cell wall.

A. Transmission electron microscopy (TEM) showing a section of a conidial cell wall (CW) and also the melanin (m) dense outer layer.

B. Scanning electron microscopy (SEM) showing the rodlets (r) on the conidial surface.

C. Diagrammatic representation showing the theoretical organisation of the polymers in the conidial cell wall. Here, the amorphous α -1,3-glucan glues the melanin to the conidial surface. PM: plasma membrane.

D. TEM showing the mycelial cell wall grown in liquid culture.

E. Diagrammatic representation of the theoretical structure of the mycelial cell wall. Soluble or GPI-anchored proteins and some polysaccharides such as mannans are produced intracellularly and transported to the cell wall space by the Golgi/secretory vesicle (G/SV) system. β -1,3-glucans and chitin are produced as linear chains by polysaccharide synthases. Individual chains are then joined non-covalently into stable triple helixes.

F. SEM showing the extracellular matrix (ECM) covering the hyphae growing on agar (and absent on hyphae grown in liquid culture).

G. Localisation of chitin around the cell wall of a germinating conidium and at the septum using a fluorescent label.

H. Surface labelling of the mycelial cell wall using a fluorescently-labelled antibody.

I. β -1,3-glucan localised with a β -1,3-glucan specific monoclonal antibody around the germinating conidia and at the germ tube apex.

J. Labelling of the entire mycelial surface with an anti-galactofuran monoclonal antibody.

All images taken from Latge, (2010).

More than 90 % of the cell wall is composed of polysaccharide, and the outer layer of the cell wall is an insoluble structure requiring solubilisation, usually by means of hot alkali treatment before it can be properly analysed (Latge, 2007). For most fungal species, the central core of the cell wall is composed of a branched β -1,3, 1,6, glucan linked to chitin via a β -1,4 linkage (Latge, 2007). In *A. fumigatus* and *S. cerevisiae*, interchain β 1,6 glucosidic linkages make up 3 % and 4 % of the total glucan linkages, respectively (Fontaine *et al.*, 2000a; Kollar *et al.*, 1995; Nguyen *et al.*, 1998; Perez & Ribas, 2004). This structural core varies between fungal species, and is thought to be fibrillar and embedded in an unstructured cement, which is alkali-soluble (Latge, 2007). The glucan-chitin complex is bound covalently to other polysaccharides, and this is variable between pathogens. In *A. fumigatus*, the polysaccharides are composed of galactomannan and β -1,3-1,4-glucan, which is absent in the human pathogenic yeast *Candida albicans* which contains mainly β -1,6-glucan, that is absent in *A. fumigatus* (Aimanianda *et al.*, 2009; Fontaine *et al.*, 2000b). In *A. fumigatus*, the alkali-soluble fraction is comprised of α -1,3-glucan with 1 % interconnecting α -1,4-linkages (Latge, 2010). β (1-3) glucans are synthesised by a plasma membrane bound glucan synthase complex, and using UDP-glucose as a substrate, linear chains are extruded through the membrane (Beauvais *et al.*, 1993). Fungal β -glucan exhibits important immunostimulatory properties, mediated by the innate immune receptor Dectin-1 (Brown, 2006; Taylor *et al.*, 2007). Dectin-1 will be discussed later in this chapter.

N-mannans and O-mannans are also found in the cell wall of *A. fumigatus*, and these often terminate in a galactofuranose residue at the non-reducing end (Leitao *et al.*, 2003; Morelle *et al.*, 2005), and these mannans are covalently bound to the glucan fibrillar core (Latge, 2010). The polysaccharide skeleton of the cell wall is coated with cell wall proteins (CWPs). The glycosylphosphatidylinositol (GPI)-modified proteins represent the major class of CWPs (de Groot *et al.*, 2003; Eisenhaber *et al.*, 2004). GPI-

modified proteins possess an N-terminal hydrophobic signal peptide sequence targeting them to the endoplasmic reticulum. A C-terminal hydrophobic domain is present that is cleaved in the endoplasmic reticulum and replaced with a GPI-anchor. The GPI moiety may then be processed and attached to 1,6- β -glucan in the cell wall (Romano *et al.*, 2006). The *S. cerevisiae* ECM33 protein has the typical features of a GPI-anchored protein, and its deletion resulted in a weakened and disorganised cell wall, defective glycosylation and activation of the cell wall integrity pathway (Pardo *et al.*, 2004). The cell wall integrity (CWI) pathway is activated in response to cell wall stress, and uses a mitogen-activated protein kinase (MAPK) cascade, to ensure maintenance of the cell wall by mediating cell wall biosynthesis, actin organization, and other events necessary to maintain CWI (Levin, 2005). The *C. albicans* ECM33 protein is required for normal cell architecture and expression of cell-surface proteins, and ECM33 mutants were reduced in the ability to invade epithelial cells, and were less virulent in a murine model of candidosis (Martinez-Lopez *et al.*, 2004; Martinez-Lopez *et al.*, 2006). These findings prompted a study which found that the *A. fumigatus* ECM33 (*AfuECM33*) homologue is involved in conidial adherence and morphogenesis (Romano *et al.*, 2006). Interestingly, an *AfuECM33* mutant exhibited rapid germination, increased cell-cell adhesion, increased resistance towards the anti-fungal caspofungin and increased virulence in a mouse model for IA (Romano *et al.*, 2006). The authors suggest that the cell wall alteration in the *AfuECM33* mutant leads to greater exposure of cell-surface proteins involved in adherence, leading to increased cell-cell adhesion, and that a softer, more pliable cell wall allows for faster germination. Reduced synthesis of (1,3)- β -glucan in the *AfuECM33* mutant may explain the increased sensitivity to caspofungin, since caspofungin inhibits the (1,3)- β -glucan synthase (Romano *et al.*, 2006).

An important feature of the fungal cell wall is that it is a highly dynamic structure that is constantly changing during the cell cycle and in response to the

environment. The majority of structural changes that occur in the cell wall are associated with the outer layer (Latge, 2010). *A. fumigatus* conidia are covered by hydrophobins and melanin, while germinating conidia expose α -1,3-glucans, galactomannan, galactosaminogalactan and N-glycosylated proteins including galactomannoproteins on their surface (Latge, 2010). In fact, the exposure of such galactomannan and associated galactomannoproteins on germinating conidia is the basis of the commercial Platelia enzyme immunoassay (EIA), which has been used widespread for the diagnosis of IA, and detection of β (1-3) glucans is also used as a diagnostic strategy for IA (Thornton, 2010).

Dormant *A. fumigatus* conidia are covered by a hydrophobic rodlet layer comprised of a thin layer of specifically arranged RodA hydrophobins (Thau *et al.*, 1994). The rodlet layer favours the buoyancy and air dispersal of conidia (Beever & Dempsey, 1978). The hydrophobin proteins are characterised by a conserved spacing of eight cysteine residues (Wessels, 1997; Wosten & de Vocht, 2000). The conidia of *A. fumigatus* contain two hydrophobins, RodA and RodB. The RodB protein, although homologous to RodA, is not essential for rodlet formation (Paris *et al.*, 2003a). Using rodlet mutants, it was shown that RodA protects *A. fumigatus* conidia against killing by alveolar macrophages (Paris *et al.*, 2003a). RodA is covalently bound to the cell wall polysaccharides, indicated by the presence of a GPI-anchoring sequence in the *rodA* gene (AFUA_5G09580) (Latge, 2007). The rodlet layer maintains *A. fumigatus* conidia immunologically silent, and is the likely reason why inhaled spores do not usually initiate inflammatory responses in immunocompetent individuals (Aimanianda *et al.*, 2009). Removal of the RodA protein chemically, by gene deletion, or through germination, resulted in conidia which induced greater immune responses compared to the wild-type (Aimanianda *et al.*, 2009). RodA has recently been shown to prevent *A. fumigatus* conidia from triggering nuclear extracellular trap (NET) formation in human

and murine neutrophils, thereby presenting a novel mechanism by which *A. fumigatus* conidia escape neutrophil attack (Bruns *et al.*, 2010). NETs will be discussed in more detail in the subsequent section.

Melanin is a blue-green pigment synthesised by the dihydroxynaphthalene (DHN)-melanin pathway, directed by a cluster of 6 genes in *A. fumigatus*, which are expressed during conidiation (Tsai *et al.*, 1999). Melanin has been shown *in vitro* to protect *A. fumigatus* conidia against phagocytosis and the effects of reactive oxygen species (ROS) produced by phagocytes (Jahn *et al.*, 2002; Tsai *et al.*, 1998), and it is a documented virulence factor for *A. fumigatus* (Latge, 1999). The polyketide synthetase PKSP, encoded by the *pksp* gene in *A. fumigatus* (also called *alb1*) mediates one of the first steps of the DHN-melanin pathway. *pksp* mutants did not produce melanin and were found to be less virulent than wild-type strains in murine models of IA (Jahn *et al.*, 1997; Tsai *et al.*, 1998). Recently, it has been shown that melanin also plays a structural role in the conidial cell wall, is essential for correct assembly of the fungal cell wall layers, and the expression of the hydrophobic rodlet layer at the outer cell wall (Pihet *et al.*, 2009).

Importantly, the fungal cell wall is an essential and major target for anti-fungal drug discovery and development for several reasons: it accounts for one quarter of the fungal cell; it is a physically rigid structure protecting the fungus from the environment; it is essential for fungal life; it is composed of unique molecules which do not have equivalents in humans (e.g. β -glucans and chitin) (Beauvais & Latge, 2001). Given the huge potential for cell wall anti-fungal drug targets and the importance of the cell wall in innate immune recognition of *A. fumigatus*, a greater understanding of the cell wall, its composition, biosynthesis and regulation is necessary.

3.1.3 The innate immune response towards *Aspergillus fumigatus*.

The innate immune response to *A. fumigatus* may be discussed under 4 different headings: the cells of the innate immune system, the antimicrobial activity of respiratory cells, pattern recognition systems and chemical immune effectors such as cytokines and chemokines (Balloy & Chignard, 2009).

3.1.3.1 The cells of the innate immune system.

The innate immune system comprises three main cell types involved in defence against pathogens; alveolar macrophages, epithelial cells, and polymorphonuclear neutrophils (PMNs). Alveolar macrophages are the most prominent phagocytic cells in the lung alveoli, and are important in controlling the early steps of innate immunity towards *Aspergillus* infections (Romani, 2004). Macrophages engulf *A. fumigatus* conidia by phagocytosis, and conidia are killed within the cells, with 90 % of spores being killed after 30 hr (Schaffner *et al.*, 1983). Alveolar macrophages are able to engulf dormant or swollen conidia; however, they can only kill swollen spores (Philippe *et al.*, 2003). Furthermore, recognition, phagocytosis, and killing of *A. fumigatus* conidia by alveolar macrophages not only plays an important role in fungal clearance, but also in triggering a pro-inflammatory immune response leading to local influx of neutrophils and their migration to the site of infection (Brakhage *et al.*, 2010). Pathogen recognition by macrophages is mediated by specialised membrane bound pathogen recognition receptors (PRRs) such as the C-type lectin receptor Dectin-1 (Reid *et al.*, 2009) and the Toll-like receptors (Akira & Takeda, 2004). Such PRRs will be discussed in more detail in subsequent sections. Once *A. fumigatus* conidia are phagocytosed by alveolar macrophages, they are processed in the phagolysosome and eventually killed (Brakhage *et al.*, 2010). It has not been fully elucidated how the macrophages kill the conidia but reactive oxygen species (ROS) are important in this process, as NADPH

oxidase mutants are unable to kill *A. fumigatus* conidia (Philippe *et al.*, 2003). However, since *A. fumigatus* mutants deficient in major oxidative stress defence regulators (AfYap1, and AfSkn7) are not attenuated in virulence in various immunosuppressed mouse models of IA (Lamarre *et al.*, 2007; Lessing *et al.*, 2007), it is unlikely that the production of ROS is crucial for the direct killing of *A. fumigatus*, but that it may be more relevant in signalling to other immune effector cells (Lessing *et al.*, 2007). This hypothesis is supported by earlier experiments that found the granular proteins in neutrophils to be responsible for the killing of microbes while the ROS were important for the activation of vacuolar enzymes (Reeves *et al.*, 2002; Segal, 2005). Segal, (2005) proposed that the mechanism by which NADPH oxidase contributes to *A. fumigatus* killing might be indirect, and due to depolarisation of the phagocytic vacuole leads to an influx of ions, resulting in the activation of degradative enzymes, such as elastase and cathepsin G.

Epithelial cells are located on the upper airways of the trachea and bronchus, and include cell types that are either ciliated or produce and secrete mucus. Inhaled spores become trapped in the mucus and are transported by ciliary beating to the oropharyngeal region, where they are either swallowed or ejected, and this is aided by mechanical defences such as coughing and sneezing (Balloy & Chignard, 2009). There are two types of epithelial cell present in alveoli, the type I and type II pneumocytes. These cell types are important in secreting pulmonary surfactant, which has been implicated in defence against microorganisms, due to the antimicrobial properties of two of its constituent proteins: surfactant proteins A and D (SP-A, SP-D) (Balloy & Chignard, 2009). SP-A and SP-D are actually pattern recognition molecules of innate immunity themselves, and are composed of an N-terminal helical domain, and a ligand recognition domain called a C-type lectin or carbohydrate recognition domain (CRD) (Madan *et al.*, 2010). These CRDs recognise patterns on the surface of pathogens such as viruses,

bacteria and fungi, and cause both direct inhibition of microbial growth, as well as enhanced phagocytosis by neutrophils and macrophages (Kuroki *et al.*, 2007). SP-A and SP-D can interact with phagocytes upon microbial challenge, increasing their chemotactic, phagocytic, antigen presentation and oxidative properties (Kishore *et al.*, 2002). SP-A and SP-D have been shown to be important in binding and clumping of *A. fumigatus* conidia leading to increased phagocytosis of germinating conidia by macrophages and neutrophils (Allen *et al.*, 2001; Madan *et al.*, 1997). In fact, surfactant proteins act as opsonins, inducing phagocytic cells and modulating inflammatory cytokine release (Wright, 2005). Indeed, mice with SP-D gene deletions showed increased susceptibility to *A. fumigatus* conidia challenge in a corticosteroid model of immunosuppression (Madan *et al.*, 2010). Many interactions have been described for pathogens and phagocytic cells, and many intracellular pathogens have been documented, such as *Mycobacteria tuberculosis* and *Chlamydia pneumoniae*, whereby the pathogens multiply inside the epithelial cell (Balloy & Chignard, 2009). To date, *A. fumigatus* has not been described as an intracellular pathogen, although the conidia of this fungus can survive in acid organelles following engulfment by respiratory epithelial cells (Botterel *et al.*, 2008; Paris *et al.*, 1997; Wasylnka & Moore, 2002; Wasylnka & Moore, 2003). In some cases, *A. fumigatus* conidia have been found to germinate inside these acid organelles without causing tissue damage (Wasylnka & Moore, 2003), a fact that suggests that *A. fumigatus* evades the action of phagocytes through residence in these epithelial organelles, and may represent a starting point for systemic spread of infection (Balloy & Chignard, 2009).

PMNs represent the most abundant population of intravascular phagocytic cells and are essential for defence against infections. At least 40 % of all human neutrophils are found in the vascular network of the lung, and these neutrophils are recruited to the alveolar spaces during infection so that they can boost immune defences (Balloy &

Chignard, 2009). During infection, PMNs may make up 90 % of the total phagocytic cells in the alveoli. Recently, it was shown that neutrophils are essential at early time-points following *A. fumigatus* infection, with mice developing IA following neutrophil depletion either before or within 3 hr of infection (Mircescu *et al.*, 2009). In contrast, alveolar-macrophage depleted animals were able to limit hyphal tissue invasion, possibly due to the presence of functioning neutrophils (Mircescu *et al.*, 2009). Neutrophils are capable of phagocytosing *A. fumigatus* conidia in the alveoli, and have been shown to be fungicidal against conidia *in vitro* (Chignard *et al.*, 2007; Levitz & Diamond, 1985). *A. fumigatus* has been found to produce metabolites which interfere with neutrophil function, including the toxic molecule fumagillin (Fallon *et al.*, 2010) and gliotoxin (Tsunawaki *et al.*, 2004). Many of the cell-mediated killing strategies discussed here refer to the phagocytic killing of *A. fumigatus* conidia by macrophages and neutrophils, as *A. fumigatus* hyphae are too large to be taken up by phagocytes. Hyphae are targeted by polymorphonuclear leucocytes (PMNLs) (Levitz, 2004; Rex *et al.*, 1990). PMNLs form aggregates around the hyphae and kill them by the granular release of ROS and antimicrobial peptides (Levitz *et al.*, 1986; Levitz & Farrell, 1990).

Despite the obvious importance of neutrophils in the defence against *A. fumigatus*, it is likely that ROS-mediated mechanisms of killing may not be the most crucial, or the only killing strategy used by neutrophils (Lessing *et al.*, 2007). In line with the need to elucidate mechanisms of neutrophil-killing independent of ROS-mediated destruction, neutrophils have recently attracted much attention following the identification of neutrophil extracellular traps (NETs). NETs were observed during neutrophil death as a final defence mechanism against bacteria (Brinkmann *et al.*, 2004). Dying PMNLs have been shown to eject nuclear DNA in response to *A. fumigatus*, forming NETs, described as a dynamic web-like structure embedded with fungicidal proteins which inhibit hyphal growth (Bruns *et al.*, 2010; McCormick *et al.*,

2010). NET formation has been observed in human neutrophils upon exposure to *A. fumigatus* and other *Aspergilli* both *in vivo* and *in vitro* (Bianchi *et al.*, 2009; Bruns *et al.*, 2010; McCormick *et al.*, 2010), and has been found to reduce hyphal activity in the respiratory tract after nine hours of co-incubation (Bruns *et al.*, 2010). Following NETosis, the final NET release from a neutrophil occurs within three hours of DNA release (Bruns *et al.*, 2010). NET formation was observed upon exposure to live and UV-killed *A. fumigatus* conidia and hyphae, and was associated with the presence of elastase, known to be characteristic of NETs (McCormick *et al.*, 2010). NETs trap *A. fumigatus* conidia (Bruns *et al.*, 2010; Jaillon *et al.*, 2007; McCormick *et al.*, 2010) and hyphae (Bruns *et al.*, 2010), and appear to be fungistatic rather than fungicidal (Bruns *et al.*, 2010; McCormick *et al.*, 2010). It is suggested that they may help recruit more neutrophils or other immune cells to the infected site (Brakhage *et al.*, 2010), as well as reducing fungal dissemination (Bruns *et al.*, 2010; McCormick *et al.*, 2010). NETs are formed following the induction of a ROS signalling cascade in neutrophils which results in breakdown of the nuclear envelope and granular membranes (Fuchs *et al.*, 2007). Once the nuclear membrane is ruptured, the NETs are formed by a mixture of nuclear DNA with granular contents and are then explosively released, in a process associated with cell death, known as NETosis (Brinkmann & Zychlinsky, 2007). These findings highlight the importance of neutrophils in the defence against *A. fumigatus*, and the NET phenomenon will be discussed in more detail later in this chapter.

3.1.3.2 The antimicrobial activity of respiratory cells.

The airway epithelial cells exert antimicrobial activity by producing a range of antimicrobial compounds, which either kill pathogens directly, or act to enhance phagocytosis-mediated elimination of pathogens. The primary role of macrophages and neutrophils in the immune response is the phagocytosis and subsequent killing of

pathogens. Oxygen-dependant oxidative mechanisms are important in this process, involving the generation of ROS and reactive nitrogen species (RNS) derived from nitric oxide (NO). The generation of ROS during phagocytosis involves the NADPH oxidase complex, which produces hypochloric acid (HOCl) (Kohchi *et al.*, 2009). Another enzyme, myeloperoxidase (MPO) produces superoxide anions. Both of these enzymes are critical for elimination of *A. fumigatus*. *In vitro* studies using murine macrophages lacking NADPH oxidase have shown that the production of ROS is an important part of the fungicidal activity of macrophages (Philippe *et al.*, 2003). However, in the same study using murine macrophages lacking NO synthase, it was shown that the fungicidal activity of macrophages is independent of the production of NO and its derivatives. This shows that the importance of different oxidative mechanisms in the defence against *A. fumigatus* needs further investigation. A study using mice NADPH oxidase mutants showed that mice lacking NADPH oxidase were more susceptible to *A. fumigatus* infection (Aratani *et al.*, 2002). The importance of the NADPH complex in defence against *A. fumigatus* explains why patients of chronic granulomatous disease (CGD), who are deficient in macrophage and neutrophil NADPH oxidase, are highly susceptible to IA (Almyroudis *et al.*, 2005).

Antimicrobial molecules are another strategy used by respiratory cells in the defence against *A. fumigatus*. Lactoferrin is produced by the neutrophils and macrophages, and binds to iron, depriving the fungus of iron, which is essential for its survival (Zarembler *et al.*, 2007). Lactoferrin is abundant in respiratory secretions (Travis *et al.*, 1999). Recently, it was found that PMNLs play a role in the defence against inhaled *A. fumigatus* conidia (Bonnett *et al.*, 2006) and that they aggregate around conidia in the airways and prevent germination by releasing lactoferrin from primary granules (Bonnett *et al.*, 2006; Zarembler *et al.*, 2007). Platelets have also recently been found to damage *A. fumigatus* conidia and germinating hyphae by

adhering to the fungus and releasing serotonin from granules (Perkhofer *et al.*, 2008a). Serotonin was previously found to exert anti-fungal effects against *Aspergillus* species *in vitro* (Perkhofer *et al.*, 2008b). Elastase and cathepsin G, two serine proteases which are present in neutrophil granules appear to be important in defence against *A. fumigatus*, as mice deficient in either of these enzymes were found to be more susceptible to *A. fumigatus* infection (Tkalcevic *et al.*, 2000). Chitinases, which are capable of degrading chitin in the fungal cell wall, are produced by epithelial cells and macrophages (Chen *et al.*, 2009).

3.1.3.3 Pattern recognition systems.

The ability of our immune system to immediately recognise and respond to microbes is dependant upon germ-line encoded pattern recognition receptors (PRRs) which recognise microbial components and initiate an immune response (Janeway, 1992). Each PRR is specific in nature, enabling it to recognise invariant molecular components of pathogens, known as pathogen associated molecular patterns (PAMPs), and this leads to an appropriate immune response that is tailored to specifically defend against the particular pathogen (Janeway, 1998; Medzhitov & Janeway, 2000). Specific PAMPs tend to be found in groups of related organisms. For example, lipopolysaccharide (LPS) is a PAMP found in Gram-negative bacteria, and β -glucans are an important fungal PAMP, allowing a limited range of PRRs to recognise a wide range of organisms (Tsoni & Brown, 2008). PRRs are also known to identify endogenous components released during tissue injury, and it has been hypothesised that rather than discriminating between self and non-self here, PRRs identify ‘danger’ signals and activate the immune system accordingly (Matzinger, 1994). Several families of PRRs exist, both inside and outside of the cell, but the main PRRs which will be discussed here are those involved in the recognition of extracellular pathogens, in particular the Toll-Like receptors (TLR) and the C-type lectin (CLR) receptors. Recognition of pathogens through these receptors results in ingestion and phagocytosis of microbes in an actin-dependant manner. Several destructive mechanisms, including the respiratory burst (Kohchi *et al.*, 2009), result in microbial killing.

TLRs are a family of innate immune receptors that are highly evolutionary conserved right across the plant and animal kingdom (Vega & Martin, 2008). TLRs derive their name from the Toll protein in *Drosophila*, with which they share a high level of sequence similarity. Toll was originally described as a protein involved in *Drosophila* embryonic development (Anderson *et al.*, 1985a; Anderson *et al.*, 1985b).

However, there are remarkable similarities between the Toll signalling pathway and the mammalian IL-1 pathway which leads to the activation of NF- κ B, a transcription factor that plays an important role in inflammation and immune response (Takeda *et al.*, 2003). In fact, the intracellular domains of Toll and IL-1 are highly conserved at the sequence level and are known as the Toll/IL-1 receptor (TIR) domain (Takeda *et al.*, 2003). These similarities prompted a series of experiments which showed that Toll protein was involved in protecting *Drosophila* against fungal and Gram-positive bacterial infections (Lemaitre *et al.*, 1996; Lemaitre *et al.*, 1997).

Shortly after Toll protein was found to be important for host defence, a mammalian homologue of Toll was discovered (Medzhitov *et al.*, 1997). Since then, a family of Toll homologues have been identified in mammals, and these are known as the Toll-like receptors. Currently, 10 functional TLRs are known, TLR 1-10, and it is likely that many more have yet to be discovered (Chuang & Ulevitch, 2000; Chuang & Ulevitch, 2001; Du *et al.*, 2000; Medzhitov *et al.*, 1997; Rock *et al.*, 1998; Takeuchi *et al.*, 1999). Members of the TLR family share a common structure, and are composed of an intracellular and an extracellular domain. Examination of human TLRs reveals that they can be placed into 5 subfamilies based on sequence similarity and genomic structure of the TLR encoding genes.

TLRs are integral membrane glycoproteins, characterised by a leucine-rich repeat (LRR) in the extracellular domains, involved in ligand recognition, and an intracellular TIR domain which is important for signal transduction following ligand binding. The actual structural basis of ligand binding to mammalian TLRs is poorly understood, and there is a deficit in experimental proof for an interaction between TLR ligands and LRR domains (Vega & Martin, 2008). However, a signalling cascade for TLRs, ultimately leading to the activation of NF- κ B and other transcription factors such as interferon (IFN) regulatory factor (IRF)-1/3/5/7, and/or activator protein-1 (AP-1)

has been well characterised (Brikos & O'Neill, 2008). Activation of these transcription factors induces the expression of genes encoding cytokines, chemokines, type 1 interferons, co-stimulatory molecules and other effectors of the immune response tailored to the particular pathogen. Upon recognition of PAMPS on microbial surfaces, TLRs form dimers and/or associate with other receptors to induce an interaction between the TIR-intracellular domain of the TLR and the TIR-domain of intracellular adaptor molecules (O'Neill & Bowie, 2007). Except for TLR3, ligand-TLR interactions trigger the binding of at least one adaptor molecule to the intracellular domain of the TLR (Chignard *et al.*, 2007). This leads to the signal cascade that eventually results in the activation of transcription factors as mentioned above. A general overview of mammalian TLR signalling using the MyD88 adaptor is presented schematically in Figure 3.2 (adapted from Chignard *et al.*, 2007; Vega & Martin, 2008). The LRR domain recognises the ligand (PAMP). The cytoplasmic or intracellular domain of the TLR (TIR) associates with MyD88, recruiting members of the IRAK family of protein kinases and a signal cascade occurs which eventually leads to the activation of the transcription factor NF κ B. In unstimulated cells, NF κ B is retained in the cytoplasm by interaction with one of seven inhibitory factor kappa B (I κ Bs) proteins. In response to a wide variety of stimuli, I κ B is phosphorylated by members of the I κ B-kinase family (IKK). Phosphorylation targets I κ B for ubiquitination and degradation. NF κ B is then free, and it subsequently translocates to the nucleus, activating the transcription of inflammatory genes encoding cytokines (such as IL-1 and TNF- α), chemokines and other inflammatory mediators and immune effectors as previously mentioned.

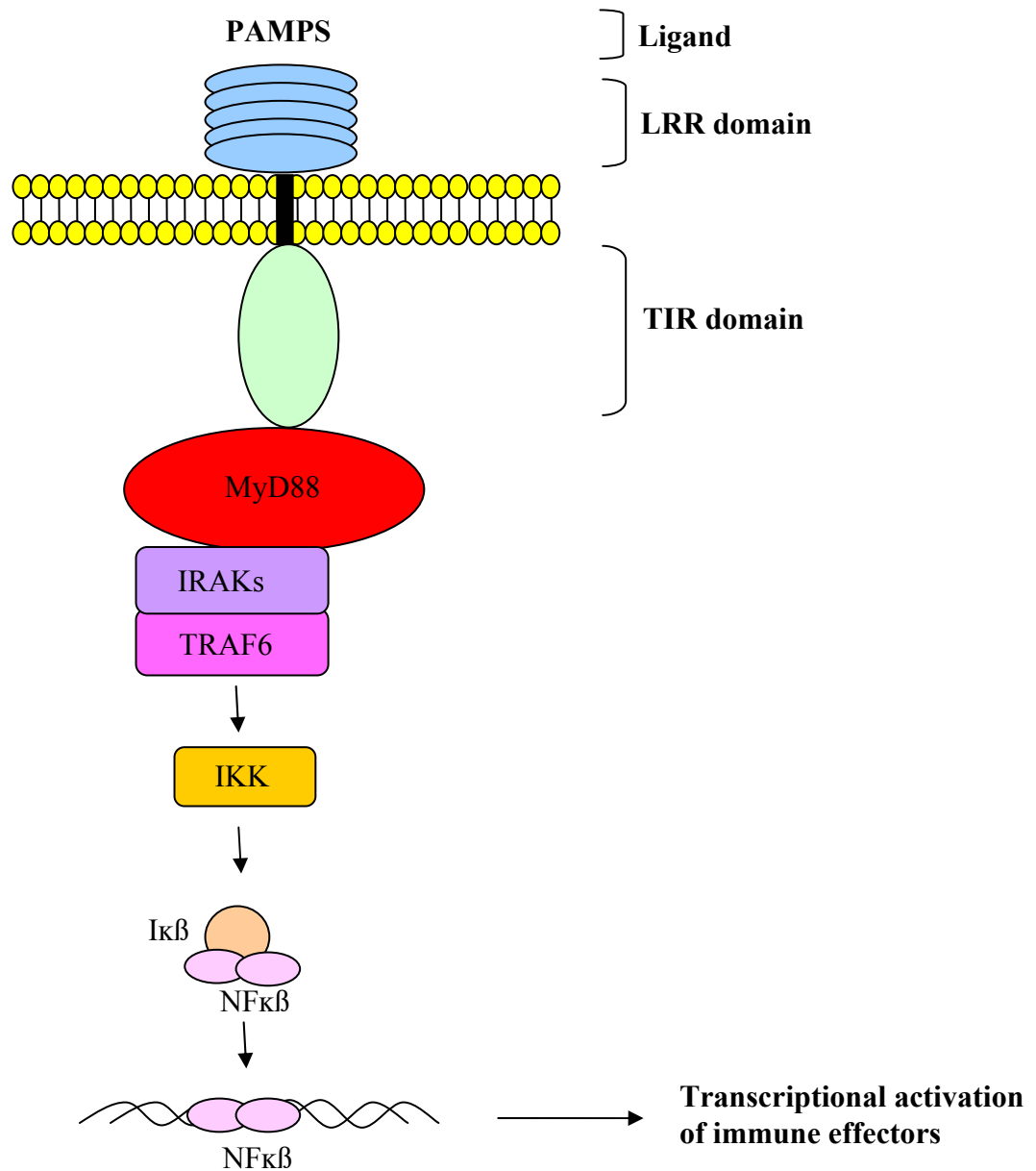


Figure 3.2. The mammalian Toll-like receptor (TLR) signalling pathway.

Mammalian TLRs possess an extracellular domain, which contains a leucine rich region (LRR). This LRR functions in ligand binding. TLR ligands are usually specific microbial patterns (PAMPs). The cytoplasmic or intracellular domain of TLRs (TIR) associates with MyD88, recruiting members of the IRAK family of protein kinases, and this eventually leads to the degradation of IκB, releasing the transcription factor NFκB. Release of NFκB causes it to become activated, where it translocates to the nucleus, activating the transcription of inflammatory genes encoding cytokines, chemokines and other inflammatory mediators and immune effectors.

The role of TLRs in the recognition of *A. fumigatus* was first reported when TLR2, but not TLR4 was proposed to be a receptor for *A. fumigatus* hyphae (Wang *et al.*, 2001). TLR2 and TLR4 have since been found to be essential for *Aspergillus*-induced activation of murine macrophages *in vivo* and *in vitro* (Meier *et al.*, 2003). Initially, HEK293 cells expressing each of the human TLRs were challenged with *A. fumigatus* conidia or hyphae, and only cells specifically expressing TLR2 or TLR4 exhibited NF κ B activation (Meier *et al.*, 2003). Immunofluorescence detection of NF κ B nuclear translocation in murine macrophages following *A. fumigatus* exposure is dependant on functional TLR4 and to a lesser extent TLR2 (Meier *et al.*, 2003). Cytokine measurement from murine macrophages stimulated with *A. fumigatus* hyphae and conidia indicated that the secretion of IL-6, TNF- α and NO are mainly TLR4-dependant (Meier *et al.*, 2003). TLR2 is also involved in recognition of *A. fumigatus*, due to the additive loss of cytokine production in TLR2/TLR4 double deficient macrophages compared to TLR4 deficient macrophages (Meier *et al.*, 2003). Lack of TLR2 and TLR4 resulted in less neutrophil infiltration *in vivo*, and also less production of a chemoattractant, MIP-2, in response to *A. fumigatus* challenge (Meier *et al.*, 2003). In all cases, the reduction in immune function was more severe with loss of TLR4 compared to TLR2. These findings prove the importance of TLR2 and TLR4 in the recognition and corresponding immune response towards *A. fumigatus* (Meier *et al.*, 2003). TLR2 and TLR4 have also been implicated in mediating the NF κ B-dependant production of pro-inflammatory cytokines during fungal keratitis cause by *A. fumigatus* (Zhao & Wu, 2008). The important of TLR4, but not TLR2 in inducing TNF- α release from human monocytes exposed to ethanol-fixed, serum-opsonised *A. fumigatus* hyphae has also been reported (Wang *et al.*, 2001). Another study found that TLR2 rather than TLR4 was the important receptor for signalling TNF- α in response to *A. fumigatus* hyphae in both the human cell line HEK293 and murine peritoneal macrophages

(Mambula *et al.*, 2002). Signalling through the PRR CD14 contributed to TNF- α production in response to *A. fumigatus* hyphae in a human monocytic cell line (THP-1) and HEK293 cells (Mambula *et al.*, 2002; Wang *et al.*, 2001). CD14 has been widely recognised as a PRR for a wide variety of microbial and non-microbial ligands (Pugin *et al.*, 1994). As alluded to above, the literature reveals several controversies regarding the role of TLR2 and TLR4 in the innate immune response to *A. fumigatus* (Chignard *et al.*, 2007). In agreement with Meier *et al.*, (2003), another study documented that TLR2 and TLR4 were necessary for immune signalling in response to *A. fumigatus* (Netea *et al.*, 2005; Netea *et al.*, 2006), and that macrophages respond differently to conidia and hyphae (Netea *et al.*, 2005). TLR2 appears to recognise both conidia and hyphae, whereas TLR4 only detects conidia (Netea *et al.*, 2005). TLR4-mediated pro-inflammatory signals, but not TLR2-induced signals, are lost on *A. fumigatus* germination to hyphae, and TLR2 induces IL-10 production upon exposure to hyphae (Netea *et al.*, 2005). This was speculated to be a strategy used by germinating *A. fumigatus* to evade the immune system (Netea *et al.*, 2005). Differential recognition of *A. fumigatus* conidia and hyphae by TLRs is most likely due to differences in the expression of cell wall components on hyphae and conidia which comprise PAMPs which are differentially recognised by TLR2 and TLR4 (Bernard & Latge, 2001). To date, specific *A. fumigatus* PAMPs which are recognised by TLRs have not been described, highlighting the importance in this area of research (Chignard *et al.*, 2007). In fact, with the exception of phospholipomannan of *C. albicans*, the fungal ligands stimulating TLR activation remain completely undefined (Levitz, 2010).

Two C-type lectin receptors on human myeloid cells; the mannose receptor (CD206) and DC-SIGN, appear to play a major role in the recognition of mannans on fungal cell walls (Levitz & Specht, 2006). These receptors have cytoplasmic regions which direct mannosylated antigens, such as fungal cell wall components, to the

endocytic pathway of dendritic cells, to be eventually presented to T cells (Levitz, 2010). Langerin and Dectin-2 are receptors which also recognise mannan (Levitz, 2010). CD206 and Dectin-2 also recognise chitin and α -glucans respectively, although redundancy exists with regard to the number of host receptors that recognise glucans, mannans and chitin (Bittencourt *et al.*, 2006; Lee *et al.*, 2008; Levitz, 2010).

Dectin-1, a type II transmembrane protein that belongs to the NK-like C-type lectin-like receptor family is a known receptor for β -1,3/ β -1,6-linked glucans (Brown *et al.*, 2002). Since the discovery that Dectin-1 is required for the generation of the alveolar macrophage proinflammatory response towards *A. fumigatus*, and that these Dectin-1 mediated responses are dependant on the stage-specific display of β -glucan (Hohl *et al.*, 2005; Steele *et al.*, 2005), Dectin-1 has received much attention for its essential role in the pulmonary defence against *A. fumigatus* (Werner *et al.*, 2009). Dectin-1 contains an extracellular C-type lectin-like domain (CTLCD) connected by a stalk region to a transmembrane domain and a cytoplasmic tail. The tail contains an immune-receptor tyrosine-based activation (ITAM)-like motif (Ariizumi *et al.*, 2000). Alternative splicing of Dectin-1 leads to two isoforms that differ by the presence or absence of the stalk region, and have different functionalities (Heinsbroek *et al.*, 2006; Jimenez-A *et al.*, 2008; Willment *et al.*, 2001). Dectin-1 is highly expressed on inflammatory cells and cells at portals of microbial entry, such as alveolar macrophages (Reid *et al.*, 2004; Taylor *et al.*, 2002). Remodelling and expansion of the cell wall during the early stages of conidial germination results in exposure of β -glucan on the fungal cell surface, and subsequently triggers Dectin-1 signalling in a dose-response manner (Hohl *et al.*, 2005). The authors propose that restricted recognition of germinating conidia focuses immune responses on spores likely to cause invasive disease (Hohl *et al.*, 2005). Dectin-1 has been shown *in vitro* to mediate the production of cytokines (TNF- α) and chemokines (G-CSF and MIP-2) by human macrophages in

response to *A. fumigatus* after 24 hr co-culture, and this induction was blocked upon addition of an anti-Dectin 1 mAb (Steele *et al.*, 2005). TLR2 was found to play an accessory role in facilitating the Dectin-1-mediated alveolar response to *A. fumigatus*, whereby loss of TLR2 function seemed to reduce the level of Dectin-1 cytokine release (Steele *et al.*, 2005). Furthermore, production of cytokines and chemokines by macrophages in response to *A. fumigatus* swollen conidia and early germlings was mediated by the recognition of exposed β -glucans by Dectin-1, and that the production of these inflammatory mediators is negligible following exposure to live *A. fumigatus* resting conidia, which are maintained in an immunologically inert state by the presence of the rodlet layer as mentioned previously (Aimanianda *et al.*, 2009; Steele *et al.*, 2005). Despite current research efforts, it is important to state that the conidial ligands that activate TLR/MyD88-dependant signals still remain unknown and it is suggested that they may involve molecules of carbohydrate, lipid or protein origin (Hohl *et al.*, 2005). The complex interactions that exist between ligands and receptors beyond the established β -glucan/ Dectin-1 interaction represents an area of research which requires further investigation.

3.1.3.4 Chemical Immune Effectors.

Activation of transcription factors, such as NF κ B, results in their translocation to the nucleus, whereby they can up-regulate the expression of a suite of inflammatory genes. Genes encoding cytokines and chemokines are targets for NF κ B. The exact repertoire of cytokines produced during an invasive aspergillosis infection varies in mice depending on the immune status and the mode of immunosuppression used (Balloy *et al.*, 2005; Duong *et al.*, 1998). The lungs of immunocompetent mice generally contain cytokines such as TNF- α , interleukin-12 (IL-12), interferon-gamma (IFN- γ), IL-18, IL-6, IL-1 β , IL-10, granulocyte macrophage-colony stimulating factor

(GM-CSF), MIP-1 α , MCP-1, MIP-2 and keratinocyte chemoattractant (KC) (Balloy *et al.*, 2005; Duong *et al.*, 1998). A selection of these cytokines will be discussed in more detail.

TNF- α is a 17-kDa cytokine produced predominantly by a range of macrophage populations, including alveolar macrophages (Mehrad *et al.*, 1999). It has been shown to be an essential proximal signal for the induction and maintenance of the innate pulmonary defence in pneumonia (Moussa *et al.*, 1994) and other important human pathogens (Gosselin *et al.*, 1995; Laichalk *et al.*, 1996). TNF- α has also been found to be important for the immune response towards *A. fumigatus in vivo*, whereby depletion of TNF- α resulted in greater fungal burden and mortality, coinciding with a reduction in the number of circulating neutrophils at the site of infection (Mehrad *et al.*, 1999). Prior administration of TNF- α to mice resulted in resistance of animals to *A. fumigatus* infection (Mehrad *et al.*, 1999). The activity of TNF- α towards *A. fumigatus* is likely to involve several mechanisms. TNF- α induces expression of adhesion molecules on leucocytes and endothelial cells, thereby controlling neutrophil abundance in the lung (Gamble *et al.*, 1985). Mehrad *et al.*, (1999) indicated that *in vivo* neutralisation of TNF- α resulted in a reduction in the level of chemokines. Chemokines have been implicated in the defence against *A. fumigatus*; *in vitro* experiments using rat alveolar macrophages showed that these cells produced MIP-1 α , MIP-2, KC and also TNF- α following exposure to *A. fumigatus* conidia (Shahan *et al.*, 1998). Mice with a deletion in CCR1, a chemokine receptor for MIP-1 α and RANTES, developed systemic infection when exposed to *A. fumigatus* intravenously, indicating the important role of these chemokines in defence (Gao *et al.*, 1997).

IL-10 is a pleiotropic cytokine that is predominantly produced by Th2 lymphocytes, but also by macrophages, dendritic cells, mast cells and B lymphocytes (de Vries, 1995; Goldman *et al.*, 1997; Ho *et al.*, 1994; Moore *et al.*, 1993). IL-10 is an

important regulatory cytokine of the innate immune system (Balloy & Chignard, 2009). IL-10 has a variety of effects on the function of immune cells, including T cells and phagocytes (de Vries, 1995; Goldman *et al.*, 1997; Ho *et al.*, 1994; Moore *et al.*, 1993). IL-10 can downregulate T cell activation and the production of pro-inflammatory cytokines (IL-1, TNF- α , IL-5), chemokines and IFN- γ . It can hinder macrophage function, inhibit NO production, enhance B cell proliferation and antibody production. It promotes a Th2 cellular response while blocking a Th1 response (Bettelli *et al.*, 1998; de Vries, 1995; Goldman *et al.*, 1997; Ho *et al.*, 1994; Moore *et al.*, 1993). While IL-10 has proven to be a beneficial cytokine for some microbial infections, IL-10 production has been found to be deleterious for others, in particular fungal infections, including those caused by *C. albicans* and *Cryptococcus neoformans* (Monari *et al.*, 1997; Romani *et al.*, 1994; Tonnetti *et al.*, 1995). IL-10 has been found to have contrasting roles in response to *A. fumigatus*; it can inhibit the oxidative and anti-fungal activity of neutrophils to *A. fumigatus* hyphae, yet it can enhance the phagocytic activity of these cells, possibly providing a sanctuary for progressive infection (Roilides *et al.*, 1997). IL-10 had no direct effect on the morphological forms of *A. fumigatus* (Roilides *et al.*, 1997). IL-10 appears to be beneficial in regulating the inflammatory response towards allergic bronchopulmonary aspergillosis, and inhibits inflammatory responses caused by IFN- γ or IL-5 (Grunig *et al.*, 1997). However, later experiments using IL-10 knockout mice have shown that IL-10 is detrimental during systemic aspergillosis infections, increasing host susceptibility to infection (Clemons *et al.*, 2000).

3.1.4 Model systems for studying *A. fumigatus* virulence.

There are a range of model systems available for the study of virulence in many important human pathogens including *A. fumigatus*. Use of the invertebrate *Galleria*

mellonella as a virulence model has been described in Chapter 1. Here, various immunocompromised murine models of invasive aspergillosis (IA) will be discussed.

Animals, in particular mouse models have played a major role in the investigation of virulence of *A. fumigatus* (Latge, 2001). The identification of virulence factors depends on the experimental model used (Shibuya *et al.*, 1999). Models can vary in animals used (weight, strain and sex), the type of immunosuppression (drugs, dose and frequency of administration), and the challenge protocol (route of inoculation and concentration of conidia) (Latge, 2001). The most commonly used animal models of IA involve the induction of neutropenia or corticosteroid-induced immunosuppression which mimic human infection (Dagenais and Keller, 2009). Neutropenia may be achieved by treatment with cyclophosphamide or other chemotherapeutic agents, whereas animals treated with corticosteroids represent the non-neutropenic model used to evaluate IA in the context of non-neutropenic patients (Dagenais and Keller, 2009). The use of different drug or neutrophil depletion regimens is known to influence survival, pathology and other outcomes in animal models of IA (Stephens-Romero *et al.*, 2005). One of the most notable examples of this is the observation that *A. fumigatus* gliotoxin mutants demonstrate wild-type virulence in a neutropenic model but reduced virulence in a non-neutropenic model, suggesting that gliotoxin is only important for pathogenicity in non-neutropenic hosts (Dagenais and Keller, 2009).

In order to induce IA in mice, conidial inoculation may be performed intratracheally, intravenously or via inhalation chamber (Dagenais and Keller, 2009). Intranasal inoculation is used routinely due to ease of handling, although inhalation chamber may represent the most reproducible strategy, and most closely resembles human infection (Sheppard *et al.*, 2004; Steinbach *et al.*, 2004). The typical outcomes often chosen to assess disease development include animal survival, histology, host cellular responses and fungal burden, which may all be influenced by the variables

mentioned above (Stephens-Romero *et al.*, 2005). Models which involve infecting separate groups of *A. fumigatus* with different strains are useful in identifying mutant strains which exhibit large differences in virulence (Latge, 2001). Models incorporating mixtures of strains are more useful in measuring slight variations in strain virulence capabilities that may not be detected when groups of animals are infected separately (Latge, 1999). Despite the advances in the development of animal models, one limitation that remains is the lack of conformity to human infection, and there currently is no model where IA can be induced by a low number of conidia (Latge, 1999). In humans, IA is often a chronic disease, caused by cumulative exposure to small numbers of conidia in an immunocompromised patient, whereas experimentally induced IA is a hyperacute infection achieved by delivering a large dose of conidia at a single time point (Latge, 1999).

The interaction of pathogenic fungi with mammalian cells has proven to be very useful in complementing *in vivo* studies, and can direct experiments towards the appropriate *in vivo* assays (Dagenais and Keller, 2009). *In vitro* studies with mammalian cell lines are frequently used to assess the role of specific fungal components during fungal-host cell interactions (Dagenais and Keller, 2009), and have been particularly useful in the discovering of the major β -glucan receptor, Dectin-1, as described above. The fact that *A. fumigatus* mutants which exhibit altered interactions with host cells *in vitro* do not always exhibit differences in virulence *in vivo* highlights the multifactorial nature of *A. fumigatus* pathogenicity and indicates the importance of examining multiple outcomes of infection, including histology and fungal burden (Dagenais and Keller, 2009).

Alternative hosts for studying *A. fumigatus* virulence have been described including the use of a *Drosophila melanogaster* model to study drug activity and virulence (Lionakis & Kontoyiannis, 2005). Rabbits and guinea pigs have also been

used to study IA and fungal keratitis (Clemons & Stevens, 2005), although these models will not be discussed further in this study. Recently, the use of embryonated chicken eggs has been described for the investigation of *A. fumigatus* virulence, and results obtained from these studies using defined mutants with previously identified virulence capabilities, showed strong agreement with murine models (Jacobsen *et al.*, 2010). The authors reported many advantages in using such a model; it bridges the gap between invertebrates and mice, is economically sustainable and easy to handle, yields highly reproducible results and histological examination of tissues post-infection is possible.

Overall, there is now a large choice of infection models in which to study *A. fumigatus* virulence traits and pathogenicity. These models are useful in discriminating between different mutant strains, whereby the contribution of a specific gene to virulence can be assessed. The use of invertebrate models provides a good starting point for screening mutants for differences in virulence, and then interesting mutants can be further analysed in one of the other models.

3.2 Aims and Objectives.

The overall aims of this work were to functionally characterise and determine a role for the non-ribosomal peptide synthetase Pes3 in *A. fumigatus*. The specific aims that were addressed are listed below.

- 1) To disrupt *pes3* function in *A. fumigatus* by a targeted gene disruption approach, in order to generate a *pes3* mutant strain (termed $\Delta pes3$).
- 2) Complementation of *pes3* disruption restoring a functional *pes3* open reading frame.
- 3) To confirm *pes3* manipulations by examining *pes3* expression in relevant strains.
- 4) To undertake comparative metabolite analysis between *A. fumigatus* wild-type and $\Delta pes3$.
- 5) To perform comparative phenotypic analysis between *A. fumigatus* wild-type and $\Delta pes3$ in order to identify possible a biological role for *pes3*.
- 6) To perform *in vivo* virulence testing in order to assess the virulence of $\Delta pes3$, in both an insect model system and murine virulence models of IA.
- 7) To measure cytokine production in a mammalian macrophage cell line following exposure to *A. fumigatus* wild-type and $\Delta pes3$ in order to investigate if deletion of *pes3* led to an immunologically silent phenotype.

3.3 Results.

3.3.1 Genetic manipulation of *pes3* gene within *A. fumigatus*.

The generation of *A. fumigatus* $\Delta pes3$ was performed by Dr. Deirdre Stack prior to commencement of this work. A summary of this is provided in Section 3.3.2. Screening for the $\Delta pes3$ genotype following transformation was part of this work, and is described in detail.

3.3.2 Generation of *pes3* disruption constructs.

For inactivation of *pes3*, a bipartite gene disruption strategy was employed (Section 2.2.3.1, Figure 2.1). The *A. fumigatus* ATCC 46645 strain was used in this study. As the *pes3* ORF very large (25 kb), the strategy employed was designed to disrupt 1.5 kb of the *pes3* coding region, corresponding to the first *pes3* module. This specifically resulted in the deletion of the first thiolation and condensation domains (nucleotides 2,046-3,528 of *pes3*). For this study, *ptrA* was released from the pSK275 plasmid via *Eco*ICRI and *Hind*III restriction digestion. PCR 1 resulted in a 1.2 kb DNA fragment corresponding to a region of *pes3* beginning approximately 800 bp downstream of the ATG start codon. This PCR product contained an *Eco*ICRI recognition site towards its 3' end which was available for restriction and subsequent ligation to *ptrA*. PCR 2 resulted in a 1.3 kb DNA fragment corresponding to a region of *pes3* beginning approximately 5.5 kb downstream from the ATG start codon. This PCR product contained a *Hind*III recognition site close to its 5' end. The products of PCR 1 and PCR 2 were restricted with *Eco*ICRI and *Hind*III respectively, and were ligated to *ptrA* via the same sites. Final *pes3* disruption constructs were 2.6 kb and 2.3 kb, respectively. Transformation of *A. fumigatus* ATCC 46645 protoplasts was performed and transformants were selected on agar plates containing pyrithiamine as described (Section 2.2.3.2).

3.3.3 Isolation of an *A. fumigatus pes3* mutant strain ($\Delta pes3$).

Potential *pes3* mutants were initially identified by resistance to pyrithiamine (PT) following transformation. There were 10 colonies that appeared PT-resistant following transformation. These colonies were isolated as described (Section 2.2.3.3) and Southern blot analysis was performed (Section 2.2.4). Genomic DNA (gDNA) from *A. fumigatus* ATCC 46645 and these transformants was restriction digested with *EcoRI* and probed for the 5' coding region of *pes3* with a DIG-labelled *pes3* probe (Section 2.2.5). Expected hybridisation patterns for wild-type and $\Delta pes3$ were 4.1 kb and 1.5 kb respectively. A schematic representation of the Southern blot and hybridisation patterns is shown in Figure 3.3. Following Southern blot analysis, colonies which yielded the correct signal for a *pes3* disruption were subjected to single spore isolation (Section 2.2.3.4). A second round of Southern blot analysis was then carried out on single-spored colonies using the Southern strategy as outlined above. *EcoRI* genomic DNA digestions and Southern blot analysis of two of the $\Delta pes3$ single spore transformants is shown in Figure 3.4.

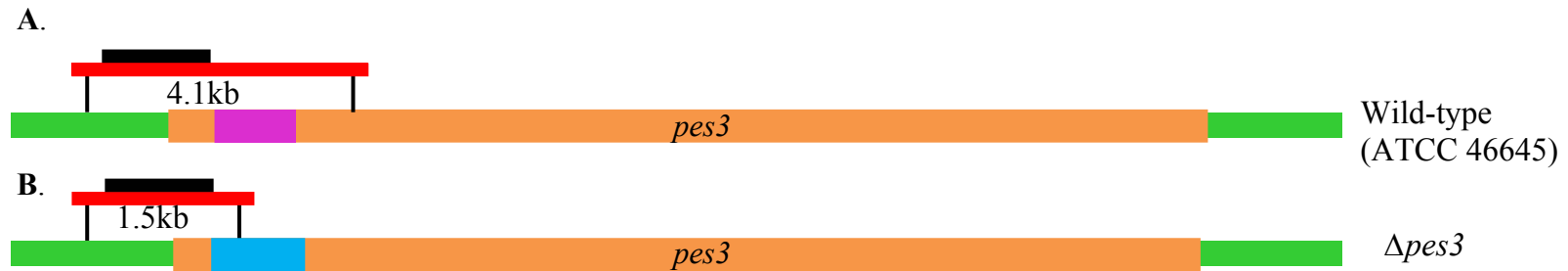


Figure 3.3. Southern blotting and hybridisation strategy used to identify *A. fumigatus* $\Delta pes3$.

This diagram illustrates the probing strategy that was used to identify $\Delta pes3$. The *pes3* locus in wild-type (A) and $\Delta pes3$ (B) is shown. The entire *pes3* coding region is indicated as an orange bar and the 5' and 3' flanking regions are shown in green. Approx. 1.5 kb of *pes3* was deleted and replaced by the pyrithiamine resistance cassette (*ptrA*) from *A. oryzae* (Kubodera *et al.*, 2000; 2002). *ptrA* is indicated in blue, while the region of *pes3* targeted for deletion is indicated in pink. Black vertical lines indicate *EcoRI* restriction sites in the genomic sequence of wild-type and $\Delta pes3$. Genomic DNA from pyrithiamine-resistance colonies was *EcoRI* digested and probed with a 1 kb DIG-labelled fragment corresponding to the 5' region of *pes3*. The probe is indicated with a black horizontal line. The positions for probe binding are indicated with red horizontal lines. Expected hybridisation patterns: ATCC 46645 wild-type-4.1 kb, $\Delta pes3$ -1.5 kb.

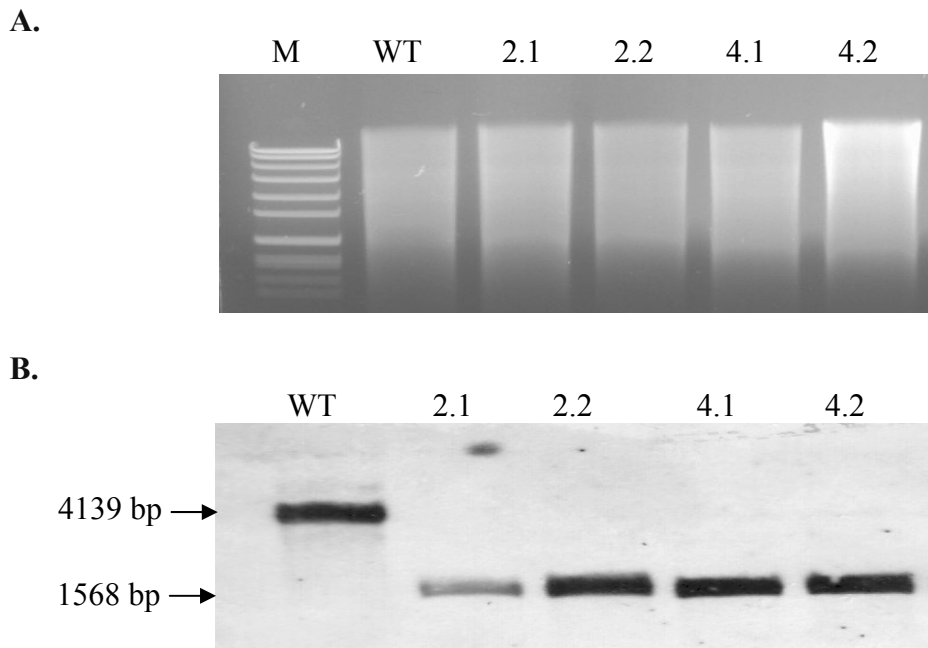


Figure 3.4. Isolation of an *A. fumigatus* $\Delta pes3$ mutant strain.

A. *EcoRI* restriction digestion of 1 μ g genomic DNA (gDNA) from PT-resistant single spored transformants # 2 and # 4 following transformation of *A. fumigatus* ATCC 46645 protoplasts with *pes3* disruption constructs. M: Molecular weight marker (Roche VII). WT: gDNA from *A. fumigatus* ATCC 46645. Lanes 2.1-4.2: gDNA from pyrithiamine-resistant single spored transformants following *EcoRI* digestion.

B. Southern blot depicting successful disruption of *pes3* gene. *EcoRI* digested genomic DNA (A) was probed with a DIG-labelled PCR product corresponding to the 5' region of *pes3*. Horizontal arrows indicate the sizes (bp) of the DNA fragments visible on the blot. WT: *A. fumigatus* WT (= ATCC 46645). Lanes 2.1-4.2: *A. fumigatus* $\Delta pes3$ single spore transformants. Expected hybridisation patterns: WT: 4,139 bp, $\Delta pes3$: 1,568 bp.

3.3.4 Generation of *pes3* replacement constructs and isolation of a *pes3* complemented strain ($\Delta pes3::PES3$).

As the *pes3* disruption strategy resulted in the deletion of 1.5 kb of the gene, it was essential to restore the deleted *pes3* region specifically at the *pes3* locus. In order to select for transformed colonies, a resistance cassette was supplied separately on a plasmid vector, Pan8.1 (a gift from Dr. Markus Schrettl). Pan8.1 contains a Phleomycin resistance cassette (*ble'*). *ble'* is comprised of 1.8 kb of the constitutive *gpdA* promoter from *Aspergillus nidulans* and the *ble*-gene fused to the *A. nidulans trpC* terminator sequence. Phleomycin resistance was used as a trait to select for transformants that had incorporated Pan8.1. Several strategies were undertaken in order to complement $\Delta pes3$ and restore an intact *pes3* coding region, and a summary of these, and outcomes are provided in Table 3.1. Ultimately, a bipartite replacement strategy was designed to specifically replace the region of *pes3* that had been deleted. This strategy was designed to replace *ptrA* which was located at the *pes3* locus in $\Delta pes3$. The *pes3* bipartite replacement constructs (referred to as *pes3*-left and *pes3*-right) comprised two overlapping fragments spanning the 1.5 kb of *pes3* which had been deleted. These were generated by PCR using specific primer pairs to generate overlapping *pes3* fragments (Table 2.3 for a list of all primers). Wild-type ATCC 46645 gDNA was used as a PCR template. The *pes3*-left and *pes3*-right PCR products are shown in Figure 3.5. Gel-purified DNA was precipitated prior to use in transformation (Section 2.2.2.2), and the precipitated PCR products are shown in Figure 3.5. In order to select for transformants and potentially complemented strains, a co-transformation procedure was employed whereby protoplasts of $\Delta pes3$ were transformed simultaneously with both the *pes3* bipartite replacement constructs and the plasmid vector Pan8.1, which was described above. Phleomycin-resistant transformants were further screened for the presence of an intact *pes3* gene, employing the same Southern blot strategy that was used to confirm

$\Delta pes3$ (Figure 3.3). *EcoRI* genomic DNA digestions and Southern blot analysis of $\Delta pes3$ complemented single spore transformants are shown in Figure 3.6. gDNA from phleomycin-resistant colony 3 showed absence of the 1,568 bp fragment specific to $\Delta pes3$ (Figure 3.6, lanes 5), while displaying the presence of a 4,139 bp band indicative of restoration of the *pes3* coding region (Figure 3.6). Single spore isolation colony 3 yielded *A. fumigatus* $\Delta pes3::PES3^{3.1}$ and $\Delta pes3::PES3^{3.2}$. Table 3.1 outlines the various transformation experiments undertaken in order to generate *A. fumigatus* $\Delta pes3::PES3$.

Table 3.1. Strategies employed to complement $\Delta pes3$. Plasmid Pan8.1 was used to confer phleomycin resistance on *A. fumigatus* transformants. $\Delta pes3$ protoplasts were either transformed with linear or bipartite replacement constructs using the indicated DNA amounts. Strategy 4 was successful with one transformant exhibiting targeted integration of the *pes3* bipartite replacement constructs at the *pes3* locus, thereby restoring *pes3* integrity.

Strategy no.	<i>pes3</i> replacement construct used	Concentration of DNA used for transformation	No. of phleomycin resistant colonies	No. of colonies with <i>pes3</i> integration	No. of targeted <i>pes3</i> integrations
1	A single <i>pes3</i> replacement construct, 3.7 kb in length, spanning the 1.5 kb deleted region, with approximately 1 kb of flanking region each side.	5 μ g <i>pes3</i> construct and 3 μ g Pan8.1 vector.	0	0	0
2	A single <i>pes3</i> replacement construct, 3.7 kb in length, spanning the 1.5 kb deleted region, with approximately 1 kb of flanking region each side.	5 μ g <i>pes3</i> linear replacement construct and 5 μ g Pan8.1.	40	0	0

Strategy no.	<i>pes3</i> replacement construct used	Concentration of DNA used for transformation	No. of phleomycin resistant colonies	No. of colonies with <i>pes3</i> integration	No. of targeted <i>pes3</i> integrations
3	<i>pes3</i> bipartite constructs - <i>pes3</i> -left and <i>pes3</i> -right.	5 µg <i>pes3</i> -left and 5 µg <i>pes3</i> -right and 10 µg Pan8.1	25	25	0
4	<i>pes3</i> bipartite constructs - <i>pes3</i> -left and <i>pes3</i> -right.	5 µg <i>pes3</i> -left and 5 µg <i>pes3</i> -right and 5 µg Pan8.1	15	9	1

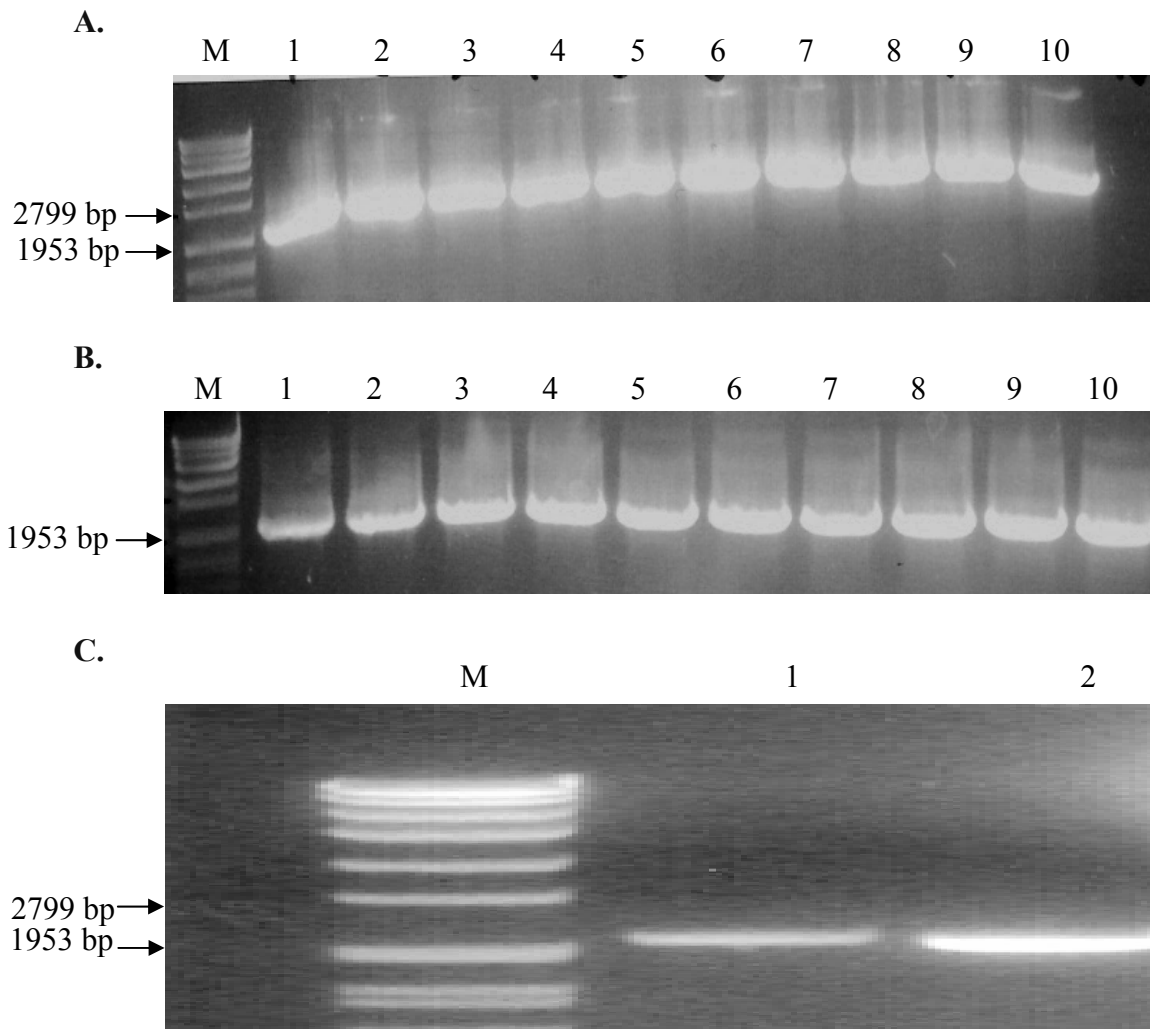


Figure 3.5. PCR amplification of *pes3* bipartite replacement constructs.

A. PCR reactions (x10) were performed to amplify the *pes3*-left construct. Lanes 1-10: *pes3*-left (2,121bp).

B. PCR reactions (x10) were performed to amplify the *pes3*-right construct. Lanes 1-10: *pes3*-right (2,091bp).

C. Precipitated *pes3* replacement constructs. Lane 1: *pes3*-left. Lane 2: *pes3*-right. Load: 1 μ l precipitated DNA.

M. Molecular weight marker (Roche VII).

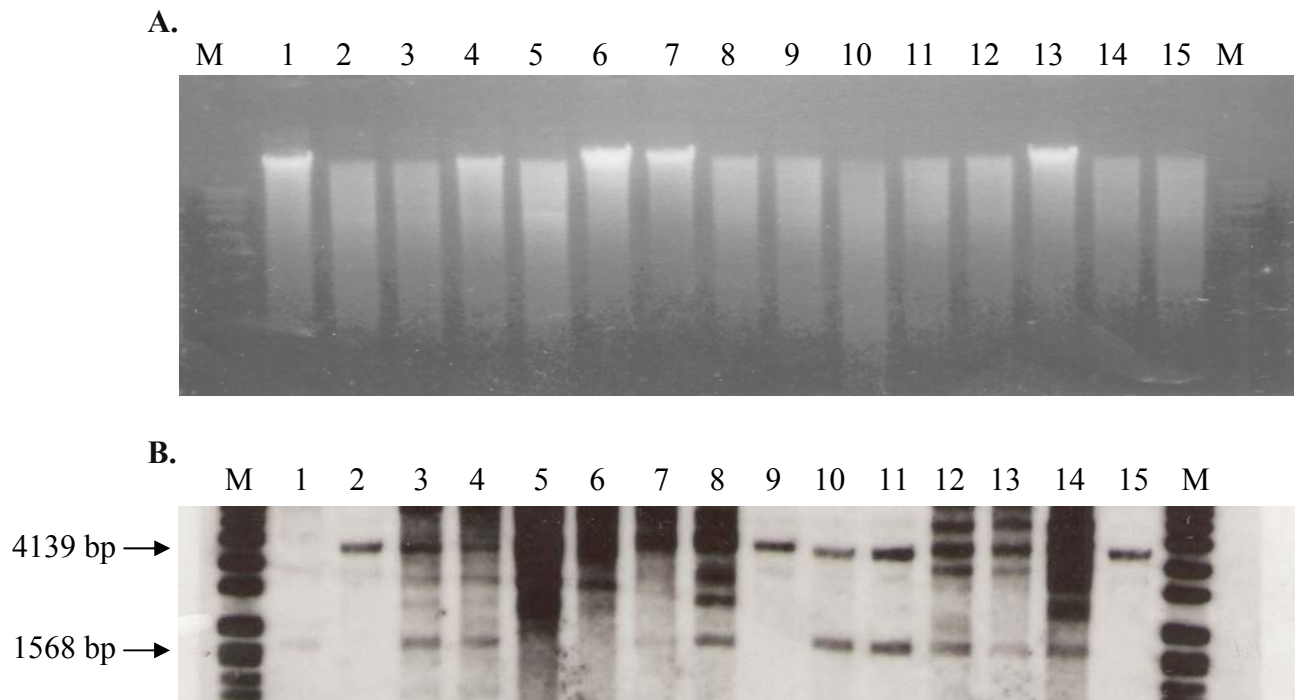


Figure 3.6. Isolation of a complemented *A. fumigatus* $\Delta pes3$ ($\Delta pes3::PES3$).

A. *EcoRI* restriction digests of 1 μ g genomic DNA (gDNA) from phleomycin transformants following transformation of *A. fumigatus* $\Delta pes3$ protoplasts with *pes3* replacement constructs and Pan8.1 vector simultaneously. Lane 1: gDNA from *A. fumigatus* $\Delta pes3$. Lanes 2, 9, 15: gDNA from *A. fumigatus* ATCC 46645. Lanes: 3-8 & 10-14: gDNA from 11 phleomycin resistant transformants.

B. Southern blot for determination of *pes3* complementation. *EcoRI* digested DNA (A) was probed with the 5' flanking region of *pes3*. Lane annotation: As for A. Expected hybridisation patterns: Wild-type (Lanes 2, 9, 15): 4,139bp, $\Delta pes3$ (Lane 1): 1,568bp, $\Delta pes3::PES3$ (Lane 5): 4,139 bp.

M. DIG-labelled 8 kb DNA Molecular weight marker (Roche VII).

3.3.5 Expression analysis of *pes3* in *A. fumigatus*.

The disruption and subsequent replacement of *pes3* was confirmed by Southern blot. A combination of RT-PCR and qReal-Time PCR was then employed to confirm that these genetic manipulations resulted in the abolition of *pes3* expression in *A. fumigatus* $\Delta pes3$ and the re-appearance of *pes3* expression in $\Delta pes3::PES3$. Expression analysis in $\Delta pes3$ and $\Delta pes3::PES3$ will be dealt with in the following two sections.

3.3.5.1 Disruption of *pes3* leads to abolition of *pes3* expression in *A. fumigatus*.

RT-PCR and qRT-PCR was performed on *A. fumigatus* wild-type ATCC 46645 and *A. fumigatus* $\Delta pes3$. RT-PCR was then performed to examine *pes3* expression under a range of culture conditions using specific primers (Table 2.3) to yield a *pes3* amplicon (248 bp). RT-PCR was also performed for the house-keeping gene, *calm* (Section 2.2.6.5). This analysis confirmed that the disruption strategy employed resulted in the expected absence of *pes3* expression. Real-Time PCR (Section 2.2.6.6) was subsequently performed on the same cDNA samples in order to quantify the gene expression levels and this is shown in Figure 3.7. Here, the relative expression of *pes3* transcripts is compared to *calm* (Burns *et al.*, 2005) in any given cDNA sample, and is given as a multiple of 1, whereby a value of 1 indicates that *pes3* and *calm* were equally abundant in that sample. The qRT-PCR analysis confirms that *pes3* expression is evident in all wild-type cultures, and absent in *A. fumigatus* $\Delta pes3$ in all culture conditions. Although expression is evident, *pes3* appears to be expressed at a low level in comparison to *calm* in all samples, with a 10-20 % level of abundance compared to *calm* in most cDNA preparations (Figure 3.7).

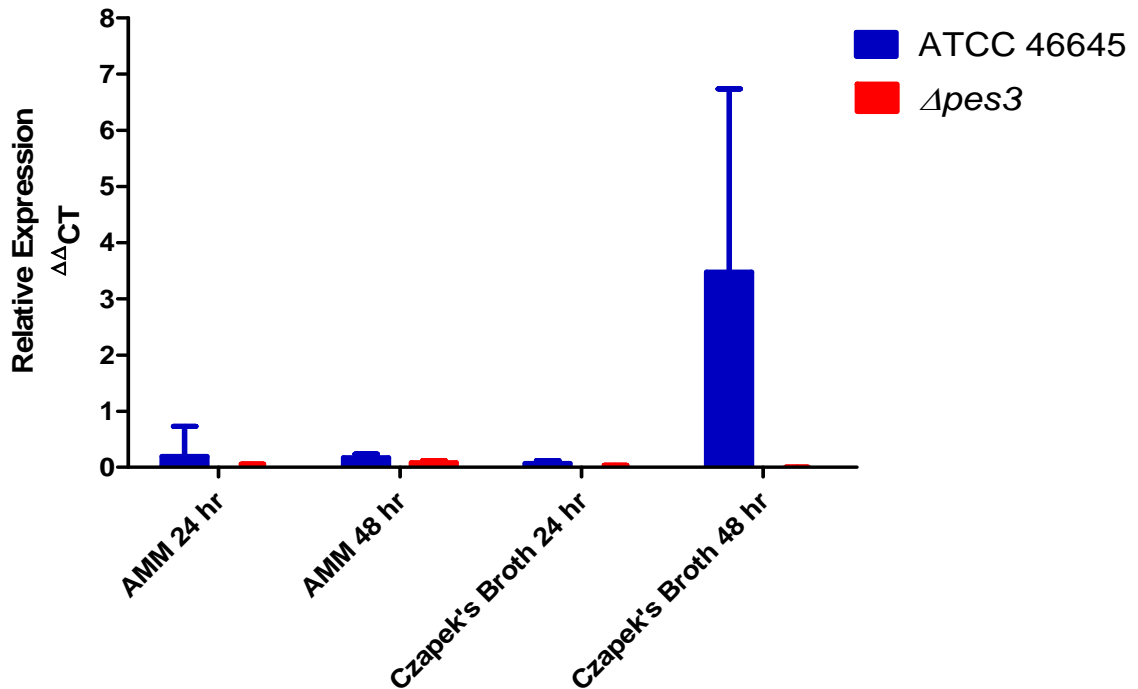


Figure 3.7. Real-Time expression analysis confirms abolition of *pes3* expression in *A. fumigatus* $\Delta pes3$.

Cultures of *A. fumigatus* wild-type and $\Delta pes3$ were grown in either AMM or Czapek's broth media for either 24 or 48 hr, and Real-Time PCR analysis was performed on the resultant cDNA samples. The relative abundances of *pes3* and the house-keeping *calm* transcripts are given. *pes3* expression is evident in *A. fumigatus* wild-type, and is absent in *A. fumigatus* $\Delta pes3$ in all conditions tested.

3.3.5.2 Restoration of *pes3* expression in $\Delta pes3::PES3$.

Complementation of $\Delta pes3$ using the strategy described in Section 3.3.4, was confirmed by Southern blot. Subsequently, RT-PCR was performed to confirm the restoration of *pes3* expression in complemented strains. *A. fumigatus* wild-type ATCC 46645, *A. fumigatus* $\Delta pes3$ and single-spored colonies of $\Delta pes3::PES3$ were analysed. These single-spored colonies are referred to as *A. fumigatus* $\Delta pes3::PES3^{3.1}$ and $\Delta pes3::PES3^{3.2}$. RT-PCR was then performed as in the preceding section. RT-PCR confirmed that the complementation strategy employed resulted in the restoration of *pes3* expression, as visualised by the reappearance of the *pes3* amplicon in $\Delta pes3::PES3^{3.1}$ and $\Delta pes3::PES3^{3.2}$ (Figure 3.8). *A. fumigatus* $\Delta pes3$ was also included in this experiment, and the absence of *pes3* gene expression was confirmed in the mutant strain by RT-PCR (Figure 3.8).

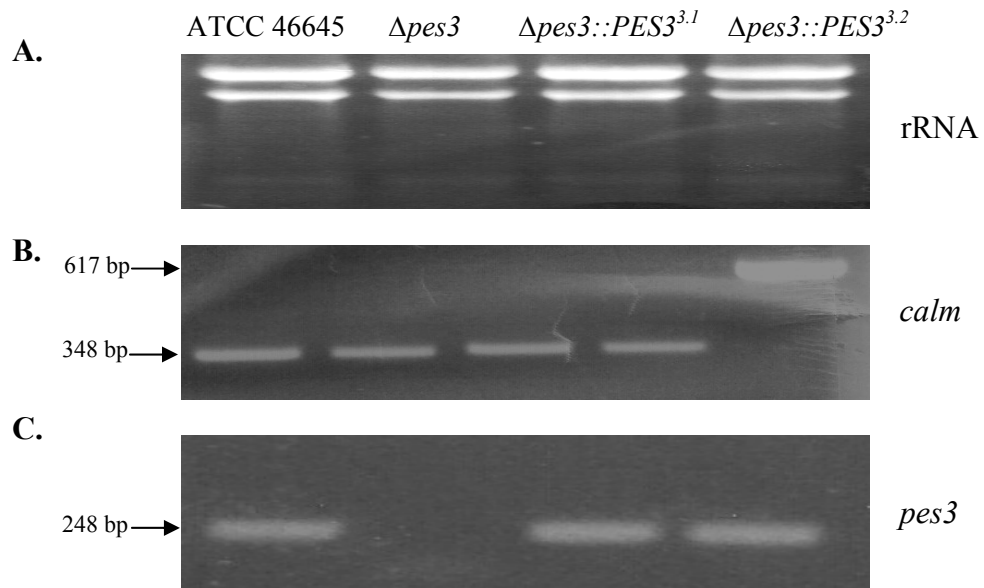


Figure 3.8. RT-PCR expression analysis confirming absence of *pes3* transcripts in *A. fumigatus* $\Delta pes3$, and restoration of *pes3* transcription in $\Delta pes3::PES3^{3.1}$ and $\Delta pes3::PES3^{3.2}$.

A. Total RNA was harvested from 48 hr cultures of *A. fumigatus* strains in Czapek's broth. The integrity of the 28, 18 and 5.8 S rRNA sub-units is evident. Load: 3 μ g RNA per lane.

B. *calm* is constitutively expressed and gDNA amplicon absence in cDNA confirms the absence of contaminating genomic DNA (gDNA) in cDNA preparations.

C. *pes3* RT-PCR. An amplicon (248 bp) of the *pes3* coding region was amplified from cDNA of *A. fumigatus* strains.

Load: 5 μ l PCR product per lane resolved on 2 % (w/v) agarose gels.

3.3.6 Restoration of *pes3* locus in *pes3* complemented strain confirmed by restriction mapping.

Due to the large size of the *pes3* gene, the disruption strategy was designed to delete a region of the gene. Subsequently, targeted complementation was required to restore the *pes3* locus. To ensure correct integration of the *pes3* replacement constructs at the *pes3* locus, a restriction mapping experiment was performed. Using genomic DNA (gDNA) from either *A. fumigatus* wild-type, $\Delta pes3$ or $\Delta pes3::PES3$ strains, a PCR reaction was carried out using primers oAf*pes3*-6 and oAf*pes3*-6 (Table 2.3). These primers span the region where the *pes3* disruption was targeted, and should lead to a PCR product in all strains. PCR reactions should generate a PCR product of 3,737 bp in wild-type and $\Delta pes3::PES3$, and 4,285 bp in $\Delta pes3$. These PCR products were gel purified and restriction digested with *AgeI* restriction enzyme (Section 2.2.2.5, 2.2.2.6). *AgeI* restriction should lead to different size bands in the wild-type and $\Delta pes3$ PCR products due to presence of *ptrA* in the $\Delta pes3$ gDNA. A list of the expected and observed fragments following *AgeI* digestion is presented in Table 3.2. This confirms that the *pes3* locus was restored in $\Delta pes3::PES3$ as all expected bands were observed (Figure 3.9). The restriction pattern for $\Delta pes3::PES3$ is identical to that of wild-type as expected. $\Delta pes3$ contains differences at this region, due to the presence of *ptrA*, and this is also evident in the restriction map. Overall, this confirms the integrity of the *pes3* locus in the $\Delta pes3::PES3$ strain, and validates the use of this strain for further analysis.

Table 3.2. Expected restriction fragments following *AgeI* restriction digestion of *pes3* PCR fragments from genomic DNA of *A. fumigatus* wild-type, $\Delta pes3$ and $\Delta pes3::PES3^{3.1}$.

Wild-type genomic DNA:	$\Delta pes3$ genomic DNA:	Successfully complemented <i>pes3</i> strain – i.e. $\Delta pes3::PES3$
1197 bp	2197 bp	1197 bp
1053 bp	1170 bp	1053 bp
694 bp	694 bp	694 bp
569 bp	224 bp	569 bp
224 bp		224 bp

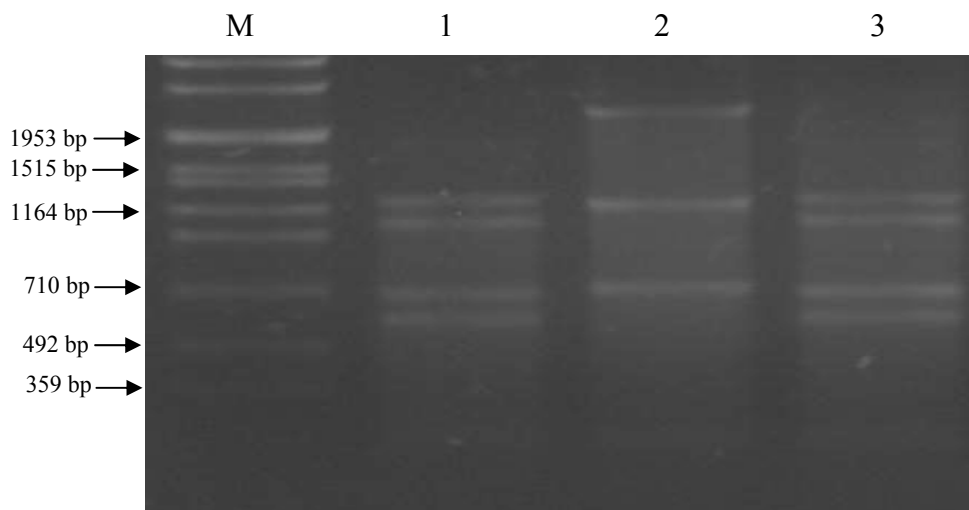


Figure 3.9. Restriction mapping of *pes3* PCR product confirms successful integration of *pes3* constructs in $\Delta pes3::PES3^{3.1}$ and $\Delta pes3::PES3^{3.2}$.

Purified PCR products were restriction digested with *AgeI* and resolved on 1 % agarose gel. All expected bands were observed as listed in Table 3.2

M. Roche VII marker. Lanes 1-3: *AgeI* digested PCR products: Lane 1: *A. fumigatus* ATCC 46645, Lane 2: $\Delta pes3$ genomic DNA, Lane 3: $\Delta pes3::PES3^{3.1}$ genomic DNA.

3.3.7. Comparative metabolite analysis reveals no difference in metabolite profile between *A. fumigatus* wild-type and $\Delta pes3$.

Availability of the *A. fumigatus* $\Delta pes3$ mutant facilitated comparative metabolite analysis to be undertaken between wild-type and mutant cultures to identify a potential Pes3 encoded non-ribosomal peptide (NRP) (Section 2.2.7). In order to do this, *A. fumigatus* wild-type and $\Delta pes3$ were cultivated in a variety of growth conditions, which are listed in Table 3.3.

The growth conditions employed comprised a variety of liquid culture media, or growth on different agar media for a defined time-point. For liquid culture media, either supernatants (Section 2.2.7.1) or organic extractions of supernatants (Section 2.2.7.2) of wild-type and $\Delta pes3$ were compared. For agar cultures, extractions were performed using two different methods, and the time-point analysed here was usually 6 days incubation at 37 °C. Extraction methods and appropriate solvents used are also listed in Table 3.3. Conditions listed as A, B, C, D and E were performed and analysed by RP- HPLC at NUI Maynooth. The material for analysis for Conditions F and G was prepared at NUI Maynooth, and analysed by LC-DAD-MS by a collaborating group at the Danish Technical University (DTU). Material resulting from condition D and E were also analysed at DTU.

For Conditions D and E, conidial suspensions were washed from agar plates with H₂O and metabolites were extracted using a protocol based on that of Moon *et al.*, (2008) (Section 2.2.7.3). This conidial metabolite extraction procedure was performed on conidia which had either been cultivated for 6 days on AMM agar or AMM agar which was supplemented with 2 mM hydrogen peroxide. Examination of metabolite profiles following exposure to hydrogen peroxide was performed in order to see if differences occurred between the strains after oxidative stress, following the observation that another NRP synthetase, Pes1, has previously been shown to protect against oxidative stress in *A.*

fumigatus (Reeves *et al.*, 2006). Preparation of plug extracts for analysis at DTU was performed using a method which was developed at DTU (Smedsgaard, 1997) (Section 2.2.7.4). Organically extracted material was analysed by LC-DAD-MS at the facilities at DTU.

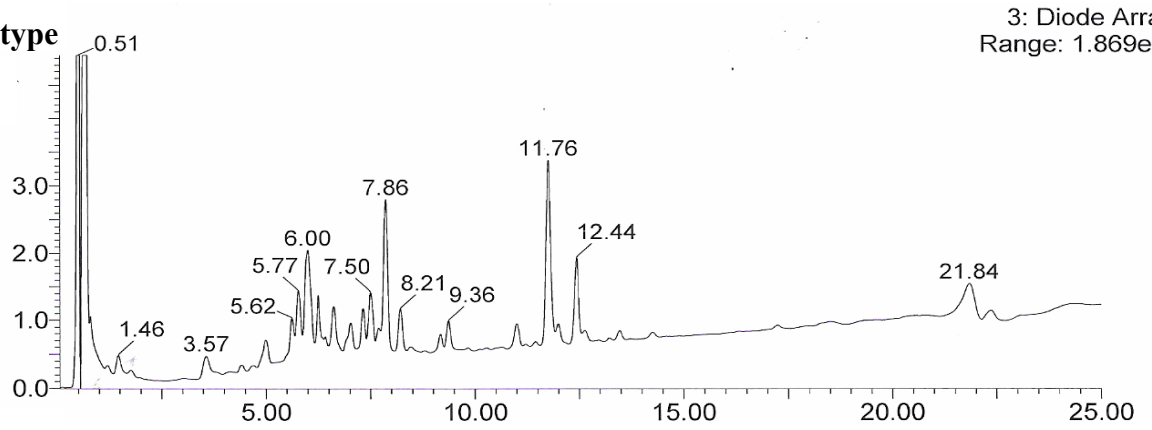
Table 3.3. Summary of conditions used for comparative metabolite analysis of wild-type *A. fumigatus* and $\Delta pes3$.

Growth Condition (all at 37 °C)	Extraction Solvent	Injection Volume	Outcome
A. RPMI 48 hr incubation, 200 rpm	1) Organic extraction of culture supernatant (SN) with SN: chloroform in a 1:1 ratio 2) Neat culture supernatant injection.	100 μ l / 20 μ l	No differences observed
B. Czapek's 48 hr incubation, 200 rpm	1) Organic extraction of culture supernatant (SN) with SN: chloroform in a 1:1 ratio 2) Neat culture supernatant injection.	100 μ l / 20 μ l	No differences observed
C. AMM 48 hr incubation, 200 rpm	1) Organic extraction of culture supernatant (SN) with SN: chloroform in a 1:1 ratio 2) Neat culture supernatant injection.	100 μ l / 20 μ l	No differences observed
D. Incubation on AMM agar for 6 days	Conidial Extraction Method (Moon <i>et al.</i> , 2008)	100 μ l	No differences observed
E. Incubation on AMM supplemented with H ₂ O ₂ (final concentration 2 mM) for 6 days	Conidial Extraction Method (Moon <i>et al.</i> , 2008)	100 μ l	No differences observed
F. Incubation on AMM agar for 6 days	Plug Extraction Method (Smedsgaard, 1997)	1 μ l	No differences observed
G. Incubation on Czapek's agar for 6 days	Plug Extraction Method (Smedsgaard, 1997)	1 μ l	No differences observed

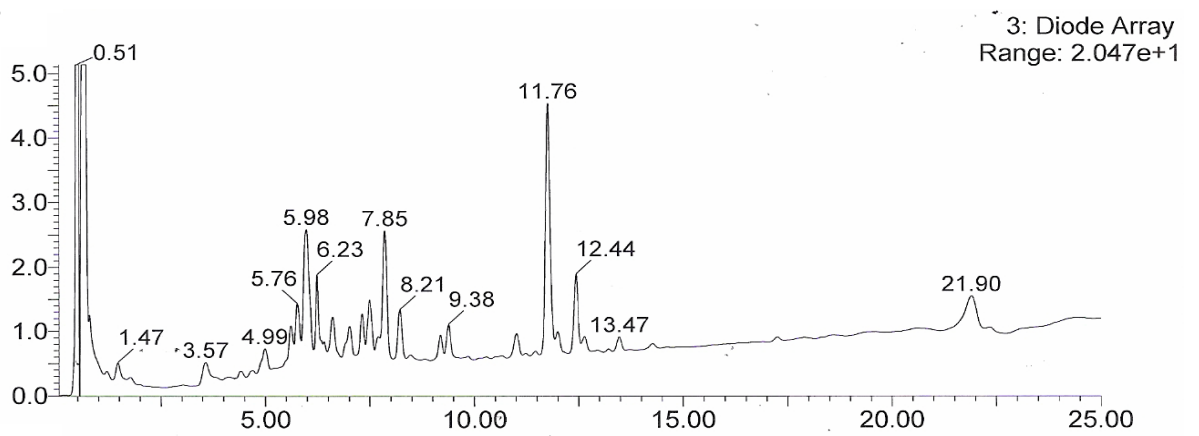
In all cases, comparative analysis between wild-type and $\Delta pes3$ revealed that there were no differences in metabolite profiles between the strains. Not all chromatograms are shown, however a selection of the chromatograms generated at DTU are presented. The remainder of the analysis is summarised in Table 3.3. The metabolite profiles of wild-type and $\Delta pes3$ following 6 days growth on Czapek's agar are given in Figures 3.10 and 3.11. Plug extracts were performed from these agar plates, and extractions were carried using two solvent mixes. Figure 3.10 shows the chromatograms following organic extractions of plugs using either a mixture of 25 % acetonitrile and 75 % water (Section 2.1.8.2.1) and the LC-DAD and total ion chromatgrams are shown for each strain. Figure 3.11 shows the chromatograms following organic extraction of plugs using a mixture of ethyl acetate, dichloromethane and methanol (Section 2.1.8.2.2). These samples were separated on a Dionex HPLC system. Wild-type and $\Delta pes3$ extracts yielded profiles that are virtually identical to one another, under all growth conditions, using all extraction methods tested in this study. This strongly suggests that *pes3* is not responsible for the synthesis of a soluble non-ribosomal peptide that is secreted or stored intracellularly in *A. fumigatus*.

A.

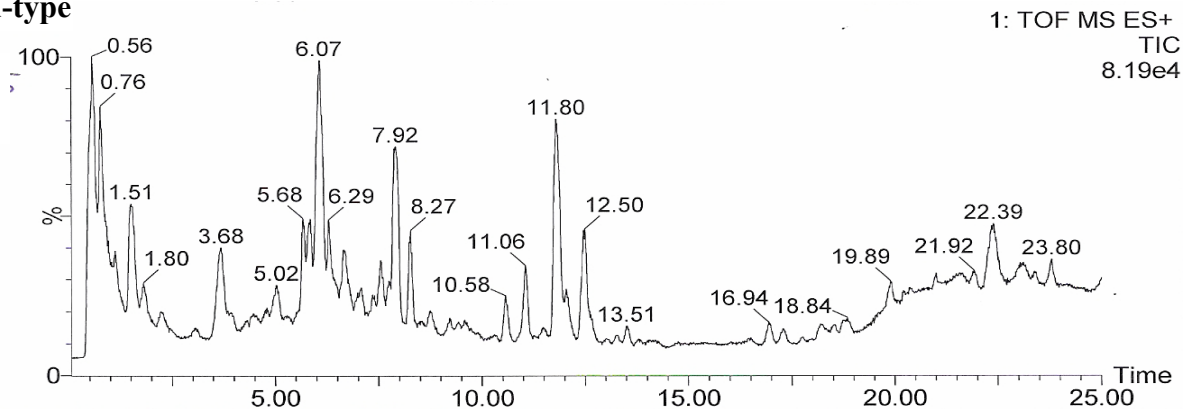
Wild-type



$\Delta pes3$



B. Wild-type



$\Delta pes3$

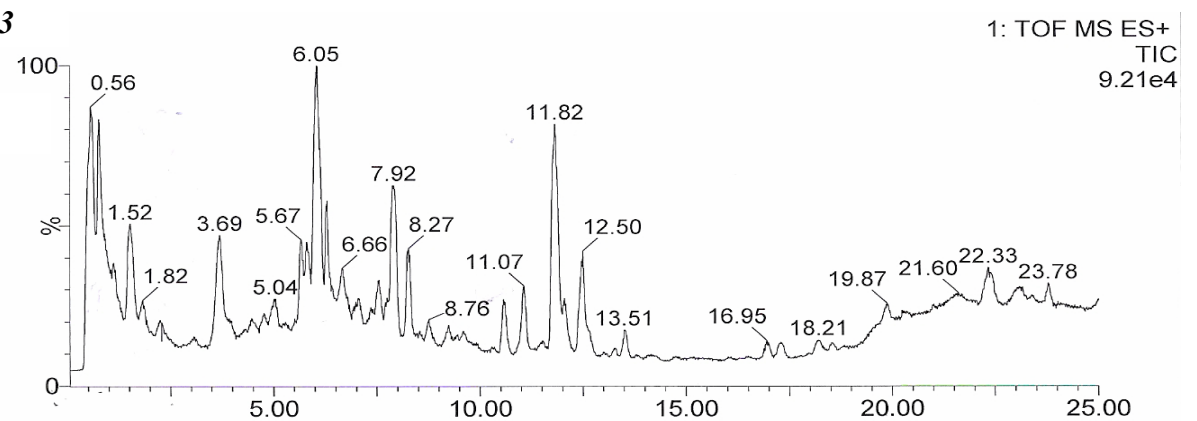
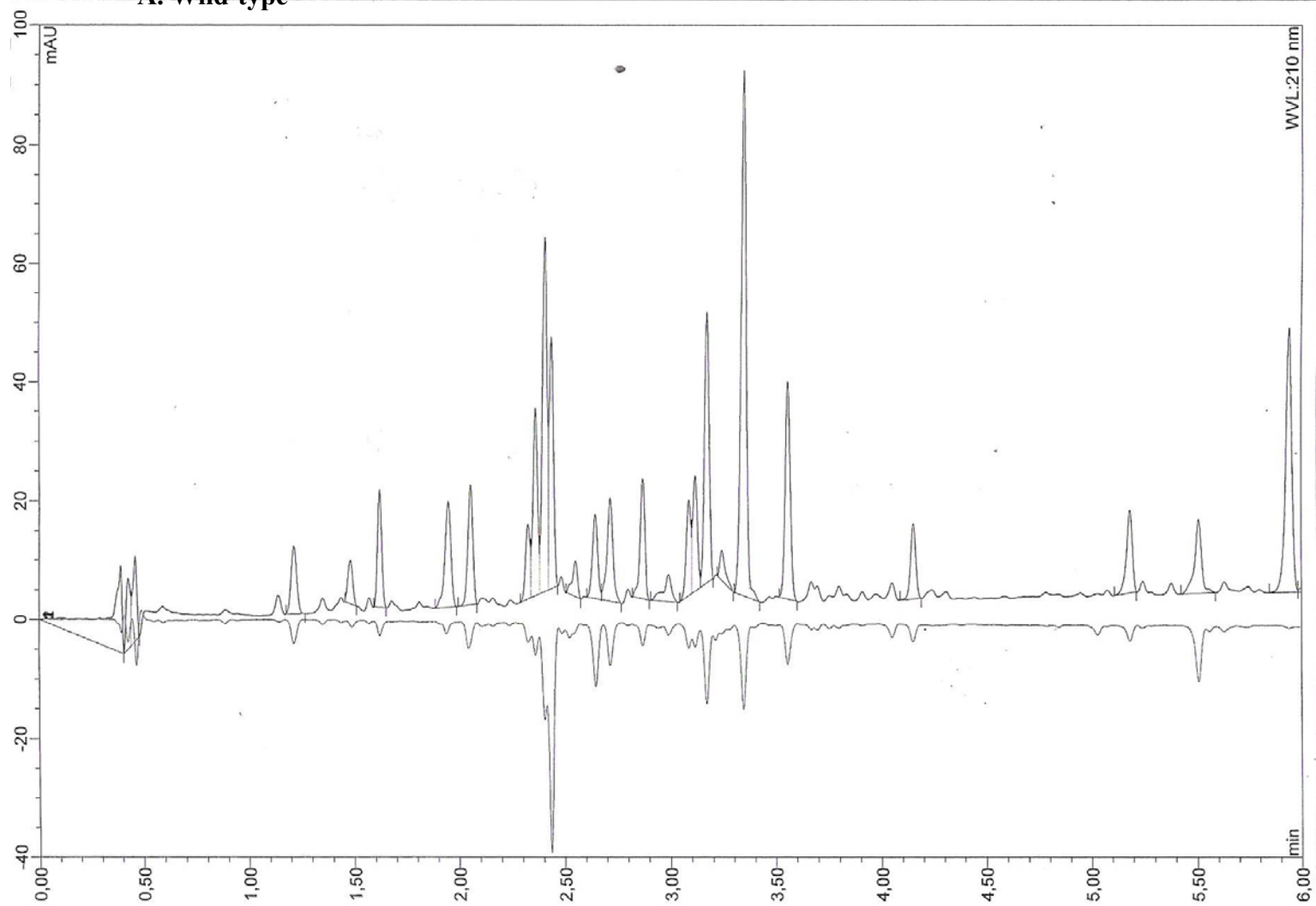


Figure 3.10. LC-DAD and mass spectra for *A. fumigatus* wild-type and $\Delta pes3$ following plug extraction with an acetonitrile/H₂O extraction solvent.

A. LC-DAD profiles for both strains. The profiles for both strains are virtually identical.

B. Mass spectra for both strains show that the metabolite profiles from wild-type and $\Delta pes3$ are the same.

A. Wild-type



B. $\Delta pes3$

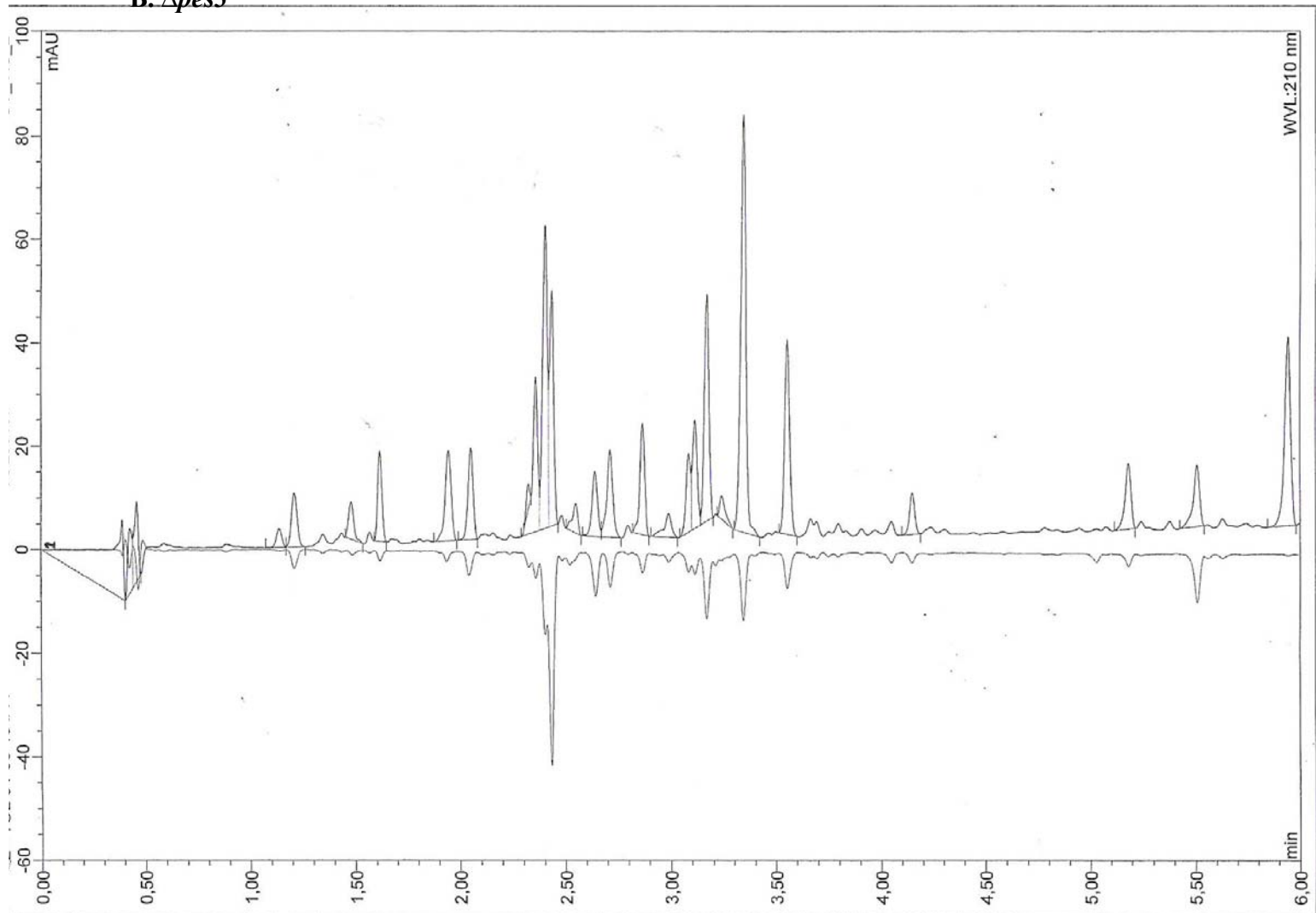


Figure 3.11. Chromatograms of *A. fumigatus* wild-type and $\Delta pes3$ metabolite profiles following plug extraction with a 3:2:1 ethyl acetate: dichloromethane: methanol mixture.

A. Wild-type.

B. $\Delta pes3$.

Profiles for both strains are identical.

3.3.8 Phenotypic Characterisation of the *A. fumigatus* $\Delta pes3$ mutant.

A. fumigatus $\Delta pes3$ was compared to wild-type under a variety of growth conditions and environmental stresses in order to investigate if it displayed an altered phenotype under any condition. A summary of all conditions tested in this study, and their outcomes, is provided in Table 3.4. For all phenotypic analysis described in Table 3.4, plate assays were used in order to compare *A. fumigatus* wild-type and $\Delta pes3$ (Section 2.2.8).

Initially, plate assays were performed in a range of different iron concentrations to see if *pes3* was involved in siderophore biosynthesis in *A. fumigatus*. This strategy was based on the fact that at least two of the non-ribosomal peptide synthetases in *A. fumigatus* have been proven to be involved in siderophore biosynthesis for iron acquisition (Schrettl *et al.*, 2007; Reiber *et al.*, 2005). Under all growth conditions examined here, $\Delta pes3$ behaved comparably to the wild-type strain. A representative of these plate assays showing the radial growth of wild-type and $\Delta pes3$ at 20, 44 and 66 hr growth is given in Figure 3.12.

A. fumigatus wild-type and $\Delta pes3$ were compared in their sensitivity to cell wall stressing agents including calcafluor white, congo red, sodium dodecyl sulphate and caffeine. The specific activity of these agents will be discussed later. For all cell wall stress experiments, *A. fumigatus* $\Delta pes3$ behaved identical to wild-type.

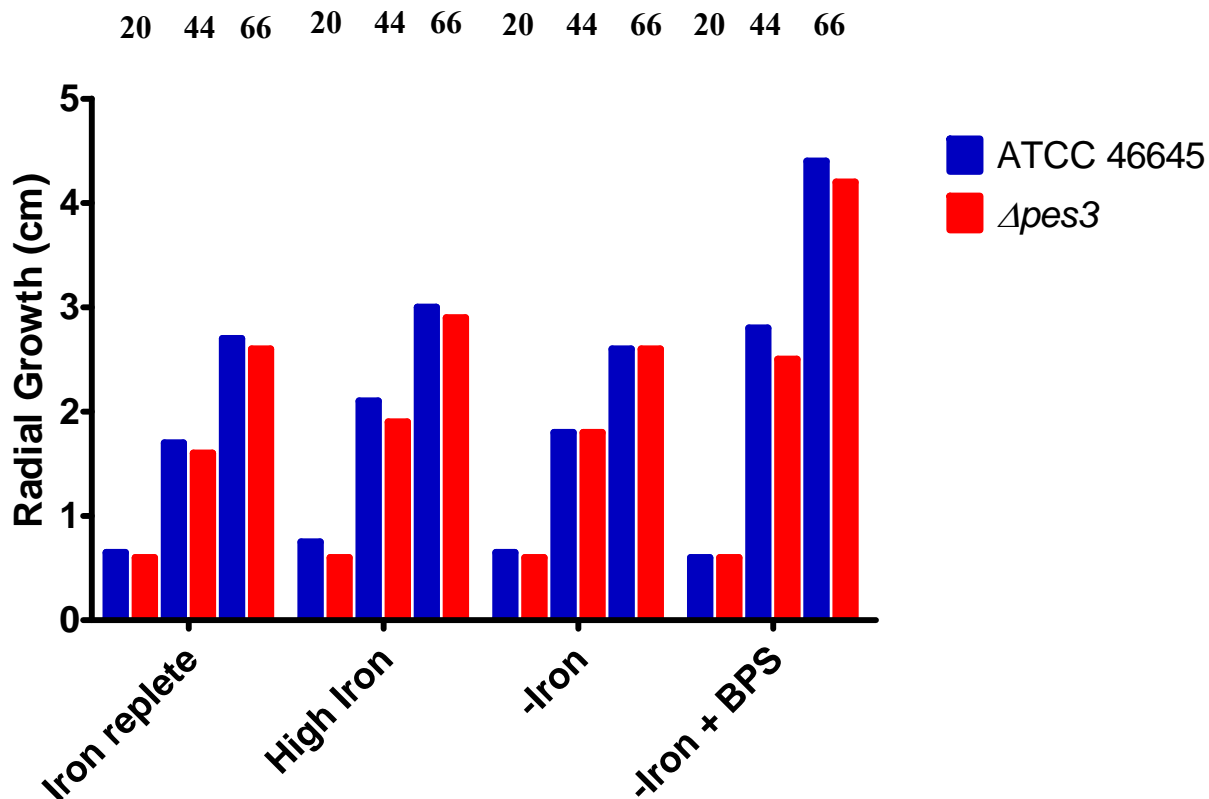


Figure 3.12. *A. fumigatus* $\Delta pes3$ behaves identical to wild-type (ATCC 46645) when grown on a range of varying iron conditions.

Wild-type and $\Delta pes3$ were exposed to a range of conditions, as indicated. Iron replete (10 μM FeSO_4), high iron (1.5 mM FeSO_4), -iron (omission of iron from growth media), iron + BPS (omission of iron from growth media, in addition to supplementation with the iron chelator bathophenanthroline disulphonate (BPS) (200 μM)). Radial growth (cm) of colonies was measured at 20, 44 and 66 hr intervals. Both wild-type and $\Delta pes3$ strains grew at comparable rates on all conditions tested.

Δpes3 was examined for sensitivity to oxidative stress by growth on AMM agar in increasing concentrations of the oxidising agents hydrogen peroxide (H₂O₂), diamide or menadione. Plate assays were performed as described and growth was monitored over a 72 hr period at 24 hr intervals. Sensitivity to the oxidising agents was tested at concentrations of; H₂O₂ – 0.3 mM, diamide – 0.2 mM, and menadione – 0.40 μM. The radial growth of *A. fumigatus* wild-type and *Δpes3* following growth under all of these oxidative stress conditions is shown in Figure 3.13. The time point is 72 hr, and the data represents the mean ± SE of three biological replicates. *A. fumigatus Δpes3* exhibited an increased growth rate compared to wild-type when exposed to 0.1 mM diamide (p < 0.05). In all other conditions tested here, *pes3* displayed no alteration in growth compared to wild-type *A. fumigatus*, indicating that *pes3* does not play a role in protection against oxidative stress in *A. fumigatus*.

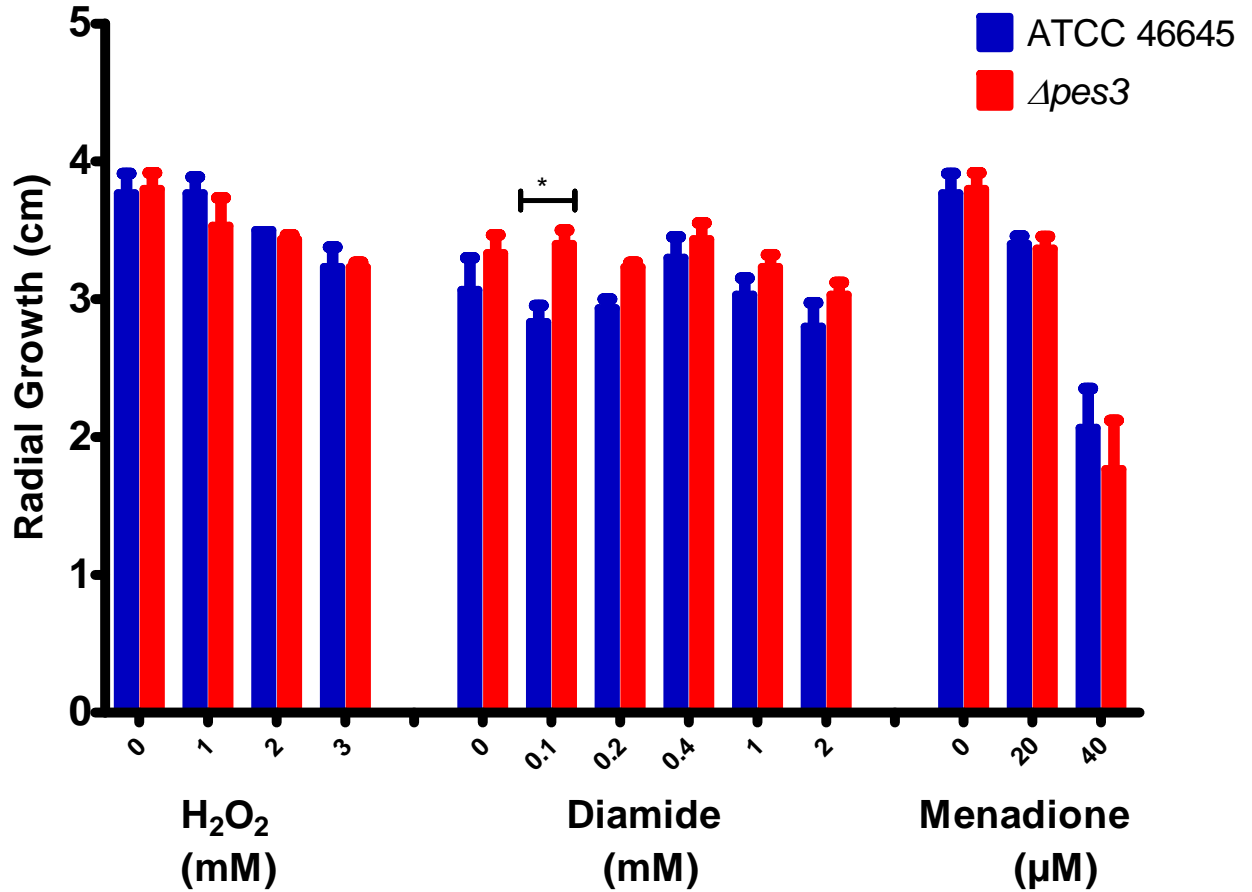


Figure 3.13. *A. fumigatus* $\Delta pes3$ behaves comparably to wild-type ATCC 46645 when exposed to a range of oxidising agents, including hydrogen peroxide (H₂O₂), diamide and menadione.

The radial growth of wild-type and $\Delta pes3$ are shown following 72 hr exposure to hydrogen peroxide, diamide or menadione which are known to cause oxidative stress. In all conditions tested, wild-type and $\Delta pes3$ exhibited comparable growth rates, with the exception of a slightly increased growth of $\Delta pes3$ compared to wild-type on the lowest concentration of diamide tested Key: *: $p < 0.05$. Data presented as mean \pm standard error of three experiments.

3.3.9 *A. fumigatus* $\Delta pes3$ exhibits increased sensitivity to the anti-fungal Voriconazole.

Anti-fungal phenotypic testing was performed in order to compare wild-type and $\Delta pes3$ upon exposure to anti-fungal agents. Sensitivity to voriconazole, amphotericin B and caspofungin were tested in this study. The concentrations of anti-fungals used in this study were: voriconazole – 0.25, 0.5, 0.75, 1.0 $\mu\text{g/ml}$, caspofungin – 0.2, 0.5, 1.0 $\mu\text{g/ml}$ and amphotericin B – 0.125, 0.25, 0.5, 1.0 $\mu\text{g/ml}$.

A. fumigatus $\Delta pes3$ exhibited increased sensitivity to voriconazole when compared to wild-type at all concentrations of voriconazole tested. This difference in sensitivity was observed by a lower growth rate of $\Delta pes3$ when exposed to the anti-fungal, and the altered phenotype was most significant at a concentration of 0.5 $\mu\text{g/ml}$ ($p < 0.001$, $n = 3$). This data is presented in Figure 3.14 which shows the radial growth rates of wild-type and $\Delta pes3$ upon either on AMM agar only or in the presence of 0.5 $\mu\text{g/ml}$ voriconazole for the indicated time points (hr). $\Delta pes3$ also displayed increased sensitivity compared to wild-type at concentrations of 0.25 $\mu\text{g/ml}$ ($p < 0.05$), and 0.75 $\mu\text{g/ml}$ ($p < 0.05$). At 1 $\mu\text{g/ml}$ voriconazole, $\Delta pes3$ was completely inhibited in growth at all time points analysed. However, since the most significant difference between wild-type and $\Delta pes3$ was observed at 0.5 $\mu\text{g/ml}$ voriconazole, this is the only data presented. Complementation with *pes3* resulted in levels of growth which were similar to wild-type when exposed to voriconazole. The radial growth of wild-type, $\Delta pes3$ and complemented strains at 72 hr growth on voriconazole (0.5 $\mu\text{g/ml}$) is shown in Figure 3.14. There appears to be an overall growth reduction on voriconazole in all strains from the data presented in Figure 3.14 (B) compared to that in Figure 3.14 (A). The fact that these experiments were carried out close to one year apart, and differences in conidial concentrations and/or voriconazole batch differences may explain this observation. What is important however, is that overall trend is constant whereby $\Delta pes3$ displays increased sensitivity to voriconazole and this reduction in

growth ($p < 0.001$) is restored in the complemented strain ($\Delta pes3::PES3^{3.1}$ and $\Delta pes3::PES3^{3.2}$). Taken together, these results indicate that *pes3* plays a role in protection against voriconazole toxicity in *A. fumigatus* and suggests an alteration at the cell wall or cell membrane of *A. fumigatus* $\Delta pes3$. $\Delta pes3$ behaved comparably to wild-type when exposed to the other anti-fungals used in this study (amphotericin B and caspofungin). Radial growths of strains upon exposure to these drugs is given in Figure 3.15.

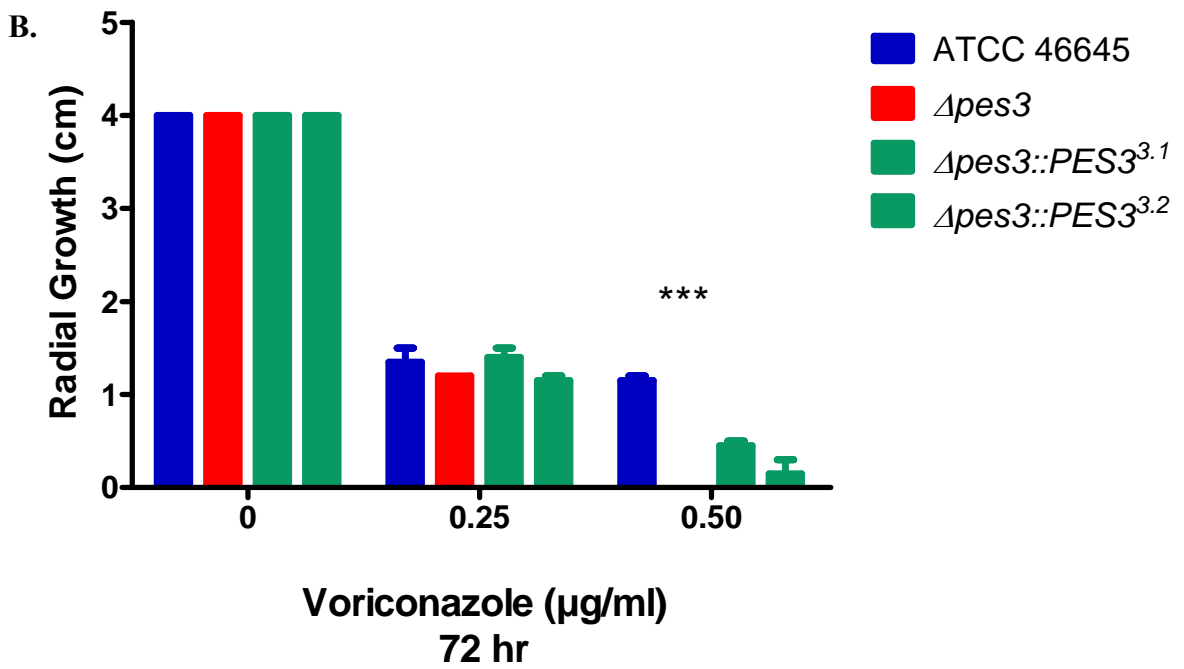
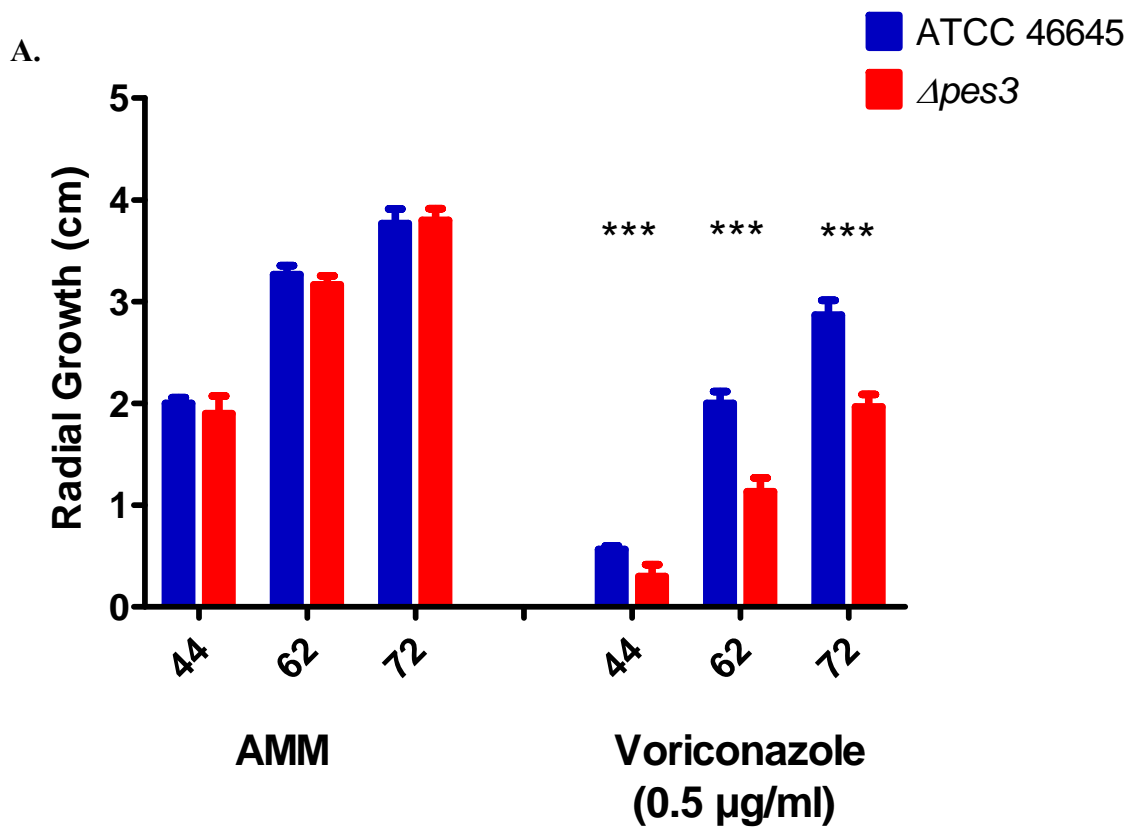


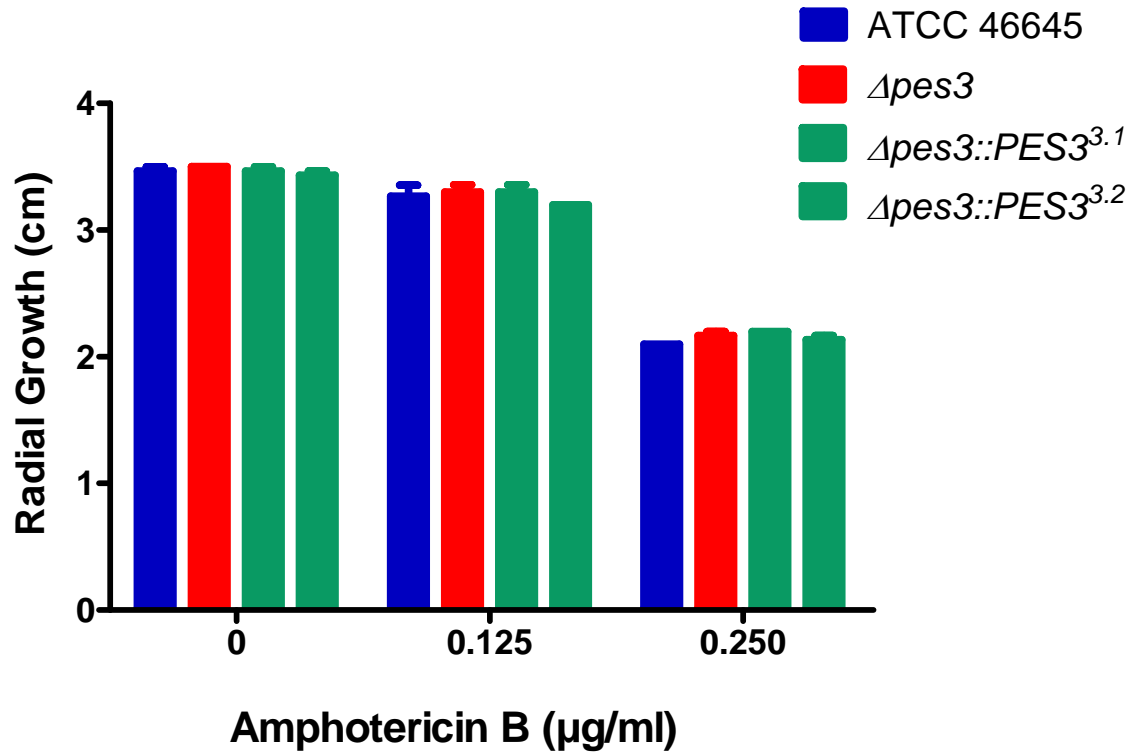
Figure 3.14. *A. fumigatus* $\Delta pes3$ displays increased sensitivity to the anti-fungal voriconazole.

A. Radial growth (cm) of wild-type and $\Delta pes3$ following exposure to voriconazole (0.5 $\mu\text{g/ml}$). Growth was monitored daily at the time points indicated. On AMM only, wild-type and $\Delta pes3$ grew at similar rates, while exposure to voriconazole led to significant differences in growth between the two strains ($p < 0.001$), with the mutant displaying reduced growth at all time points.

B. Restoration of growth upon exposure to voriconazole is restored once *pes3* is complemented. Exposure of wild-type, $\Delta pes3$ and *pes3* complemented strains is presented following 72 hr growth on voriconazole at 0, 0.25, 0.5 $\mu\text{g/ml}$. All strains grew equally in the absence of voriconazole, and the lack of growth observed for $\Delta pes3$ (0.5 $\mu\text{g/ml}$) is restored in both complemented strains tested here ($p < 0.001$).

Each graph displays the mean \pm standard error of three experiments. Key: ***: $p < 0.001$.

A.



B.

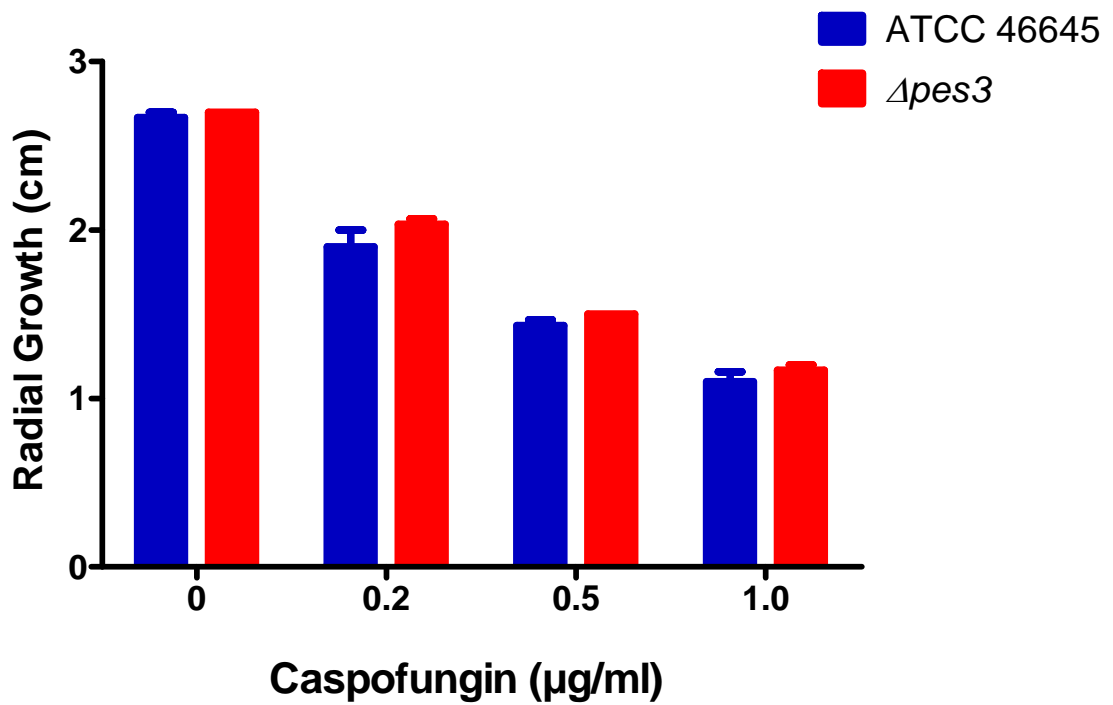


Figure 3.15. *A. fumigatus* wild-type and $\Delta pes3$ display similar growth rates on exposure to amphotericin B and caspofungin.

A. Radial growth (cm) of wild-type and $\Delta pes3$ following exposure to amphotericin B (0-0.25 $\mu\text{g/ml}$). Growth was monitored daily and the 72 hr time-point is shown here. Both strains showed equal growth rates on all concentrations tested. Data represents the mean \pm standard error of three experiments.

B. Radial growth (cm) of wild-type and $\Delta pes3$ following exposure to caspofungin (0-1.0 $\mu\text{g/ml}$). Growth was monitored daily and the 48 hr time-point is shown here. Both strains showed equal growth rates on all concentrations tested. Data represents the mean \pm standard error of three experiments.

Table 3.4. A summary of the phenotypic assays, and their outcomes, performed for *A. fumigatus* wild-type (ATCC 46645) and $\Delta pes3$ in this study.

Phenotypic Test	Reagents Used	Concentrations Tested	Result (i.e. growth of $\Delta pes3$ compared to wild-type)
Role of <i>pes3</i> in Siderophore Biosynthesis	Iron Stresses (High, Low, none)	10 μ M, 1.5 mM, 200 μ M BPS	No difference.
Oxidative Stress	Menadione	20, 30, 40 μ M	No difference.
	Diamide	0.1, 0.2, 0.4, 1, 2 mM	$\Delta pes3$ more resistant to diamide (0.1 mM, $p < 0.05$) for <i>A. fumigatus</i> $\Delta pes3$
	Hydrogen Peroxide	1, 2, 3 mM	No difference.
Anti-fungal Susceptibility	Voriconazole (vrc)	0.25, 0.5, 0.75, 1.0 μ g/ml	$\Delta pes3$ displays increased sensitivity to vrc at 0.5 μ g/ml ($p < 0.001$). Restored in $\Delta pes3::PES3$.
	Amphotericin B	0.125, 0.25, 0.5, 1.0 μ g/ml	No difference.
	Caspofungin	0.2, 0.5, 1.0 μ g/ml	No difference.

Phenotypic Test	Reagents Used	Concentrations Tested	Result (i.e. growth of $\Delta pes3$ compared to wild-type)
Cell Wall Stress	Caffeine	2, 5 mM	No difference.
	Congo Red	5, 10, 15 $\mu\text{g/ml}$	No difference.
	Calcafluor White	100, 200 $\mu\text{g/ml}$	No difference.
	High temperature (48 °)	n/a	No difference.
Membrane Stress	SDS	0.01, 0.02 % (w/v)	No difference.

3.3.10 *A. fumigatus* $\Delta pes3$ grows and undergoes conidial germination at a rate comparable to wild-type.

In order to compare the growth rates for *A. fumigatus* ATCC 46645 and $\Delta pes3$, both conidial germination rates and vegetative growth were measured. To measure the conidial germination rates, a germination assay was performed (Section 2.2.10). The result of the germination assay is presented in Figure 3.16. Germination began in both strains after 3 hr growth, and after 5 hr, the rate of germination was about 5 % for both strains. By 6 hr, germination was underway for about 25 % of the wild-type conidia, while a 35 % germination rate for $\Delta pes3$ was observed at this time, indicating a slightly faster germination rate for $\Delta pes3$. $\Delta pes3$ also exhibited a slightly faster germination rate after 7 hr incubation (wild-type – 55 %, $\Delta pes3$ – 65 %). At 9 hr, the wild-type cultures contained more germinated conidia compared to $\Delta pes3$ (wild-type – 85 %, $\Delta pes3$ – 80 %). While moderate differences were observed between the two strains, statistical analysis (Students t-test), indicated that these differences were not significant.

Growth curves were then carried out for both strains (Section 2.2.9), whereby the dry weights of mycelial biomass following a 96 hr incubation period were recorded. The dry weights (g) of the total biomass harvested from cultures at 24, 48, 72 and 96 hr is presented in Figure 3.17. Growth curves for these two strains showed that the exponential growth phase lasted until 48 hr, with growth rates remaining stationary after this time-point. Overall, there is no significant difference between the growth rates of *A. fumigatus* wild-type and $\Delta pes3$ in liquid shake cultures.

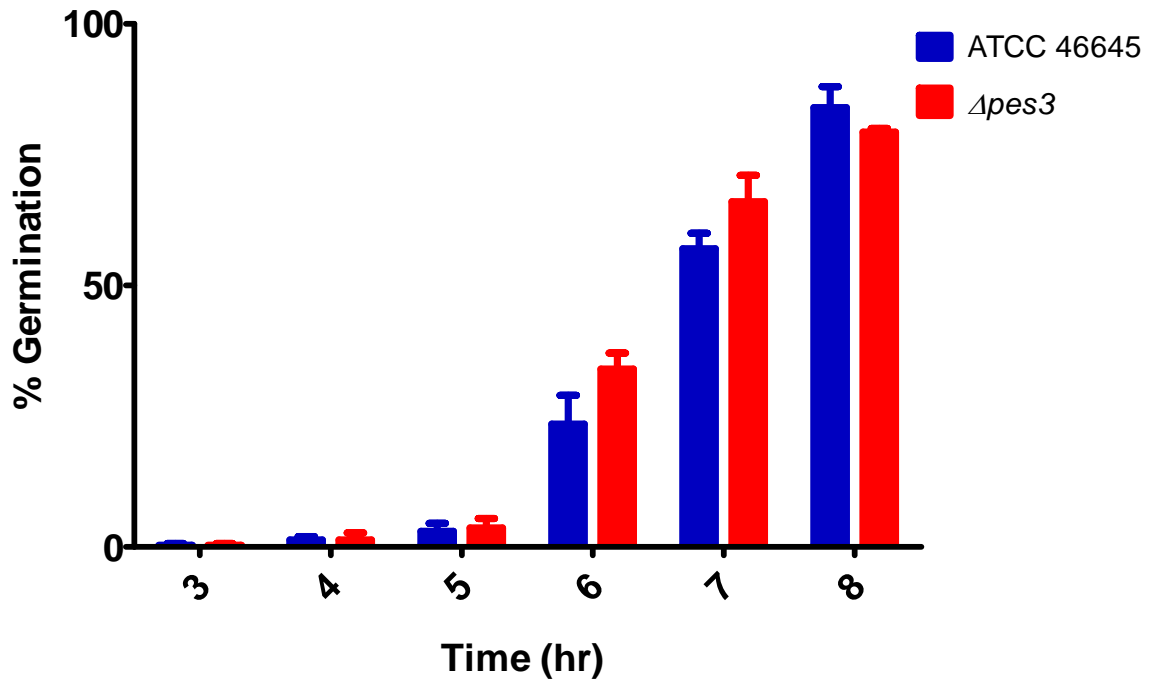


Figure 3.16. *A. fumigatus* ATCC 46645 and $\Delta pes3$ have similar conidial germination rates.

Germination rates of wild-type and $\Delta pes3$ were recorded over an 8 hr time period following growth of conidia in AMM. Germination was first observed at 3 hr, and the % of conidia in germination (of 100 counted in total) is indicated on the Y-axis. No significant differences in the germination rate between both strains was observed. The mean \pm standard error of 2 replicates for wild-type and 3 replicates for $\Delta pes3$ is displayed.

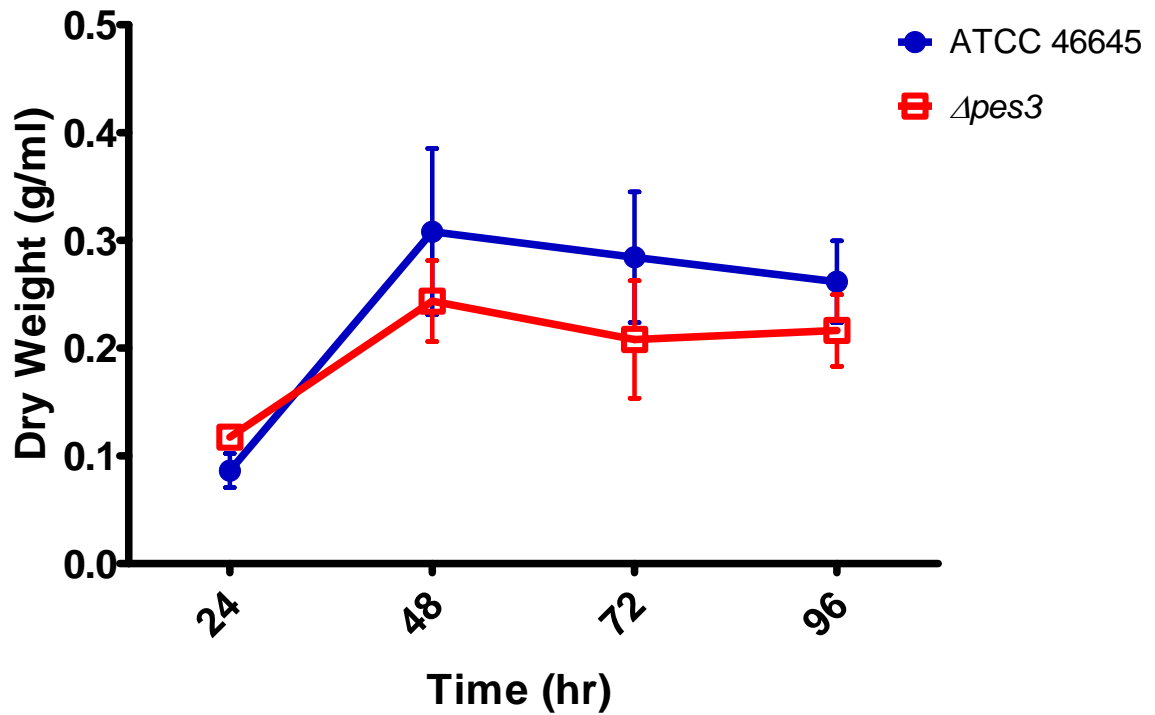


Figure 3.17. Vegetative growth curves are similar for *Aspergillus fumigatus* ATCC 46645 and $\Delta pes3$.

Cultures ($n = 3$ for each time point) were grown in AMM (100 ml) at 37 °C. A comparison of the dry weights (g) of resulting mycelia indicates that there were no significant differences between strains. The mean \pm the standard error of three experiments is displayed.

3.3.11. *A. fumigatus* $\Delta pes3$ is more virulent than wild-type *A. fumigatus*.

In order to assess any contribution of *pes3* in the virulence of *A. fumigatus*, the $\Delta pes3$ mutant and its wild-type progenitor ATCC 46645 were tested in two distinct models of infection. The major result of these experiments was that *A. fumigatus* $\Delta pes3$ was more virulent than wild-type, and increased virulence was recorded using both the *G.mellonella* insect model (Cotter *et al.*, 2000) and a hydrocortisone acetate (HCA) immunocompromised mouse model of invasive aspergillosis (Smith *et al.*, 1994). Interestingly, no difference in virulence between the two strains was observed in a neutropenic model of invasive aspergillosis, suggesting that the hypervirulence of $\Delta pes3$ is dependant on neutrophil presence. Murine virulence testing was carried out in collaboration with Dr. Elaine Bignell and Timothy Cairns at Imperial College London, UK.

3.3.11.1 Deletion of *A. fumigatus pes3* leads to increased virulence in the *Galleria mellonella* model of infection.

To assess the relative contribution of *pes3* to the virulence of *A. fumigatus*, the survival of larvae ($n = 20$) of the greater wax moth *G. mellonella* was compared following infection with 10^7 conidia/larvae of *A. fumigatus* ATCC 46645 or the same dose of $\Delta pes3$ conidia (Section 2.2.12). Larvae ($n = 20$) were injected with sterile PBS as an injection control. Larvae infected with wild-type had a greater survival compared to those infected with $\Delta pes3$ ($p < 0.001$) indicating increased virulence of the $\Delta pes3$ strain. The experiment was repeated four times. Larval survival (%) is shown in Figure 3.18. Apart from the PBS control, 100 % mortality was recorded at 96 hr post infection for all groups of larvae. At 24 hr following infection, approx. 95 % of the larva infected with wild-type remained alive, while an 85 % survival rate was observed for those infected with the mutant, indicating increased mortality associated with the loss of *pes3*. This difference is more pronounced at

48 hr and 72 hr time-points. At 48 hr post infection, 55 % of larvae infected with wild-type remain alive, in contrast to only 30 % of larvae infected with $\Delta pes3$. By 72 hr, only 3 % of larvae infected with $\Delta pes3$ are viable, versus 23 % in the wild-type group. The increased mortality associated with the higher virulence potential of $\Delta pes3$ is restored to wild-type survival levels in both complemented strains ($\Delta pes3::PES33.1$ and $\Delta pes3::PES33.1$) tested here, and the overall differences in survival proportions between larvae infected with wild-type or mutant is highly significant ($p < 0.001$) (Figure 3.18). Survival curves were generated using Kaplan-Meier survival plot with the Log-Rank (Mantel-Cox) test for significance. As stated above, virulence is restored to wild-type levels in $pes3$ complemented strains, indicating that the hypervirulence of $\Delta pes3$ is solely due to the disruption of $pes3$ (Figure 3.18). It is clear that *A. fumigatus* $\Delta pes3$ is more virulent than wild-type in the *G. mellonella* model of infection.

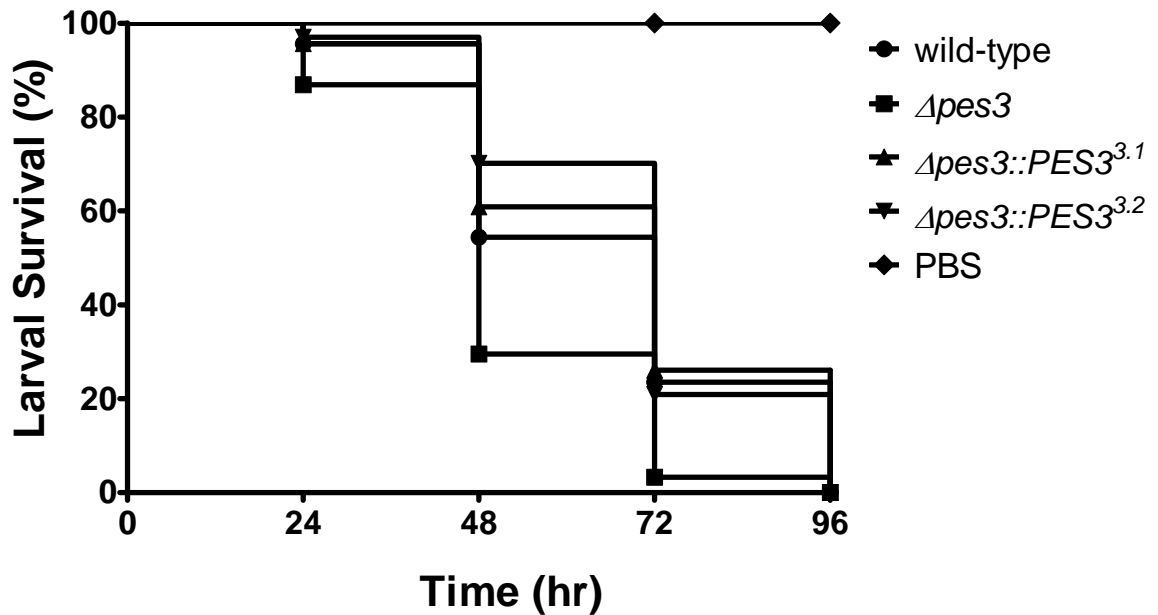


Figure 3.18. *A. fumigatus* $\Delta pes3$ is more virulent in the *Galleria mellonella* insect model.

The survival proportions of larvae ($n = 20$) infected with either wild-type, $\Delta pes3$ or $\Delta pes3::PES3^{3.1}$ and $\Delta pes3::PES3^{3.2}$ strains are shown. Larval viability (%) was assessed at 24 hr intervals following infection. *A. fumigatus* $\Delta pes3$ is more virulent than wild-type and is associated with reduced larval survival ($p < 0.001$) at all time points observed. Virulence is restored to wild-type levels in two complemented strains ($\Delta pes3::PES3^{3.1}$ and $\Delta pes3::PES3^{3.2}$). PBS was used as an injection control and all larvae in this group remained viable for the entire experiment.

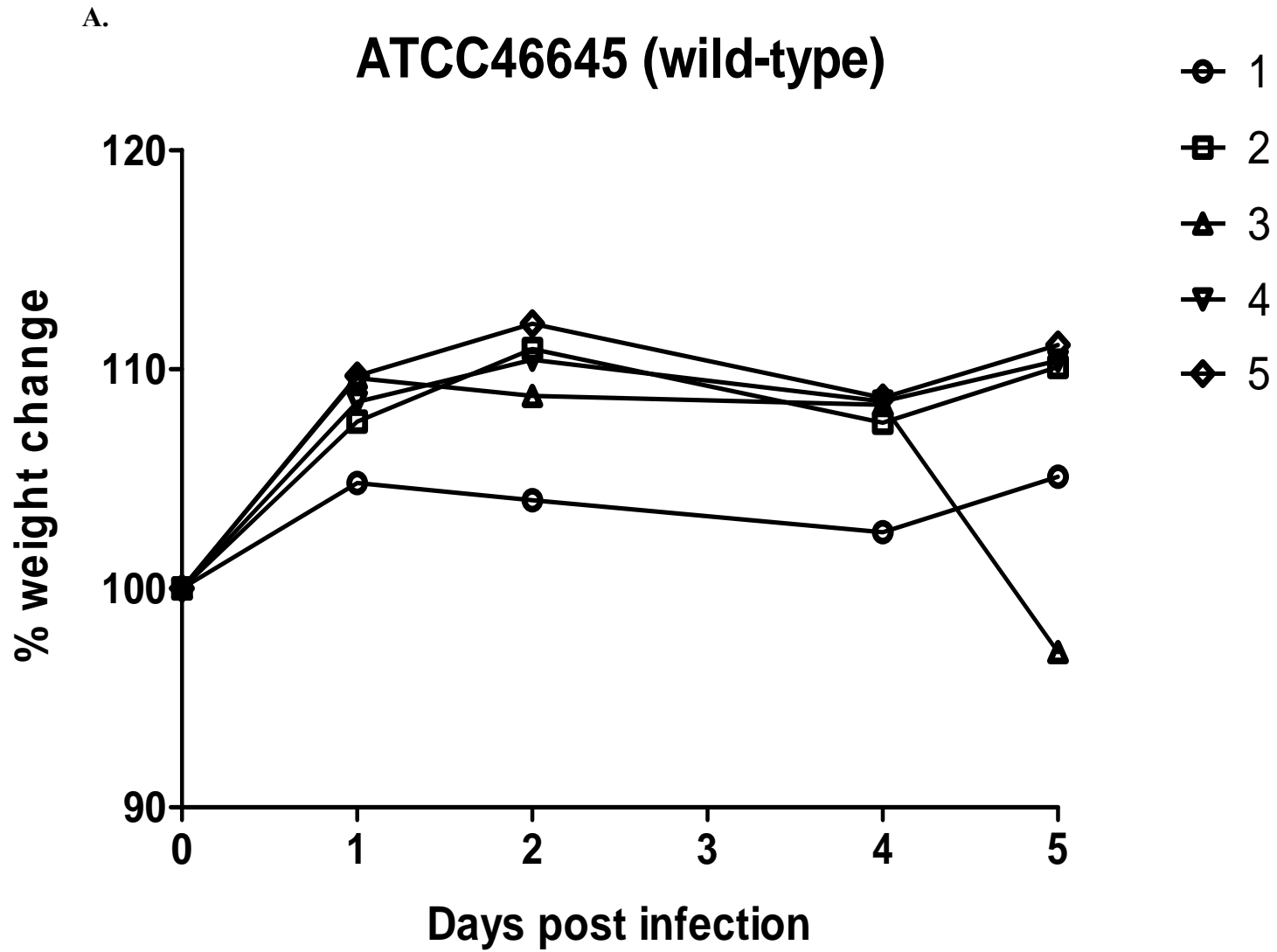
3.3.11.2 Deletion of *A. fumigatus pes3* leads to increased virulence in a Murine Hydrocortisone Acetate (HCA) Immunocompromised model of Invasive Aspergillosis (IA).

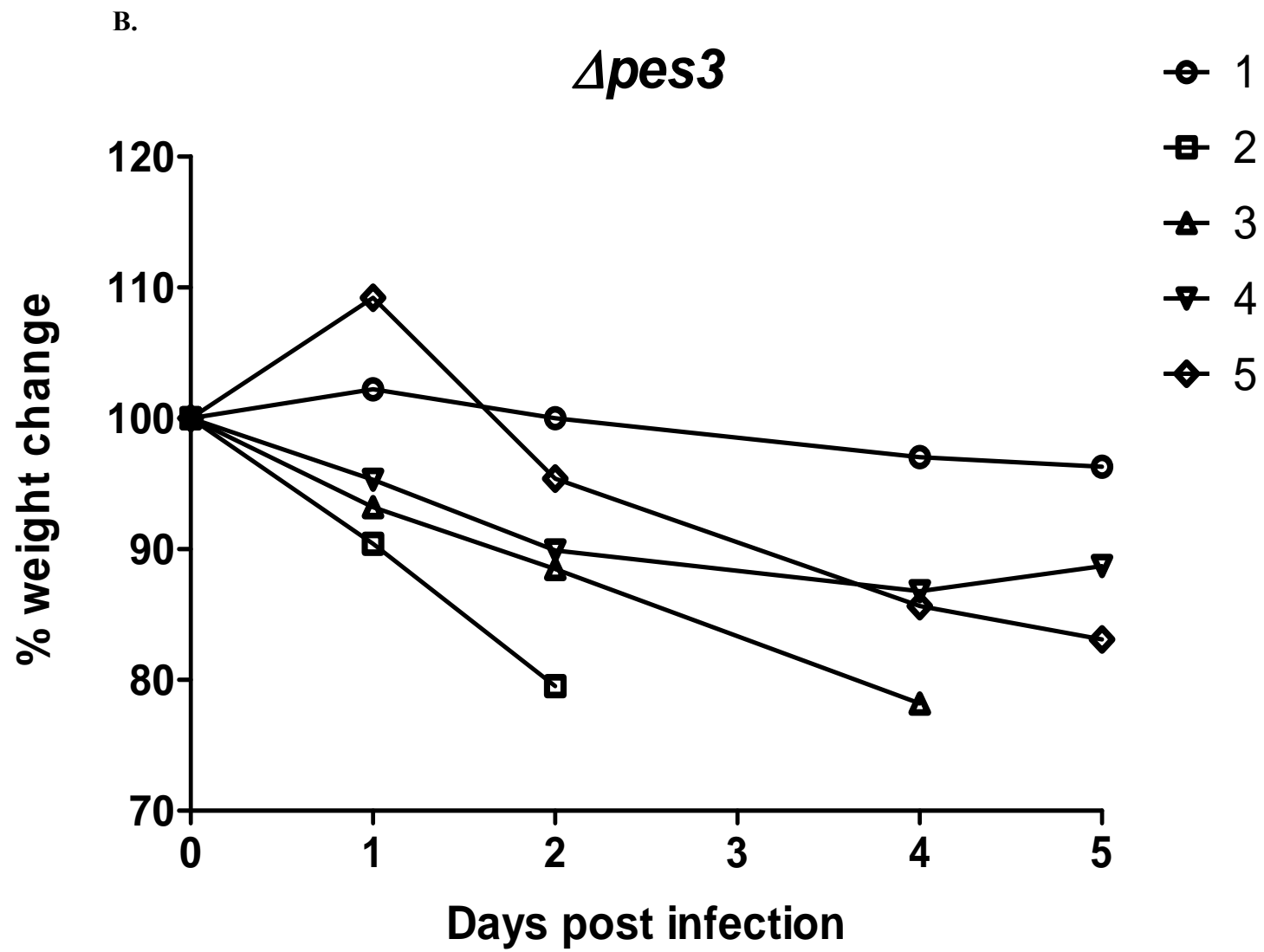
Mice were immunosuppressed with hydrocortisone acetate (HCA) as described (Section 2.2.11), and were infected with conidia (10^4) of either *A. fumigatus* wild-type (ATCC 46645) or $\Delta pes3$ and weights of the animals were recorded daily as a measure of health in this model. The experiment took place over a period of 5 days. Animals that dropped below 20 % of their starting weight before the end of the infection were culled, and were regarded as having succumbed to infection. The weight data for each strain in the HCA model is given in Figure 3.19. The $\Delta pes3$ strain exhibits increased virulence in this model, as observed by weight loss in these animals, and two animals exhibited > 20 % weight loss by day 4 of the infection; animal 2 at day 2 and animal 3 at day 4. These animals were culled. Every animal infected with $\Delta pes3$ exhibited some weight loss over the course of the infection. Animals infected with wild-type displayed moderate fluctuations in weight during the infection, but none of them dropped below 20 % of their starting weight (Figure 3.19). The mean weights of animals at day 5 of the infection were significantly lower for the *A. fumigatus* $\Delta pes3$ infection group (93.00 ± 2.5 % of starting weight) than the wild-type counterpart (106.2 ± 1.62 % of starting weight) ($p < 0.01$). As a control for this experiment, mice ($n = 5$) were HCA treated, and inoculated with conidia (10^4) of an *A. fumigatus* para-aminobenzoic (PABA) acid auxotroph (referred to as *A. fumigatus* H515) which is unable to germinate in the murine lung (Brown *et al.*, 2000). Weights for animals in the H515 group are also shown in Figure 3.19. Animals in this group remained at a steady weight over the course of the infection.

In addition to weight loss determination, fungal burden was assessed in the lungs of infected animals as a measure of fungal virulence. Lungs of infected animals were isolated

at 4 days post-infection and genomic DNA was extracted from homogenised tissue. From these samples the fractions of fungal DNA, corresponding to the fungal burden in the respective organ, were determined by quantitative PCR by amplifying the fungal beta-tubulin (BT) gene product and comparing this to the murine actin gene product (Bergmann *et al.*, 2009; Timothy Cairns, Imperial College London – personal communication) (Figure 3.20). In this assay, the cycle threshold (Ct) values are calculated for each specimen, and normalised to give a value corresponding to Ct fungal BT/ Ct murine actin. A lower value indicates a higher fungal: murine DNA ratio, because the higher the concentration of fungal DNA, the lower the cycle threshold value for BT, and therefore increased fungal burden. This analysis revealed a higher fungal burden in the lungs of animals infected with $\Delta pes3$ compared to wild-type ($p = 0.02$), as indicated by a higher fungal: murine DNA ratio (Figure 3.20). There was a large difference between the fungal burden in mice challenged with the negative control H515 strain compared to wild-type ($p = 0.03$) or $\Delta pes3$ ($p = 0.03$), as expected, since this strain is unable to germinate in the murine lung.

In summary, the hypervirulent phenotype observed for $\Delta pes3$ in the HCA model is associated with a reduction in weight loss and an increase in fungal burden in the murine lung (Figures 3.19 and 3.20).





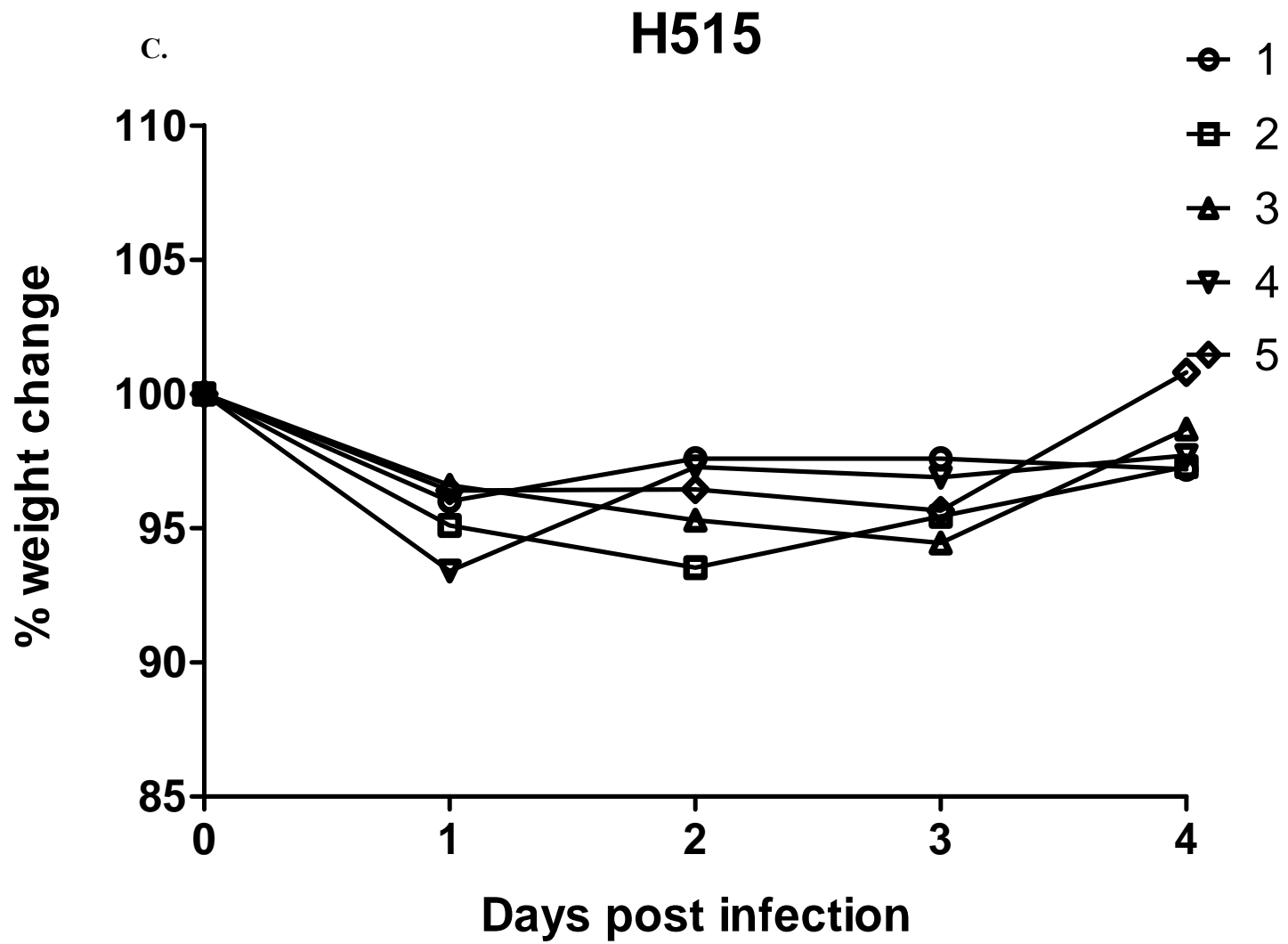


Figure 3.19. *A. fumigatus* $\Delta pes3$ is more virulent than wild-type in a HCA immunocompromised model of IA.

Immunosuppressed animals ($n = 5$) were infected with either wild-type or $\Delta pes3$ and weight was measured daily. A strain unable to germinate in the murine lung (H515) was included as a negative control in this experiment. Shown are the weight data for infected animals in each group; wild-type (A), or $\Delta pes3$ (B), or control group (C). The weight was recorded as a % of the original starting weight, whereby weight gain is $> 100\%$, and weight loss is $< 100\%$. The weight for each of the 5 animals in each group is displayed. Animals infected with $\Delta pes3$ exhibited a greater weight loss compared to wild-type over the course of the experiment, and two animals were culled early due to severe weight loss (animal 2 and animal 3).

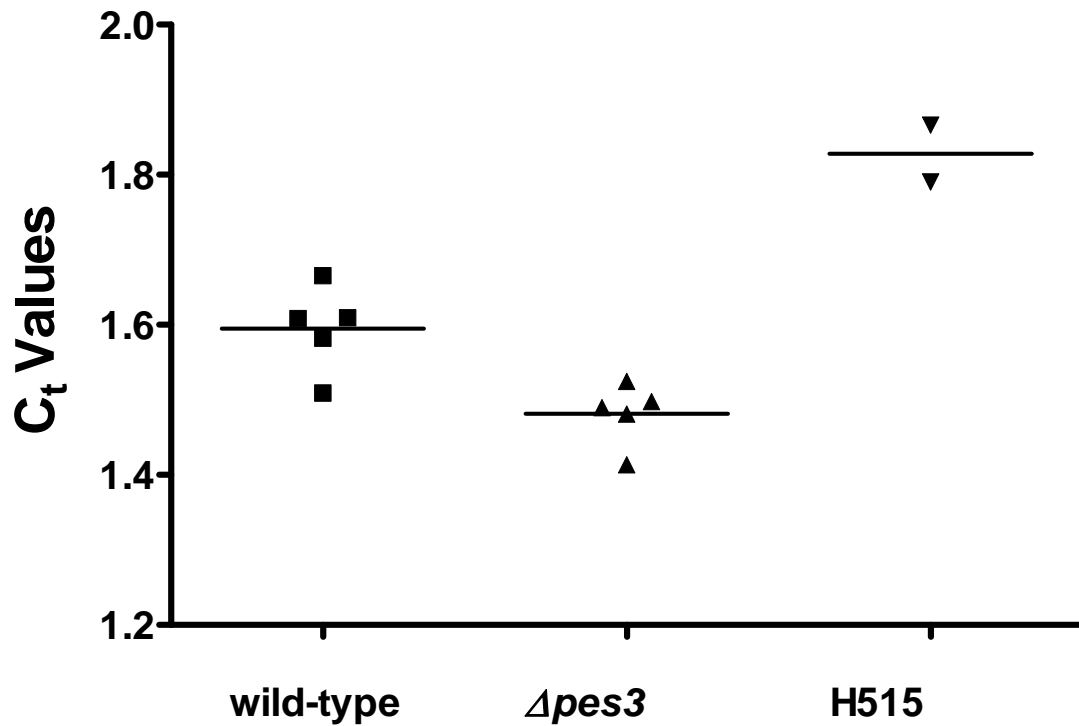
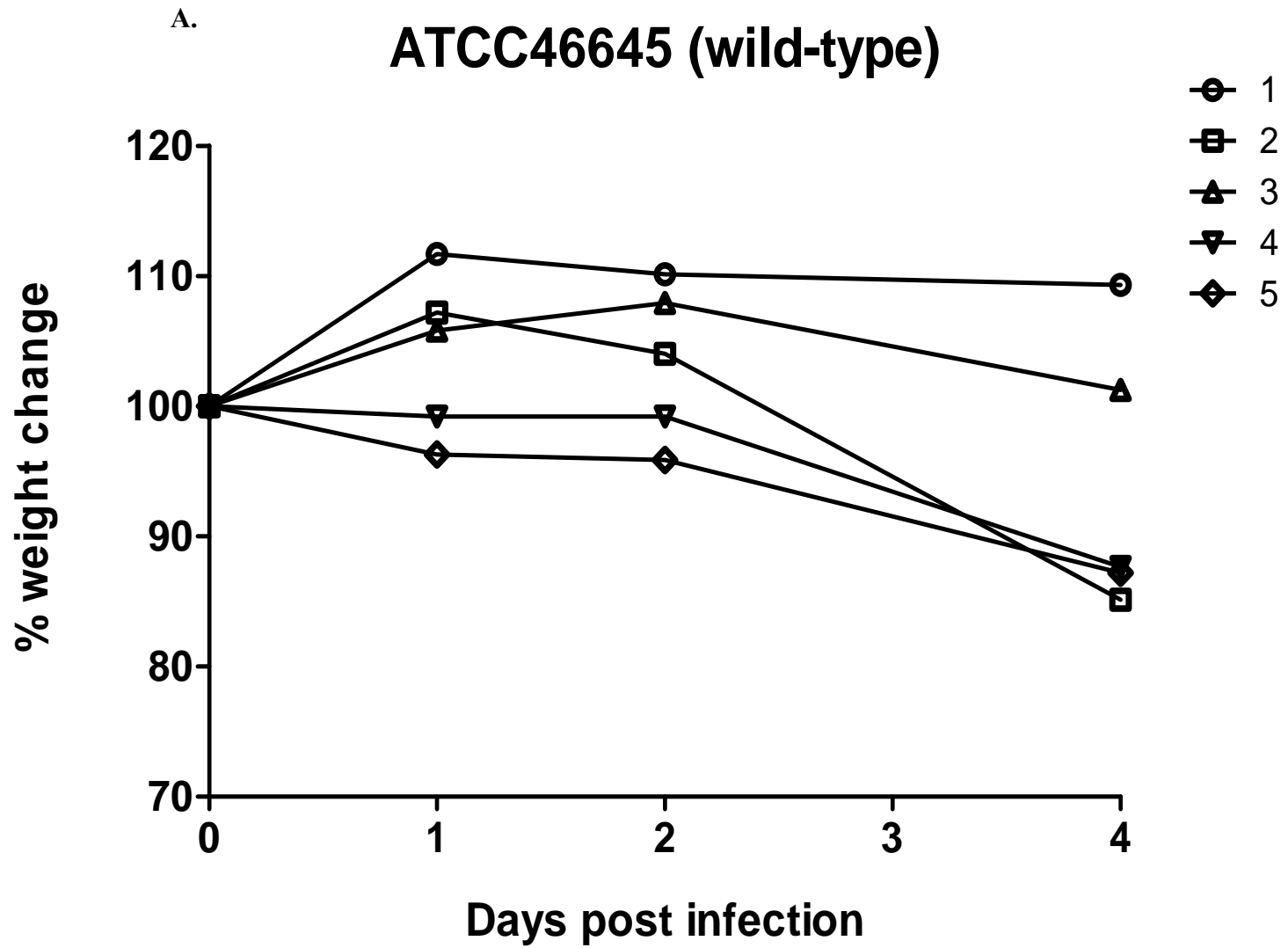


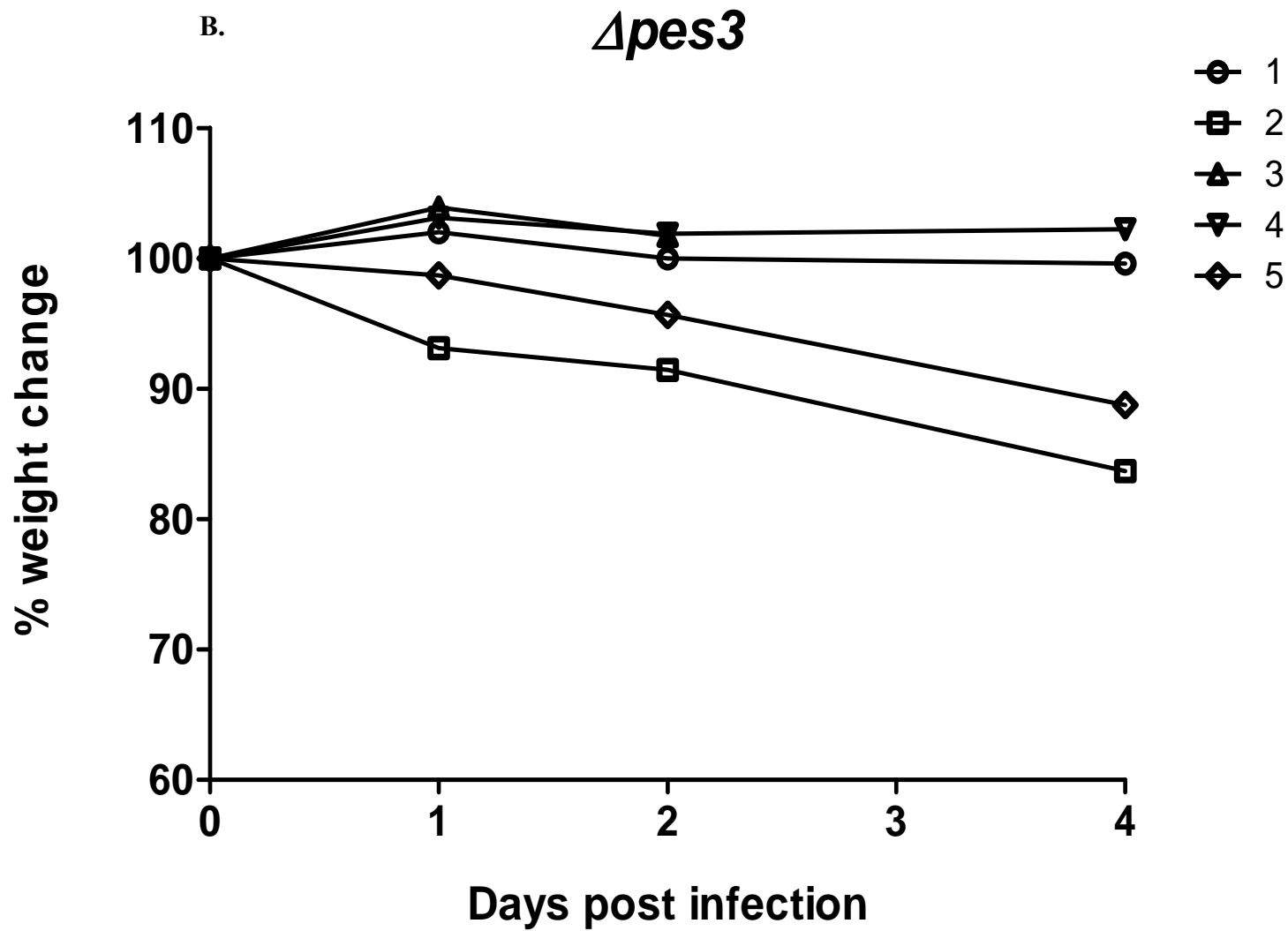
Figure 3.20. Fungal burden in the murine lung following infection in the HCA model of IA.

The threshold cycle values (C_t) from qPCR performed on DNA extracted from corresponding lung tissues of infected animals are given. The values shown represent C_t fungal BT/ C_t murine actin (X – axis). The lungs of animals infected with $\Delta pes3$ display a greater fungal burden than those infected with wild-type, as observed by a lower C_t value for $\Delta pes3$ ($p = 0.02$). The fungal burden associated with the negative control (H515) was significantly lower than for all other strains ($p = 0.03$).

3.3.11.3 The deletion of *pes3* within *A. fumigatus* does not affect virulence in a murine neutropenic model of Invasive Aspergillosis (IA).

Neutropenic mice ($n = 5$ for each strain) were infected with conidia (10^4) of wild-type, $\Delta pes3$, or H515 strains of *A. fumigatus* and weight of the animals was monitored daily as in the HCA model. In this model of IA, there is no difference in weight between animals infected with either wild-type or $\Delta pes3$. Animals in the wild-type and $\Delta pes3$ group show similar weights over the course of the experiment (Figure 3.21). Weight loss was observed for animals in both groups by day 5 of the experiment, but the overall trends in weight loss were the same for both groups. Animals in the negative control group (H515) showed no overall weight loss or gain, with all weights remaining more or less stationary over the course of the experiment (Figure 3.21). Fungal burden was also assessed in the neutropenic mice following infection, and in agreement with the weight loss data, there appears to be no difference in fungal burden between animals infected with wild-type or $\Delta pes3$ ($p = 0.5204$) (Figure 3.22). Taken together, these data indicate that there is no attenuation of virulence or hypervirulence associated with *A. fumigatus* $\Delta pes3$ in neutropenic mice.





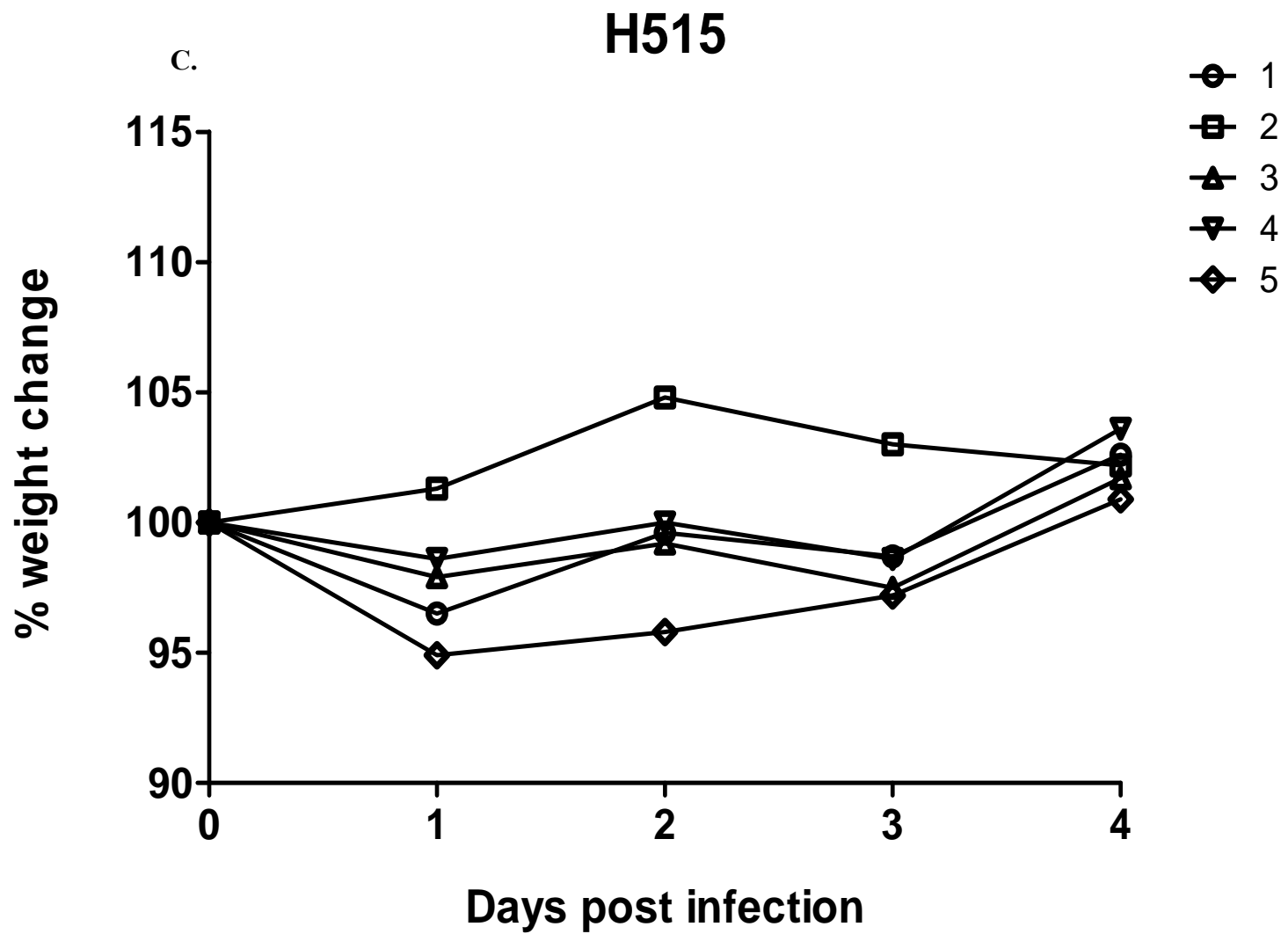


Figure 3.21. *A. fumigatus* $\Delta pes3$ is equally as virulent as wild-type in a neutropenic model of IA.

Neutropenic animals ($n = 5$) were infected with either wild-type or $\Delta pes3$ and weight was measured daily. *A. fumigatus* H515 (a strain unable to germinate in the murine lung) was included as a negative control in this experiment. The weight data for infected animals in each group is shown; wild-type (A), or $\Delta pes3$ (B), or control group (C). The weight was recorded as a % of the original starting weight, whereby weight gain is $> 100\%$, and weight loss is $< 100\%$. Overall, animals infected with *A. fumigatus* wild-type or $\Delta pes3$ exhibited moderate weight loss over the course of the experiment. However, no differences in weight loss or gain were observed for animals infected with either strain, indicating equal virulence of both strains in a neutropenic model of IA. Animals in the control group (H515) showed no net weight loss or gain, and weights were close to the starting weight by day 5 of the experiment. The weight for each of the 5 animals in each group is displayed.

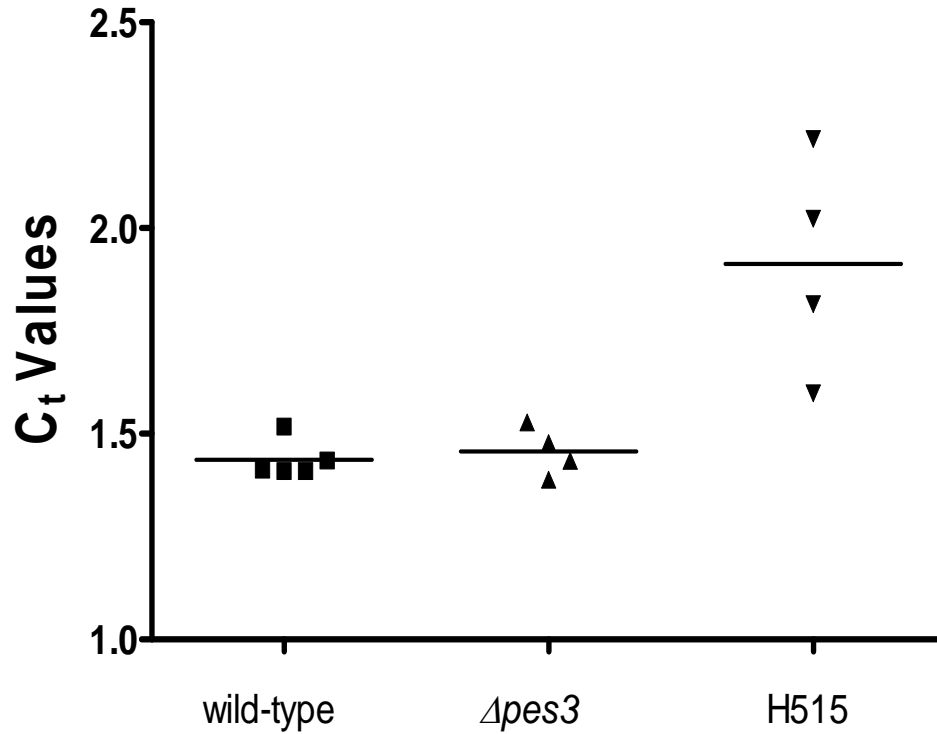


Figure 3.22. Fungal burden in the murine lung following infection in the neutropenic model of IA.

The threshold cycle values (C_t) from qPCR performed on DNA extracted from corresponding lung tissues of infected animals are given. The values shown represent C_t fungal BT/ C_t murine actin (X – axis). The lungs of animals infected with $\Delta pes3$ display a similar fungal burden to those infected with wild-type, as observed by a lower C_t value for $\Delta pes3$ ($p = 0.5204$). The fungal burden associated with the negative control (H515) was significantly lower than for all other strains ($p = 0.04$).

In summary, the data presented here shows that *A. fumigatus* $\Delta pes3$ is more virulent than wild-type in both an insect and animal model of IA. Initially, virulence testing was performed using the *Galleria* wax moth larvae as a model, and measuring larval survival as an indicator of virulence. In this model, $\Delta pes3$ led to a dramatic reduction in survival compared to wild-type and this reduction in survival was observed as early as 24 hr following infection, and difference in survival was maintained throughout the course of the experiment ($p < 0.001$). Virulence was subsequently investigated in two murine models of IA, a hydrocortisone acetate (HCA) immunosuppressed model, and a neutropenic model. Using weight loss as an indicator of virulence, it was revealed that *A. fumigatus* $\Delta pes3$ is more virulent than wild-type in the HCA model compared to wild-type with 2 animals infected with $\Delta pes3$ being sacrificed before the end of the experiment due to severe weight loss ($> 20\%$ of starting weight). There is an obvious increase in weight loss in animals infected with $\Delta pes3$ compared to wild-type in this model and this coincided with increased fungal burden in the lungs of $\Delta pes3$ infected mice ($p = 0.02$). In contrast, no difference in weight loss or fungal burden was observed between groups of animals infected with either *A. fumigatus* wild-type or $\Delta pes3$ in a neutropenic model, with overall weights remaining similar for both groups, and similar fungal burden in the lungs in animals infected with either strain.

3.3.12 *A. fumigatus* $\Delta pes3$ is immunologically silenced compare to wild-type.

It was decided to investigate if *A. fumigatus* $\Delta pes3$ manifested as immunologically silenced or less immunogenic upon inoculation in comparison to wild-type in order to explain the observed hypervirulence. In order to investigate this, a series of experiments were carried out whereby murine bone-derived macrophages (BMMØS) were co-incubated with *A. fumigatus* wild-type or $\Delta pes3$ for 18 hr and cytokine production was measured as

described (Section 2.2.13). In all cell signalling experiments, known TLR ligands were included and a list of these is presented in Table 3.5. BMMØS were usually stimulated with fungal cells (either germlings or conidia) at a ratio of 5:1 fungal cells: macrophages. The set-up of the immune signalling experiments is represented schematically in Figure 3.23.

Less TNF- α was produced in response to $\Delta pes3$ germlings which had been germinating for 9 hr, prior to incubation with macrophages, in comparison to the wild-type counterpart, with approximately 40 % less TNF- α released from BMMØS when incubated with $\Delta pes3$ (Figure 3.24). TNF- α was also measured from BMMØS exposed to *A. fumigatus* conidia, either live or heat-killed. No overall difference was observed between the levels of TNF- α induced by wild-type and $\Delta pes3$ exposure regardless of whether conidia were alive or dead (Figure 3.24). Similarly, less IL-6 (68 % reduction) was produced by BMMØS in response to $\Delta pes3$ germlings (pre-incubated for 9 hr) and no differences were observed in the response of BMMØS to conidia of either strain, with respect to IL-6 (Figure 3.25). Production of IL-6 by BMMØS was also measured in response to *A. fumigatus* culture supernatant (SN) in which conidia of wild-type and $\Delta pes3$ had been germinating for either 6 hr or 9 hr. In all cases, no IL-6 was produced in response to SN, with less than < 100 pg/ml for all samples (Figure 3.25).

The levels of RANTES (CCL5) and an anti-inflammatory cytokine IL-10 were measured following stimulation of BMMØS, in order to get a wider view on the extent of the reduced immune response towards $\Delta pes3$. As observed for both TNF- α and IL-6, the production of RANTES and IL-10 were also reduced upon exposure of BMMØS to *A. fumigatus* $\Delta pes3$ compared to wild-type (Figure 3.26). A 25 % reduction in RANTES was observed when macrophages were co-incubated with $\Delta pes3$ germlings which had been germinated for 9 hr prior to co-incubation. A 10 % reduction in IL-10 was observed following macrophage exposure to $\Delta pes3$ germlings which had been germinated for 9 hr.

Table 3.5. Known TLR ligands used in this study.

Ligand	Toll Like Receptor (TLR) Activated	Final Concentration
LPS	TLR 4	100 ng/ml
Pam-2-cys	TLR 2	1 µg/ml
Poly IC	TLR 3	10 µg/ml

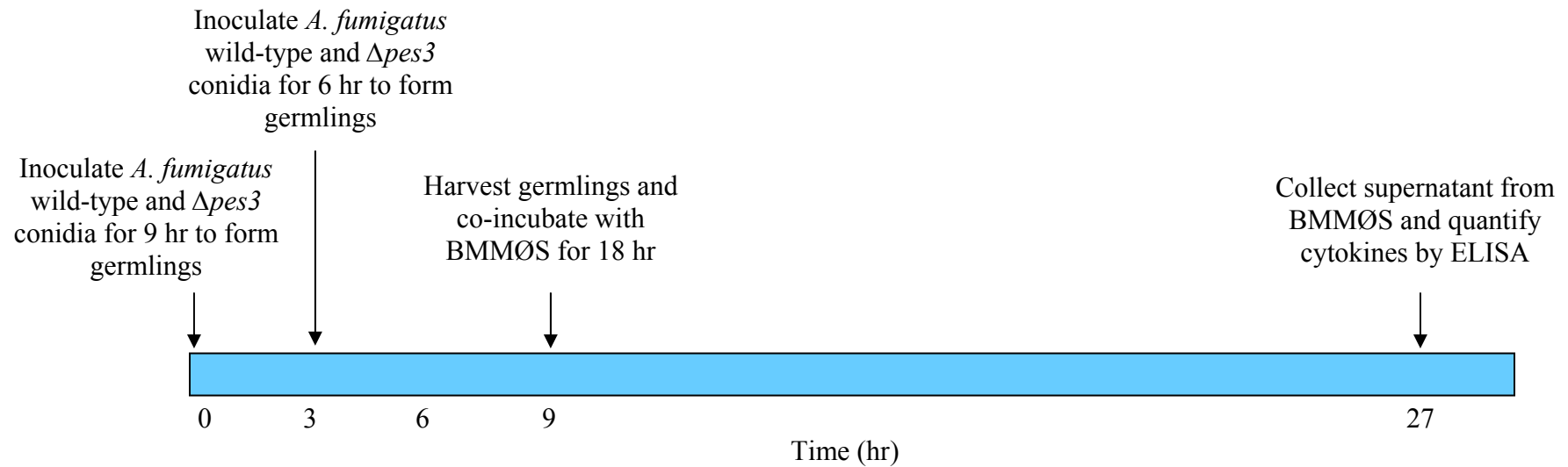
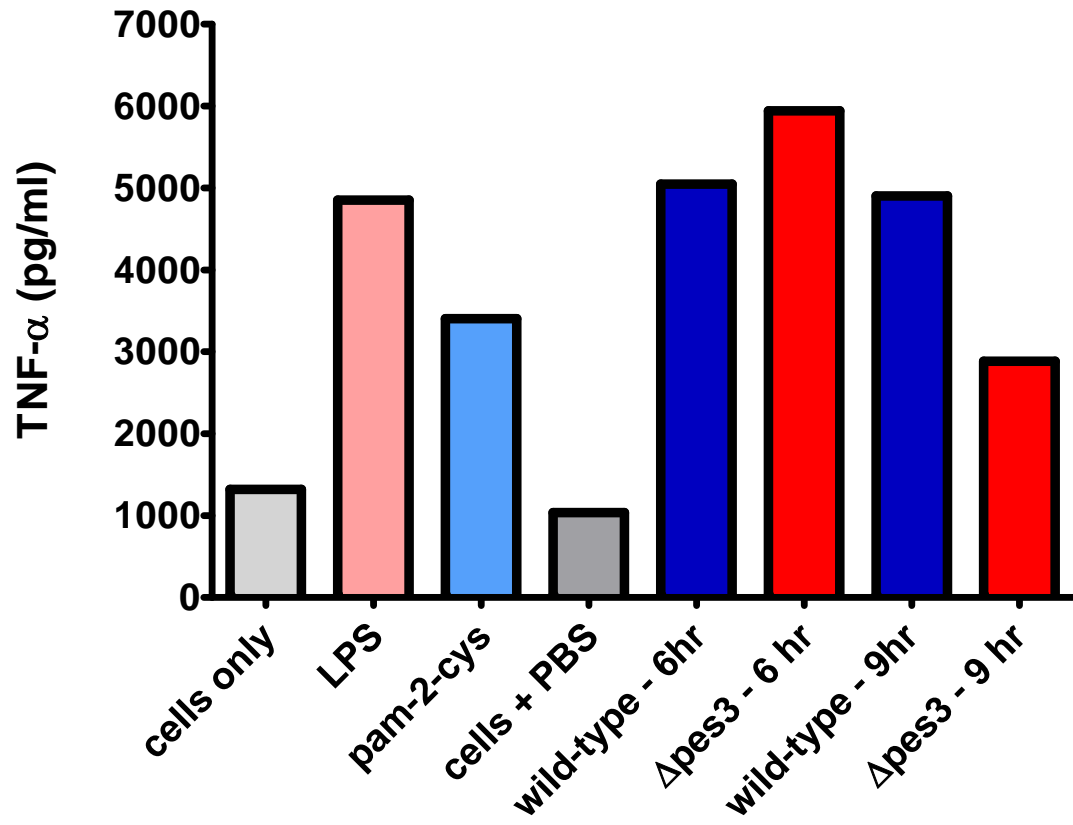


Figure 3.23. Schematic representation time-line for immune signalling experiments.

Conidia of *A. fumigatus* wild-type (ATCC 46645) and $\Delta pes3$ were harvested and used to inoculate cultures of AMM in order to allow germling formation as described (Section 2.2.13.3). Conidia were allowed to germinate for either 6 hr or 9 hr after which an aliquot of the culture corresponding to 5×10^6 conidia was added to murine BMMØS and co-incubated for 18 hr. Supernatants were then collected from cells, and cytokines of interest were determined by ELISA.

A.



B.

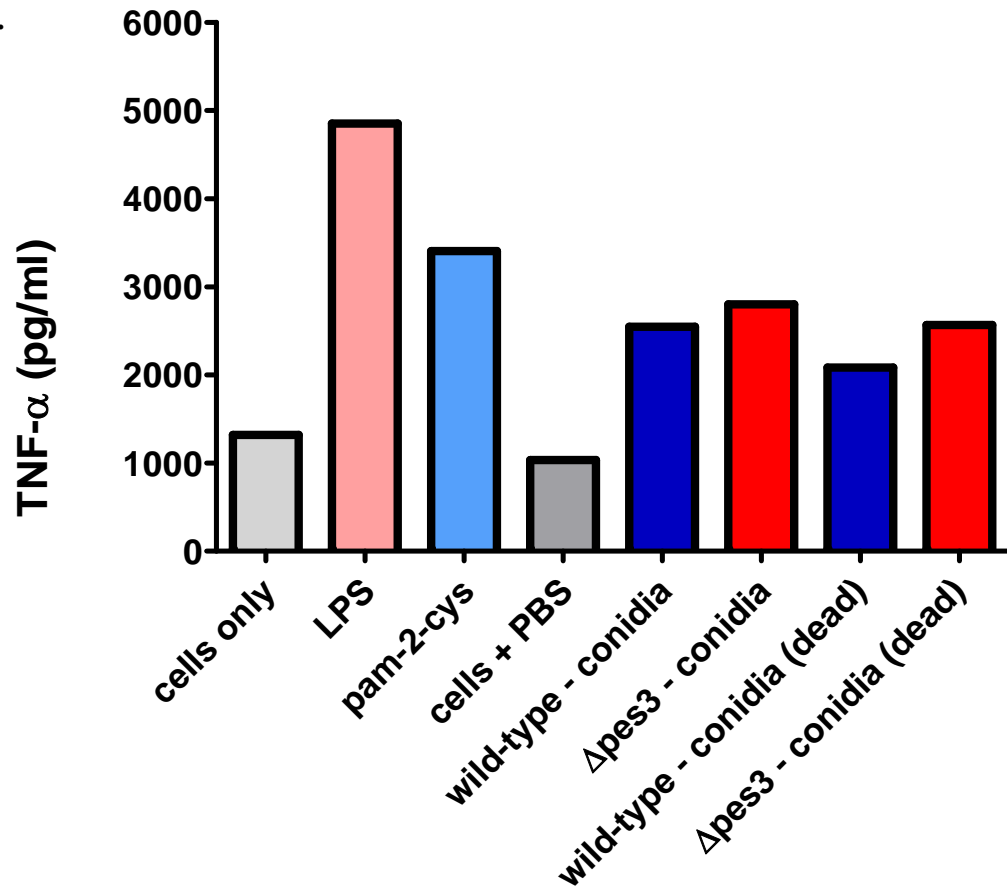
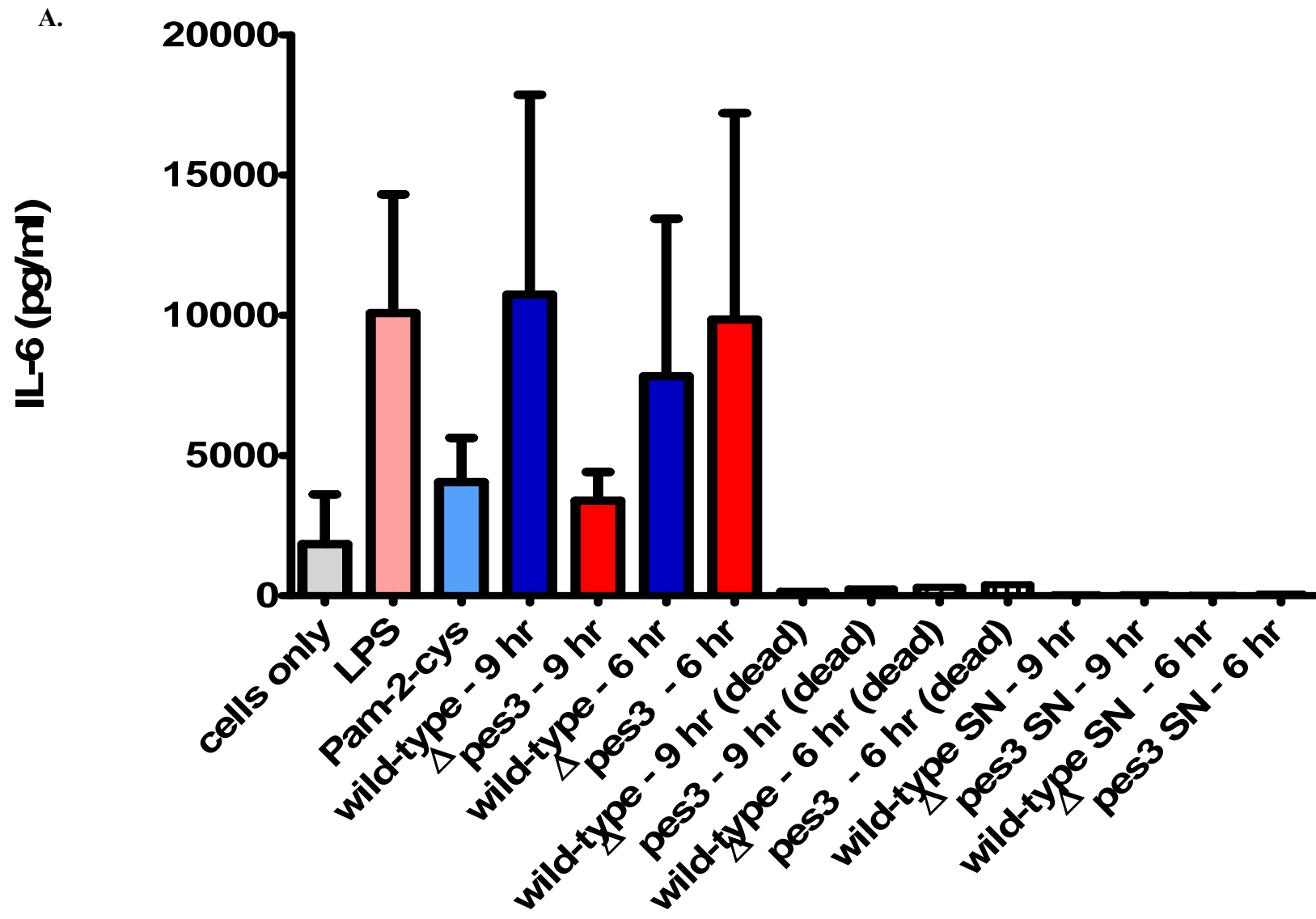


Figure 3.24. ELISA determination of TNF- α released from BMMØS following co-incubation with *A. fumigatus* germlings and conidia.

A. Less TNF- α is produced when murine BMMØS are exposed to *A. fumigatus* $\Delta pes3$ germlings (2,900 pg/ml) in comparison to wild-type germlings (4,900 pg/ml) following a 9 hr germination period of conidia prior to 18 hr co-incubation with BMMØS. *A. fumigatus* germlings following 6 or 9 hour germination from conidia were added to BMMØS at a ratio of 5:1. Cells are responsive towards the TLR 4 and TLR 2 ligands LPS and pam-2-cys respectively. Data is representative of two independent experiments.

B. No overall differences between the level of TNF- α produced by BMMØS was observed in response to *A. fumigatus* wild-type or $\Delta pes3$, whether conidia were live or dead. Conidia of wild-type or $\Delta pes3$ (1×10^7) were added to BMMØS at 5: 1 ratio. Data is representative of two independent experiments.



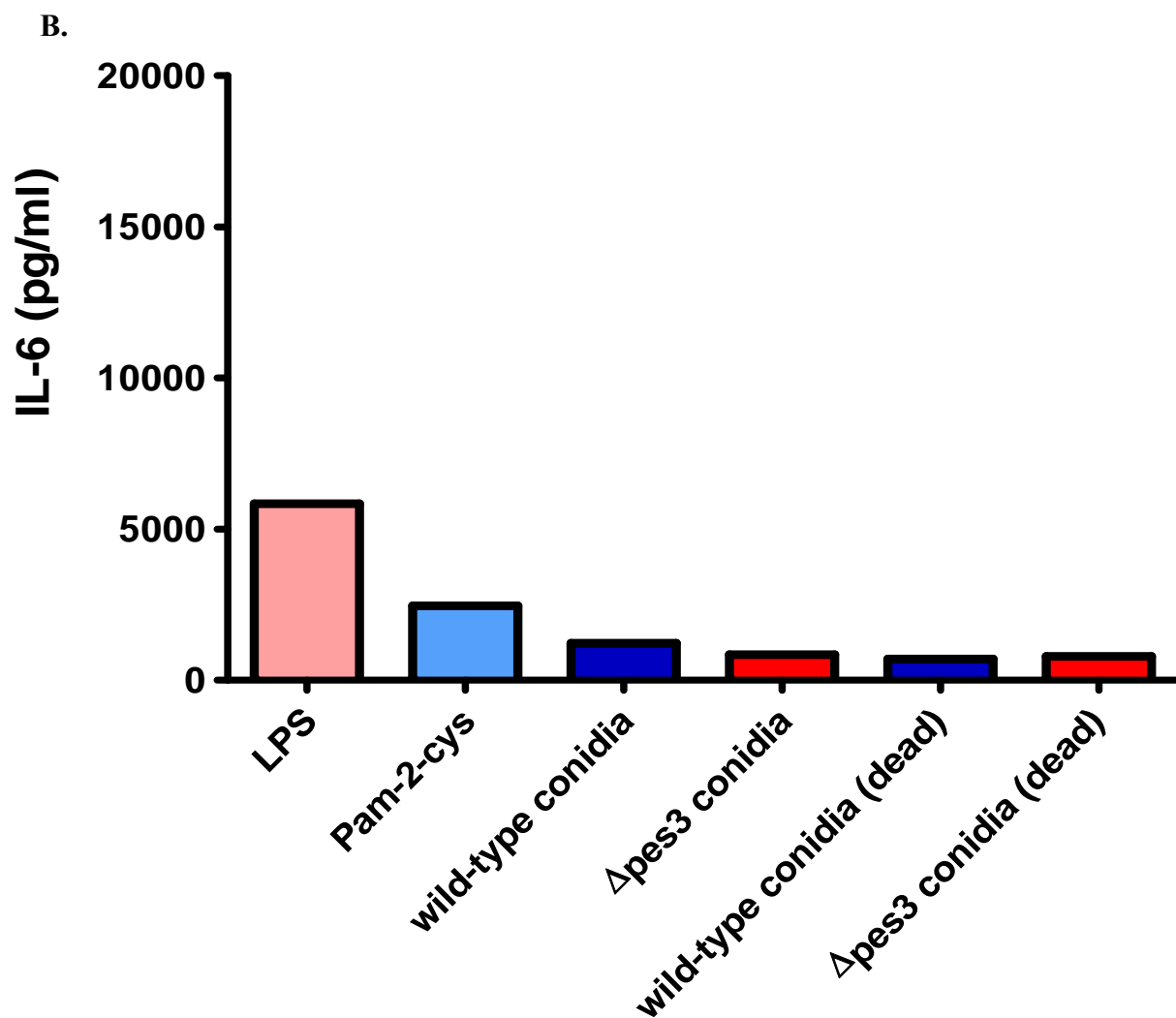


Figure 3.25. IL-6 production from BMMØS is reduced following exposure to *A. fumigatus* $\Delta pes3$ germlings.

A. BMMØS produce less IL-6 (68 % reduction) upon exposure to *A. fumigatus* $\Delta pes3$ germlings compared to wild-type, when macrophages are exposed to germlings which had undergone 9 hr germination prior to stimulation of cells. BMMØS produced 3,400 pg/ml IL-6 upon exposure to *A. fumigatus* $\Delta pes3$ in comparison to wild-type (10,100 pg/ml). The mean \pm standard error of two experiments is shown. Cells are responsive towards the TLR 4 and TLR 2 ligands LPS and pam-2-cys respectively. Cells did not produce IL-6 in response to dead hyphae of either wild-type or $\Delta pes3$, and similarly did not produce IL-6 in response to *A. fumigatus* culture supernatant (SN) of either strain, following germination of conidia of each strain for either 6 hr or 9 hr in AMM media.

B. Conidia of wild-type or $\Delta pes3$ (1×10^7) were added to BMMØS and incubated for 18 hr, after which IL-6 levels were measured by ELISA. No overall differences between the level of cytokine produced in response to wild-type or $\Delta pes3$, whether conidia were live or dead. Data is representative of two independent experiments.

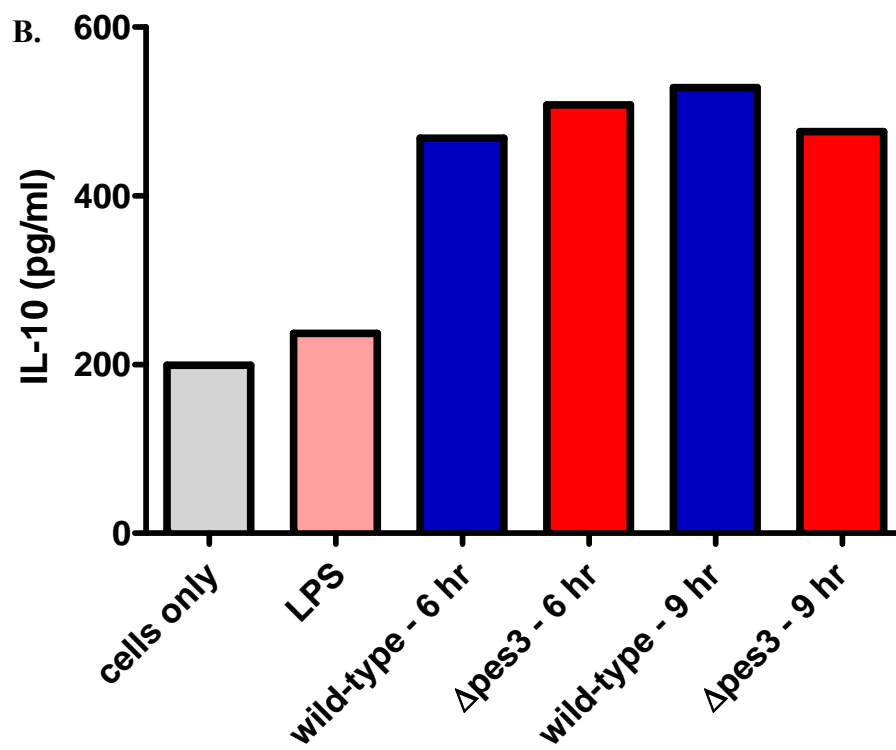
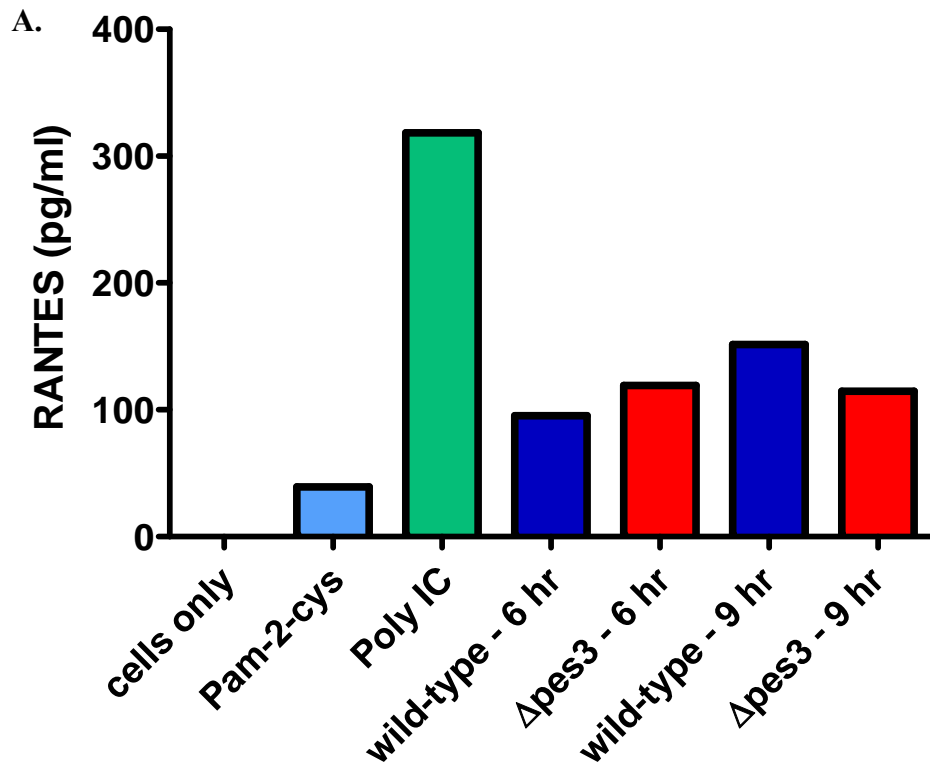


Figure 3.26. RANTES (CCL5) and IL-10 production by BMMØS is reduced upon exposure *A. fumigatus* $\Delta pes3$ compared to wild-type.

A. BMMØS produce less RANTES (24 % reduction) upon exposure to *A. fumigatus* $\Delta pes3$ germlings compared to wild-type, when macrophages are exposed to germlings which had undergone 9 hr germination prior to stimulation of cells. BMMØS produce 152 pg/ml IL-6 upon exposure to *A. fumigatus* $\Delta pes3$ in comparison to wild-type (115 pg/ml). Data is representative of two independent experiments.

B. BMMØS produce less IL-10 (10 % reduction) upon exposure to *A. fumigatus* $\Delta pes3$ germlings compared to wild-type, when macrophages are exposed to germlings which had undergone 9 hr germination prior to stimulation of cells. BMMØS produce 507 pg/ml IL-10 upon exposure to *A. fumigatus* $\Delta pes3$ in comparison to wild-type (528 pg/ml). Data is representative of two independent experiments.

3.4 Discussion.

This work has confirmed that *pes3* is expressed in *A. fumigatus* ATCC 46645 under a range of growth conditions. *pes3* was subsequently disrupted and restored. Comparative metabolite profiling was undertaken in order to identify a peptide that might be encoded by the NRP synthetase, Pes3. Despite thorough metabolite profiling using conditions in which *pes3* was found to be expressed, no differences were detected between *A. fumigatus* wild-type and $\Delta pes3$, strongly suggesting that Pes3 does not encode a secreted peptide, or one that is stored intracellularly. This hinted that Pes3 encodes a peptide with a structural role in the fungus. Extensive phenotypic revealed that *pes3* is involved against protection against voriconazole toxicity ($p < 0.001$), suggesting an alteration in the cell wall of *A. fumigatus* $\Delta pes3$ rendering it more susceptible to voriconazole. This phenotype supports the hypothesis that Pes3 encodes a structural peptide within *A. fumigatus*. Extensive phenotypic analyses convincingly eliminated a role for *pes3* in siderophore biosynthesis and oxidative stress resistance, despite NRP synthetases previously reported to have roles in these pathways. Surprisingly, *A. fumigatus* $\Delta pes3$ is more virulent compared to wild-type in both insect and mammalian models of infection, and this is accompanied by an increased fungal burden in animals infected with $\Delta pes3$ compared to wild-type. This observation suggested that $\Delta pes3$ was immunologically silenced compared to wild-type, which explains the reduced fungal clearance observed in lungs of infected animals. Immune signalling experiments revealed that murine macrophages produce less pro- and anti-inflammatory cytokines when exposed to *A. fumigatus* $\Delta pes3$ compared to wild-type. Reduced immune responses towards *A. fumigatus* $\Delta pes3$ further supports the hypothesis that *pes3* plays a structural role in *A. fumigatus*, since immune recognition of *A. fumigatus* is mediated by recognition of fungal cell wall components by pattern recognition receptors (PRRs) of the innate immune system.

pes3 transcripts were detected at both 24 and 48 hr following liquid culture in Czapek's broth and AMM media. Expression of *pes3* was also observed following 48 hr growth in Czapek's broth in *A. fumigatus* Af293 (Cramer *et al.*, 2006b). The housekeeping gene used by Cramer *et al.*, (2006), was actin, and *pes3* (referred to as NRPS-8 in that study) was found to be expressed at a low relative abundance in comparison to actin (< 10 %). The data presented here also shows that *pes3* has a low relative abundance (10 %) in comparison to the housekeeping gene, *calmodulin (calm)* (Burns *et al.*, 2005). Cramer *et al.*, (2006) also reported a high level of *pes3* expression in ungerminated spores relative to the housekeeper gene, actin (> 60 % relative abundance), and this pattern of expression was unique in comparison to all the other NRP synthetase genes examined in *A. fumigatus*. As the overall starting goal of this work was to identify a peptide that may be the product of the Pes3 NRP synthetase, it was necessary to confirm the expression of *pes3* in the strain of choice. NRP synthetase and other secondary metabolite encoding genes are often not expressed under standard laboratory conditions and may require certain triggers for their activation (Schroeckh *et al.*, 2009). Knowing that *pes3* was expressed in the ATCC 46645 strain was sufficient to further characterise the gene in this strain.

pes3 was successfully disrupted by a bipartite gene deletion strategy (Nielsen *et al.*, 2006), designed to delete 1.5 kb of the 25 kb gene. This resulted in the generation of a mutant strain ($\Delta pes3$) and *pes3* disruption was confirmed by Southern blotting and gene expression analysis. Subsequently, complementation of *pes3* was undertaken, to restore the locus. Strategies that are commonly used to complement gene deletions involve amplifying the entire gene of interest by PCR, cloning it into a plasmid vector which usually contains a resistance cassette for selection and transforming this construct (either linearised or intact) into protoplasts of the recipient strain (Personal communication, Dr. Markus Schrettl). This method can be used to replace genes (either targeted or ectopically) which have been

partially or completely deleted, and can be useful when the gene of interest is of a suitable size for amplification by PCR. This approach has been reported recently for the complementation of *A. fumigatus dvrA* (AFUA_3G09820) (Ejzykiewicz *et al.*, 2010).

A similar strategy was used to complement the *A. fumigatus* glucokinase and hexokinase encoding genes; *glkA* and *hskA* respectively, whereby the entire genes were amplified, cloned into a vector, subsequently fused to a resistance cassette, and the entire construct was transformed into protoplasts of the recipient strain (Fleck & Brock, 2010). In these cases the genes of interest were usually about 2 kb in size, making them suitable for whole amplification by PCR. However, to alleviate problems in attempting to amplify a 25 kb construct for *pes3*, a strategy was designed to specifically replace only the region that was deleted in $\Delta pes3$. The advantage of this is to ensure a specific targeted replacement of *pes3*. The strategies employed are summarised (Table 3.1) and eventually successful complementation of *pes3* was achieved. A bipartite replacement strategy was employed, whereby two overlapping DNA fragments, flanking the *pes3* disrupted region were generated by PCR. These were simultaneously transformed into protoplasts of $\Delta pes3$ along with a plasmid conferring phleomycin resistance (Pan 8.1), to allow for selection of transformed colonies. This complementation strategy represents a unique approach towards reconstituting deleted genes, and is a very useful way for restoring large coding regions which have undergone partial deletion, and overcomes the difficulty in amplifying very large genes by PCR. Complementation of *pes3* was confirmed thoroughly by Southern blotting, gene expression analysis, and restriction mapping of part of the *pes3* locus.

Comparative metabolite profiling of *A. fumigatus* wild-type and $\Delta pes3$ by RP-HPLC was undertaken in order to identify a specific non-ribosomal peptide (NRP) produced by Pes3. Extensive comparative analysis was performed at both NUIM, and with a collaborating group at the Danish Technical University. A wide range of growth

conditions, and metabolite extraction methods were explored. In all cases, the metabolite profiles generated for wild-type and mutant were identical. The plug extraction method used in this study has been found to be sufficient to determine all secondary metabolites reported to be produced as well as some previously unknown metabolites from 395 fungal isolates (Smedsgaard *et al.*, 1997). Furthermore, this work included comparative analysis between wild-type and $\Delta pes3$ using culture conditions in which *pes3* expression was detected in this study and others (Cramer *et al.*, 2006b). Comparison of wild-type vs. $\Delta pes3$ ungerminated spores, where *pes3* expression was found to be most abundant (Cramer *et al.*, 2006b) was also included in this study, and this also revealed no differences in metabolite profiles. Taken together, these findings imply that the NRP synthetase, Pes3, does not produce either a secreted or an intracellularly stored metabolite in *A. fumigatus*.

This is a unique finding for an NRP synthetase, as to date, documented NRP synthetase-encoded peptides can usually be found in the culture supernatant (or located intracellularly) of the producing organism under specific culture conditions. For example, *A. fumigatus* uses the NRP synthetase encoded siderophore, hydroxyferricrocin, to store iron in conidia (Schrettl *et al.*, 2007). The lack of a *pes3* candidate peptide despite extensive metabolite analysis hinted that the Pes3-encoded peptide might be structural in nature, an unusual property for a non-ribosomal peptide. Ergot alkaloids, a family of secondary metabolites of NRP synthetase origin have been found to be associated with *A. fumigatus* conidia (Panaccione and Coyle, 2005), but they were extracted relatively easily by sonication of conidia in methanol (Panaccione and Coyle, 2005). It is highly likely that the Pes3-encoded peptide is more tightly bound to the *A. fumigatus* cell wall, perhaps covalently, as it was not extracted by any of the means used in this study.

A range of phenotypic analyses were performed in order to compare *A. fumigatus* wild-type and $\Delta pes3$, to identify a biochemical role for *pes3*. Since little is known about the

roles of the individual NRP synthetases in *A. fumigatus*, a starting point for investigation was to probe pathways in which NRP synthetases are already known to be involved. Two non-ribosomal peptide synthetases have been proven to play essential roles in siderophore biosynthesis in *A. fumigatus*, namely the genes encoding SidD and SidC (Schrettl *et al.*, 2007; Reiber *et al.*, 2005). A role for Pes3 in this pathway was investigated. Plate assays were performed with various iron conditions; high iron, low iron, and depletion of iron by the addition of an iron chelating compound, BPS, which blocks reductive iron assimilation in *A. fumigatus*. Wild-type and $\Delta pes3$ showed exactly the same growth rate in all conditions tested. Schrettl and co-workers found that in the absence of siderophore mediated iron mobilisation, reductive iron assimilation is absolutely essential for the growth of the fungus in iron starvation conditions (Schrettl *et al.*, 2007). Taking this into account, it is highly likely that the *pes3* mutant is able to produce siderophores, as it can grow normally in the presence of BPS, therefore eliminating a role for Pes3 in the siderophore biosynthesis pathway.

Other phenotypic analyses performed were oxidative stress testing, heavy metal stress testing, and testing with various cell wall damaging agents. The outcomes of these assays are summarised in Table 3.4. Plate assays were carried out to measure radial growth rates of *A. fumigatus* wild-type and $\Delta pes3$ upon exposure to the various stresses. Strains were compared for response to oxidative stress as fungal NRP synthetases have previously been reported to be involved in protection against oxidative stress. *A. fumigatus* Pes1 has been found to confer protection against oxidative stress (Reeves *et al.*, 2006) and NPS6 in the plant pathogen *Cochliobolus heterostrophus*, is involved in both virulence and resistance to oxidative stress (Lee *et al.*, 2005, Oide *et al.*, 2006). Also, Indigoidine, a blue pigment involved in virulence produced by the plant pathogenic bacteria, *Erwinia chrysanthemi*, is produced non-ribosomally, and increases tolerance to oxidative stress in

this species (Reverchon *et al.*, 2002). *A. fumigatus* Pes3 doesn't appear to play a role in protection against oxidative stress, with disruption of *pes3* leading to no alteration in sensitivity towards hydrogen peroxide or menadione. *A. fumigatus* $\Delta pes3$ did exhibit increased resistance to the oxidising agent diamide, with a significant difference between *A. fumigatus* wild-type and $\Delta pes3$ ($p < 0.05$) at 72 hr growth in the presence of diamide (0.1 mM). One possibility is that an altered cell wall in *A. fumigatus* $\Delta pes3$ hinders diamide entering the cell, and so *A. fumigatus* $\Delta pes3$ is exposed to less diamide-induced oxidative stress than wild-type, leading to the increased growth observed. More recently, a mutagenic compound NG-391, produced by a hybrid PKS-NRPS, from the fungal entomopathogen *Metarhizium robertsii*, was described, which appears to play no role in virulence or protection against oxidative stress caused by hydrogen peroxide in this species (Donzelli *et al.*, 2010).

Sensitivity to cell wall damaging and membrane perturbing agents (calcafluor white, congo red, sodium dodecyl sulphate (SDS) or caffeine) was investigated. Congo red and calcafluor white were used following a recent protocol for identification of fungal cell wall mutants (Ram & Klis, 2006). Testing for altered sensitivity to Congo red (CR) and calcafluor white (CFW) is routinely used to identify fungal cell wall mutants (Ram and Klis, 2006). Increased susceptibility to these agents has indicated cell wall defects in many species including *S. cerevisiae*, *C. albicans* (Popolo & Vai, 1998) various *Aspergillus* species (Oka *et al.*, 2005; Shaw & Momany, 2002), and *Cryptococcus neoformans* (Gerik *et al.*, 2005). CR and CFW have been shown to interact with β -linked glucans *in vitro* (Wood, 1980), whereas *in vivo* they have been shown to interact with growing chitin chains (Herth, 1980). Exposure to these cell wall damaging agents has been shown to induce cell wall-related morphological changes, and leads to incomplete mother and daughter cell separation in *S. cerevisiae* (Roncero & Duran, 1985; Vannini *et al.*, 1983) and it is

suggested that this may be due to inhibition of chitin synthesis (Ram & Klis, 2006). These compounds also caused swelling or lysis of the hyphal tips in the filamentous fungi *A. niger* and *Geotrichum lactis*, due to cell wall weakening and internal turgor pressure (Damveld *et al.*, 2005; Pancaldi *et al.*, 1984; Roncero & Duran, 1985). Exposure to CR or CFW ultimately leads to the activation of the cell wall stress response, whereby cell wall-reinforcing genes are activated, and increased chitin is deposited in the cell wall (Levin, 2005) Caffeine inhibits cAMP phosphodiesterases (Parsons *et al.*, 1988), which have been found to be important in the regulation of the cell wall organisation in both *S. cerevisiae* and *C. albicans* (Jung *et al.*, 2005). Caffeine has also be found to stimulate dual phosphorylation of Slt2, the MAP kinase involved in the cell wall integrity signal transduction pathway and mutants in this pathway are found to be more sensitive to caffeine (Martin *et al.*, 1993). SDS compromises the integrity of the cell membrane, and testing with SDS indicates the accessibility of SDS to the membrane through the cell wall and has been used for identifying cell wall mutants from a mutant library in *C. albicans* (Plaine *et al.*, 2008).

Sensitivity testing to all of the cell wall damaging and membrane perturbing agents discussed here revealed no differences in growth between wild-type and $\Delta pes3$ under all conditions tested, ruling out an essential role for Pes3 in cell wall or membrane maintenance, integrity or synthesis. However, anti-fungal susceptibility testing revealed that *A. fumigatus* $\Delta pes3$ was more sensitive to voriconazole (0.5 $\mu\text{g/ml}$) than wild-type ($p < 0.001$). Voriconazole blocks ergosterol biosynthesis, thereby hindering cell membrane synthesis, resulting in membrane leakage. Perhaps one hypothesis could explain the increased susceptibility of *A. fumigatus* $\Delta pes3$ to voriconazole; an altered cell wall in *A. fumigatus* $\Delta pes3$ leads to increased entry of voriconazole, resulting in increased exposure to the membrane damaging effects of voriconazole. Pes3 does not play any role in protection

against the other anti-fungals examined in this study, and this may be due to the differences in targets for these drugs. A similar hypothesis might explain the increased resistance to diamide; an altered cell wall may alter diamide entry into the cells, possibly resulting in differences in the intracellular diamide concentration between *A. fumigatus* and $\Delta pes3$.

Growth rate comparisons between wild-type and $\Delta pes3$ strains were performed in this study. Both vegetative and conidial germination rates were assessed by performing growth curves in liquid media and microscopic examination of germinating conidia in culture (Reeves *et al.*, 2004; Professor Robert Cramer Jr. – personal communication). Conidial germination was investigated as previous gene expression analysis on all of the NRP synthetase genes within *A. fumigatus* revealed that *pes3* displayed a unique pattern of gene expression in comparison to the other NRP synthetase genes, with a high level of transcripts occurring in ungerminated spores (Cramer *et al.*, 2006b). This observation hinted that *pes3* could possibly be playing a role in conidial germination in this fungus, and if so, that the *pes3* mutant might exhibit a different germination rate to the wild-type. However, no differences with respect to rates of germination were observed in this study. Similarly, no differences in vegetative growth between wild-type and $\Delta pes3$ indicating that *pes3* does not appear to be important for germination of conidia into mycelia over a longer time period. Interestingly, a transcriptomic analysis of genes expressed within *A. fumigatus* fresh or one-year old conidia at various stages of germination did not find *pes3* transcripts to be stored constitutively in the conidia or indeed in any of the other conditions analysed in the study (Lamarre *et al.*, 2008). The strain of choice in this study was *A. fumigatus* Af293, as was used in the study mentioned earlier (Cramer *et al.*, 2006b).

In vivo virulence testing of *A. fumigatus* wild-type and $\Delta pes3$ was carried out to investigate if *pes3* contributed towards *A. fumigatus* virulence. NRP peptides have been widely reported as being important virulence factors for the producing species, whereby

NRP synthetase mutants strains exhibit reduced virulence compared to wild-type. For example, the NRP bassianolide from *Beauveria bassiana* is important for the virulence of this pathogen in its insect host (Xu *et al.*, 2009). Non-ribosomally synthesised siderophores are essential for virulence in *A. fumigatus* (Schrettl *et al.*, 2004), and the ETP gliotoxin, also produced non-ribosomally in *A. fumigatus*, is implicated in the virulence of this pathogen (Kwon-Chung & Sugui, 2009). Virulence testing was initially performed using the well-established *G. mellonella* insect infection model (Cotter *et al.*, 2000). Surprisingly, this work revealed that $\Delta pes3$ was more virulent compared to wild-type in the *G. mellonella* model with a highly reduced larval survival rate associated with the $\Delta pes3$ strain ($p < 0.001$) (Figure 3.18). Virulence was observed at levels similar to wild-type when *pes3* was complemented. Virulence was subsequently assessed in two murine models of invasive aspergillosis, including a hydrocortisone acetate immunocompromised (HCA) model, and a neutropenic model (Bergmann *et al.*, 2009). Virulence testing in the HCA model revealed that the $\Delta pes3$ mutant was more virulent as observed by the dramatic weight loss in animals infected with the $\Delta pes3$ strain compared to the wild-type strain. Indeed, two of the animals in the $\Delta pes3$ group reached critical weight loss ($> 20\%$ of starting weight) and had to be culled during the infection. Virulence was further measured by determination of fungal burden in the murine lung following 4 days infection. Increased virulence of the $\Delta pes3$ strain coincided with increased fungal burden in the lungs of these animals in comparison to wild-type ($p = 0.02$). Conversely, virulence testing in a neutropenic model for IA indicated no difference in survival between animals either infected with wild-type or $\Delta pes3$ in this model. The overall weights of animals in both neutropenic groups followed a similar trend over the course of the infection. These findings were also further investigated by determination of fungal burden in the lungs of neutropenic animals on day 4 of infection. Equal fungal burden was found in animals infected with either wild-type or $\Delta pes3$,

indicating equal clearance of the fungus from animals in each group. In both models of infection, a para-aminobenzoic acid (PABA) mutant (H515 strain) was included as a negative control, as this strain is completely attenuated in virulence and unable to germinate in the murine lung (Brown *et al.*, 2000). In both models of infection, the fungal burden associated with the H515 strain was much lower than for the two strains being investigated in this study.

In order to explain the increased virulence associated with the *pes3* disruption, many possibilities were considered. Hypothesis 1: The hypervirulence of $\Delta pes3$ observed in both *Galleria* and the HCA murine model, and the increased $\Delta pes3$ fungal burden also observed in the HCA model might be explained if $\Delta pes3$ exhibited an altered growth rate compared to wild-type. A reduced growth rate could potentially lead to a lower immune response, by virtue of less fungal components present and available for recognition by the pattern recognition receptors of the innate immune system in both *Galleria* and mouse. Similarly, an increased growth rate could mean more fungal material is available for recognition, for example increased β -glucan exposure for recognition by Dectin-1 (Hohl *et al.*, 2005). This could lead to a hyperactive immune response, and therefore increased mortality associated with inflammation and over-activation of immune effectors (Vega & Martin, 2008). Alternatively, increased growth of the fungus could mean increased production of toxic secondary metabolites, which might also explain increased virulence. This study confirms that there is no difference in growth rate, either in a vegetative state, or in the process of conidial germination between wild-type and $\Delta pes3$, eliminating this hypothesis as a reason for the increased virulence of $\Delta pes3$.

Hypothesis 2: *Pes3* encodes an immuno-suppressive peptide, and that loss of such a peptide from *A. fumigatus* $\Delta pes3$ leads to an over-active immune response in the *Galleria* larvae and in the HCA murine model and this might contribute to increased disease and

mortality. This possibility was considered plausible by the fact that *A. fumigatus* is known to produce immunosuppressive mycotoxins, one of which is gliotoxin, of NRPS origin (Kamei & Watanabe, 2005). Fumagillin, also produced by *A. fumigatus* has also been shown to suppress neutrophil function (Fallon *et al.*, 2010). However, extensive comparative metabolite analysis between wild-type and $\Delta pes3$ undertaken here indicates that Pes3 does not produce and secrete a peptide in *A. fumigatus*, convincingly eliminating this possibility to explain the hypervirulence of the $\Delta pes3$ strain. Further support for this comes from the fact that *pes3* was not found to be under the control of LaeA, the master regulator for secondary metabolism in filamentous fungi, upon a transcriptional analysis of a LaeA deletion mutant (Perrin *et al.*, 2007). Furthermore, the increase in $\Delta pes3$ fungal burden observed in the HCA model would not be in agreement with an overactive immune response, as one might expect an overactive immune response to result in enhanced fungal clearance. Moreover, the scenarios above could only partially explain the increased virulence observed for $\Delta pes3$, in that they do not explain why there was no increase in virulence observed in the neutropenic murine model.

Hypothesis 3: A more feasible hypothesis to explain the hypervirulence associated with *A. fumigatus* $\Delta pes3$ is that this strain is immunologically silent in comparison to the wild-type strain. Increased fungal burden in the lungs of animals infected with *A. fumigatus* $\Delta pes3$ compared to wild-type in a HCA model of infection suggests that the immune system is unable to clear the fungus efficiently. Increased growth of *A. fumigatus* $\Delta pes3$ has been eliminated as a cause for increased fungal burden, so it is more plausible that *A. fumigatus* $\Delta pes3$ is not recognised by the immune system as efficiently as wild-type and that it is somehow escaping the immune response. This hypothesis was investigated and supported through *in vitro* cell signalling experiments. An overall reduction in cytokine production was observed when murine BMMØS (bone-marrow-derived macrophages) were

exposed to *A. fumigatus* $\Delta pes3$, compared to wild-type. Reductions in TNF- α (40 %), IL-6 (68 %), RANTES (25 %), and IL-10 (10 %) was observed following co-incubation of macrophages with *A. fumigatus* germlings which had been previously incubated for 9 hr in AMM media to allow germling formation, prior to co-incubation with macrophages for 18 hr. Germination assays that were undertaken in this study revealed that by 8 hr, a germination rate of > 80 % was observed for both wild-type and $\Delta pes3$, and beyond 8 hr it was difficult to visually enumerate germlings. Subsequently, 9 hr was chosen as a time point in the cell signalling experiments, as it is likely that close to 100 % germination is achieved at this point. Differences in the *in vitro* murine response to both strains, despite equal growth rates, and germination rates, implies that a structural difference between the strains is leading to a difference in immune recognition of pattern associated molecular patterns (PAMPs) on the cell surface. Specific reduction in TNF- α and IL-6 upon exposure to *A. fumigatus* $\Delta pes3$ suggests a reduction in recognition through TLR4 as production of these pro-inflammatory cytokines from murine macrophages in response to *A. fumigatus* hyphae is largely dependant on TLR4 (Meier *et al.*, 2003). It is currently not known which PAMPs are involved in recognition of *Aspergillus* through TLR2 and/or TLR4, but TLR4 has been shown to recognise fungal mannan *in vitro* (Tada *et al.*, 2002).

Interestingly, the literature revealed that the majority of *A. fumigatus* mutants for which hypervirulent phenotypes have been reported relate to a defect in the cell wall or conidial surface of the mutant. Disruption of *ecm33* (AFUA4G06820), encoding the GPI-anchored protein ECM33 in *A. fumigatus* resulted in a mutant strain that was more virulent than wild-type in an immunocompromised mouse model for IA (Romano *et al.*, 2006). *A. fumigatus* $\Delta ecm33$ exhibited rapid conidial germination, increased resistance to caspofungin, and increased cell-cell adhesion, and the authors suggest that deletion of ECM33 leads to a softer cell wall, allowing faster germination (Romano *et al.*, 2006).

3)-glucan is a major polysaccharide in the cell wall of *A. fumigatus*, and several α (1-3)-glucan synthases (AGS) have been identified to date with AGS1 being responsible for α (1-3)-glucan biosynthesis (Beauvais *et al.*, 2005). AGS3, another α (1-3)-glucan synthase has since been identified and is involved in α (1-3)-glucan biosynthesis. Interestingly, an AGS-3 deletion mutant was found to be hypervirulent in a murine model of IA and this coincided with increased melanin at the conidial cell wall, increased resistance to ROS and faster germination (Maubon *et al.*, 2006). An *A. fumigatus* transcription factor, ACE2, which regulates pigment production, conidiation and virulence, was deleted and a range of mutant phenotypes were reported (Ejzykowicz *et al.*, 2009), including the production of a yellow-orange pigment on certain media, abnormal conidiation, accelerated germination, and difference in the conidial surface ($\Delta ace2$ conidia appeared smooth, while wild-type conidia generally have a rough undulating appearance). Furthermore, the ACE2 mutant was hypervirulent in a non-neutropenic mouse model of IA, but no difference in virulence was observed in neutropenic mice (Ejzykowicz *et al.*, 2009). These findings indicate that, like *A. fumigatus* $\Delta pes3$, the presence of neutrophils was necessary for the increased virulence of *A. fumigatus* $\Delta ace2$. The fatty acid oxygenases PpoA, PpoB and PpoC synthesise prostaglandins and other oxylipins (Tsitsigiannis *et al.*, 2005). PpoA, B and C silencing by RNAi lead to a hypervirulent strain of *A. fumigatus* (Maubon *et al.*, 2006). ACE2 was shown to regulate the expression of genes encoding PpoA, PpoB and PpoC, ECM33, and AGS-3, which may explain the increased virulence observed in *A. fumigatus* $\Delta ace2$ (Ejzykowicz *et al.*, 2009). Furthermore, *A. fumigatus* $\Delta ace2$ exhibited abnormal conidial cell wall architecture (Ejzykowicz *et al.*, 2009). The inner layer of the $\Delta ace2$ conidial cell wall was 2-fold thicker than wild-type, and the authors suggest that the increased thickness of this layer is due to an increased amount of chitin, as *ecm33* expression is decreased in $\Delta ace2$, and deletion of *ecm33* is known to lead to increased chitin content in the cell wall

(Chabane *et al.*, 2006; Ejzykiewicz *et al.*, 2009). Finally, genes encoding trehalose synthases (TPSs) were investigated in *A. fumigatus*, and a trehalose synthase double mutant ($\Delta tpsAB$), was hypervirulent in a non-neutropenic model of IA, consistent with greater pulmonary fungal burden (determined by measuring galactomannan content), and increased pulmonary inflammation. This mutant exhibited major alterations in the conidial and hyphal cell wall with loss of the electron dense outer layer. Furthermore, expression of AGS-3 was down-regulated in $\Delta tpsAB$, possibly contributing to the increased virulence observed for $\Delta tpsAB$ (Al-Bader *et al.*, 2010). Taking all the data presented here, and the hypervirulent mutants reported in the literature into consideration, it is highly plausible that the hypervirulence of *A. fumigatus* $\Delta pes3$ is associated with an alteration at the cell surface of the mutant strain that interferes or reduces the recognition of the fungus by the innate immune system.

The similarity in virulence between both strains in the neutropenic model could be explained if the absence of the *pes3* gene product resulted in a reduced immune response (and therefore higher fungal burden) via the neutrophil. This could also be stated as; the *pes3* gene product elicits an intact immune response when present in *A. fumigatus*, and that the particular recognition and response mediated by *pes3* is reliant on the neutrophil. Recognition of *A. fumigatus* by the innate immune system, leads to clearing of fungal burden and the neutrophils are extremely important in this process, as discussed earlier in this chapter. Full recognition of the wild-type strain could be dependent on *pes3*, and this eventually leads to recruitment of neutrophils, which are important in the defence against *A. fumigatus*. Upon exposure to $\Delta pes3$, fungal recognition by the immune system is impaired, manifesting as a reduced neutrophil function which could slow the clearance of fungal burden, and increase virulence, as observed in this study. The fact that no difference is observed between wild-type and $\Delta pes3$ in the neutropenic model is compatible with this

hypothesis. Certain hypotheses can explain the immunological silencing of *A. fumigatus* $\Delta pes3$. As described earlier, *A. fumigatus* dormant conidia are covered by a hydrophobic rodlet layer (Thau *et al.*, 1994). This rodlet layer is made of hydrophobic proteins, and the rodlet layer maintains conidia in an immunologically silent state (Aimanianda *et al.*, 2009). Recently, it has been shown that RodA (one of the rodlet hydrophobins) prevents *A. fumigatus* conidia from triggering NET formation by human neutrophils (Bruns *et al.*, 2010), indicating the importance of rodlet removal in leading to a neutrophil-mediated immune response.

Pes3 may encode a peptide which functions in removal of the rodlet layer from germinating conidia, thereby facilitating recognition of fungal PAMPs by the receptors of the innate immune system. Loss of a Pes3-encoded peptide could result in incomplete or delayed removal of the rodlet layer during conidial germination, thereby keeping *A. fumigatus* in a silent state, resulting in increased virulence, and reduced cytokine induction in response to *A. fumigatus* $\Delta pes3$ as observed. Alternatively, Pes3 might encode a peptide which functions in linking the rodlet layer to the cell wall. Loss of Pes3 could result in aberrant linking of this rodlet layer to the cell wall, and may hinder other enzymes involved in the removal of the rodlet layer upon germination. Either hypothesis would lead to a reduction in exposure of fungal cell wall components, and would maintain the conidia of *A. fumigatus* $\Delta pes3$ in an immunologically inert state. Either hypothesis could explain the abundance of *pes3* transcripts in ungerminated conidia (Cramer *et al.*, 2006b). The storage of *pes3* transcripts in conidia would make them available for immediate translation of Pes3, allowing rapid removal of, or attachment of proteins to, the rodlet layer upon commencement of conidial germination. Failure to remove the rodlet layer in *A. fumigatus* $\Delta pes3$ would lead to the prevention of NET formation right through the infection process (Bruns *et al.*, 2010), leading to hypervirulence of $\Delta pes3$ and increased fungal burden as

observed. Furthermore, the involvement of a Pes3-encoded peptide in the rodlet layer might explain the reason no difference in virulence was observed between *A. fumigatus* wild-type and $\Delta pes3$ in a neutropenic model of IA. Alternatively, a Pes3-encoded non-ribosomal peptide could be involved in binding or linking the fibrillar to amorphous polysaccharides in the cell wall, as to date, the linkages that are removed upon NaOH treatment are completely unknown (Latgé, 2010). It has been suggested that antibodies recognising specific linkages between the carbohydrates of the cell wall would be useful in elucidating the exact cell wall structure, and this has recently been used to elucidate the structure of plant cell walls (Knox, 2008). Unfortunately, one limitation in applying this technique to determine if *pes3* is involved in linking components of the cell wall together is that the peptide encoded by Pes3 is unknown, and so it would be impossible to raise an antibody against it, at present. Nevertheless, the lack of information currently available on these linkages, together with the phenotypes observed for $\Delta pes3$, and the high level of *pes3* transcripts present in conidia (Cramer *et al.*, 2006b) do make these hypotheses valid and worthy of further investigation.

Interestingly, a genome-wide transcriptional analysis of the *A. fumigatus* genes differentially expressed in conidia upon exposure to human neutrophils did not record *pes3* expression as having changed in this study (Sugui *et al.*, 2008). This finding could be seen to support the hypothesis that *pes3* plays a structural role in *A. fumigatus*, because even though *pes3* is important for immune recognition, and this does seem to involve the neutrophil in some way, i.e. its expression is not something that needs to be altered in response to neutrophil presence, as it is a structural component which is constitutively present.

The role of a fungal NRP synthetase in synthesising a peptide with a structural role has not been described before, so this may be a novel role for an NRP synthetase.

Phenotypic assays carried out in this study to investigate the response towards cell wall damaging agents revealed no difference between wild-type and $\Delta pes3$. However, *A. fumigatus* $\Delta pes3$ is more sensitive to the anti-fungal voriconazole than wild-type, which does point towards some alteration at the cell surface of this strain. In order to further validate the hypothesis that $\Delta pes3$ is immunologically silenced, histological analysis of murine tissue during and following fungal infection would be very useful. Neutrophil infiltration is dependant on the production and release of cytokines such as TNF- α and chemoattractants (eg. IL-8) at the site of infection (Wagner & Roth, 2000), and reduction in TNF- α and the chemoattractant RANTES observed upon exposure to *A. fumigatus* $\Delta pes3$ should lead to impairment of neutrophil migration. If the hypothesis is correct, one might expect to see less infiltration of neutrophils in the tissue of animals infected with *A. fumigatus* $\Delta pes3$, resulting in reduced clearance of the fungus, and the higher fungal burden observed. Furthermore, an investigation of cytokine production *in vivo* in response to both strains is desirable. As well as *in vivo* cytokine measurements, it would be very useful to measure the expression of Toll like and other receptors known to be involved in the innate response against *A. fumigatus* infections, namely TLR 2, TLR 4 and Dectin-1 as discussed earlier. Further experiments to visualise *A. fumigatus* wild-type and $\Delta pes3$ microscopically during different stages of growth; i.e. germination and mycelial growth would address and possibly confirm this hypothesis that the hyper-virulence and reduction in immune response associated with *A. fumigatus* $\Delta pes3$ is related to a cell wall defect.

4.1 Introduction.

4.1.1. *pesL* in the genome of *A. fumigatus*.

PesL (Cadre identifier: AFUA_6G12050) is a putative non-ribosomal peptide (NRP) synthetase encoded in the genome of *Aspergillus fumigatus*. A phylogenomic analysis of NRP synthetases within the genus *Aspergillus* revealed that PesL is one of two mono-modular NRP synthetases in *A. fumigatus*, and in this study PesL is referred to as NRPS11 (Cramer *et al.*, 2006b; Stack *et al.*, 2007). PesL is predicted to possess a single module containing an Adenylation (A), Thiolation (T) and Condensation (C) Domain (Cramer *et al.*, 2006b; Stack *et al.*, 2007). The *pesL* open reading frame is 3,915 bp in length, including an annotated intron of 432 bp occurring 87 bp after the ATG start codon. Assuming the correct annotation of the intron, the translated protein encoded by *pesL* is comprised of 1,160 amino acid residues and has a predicted molecular weight of approximately 129 kDa. Blast homology searching at NCBI reveals that the PesL amino acid sequence is most homologous to a putative NRP synthetase (ACLA_017900) from the fully-sequenced genome of *Aspergillus clavatus* NRRL 1 strain. The next most homologous sequence is that of a putative NRP synthetase (NFIA_057990) from *Neosartorya fischeri* NRRL 181 strain. Similar results were found when using the blastp function at CADRE. Table 4.1 shows the Blast results obtained using the TBLASTN 2.2.23+ program with the *pesL* translated nucleotide sequence as a query (Altschul *et al.*, 1997). Upon examining the Blast results, it is clear that for almost all of the homologues of PesL, there are no specific references for any of these genes relating the encoded NRP synthetase to a downstream peptide product. The lack of information relating NRP synthetases to a specific product highlights the large amount of work that remains to be done in order to elucidate the role of NRP synthetases in fungi in general, but also within the important pathogen, *A. fumigatus*.

Table 4.1. Blast results obtained using the TBLASTN 2.2.23+ program with the *pesL* translated nucleotide sequence as a query. The top 5 Blast hits are included.

#	Accession	Description	Query coverage	E value	Max identity
1	XM_745991.1	<i>Aspergillus fumigatus</i> Af293 non-ribosomal peptide synthase, putative (AFUA_6G12050), partial mRNA	100%	0.0	97%
2	XM_001268512.1	<i>Aspergillus clavatus</i> NRRL 1 non-ribosomal peptide synthase, putative (ACLA_017900), partial mRNA	95%	0.0	53%
3	XM_001258345.1	<i>Neosartorya fischeri</i> NRRL 181 non-ribosomal peptide synthase, putative (NFIA_057990) partial mRNA	83%	5e-152	35%
4	XM_001270090.1	<i>Aspergillus clavatus</i> NRRL 1 non-ribosomal peptide synthase, putative (ACLA_095980), partial mRNA	91%	2e-151	32%
5	XM_001258342.1	<i>Neosartorya fischeri</i> NRRL 181 non-ribosomal peptide synthase, putative (NFIA_057960) partial mRNA	84%	9e-150	35%

PesL was chosen for investigation in this study as it represents one of two monomodular NRP synthetases in *A. fumigatus* (Cramer *et al.*, 2006b; Stack *et al.*, 2007), and identification of the peptide encoded by PesL might provide information on the substrate specificity of fungal NRP synthetase adenylation domains, for which information is greatly lacking (Stack *et al.*, 2007; Stack *et al.*, 2009). Furthermore, with the publishing of the complete genome sequence of *A. fumigatus*, it was proposed that *pesL* was part of a secondary metabolite biosynthetic gene cluster containing four other genes (Nierman *et al.*, 2005). Table 4.2 shows the genes surrounding *pesL* in the genome of *A. fumigatus* and their putative functions. For convenience, this cluster is referred to as the *pesL* cluster during this thesis. The total cluster spanned from AFUA_6G12040 to AFUA_6G12080 and no orthologous clusters are found in two other *Aspergillus* species, *A. oryzae* or *A. nidulans* according to Nierman *et al.*, (2005). This proposed cluster contains another putative NRP synthetase encoded by the gene AFUA_6G12080 which is referred to as NRPS 12 by Cramer *et al.*, (2006a), and is also referred to as PesM (Stack *et al.*, 2007). LaeA is a transcriptional regulator of secondary metabolite biosynthetic gene clusters in *A. fumigatus* and *A. nidulans*, and is known to influence transcription by acting on a chromatin remodelling level (Bok *et al.*, 2005; Bok *et al.*, 2006). *pesL* and all other genes in the *pesL* cluster were found to be under the regulation of the global secondary metabolite transcriptional regulator, LaeA, in a transcriptional analysis of a LaeA mutant (Perrin *et al.*, 2007). Therefore, it was likely that PesL encoded a secondary metabolite peptide in *A. fumigatus*. The next section will focus on the major secondary metabolites produced by *A. fumigatus* and will give an overview of the state on knowledge on the biosynthetic pathways involved in their biosynthesis.

Table 4.2. Transcript neighbourhood for *A. fumigatus pesL*. This table shows 5 genes proposed to be part of a secondary metabolite gene cluster with *pesL* in the genome of *A. fumigatus* Af293 (Nierman *et al.*, 2005). Data was taken from CADRE (Mabey *et al.*, 2004). *pesL* (AFUA_6G12050) is underlined.

Gene Number	Function/Putative	References
AFUA_6G12040	MFS sugar permease, putative	N/A
<u>AFUA_6G12050</u>	Non-ribosomal peptide synthase, putative, similar to non-ribosomal peptide synthase (GI:32264582) (<i>Alternaria brassicae</i>), (6.3.2.-)	(Ames <i>et al.</i> , 2010)
AFUA_6G12060	MAK1-like monooxygenase, putative, similar to PIR:S70702: maackiain detoxification protein 1 (<i>Nectria haematococca</i>) similar to Salicylate hydroxylase (EC 1.14.13.1) (Salicylate 1-monooxygenase). (Swiss-Prot:P23262) (<i>Pseudomonas putida</i>), (1.14.13.-)	Ames <i>et al.</i> (2010)
AFUA_6G12070	FAD binding domain protein, similar to GB:BAC61978.1: putative oxidoreductase, oxygen dependent, FAD-dependent protein (<i>Vibrio parahaemolyticus</i>), (1.5.3.-)	N/A
AFUA_6G12080	non-ribosomal peptide synthase, putative, similar to non-ribosomal peptide synthase (GI:32264582) (<i>Alternaria brassicae</i>) PMID: 14727058, (6.3.2.-)	Ames & Walsh) 2010

4.1.2. Secondary metabolite production in *A. fumigatus*.

At least 226 secondary metabolites in 24 distinct biosynthetic families have been reported from *A. fumigatus* (Frisvad *et al.*, 2009). A recent metabolomic analysis of various isolates of *A. fumigatus* indicated that the metabolites consistently produced were fumiquinazolines A/B, C/D and F/G (100 %), fumigaclavine C (100 %), fumitremorgins (100 %), fumagillin (100 %), pseurotin A (100 %), melanins (100%) and helvolic acid (98 %), with other metabolites such as gliotoxin and fumigatins produced by approximately half of the isolates examined (Frisvad *et al.*, 2009). It has been widely reported that the production of secondary metabolites depends on the growth media used and environmental factors (Furtado *et al.*, 2002; Furtado *et al.*, 2005). Czapek's yeast autolysate (CYA) agar and yeast extract sucrose (YES) were found to be suitable for the production of representatives of all known families of secondary metabolites in *A. fumigatus* detected using HPLC coupled with diode array detection (DAD) (Frisvad *et al.*, 2007; Frisvad *et al.*, 2009). The three major groups of secondary metabolites produced by *A. fumigatus*; the fumiquinazolines, the fumitremorgins, and the ergot alkaloids will be discussed in more detail in the following sections.

4.1.2.1. The fumiquinazolines.

Fumiquinazolines A-G were first detected from a strain of *A. fumigatus* isolated from the gastrointestinal tract of the marine fish *Pseudolabrus japonicus* (Takahashi *et al.*, 1995). The structures of these compounds were elucidated on the basis of spectral and X-ray analyses and some chemical transformations (Takahashi *et al.*, 1995). These compounds are among a variety of quinazoline-containing natural product scaffolds produced by fungi (Dyakonov & Telezhenetskaya, 1997). Upon examination of their structure it was proposed that anthranilate (Ant) (a non-proteinogenic aryl β -amino acid)

was a building block for these compounds (Ames & Walsh, 2010). These authors used a biochemical approach to confirm that an NRPS module (AnaPS module 1) from the known gene cluster for acetylaszonalenin from the *Neosartorya fisheri* NRRL 181 strain (Yin *et al.*, 2009) activates Ant. Subsequently, they chose an *A. fumigatus* NRP synthetase module as a candidate for Ant selectivity based on its similarity to AnaPS module 1, and this module corresponded to the first module encoded by *A. fumigatus pesM* (AFUA_6G12080) which is proposed to be part of a cluster with *pesL*. In contrast to earlier findings about the clustering of genes with *pesL* (Nierman *et al.*, 2005), the authors state that *pesM* is actually part of an eight-gene cluster along with *pesL*, that they predict to be involved in the production of the Ant-containing alkaloid fumiquinazoline A (Ames *et al.*, 2010). Module 1 of a recombinantly expressed PesM was shown to preferably activate Ant (Ames & Walsh, 2010). The authors propose that the three-module NRPS PesM is likely to produce fumiquinazoline F, and that PesL (AFUA_6G12050) could function in the conversion of fumiquinazoline F to fumiquinazoline A, by activating alanine and acting with an N-acyltransferase (AFUA_6G12100), which also encoded by the cluster, to couple alanine to the indole N1 of fumiquinazoline F (Ames & Walsh, 2010). More recently, these same authors have shown biochemically that recombinantly expressed PesL and an FAD-dependant monooxygenase (encoded by AFUA_6G12060) are necessary and sufficient to convert fumiquinazoline F into fumiquinazoline A (Ames *et al.*, 2010). The biosynthesis of fumiquinazolines in *A. fumigatus* will be discussed again later in this chapter. The chemical structures for a selection of quinazoline-containing fungal metabolites are presented in Figure 4.1.

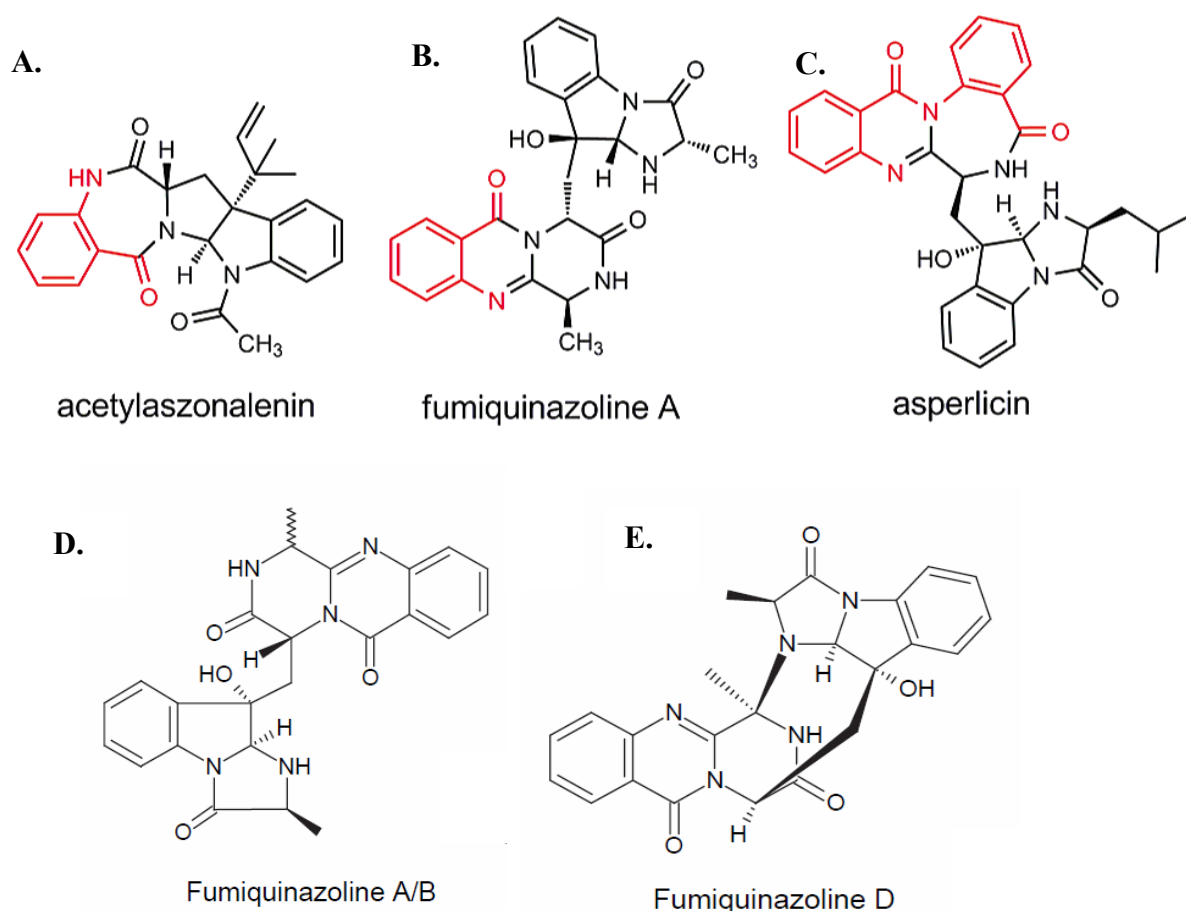


Figure 4.1. Examples of fungal natural products that use anthranilic acid (Ant) as a building block. The Ant-derived portion is shown in red in A-C. A. Acetylaszonalenin biosynthesis is directed by a gene cluster in *Neosartorya fisheri* (Yin *et al.*, 2009). B. Fumiquinazoline A is produced by *A. fumigatus* and its biosynthesis appears to be directed by a gene cluster containing two NRP synthetases (Ames *et al.*, 2010; Ames & Walsh, 2010). C. Asperlicin was first detected in *Aspergillus alliaceus* (Chang *et al.*, 1985) and has received much attention for its therapeutic potential in the treatment of a variety of human disorders (Herranz, 2003). D, E. Fumiquinazoline A, B and D are also produced by *A. fumigatus* and along with other fumiquinazolines were consistently found in 40 isolates of *A. fumigatus* examined (Frisvad *et al.*, 2009). A-C from Ames & Walsh (2010). D-E from Frisvad *et al.*, (2009).

4.1.2.2. The fumitremorgins.

The fumitremorgins are a family of tremorgenic mycotoxins, which are produced by *A. fumigatus* and other fungi (Horie & Yamazaki, 1981; Yamazaki *et al.*, 1971). Tremorgenic mycotoxins, the most potent being verruculogen, cause tremors in animals, and are the reported cause of certain naturally occurring neurological disorders of farm animals (Perera *et al.*, 1982). Fumitremorgins belong to a 20 member family of prenylated indole alkaloids derived from tryptophan and proline, including fumitremorgin A-C, verruculogen and derivatives, TR-2, tryprostatins, cyclotryprostatins and spirotryprostatins (Cui *et al.*, 1996a; Cui *et al.*, 1996b; Frisvad *et al.*, 2009). There is interest in the fumitremorgin biosynthetic pathway, as some of the compounds; tryprostatin A and fumitremorgin C have been found to exhibit anti-cancer activity (Williams *et al.*, 2000; Zhao *et al.*, 2002).

It was hypothesised that these metabolites were derived from the diketopiperazine cyclo-L-Trp-L-Pro, derived from tryptophan and proline, known as brevianamide F (Williams *et al.*, 2000). A prenyltransferase FtmPT1 (AFUA_8G00210) was characterised and found to convert brevianamide F into tryprostatin B and a biosynthetic gene cluster for fumitremorgins was proposed, which contained a di-modular NRP synthetase gene, hypothesised to form the di-peptide *cyclo*-L-Trp-L-Pro precursor of the fumitremorgins, Brevianamide F (Grundmann & Li, 2005). Since then, the dimodular NRP synthetase gene, *ftmA* (AFUA_8G00170), has been characterised and proven to be responsible for the condensation of tryptophan and proline into brevianamide F, which is the first committed step of the fumitremorgin biosynthetic pathway (Maiya *et al.*, 2006). Since then, several enzymes in the fumitremorgin biosynthetic gene cluster have been characterised. Three p450 monooxygenases (FtmC, FtmE and FtmG) have been identified and these catalyse important steps in the conversion of tryprostatin B to tryprostatin A and eventually to

fumitremorgin C (Kato *et al.*, 2009). FtmPT2 (AFUA_8G00250) is an *N*-prenyltransferase which catalyses the last step in the fumitremorgin biosynthetic pathway, resulting in the production of fumitremorgin B (Grundmann *et al.*, 2008). There are still several genes within the cluster which remain to be characterised; *ftmD*, *ftmF* and *ftmL*, however gene deletion indicated that *ftmL* is probably not involved in this biosynthesis of fumitremorgins (Kato *et al.*, 2009). *ftmF*, which encodes a putative oxygenase, is hypothesised to be involved in the biosynthesis of verruculogen, a fumitremorgin-related compound whose biosynthesis had not been fully elucidated to date (Kato *et al.*, 2009). The proposed biosynthetic pathway for fumitremorgins in *A. fumigatus* is presented in Figure 4.2.

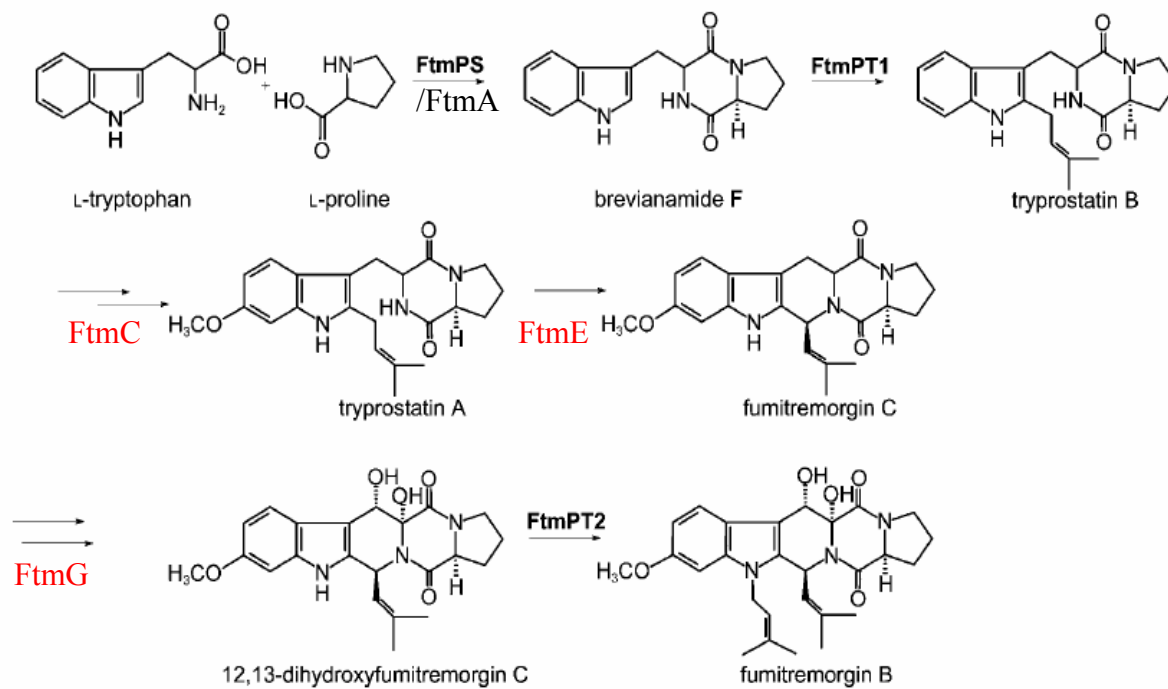


Figure 4.2. The fumitremorgin biosynthetic pathway in *A. fumigatus* (Grundmann *et al.*, 2008). Missing links in the original pathway which were later determined are added in red (Kato *et al.*, 2009).

4.1.2.3. The ergot alkaloids.

The ergot alkaloids are a complex family of indole-derived alkaloids that have long been known for their association with human suffering (Panaccione & Coyle, 2005), and ergots produced by the ergot fungus *Claviceps purpurea* are the causative agents of gangrenous and convulsive forms of ergotism known as St. Anthony's fire (Walter, 1990). Ergot alkaloids are produced by many fungal species, covering two divergent ascomycete orders (*Hypocreales* and *Eurotiales*), including endophytic fungi of the genera *Neotyphodium*, *Epichloë* and *Balansia*, ergot *Claviceps* spp. (order *Hypocreales*) and *A. fumigatus* (order *Eurotiales*) (Clay & Schardl, 2002; Flieger *et al.*, 1997; Kozlovsky, 1999; Panaccione & Coyle, 2005; Spilsbury & Wilkinson, 1961). Ergot alkaloids have been reported to be associated with conidia in *A. fumigatus*, and were found to be present on or in conidia in quantities that collectively represent about 1 % of the dry mass of the conidium (Panaccione & Coyle, 2005). Since these initial observations, deletion of the *A. fumigatus brlA* gene, which controls conidiophore development in *A. nidulans* (Adams *et al.*, 1988; Boylan *et al.*, 1987), resulted in a non-conidiating *A. fumigatus* mutant from which no ergot alkaloids were detected in mycelia, indicating that ergot alkaloids are not produced during the vegetative growth of *A. fumigatus*, and are solely associated with conidiation (Coyle *et al.*, 2007).

Ergot-producing *Claviceps* species produce a wide variety of clavine and lysergyl-derived ergot alkaloids but commonly accumulate ergopeptines or simple amides of lysergic acid, such as ergine and ergonovine (Coyle & Panaccione, 2005; Flieger *et al.*, 1997; Floss, 1976). The lysergyl moiety of ergot alkaloids, e.g. ergotamine, is derived from tryptophan and dimethylallylphosphate (DMAPP) (Williams *et al.*, 2000). Most of the clavine and lysergyl-derived ergot alkaloids contain the same four-member ergoline ring system, but they differ in the number, type and position of the side chains (Coyle &

Panaccione, 2005; Flieger *et al.*, 1997; Floss, 1976). Ergopeptines are non-ribosomally synthesised peptides consisting of lysergic acid and three amino acids. *A. fumigatus* produces several clavine ergot alkaloids, such as festuclavine and fumigaclavines A, B and C (Cole *et al.*, 1977; Panaccione & Coyle, 2005; Spilsbury & Wilkinson, 1961). One important difference between the ergot alkaloids of the clavicipitaceous fungi and *A. fumigatus* is the saturation of the fourth ring of the ergoline structure in *A. fumigatus* (Coyle *et al.*, 2010). Festuclavine was first described in *Claviceps purpurea* (Flieger *et al.*, 1997; Floss, 1976) and has also been found in *Neotyphodium species* (Panaccione *et al.*, 2003; Porter *et al.*, 1981). However, none of the fumigaclavines produced by *A. fumigatus* have been found in any of the *Claviceps* species, and likewise, the end-products (ergopeptines and lysergic acid amides) of the *Claviceps* and *Neotyphodium spp.* ergot alkaloid biosynthetic pathways have not been found in *A. fumigatus* (Coyle & Panaccione, 2005). This differential biosynthesis of alkaloids between different species is in agreement with the hypothesis that early steps of the ergot biosynthetic pathway are shared by these evolutionary diverse fungal species but later steps in the pathway are different for *A. fumigatus* and the *Clavicipitaceous* fungi (Coyle & Panaccione, 2005).

According to Frisvad *et al.* (2009), *A. fumigatus* produces 8 ergot alkaloids including agroclavine, festuclavine, elymoclavine, chanoclavine I and fumigaclavines A, B and C. Fumigaclavine C is the end product of the ergot alkaloid pathway in *A. fumigatus*, with festuclavine, fumigaclavine B and fumigaclavine A (in that specific order) acting as the final three intermediates in its biosynthesis (Panaccione, 2005; Unsold & Li, 2006). Chemical structures for a selection of ergot alkaloids produced by *A. fumigatus* are shown in Figure 4.3. Clustered arrangements of genes involved in ergot alkaloid (EA) biosynthesis have been found in *A. fumigatus* (Coyle & Panaccione, 2005), *Claviceps fusiformis* (Lorenz *et al.*, 2007), *C. purpurea* (Tudzynski *et al.*, 1999) and *Neotyphodium lolli* (Fleetwood *et*

al., 2007). The *dmaW* gene encodes dimethylallyltryptophan synthase (DMAT synthase), which performs the determinant step in EA biosynthesis (Tsai *et al.*, 1995; Vazquez *et al.*, 2003; Wang *et al.*, 2004). DMAT synthase specifically catalyses the prenylation of tryptophan, and the biochemical properties of DMAT synthase have been characterised many times using purified proteins from different ergot alkaloid producing *Claviceps* strains (Cress *et al.*, 1981; Gebler & Poulter, 1992; Lee *et al.*, 1976). Deletion of the *dmaW* gene in *Neotyphodium sp. Strain Lp1*, resulted in complete loss of ergot alkaloids in the resulting mutant (Wang *et al.*, 2004). Based on the high sequence identity of *dmaW* genes and clustering of other EA biosynthesis genes, it was proposed that the EA biosynthesis pathway in *A. fumigatus* has a common origin with the clavicipitaceous fungi (Coyle & Panaccione, 2005). However, the arrangement of the *A. fumigatus* EA cluster is dramatically different to that of *C. purpurea* and *C. fusiformis* (Liu *et al.*, 2009a; Lorenz *et al.*, 2007). This observation sparked phylogenetic analyses to be undertaken which revealed a monophyletic origin for the *dmaW* gene in fungi, implying that the *A. fumigatus dmaW* gene has the same origin as corresponding genes from the clavicipitaceous fungi (Liu *et al.*, 2009a). Functions for a few of the other genes in EA biosynthetic clusters have been characterised. The EA biosynthetic cluster in *A. fumigatus* was identified by functional analysis of the *dmaW* gene controlling the determinant step in the pathway and by analysing flanking regions of *dmaW* for other potential EA biosynthetic genes (Coyle & Panaccione, 2005). Current understandings on EA biosynthetic pathways will be discussed in more detail later in this chapter.

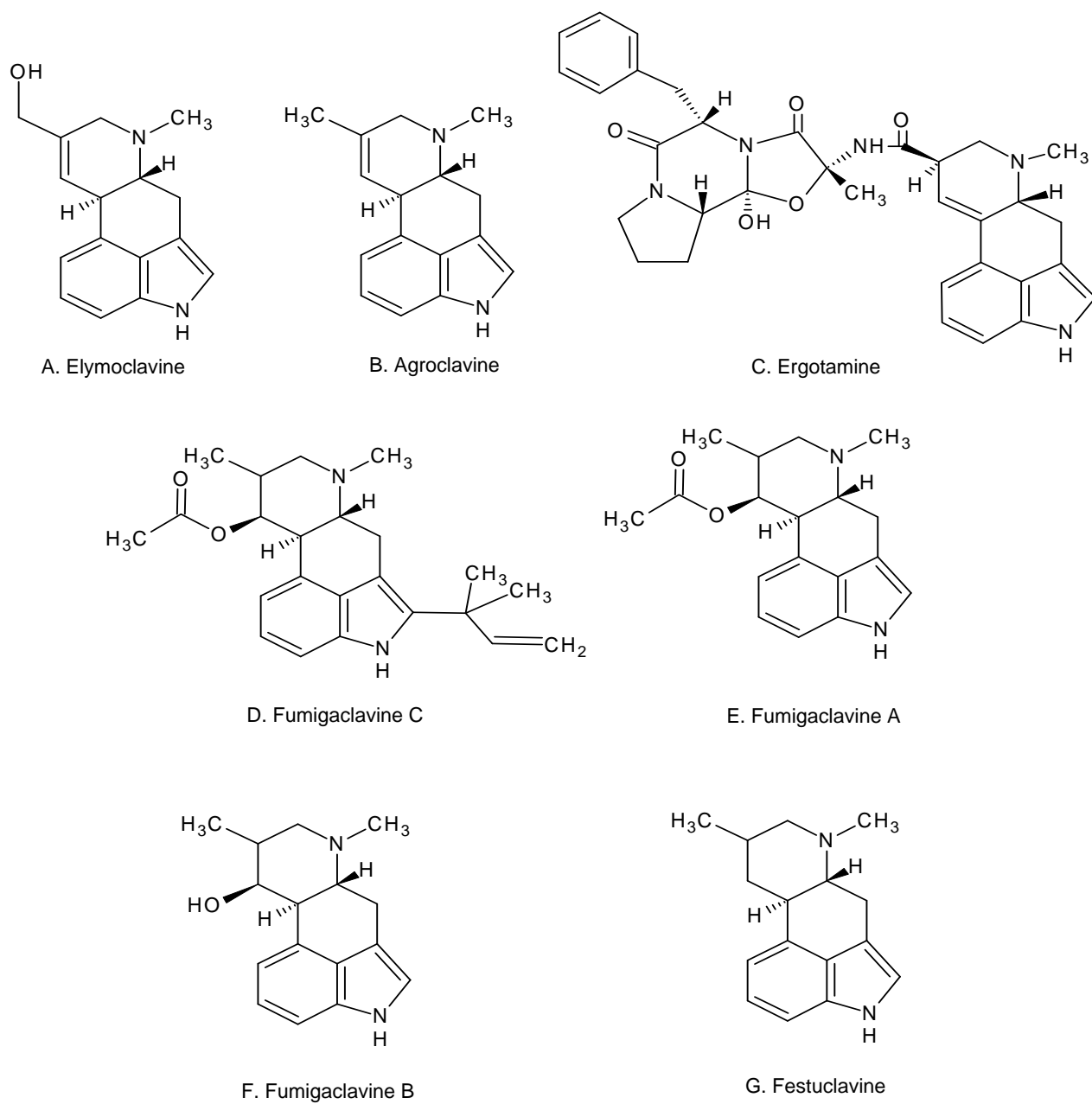


Figure 4.3. Chemical structure of a selection of fungal ergot alkaloids. Professor

Thomas Larsen – DTU.

4.2 Aims and Objectives.

The overall aims of this work were to functionally characterise and identify a non-ribosomal peptide encoded by *PesL* in *A. fumigatus*.

The specific aims that were addressed are listed below.

- 1) To disrupt *pesL* function in *A. fumigatus* using a gene deletion strategy, to generate a *pesL* mutant strain ($\Delta pesL$), and to confirm corresponding loss of *pesL* expression upon disruption.
- 2) To perform comparative phenotypic analysis between *A. fumigatus* wild-type and $\Delta pesL$ in order to identify a possible biological role for *pesL*.
- 3) To undertake comparative metabolite analysis between *A. fumigatus* wild-type and $\Delta pesL$.
- 4) To perform *in vivo* virulence testing in order to assess the virulence of $\Delta pesL$, in the *G. mellonella* insect model system.

4.3. Results.

4.3.1. Generation of *pesL* disruption constructs.

For inactivation of *pesL*, a bipartite gene disruption strategy was employed (Nielsen *et al.*, 2006). An *A. fumigatus* strain (\DeltaakuB) deficient in non-homologous end joining (NHEJ) was transformed with *pesL* disruption constructs. All primers used in this study are listed in Table 2.3. This strategy resulted in the deletion of nucleotides 1-2,875 of *pesL* corresponding to amino acids 1-959 of PesL. For this study, *ptrA* was released from the pSK275 plasmid via *PstI* and *HindIII* restriction digestion. PCR 1 resulted in a 1.2 kb DNA flanking the 5' end of *pesL*. PCR 2 resulted in a 1.3 kb DNA fragment corresponding to a region at the 3' end of *pesL*. PCR 1 and PCR 2 are shown in Figure 4.4. PCR 1 and PCR 2 were restricted with *PstI* and *HindIII* respectively, and were ligated to *ptrA* via the same sites. Final *pesL* disruption constructs (PCR 3 and 4) were 2.6 kb and 2.1 kb, respectively (Figure 4.5). Transformation of *A. fumigatus* protoplasts was performed and transformants were selected on agar plates containing pyrithiamine as described (Section 2.2.3.2).

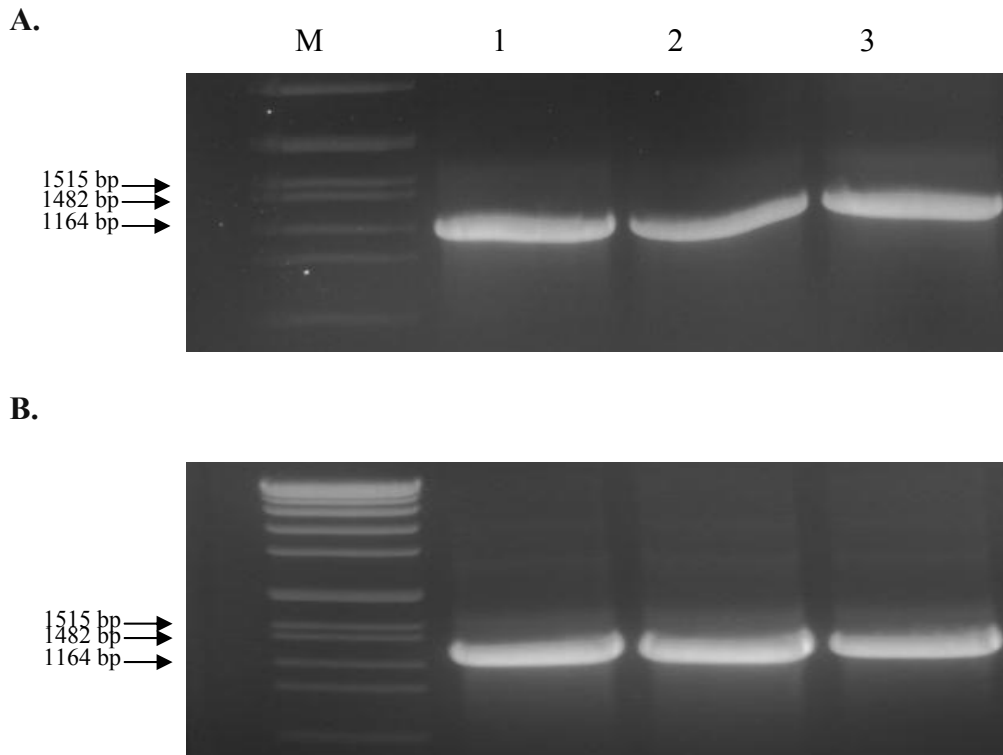


Figure 4.4. PCR 1 and PCR 2 for generation of *pesL* disruption constructs.

A. PCR 1 products (1,194 bp).

B. PCR 2 products (1,313 bp).

M: Molecular weight marker (Roche VII). Lane 1-3: PCR products from three PCR reactions.

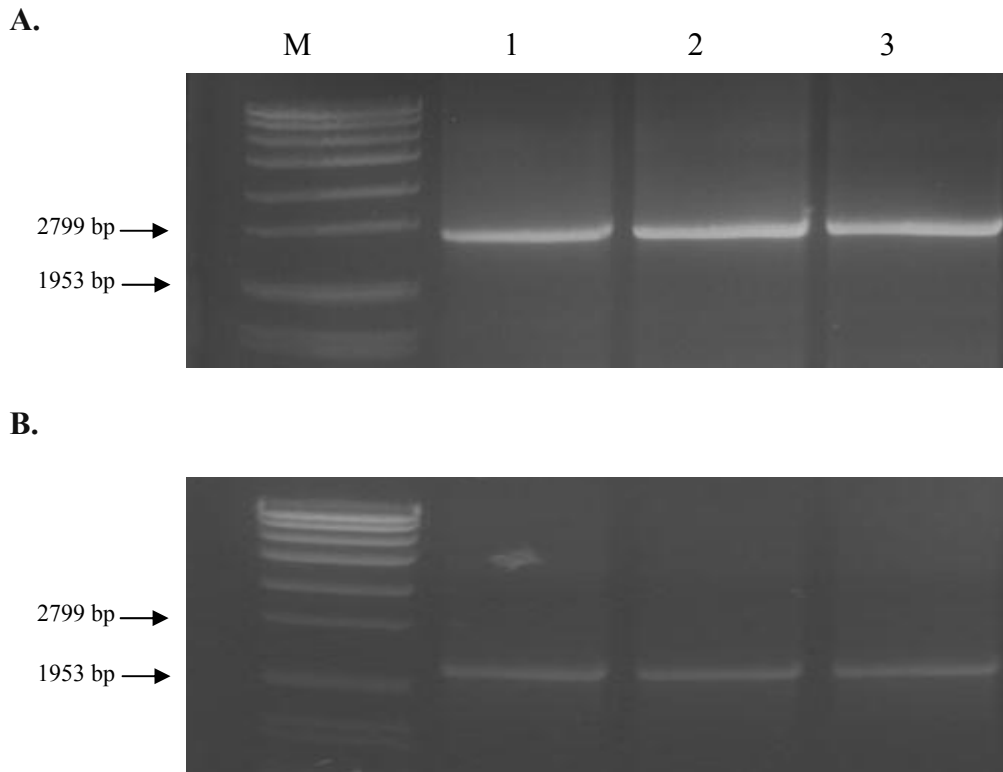


Figure 4.5. *pesL* Final disruption constructs PCR 3 and PCR 4.

A. PCR 3 products (2.6 kb).

B. PCR 2 products (2.0 kb).

M: Molecular weight marker (Roche VII). Lane 1-3: PCR products from three PCR reactions.

4.3.2. Isolation of an *A. fumigatus pesL* mutant strain ($\Delta pesL$).

Potential *pesL* mutants were initially identified by resistance to pyrithiamine following transformation. There were 40 colonies that appeared resistant to pyrithiamine, and 10 of these were selected for further analysis. These colonies were isolated as described (Section 2.2.3.3) and Southern blot analysis was performed (Section 2.2.4). Genomic DNA (gDNA) from *A. fumigatus* \DeltaakuB and these transformants was restriction digested with *XbaI* and probed for the 3' coding region of *pesL* with a DIG-labelled *pesL* probe (Section 2.2.5). Expected hybridisation patterns for wild-type and $\Delta pesL$ were 6.6 kb and 3.3 kb, respectively. The expected $\Delta pesL$ pattern was observed in 4 of the 10 transformants, indicating that *pesL* had been successfully deleted. A schematic representation of the Southern blot and hybridisation patterns is shown in Figure 4.6. Following Southern blot analysis, colonies which yielded the expected signal for a *pesL* disruption were subjected to single spore isolation (Section 2.2.3.4). A second round of Southern blot analysis was then carried out on single-spored colonies using the probing strategy as outlined above. *XbaI* genomic DNA digestions and Southern blot analysis of a single spore transformant ($\Delta pesL$) is shown in Figure 4.7.

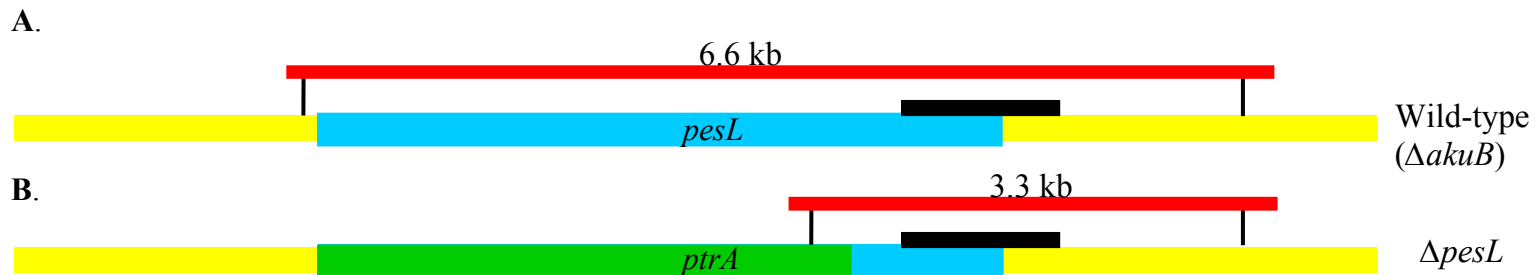


Figure 4.6. Southern blotting and hybridisation strategy used to identify *A. fumigatus* $\Delta pesL$.

This diagram illustrates the probing strategy that was used to identify $\Delta pesL$. The *pesL* locus in wild-type (A) and $\Delta pesL$ (B) is shown. The entire *pesL* coding region is indicated as a blue bar and the 5' and 3' flanking regions are shown in yellow. Approx. 3.0 kb of *pesL* was deleted and replaced by the pyrithiamine resistance cassette (*ptrA*) from *A. oryzae* (Kubodera *et al.*, 2000; Kubodera *et al.*, 2002) *ptrA* is indicated in green. Black vertical lines indicate *XbaI* restriction sites in the genomic sequence of wild-type and $\Delta pesL$. Genomic DNA from pyrithimane-resistance colonies was *EcoRI* digested and probed with a 1 kb DIG-labelled fragment corresponding to the 3' flanking region of *pesL*. The probe is indicated with a black horizontal line. The positions for probe binding are indicated with red horizontal lines. Expected hybridisation patterns: wild-type-6.6 kb, $\Delta pesL$ -3.3 kb.



Figure 4.7. Isolation of an *A. fumigatus* $\Delta pesL$ mutant strain.

*Xba*I digested genomic DNA (gDNA) was probed with a DIG-labelled PCR product corresponding to the 3' flanking region of *pesL*. Horizontal arrows indicate the sizes (bp) of the DNA fragments visible on the blot. Lane 1: *A. fumigatus* wild-type (= *A. fumigatus* $\Delta akuB$), Lane 2: *A. fumigatus* $\Delta pesL$ single spore transformant. Expected hybridisation pattern: wild-type- 6.6 kb, $\Delta pesL$: 3.3 kb.

4.3.3. Expression analysis of *pesL* in *A. fumigatus*.

Expression analysis was undertaken by a combination of RT-PCR and Real-Time PCR to confirm that disruption of *pesL* corresponded to a loss of *pesL* expression. The expression of *pesL* in a variety of growth conditions, and genes proposed to be a cluster with *pesL* (Nierman *et al.*, 2005) were also investigated.

4.3.3.1. Disruption of *pesL* leads to abolition of *pesL* expression in *A. fumigatus*.

RT-PCR and Real-Time PCR analyses were undertaken following growth of *A. fumigatus* wild-type and $\Delta pesL$ in either RPMI media or Czpaek's Broth for 48 hr at 37 °C. *pesL* / NRPS 11 expression had previously been observed under these conditions (Cramer *et al.*, 2006b). Primers were used to amplify a 228 bp amplicon within the *pesL* coding region (Table 2.3). This analysis confirmed that *pesL* expression was completely abolished following *pesL* disruption, as observed by the lack of a *pesL* amplicon from $\Delta pesL$ cDNA preparations (Figure 4.8).

Real-Time PCR analysis was then undertaken (Section 2.2.6.6) using the same cDNA preparations in order to quantify the levels of *pesL* expression in the wild-type and once again confirm absence of *pesL* expression in $\Delta pesL$. The expression of *pesL* was compared to the expression of *calm* in all samples, and relative expression is given as a multiple of 1, whereby a value of 1 indicates that *pesL* and *calm* were equally abundant in that sample. Real-time PCR provided further confirmation that *pesL* expression had been abolished in *A. fumigatus* $\Delta pesL$ (Figure 4.9) Also, *pesL* is expressed at a low level in RPMI with a low relative abundance compared to *calm* (30 % relative abundance), and *pesL* expression is extremely low in Czapek's broth (Figure 4.9).

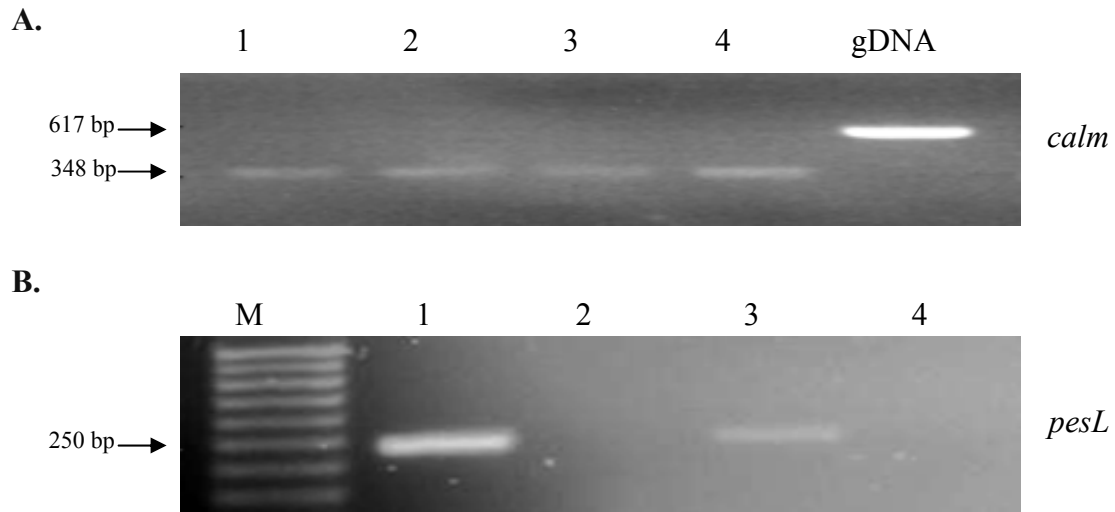


Figure 4.8. RT-PCR analysis confirms absence of *pesL* gene expression in *A. fumigatus* $\Delta pesL$.

RT-PCR to examine expression of *pesL* in *A. fumigatus* $\Delta akuB$ (wild-type) and $\Delta pesL$ following growth in liquid RPMI (R) or Czapek's Broth (CB) for 48 hr confirms the abolition of *pesL* expression in $\Delta pesL$.

A. *calm* is constitutively expressed in *A. fumigatus* was used as a control for RT-PCR experiments, and gDNA amplicon absence in cDNA confirms the absence of contaminating genomic DNA (gDNA) in cDNA preparations.

B. RT-PCR analysis for *pesL* amplicon (228 bp). M: Roche 50 bp DNA ruler.

Lanes: 1- wild-type (R), 2- $\Delta pesL$ (R), 3-wild-type (CB), 4- $\Delta pesL$ (CB).

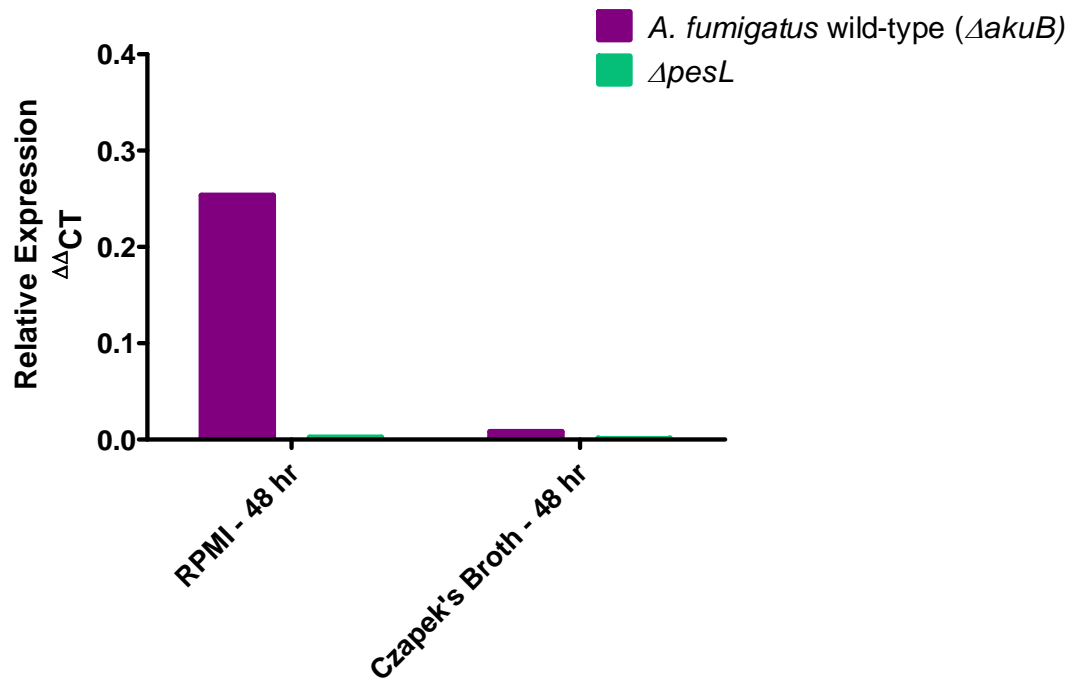


Figure 4.9. Confirmation of absence of *pesL* gene expression in *A. fumigatus* $\Delta pesL$ by Real-Time PCR.

Real-Time PCR analysis of *pesL* expression following *A. fumigatus* wild-type and $\Delta pesL$ growth in RPMI or Czapek's broth media for 48 hr. The relative abundances of *pesL* and the house-keeping *calm* transcripts are given. *pesL* expression is evident in *A. fumigatus* wild-type following growth in RPMI, and lowly expressed in Czapek's broth. *pesL* expression is absent in *A. fumigatus* $\Delta pesL$ in all conditions tested.

4.3.3.2. *pesL* is expressed under a range of conditions in *A. fumigatus*.

Once *pesL* was successfully disrupted, comparative metabolite profiling between *A. fumigatus* wild-type and $\Delta pesL$ could be undertaken, in order to identify a non-ribosomal peptide encoded by PesL. In order to do this, it was necessary to identify culture conditions where *pesL* was actually expressed. To this end, *pesL* expression was examined by RT-PCR in a range of culture conditions, usually over a 96 hr time period. A summary of these conditions, and the status of *pesL* expression (qualitative) is presented in Table 4.3.

RT-PCR analysis indicated that *pesL* was expressed in almost all culture conditions examined. *pesL* was expressed at a constant level in Czapek's broth over a 96 hr time period, whereas *pesL* expression varied greatly when *A. fumigatus* was grown in MEM (FCS) media (Figure 4.10). Under these conditions, *pesL* was most highly expressed at 48 hr, less abundant at 24 and 72 hr, and expression was also evident to a lower extent at 96 hr. (Figure 4.10). *pesL* expression was also detected, albeit weakly in YG media at 48 and 72 hr (Figure 4.11).

Table 4.3. A summary of all the culture conditions used to examine *pesL* expression.

Culture condition	Time period	<i>pesL</i> expressed yes (✓) / no (x)
Minimal Eagle's Media	24 hr	✓
(MEM) supplemented with 5	48 hr	✓
% Foetal Calf Serum (FCS)	72 hr	✓
Shaking at 37 °C	96 hr	✓
Yeast Glucose (YG) media	24 hr	X
Shaking at 37 °C	48 hr	✓
	72 hr	✓
	96 hr	X
Czapek's Media	24 hr	✓
Shaking at 37 °C	48 hr	✓
	72 hr	✓
	96 hr	✓
<i>Aspergillus</i> minimal media	24 hr	✓
(AMM)	48 hr	X
Shaking at 37 °C		

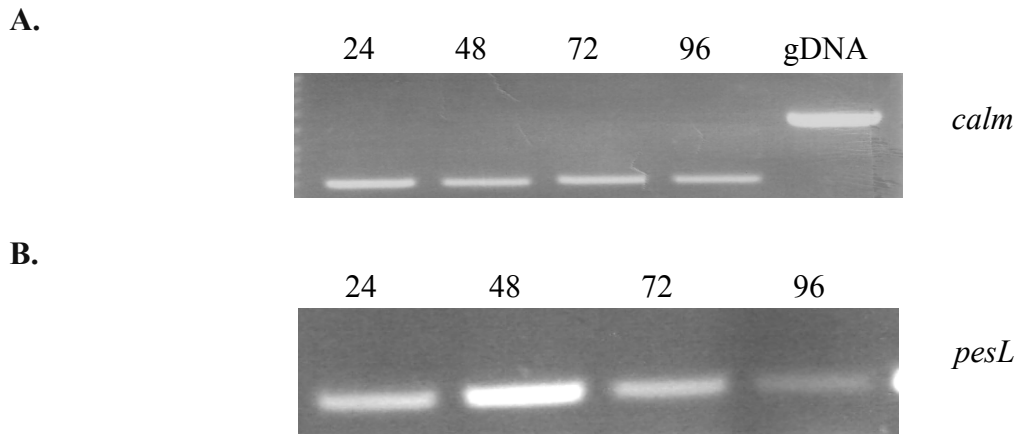


Figure 4.10. *pesL* is expressed in MEM-FCS culture media over a 96 hr time period.

Expression of *calm* and *pesL* at 24, 48, 72, and 92 hr as indicated above.

A. RT-PCR for the *calm* and gDNA amplicon absence in cDNA confirms the absence of contaminating genomic DNA (gDNA) in cDNA preparations.

B. *pesL* cDNA amplicon (250 bp) indicates expression in MEM-FCS at all time points examined, with highest abundance at 48 hr. Expression appears somewhat similar at 24 and 72 hr time-points, and *pesL* expression is least abundant at 96 hr.

4.3.3.3. The 5 genes in the putative *pesL* cluster are expressed in the *A. fumigatus* \DeltaakuB strain.

When the genome of *A. fumigatus* was sequenced, the *pesL* cluster was proposed to contain 5 genes. These genes and putative assigned functions are presented in Table 4.4. RT-PCR analysis following growth of *A. fumigatus* in YG media over a 96 hr time period showed that all genes within the proposed *pesL* cluster were expressed (Figure 4.11). While no major changes in gene expression were observed over a 96 hr time period, it is clear that all 5 genes did not show the same pattern of expression. All genes are expressed at 48 hr and 72 hr, while all genes except *pesL* are expressed at 24 hr and 96 hr. Observation of gene expression was important as secondary metabolite gene clusters are often found to be suppressed and silent under standard laboratory conditions (Fisch *et al.*, 2009; Tamano *et al.*, 2008).

Table 4.4. Putative genes in *pesL* cluster in *A. fumigatus*. Nierman *et al.* (2005).

Cadre Identifier (Afu)	Putative function
AFUA_6G12040	maltose permease, putative
AFUA_6G12050	non-ribosomal peptide (NRP) synthetase, putative, PesL
AFUA_6G12060	MAK1-like monooxygenase, putative
AFUA_6G12070	FAD binding domain protein
AFUA_6G12080	non-ribosomal peptide (NRP) synthetase, putative, PesM

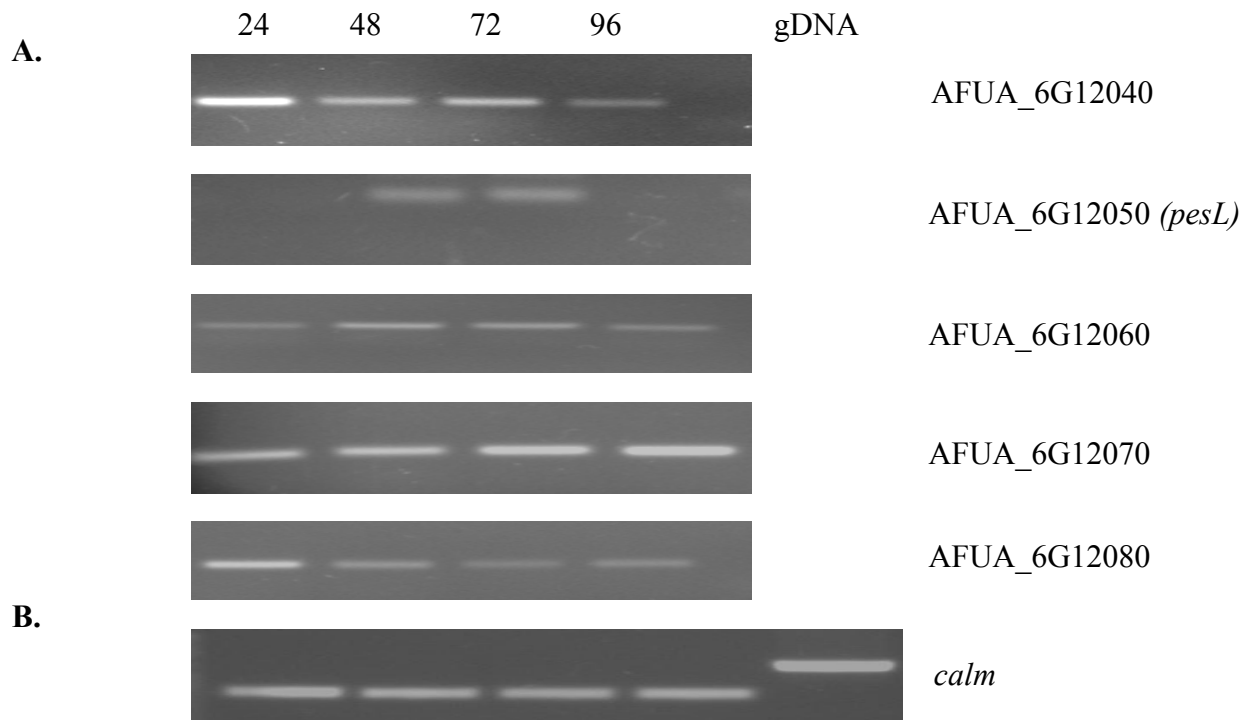


Figure 4.11. All genes in the proposed *pesL* cluster are expressed in *A. fumigatus*.

A. RT-PCR was carried out for all genes in the *pesL* cluster, following growth in YG media. Amplicons were generated for all genes as indicated. Expression of all genes was observed over a 96 hr time period, with no major changes in expression occurring over the time period examined. However, the 5 genes display differential patterns of expression.

B. RT-PCR for *calm*, confirms no contaminating gDNA in cDNA preparations and equal loading of cDNA in all PCR reactions.

4.3.4. Phenotypic characterisation of *A. fumigatus* $\Delta pesL$.

A. fumigatus $\Delta pesL$ was compared to wild-type under a variety of growth conditions and environmental stresses in order to investigate if it displayed altered phenotypes under any condition. A summary of all conditions tested in this study and outcomes is provided in Table 4.5. For all phenotypic analyses, plate assays were used in order to compare *A. fumigatus* wild-type and $\Delta pesL$ (Section 2.2.8). Conditions analysed were similar to those described for analysis of *A. fumigatus* $\Delta pes3$ in the previous chapter. Under conditions of varying iron availability, *A. fumigatus* $\Delta pesL$ behaved comparably to wild-type, indicating no role for *pesL* in the biosynthesis of siderophores in *A. fumigatus* (Figure 4.12). This finding is important as NRPS has previously been shown to be important for siderophore biosynthesis in *A. fumigatus* (Schrettl *et al.*, 2004; Schrettl *et al.*, 2007), and these findings clearly demonstrate that *pesL* is not involved in this process. Other phenotypic analysis performed including testing for heavy metal stress in the presence of cobalt chloride, revealed no differences between wild-type and $\Delta pesL$ (not shown). A range of cell wall damaging and membrane perturbing agents, previously described in Chapter 3, were tested, and in all cases, *A. fumigatus* $\Delta pesL$ grew at equal rates compared to wild-type upon exposure to all of these agents (caffeine, SDS, congo red, calcafluor white, and growth at elevated temperatures), eliminating a role for *pesL* in cell wall synthesis, structure or integrity in *A. fumigatus*. However, some interesting phenotypes were observed for *A. fumigatus* $\Delta pesL$ and these will be dealt with individually in the subsequent sections.

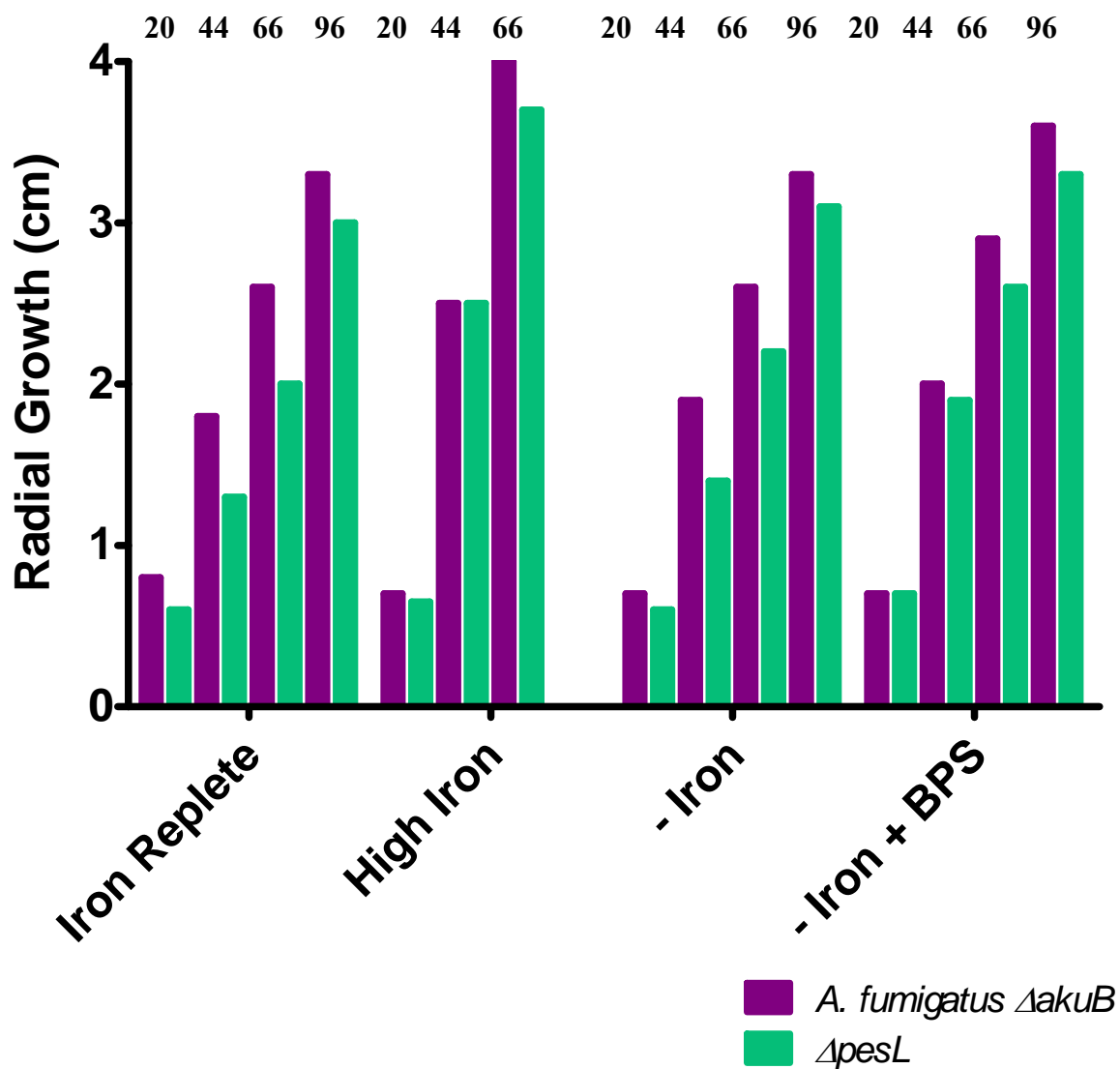


Figure 4.12. *A. fumigatus* $\Delta pesL$ behaves comparably to wild-type ($\Delta akuB$) when grown on a range of varying iron conditions.

Wild-type and $\Delta pesL$ were exposed to a range of varying iron conditions, as indicated on the graph. The graph shows that *A. fumigatus* wild-type and $\Delta pesL$ strains grew at comparable rates on all conditions tested. Radial growth (cm) of colonies was measured at 20, 44 and 66 hr intervals as indicated above the graph.

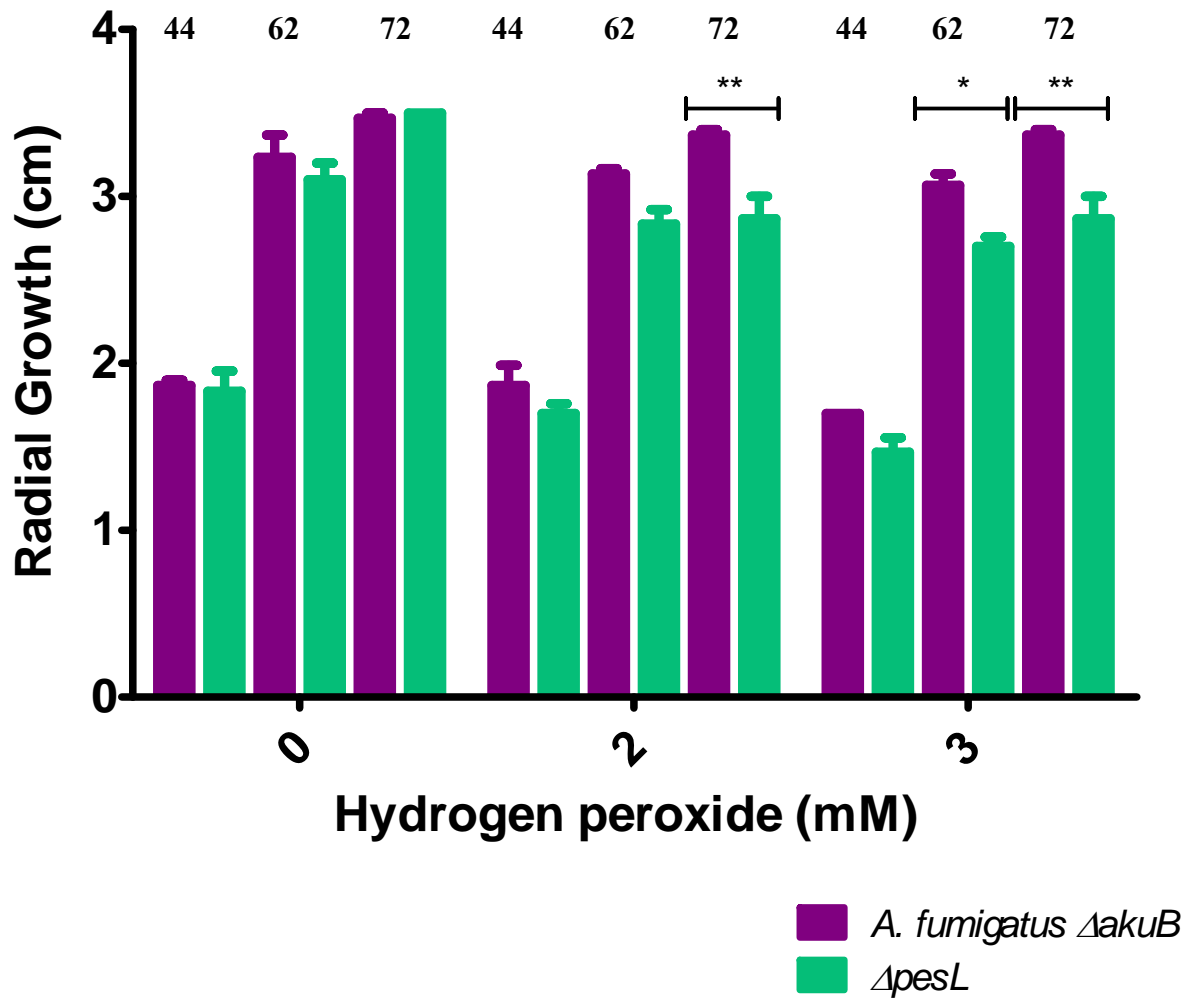
4.3.4.1. *pesL* protects *A. fumigatus* against oxidative stress caused by hydrogen peroxide.

A. fumigatus $\Delta pesL$ was examined for sensitivity to oxidative stress by growth on AMM agar in increasing concentrations agents which are known to cause oxidative stress. Sensitivity to the oxidising agents described was tested by performing plate assays (Section 2.2.8) using concentration ranges summarised in Table 4.5. In these investigations, *A. fumigatus* $\Delta pesL$ was more sensitive to H₂O₂ compared to the wild-type strain, and this is shown in Figure 4.13, as indicated by reduced growth upon exposure to 2 mM H₂O₂ at 72 hr growth ($p < 0.01$). This phenotype is more pronounced when the strains are exposed to 3 mM H₂O₂, at an earlier time of 62 hr ($p < 0.05$), and 72 hr ($p < 0.01$). Overall, these data indicated that *pesL* is involved in protection against the effects of H₂O₂ in *A. fumigatus*. Furthermore, the morphologies of wild-type and $\Delta pesL$ colonies were different following growth in the presence of H₂O₂. A loopful (5 μ l) of a conidial suspension was spread onto an AMM plate supplemented with H₂O₂ (final concentration 2 mM) and incubated for 5 days, and the plates were then photographed. Wild-type colonies were much darker green in colour, while $\Delta pesL$ were pale with less sporulation (Figure 4.13). These results indicated that exposure to H₂O₂ hinders conidial germination and further sporulation, strongly suggesting that *pesL* is important in the protection against oxidative stress caused by H₂O₂ in *A. fumigatus*.

In contrast, *A. fumigatus* $\Delta pesL$ exhibited increased growth compared to wild-type upon exposure to another oxidising agent, menadione, at all concentrations tested (Figure 4.14). At 62 and 72 hr growth, *A. fumigatus* $\Delta pesL$ shows increased growth in comparison to the wild-type strain on 20 μ M menadione ($p < 0.05$). This increased resistance of $\Delta pesL$ to menadione is more pronounced at a higher concentration (40 μ M), and this is evident at an earlier time point of 44 hr growth ($p < 0.01$). Upon exposure to diamide, *A. fumigatus*

wild-type and $\Delta pesL$ grew at similar rates (Figure 4.15). There appears to be an increase in growth of *A. fumigatus* $\Delta pesL$ compared to wild-type upon exposure to diamide but this is also seen in the absence of diamide, and may be due to slight differences in the starting conidial concentration. No statistical significance was observed between wild-type and $\Delta pesL$ upon diamide exposure. Overall, the oxidative stress phenotypic tests highlight a role for *pesL* in protection against hydrogen peroxide. The absence of *pesL* leads to greater growth of *A. fumigatus* in the presence of menadione, and no difference was observed upon exposure to diamide. Possible explanations for these contrasting findings will be discussed later in this chapter.

A.



B.



A. fumigatus wild-type

$\Delta pesL$

Figure 4.13. *A. fumigatus* $\Delta pesL$ exhibits increased sensitivity to hydrogen peroxide compared to wild-type.

A. The radial growth (cm) of strains exposed to increasing concentrations of H₂O₂ shows that $\Delta pesL$ is more sensitive to wild-type as indicated by reduced growth upon exposure to 2 mM H₂O₂ at 72 hr growth ($p < 0.01$). Growth was monitored at 44, 62 and 72 hr as indicated. Increased sensitivity of $\Delta pesL$ is more pronounced when the strains are exposed to 3 mM H₂O₂, at an earlier time of 62 hr ($p < 0.05$), and 72 hr ($p < 0.01$). Overall, these data indicated that *pesL* is involved in protection against the effects of H₂O₂ in *A. fumigatus*. Key: * = $p < 0.05$, ** = $P < 0.01$. Data represents the mean \pm standard error of three experiments.

B. $\Delta pesL$ displays severely reduced growth in the presence of 2mM H₂O₂ compared to wild-type 5 days post-inoculation. Colonies of wild-type growing in 2mM H₂O₂ were much darker in colour and sporulating more extensively than $\Delta pesL$. The data indicates that both germination and conidiation are reduced in $\Delta pesL$ when 2mM H₂O₂ is present, strongly implying a role for *pesL* in resistance to oxidative stress in *A. fumigatus*.

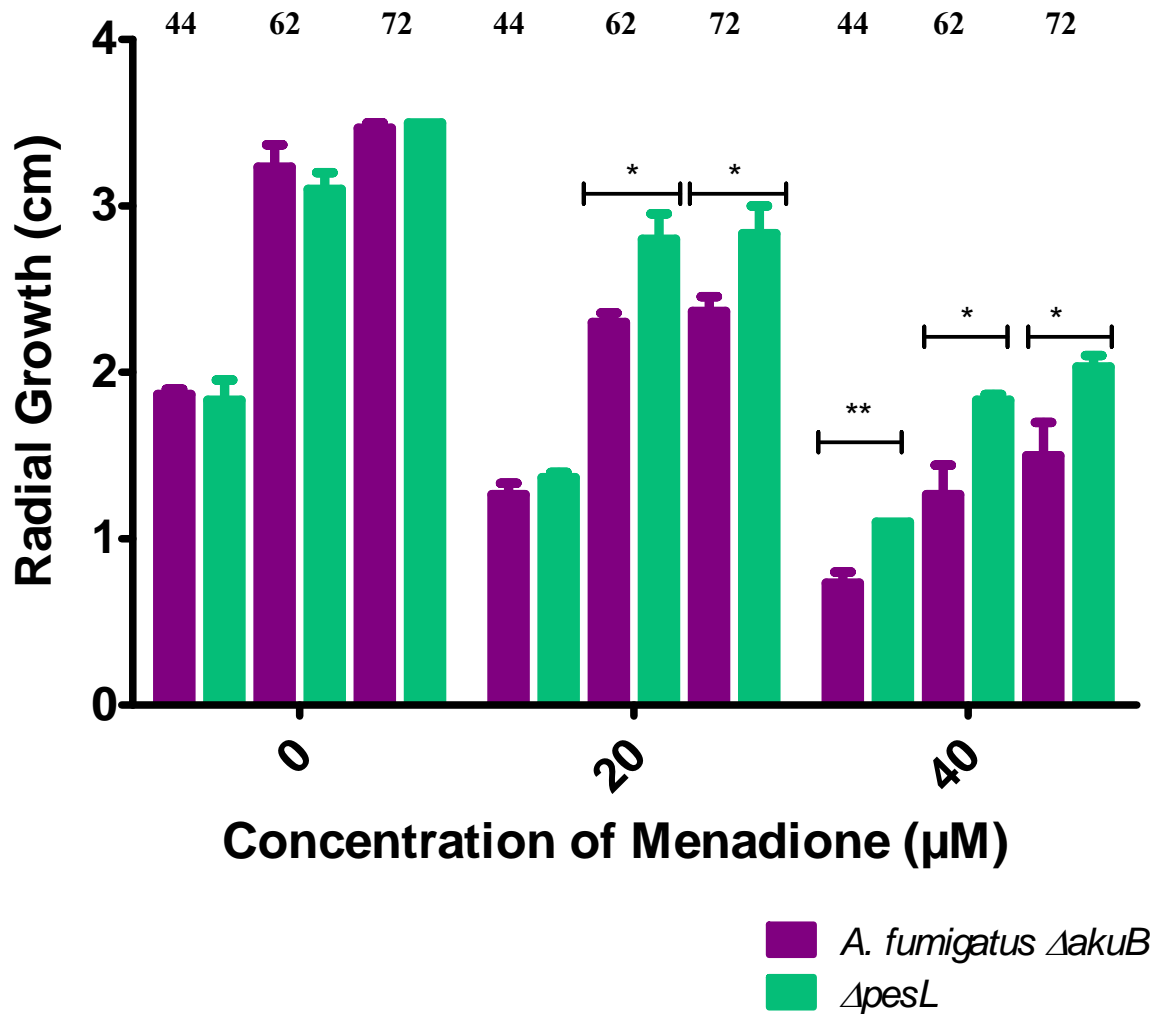


Figure 4.14. *A. fumigatus* $\Delta pesL$ is more resistant to the effects of menadione.

The radial growth (cm) of *A. fumigatus* wild-type and $\Delta pesL$ exposed to increasing concentrations of menadione shows that $\Delta pesL$ is more resistant than wild-type as increased growth is observed for $\Delta pesL$ at all concentrations of menadione. Growth was monitored at 44, 62 and 72 hr as indicated. Key: * = $p < 0.05$, ** = $P < 0.01$. Data represents the mean \pm standard error of three experiments.

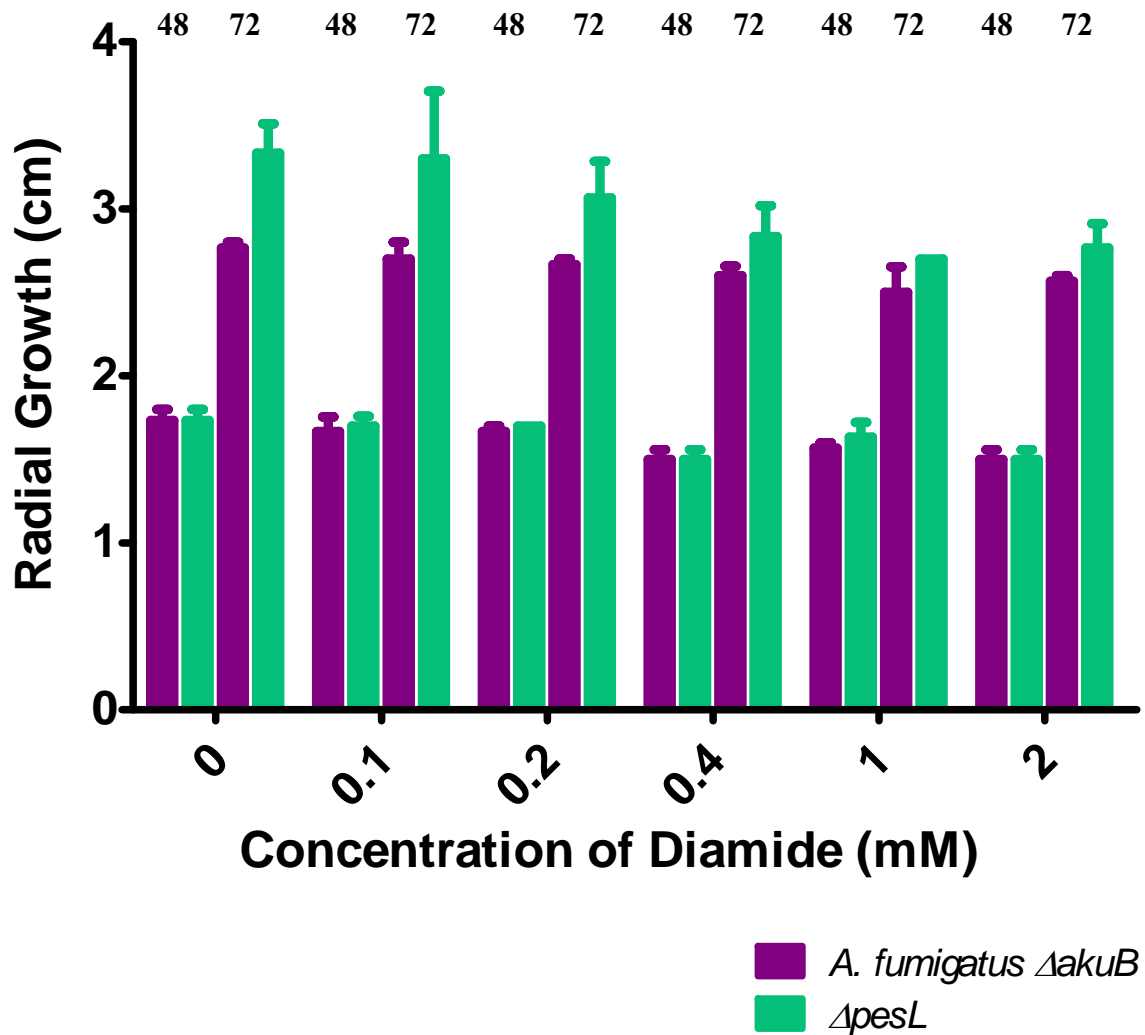


Figure 4.15. *A. fumigatus* $\Delta pesL$ behaves comparable to wild-type upon exposure to diamide.

The radial growth (cm) of *A. fumigatus* wild-type and $\Delta pesL$ exposed to increasing concentrations of diamide shows no statistical difference between the growth rates of strains. It may be seen however, that $\Delta pesL$ appears to exhibit a slightly enhanced growth rate compared to wild-type, particularly at the 72 time point. Data represents the mean \pm standard error of three experiments.

4.3.4.2. *pesL* protects *A. fumigatus* against voriconazole toxicity.

Anti-fungal phenotypic testing was performed for *A. fumigatus* wild-type and $\Delta pesL$ upon exposure to the anti-fungal agents; voriconazole, amphotericin B and caspofungin as have been described in Chapter 3. The concentrations of anti-fungals used in this study are summarised in Table 4.5.

A. fumigatus $\Delta pesL$ exhibited increased sensitivity to voriconazole when compared to wild-type at all concentrations of voriconazole tested, corresponding to a lower growth rate upon exposure to voriconazole and this was most significant at concentrations of 0.5 $\mu\text{g/ml}$ following 44 hr ($p < 0.05$), 62 hr ($p < 0.001$), and 72 hr growth ($p < 0.01$). Exposure to the highest concentration of voriconazole tested (1.0 $\mu\text{g/ml}$) resulted in complete growth inhibition of $\Delta pesL$ after 44 hr growth ($p < 0.05$), and even though $\Delta pesL$ had begun to grow by 62 hr, the growth rate was still only 50 % of the wild-type ($p < 0.05$). A steady decrease in the overall growth of both strains was observed as the concentration of voriconazole increased, indicating that the concentration range used was sufficient to detect differences in susceptibility between strains. This data is presented in Figure 4.16, and strongly indicates a role for *pesL* in protection against voriconazole toxicity in *A. fumigatus*.

A. fumigatus $\Delta pesL$ exhibited slightly reduced growth compared to wild-type when exposed to 0.5 $\mu\text{g/ml}$ amphotericin B ($p < 0.05$), but behaved comparably to wild-type at all other concentrations tested (Figure 4.17). Testing with caspofungin showed no differences in susceptibility between *A. fumigatus* wild-type and $\Delta pesL$.

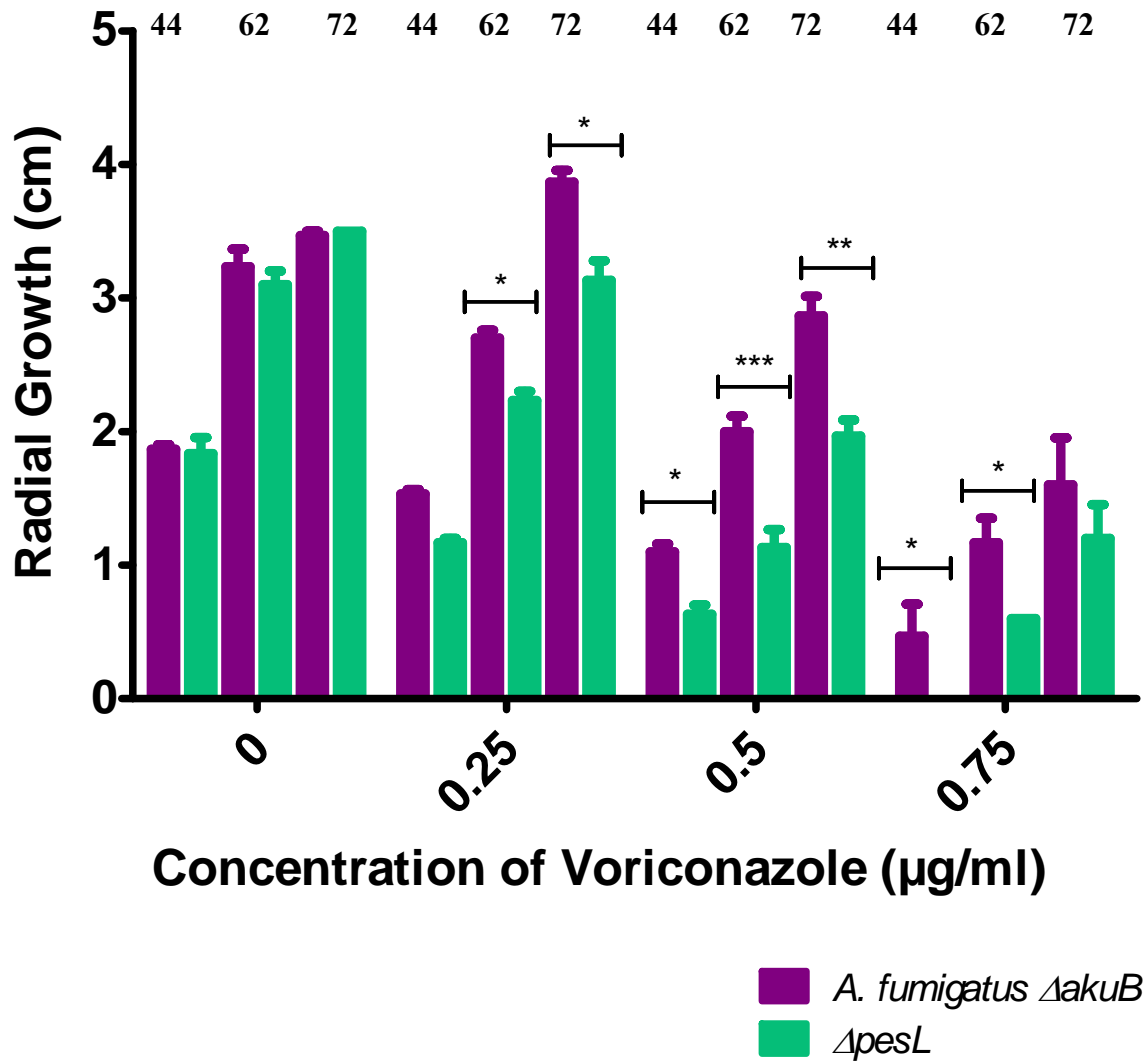


Figure 4.16. *A. fumigatus* $\Delta pesL$ displays increased sensitivity to the anti-fungal voriconazole.

A. Radial growth (cm) of wild-type and $\Delta pesL$ following exposure to increasing concentrations of voriconazole show that $\Delta pesL$ exhibits increased susceptibility at all concentrations tested. Growth was monitored at 44, 62 and 72 hr time points as indicated. On AMM only, wild-type and $\Delta pesL$ grew at similar rates, while exposure to voriconazole led to significant differences in growth between the two strains ($p < 0.001$), with the mutant displaying reduced growth at all time points. Each graph displays the mean \pm standard error of three experiments. Key: * = $p < 0.05$, ** = $p < 0.01$, *** = $p < 0.001$.

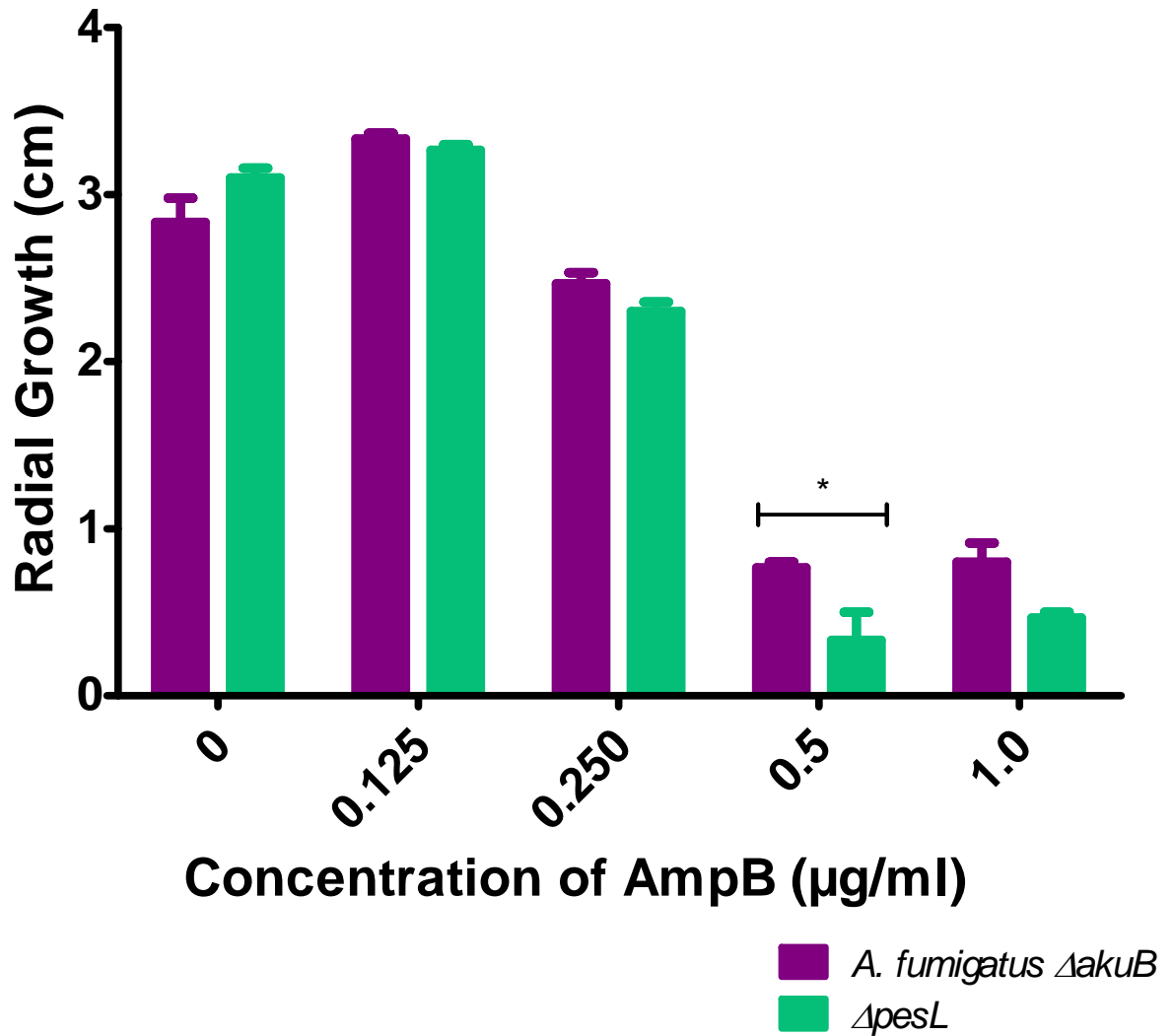


Figure 4.17. *A. fumigatus* $\Delta pesL$ displays moderately increased sensitivity to the anti-fungal amphotericin B.

A. Radial growth (cm) of wild-type and $\Delta pesL$ following exposure to increasing concentrations of amphotericin B show that $\Delta pesL$ exhibits increased susceptibility 0.5 μg/ml. Growth was monitored at 24, 48 and 72 hr time points and growth at 72 hr is shown.

Data represents the mean ± standard error of three experiments. Key: * = p < 0.05.

Table 4.5. A summary of the phenotypic assays, and their outcomes, performed for *A. fumigatus* wild-type (\DeltaakuB) and $\Delta pesL$ in this study.

Phenotypic Test	Reagents Used	Concentrations Tested	Result (i.e. growth of $\Delta pesL$ compared to wild-type)
Role of <i>pesL</i> in Siderophore Biosynthesis	Iron Stresses (High, Low, none)	10 μ M, 1.5 mM, 200 μ M BPS	No difference.
Oxidative Stress	Menadione	20, 40 μ M	$\Delta pesL$ more resistant to menadione at all concentrations tested ($p < 0.05$).
	Diamide	0.1, 0.2, 0.4, 1, 2 mM	No difference.
	Hydrogen Peroxide (H_2O_2)	1, 2, 3 mM	$\Delta pesL$ displays increased sensitivity to H_2O_2 at 62 hr ($p < 0.05$) and 72 hr ($p < 0.01$) growth.
Anti-fungal Susceptibility	Voriconazole (vrc)	0.25, 0.5, 0.75, 1.0 μ g/ml	$\Delta pesL$ displays increased sensitivity at all concentrations of vrc tested ($p < 0.05$).
	Amphotericin B	0.125, 0.25, 0.5, 1.0 μ g/ml	$\Delta pesL$ displays increased sensitivity at 0.5 μ g/ml ($p < 0.05$).
	Caspofungin	0.2, 0.5, 1.0 μ g/ml	No difference.
Heavy Metal Stress	Cobalt Chloride	0.1, 0.5, 1 mM	No difference.

Phenotypic Test	Reagents Used	Concentrations Tested	Result (i.e. growth of $\Delta pesL$ compared to wild-type)
Cell Wall Stress	Congo Red	5, 10, 15 $\mu\text{g/ml}$	No difference.
	Calcafluor White	100, 200 $\mu\text{g/ml}$	No difference.
	High temperature (48 ° C)	n/a	No difference.
	Caffeine	2, 5 mM	No difference.
Membrane Stress	SDS	0.01, 0.02 % (w/v)	No difference.

4.3.5. *pesL* contributes to *A. fumigatus* virulence in an insect model of infection.

To investigate if *pesL* contributes to virulence in *A. fumigatus*, the survival of larvae ($n = 20$) of the greater wax moth *G. mellonella* was compared following infection with 10^7 conidia/larvae of *A. fumigatus* wild-type (\DeltaakuB) or the same dose of $\Delta pesL$. Larvae ($n = 20$) were injected with sterile PBS as an injection control. Larvae infected with wild-type had a lower survival compared to those infected with $\Delta pesL$ ($p < 0.001$) indicating decreased virulence of the $\Delta pesL$ strain. Larval survival (%) is shown in Figure 4.18. Larvae injected with PBS exhibited 100 % survival throughout the experiment. At 24 hr following infection, 97 % of larvae infected with wild-type remained alive, while 100 % survival rate was observed for those infected with $\Delta pesL$. The difference in virulence between strains is more pronounced at 48 hr and 72 hr time-points, indicating reduced mortality upon the loss of *pesL* and its encoded peptide. At 48 hr post infection, 96 % of larvae infected with $\Delta pesL$ remain alive, in contrast to only 71 % of larvae infected with wild-type. By 72 hr, 82 % of larvae infected with $\Delta pesL$ are viable, versus 37 % in the wild-type group. The overall survival proportions between larvae infected with wild-type or $\Delta pesL$ is highly significant ($p < 0.001$) (Figure 4.18). Survival curves were generated using Kaplan-Meier survival plot with the Log-Rank (Mantel-Cox) test for significance. The experiment was repeated three times. Overall, these findings show that loss of *pesL* and its encoded peptide leads to reduced virulence in the *G. mellonella* model, strongly suggesting that the peptide encoded by *PesL* contributes to the virulence of *A. fumigatus*.

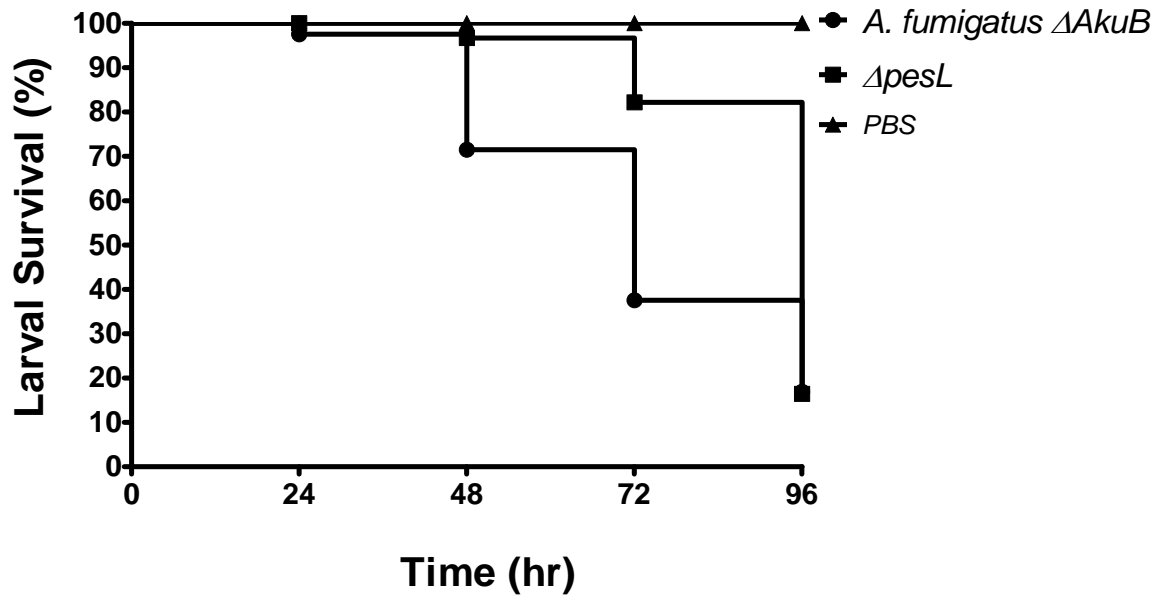


Figure 4.18. *A. fumigatus* Δ *pesL* is less virulent than wild-type in the *Galleria mellonella* insect model.

The survival proportions of larvae ($n = 20$) infected with either wild-type or Δ *pesL* are shown. *A. fumigatus* Δ *pesL* is less virulent than wild-type and larvae infected with Δ *pesL* exhibit increased survival compared to those infected with wild-type ($p < 0.001$). Larval viability (%) was assessed at 24 hr intervals following infection. At 48 hr post-infection, a 25 % difference in survival was observed between groups of infected larvae (wild-type – 70 % survival, Δ *pesL* – 95 % survival). By 72 hr, the difference was more pronounced with a 45 % survival difference observed between between larval infected with wild-type and Δ *pesL*. PBS was used as an injection control and all larvae in this group remained viable for the entire experiment.

4.3.6. Comparative metabolite profiling reveals that *pesL* encodes a peptide(s) that is up-regulated during oxidative stress caused by hydrogen peroxide.

The NRP synthetase encoded by *pesL* is likely to be involved in the biosynthesis of a secondary metabolite based on the observation that *pesL* and other genes within the proposed *pesL* cluster are under the transcriptional regulation of the master regulator of secondary metabolism in *A. fumigatus*, LaeA (Perrin *et al.*, 2007). Availability of the *A. fumigatus* $\Delta pesL$ mutant facilitated comparative metabolite analysis to be undertaken between wild-type and mutant cultures to identify a potential PesL-encoded non-ribosomal peptide (NRP) (Section 2.2.10). *A. fumigatus* wild-type and $\Delta pesL$ were cultivated in a variety of growth conditions, in which *pesL* was known to be expressed (Tables 4.3, 4.6), and metabolite extractions were performed for analysis by RP-HPLC either at NUIM or at the Danish Technical University.

Initially, culture supernatants (SN) were collected following growth of *A. fumigatus* wild-type ($\Delta akuB$) and $\Delta pesL$ in conditions A, B and C (Table 4.6) SN were either injected directly on the column or were subjected to organic extraction prior to injection (Sections 2.2.7.1, 2.2.7.2). These analyses were conducted at NUIM, and in all cases, no differences were observed between wild-type and $\Delta pesL$ strains with respect to metabolite profiles, and all conditions are summarised in Table 4.6. Since all of the conditions tested in A-C were liquid culture conditions, these analyses alone were not sufficient to analyse metabolites which may be present on the surface of, or associated with, conidia. Conditions D and E were then explored whereby relevant *A. fumigatus* strains were grown on AMM agar for 6 days and conidial extraction was carried out following the protocol of Moon *et al.*, (2008) (Section 2.2.7.3).

Table 4.6. Summary of conditions used for comparative metabolite analysis of wild-type *A. fumigatus* and $\Delta pesL$.

Growth Condition (all at 37 °C)	Extraction Solvent	Injection Volume	Outcome
A. RPMI 48 hr incubation, 200 rpm	1) Organic extraction of culture supernatant (SN) with SN: chloroform in a 1:1 ratio 2) Neat culture supernatant injection.	100 μ l / 20 μ l	No differences observed
B. Czapek's 48 hr incubation, 200 rpm	1) Organic extraction of culture supernatant (SN) with SN: chloroform in a 1:1 ratio 2) Neat culture supernatant injection.	100 μ l / 20 μ l	No differences observed
C. AMM 48 hr incubation, 200 rpm	1) Organic extraction of culture supernatant (SN) with SN: chloroform in a 1:1 ratio 2) Neat culture supernatant injection.	100 μ l / 20 μ l	No differences observed
D. Incubation on AMM agar for 6 days	Conidial Extraction Method (Moon <i>et al.</i> , 2008)	100 μ l	See section 4.3.6
E. Incubation on AMM supplemented with H ₂ O ₂ (final concentration 2 mM) for 6 days	Conidial Extraction Method (Moon <i>et al.</i> , 2008)	100 μ l	See section 4.3.6
F. Incubation on AMM agar for 6 days	Plug Extraction Method (Smedsgaard, 1997)	1 μ l	See section 4.3.7
G. Incubation on Czapek's agar for 6 days	Plug Extraction Method (Smedsgaard, 1997)	1 μ l	See section 4.3.7

For E, AMM agar was supplemented with H₂O₂ to a final concentration of 2 mM. This was done as phenotypic analysis revealed that *A. fumigatus* $\Delta pesL$ was more sensitive to H₂O₂ than wild-type (Section 4.3.4.1), so if PesL produces a peptide which protects *A. fumigatus* against oxidative stress, this peptide is likely to be produced more abundantly when the fungus is exposed to H₂O₂, possibly aiding PesL NRP identification. These analyses revealed two peaks present in extracts of *A. fumigatus* wild-type (Rt = 14.479 min, and 15.927 min) that were absent in $\Delta pesL$ at 220 nm (Figure 4.19). Aside from these peaks, metabolite profiles were otherwise identical between the two strains. These peaks represented candidate PesL-encoded non-ribosomal peptide(s), and are referred to as peptide(s) due to the absence of more than one peak in $\Delta pesL$. Examination of *A. fumigatus* wild-type and $\Delta pesL$ metabolite profiles at 280 nm indicated one of the candidate PesL-encoded peptides exhibited absorbance at 280 nm, indicating the presence of aromatic amino acids, such as phenylalanine, tyrosine, or tryptophan (Figure 4.20). Furthermore, this material was more abundant (approximately 2-fold) in extracts from conidia which had been exposed to H₂O₂ (1,200 mAU) compared to extracts which were taken from AMM agar plates only (600 mAU) (Figure 4.21).

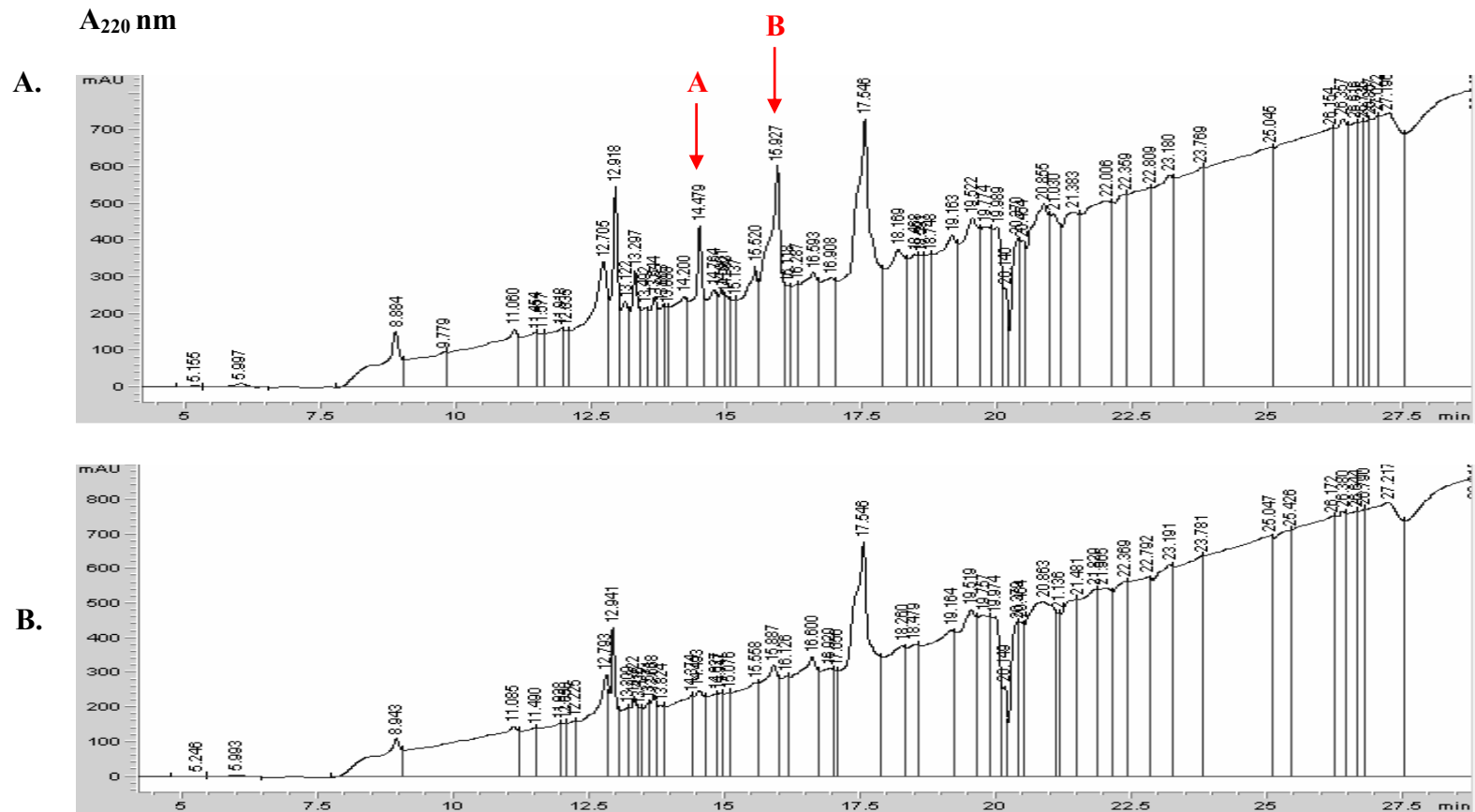
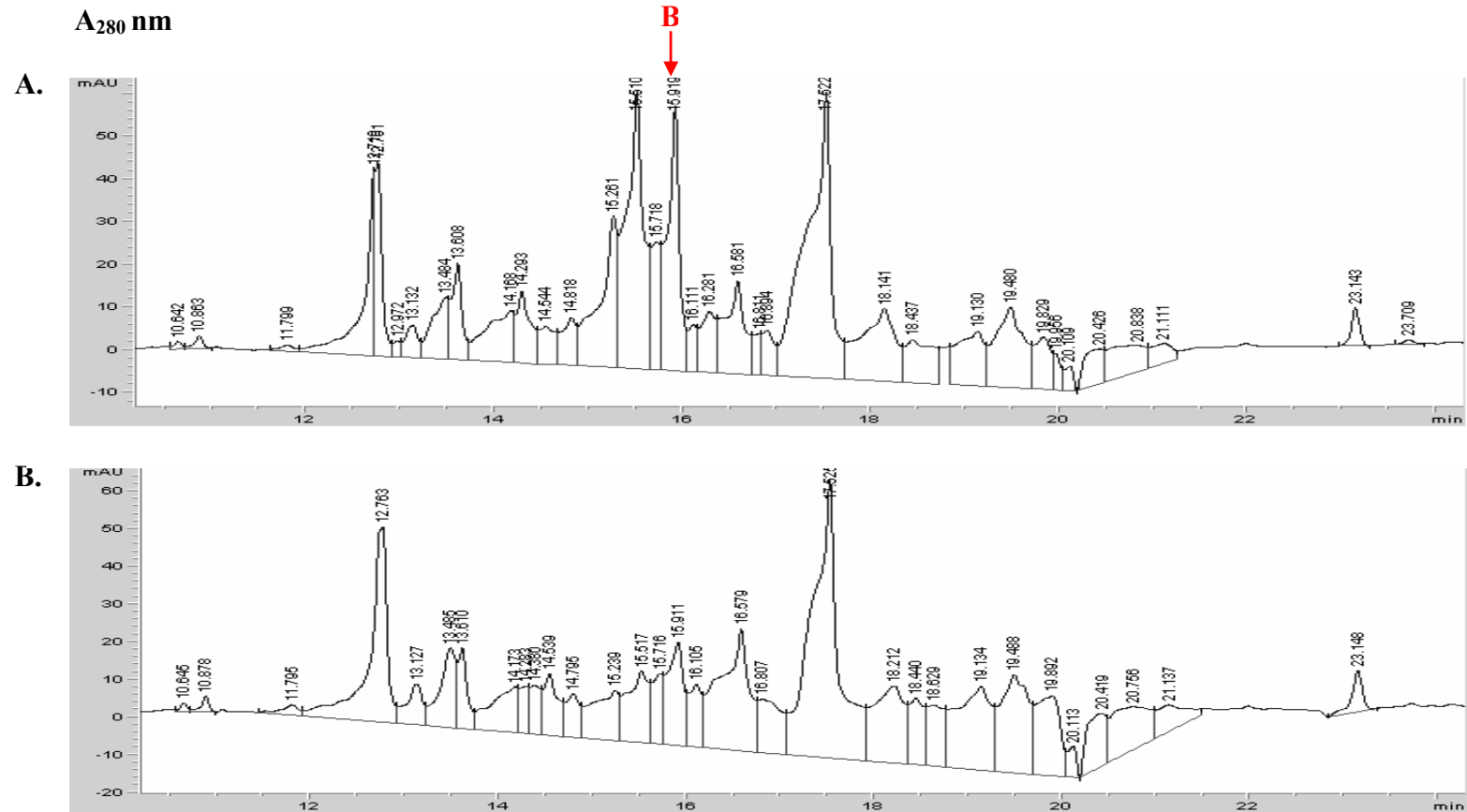


Figure 4.19. HPLC chromatograms detailing the fractionation of metabolites (0-30 min) following conidial extractions from *A. fumigatus* wild-type (A), and *A. fumigatus* $\Delta pesL$ (B), at 220 nm. Two peaks were present in wild-type (A: 14.479 min and B: 15.927 min) and absent in $\Delta pesL$ and these are indicated with red arrows.



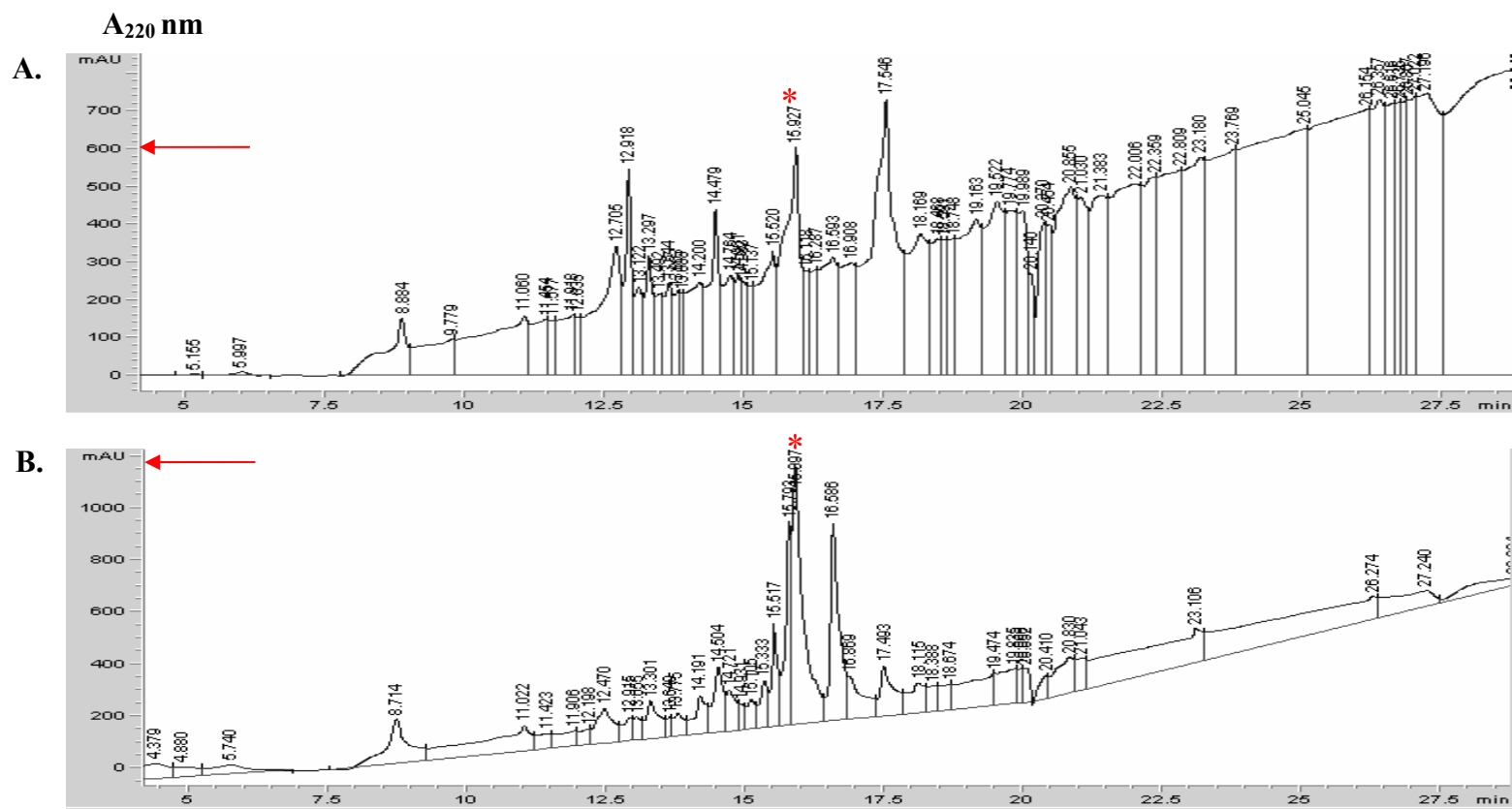


Figure 4.21. HPLC chromatograms detailing the fractionation of metabolites (0-30 min) following conidial extractions from *A. fumigatus* wild-type from AMM agar (A) or AMM agar supplemented with H_2O_2 (2 mM) (B) at 220 nm. Candidate PesL-encoded peptide (B: 15.927 min), is indicated with a red asterisk, and is more abundant following conidial exposure to H_2O_2 with approximately two-fold increase in absorbance at 220 nm, indicated by a red arrow.

4.3.7. PesL is essential for Fumigaclavine C biosynthesis in *A. fumigatus*.

Following these observations, samples were prepared for analysis at DTU in order to identify these PesL candidate peptides. A plug extraction method was used according to Smedsgaard, (1997) (Section 2.2.7.4), as this method was successful in generating extracts for the metabolite profiling of 395 fungal isolates (Smedsgaard, 1997) and allows simultaneous extraction of intracellular metabolites stored in mycelia, secreted metabolites that are present in the agar, and conidial associated metabolites (Professor Thomas Larsen – personal communication). Plug extractions were prepared for *A. fumigatus* wild-type and $\Delta pesL$ following Conditions F and G (Table 4.6). Briefly, metabolites were extracted from each strain following growth on either AMM or Czapek’s agar for 6 days. Extractions were carried out using two protocols; a mixture of 25 % acetonitrile and 75 % water (Section 2.1.8.2.1), or a mixture of ethyl acetate, dichloromethane and methanol (Section 2.1.8.2.2).

Analysis of these samples at DTU revealed that the deletion of *pesL* led to the loss of fumigaclavine C production in *A. fumigatus* $\Delta pesL$ (Figure 4.22), and this was observed under both conditions, following growth on both AMM and Czapek’s media. Figure 4.22 shows metabolite profiles following growth on Czapek’s agar, and extraction with ethyl acetate, dichloromethane and methanol. The RP-HPLC chromatograms clearly indicate that *A. fumigatus* wild-type produces fumigaclavine C, represented by a single peak at 5.13 min, and this peak is completely absent in *A. fumigatus* $\Delta pesL$. Interestingly, a metabolite was observed in the *A. fumigatus* $\Delta pesL$ profile (approx 3.60 min) that was not found in wild-type extracts (Figure 4.22). Identification of fumigaclavine C was confirmed by searching for the specific mass of fumigaclavine C; 367 [M + H]⁺, and a metabolite with this molecular mass was observed at a retention time of 5.17 min (Figure 4.23). Analysis of the UV spectrum of the peak at 3.60 min revealed that this peak represented a compound related to the fomitremorgin family of secondary metabolites, and is very similar to that of

Fumitremorgin C and TR-2 (Professor Thomas Larsen – personal communication) (Figure 4.24).

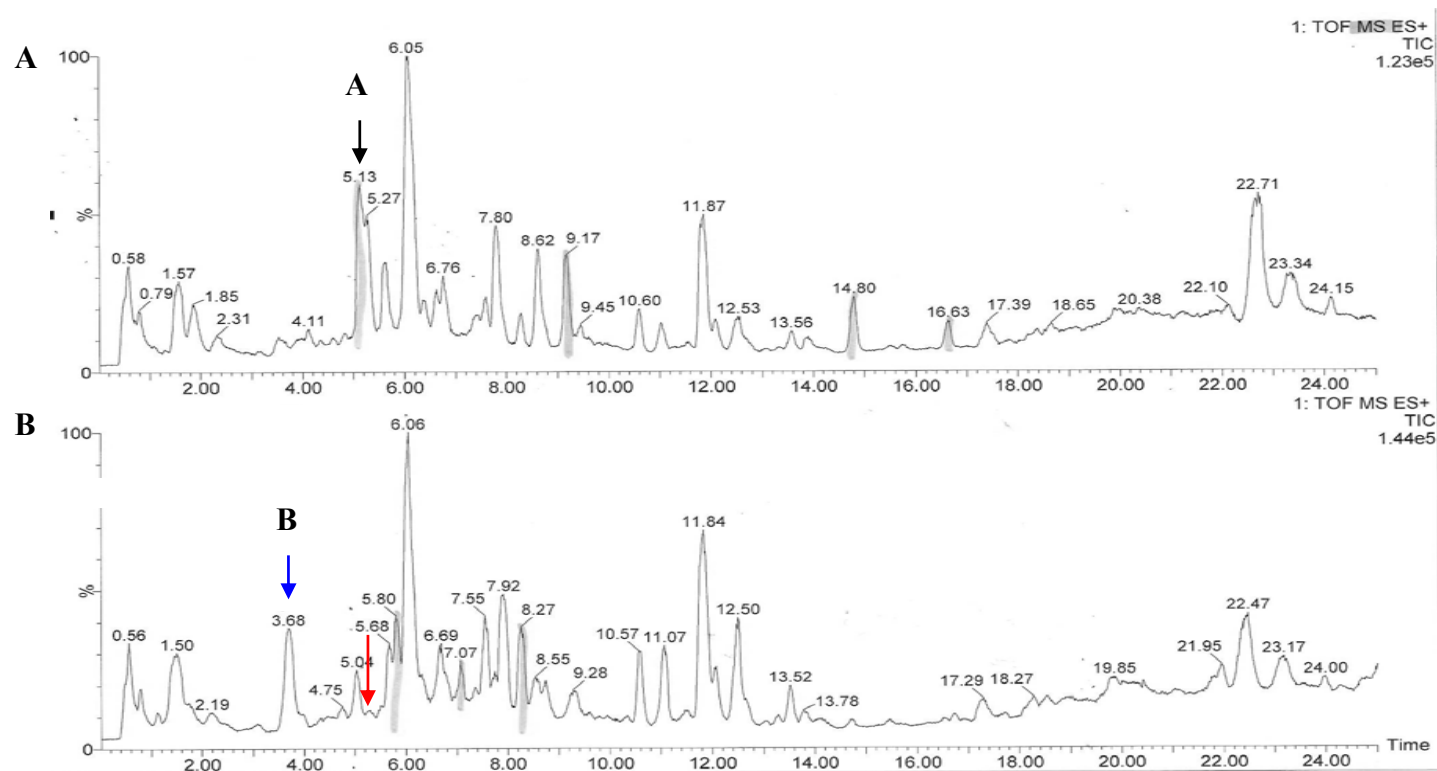


Figure 4.22. Total ion chromatograms (0-25 min) representative of metabolites detected from *A. fumigatus* (A) wild-type \DeltaakuB and (B) *A. fumigatus* $\Delta pesL$ following 6 days growth on Czapek's agar. Major differences between the extracts are annotated as follows: A; Fumigaclavine C (5.13 min), B; unknown peak (3.68 min). Red arrow highlights the absence of fumigaclavine C in *A. fumigatus* $\Delta pesL$, while a blue arrow indicates the presence of a new peak appearing in $\Delta pesL$ at 3.68 min.

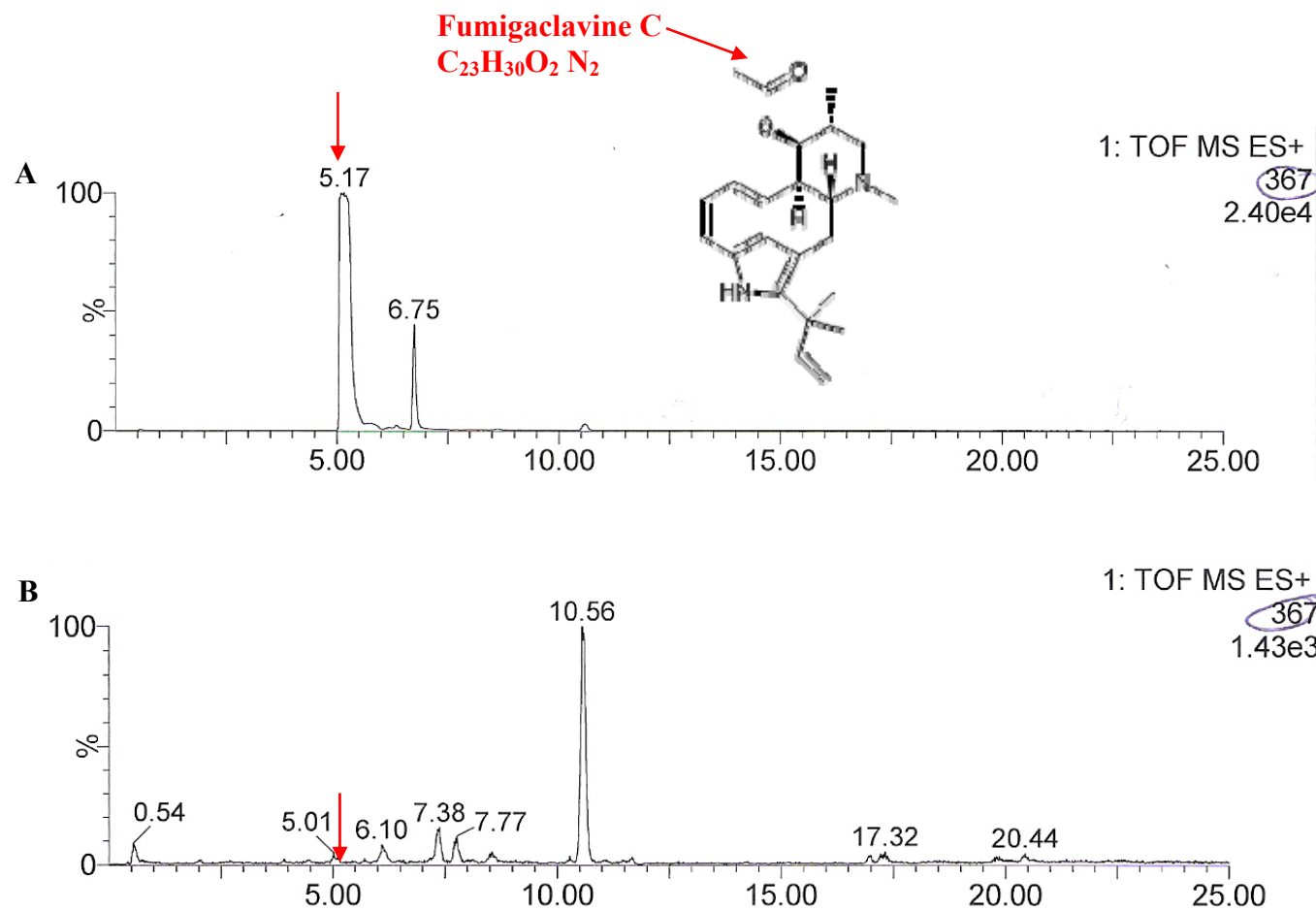


Figure 4.23. Fumigaclavine C identification by mass spectrometry. (A) Fumigaclavine C in *A. fumigatus* wild-type \DeltaakuB identifying at m/z 367 $[M + H]^+$ (retention time 5.17 min) and (B) absence of relevant peak in *A. fumigatus* $\Delta pesL$. Fumigaclavine C structure is also shown. Mass indicated on top right of each chromatogram.

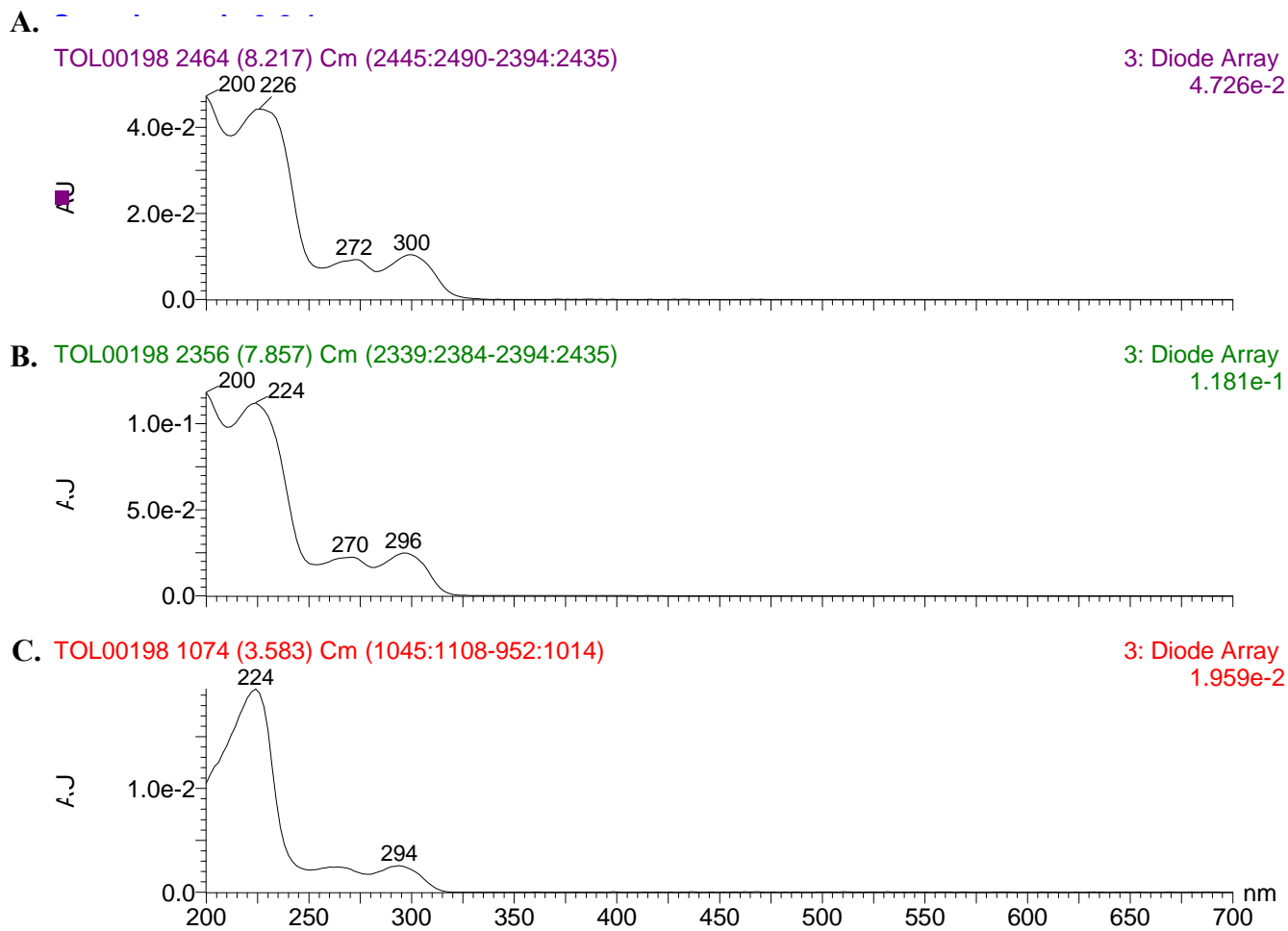


Figure 4.24. A metabolite (3.68 min) observed in *A. fumigatus* $\Delta pesL$ has a similar UV profile to the fumitremorgin family of compounds.

A. UV spectrum analysis for Fumitremorgin C.

B. UV spectrum for the unidentified metabolite at 3.60 min.

C. UV spectrum analysis for TR-2.

A-C indicate that the new unidentified metabolite observed in *A. fumigatus* $\Delta pesL$ is closely related to the fumitremorgin family of compounds, deduced from the similar UV absorbance of this compound to Fumitremorgin C (A) and TR-2 (C).

4.3.8. *PesL* is not essential for fumiquinazoline production in *A. fumigatus*.

An investigation into the secondary metabolites produced by *A. fumigatus* and other closely related species (including *A. lentulus*, *A. novofumigatus*, *A. fumigatiaffinis*, *Neosartoria fisheri* and *N. pseudofisheri*) revealed that one of the major metabolite families produced by *A. fumigatus* were the fumiquinazolines (A-G), and all were consistently produced in all strains tested (Larsen *et al.*, 2007). Recently, *PesL* has been implicated in fumiquinazoline biosynthesis in *A. fumigatus* (Ames *et al.*, 2010; Ames & Walsh, 2010). The authors show that recombinantly-expressed *PesL* (Af12050) was able to activate L-alanine as an adenylate, install it on its PCP domain and acylate the oxidised indole of fumiquinazoline F for subsequent intramolecular cyclization to create fumiquinazoline A, thereby implying that *PesL* is essential for the conversion of fumiquinazoline F to fumiquinazoline A (Ames *et al.*, 2010).

With the availability of *A. fumigatus* $\Delta pesL$, the metabolite profiles of wild-type and $\Delta pesL$ were thoroughly examined for the presence of the fumiquinazoline compounds. Table 4.7 shows a list of the compounds in this family, molecular formula, and molecular weight. LC-DAD-MS analysis following plug extracts (Smedsgaard, 1997) of wild-type and $\Delta pesL$, revealed the presence of all known fumiquinazolines in both strains (Figure 4.25).

Table 4.7. Structure and molecular weight (m/z) of the fumiquinazoline compounds produced by *A. fumigatus* (Larsen *et al.*, 2007; Takahashi *et al.*, 1995).

Compound	Molecular formula	M/Z	Retention time (RP-HPLC) – this study
Fumiquinazoline A	C ₂₄ H ₂₃ N ₅ O ₄	445.1744	7.32-7.34 min
Fumiquinazoline B	C ₂₄ H ₂₃ N ₅ O ₄	445.1744	7.32-7.34 min
Fumiquinazoline C	C ₂₄ H ₂₁ O ₄ N ₅	443.1588	7.6 min
Fumiquinazoline D	C ₂₄ H ₂₁ O ₄ N ₅	443.1588	7.6 min
Fumiquinazoline F	C ₂₁ H ₁₈ O ₂ N ₅	358.1430	6.12-6.15 min
Fumiquinazoline G	C ₂₁ H ₁₈ O ₂ N ₅	358.1430	6.12-6.15 min

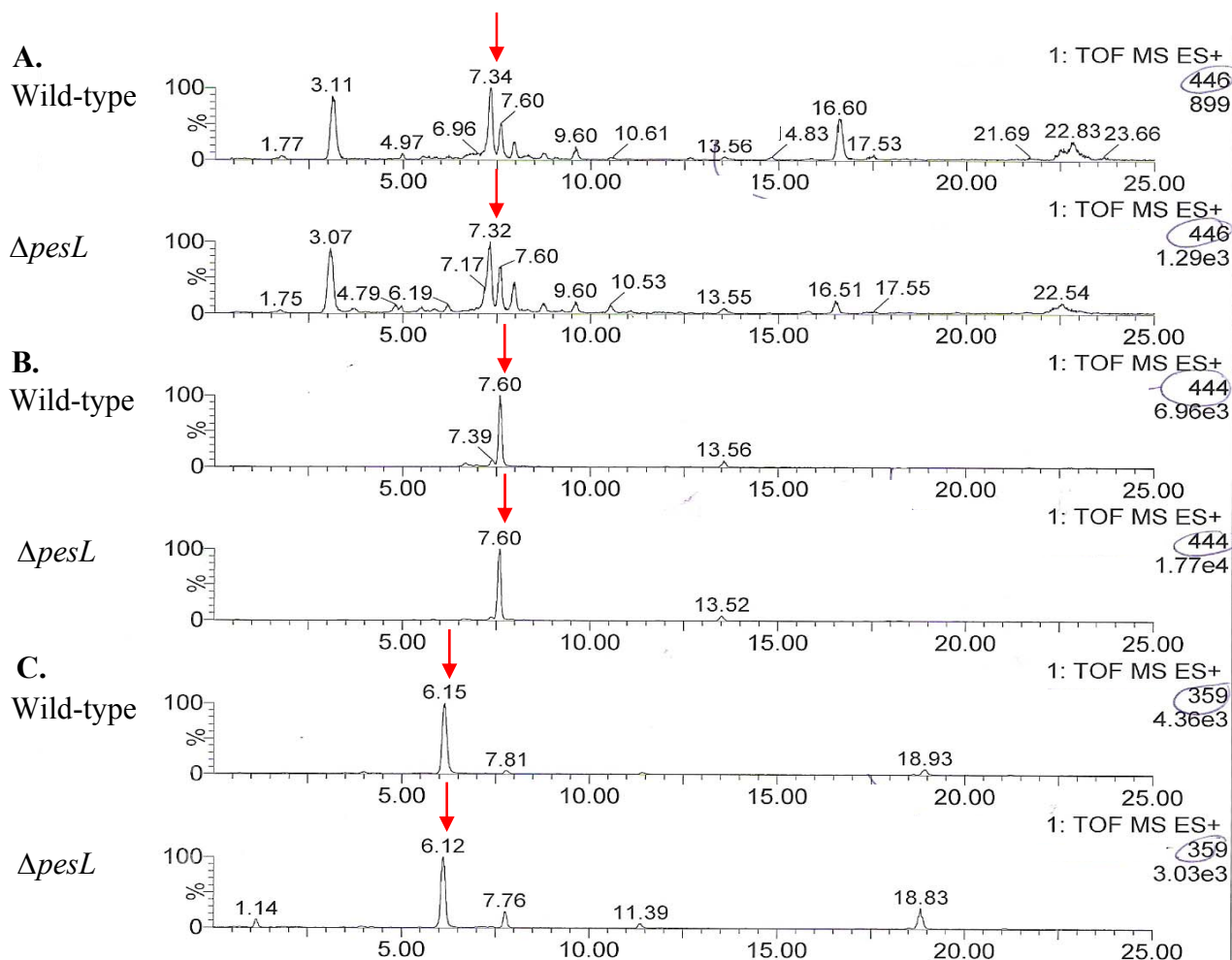


Figure 4.25. *A. fumigatus* PesL is not essential for production of any of the fumiquinazoline family of compounds.

A-C. Mass spectrometry analysis of metabolites from *A. fumigatus* wild-type and $\Delta pesL$.

The molecular masses of fumiquinazolines A, B, C, D, F and G (Table 4.7) were searched and the major peak representing each compound is indicated with an arrow for each strain.

A. Fumiquinazolines A and B: 446 [M + H]⁺

B. Fumiquinazolines C and D: 444 [M + H]⁺

C. Fumiquinazolines F and G: 359 [M + H]⁺

All fumiquinazolines were found in both *A. fumigatus* wild-type and $\Delta pesL$

4.4. Discussion.

The overall objective of this work was to identify the peptide encoded by the modular NRP synthetase, PesL, within *A. fumigatus*. A bipartite gene deletion strategy (Nielsen *et al.*, 2006) was employed to generate a *pesL* mutant ($\Delta pesL$). Corresponding loss of *pesL* expression was subsequently confirmed by RT-PCR and Real-Time PCR. In addition to this, *pesL* expression was observed in a range of culture conditions therefore providing an opportunity to compare *A. fumigatus* wild-type and $\Delta pesL$ to infer a biological function and/or peptide product produced by PesL. Extensive phenotypic analysis undertaken eliminated a role for *pesL* in siderophore biosynthesis in *A. fumigatus*, but provided evidence that *pesL* is important in protection against both oxidative stress caused by hydrogen peroxide, and voriconazole toxicity. *A. fumigatus* $\Delta pesL$ exhibited reduced virulence in the *Galleria mellonella* virulence model ($p < 0.001$). Comparative metabolite analysis undertaken indicated that fumigaclavine C, the end product of the complex ergot alkaloid pathway, was absent in *A. fumigatus* $\Delta pesL$. This strongly implies a role for PesL in the biosynthesis of fumigaclavine C in *A. fumigatus*, despite the apparent absence of NRP synthetase genes in the *A. fumigatus* EA biosynthetic cluster described to date. Interestingly, despite recent reports linking PesL to fumiquinazoline biosynthesis (Ames *et al.*, 2010), the entire family of fumiquinazolines were intact in both *A. fumigatus* wild-type and $\Delta pesL$, therefore suggesting an alternative route to fumiquinazole biosynthesis in *A. fumigatus*, and indicating that the fumiquinazoline biosynthetic pathway is more complex than currently thought.

A. fumigatus pesL was disrupted using a strain ($\Delta akuB$) which is impaired in the non-homologous end joining (NHEJ) pathway of DNA repair. Deletion of 3 kb of *pesL* was confirmed by Southern blot analysis. Corresponding abolition of *pesL* expression was then confirmed by RT-PCR and Real-Time PCR. Cramer *et al.*, (2006b), reported that *pesL*

expression was observed following 48 hr growth in RPMI and Czapek's broth. Expression was higher in RPMI (75 % relative abundance compared to *actin*), than Czapek's broth, with approx. 35 % relative abundance compared to *actin* (Cramer *et al.*, 2006b). In the work presented here, *pesL* was also found to be more abundant following growth in RPMI (approx. 25 % relative to *calmodulin*), while *pesL* expression was negligible following growth in Czapek's broth. It should be noted however, that the *A. fumigatus* strain used in this study differed to that of Cramer *et al.*, (2006b) who used the reference strain *A. fumigatus* Af293. Furthermore, the housekeeping genes used varied between the two studies. *Calmodulin* was the housekeeping gene used in this work, while *actin* was used by Cramer *et al.*, (2006b). These experimental differences might explain the differences in *pesL* expression observed between the two studies. Importantly, conditions were identified under which *pesL* was expressed, providing a starting point for comparative metabolite profiling between *A. fumigatus* wild-type and $\Delta pesL$.

pesL was proposed to be part of a putative five-gene SM cluster upon sequencing of the *A. fumigatus* genome (Nierman *et al.*, 2005), and more recently as part of an eight-gene cluster proposed to be responsible for the biosynthesis of the fumiquinazoline family of secondary metabolites in *A. fumigatus* (Ames *et al.*, 2010). However, neither group showed co-regulated expression of the cluster genes, with or without simultaneous secondary metabolite production, a feature that is a hallmark of SM biosynthetic gene clusters (Gardiner *et al.*, 2004; Gardiner & Howlett, 2005). All genes in the proposed *pesL* cluster (AFUA_6G12040-AFUA_6G12080), according to Nierman *et al.*, (2005), were found to be expressed in this study in yeast glucose media over a 96 hr time period, which means all genes are capable of being transcriptionally active. This observation was important as secondary metabolite gene clusters have been found to be transcriptionally silent under standard laboratory conditions, making identification of peptides very difficult (Schroeckh

et al., 2009). However, the proposed cluster genes did not all exhibit the same pattern of expression, suggesting that they are not co-regulated in the production of a particular secondary metabolite.

Since at least two NRP synthetases are known to be essential for siderophore production in *A. fumigatus* (Schrettl *et al.*, 2004; Schrettl *et al.*, 2007), a role for PesL in this process was investigated. Plate assays under varying iron conditions eliminated a role for PesL in siderophore biosynthesis in *A. fumigatus*. Further phenotypic analysis indicated that deletion of *pesL* resulted in increased sensitivity to the oxidising agent H₂O₂ (2 mM and above) ($p < 0.01$), while in contrast, *A. fumigatus* $\Delta pesL$ was more resistant to menadione at concentrations of 20 μ M ($p < 0.05$) and 40 μ M ($p < 0.01$). A third agent, diamide, known to cause oxidative stress, appeared to cause no difference between wild-type and $\Delta pesL$. A range of oxidising agents was chosen since no one agent can fully represent conditions of oxidative stress (Temple *et al.*, 2005; Zhao *et al.*, 2006). These data indicate that PesL is important for protection against H₂O₂-mediated oxidative stress in *A. fumigatus*, as has also been observed for another *A. fumigatus* NRP synthetase, Pes1 (Reeves *et al.*, 2006), but deletion of *pesL* did not hinder growth of *A. fumigatus* when exposed to the other oxidising agents in this study. One possible explanation for the increased resistance of *A. fumigatus* $\Delta pesL$ to menadione is that exposure to menadione triggered an oxidant defence response that was somehow elevated in $\Delta pesL$ as a protective mechanism. In other words, the loss of *pesL* might have been compensated for upon exposure to menadione. The transcriptional responses to various oxidising agents, including the ones used here, was shown to differ substantially in *S. cerevisiae*, with respiratory genes being influenced by hydrogen peroxide, while menadione influenced the NADPH-producing pentose phosphate pathway (Thorpe *et al.*, 2004). Furthermore, a genome wide comparison of gene expression profiles upon exposure to menadione, hydrogen peroxide

and diamide in *A. nidulans* revealed that separate response gene groups existed for the different agents (Pocsi *et al.*, 2005). Interestingly, the role of NRPS in protection of fungal species against oxidative stress has been widely reported. Another NRP synthetase, Pes1 has found to be important for protection against hydrogen peroxide in *A. fumigatus* (Lorna Gallagher – personal communication). NPS6, in the plant pathogen *Cochliobolus heterostrophus*, was found to be involved in both virulence and resistance to oxidative stress (Lee *et al.*, 2005). NPS6 was later shown to be responsible for extracellular siderophore biosynthesis in *C. heterostrophus*, which is essential for virulence on its host, maize (Oide *et al.*, 2006).

A. fumigatus $\Delta pesL$ also exhibited increased sensitivity to the anti-fungal voriconazole, when compared to wild-type, with the most significant difference observed at a concentration of 0.5 $\mu\text{g/ml}$ over a 72 hr time period ($p < 0.01$). This indicates that the peptide encoded by PesL is important in mediating resistance to the toxic effects of voriconazole. This phenotype was also observed for another *A. fumigatus* mutant, in which the NRP synthetase Pes1, was disrupted (Lorna Gallagher – personal communication). *A. fumigatus* $\Delta pesL$ exhibited moderately increased sensitivity to amphotericin B at 0.5 $\mu\text{g/ml}$ ($p < 0.05$). In contrast, sensitivity testing with caspofungin revealed no difference between *A. fumigatus* wild-type and $\Delta pesL$. The specific mechanism by which PesL protects *A. fumigatus* against voriconazole and amphotericin B toxicity was not investigated further in this study.

Availability of *A. fumigatus* $\Delta pesL$ facilitated comparative metabolite profiling in order to identify a PesL-encoded non-ribosomal peptide. Initial profiling experiments involving comparison of metabolites in *A. fumigatus* wild-type versus $\Delta pesL$ following a range of liquid culturing conditions revealed no differences in metabolite profiles. It was considered that PesL might encode a peptide associated with conidia rather than vegetative

growth. Disruption of a NRP synthetase, MaNPS1, in the insect pathogenic fungus *Metarhizium anisopliae* led to the discovery that serinocyclins, a family of peptides that are associated with the conidia of this fungus, are actually non-ribosomally synthesised (Krasnoff *et al.*, 2007; Moon *et al.*, 2008). The black mold fungus *Stachybotrys chartarum* produces trichothecenes which are associated with its spores (Sorenson *et al.*, 1987). Furthermore, the ergot alkaloids (fumigaclavine A, B, C and festuclavine) of *A. fumigatus* are associated with the conidia (Coyle *et al.*, 2007).

With these considerations, conidial extracts of *A. fumigatus* wild-type and $\Delta pesL$ were compared and two peaks representing candidate PesL-encoded peptides were identified by RP-HPLC which were absent in extracts of *A. fumigatus* $\Delta pesL$. The abundance of one of these metabolites (retention time = 15.927 min) was elevated when *A. fumigatus* was grown in the presence of H₂O₂ (2 mM). These data together indicated that PesL is involved in the biosynthesis of peptide(s) which are found associated with the conidia of *A. fumigatus*, and up-regulated in response to oxidative stress caused by H₂O₂, in agreement with increased sensitivity to H₂O₂ upon deletion of *pesL*. LC-DAD-MS analysis at DTU revealed that the metabolite specifically absent in *A. fumigatus* $\Delta pesL$ was fumigaclavine C, the end product of the complex ergot alkaloid (EA) biosynthetic pathway (Frisvad *et al.*, 2009). Complete loss fumigaclavine C in *A. fumigatus* $\Delta pesL$ was observed in all conditions explored where conidia were examined, in agreement with the known ergot alkaloid association with *A. fumigatus* conidia (Coyle *et al.*, 2007). Interestingly, another NRP synthetase mutant generated at NUIM, *A. fumigatus* $\Delta pes1$ (AFUA_1G10380), exhibited similar phenotypes to the *A. fumigatus* $\Delta pesL$ phenotypes described here (Lorna Gallagher – personal communication), suggesting redundancy among NRP synthetases.

The loss of fumigaclavine C biosynthesis in *A. fumigatus* $\Delta pesL$ and the corresponding sensitivity of $\Delta pesL$ to oxidative stress caused by hydrogen peroxide, and increased susceptibility to voriconazole and amphotericin B, strongly suggests that fumigaclavine C plays a role in protecting *A. fumigatus* against H₂O₂ -mediated oxidative stress, voriconazole and amphotericin B toxicity. Furthermore, initial experiments indicated that a metabolite absent in *A. fumigatus* $\Delta pesL$ was up-regulated following exposure to 2 mM H₂O₂ (Figure 4.20). These findings are in agreement with previously established links between fungal secondary metabolism and oxidative stress (Reverberi *et al.*, 2010).

With the observation that *A. fumigatus* PesL is essential for fumigaclavine C biosynthesis, it was necessary to review the EA biosynthetic pathway in *A. fumigatus* with a view to clarifying a role for PesL. The EA biosynthetic pathway is complex, and only some of the enzymes involved have been functionally characterised, mainly through *in vitro* biochemical characterisation of proteins (native or recombinant). This discussion will focus on the current understandings of the biosynthetic clusters which direct EA biosynthesis in *A. fumigatus*, *C. purpurea* and *Neotyphodium lolli*. Schematic representations of the arrangement of the published EA biosynthetic clusters in *A. fumigatus*, *C. purpurea* and *N. lolli* are shown in Figure 4.26. Although gene sequence is relatively conserved between the three EA gene clusters, there are differences in gene orientation and organisation, and the *N. lolli* cluster is more complex in structure and organisation (Fleetwood *et al.*, 2007). Genes that are shared by *C. purpurea* and *N. lolli*, but absent from *A. fumigatus* – *lpsA*, *lpsB*, and *cloA*- have been shown to be necessary for steps leading to ergopeptine biosynthesis (Correia *et al.*, 2003; Haarmann *et al.*, 2006; Panaccione *et al.*, 2001). The most striking difference between the three clusters is the presence of non-ribosomal peptide synthetase genes in the *C. purpurea* and *N. lolli* clusters, and the complete absence of NRP synthetase genes in the proposed *A. fumigatus* EA

cluster. The requirement for PesL in fumigaclavine C biosynthesis in *A. fumigatus* shown here indicates that the proposed *A. fumigatus* EA cluster has not been fully elucidated.

As there has been frequent renaming of genes within all three clusters, these clusters have been re-depicted and colour coded to show the different gene functions with the most recent gene names associated with putative functions, and this is shown in Figure 4.27. This information was compiled from publications that displayed one or more of these gene clusters, with or without gene function alignment (Fleetwood *et al.*, 2007; Haarmann *et al.*, 2005; Lorenz *et al.*, 2007).

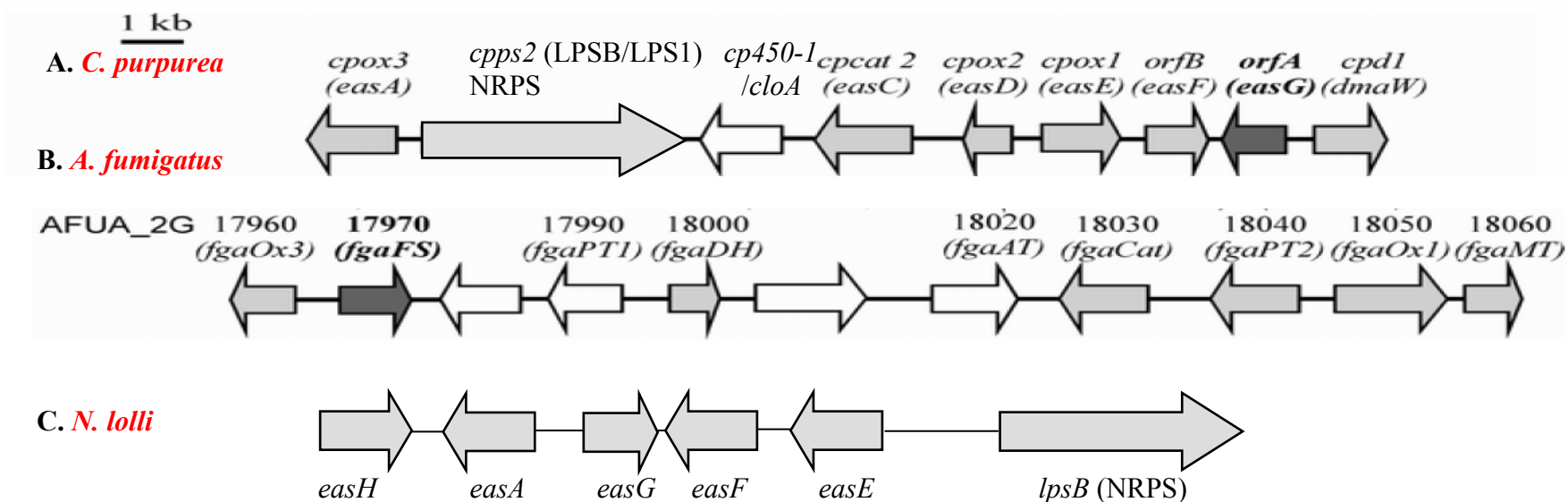
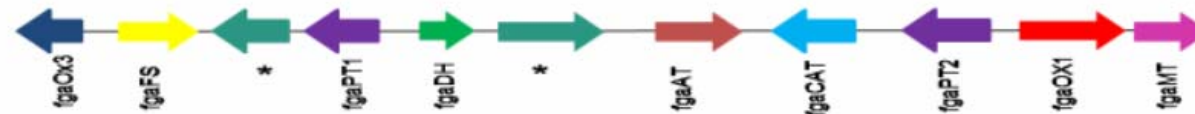


Figure 4.26. The proposed EA biosynthetic gene clusters from *A. fumigatus*, *C. purpurea*, and *N. lolli*. A. Two NRP synthetase genes are present in the *C. purpurea* EA cluster; *cp450-1* and *cp450-2* (which occurs downstream of *cpd1*) and these are absent in the *A. fumigatus* EA cluster. Later, several other genes not shown here were found including two more NRP synthetases, *lpsC* (*cp450-3*) and *lpsA2* (*cp450-4*), which is highly homologous to *cp450-1*. *cpimd* was found, which likely encodes a protein of primary metabolism (Haarmann *et al.*, 2005). B. EA gene cluster from *A. fumigatus* Af293 (Coyle & Panaccione, 2005; Unsold & Li, 2005), showing absence of NRP synthetase genes. C. EA cluster from *N. lolli*. This figure is the most up-to-date representation of the cluster with gene names. Genes with homologues between the clusters are marked in grey, while unique genes are in white. Figures adapted from (Wallwey *et al.*, 2010b).

A. fumigatus
Fumigaclavine cluster



C. purpurea
Ergotamine cluster



N. lollii
Ergovaline cluster

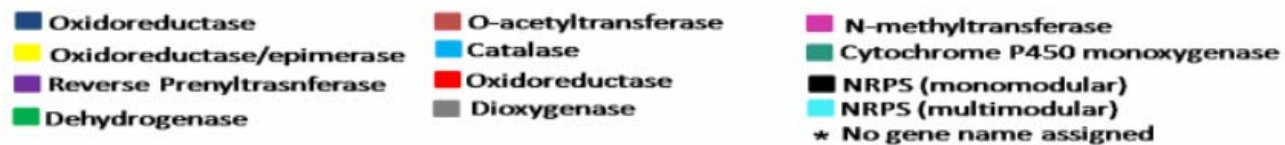
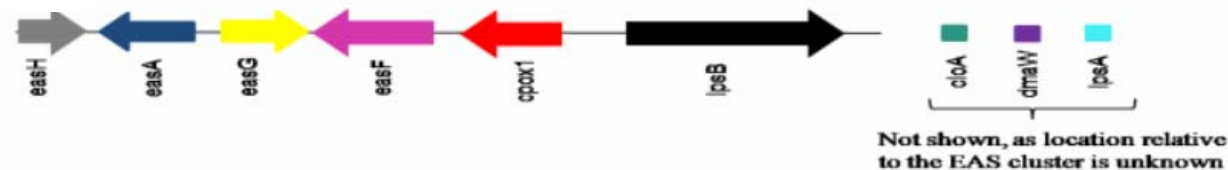


Figure 4.27. The proposed EA biosynthetic clusters in *A. fumigatus*, *C. purpurea* and *N. lollii*. These colour coded clusters have been redrawn from various sources to highlight both the similarities and major differences between the clusters (Lorna Gallagher – NUI Maynooth). (Correia *et al.*, 2003; Coyle & Panaccione, 2005; Fleetwood *et al.*, 2007; Haarmann *et al.*, 2005; Lorenz *et al.*, 2007; Tudzynski *et al.*, 1999; Unsold & Li, 2005; Wallwey *et al.*, 2010b).

A gene cluster directing EA biosynthesis in *A. fumigatus* was identified independently by two groups (Coyle & Panaccione, 2005; Unsold & Li, 2005). Deletion of *A. fumigatus dmaW* resulted in loss of all known ergot alkaloids in the resultant mutant strain, and sequence analysis examining genes in the vicinity of *dmaW* in the genome led to the proposal of an EA cluster (Coyle & Panaccione, 2005). In that study, *A. fumigatus dmaW* was identified through sequence analysis and the deduced protein exhibited 50 % sequence identity to the DMAT synthase in *C. fusiformis* (Tsai *et al.*, 1995), 53 % identity to DMAT synthase from *C. purpurea* (Tudzynski *et al.*, 1999), and 59 % identity to DMAT synthase from *Neotyphodium sp. strain Lp1* (Wang *et al.*, 2004). *Neotyphodium sp. strain Lp1* is a naturally occurring hybrid of *Neotyphodium lolli* and *Epichloë typhina* (Schardl *et al.*, 1994).

In another study, the *A. fumigatus fgaPT2 (dmaW)* gene, was over-expressed to produce a heterologous DMAT synthase in *S. cerevisiae*, and biochemical analysis confirmed that FgaPT2 catalyses the conversion of L-tryptophan to 4-dimethylallyltryptophan, the first committed step in ergot alkaloid biosynthesis (Unsold & Li, 2005). The specific substrates for FgaPT2 were L-tryptophan and dimethylallyl disphosphate (DMAPP) (Unsold & Li, 2005). FgaPT2 was the first enzyme involved in EA biosynthesis to be heterologously overproduced and purified to homogeneity (Unsold & Li, 2005). The work presented by Unsold and Li (2005) showed that FgaPT2 was capable of converting L-tryptophan to 4-dimethylallyltryptophan *in vitro*. An EA cluster for *A. fumigatus* was also proposed and this cluster contained at least 7 genes which had orthologues in the *C. purpurea* EA biosynthetic cluster (Unsold & Li, 2005). These 7 genes are proposed to be responsible for the common steps in the biosynthesis of EA in both species (Unsold & Li, 2006). The EA cluster in *A. fumigatus* contains another homologue of *cpd1* (the *C. purpurea* DMAT gene), termed *fgaPT1*, which is separated from *fgaPT2* by

only 10 kb (Unsold & Li, 2005). Four genes referred to as *fgaOX1*, *fgaOX2*, *fgaOX3* and *fgaCAT* were identified nearby *fgaPT1* and *fgaPT2*, which appear to be homologues of *cpox1*, *cpox2*, *cpox3* and *cpcat2* from the *C. purpurea* EA biosynthetic cluster (Unsold & Li, 2005). Together with the DMATS, it is suggested that the four genes (*fgaOX1*, *fgaOX2*, *fgaOX3* and *fgaCAT*), could be involved in the assembly of the clavinet skeleton, as this is a common structural feature of ergot alkaloids from all producing organisms (Coyle & Panaccione, 2005).

Interestingly, neither group reported the presence of NRP synthetase genes within the EA clusters of *A. fumigatus* (Coyle & Panaccione, 2005; Unsold & Li, 2005), presumably due to the absence of NRP synthetase genes in the genomic location of the characterised EA biosynthetic genes within *A. fumigatus*. There is, however, a gene encoding a catalase (AFUA_2G18030) in the EA cluster vicinity in the *A. fumigatus* genome (Mabey *et al.*, 2004). A putative catalase gene (*cpcat2*) has also been identified in the EA cluster of *C. purpurea*, though no function has yet been assigned (Correia *et al.*, 2003). If these catalases play a role in the EA biosynthetic pathway, it may suggest a link between the production of EA and oxidative stress, since catalases are known anti-oxidant enzymes (Chauhan *et al.*, 2006). This is also reflected in the increased sensitivity of *A. fumigatus* $\Delta pesL$ to H₂O₂-mediated oxidative stress. Furthermore, the inclusion of the catalase in the *C. purpurea* EA cluster, in contrast to the *A. fumigatus* EA cluster, suggests that the core EA cluster in general needs further refinement between different EA producing fungi.

Cloning and expression of an N-methyltransferase, FgaMT (AFUA_2G18060) from the *A. fumigatus* EA cluster confirmed that this enzyme catalyses the second step of EA biosynthesis by methylating the NH₂ group of 4-DMAT to produce 4-dimethylallyl-L-abrine in the presence of S-adenosyl methionine (SAM) (Rigbers & Li, 2008). FgaMT

homologues are found in the EA clusters of *C. purpurea* and *C. fusiformis* (53 % identity with *easF*) and *N. lolli* (60 % identity with *easF*), and it is expected that these homologues catalyse the same reaction as FgaMT (Rigbers & Li, 2008). A homologue of *A. fumigatus* FgaOX1 in *C. purpurea* (encoded by *cpox1/easE*) has been shown to convert N-methylallyl-4-tryptophan to chanoclavine-1 (Lorenz *et al.*, 2010). A similar reaction is likely to occur in *A. fumigatus* with FgaOX1 converting 4-dimethylallyl-L-abrine to chanoclavine-1 (Wallwey *et al.*, 2010b), although this has not been biochemically proven. *A. fumigatus* FgaDH (AFUA_2G18000), a short-chain alcohol dehydrogenase, catalyses the conversion of chanoclavine-I to chanoclavine-I aldehyde (Wallwey *et al.*, 2010a). The conversion of chanoclavine-I aldehyde to festuclavine is dependant on an old yellow enzyme FgaOX3 (a homologue of EasA from *C. purpurea* and *C. fusiformis*) and FgaFS (a homologue of EasG from *C. purpurea* and *C. fusiformis*) (Wallwey *et al.*, 2010b). Disruption of *A. fumigatus easA (fgaOx3)* resulted in a mutant which failed to produce festuclavine or fumigaclavines A, B and C, which are ergot alkaloids typically specific to *A. fumigatus* (Coyle *et al.*, 2010). However, chanoclavine-I, an important intermediate in EA biosynthesis, mentioned above, was found, in addition to accumulation of chanoclavine-I aldehyde, in mutant metabolite profiles (Coyle *et al.*, 2010). Transformation of the *C. purpurea easA* homologue into the *A. fumigatus easA* mutant resulted in a distinct ergot alkaloid profile, resembling the typical profile of ergot alkaloids from *C. purpurea*. These important findings indicate that the old yellow enzyme controls the branch point between *A. fumigatus* and *C. purpurea* EA biosynthesis, and that chanoclavine-I aldehyde is the last shared intermediate between the two pathways (Coyle *et al.*, 2010).

Comparison of EA biosynthesis clusters helps to find candidate genes that mediate later steps of ergot alkaloid production; that is, after agroclavine (*C. purpurea*) and festuclavine (*A. fumigatus*), and are useful to identify species-specific EA biosynthesis

pathway steps. This strategy was used to identify the acetyltransferase (FgaAT) that catalyses the conversion of fumigaclavine B to fumigaclavine A, and this was experimentally proven using a heterologously produced FgaAT (Liu *et al.*, 2009b). FgaAT is encoded by a gene unique to the *A. fumigatus* EA cluster (AFUA_2G18020), and is in agreement with the presence of an acetyl moiety in the structure of fumigaclavine A and C, but not in the structure of the *C. purpurea* ergot alkaloids (Liu *et al.*, 2009b). The second putative prenyltransferase gene *fgaPT1* in *A. fumigatus* was proposed to function in orchestration of the additional prenyl moiety at C-2 of the indole nucleus in fumigaclavine C (Coyle & Panaccione, 2005). Since then, *fgaPT1* has been cloned, heterologously expressed and biochemically characterised. FgaPT1 was shown to catalyse the prenylation of fumigaclavine A to fumigaclavine C, which is the last known step in EA biosynthesis in *A. fumigatus* (Unsold & Li, 2006). As mentioned earlier, many of the enzymes involved in EA biosynthesis have been biochemically characterised *in vitro*, and while FgaPT1 is sufficient to convert fumigaclavine A into fumigaclavine C *in vitro*, this step may require tethering of fumigaclavine A to a non-ribosomal peptide synthetase module, i.e. PesL, *in vivo*. The findings presented here clearly demonstrated that deletion of the NRP synthetase PesL, results in complete loss of fumigaclavine C, validating this hypothesis.

Two other unique genes in the *A. fumigatus* EA cluster (AFUA_2G17980 and AFUA_2G18010) encode putative P450 monooxygenases according to functions assigned at the CADRE database (Mabey *et al.*, 2004), and functions for these within the EA biosynthetic pathway have yet to be assigned. The proposed biosynthetic pathways for *A. fumigatus*, and *C. purpurea* including all known steps is presented in Figure 4.28 (Wallwey *et al.*, 2010b).

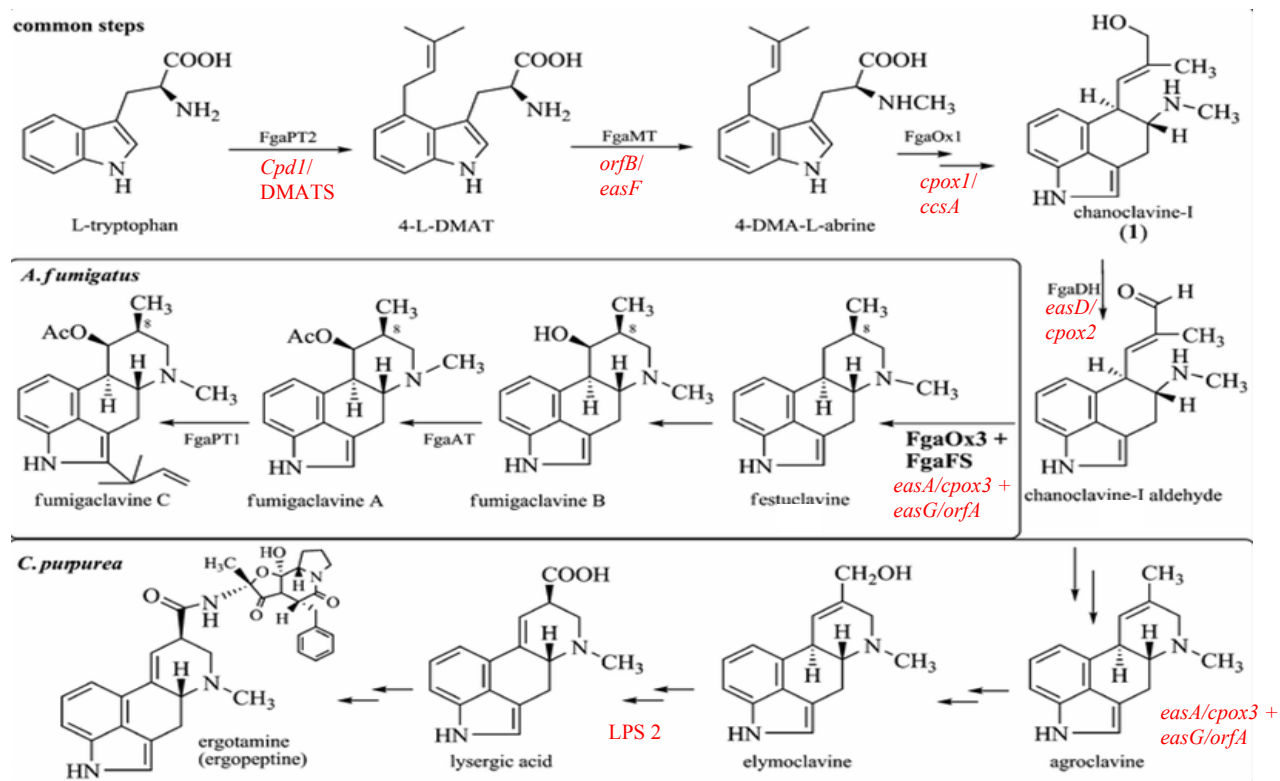


Figure 4.28. Proposed EA biosynthetic pathway for ergot alkaloids in *A. fumigatus* and *C. purpurea* with both common steps and divergent steps shown resulting in a different fga profile of ergot alkaloids for the two species as shown. As described in text, chanoclavine-I aldehyde is the last shared intermediate between the two pathways (Wallwey *et al.*, 2010b). Enzyme names in black are for *A. fumigatus* pathway, while *C. purpurea* equivalents have been added in red.

The functions of several genes of the *C. purpurea* EA cluster have now been proven experimentally. The gene cluster for EA biosynthesis was identified in *C. purpurea* by chromosome walking on the flanking regions of the DMAT synthase gene, *cpd1*, and the genetic organisation of putative EA genes were described (Correia *et al.*, 2003; Tudzynski *et al.*, 1999). A NRP synthetase gene, *cpps1*, was identified, which was shown to encode the tri-modular NRP synthetase LPS1, previously characterised by Riederer *et al.*, (1996). Two ORFs encoding proteins of unknown function, and two putative oxidoreductase encoding genes, *cpox1* and *cpox2*, were also identified (Tudzynski *et al.*, 1999). A putative P450 mono-oxygenase gene (*cpP450-1*), a putative catalase gene (*cpcat2*), another putative oxidase gene (*cpox3*), and another NRP synthetase gene, *cpps2* (LPS2), were later identified (Correia *et al.*, 2003). RT-PCR and Northern blot experiments indicated that all genes are expressed under alkaloid producing conditions (Correia *et al.*, 2003; Tudzynski *et al.*, 1999). Further sequencing of the *C. purpurea* cluster revealed the presence of a third NRP synthetase gene, *lpsC* (Lorenz *et al.*, 2007), and a fourth NRP synthetase gene (Haarmann *et al.*, 2005). *C. purpurea dmaW* (*cpd1*) was cloned and expressed in yeast and proven unambiguously to perform the first committed step for EA biosynthesis (Tsai *et al.*, 1995). A lysergyl peptide synthetase complex (LPS) was purified as two NRP synthetase enzymes, lysergyl peptide synthetase 1 (LPS1) (*cpps1*) and LPS2 (*cpps2*). (Riederer *et al.*, 1996) These are responsible for the formation of the non-cyclo peptide precursor of ergotamine in *C. purpurea* from lysergic acid and three amino acids (Riederer *et al.*, 1996; Walzel *et al.*, 1997).

The early steps in the *C. purpurea* EA pathway are shared with *A. fumigatus*, as described above, and homologues for all steps are found in both species (Figure 4.24). Where festuclavine is produced by *A. fumigatus*, agroclavine is produced by *C. purpurea*. Agroclavine is converted to elymoclavine by an unknown enzyme. The *cloA* gene,

encoding the cytochrome p450 enzyme CloA, catalyses the conversion of elymoclavine to paspalic acid (Haarmann *et al.*, 2006). The orientation of the COOH in paspalic acid is changed by an unknown reaction resulting in lysergic acid. Synthesis of the typical ergot alkaloids then occurs using lysergic acid as starting material. Synthesis starts with binding of D-lysergic acid to the monomodular LPS2 (also called LpsB) as thioester, and successive condensation of the D-lysergic acid with three amino acids by the trimodular NRP synthetase LPS1 (LpsA), and modification and cyclization of the resulting D-lysergyl tripeptide yields the peptide alkaloids (ergopeptines) that are characteristic of the *C. purpurea* EA pathway (Riederer *et al.*, 1996; Walzel *et al.*, 1997). Ergotamine, the typical end product of the *C. purpurea* EA pathway is specifically produced when alanine, phenylalanine and proline are condensed with D-lysergic acid by LPS1 (Walzel *et al.*, 1997). The *cpps2* gene, encoding lysergyl peptide synthetase 2 (LPS2), the lysergic acid-activating portion of the LPS complex, has been functionally characterised by cloning and deletion in *C. purpurea*, with deletion resulting in loss of ergopeptine biosynthesis (Correia *et al.*, 2003). Accumulation of D-lysergic acid was observed in the *C. purpurea* LPS2 mutant ($\Delta cpps2$), as a result of blocking ergopeptine biosynthesis, which indicates that ergoline ring biosynthesis was unaffected by the loss of LPS2 (Correia *et al.*, 2003).

Interestingly, a number of *C. purpurea* strains can produce both two different races of ergopeptines (derived from D-lysergyl alanine) simultaneously (Flieger *et al.*, 1997), indicating the presence of two different biosynthesis systems within the one strain, which both use D-lysergic acid as substrate (Correia *et al.*, 2003). Strains can produce a different suite of ergot alkaloids through processing of activated lysergic acid by either of the two trimodular NRP synthetases LPSA1/LPSA2, which appear to be two different variations of LPS1 (Haarmann *et al.*, 2008). It was shown that the variability of alkaloid production observed by different chemical races of *C. purpurea* species P1 (ergotamine and

ergopeptine) and ECC93 (mainly ergocristine) corresponds to differences in the substrate specificity of the NRP synthetase modules (Haarmann *et al.*, 2005). Comparison of the cluster sequences of strain P1, an ergotamine producer, with that of strain ECC93, an ergocristine producer, showed high conservation of most of the cluster genes, but significant variation in the NRPS modules (Haarmann *et al.*, 2005). The development of a *C. purpurea* $\Delta ku70$ strain, deficient in nonhomologous end joining (NHEJ), aided the disruption of the first module of *lpsA1*, and inactivation of this gene led to loss of ergotamine, as expected (Haarmann *et al.*, 2005) (Haarmann *et al.*, 2008). Loss of *lpsA1* did not affect the production of ergocryptine (Haarmann *et al.*, 2008), supporting the hypothesis that evolution of chemical races correlates with evolution of NRP synthetase module specificity (Haarmann *et al.*, 2005). LPS2-A most likely catalyses the synthesis of ergocryptine (Haarmann *et al.*, 2008), while *lpsC* probably encodes a monomodular NRP synthetase that catalyses the formation of ergometrine, an ergopeptine with one amino acid side chain (Ortel & Keller, 2009). The observation of chemical races of ergot alkaloids in *C. purpurea* highlights that versatility exists in the EA biosynthetic pathway, a characteristic which might be occurring in other fungal secondary metabolite pathways, aiding to the diversity of the metabolites produced.

The ergot alkaloid pathway in *N. lolii* results in the production of the ergopeptine, ergovaline. Gene knockout of the DMAT synthase (*dmaW*) in *N. lolii* proved that DMAT is essential for the production of ergovaline, ergine (an alternative product of the EA pathway) and chanoclavine (Wang *et al.*, 2004). Ergovaline production could be restored in the *N. lolii* *dmaW* mutant by transformation with the *C. fusiformis* *dmaW* homologue, indicating the conservation of the DMAT synthases (Wang *et al.*, 2004). Ergovaline, similar to ergotamine in *C. purpurea*, is composed of activated lysergic acid and a tripeptide moiety. The tripeptide is composed of alanine, valine and proline (Brunner *et al.*,

1979). The trimodular NRP synthetase, LPS1 (*lpsA* gene) has been characterised in *Neophytodium sp. strain 1* (Damrongkool *et al.*, 2005; Panaccione *et al.*, 2001). The gene encoding LPS1 was deleted in *Neotyphodium sp. Strain Lp1*, and mutants did not produce ergopeptines and simple amides of lysergic acid but still produced clavinet ergot alkaloids (Panaccione *et al.*, 2001; Panaccione *et al.*, 2003). A putative gene cluster for EA biosynthesis has been proposed in *N. lolli* and this followed from the discovery of a second NRP synthetase gene, *lspB*, which encodes a monomodular NRP synthetase (Fleetwood *et al.*, 2007). *lpsB* was functionally characterised by gene knockout and the *lpsB* mutant did not produce ergovaline (Fleetwood *et al.*, 2007). The EA gene cluster in *N. lolli* is very similar to those described for *C. purpurea* (Correia *et al.*, 2003; Haarmann *et al.*, 2005; Tudzynski *et al.*, 1999) and *A. fumigatus* (Coyle & Panaccione, 2005; Unsold & Li, 2005) (Figures 4.25, 4.26). However, the *N. lolli* cluster is more complex in structure organisation and gene orders varies in comparison with the other clusters (Fleetwood *et al.*, 2007).

Reviewing the biosynthetic pathways for EA biosynthesis highlighted that the *A. fumigatus* EA cluster is not reported to contain NRP synthetase genes. However, deletion of *pesL*, a monomodular NRP synthetase gene, in this study, resulted in the complete loss of fumigaclavine C, the final product of the EA biosynthetic pathway in *A. fumigatus*. This indicates that NRPS does play a role in ergot alkaloid biosynthesis, after all, in *A. fumigatus*. No homologues for the *C. purpurea* NRP synthetase encoding genes *cppls1* or *cppls2* were found in the vicinity of *fgaPT2* in the *A. fumigatus* EA gene cluster, thought to be consistent with the absence of a peptide moiety in fumigaclavines (Unsold & Li, 2005). However, the findings presented here contradict earlier hypotheses. We hypothesise that *PesL* is necessary to facilitate the reverse prenylation of fumigaclavine A by *FgaPT1*, possibly by tethering fumigaclavine A making it accessible to *FgaPT1*, to yield fumigaclavine C in *A. fumigatus*. Further characterisation of EA and other secondary

metabolite biosynthetic pathways in *A. fumigatus* and other fungi might reveal that NRP synthetases play an important role in tethering of biosynthetic intermediates in complex biosynthetic pathways, and these findings highlight the importance of gene deletion studies for functional assignment of NRP synthetases.

Gene clusters encoding secondary metabolites are usually co-regulated with the production of the specific metabolite(s) (Gardiner *et al.*, 2004; Gardiner & Howlett, 2005), and this also been observed for the *C. purpurea* EA biosynthetic cluster (Correia *et al.*, 2003; Tudzynski *et al.*, 1999). Such a study had not been reported for the genes involved in EA biosynthesis in *A. fumigatus*. *PesL* has been proposed to be part of a gene cluster, as described earlier, yet it does not show a co-regulated pattern of expression with other genes in the proposed cluster. However, the proven role for *PesL* in fumigaclavine C biosynthesis could suggest that *PesL* was once in a cluster with the other EA genes and has been translocated to its current location throughout the evolution of *A. fumigatus*.

Interestingly, transposable elements were found interspersed between the genes of the EA cluster in *N. lolli* and these have also been found upstream of *Epichloë dmaW* (Fleetwood *et al.*, 2007). The transposable elements have created several repeated sequences that could be reminiscent of previous recombination events leading to the different organisation of the *N. lolli* EA cluster, compared to EA clusters in other fungi (Fleetwood *et al.*, 2007). Perhaps transposable elements are a similar feature associated with the EA cluster of *A. fumigatus*, and have facilitated rearrangement of the cluster, leading to the translocation of the NRP synthetase gene *pesL* to its current position in the genome. A transcriptional analysis of the genes regulated by *StuA*, a regulatory protein controlling development in *A. fumigatus* and other fungi, revealed that the EA biosynthetic gene cluster is under the regulation of *StuA* (Sheppard *et al.*, 2005) and, interestingly, there is a possible retrotransposon element between the EA cluster and an adjacent aflatoxin gene

cluster in the genome of *A. fumigatus* (Sheppard *et al.*, 2005). This might allow gene rearrangements to occur between these two adjacent gene clusters and with other parts of the genome. In *Magnaporthe oryzae*, transposable elements have been found to influence recombination rate, loss of synteny and other features indicative of genome evolution (Thon *et al.*, 2006). In fact, transposable elements have been reported to be associated with other biosynthetic gene clusters in *Epichloë* (Fleetwood *et al.*, 2007).

The *G. mellonella* infection model (Cotter *et al.*, 2000) was used in order to assess the contribution of *pesL* to *A. fumigatus* virulence. Reeves *et al.*, (2004) employed this model to determine the virulence of different isolates of *A. fumigatus*, and strong correlations were observed between the *G. mellonella* and murine response to fungal infection (Brennan *et al.*, 2002). Furthermore, correlations were observed between *G. mellonella* and murine models of infection with respect to *A. fumigatus* $\Delta pes3$ (Chapter 3 of this thesis). The virulence of *A. fumigatus* $\Delta pesL$ was attenuated compared to wild-type ($p < 0.0001$) in this model, consistent with increased survival of larvae following infection with $\Delta pesL$ over a 96 hr time period. The largest difference in larval survival was observed at the 72 hr time point with 38 % survival following infection with *A. fumigatus* wild-type compared to 82 % survival following infection with $\Delta pesL$. Several explanations can be given for the reduced virulence observed upon deletion of *pesL*. *A. fumigatus* $\Delta pesL$ was more sensitive to H₂O₂-mediated oxidative stress, it is likely that it was less able to resist the reactive oxygen intermediates (ROS) produced by the *Galleria* NADPH oxidase complex during the innate immune response (Bergin *et al.*, 2005). Furthermore, loss of fumigaclavine C, the end product of the ergot alkaloid biosynthetic pathway in *A. fumigatus*, is likely contributing to reduced virulence of *A. fumigatus* $\Delta pesL$ since ergot alkaloids have a long history of association with animal infection (Panaccione & Coyle, 2005).

In conclusion, the work presented here demonstrates for the first time, a role for an NRP synthetase in the ergot alkaloid biosynthetic pathway, specifically in fumigaclavine C biosynthesis, within *A. fumigatus*. Furthermore, it appears to be the first characterisation of a monomodular NRP synthetase in the *Aspergilli*, and characterisation of other such enzymes might reveal that they serve as discrete modules that might be used by several biosynthetic pathways in order to facilitate maximum diversity and evolution of secondary metabolite biosynthesis. Perhaps the appearance of an apparently new metabolite in *A. fumigatus* $\Delta pesL$, which appears to be related to the fumitremorgin family of compounds, is an example of secondary metabolite diversity in action – since the available isoprene moieties not used for fumigaclavine C biosynthesis might be now available for biosynthesis of a new fumitremorgin-type metabolite. Since the new compound appears to be closely related to the fumitremorgins, it probably contains tryptophan, making this hypothesis plausible. To date, a role for ergot alkaloid biosynthesis in *A. fumigatus* pathogenesis has not been investigated, and the data presented here indicates that ergot alkaloids contribute to the virulence of *A. fumigatus*, and highlights the potential of the ergot alkaloid biosynthetic pathway as a novel drug target for the treatment of IA.

5.1. Introduction.

A. fumigatus is responsible for a range of human diseases, which have been described earlier in this thesis. Currently, there are several classes of anti-fungal therapy in use, and there is a growing concern following evidence of resistance to several major anti-fungal drugs (Loeffler & Stevens, 2003; Morschhauser, 2010). Subsequently, there is a great need for both the discovery and development of new classes of drugs. Moreover, understanding the many biochemical pathways within the organism may reveal novel drug targets worthy of further investigation.

All living organisms encounter potentially damaging environmental stresses, by exposure to specific damaging agents present in their habitat (Folch-Mallol *et al.*, 2004). Organisms are also challenged with the threat of cellular damage from the by-products of cellular metabolism (Dowling & Simmons, 2009). In order to overcome and survive these serious challenges, they need to possess highly effective defence systems which are able to both counteract and repair the damage caused by cellular insults. A clear understanding, and subsequent targeting, of these defence systems, particularly in pathogenic organisms such as *A. fumigatus*, may present novel drug targets for the treatment of human disease. The identification and elucidation of pathogen-specific pathways, absent in mammalian systems, can provide promising targets worthy of further investigation, as it may be possible to inactivate these systems therapeutically, thereby leading to new treatments for important pathogenic diseases, for example, inhibition of siderophore biosynthesis (Monfeli & Beeson, 2007).

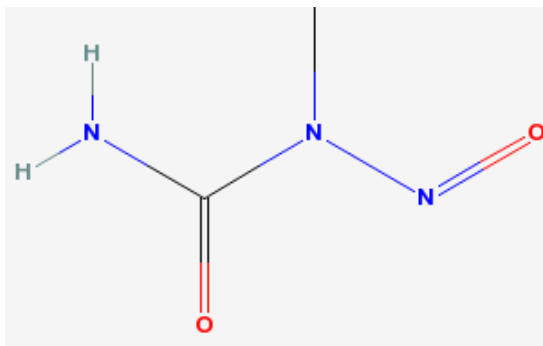
Among the defence systems shared by all organisms is the well-characterised heat-shock response, which is probably most thoroughly documented in the yeast model organism, *Saccharomyces cerevisiae* (Palotai *et al.*, 2008). *A. fumigatus* also possesses a heat-shock system which has recently been investigated (Albrecht *et al.*, 2010; Do *et al.*,

2009). While further investigation of this system would shed interesting information on the biology of this fungus, the high level of conservation of the heat-shock response makes this system a poor choice of drug target, as drugs aimed at the heat-shock response of a pathogen will target the host cells also.

Other adaptive systems have been documented in microorganisms, including the adaptive response to alkylating DNA damage. Mono-functional alkylating agents such as *N*-methyl-*N*-nitrosourea (MNU), *N*-methyl-*N*-nitro-*N*-nitrosoguanidine (MNNG), and the metabolically active form of dimethylnitrosamine are efficient mutagens and carcinogens (Dempfle *et al.*, 1985). Chemical structures for the alkylating compounds mentioned in this study are shown in Figure 5.1. Electrophilic methylating agents can react with a number of nucleophilic sites on DNA molecules (Wyatt & Pittman, 2006). The major mutagenic lesion that results in DNA from MNU, MNNG and dimethylnitrosamine is O⁶-methylguanine (O⁶MeGua), which leads to mis-pairing of thymine residues during DNA replication (Hall & Saffhill, 1983; Loechler *et al.*, 1984). This mis-pairing results in G-C → A-T transitions mutations, thereby disrupting the coding potential of affected DNA regions (Coulondre & Miller, 1977). Ethyl methanesulfonate (EMS) has been employed in numerous genotoxicity studies as a model alkylating agent (Recio *et al.*, 2010). EMS is a direct acting clastogen, causing specific breaks in chromosomes. EMS can cause micronucleus (MN) formation in animal cells, and this is the basis of many genotoxicity assays (Recio *et al.*, 2010). MN are surrogate markers of chromosomal aberrations that are associated with increased cancer risks (Bonassi *et al.*, 2007). EMS readily reacts with DNA producing alkylated (specifically ethylated) nucleotides. Alkylation can occur at various locations on nucleotide bases, depending on the physico-chemical properties of the agent, leading to mutations in the DNA (Gocke *et al.*, 2009). MMS and MNNG modify DNA by adding methyl groups to a number of nucleophilic sites on the DNA bases, although

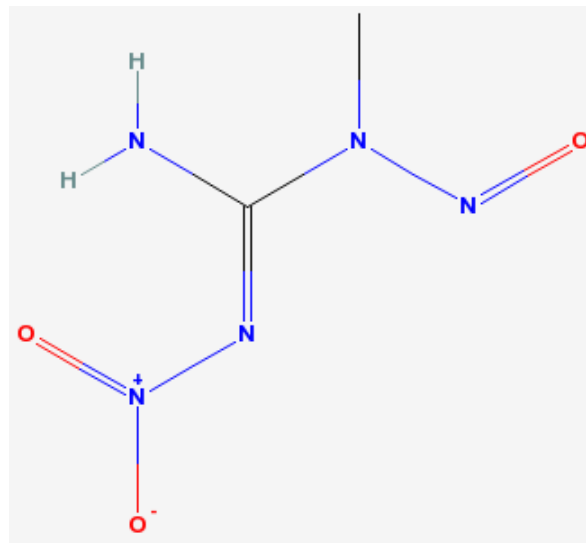
MNNG produces a greater percentage of O-methyl adducts (Wyatt & Pittman, 2006). MMS and MNNG are known to cause sister chromatic exchanges (SCE) during the S-phase of the cell cycle (Kaina, 2004). An overview of the different lesions and adducts caused by some of the methylating agents discussed here is presented in Figure 5.2.

A.



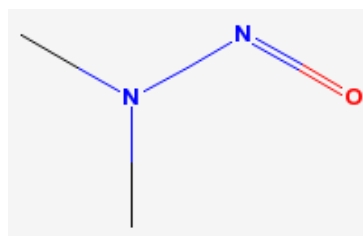
N-methyl-*N*-nitrosourea (MNU)

B.



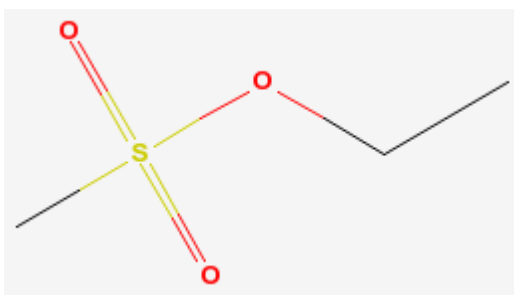
N-methyl-*N*-nitro-*N*-nitrosoguanidine (MNNG)

C.



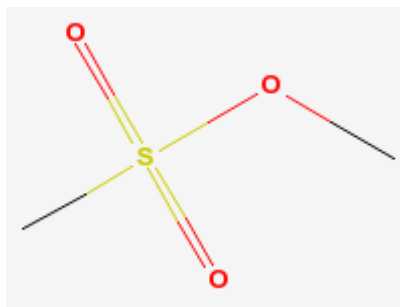
dimethylnitrosamine

D.



Ethyl Methanesulfonate (EMS)

E.



Methyl Methanesulfonate (MMS)

Figure 5.1. Chemical structures of the mono-functional alkylating agents. (A) MNU (B) MNNG and (C) dimethylnitrosamine, (D) EMS, (E) MMS. These structures were retrieved from the PubChem Compound database (<http://pubchem.ncbi.nlm.nih.gov/>).

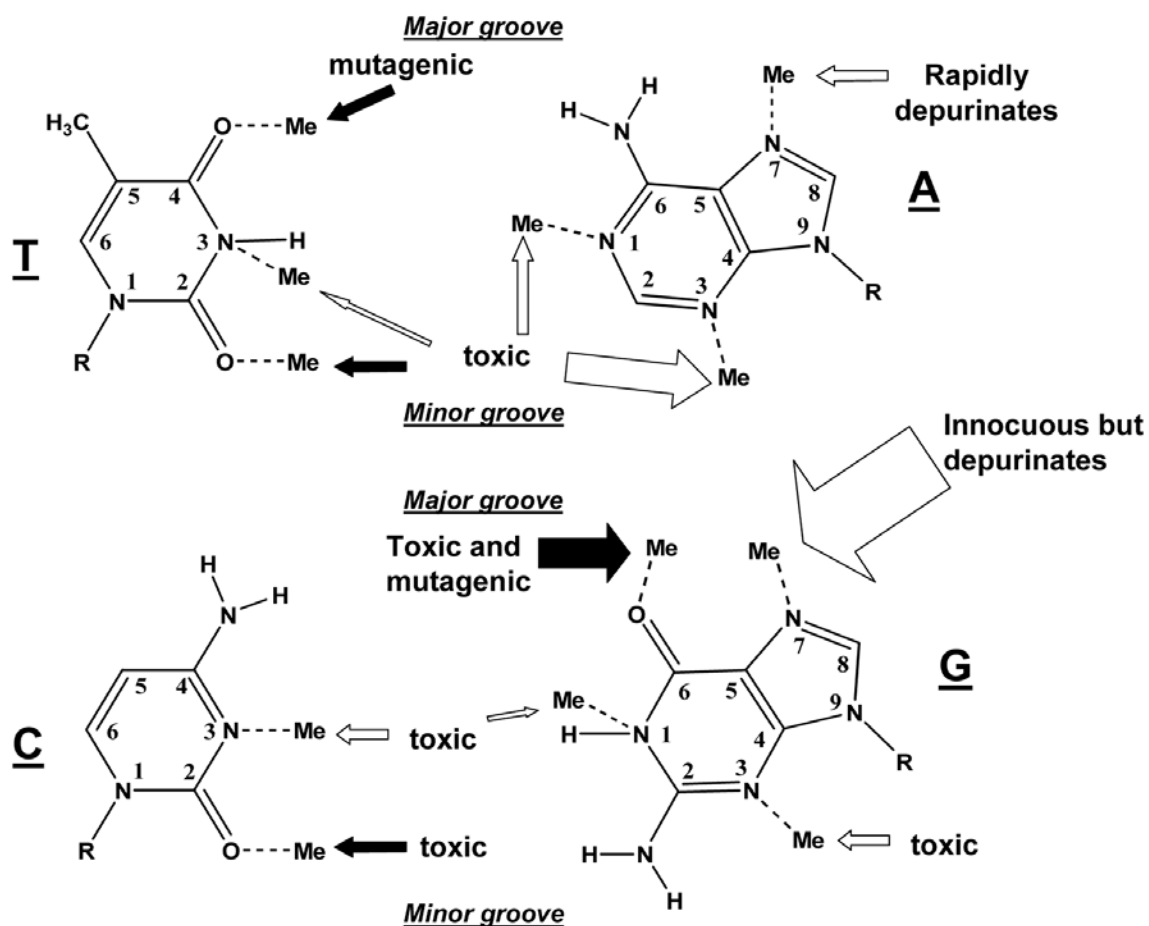


Figure 5.2. Potential sites of chemical methylation in double-stranded DNA. The arrows point to each methyl adduct and describes whether each adduct is known to be predominantly toxic or mutagenic. The open arrows represent sites that are methylated by MMS, MNNG, and MNU. The filled arrows point to sites that are methylated by MNNG and MNU, but not detectably by MMS. Note that methylation of different sites on the same base at the same time is extremely rare. The size of the arrows roughly represent the relative proportion of adducts. In single-stranded DNA, the N1- adenine and N3-cytosine positions display a greater reactivity. (Wyatt & Pittman, 2006).

Escherichia coli responds to alkylation damage by induction of an adaptive DNA repair pathway which increases the cellular resistance to the mutagenic and toxic effects of alkylating agents (Samson & Cairns, 1977). *E. coli* contains two genes which encode DNA methyltransferases, the inducible *ada* of the Ada regulon, and *ogt*, which is a constitutively expressed gene (Friedberg *et al.*, 1995; Sedgwick & Lindahl, 2002). Since the focus of this work was the investigation of an adaptive response towards alkylating DNA damage, the literature reviewed here will focus mainly on the adaptive response in *E. coli*. As mentioned above, the key player in the *E. coli* adaptive response is the Ada protein, which has been extensively studied and well characterised over the last 30 years (reviewed in Sedgwick and Lindahl, 2002). The Ada protein is 354 amino acids in length and has a molecular weight of 39 kDa. This protein has a dual function as a positive regulator of the adaptive response to alkylation damage, and as a direct DNA repair enzyme, by demethylating O⁶-methylguanine, O⁴-methylthymine and phosphotriester residues formed by alkylating agents such as MNNG (Nakabeppu & Sekiguchi, 1986; Teo *et al.*, 1984). Ada positively regulates the adaptive response to alkylation damage by acting as a transcriptional activator for certain genes involved in the alkylation response pathway, namely *alkB*, *alkA*, and *aidB* and also *ada* itself. The *alkA* gene encodes a DNA glycosylase, which is constitutively expressed in low levels in *E. coli* (Karran *et al.*, 1982; Samson & Cairns, 1977). AlkA removes O²-methylpyrimidines and 3-methylpurines (Evensen & Seeberg, 1982; Karran *et al.*, 1982), lethal lesions that block DNA replication and thus cause cell death. A homologue of AlkA has been identified in mammalian cells. This is known as AAG/APNG/MPG and it removes 3-meA lesions (Chakravarti *et al.*, 1991; O' Connor & Laval, 1990). Both AlkA and AAG have been shown to remove a wide range of lesions, e.g., 3-meA, N³-methylguanine, 1, N⁶-ethenoadenine and others (Dosanjh *et al.*, 1994a; Dosanjh *et al.*, 1994b; Hang *et al.*, 1997). The *alkB* gene forms a small operon with *ada*

and is required for error-free replication of methylated single-stranded DNA (Dinglay *et al.*, 2000). The *alkB* gene counteracts this lethal alkylation damage independently of the adaptive response (Kataoka & Sekiguchi, 1985). More recently, it has been shown that *E. coli* AlkB repairs the cytotoxic lesions 1-methyladenine and 3-methylcytosine in single- and double-stranded DNA in a reaction that is dependent on oxygen, alpha-ketoglutarate and Fe (Trewick *et al.*, 2002). The *aidB* gene encodes a product which appears to detoxify nitrosoguanines, reducing the level of methylation by these agents (Landini *et al.*, 1994). Recent observations suggest that AidB might be able to bind double-stranded DNA and take part in its dealkylation (Rohankhedkar *et al.*, 2006).

Ada acts as a DNA repair enzyme by repairing one of the two diastereoisomers of methylphosphotriesters in DNA, by transferring the methyl group on to one of its own cysteine residues (McCarthy & Lindahl, 1985). This self-methylation converts the Ada protein to methylated Ada (^{me}Ada), a form of Ada that is capable of binding the promoter regions of specific genes and enhancing their transcription (Teo *et al.*, 1984). In this way, activation of Ada is a direct consequence of one of its DNA repair activities (Volkert & Landini, 2001). This transcriptional regulator function is mediated by the N-terminal domain of the Ada protein (Kataoka *et al.*, 1986). Specifically, cysteine residue 38 (Cys-38) has been shown to be the critical residue for the self methylation of Ada, thereby turning it into an active transcriptional regulator (Takinowaki *et al.*, 2004). N-Ada contains a zinc ion tightly bound to four cysteines, of which one is Cys-38. Metal coordination is linked with the methyl acceptor function of Cys-38, pointing to a novel mechanism involving metallo-activation of the cysteine sulphur atom by its bound metal (He *et al.*, 2003). The Ada protein also accepts methyl groups from the highly mutagenic lesions O⁶- methylguanine and O⁴- methylthiamine onto a different cysteine, known to be residue 321 (Cys-321), located in the COOH-terminal region of the protein (Demple *et al.*, 1985). Transfer of a

methyl group from damaged DNA to the C-terminal cysteine (Cys-321) results in the inactivation of the O⁶-AlkG repair ability of Ada (Olsson & Lindahl, 1980), and as already stated, transfer to the N-terminal site (Cys-38) results in conversion of Ada to a strong transcriptional activator (Teo *et al.*, 1984). Activated Ada binds to a conserved nucleotide sequence, known as the *ada* box, composed of an A-box and a B-box, which is associated with the regulatory regions of at least two genes in *E. coli*, *ada* itself, and *alkA*, an inducible 3-methyladenine DNA glycosylase II (Nakamura *et al.*, 1988; Teo *et al.*, 1984). The induction of the adaptive response after exposure to alkylating agents protects *E. coli* from both the mutagenic and the lethal effects of alkylation damage (Samson & Cairns, 1977). A schematic diagram depicting the current understanding of this adaptive response in *E. coli* is presented in Figure 5.3. A diagrammatic representation of the transcriptional activator function of Ada, including the *ada* box region is depicted in Figure 5.4.

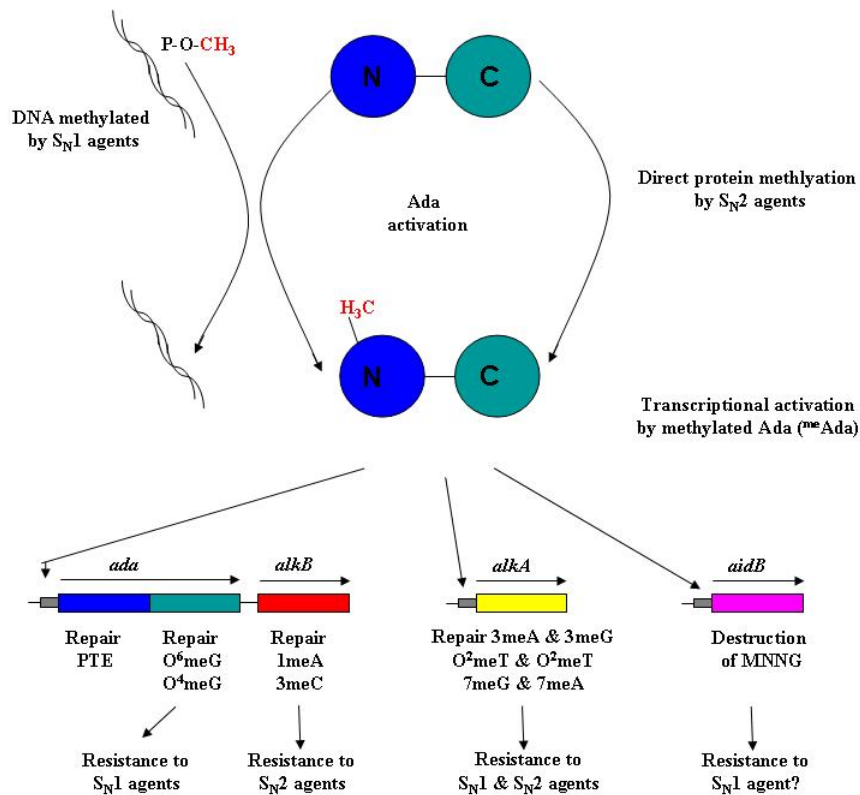


Figure 5.3. Schematic representation of the *E. coli* Ada response. The Ada protein is a positive regulator of the response by acting as a transcriptional regulator for the expression of enzymes including *ada* itself, *alkB*, *alkA* and *aidB*. Genes are depicted by various coloured boxes in diagram. Ada becomes activated (^mAda) when it repairs methylphosphotriester (PTE) lesions in DNA, and the methyl group is transferred by Ada to Cys-38 in the N-terminal domain of the protein. ^mAda can bind the promoter region of specific genes (indicated by the grey boxes in the diagram). The activation of these genes results in increased repair of alkylating DNA damage and probable destruction of certain alkylating agents, as stated in the diagram. Adapted from Sedgwick and Lindahl (2002).

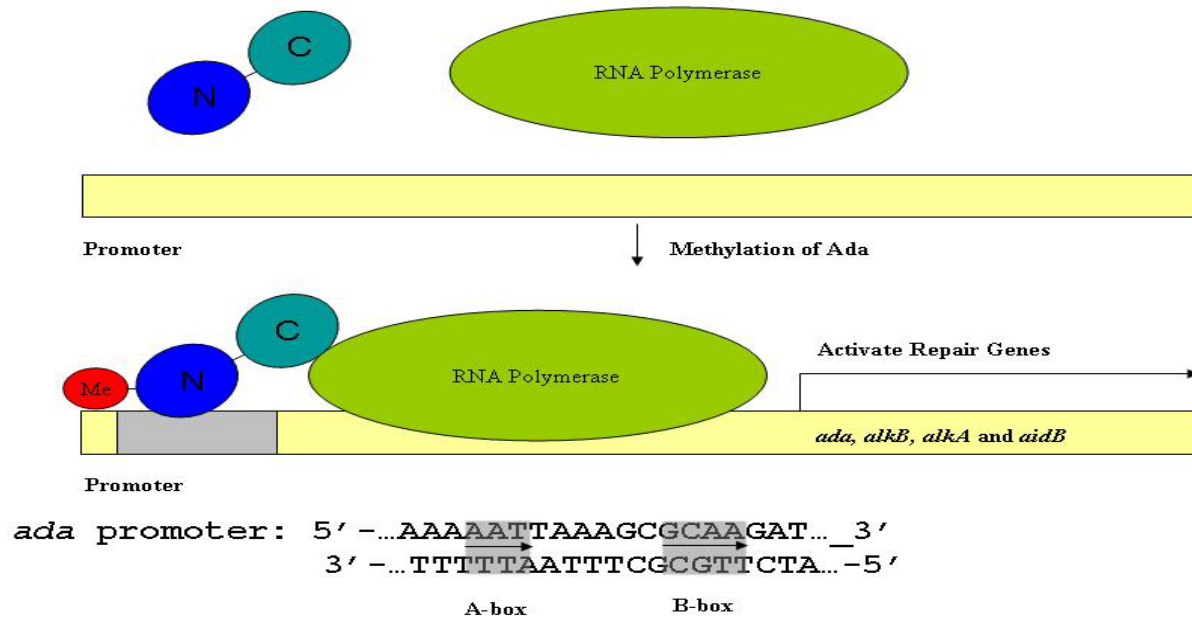


Figure 5.4. Schematic Representation of the transcriptional activator activity of *E. coli* Ada.

Ada is composed of two domains, an N-terminal and a C-terminal domain, each possessing distinct functions. The N-terminal domain becomes methylated at Cys-38 (^{me}Ada) to become a strong transcriptional regulator for the adaptive response in *E. coli*. ^{me}Ada can bind a defined region in the promoter of downstream target genes such as *alkA*, *alkB*, *aidB* and *ada* itself. This defined region is known as the *ada* promoter and is comprised of two regions, known as the A-box and B-box, and the sequence of the *ada* promoter is shown in the diagram above.

Currently, there is a large amount of literature describing and characterising this adaptive response in *E. coli*. A similar adaptive response exists in the gram positive bacterium *Bacillus subtilis* (Morohoshi & Munakata, 1987). However, in *B. subtilis*, the dual activities described for Ada in *E. coli* are performed by two separate proteins, namely AdaB, an inducible O⁶-AlkG ATase, and AdaA, an Alk-PT ATase (Morohoshi *et al.*, 1990). In *B. subtilis*, the alkylated form of the Alk-PT ATase also promotes transcription of the *ada* operon (Morohoshi *et al.*, 1990). Furthermore, there are differences in the organisation of the *ada* operon between *E. coli* and *B. subtilis* and no *alkB* gene has been found in *B. subtilis* (Demple *et al.*, 1985). The yeast *Saccharomyces cerevisiae* does not possess an adaptive response to alkylating damage (Maga & McEntee, 1985; Polakowska *et al.*, 1986). However, an AlkA homologue has been identified in *S. cerevisiae* through complementation experiments in *E. coli* adaptive response mutants (Berdal *et al.*, 1990; Chen *et al.*, 1990). This yeast AlkA homologue (MAG) was able to remove 7-methylguanine as well as 3-methyladenine from dimethyl-sulphate treated DNA, confirming the related nature of this enzyme to the AlkA DNA glycosylase from *E. coli*. (Berdal *et al.*, 1990). A gene for O⁶-alkylguanine DNA alkyltransferase has been cloned from *S. cerevisiae* by functional complementation of an *E. coli ada ogt* double mutant, and this gene has been designated *MGT1* (Sassanfar & Samson, 1990; Xiao *et al.*, 1991). Mutants, in whom the *MGT1* gene is disrupted, are sensitive to killing and mutagenesis following exposure to alkylating agents. In agreement with the lack of an adaptive response in *S. cerevisiae*, *MGT1* transcript levels were not increased in response to alkylation treatment (Xiao *et al.*, 1991). An improved growth response in the presence of MNNG was observed for *Aspergillus nidulans*, following exposure with a sub-lethal dose (Hooley *et al.*, 1988), and DNA alkyltransferase activity was also observed in this fungus (Baker *et al.*, 1992; Swirski *et al.*, 1988) This activity has been shown to be highly inducible, and

effective at repairing O⁶-methylguanine and O⁴-methylguanine lesions, suggesting that an adaptive response is present in *A. nidulans*. To date, no corresponding response has ever been described for the closely related human pathogen *Aspergillus fumigatus*.

5.2. Aims and Objectives.

- 1) Establish if an adaptive response towards alkylating DNA damage exists in *Aspergillus fumigatus*.
- 2) Identify the candidate key genes responsible for any adaptive response.
- 3) Investigate the function of putative DNA repair genes by using a targeted gene deletion strategy, for the generation of specific *A. fumigatus* DNA repair mutants.
- 4) To perform phenotypic analysis for these mutants with respect to sensitivity to DNA damaging agents, in particular alkylating agents.
- 5) To investigate gene expression levels of key response genes upon exposure to the DNA alkylating agent, MNNG.
- 6) To clone key response genes from *A. fumigatus* into *S. cerevisiae* to investigate if the *A. fumigatus* genes are capable of complementing a yeast *MGT1* deletion.

5.3. Results.

5.3.1. Identification of candidate genes for an adaptive response to alkylation damage in *A. fumigatus*.

The *E. coli* Ada protein sequence (NCBI Accession No. *E. coli* NP_416717.1) was used as a query sequence in order to perform a Blast search against all the available *Aspergillus* protein sequences at the CADRE database (Mabey *et al.*, 2004). Currently, there are nine available *Aspergillus* genomes. Blast homology searching using the BLASTX function at CADRE revealed that the top two homology hits for *E. coli* Ada were in the *A. fumigatus* genome and that these were encoded by the genes AFUA_5G06350 and AFUA_2G02090. According to annotation on CADRE, these genes encode for a putative DNA repair and transcription factor Ada, and a methylated-DNA-protein-cysteine methyltransferase respectively. Following this, the *E. coli* Ada protein sequence was aligned with the AFUA_5G06350 or the AFUA_2G02090 protein sequences to look for specific regions of homology. To this end, an online alignment program, SIM Alignment Tool at the Swiss Institute of Bioinformatics (<http://www.expasy.ch/tools/sim-prot.html>) was used. Partial alignments were obtained using this online program and these alignments are presented in Figures 5.5 and 5.6. Alignment of Ada with AFUA_5G06350 indicated that there was 44.9% sequence identity in 136 residues of overlap between the two proteins (Figure 5.5). Alignment of Ada with AFUA_2G02090 indicated that there was 37.3 % sequence identity in 67 residues of overlap between the two proteins (Figure 5.6). Interestingly, the N-terminal domain of Ada aligned well with the putative DNA repair and transcription factor (AFUA_5G06350), while the C-terminal region of Ada aligned with the *A. fumigatus* putative methylated-DNA-protein cysteine methyltransferase (AFUA_2G02090). AFUA_5G06350 is thus likely to encode the methylphosphotransferase (MPT) and AFUA_2G0290 likely encodes an alkylguaninetransferase (AGT) analogous to

the N- and C-terminal domains of *E. coli* Ada (Kataoka *et al.*, 1986; Demple *et al.*, 1985). These alignments also revealed that the critical residues for methyl acceptance in *E. coli* Ada are also present in AfMPT and AfAGT. The N-terminal Ada domain accepts methyl groups from methylphosphotriesters and this is mediated by cysteine residue 38 (cys-38), which is also present in AfMPT (Figure 5.5). The C-terminal Ada domain accepts methyl groups from O⁶- methylguanine and O⁴- methylthymine residues, for which the critical residue is cys-321, and this is also conserved in AfAGT (Figure 5.6). Examination of the upstream regions (approx. 300 bp) of the AFUA_5G06350 and AFUA_2G02090 open reading frames revealed that there are potential *ada* binding sites in the promoter regions of these genes, using the *E. coli* A-box and B-box sequences as possible binding sites. These potential *ada* box regions are shown in Figure 5.7. To look for other genes known to be involved in the adaptive response in *E. coli*, further protein blast (NCBI) searching using bacterial sequences of *alkB* and *alkA* proteins revealed that there were also homologues in *A. fumigatus* encoded by the genes AFUA_6G07990 and AFUA_4G06800 respectively. Based on these results, the *A. fumigatus* genes are now referred to as AFUA_5G06350 (*Afmpt*), AFUA_2G02090 (*Afagt*), AFUA_4G06800 (*AfalkA*) and AFUA_6G07990 (*AfalkB*). The presence of these 4 specific genes in the genome of *A. fumigatus*, which are homologous to the key adaptive response genes in *E. coli*, provided a strong basis for the further investigation of an adaptive response to alkylation in this filamentous fungus.

A.

AGAGCCAGCCCTTGCATTCCTCTTTTCAAATGACCACATGCTCAATCTCACTAATTATGTGTGGATACAGATGAGTGAGATCG
GTTACCTACCTAAGGCACCGTGGTGGTTGGTTCC **AAT**CCTG**GCAA**CTGATGGAAACGAGGGTCTGCTCTCAAAGTGGCCAAT
CAGCAGCGCAGACTGCACAAAGAGGGTTCAAGTTGTCGTATTCAATCAAC **AAT**CCCAAGTGTT **GCAA**AAATCCCATAACCCA
TCACTATCCTGGGTTACTCTTCATCCCATTATTGTCTGTAATACCTCAAAATGCATGTGGT.....etc.

B.

CTCTGATTTGCTACATTGAGAGCAGCGGCTTGAGCCACCCAAACAACAGTCTCTCATATAAAACAAGTCGCGTAGCCATTTGC
ACTCTTCTTAGACTACATAACTACCCAGAACA ACTAGACTAGGTGAGTCTCATCATTCCACTGATAAAGTTCATATTATTGAT
GAAAGATATAGGTCCCTGTATGATCACATGC **GAT**CCACCTCT **GCAA**AGGTCACATCACCGTTATCCAATACTTGCAGAAGAG
AGCTTGGTGGTTCATATTGGATAACCACCCGAG **AAT**AACTAT **GGCA**TCTCTTATGGAGAACCAA.....etc.

Figure 5.7. Potential Ada promoter binding site(s) in the 5' upstream region of *A. fumigatus* AFUA_5G06350 and *A. fumigatus* AFUA_2G02090

A. 300 bp sequence upstream of AFUA_5G06350 start site.

B. 300 bp sequence upstream of AFUA_3G02090 start site.

Possible *ada* promoter sites are highlighted in yellow. Start site (ATG) for each gene is underlined in black.

5.3.2. Confirmation of an adaptive response towards alkylating agents in *Aspergillus fumigatus*.

The presence of key genes in the *A. fumigatus* genome, the high degree of sequence conservation of the encoded proteins with the well described *E. coli* Ada (Sedgwick and Lindahl, 2002), and the observed adaptive response in *Aspergillus nidulans* (Hooley et al., 1988; Swirski et al., 1988; Baker et al., 1992) strongly suggested the presence of a similar adaptive response to alkylating agents in *A. fumigatus*. This possibility was investigated initially on the phenotypic level by performing plate assays containing the highly mutagenic alkylating agent, MNNG. To this end, *A. fumigatus* Af293 conidia were used to inoculate MEA agar plates or MEA plates supplemented with a non-lethal dose of MNNG (0.5 µg/ml). This dose of MNNG has been used by others as an inducing dose for the induction of alkyltransferase activity in *A. nidulans* (Baker et al., 1992). Following overnight growth, plugs were taken from these plates and transferred to fresh MEA plates supplemented with concentrations of MNNG (0-4 µg/ml). Plates were incubated for a further 72 hr until colonies became clearly visible. The radial growth of the colonies was measured (mm) at 72 hr. *A. fumigatus* colonies which had been pre-incubated/adapted overnight on MEA containing an inducing dose of MNNG (0.5 µg/ml) exhibited a greater growth rate than colonies which were pre-incubated on MEA media only ($p < 0.001$). This work provides evidence for the presence of an adaptive response towards the alkylating agent MNNG in *A. fumigatus* (Figure 5.8).

Gene expression analysis was performed in order to investigate if this adaptive response seen in the plate assays described above coincided with the induction of specific genes upon treatment of *A. fumigatus* cultures with MNNG. *A. fumigatus* Af293 cultures ($n = 9$, 100 ml each) were incubated overnight at 37 °C. MNNG (0.5 µg/ml final concentration) was added the following morning to four of the cultures in order to induce

the adaptive response. Prior to the addition of MNNG to any of the cultures, one was taken and harvested as an uninduced reference at T = 0 hr. The remaining eight cultures (four of which had MNNG added) were harvested at the following time points: 30 min, 1 hr, 2 hr and 3 hr post induction (Section 2.2.1.1). Total RNA was isolated (Section 2.2.11.1) and quantified using spectrophotometry. RNA was DNase treated, reverse-transcribed to cDNA and RT-PCR was performed (Sections 2.2.11.3, 2.2.11.4, 2.2.11.5). RT-PCR indicated that AFUA_5G06350 (*Afmpt*) and AFUA_2G02090 (*Afagt*) were up-regulated in the presence of MNNG, while neither AFUA_6G07990 (*AfalkB*) or AFUA_4G46800 (*AfalkA*) gene expression appeared to be altered upon exposure to MNNG (Figure 5.9). Induction of *Afagt* was observed at 30 min following MNNG addition and this elevated gene expression was maintained for at least 3 hr following MNNG addition (Figure 5.9). *Afmpt* expression was elevated at one hour following addition of MNNG and this was also persistent throughout the 3 hr period investigated in this work (Figure 5.9). The *calmodulin* (*calm*) gene, expressed constitutively in *A. fumigatus*, was used as a control for all RT-PCR experiments (Section 2.2.11.15) as described previously.

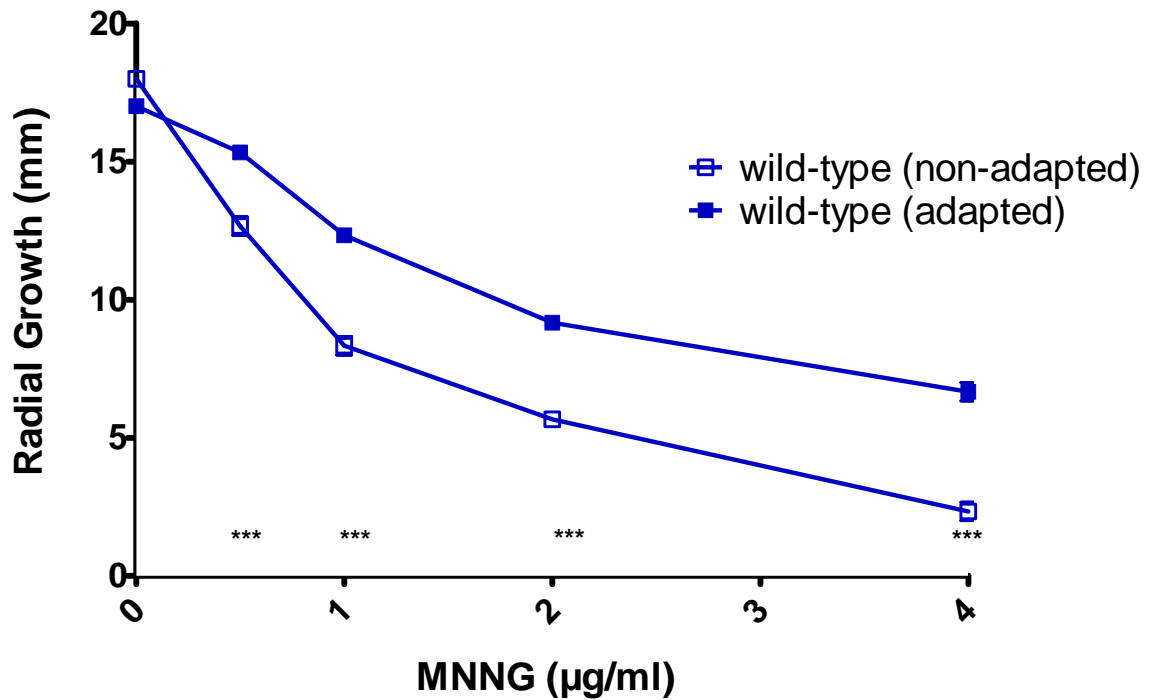


Figure 5.8. An adaptive response towards alkylating agents exists in *Aspergillus fumigatus*.

Radial growth (mm) of *Aspergillus fumigatus* Af293 on MEA agar supplemented with increasing concentrations of the alkylating agent MNNG (0-4 µg/ml). Growth was monitored at 72 h incubation at 37 °C following at overnight induction with a sub-lethal dose of MNNG (0.5 µg/ml). This data displays the mean of three independent experiments ± the standard error or the mean. Key *** = $p < 0.001$.

Figure 5.9. RT-PCR analysis of *A. fumigatus* genes (*Afmpt*, *Afagt*, *AfalkA* and *AfalkB*) with or without addition of an inducing dose of MNNG (0.5 µg/ml).

A. RNA integrity was determined by the presence of intact 26S and 18S ribosomal subunits (rRNA).

B-E. RT-PCR products (5 µl) for *A. fumigatus* genes as listed.

F. RT-PCR for the *calmodulin* (*calm*) gene confirms absence of genomic DNA (gDNA) in cDNA preparations.

T = 0: RT-PCR analysis from overnight un-induced cultures.

U = 30 min, U = 1 hr, U = 2 hr, U = 2 hr: RT-PCR analysis from un-induced cultures at relevant time points.

I = 30 min, I = 1 hr, I = 2 hr, I = 3 hr: RT-PCR analysis from induced cultures at relevant time points.

All RT-PCR products were resolved on 2 % (w/v) agarose gels.

5.3.3. Deletion of *Afmpt* and *Afagt* from the genome of *A. fumigatus*.

For inactivation of AFUA_5G06350 (*Afmpt*) and AFUA_2G02090 (*Afagt*), a bipartite gene disruption strategy was employed (Section 2.2.4). The fully sequenced *A. fumigatus* Af293 strain was used in this study. Respective fragments including flanking regions were amplified from *A. fumigatus* genomic DNA by PCR (Section 2.2.2.3). Ligations were carried out overnight with T4 DNA Ligase (Promega) and ligation products were used as the DNA template for the generation of the final bipartite disruption constructs (Section 2.2.2.7). *ptrA* was released from the pSK275 plasmid (a kind gift from Professor Sven Krappmann) via restriction digestion (Section 2.2.6). PCR reactions were performed using the Expand Long Range Template PCR System (Roche).

5.3.3.1. Generation of AFUA_5G06350 and AFUA_2G02090 bipartite disruption constructs.

The AFUA_5G06350 and AFUA_2G02090 have coding regions of 687 bp and 453 bp in length respectively. The disruption strategies that were employed in this work resulted in the deletion of the entire coding region of these genes from the genome. For both genes, PCR 1 and PCR 2 amplified 1.2 kb corresponding to the 5' and 3' flanking regions. For AFUA_5G06350, PCR 1 and PCR 2 were engineered to contain an *MfeI* and a *HindIII* site respectively. For AFUA_2G02090, PCR 1 and PCR 2 were engineered to contain an *XmaI* and a *KpnI* site respectively. PCR products and pSK275 were digested with either *MfeI* or *HindIII* (for AFUA_5G06350), or *XmaI* or *KpnI* (AFUA_2G02090). pSK275 was digested with *MfeI* and *HindIII* or *XmaI* and *KpnI* to release *ptrA*. Digested PCR products and *ptrA* were ligated to yield Ligation 1 (PCR 1 ligated to *ptrA*) and Ligation 2 (PCR 2 ligated to *ptrA*). These ligations were used as a template for the PCR amplification of the final bipartite disruption constructs. Agarose gel images of PCR 1, 2, 3 and 4 products and

digested *ptrA* for the generation of AFUA_5G06350 disruption constructs can be visualised in Figure 5.10, while disruption constructs for AFUA_2G02090 are displayed in Figure 5.11.

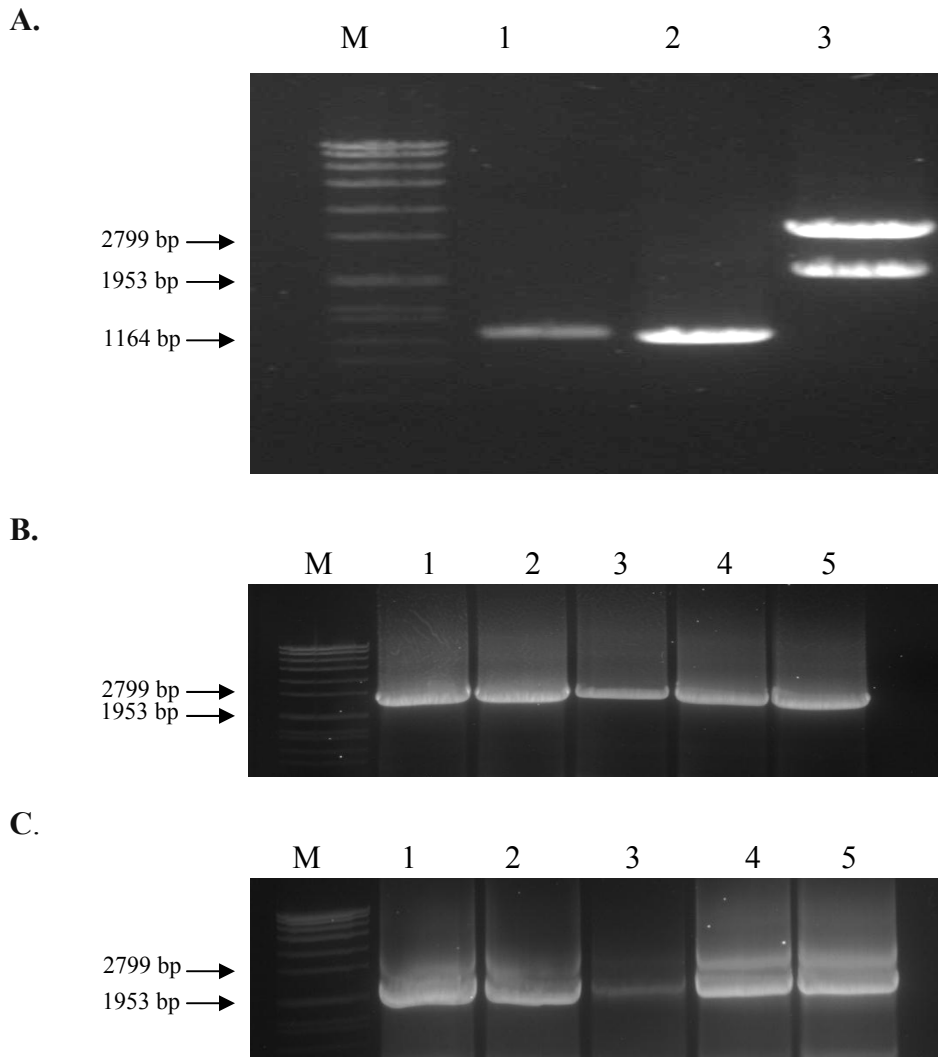


Figure 5.10. AFUA_5G06350 disruption constructs.

A. PCR 1 and PCR 2 products and *ptrA* released from pSK275 plasmid.

Lane 1: purified PCR 1 product, Lane 2: purified PCR 2 product, Lane 3: pSK275 digested with *Mfe*I and *Hind*III, yielding 2 fragments; 2.9 kb (pSK275 backbone) and 2.0 kb (*ptrA*).

B. Lane 1-5: PCR 3 products (2.6 kb).

C. Lanes 1-5: PCR 4 products (2.2 kb).

M: Molecular weight marker (Roche VII).

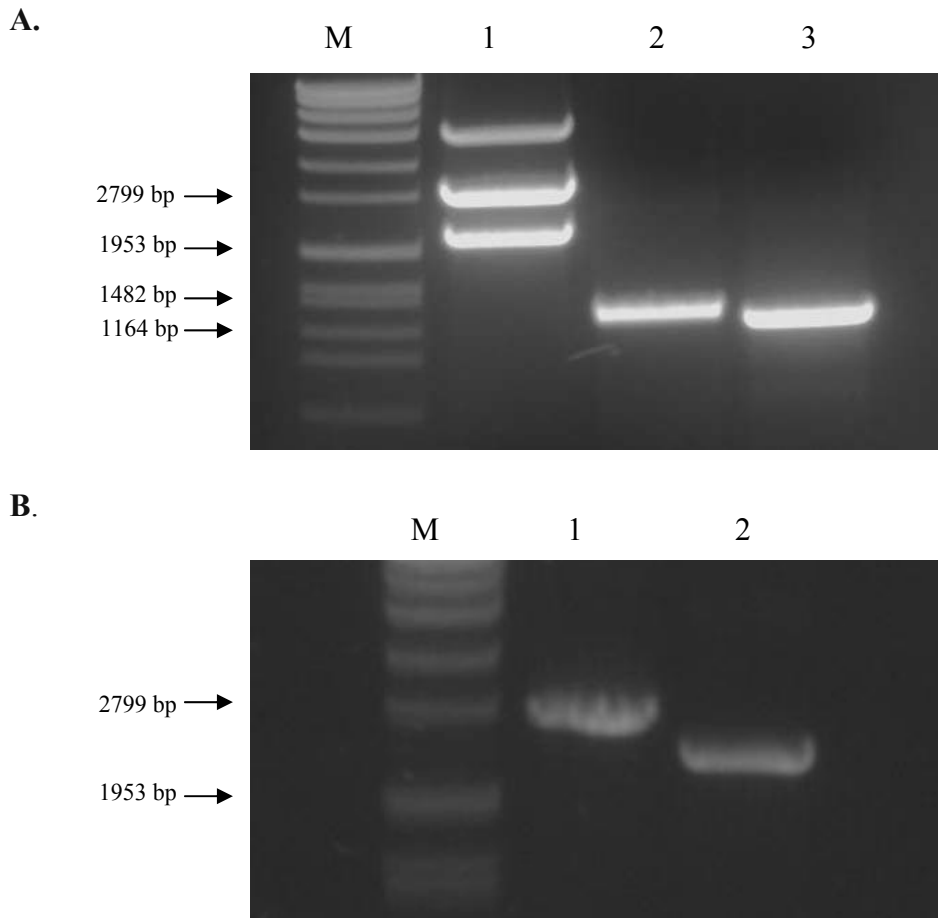


Figure 5.11. AFUA_2G02090 disruption constructs.

A. PCR 1 and PCR 2 products and *ptrA* released from pSK275 plasmid.

Lane 1: pSK275 digested with *Xma*I and *Kpn*I, yielding 2 fragments; 2.9 kb (pSK275 backbone) and 2.0 kb (*ptrA*), Lane 2: purified PCR 1 product, Lane 3: purified PCR 2 product.

B. Lane 1: PCR 3 (2.6 kb), Lane 2: PCR 4 products (2.3 kb).

M: Molecular weight marker (Roche VII).

5.3.3.2. Identification of *A. fumigatus* AFUA_5G06350 and AFUA_2G02090 mutant strains.

For generation of *A. fumigatus* mutant strains, protoplasts were transformed with 5 µg DNA for of each side of the bipartite construct and transformed protoplasts were selected in the presence of pyrithiamine (0.1 µg/ml) (Section 2.2.23). Transformants were isolated and Southern blot analysis was performed as described earlier. The identification of AFUA_5G06350 and AFUA_2G02090 mutant strains will be dealt with separately in the two following sections.

5.3.3.2.1. Identification of *A. fumigatus* AFUA_5G06350 mutant strain (termed $\Delta Afmpt$).

Ten colonies were picked from transformation plates and Southern blot analysis was performed on these. gDNA from *A. fumigatus* Af293 and these transformants was restriction digested with *AfeI* and Southern blotting was performed. A DIG-labelled probe was generated using the primers AFUA_5G06350 Primer 2 R and AFUA_5G06350 Primer 5 F, which amplified a 1 kb product, corresponding to the 5' flanking region of AFUA_5G06350. This probe was used to hybridise *AfeI* digested DNA. A schematic representation of the Southern blot strategy and hybridisation patterns is shown in Figure 5.12. DIG Detection was performed in order to detect hybridisation of DIG-labelled probes (Section 2.1.18). Using this detection strategy, expected hybridisation patterns were as follows: Af293: 3,951 bp, $\Delta Afmpt$: 5,172 bp. This analysis revealed one integration of the disruption construct in colony number 10, by the observation of a band at the correct size of 5,172 bp and the absence of a wild-type band (3951 bp) (Figure 5.13). Colony number 10 was single spore isolated as described in Methods section, and Southern blot analysis was performed on 5 of these colonies, number 10.1 – 10.5. gDNA from these colonies was

digested with *StuI* and probed for the pyrithimine coding sequence. Using the primers, *OptrA1* and *OptrA2*, a 560 bp DIG-labelled probe corresponding to *ptrA* was prepared by PCR using pSK275 as a template. This probe was used to hybridise *StuI* digested DNA. This analysis confirmed a single integration of *ptrA* into 4 of the single spored transformants 10.1 – 10.4, and no *ptrA* in wild-type as expected (Figure 5.13).

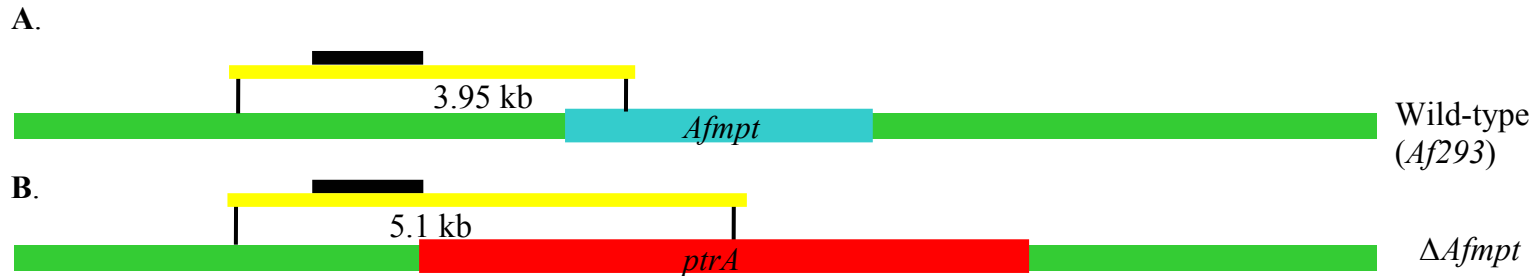
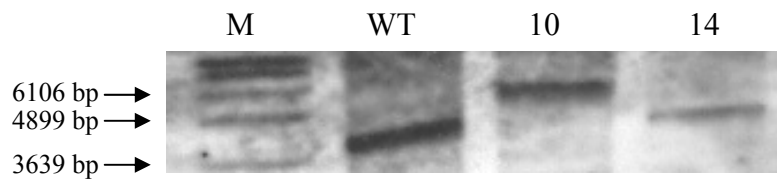


Figure 5.12. Southern blotting and hybridisation strategy used to identify *A. fumigatus* $\Delta Afmpt$.

The *Afmpt* locus in wild-type (A) and $\Delta Afmpt$ (B) is shown. The entire *Afmpt* coding region is indicated as a blue bar and the 5' and 3' flanking regions are shown in green. The entire *Afmpt* gene was deleted and replaced by the pyrithiamine resistance cassette (*ptrA*) from *A. oryzae* (Kubodera *et al.*, 2000; 2002). *ptrA* is indicated in red. Black vertical lines indicate *AfeI* restriction sites in the genomic sequence of wild-type and $\Delta Afmpt$. Genomic DNA from pyrithiamine-resistance colonies was *AfeI* digested and probed with a 1 kb DIG-labelled fragment corresponding to the 5' region of *Afmpt*. The probe is indicated with a black horizontal line. The positions for probe binding are indicated with yellow horizontal lines. Expected hybridisation patterns: Af293 wild-type-3.95 kb, $\Delta Afmpt$ -5.1 kb.

A.



B.

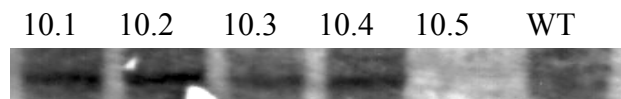


Figure 5.13. Southern blot confirming deletion of AFUA_5G06350 ($\Delta Afmpt$) in *A. fumigatus*.

A. *AfeI* digested gDNA probed with the 5' flanking region of AFUA_5G06350. WT: Af293 gDNA, 10, 14: gDNA from 2 of the pyrithiamine resistant transformants.

B. *StuI* digested gDNA probed with a pyrithimine coding region probe. 10.1 – 10.5: gDNA from 5 single spore colonies from transformant 10. WT: Af293 gDNA.

M. Molecular weight marker (Roche VII).

5.3.3.2.2. Identification of *A. fumigatus* AFUA_2G02090 mutant strain (termed $\Delta Afagt$).

Fifteen colonies were picked from transformation plates and Southern blot analysis was performed on these. gDNA from *A. fumigatus* Af293 and these transformants was restriction digested with *Mfe*I and Southern blotting was performed. A 1.2 kb DIG-labelled probe was generated using the primers AFUA_2G02090 Primer 1 and AFUA_2G02090 Primer 2, corresponding to the 5' flanking region of AFU_2G02090. This probe was used to hybridise *Mfe*I digested DNA. Using this detection strategy, expected hybridisation patterns were as follows: Af293: 3,969 bp, $\Delta Afagt$: 2,619 bp. A schematic representation of this strategy is shown in Figure 5.14. This analysis revealed several integrations of the disruption construct in many of the transformants, but three transformants (transformants 9, 11 and 24) in particular appeared to contain only one integration by the visualisation of the correct band size and absence of a wild-type band. Hybridised gDNA from transformants 9, 11 and 24 are circled in red in Figure 5.15. Colonies number 9, 11 and 24 were single spore isolated (Section 2.2.25) and Southern blot analysis was performed on 9 representative colonies from these transformants. gDNA from these colonies was digested with *Mfe*I and probed for the 5' flanking region of AFUA_2G0290. This blot is shown in Figure 5.15 and confirms the disruption of AFUA_2G02090 in all single spored transformants, with the correct hybridisation pattern seen in all lanes.

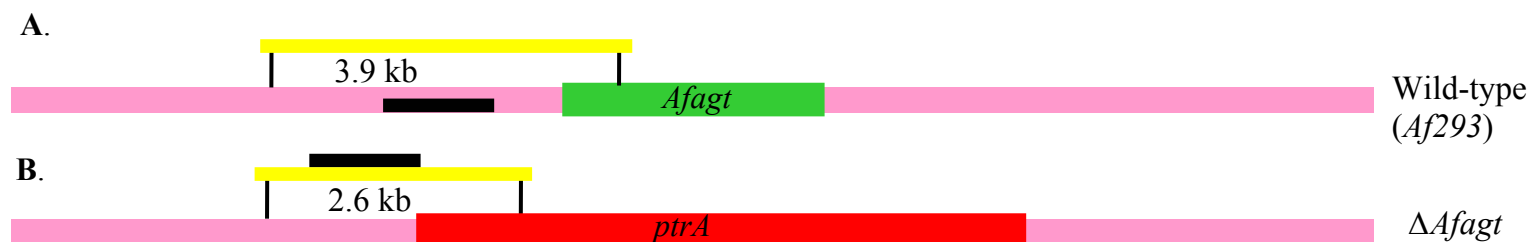


Figure 5.14. Southern blotting and hybridisation strategy used to identify *A. fumigatus* $\Delta Afmpt$.

The *Afmpt* locus in wild-type (A) and $\Delta Afmpt$ (B) is shown. The entire *Afmpt* coding region is indicated as a blue bar and the 5' and 3' flanking regions are shown in pink. The entire *Afmpt* gene was deleted and replaced by the pyrithiamine resistance cassette (*ptrA*) from *A. oryzae* (Kubodera *et al.*, 2000; 2002). *ptrA* is indicated in red. Black vertical lines indicate *MfeI* restriction sites in the genomic sequence of wild-type and $\Delta Afmpt$. Genomic DNA from pyrithiamine-resistance colonies was *MfeI* digested and probed with a 1.2 kb DIG-labelled fragment corresponding to the 5' region of *Afmpt*. The probe is indicated with a black horizontal line. The positions for probe binding are indicated with yellow horizontal lines. Expected hybridisation patterns: Af293 wild-type-3.9 kb, $\Delta Afmpt$ -2.6 kb.

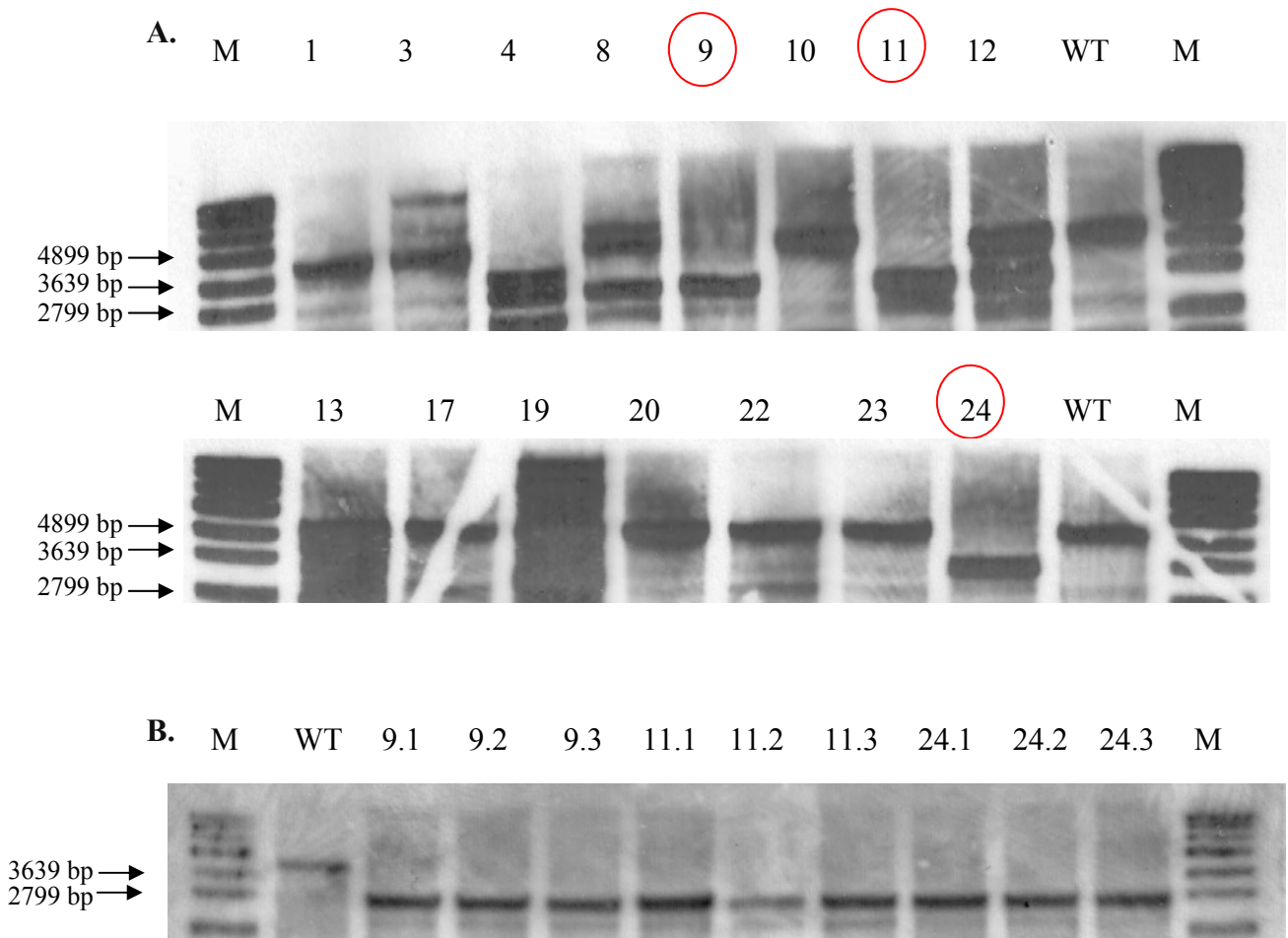


Figure 5.15. Southern blot confirming deletion of AFUA_2G02090 ($\Delta Afagt$) in *A. fumigatus*.

A. Southern blot on gDNA of pyrithimaine resistant transformants. gDNA was digested with *MfeI*, and subsequently probed for the 5' flanking region of AFUA_2G02090. WT: Af293 gDNA, 1-24: gDNA from each of the transformants.

B. Southern blot analysis on single-spored colonies confirming disruption of AFUA2G02090 ($\Delta Afagt$) in *A. fumigatus*. gDNA of Transformants 9, 11 and 24 (Figure 13A) was digested with *MfeI*, and subsequently probed for the 5' flanking region of AFUA_2G02090. WT: Af293 gDNA, 9.1-3, 11.1-3, 24.1-3: gDNA from 3 representative colonies of each of transformants 9, 11 and 24.

M. Molecular weight marker (Roche VII).

5.3.4. *A. fumigatus* $\Delta Afmpt$ and $\Delta Afagt$ are impaired in the response to alkylating DNA damage.

To establish a role for *Afmpt* in mediating the adaptive response to MNNG that was observed, plate assays were performed in increasing concentrations of MNNG as described (Section 2.2.26) and *A. fumigatus* wild-type and $\Delta Afmpt$ were compared by radial growth of colonies. Both strains showed identical growth rates in the absence of MNNG (Figure 5.14). The experiment indicated that $\Delta Afmpt$ was completely deficient in the adaptive response (Figure 5.14). $\Delta Afmpt$ showed identical growth rates on all concentrations of MNNG tested regardless of whether this strain was pre-treated or not with an inducing dose of MNNG. In addition, these growth rates were significantly lower than growth of the wild-type strain ($p < 0.001$). In fact, the $\Delta Afmpt$ strain showed complete inability to grow at the highest MNNG concentration tested (4 $\mu\text{g/ml}$) (Figure 5.14). This experiment also revealed that the $\Delta Afmpt$ mutant was more sensitive to MNNG than wild-type at all concentrations tested when both strains were uninduced ($p < 0.001$) (Figure 5.14).

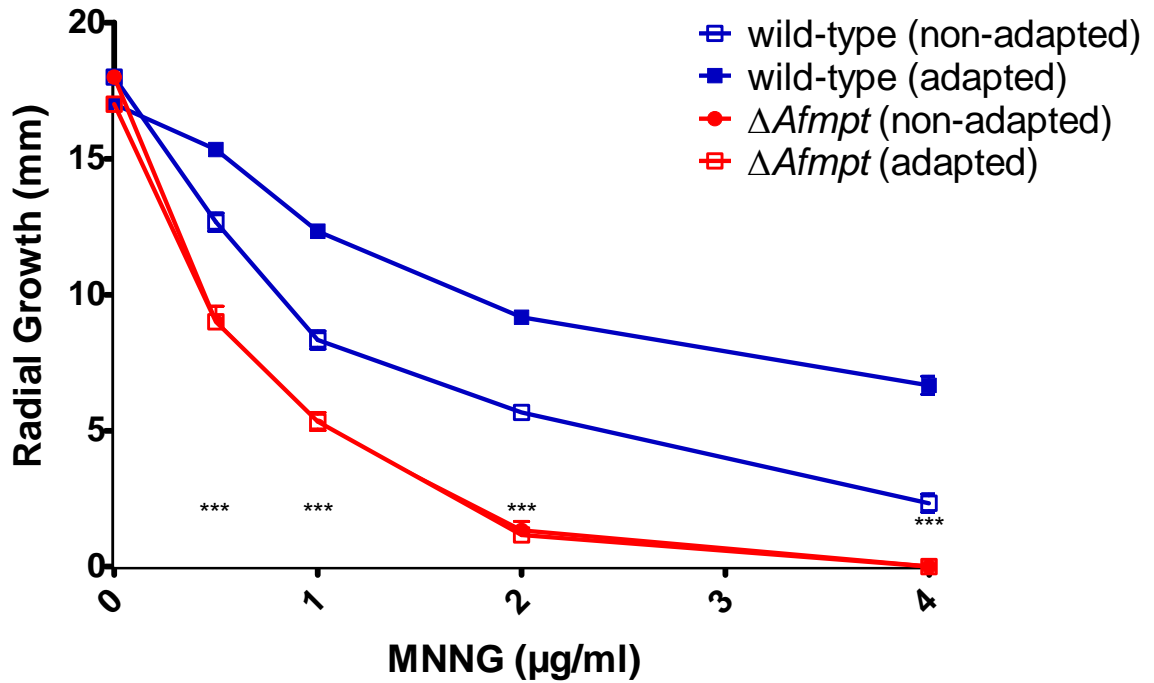


Figure 5.16. *Afmpt* is essential for the adaptive response to MNNG in *A. fumigatus*.

Radial growth (mm) of *Aspergillus fumigatus* wild-type Af293 or $\Delta Afmpt$ on MEA agar supplemented with increasing concentrations of the alkylating agent MNNG (0-4 $\mu\text{g/ml}$). Growth was monitored at 72 hr incubation at 37 °C following at overnight induction with a sub-lethal dose of MNNG (0.5 $\mu\text{g/ml}$). Data represents the mean \pm standard error of three experiments. Key *** = $p < 0.001$.

Upon observing that the $\Delta Afmpt$ mutant was more sensitive to MNNG than wild-type at all concentrations tested even when both strains were uninduced, sensitivity to a range of other DNA alkylating and damaging agents was tested in the mutants, and a summary of the conditions tested is presented in Table 2.2. Alkylating agents tested include EMS and MMS. Other agents that may lead to DNA damage by indirect means were also tested in this study to investigate the extent of disruption of the alkylation damage response. The various agents examined in this study were gliotoxin, phleomycin and hydrogen peroxide. Gliotoxin, described earlier, is a member of the epipolythiodioxopiperazine (ETP) family of highly reactive molecules which have been reported to lead to oxygen free radical formation during redox cycling (Munday, 1982). Hydrogen peroxide is a strong oxidising agent, and is known to cause oxidative stress in cells, of which one of the downstream effects is DNA damage (Klaunig *et al.*, 2010). Phleomycin blocks S-phase entry in the cell cycle (Robles *et al.*, 1999). Although the mechanism of action of phleomycin has not been clearly defined, it reportedly damages DNA by causing strand breakage and degradation (Sleigh, 1976; Sleigh & Grigg, 1976). Both $\Delta Afmpt$ and $\Delta Afagt$ were extremely sensitive to MNNG at all concentrations tested, compared to wild-type ($p < 0.001$) (Figure 5.17a and 5.17b). Neither of the mutants exhibited increased sensitivity to MMS (Figure 5.18), EMS (Figure 5.19), phleomycin or gliotoxin when compared to wild-type. MNNG, MMS and EMS plates shown in the figures contain two concentrations of conidia (5000 spores (top of plates) or 50 spores (bottom of plates)) of the relevant strain and each plate was inoculated in duplicate. Both $\Delta Afmpt$ and $\Delta Afagt$ displayed a slight sensitivity to the highest concentration of hydrogen peroxide tested (3 mM), when compared to wild-type ($p < 0.01$) (Figure 5.20).

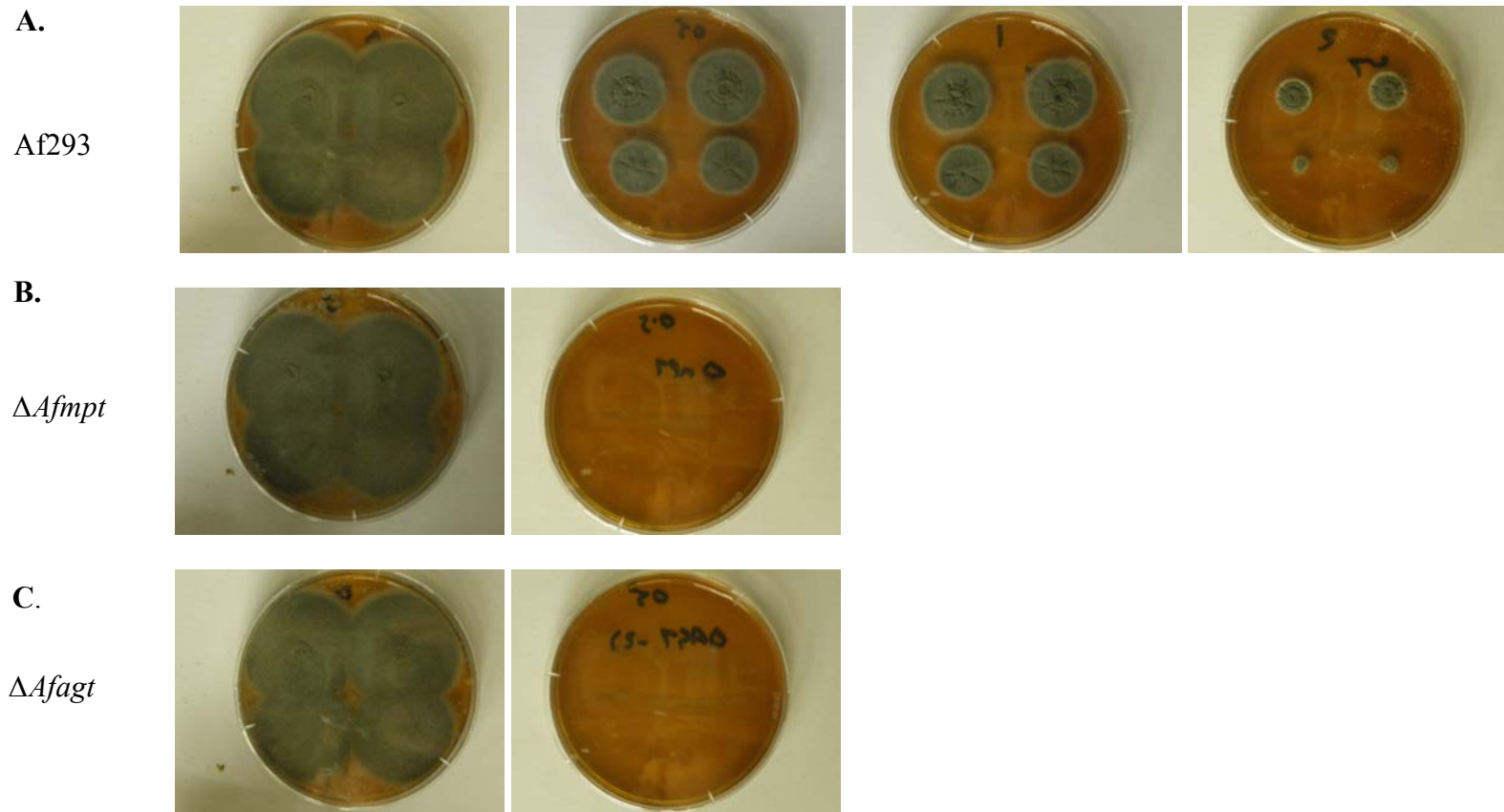


Figure 5.17a. Phenotypic analysis of *A. fumigatus* strains exposed to the DNA damaging agent MNNG. Rows A: *A. fumigatus* Af293, B: *A. fumigatus* Δmpt , C: *A. fumigatus* Δagt . Columns 1: 0 MNNG, 2: 0.5 $\mu\text{g/ml}$ MNNG, 3: 1 $\mu\text{g/ml}$ MNNG, 4: 2 $\mu\text{g/ml}$ MNNG. All plates were photographed following 72 hr incubation at 37 °C.

B.

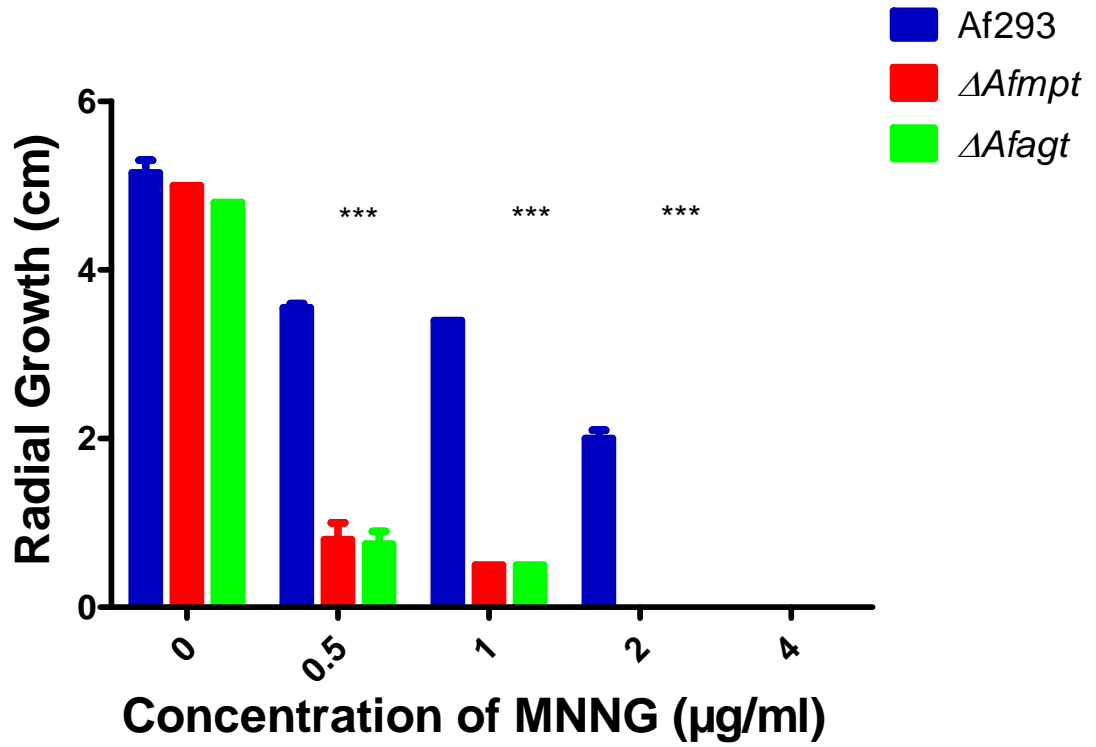


Figure 5.17b. *A. fumigatus* $\Delta Afmpt$ and $\Delta Afangt$ are extremely sensitive to MNNG exposure.

Radial growths of *A. fumigatus* strains following MNNG exposure indicates that both $\Delta Afmpt$ and $\Delta Afangt$ are more sensitive to all concentrations tested ($p < 0.001$) compared to wild-type Af293. Data represent the mean \pm standard error of three experiments.

Key: *** = $p < 0.001$.

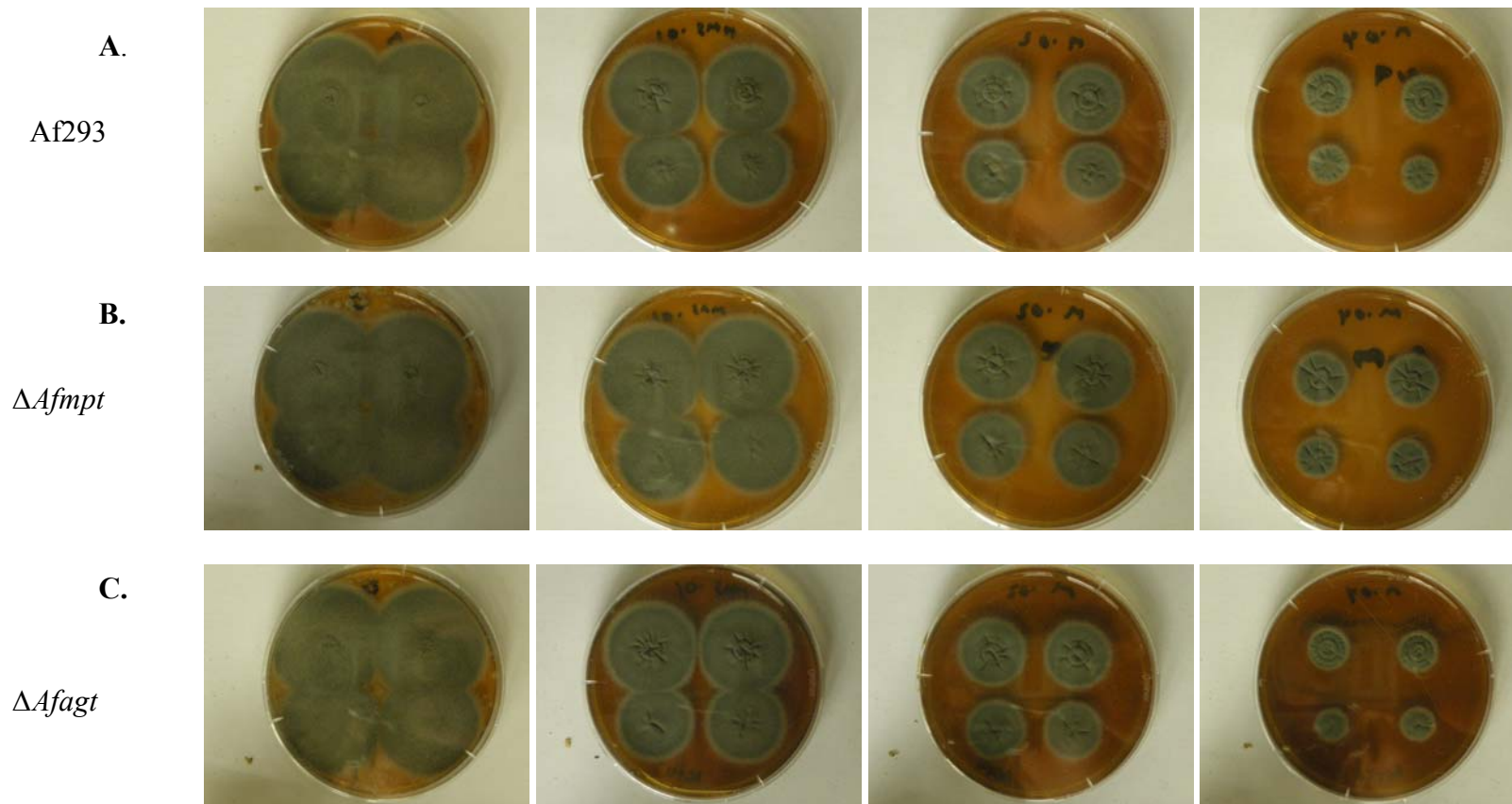


Figure 5.18. Phenotypic analysis of *A. fumigatus* strains exposed to the DNA damaging agent MMS. Rows A: *A. fumigatus* Af293, B: *A. fumigatus* Δmpt , C: *A. fumigatus* Δagt . Columns 1: 0 MMS, 2: 0.01 % (w/v) MMS, 3: 0.02 % (w/v) MMS, 4: 0.04 % (w/v) MMS. All plates were photographed following 72 hr incubation at 37 °C.

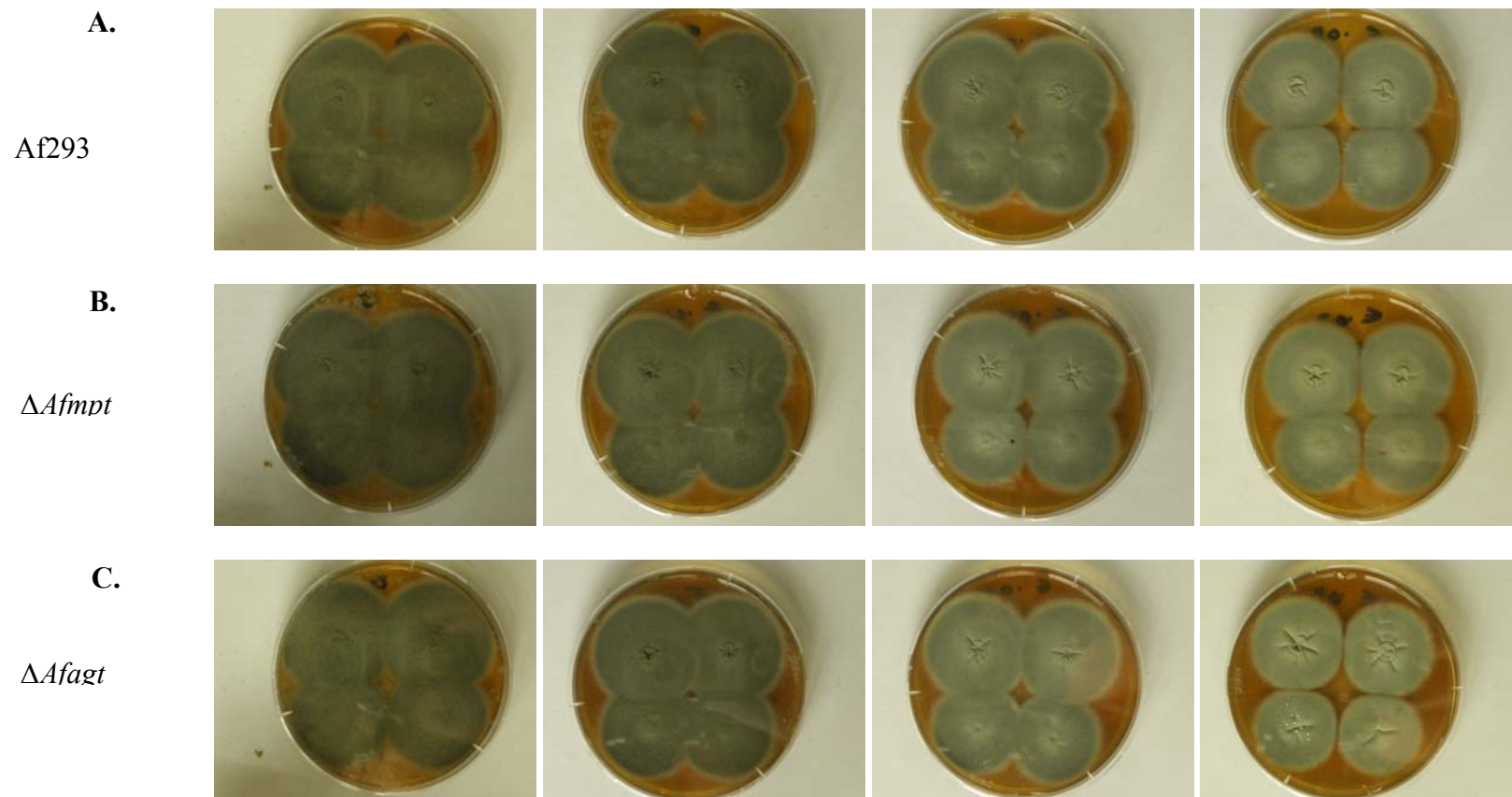


Figure 5.19. Phenotypic analysis of *A. fumigatus* strains exposed to the DNA damaging agent EMS. Rows A: *A. fumigatus* Af293, B: *A. fumigatus* $\Delta fmp1$, C: *A. fumigatus* Δagt . Columns 1: 0 EMS, 2: 0.02 % (w/v) EMS, 3: 0.04 % (w/v) EMS, 4: 0.08 % (w/v) EMS. All plates were photographed following 72 hr incubation at 37 °C.

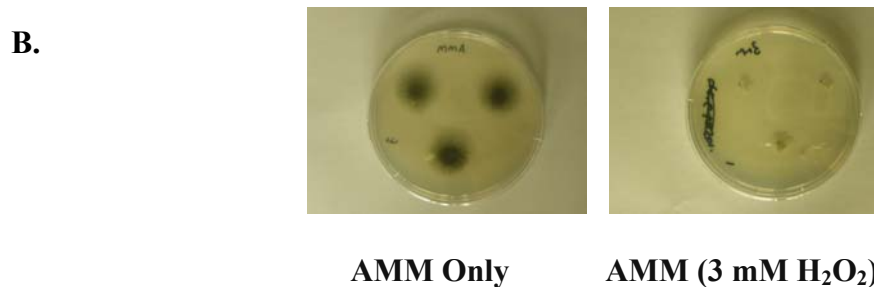
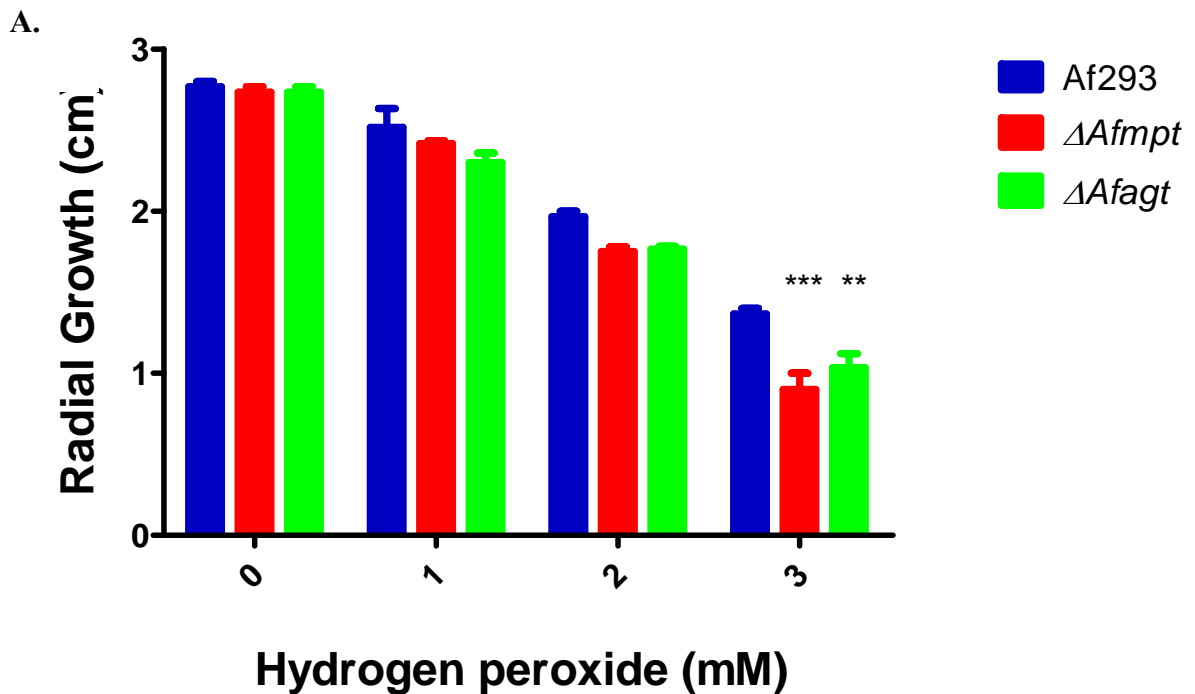


Figure 5.20. *A. fumigatus* $\Delta Afmpt$ and $\Delta Afagt$ display increased sensitivity to 3 mM Hydrogen peroxide (H₂O₂).

A. Exposure of *A. fumigatus* strains to increasing concentrations of H₂O₂. Radial growth was measured (cm) and graph depicts growth at 72 hr incubation at 37 °C. This data displays the mean radial growth from three independent experiments \pm standard error of three experiments. Key: *** = $p < 0.001$, ** = $p < 0.01$.

B. Colonies following 72 hr growth on AMM plates containing hydrogen peroxide. Bottom colony in each photo represents Af293 (wt), while $\Delta Afagt$ and $\Delta Afmpt$ are on the upper left and right portion of the plate respectively.

5.3.5. *A. fumigatus mpt* is essential for the induction of *A. fumigatus agt* in response to alkylating DNA damage.

To investigate if the loss of an adaptive response to MNNG in $\Delta Afmpt$ and increased sensitivity of both $\Delta Afmpt$ and $\Delta Afagt$ to MNNG coincided with a loss of protective gene expression of *Afmpt* and *Afagt*, RT-PCR analysis was performed on cultures which were exposed to MNNG (0.5 $\mu\text{g/ml}$). The set-up of this experiment is described earlier in this chapter, and this was repeated for both mutant strains. This gene expression analysis indicated that in $\Delta Afmpt$, loss of *Afagt* induction upon MNNG addition was apparent. Figure 5.21 displays the expression of *Afagt* in the $\Delta Afmpt$ mutant strain either with or without the addition of MNNG to growing cultures. The expression of *calm* is also shown. Similar to *calm*, *Afagt* shows almost constitutive transcript levels when cultures were un-induced or induced. This is in contrast to the pattern of *Afagt* expression observed in induced cultures wild-type Af293 (Figure 5.9). As observed for *A. fumigatus* Af293 (Figure 5.9), no changes in gene expression of *AfAlkA* or *AfAlkB* was observed in any of the strains tested with or without addition of MNNG. In addition, *Afmpt* gene expression in *A. fumigatus* $\Delta Afagt$ (Figure 5.22) shows a similar pattern to that of *A. fumigatus* Af293 (Figure 5.9). *Afmpt* expression is increased in response to MNNG addition and this elevated gene expression is maintained over the 3 hr time period observed in this study (Figure 5.22). *Afmpt* expression was absent in the $\Delta Afmpt$ strain (Figure 5.21), and *Afagt* expression was absent in the $\Delta Afagt$ strain (Figure 5.22).

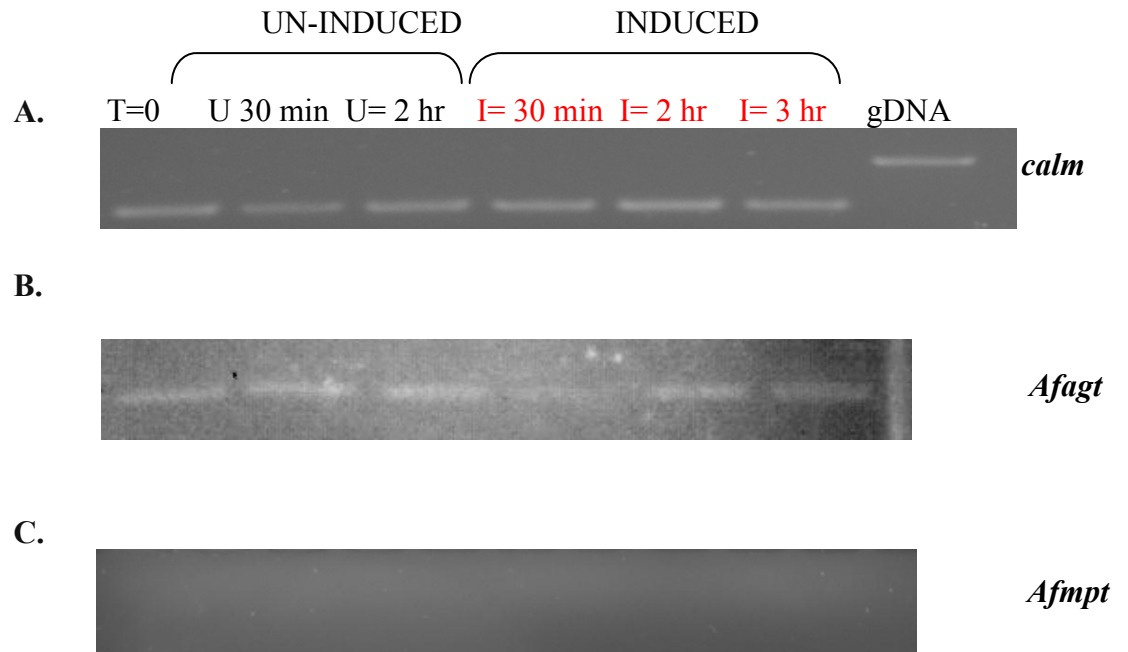


Figure 5.21. Expression of *Afagt* is not induced upon MNNG exposure in the Δmpt strain.

RT-PCR analysis of *Afagt* and *Afmpt* gene expression with or without MNNG exposure in *A. fumigatus* Δmpt .

A. Expression of the housekeeper gene *calmodulin* (*calm*).

B. *Afagt* expression.

C. *Afmpt* expression

The time points as which gene expression was examined is as follows, and these time points are relevant for A, B and C.

T = 0: RT-PCR analysis from overnight un-induced cultures.

U: Un-induced cultures: U = 30 min U = 2 hr.

I: Induced cultures: I = 30 min, I = 1 hr, I = 2 hr (post MNNG addition).

All RT-PCR products were resolved in 2 % (w/v) agarose gels.

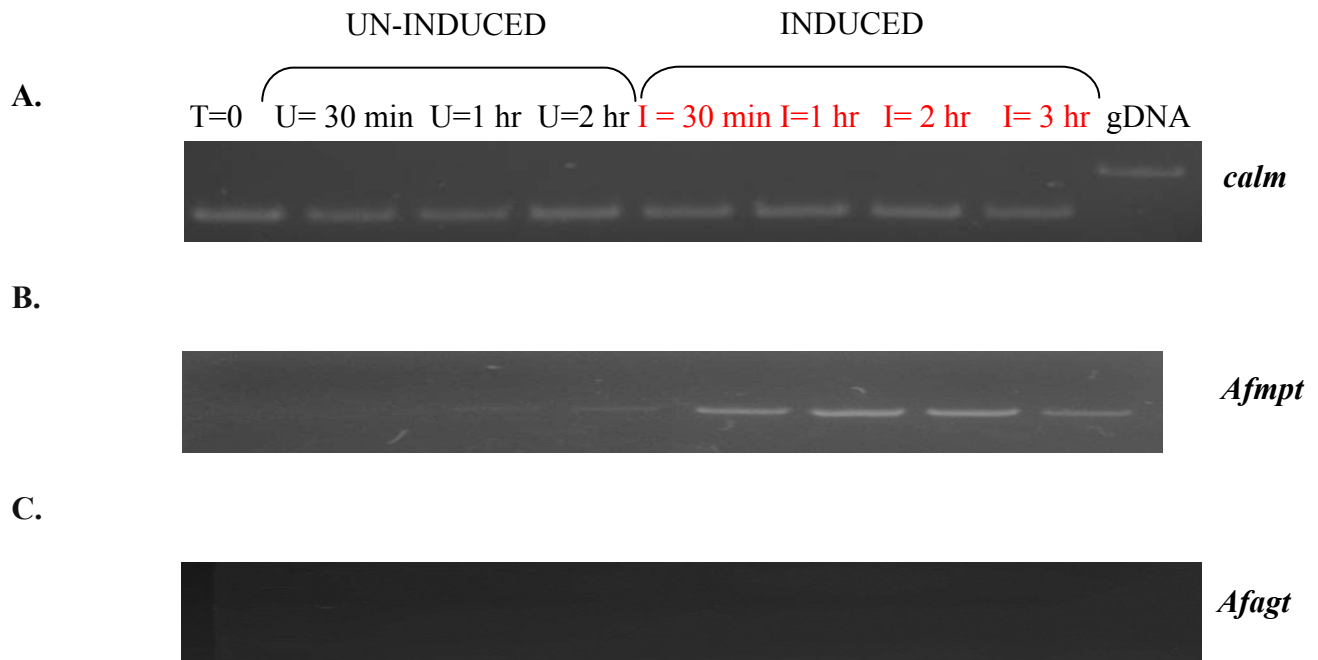


Figure 5.22. *A. fumigatus mpt* is induced upon exposure to MNNG and this is not dependant on *Afagt*.

RT-PCR analysis of *Afmpt* and *Afagt* gene expression with or without MNNG exposure in in *A. fumigatus* Δagt .

A. Expression of the housekeeper gene *calmodulin* (*calm*).

B. *Afmpt* expression.

C. *Afagt* expression.

The time points as which gene expression was examined is as follows, and these time points are relevant for A, B and C.

T = 0: RT-PCR analysis from overnight un-induced cultures.

U: Un-induced cultures: U = 30 min, U = 1 hr, U = 2 hr.

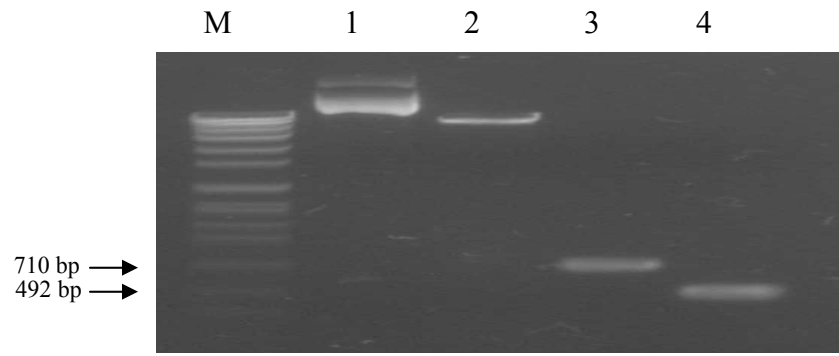
I: Induced cultures: I = 30 min, I = 1 hr, I = 2 hr, I = 3 hr (post MNNG addition).

All RT-PCR products were resolved in 2 % (w/v) agarose gels.

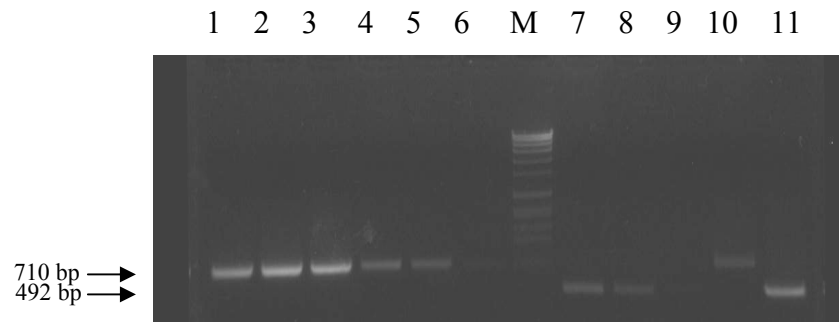
5.3.6. Cloning of AFUA_5G06350 and AFUA_2G02090 into PC210 vector for expression in *Saccharomyces cerevisiae*.

To introduce *Afmpt* (AFUA_5G06350) and *Afagt* (AFUA_2G02090) into *S. cerevisiae*, plasmids were constructed with either of the *A. fumigatus* coding regions inserted under the control of a constitutive yeast promoter. Plasmid pC210 harbours the *SSA1* coding sequence under the control of the constitutive *SSA2* promoter. The cloning strategy is described in Section 2.2.19. Colony PCR (Section 2.2.16) confirmed the presence of *Afmpt* or *Afagt* in the majority of plasmids screened (Figure 5.23). Recombinant plasmids were checked for the orientation of *Afmpt* or *Afagt* by restriction digestion with *Age1* and *Sph1* and the expected fragments for were: 4,500 bp and 2,892 bp for pC-AFUA_2G02090 and 4,500 bp and 2,892 bp for pC-AFUA_5G06350 respectively. These restriction digests are shown in Figure 5.23. This confirmed directional cloning of the *A. fumigatus* genes into pC210 vector, which resulted in pC-AFUA_5G06350 and pC-AFUA_2G02090. The pC-AFUA_5G06350 construct from colonies 1 and 3, and the pC-AFUA_2G02090 construct from colony 5 were chosen for sequencing, and the integrity of these constructs was by sequencing by commercial arrangement.

A.



B.



C.

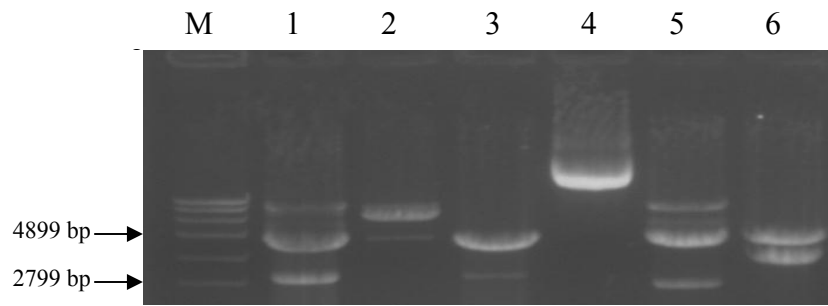


Figure 5.23. Cloning and confirmation of AFUA_5G06350 and AFUA_2G02090 into pC210.

A. Preparation of *A. fumigatus* genes and pC210 for cloning. Lane 1: Undigested pC210, Lane 2: pC210 cut with NdeI and SphI, Lane 3: AFUA_5G06350 PCR product, Lane 4: AFUA_2G02090 PCR product.

B. Colony PCR to check for presence of *A. fumigatus* genes in *E. coli* transformants. Lanes 1-6: AFUA_5G06350 amplified from *E. coli* colonies. Lanes 7-9: AFUA_2G02090 amplified from *E. coli* colonies. Lane 10: AFUA_5G06350 amplified from genomic DNA, Lane 11: gDNA control.

C. Restriction digestion to check for directional cloning of *A. fumigatus* genes into pC210. Lanes 1-3: Plasmids from *E. coli* colonies (AFUA_5G06350) 1-3. Lane 4: pC210 uncut. Lane 5-6: Plasmids from *E. coli* colonies (AFUA_2G02090).

M. Molecular weight marker (Roche VII).

5.3.7. Transformation of pC-AFUA_5G06350 and pC-AFUA_2G02090 into *S. cerevisiae*.

Directional cloning of AFUA_5G06350 or AFUA_2G02090 into pC210 resulted in two plasmids; pC-AFUA_5G06350 and pC-AFUA_2G02090 respectively. Once the generation of pC-AFUA_5G06350 and pC-AFUA_2G02090 was confirmed, these constructs were individually transformed into *S. cerevisiae* (Section 2.2.20). The *S. cerevisiae* strain used in this study was BY4741 (Table 2.4). This yeast strain has a deletion in the *MGT1* gene (analogous to the constitutive *ogt* alkylation repair gene from *E. coli*) (Sedgwick and Lindahl, 2002). Eight colonies from each transformation plate were selected, restreaked on fresh selective medium and subjected to colony PCR (Section 2.2.16) to ensure the presence of either AFUA_2G02090 or AFUA_5G06350. PCR reactions were performed using the primer pairs AFUA5G06350 PC210 F and AFUA5G06350 PC210 R or AFUA_2G02090 PC210 F and AFUA_2G02090 PC210 R. These PCR reactions should yield products sizes of approximately 700 bp and 460 bp indicating successful transformation of pC-AFUA_5G06350 and pC-AFUA_2G02090 respectively. PCR products were resolved on 1% (w/v) agarose gels (Figure 5.24). This confirmed that either pC-AFUA_5G06350 or pC-AFUA_2G02090 had been successfully transformed in all yeast colonies selected.

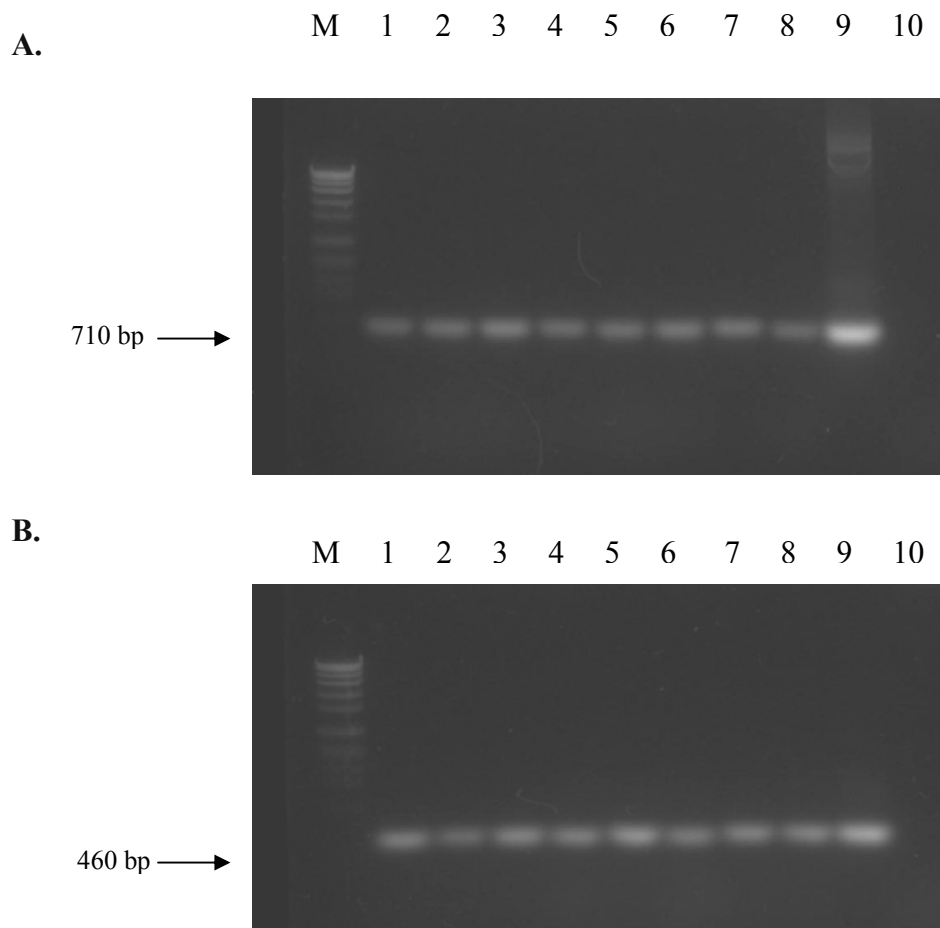


Figure 5.24. Confirmation of *S. cerevisiae* transformed with pC-AFUA_5G06350 and pC-AFUA_2G02090.

A. PCR reactions from yeast colonies transformed with pC-AFUA_5G06350. Lane 1-8: PCR reactions from transformed yeast colonies 1-8, Lane 9: genomic DNA positive control, Lane 10: *S. cerevisiae* BY4741 negative control.

B. PCR reactions from yeast colonies transformed with pC-AFUA_2G02090. Lane 1-8: PCR reactions from transformed yeast colonies 1-8, Lane 9: genomic DNA positive control, Lane 10: *S. cerevisiae* BY4741 negative control.

M. Molecular weight marker (Roche VII).

5.3.8. *Aspergillus fumigatus Afmpt* and *Afagt* are capable of complementing an *MGT1* deletion in *Saccharomyces cerevisiae*.

S. cerevisiae BY4741 strains bearing *Afmpt* or *Afagt* are referred to as Sc + *Afmpt* and Sc + *Afagt* respectively. The BY4741 YDL200c strain was also transformed with the pPRS315 vector containing the *SSA2* promoter but no downstream gene. This strain is referred to as Sc +Empty Vector and served as the control strain for yeast dot growth experiments. Dot growth assays (Section 2.2.21) were performed on these strains in the presence of increasing concentrations of MNNG in order to determine if either of the *A. fumigatus* genes could complement the yeast *MGT1* deletion. Cells were tested for growth on YPD (Section 2.1.1.23) containing MNNG at concentrations of 0, 4, 8, 16, 32 and 64 µg/ml. Growth was monitored at 2 and 3 days post incubation at 30 °C. Cells were photographed at 3 days post incubation and this is displayed in Figure 5.25. All strains displayed equal growth rates on YPD (Figure 5.25 A). Sc + *Afagt* was the only strain to display growth at all concentrations of MNNG tested (Figure 5.25 B-F). At MNNG concentrations of 4-8 µg/ml, Sc + *Afagt* displayed increased growth compared to the control and Sc + *Afmpt* strains. At 8 µg/ml MNNG, the control strain displays severely hindered growth, with no growth whatsoever from 16 µg/ml MNNG and above. At MNNG concentrations of 8 µg/ml and 16 µg/ml, Sc + *Afmpt* displays greater growth compared to the control strain (Figure 5.25 C-D).

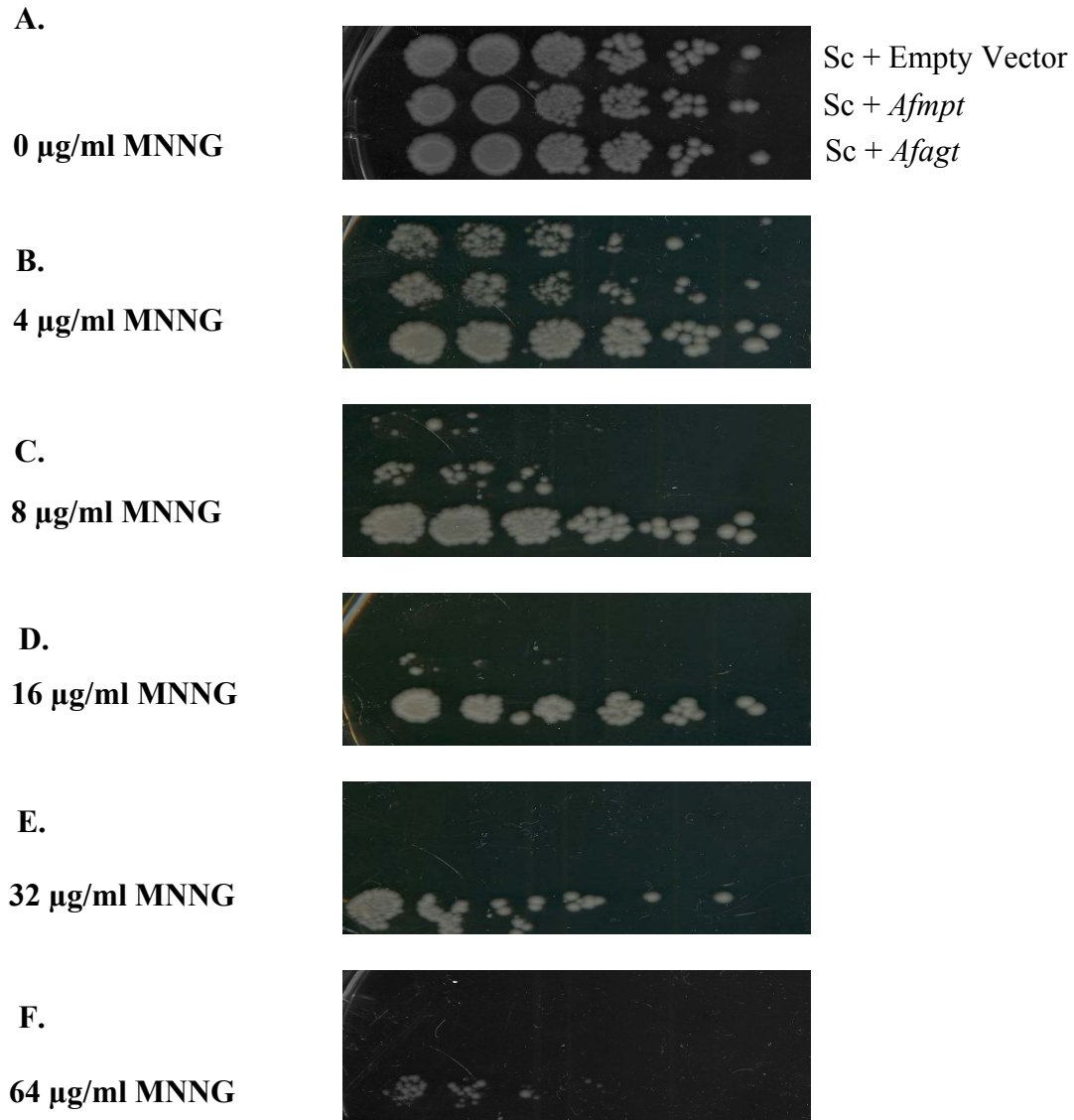


Figure 5.25. Complementation of *Saccharomyces cerevisiae* *MGT1* deletion with *A. fumigatus* adaptive response genes..

A-F: *S. cerevisiae* strains were spotted onto YPD agar plates containing increasing concentrations of the alkylating agent MNNG; A: YPD only, B: 4 $\mu\text{g/ml}$ MNNG, C: 8 $\mu\text{g/ml}$ MNNG, D: 16 $\mu\text{g/ml}$ MNNG, E: 32 $\mu\text{g/ml}$ MNNG, F: 64 $\mu\text{g/ml}$ MNNG. The order of strains from top to bottom of each panel is Sc + Empty Vector, Sc + *Afmpt* and Sc + *Afagt*.

5.4. Discussion.

The Ada protein of *E. coli* confers resistance to the biological effects of alkylating agents through its dual functions as both a transcriptional activator of the adaptive response genes (*ada*, *aidB*, *alkA* and *alkB*), and as a direct repair enzyme for the mutagenic lesions caused by alkylating agents such as N-Methyl-N'-Nitro-N-Nitrosoguanidine (MNNG) (Teo *et al.*, 1984; Nakabeppu *et al.*, 1986). Bioinformatic analysis indicated that there are homologues of *ada* in the genome of *A. fumigatus*, and two genes in particular, *Afmpt* (AFUA_5G06350) and *Afagt* (AFUA_2G02090) encode proteins which seem to correspond to the transcriptional activating domain or the methylguanine transferase domain of *E. coli* Ada respectively. Also, there were genes homologous to *E. coli* *alkB* and *alkA* in the *A. fumigatus* genome; AFUA_6G07990 (*AfalkB*) and AFUA_4G46800 (*AfalkA*), respectively. The presence of these four genes strongly suggested that an adaptive response to alkylating agents was present in *A. fumigatus*, despite no previous reports of this in the literature.

Protein sequence alignment of *A. fumigatus* AfMPT indicated a high level of sequence conservation with the N-terminal transcriptional activator domain of *E. coli* Ada, strongly indicating that AfMPT could be acting as a transcriptional activator for the adaptive response in *A. fumigatus*. Alignment of AfAGT with *E. coli* Ada indicates that AfAGT is likely to be a functional homologue of the C-terminal domain of Ada, possessing the O⁶-methylguanine and O⁴-methylthiamine methyltransferase activities. Indeed, both AfMPT and AfAGT possess the conserved cysteine residues which have been proven to be the critical sites for acceptance of the methyl groups in *E. coli* Ada. The N-terminal Ada domain accepts methyl groups from methylphosphotriesters and this is mediated by cysteine residue 38 (cys-38) (Takinowaki *et al.*, 2005), which is conserved in AfMPT. The C-terminal Ada domain accepts methyl groups from O⁶-methylguanine and O⁴-

methylthymine residues, thereby detoxifying these bases in the DNA. The critical C-terminal residue in Ada is cys-321 (Demple *et al.*, 1985), and this is also conserved in AfAGT.

It has been reported that an adaptive response exists in the closely related fungus, *Aspergillus nidulans* (Hooley *et al.*, 1988). DNA alkyltransferase activity was also observed in this fungus (Baker *et al.*, 1992; Swirski *et al.*, 1988). This activity has been shown to be highly inducible, and effective at repairing O⁶-methylguanine and O⁴-methylthymine lesions, indicative of an adaptive response present in *A. nidulans* (Baker *et al.*, 1992). However, there have not been any functional genomic studies performed to investigate what genes are responsible for this response in a filamentous fungus. Hooley and co-workers have shown an improvement in the growth of wild-type *A. nidulans* upon MNNG challenge following a pre-treatment or induction with a non-lethal dose of MNNG (Hooley *et al.*, 1988). The same approach was taken in the work presented here to investigate if an adaptive response was functional in *A. fumigatus*. In all experiments in this study, adaptation or induction of the adaptive response was mediated by culturing *A. fumigatus* strains in MNNG at a concentration of 0.5 µg/ml. Indeed, pre-treatment of *A. fumigatus* Af293 with MNNG led to a significant improvement in radial growth on subsequent exposure to MNNG (0.5-4 µg/ml) compared to un-induced cultures ($p < 0.001$). On all MNNG concentrations tested, wild-type induced cultures displayed 1.5-2 fold greater radial growth compared to un-induced controls. This clearly demonstrates a functional adaptive response to alkylating agents in *A. fumigatus*.

The adaptive response was further investigated by examining the expression levels of genes likely to be responsible for this response. The expression levels of *Afmpt*, *Afagt*, *AfalkB* and *AfalkA* was examined following addition of MNNG (0.5 µg/ml) to overnight liquid cultures. Gene expression was monitored over a three hour time period, specifically

at 30 min, 1, 2 and 3 hr following addition of MNNG as this dose was non-lethal and sufficient to induce the adaptive response on agar plates. Total RNA was extracted and reverse-transcribed to cDNA and RT-PCR was carried out for the 4 genes of interest. RT-PCR indicated that the expression levels of *Afmpt* and *Afagt* were increased upon exposure to MNNG, while no obvious change in gene expression was observed for *AfalkB* or *AfalkA*. This suggests that *Afmpt* and *Afagt* are important in the adaptive response in *A. fumigatus*. The *alkB* and *alkA* homologues could also play important roles in repair of alkylation damage but did not appear to be induced in the conditions used in this study. Induction of *Afagt* was observed at 30 min following MNNG addition and this elevated gene expression was maintained for at least 3 hr following MNNG addition. This indicates that the repair activity of *Afagt* is initiated rapidly following exposure to MNNG and that this response is persistent for several hours. *Afmpt* expression was elevated at 1 hr following addition of MNNG and this was also persistent throughout the 3 hr investigated in this work.

After confirming an adaptive response, and identifying two key genes highly induced upon exposure to MNNG, the roles of the *Afmpt* and *Afagt* encoded proteins within *A. fumigatus* were investigated further using a gene disruption approach. Both these genes were individually deleted in *A. fumigatus* Af293 (Nierman *et al.*, 2005) using a bipartite strategy and the pyrithiamine resistance marker (*ptrA*) for selection (Kubodera *et al.*, 2000; Kubodera *et al.*, 2002; Nielsen *et al.*, 2006). Single homologous integrations of *ptrA* in place of either *Afmpt* or *Afagt* were confirmed by Southern blot analysis, and abolition of corresponding gene expression was confirmed by RT-PCR. These mutant strains were termed Δ *Afmpt* and Δ *Afagt* respectively. Δ *Afmpt* was characterised for adaptation to alkylating agents, specifically MNNG, while both Δ *Afmpt* and Δ *Afagt* were characterised for sensitivity to a range of alkylating and other DNA damaging agents. Gene induction of adaptive response genes in response to MNNG was also investigated in these mutants.

When tested for an adaptive response, $\Delta Afmpt$ failed to adapt to MNNG following induction with a non-lethal dose when compared to wild-type *A. fumigatus* Af293. This was significant at all concentrations of MNNG tested ($p < 0.001$). In fact, $\Delta Afmpt$ displayed almost identical growth rate on MNNG from 0-4 $\mu\text{g/ml}$ whether or not it was induced with MNNG (0.5 $\mu\text{g/ml}$) overnight, indicating complete loss of the adaptive response when *Afmpt* was absent, and confirming that adaptation, at least to MNNG, is solely mediated by this protein within *A. fumigatus*.

Both $\Delta Afmpt$ and $\Delta Afagt$ were tested for sensitivity to a range of alkylating agents, including MNNG, Methyl methanesulfonate (MMS) and Ethyl methanesulfonate (EMS). Deletion of either *Afmpt* or *Afagt* lead to significantly increased sensitivity to MNNG (0.5-2 $\mu\text{g/ml}$) when compared to wild-type ($p < 0.001$). No growth was observed for any strain at 4 $\mu\text{g/ml}$ indicating that the concentration range chosen was adequate for illustrating differences between the mutant strains. No differences were observed between wild-type, $\Delta Afmpt$ or $\Delta Afagt$ regarding sensitivity to MMS or EMS, indicating that AfMPT or AfAGT are most likely not involved in protection against or repair of the specific lesions caused by these alkylating agents. The equal reduction in growth rate of all strains when tested on increasing MMS concentrations indicates that the range of MMS concentrations used (0.01 – 0.04 %) was a useful range to detect any differences in the mutant strains compared to wild-type. Other agents were also tested which are known to caused DNA damage or oxidative stress. Phleomycin, which is known to cause DNA breakages (Sleigh, 1976; Sleigh & Grigg, 1976), was tested, and no difference was observed between wild-type and either mutant. Sensitivity to hydrogen peroxide (H_2O_2) was also tested. For the most part, wild-type and both mutants displayed similar growth rates on H_2O_2 . *A. fumigatus* $\Delta Afmpt$ and $\Delta Afagt$, however, displayed a reduced growth rate on the highest concentration (3 mM) of H_2O_2 tested, when compared to wild-type ($p < 0.01$). This result was not investigated

further but it was an interesting observation. One possible explanation is that the mutant strains have a slightly reduced fitness, which is undetected in our study, but which is amplified in the presence of H₂O₂. Of course, it cannot be ruled out that there is a link between the oxidative stress response and the adaptive response to alkylating damage in *A. fumigatus*. Overall, these phenotypic analyses indicate that the roles of *Afmpt* and *Afagt* are specific in the response to and protection against specific alkylation lesions caused by MNNG, of which the main lesion is O⁶-methylguanine.

RT-PCR analysis was performed to determine gene expression of *Afmpt*, *Afagt*, *AfalkB* and *AfalkA* in *A. fumigatus* Δ *Afmpt* and Δ *Afagt* upon addition of MNNG as described previously for wild-type gene expression analysis. As expected, no change in *AfalkB* or *AfalkA* expression was observed in either mutant strain, once again indicating that these genes are not affected following MNNG addition. This result was expected since examination of the upstream non-coding regions (300 bp approximately) of either *AfalkA* or *AfalkB* did not reveal any potential Ada-promoter binding sites. While *Afagt* expression was evident in *A. fumigatus* Δ *Afmpt*, there was no difference in the level of expression between un-induced and induced conditions, indicating loss of *Afagt* induction upon MNNG addition in the Δ *Afmpt* mutant strain. This result is indicating that *Afmpt* is essential for the elevated transcription of *Afagt* upon exposure to MNNG in *A. fumigatus*, providing solid support for its role as the fungal equivalent of the *E. coli* Ada transcriptional activator of the adaptive response (Teo *et al.*, 1984). Complete absence of *Afagt* or *Afmpt* expression was observed in Δ *Afagt* or Δ *Afmpt*, under both un-inducing and inducing conditions, which supports the gene disruption strategy used in this study. As expected, the expression level of *Afmpt* was markedly increased in the Δ *Afagt* strain under inducing conditions and this increased expression was maintained throughout the 3 hr time period examined in this study. Once again, this indicates the importance of *Afmpt* gene expression upon exposure to

MNNG, and it also indicates that *Afmpt* expression in response to MNNG is not dependent on the presence of *Afagt*. At this point, it cannot be excluded that *Afmpt* could be affecting the transcription of other gene targets when *Afagt* is deleted. However, the severely increased sensitivity towards MNNG in *A. fumigatus* $\Delta Afagt$ discussed earlier unarguably proves that *Afagt* is essential for repair of DNA lesions caused by MNNG. *AfMPT* expression levels could be elevated in $\Delta Afagt$ in an attempt to repair the damage caused by MNNG. Overall, the gene expression analysis undertaken in this study has yielded the following: *Afmpt* and *Afagt* are induced upon exposure to MNNG, the induction of *Afagt* is lost when *Afmpt* is deleted, proving that *Afmpt* is transcriptionally activating the adaptive response in *A. fumigatus*. Despite the reported roles of *AlkA* and *AlkB* in the adaptive response in *E. coli*, these genes do not seem to be involved in the adaptive response in *A. fumigatus*, at least to MNNG. Expression of these genes in response to other alkylating agents (e.g. MMS or EMS) was not examined in this study. However, plate assay analysis of MMS and EMS indicated that deletion of *Afmpt* had no adverse effect towards these agents. If *AfalkA* or *AfalkB* are somehow involved in response to these agents, they do not appear to be transcriptionally regulated by *Afmpt*, as observed in *E. coli* (Sedgwick & Lindahl, 2002).

This work also investigated whether each of the *A. fumigatus* alkylation repair genes could complement a yeast *MGT1* deletion. As mentioned earlier in this chapter, *MGT1* is a gene which encodes an O⁶-alkylguanine DNA alkyltransferase in *S. cerevisiae* (Xiao *et al.*, 1991) (Sassanfar and Samson, 1990). The *MGT1* gene is constitutively expressed, and is not up-regulated in response to exposure to alkylating agents, in agreement with the lack of an adaptive response in *S. cerevisiae* (Xiao *et al.*, 1991). Protein blast searching of the *A. fumigatus* genome at CADRE using the *S. cerevisiae* *MGT1* protein sequence as a query revealed that the top hit in the *A. fumigatus* is the *AfAGT* protein, and that these two

proteins share 41 % sequence identity. Yeast dot growth assays indicated that *Afagt* confers resistance to MNNG in a yeast *MGT1* deletion strain. Assays were performed using MNNG concentrations between 4 – 64 µg/ml, and a yeast strain expressing *Afagt* (Sc + *Afagt*) exhibited increased resistance to MNNG compared to an empty vector control at all MNNG concentrations. The empty vector control failed to grow at concentrations greater than 8 µg/ml MNNG, while Sc + *Afagt* grew at all MNNG concentrations tested. These findings confirm that *Afagt* is capable of complementing the yeast *MGT1* deletion, and confirms that these two proteins are functionally related in agreement with the sequence similarity observed through Blast analysis. Interestingly, this work also revealed that *Afmpt* can also confer resistance to MNNG when transformed into the *MGT1* deletion strain. The increased resistance to MNNG observed in this strain is intermediate between the Sc + *Afagt* and the empty vector control strains, and is evident at MNNG concentrations up to 16 µg/ml. This is an interesting observation as *S. cerevisiae* is reported not to possess an adaptive response to alkylating agents (Polakowska *et al.*, 1986). Furthermore, no homologues of *Afmpt* were identified in *S. cerevisiae* through Blast searching at NCBI. It is not possible to say exactly how this increased resistance is mediated by *Afmpt*, but the results imply that AfMPT can repair MNNG-induced alkylation damage to some extent, perhaps transfer of methyl onto cys-38 of *Afmpt* might be sufficient to repair some of the alkylation damage, leading to slightly enhanced growth observed for Sc + *Afmpt*. Another possible explanation is that there may be some *S. cerevisiae* genes with an *ada* promoter binding site, or similar sites, which are adequate for the binding of *Afmpt* when this gene is transformed into the yeast strain (Sc + *Afmpt*). Some of these genes may be involved in protection against DNA alkylation damage, and could be transcriptionally activated by the AfMPT protein to confer the increased resistance to MNNG that is observed in this strain. Further investigation into this would require extensive bioinformatic analysis as a starting point, followed by whole-

genome transcriptional analysis, which was beyond the scope of this study. Nevertheless, the yeast experiments undertaken here do confirm the important role of the *Afagt* in DNA alkylation repair, and the complementation of the yeast *MGT1* deletion by the *Afagt* supports undoubtedly that the phenotypes observed in the *A. fumigatus* Δagt strain are specifically due to the deletion of *Afagt*.

In conclusion, this work provides the first evidence of an adaptive response to alkylating DNA damage in the opportunistic pathogen *A. fumigatus*. The key components of this adaptive response have been identified through homology searching with *E. coli* adaptive response genes, and investigated further using a targeted gene deletion strategy. The adaptive response appears to be very similar to the adaptive response which has been well documented in *E. coli*. The *A. fumigatus* adaptive response has been characterised genetically and phenotypically in this study. Previous work reported an adaptive response to MNNG, in *A. nidulans*, however, there are no further reports of this in *A. nidulans*. The findings reported here represent the first molecular characterisation of an adaptive response to alkylating agents in a eukaryotic organism. Lack of an equivalent adaptive response pathway in mammalian systems makes this pathway an interesting topic for further characterisation, as it could prove to be an interesting drug target.

This work describes the functional characterisation of two NRP synthetases; Pes3 and PesL, within the important human pathogen *A. fumigatus*. An adaptive response towards alkylating DNA damage in *A. fumigatus* was also characterised, representing the first functional characterisation of this pathway in a eukaryotic organism.

pes3 (25 kb in size) is the largest gene in *A. fumigatus*, encoding a multi-modular NRP synthetase, and represents a gene unique to *A. fumigatus*. Pes3 contains 6 adenylation domains, and is therefore predicted to encode a peptide with 6 amino acid residues, however, the non-traditional domain architecture of Pes3 has led to suggestions that it may produce a complex final product (Cramer *et al.*, 2006b). Pes3 does not appear to encode a secreted secondary metabolite, and we hypothesise that the Pes3-encoded peptide plays a structural role within *A. fumigatus*. Support for this hypothesis comes from several observations, as discussed in Chapter 3. In summary, *A. fumigatus* $\Delta pes3$ exhibits hypervirulence compared to wild-type in both murine ($p = 0.02$) and insect models ($p < 0.001$) of IA, coinciding with increased fungal burden in murine lungs *in vivo*, and reduced cytokine production by murine macrophages upon exposure to $\Delta pes3$ *in vitro*, indicating reduced immune recognition of *A. fumigatus* $\Delta pes3$. This is likely due to an alteration at the cell wall surface, resulting in a modified pathogen associated molecular pattern, and reduced immune recognition. Further support for a structural role for the Pes3 peptide comes from our observation that *pes3* protects *A. fumigatus* against voriconazole toxicity, as deduced from the reduced growth of *A. fumigatus* $\Delta pes3$ compared to wild-type ($p < 0.001$). An earlier observation that *pes3* expression was most abundant in ungerminated spores of *A. fumigatus* (Cramer *et al.*, 2006b) hinted that *pes3* may be involved in germination or cell wall structure in *A. fumigatus*.

There has been one other report in the literature describing a fungal NRP synthetase gene which is likely to encode an NRP with a structural role. An NRP synthetase gene, *AbNPS2* in the plant pathogen *Alternaria brassicola*, was identified, and encodes a large multi-modular NRP synthetase containing 4 adenylation domains, 6 thiolation (PCP) domains, 6 condensation domains, and 3 epimerisation domains (Kim *et al.*, 2007). Deletion of *AbNPS2* resulted in several altered phenotypes in the resultant mutant; reduced virulence on cabbage leaves, lower conidial germination rates, reduced hydrophobicity of conidia, and an altered conidial surface. The conidial surface in the wild-type was smooth and had a compact cell wall whereas the surface of *AbNPS2* mutant conidia was fluffy and the cell wall layers were separated, discernable by TEM (Kim *et al.*, 2007). The authors hypothesised that the *AbNPS2*-encoded NRP may be a component of, or facilitates linkage of, the outermost layer and the middle layer of the fungal conidial cell wall, a hypothesis that is similar to the suggestions made for the *Pes3*-encoded NRP in Chapter 3; *Pes3* may encode a peptide which is involved in removal of the rodlet layer from the surface of *A. fumigatus* conidia, or in linking the rodlet layer to the conidial cell wall. The exact nature of *AbNPS2* and the encoded NRP remains to be elucidated (Kim *et al.*, 2007), highlighting the challenge that exists for relating NRP synthetases to their respective NRP product. Future experiments will include hydrophobicity analyses of *A. fumigatus* wild-type and $\Delta pes3$, and SEM and/or TEM to investigate if differences at the conidial cell wall can be seen between *A. fumigatus* wild-type and $\Delta pes3$.

pesL, encoding a mono-modular NRP synthetase in *A. fumigatus*, was found to protect *A. fumigatus* against H₂O₂-mediated oxidative stress ($p < 0.01$) and voriconazole toxicity ($p < 0.01$). Comparative metabolite profiling revealed that *PesL* is essential for fumigaclavine C biosynthesis in *A. fumigatus*, as deletion of *pesL* (*A. fumigatus* $\Delta pesL$)

resulted in the complete loss of fumigaclavine C from *A. fumigatus* $\Delta pesL$ metabolite extracts. We propose that PesL anchors or tethers fumigaclavine A to facilitate reverse prenylation by FgaPT1 (Unsold and Li, 2006).

The absolute requirement for a mono-modular NRP synthetase, such as PesL, for the biosynthesis of fumigaclavine C in *A. fumigatus* suggests that similar roles might be played by NRP synthetases in other complex biosynthetic pathways, whereby NRP synthetase modules tether biosynthetic intermediates, facilitating subsequent modification by down-stream acting enzymes. Functional characterisation of NRP synthetases by gene deletion studies is required in order to investigate this. PesL has recently been implicated in fumiquinazoline biosynthesis (Ames et al., 2010), and the observed role for PesL in fumigaclavine C biosynthesis reported here suggests redundant roles for PesL. It remains to be seen whether this is a feature of the remainder of the uncharacterised NRP synthetases within *A. fumigatus* and other fungi. This is supported by observations that NRP synthetases shows less strict substrate selection and incorporation than other adenylating enzymes as mentioned previously (Stachelhaus *et al.*, 1999).

A. fumigatus $\Delta pesL$ exhibited reduced virulence compared to wild-type in the *G. mellonella* infection model ($p < 0.001$), indicating an important role for EA in the pathogenesis and virulence of *A. fumigatus*, a finding which is in agreement with the long standing association of EA with human infection (Panaccione & Coyle, 2005), and which suggests that EA may be a suitable drug target in *A. fumigatus*, and other EA producing fungi. Furthermore, the work presented here indicates a link between the production of EA metabolites and protection against oxidative stress; links between fungal secondary metabolite production and oxidative stress have attracted attention in recent reviews (Reverberi *et al.*, 2010).

The availability of the complete genome sequence of *A. fumigatus* (Nierman *et al.*, 2005) allows the identification of genes, which might be involved in previously uncharacterised pathways, through Blast searching against other sequenced genomes. This approach led to the identification of genes within the *A. fumigatus* genome which are homologous to genes known to mediate an adaptive response to alkylating DNA damage in *E. coli* (Sedgwick & Vaughan, 1991; Sedgwick & Lindahl, 2002) and other bacteria. This work reports the presence of two key genes which were found to mediate an adaptive response towards alkylating DNA damage in *A. fumigatus*; a methylphosphotransferase (*Afmpt*), and an alkylguaninetransferase (*Afagt*) which are homologous to the N- and C-terminal domains of *E. coli* Ada protein respectively. Both were found to be inducible by exposure to MNNG in this study. Targeted gene deletions of *Afmpt* and *Afagt* followed by extensive phenotypic analysis confirmed that these genes are responsible for the adaptive response, and expression analysis confirmed that the presence of *Afmpt* is essential for the induction of *Afagt* upon exposure to the alkylating agent MNNG, a finding that is paralleled with earlier findings in *E. coli* (Teo *et al.*, 1984), and implying that *Afmpt* is a transcriptional regulator for the adaptive response in *A. fumigatus*. Furthermore, introduction of *Afmpt* or *Afagt* into an *S. cerevisiae* strain deleted for a constitutive O⁶-alkylguanine DNA alkyltransferase (MGT1) (Xiao *et al.*, 1991) (Sassanfar and Samson, 1990), led to an increased growth of *S. cerevisiae* following exposure to MNNG compared to empty vector controls, proving the function of these genes in *A. fumigatus*.

Prior to this work, other workers observed an improved growth response of *A. nidulans* in the presence of MNNG following pre-exposure with a sub-lethal dose of MNNG (Hooley *et al.*, 1988), and DNA alkyltransferase activity was also detected, suggesting a repair mechanism towards alkylating DNA damage (Swirski *et al.*, 1988). However, no functional characterisation of this response was undertaken, and an adaptive

response to alkylating agents such as the *E. coli* response had not been described in a eukaryotic organism to date. The identification of key genes involved in the adaptive response, coupled with the lack of a corresponding adaptive response in mammalian cells highlights the potential of this response as a novel drug target for the treatment of *Aspergillus*-related infection.

Overall, the findings presented in this thesis raise many interesting issues. This work showed that an NRP synthetase, PesL is essential for fumigaclavine C biosynthesis, while another group have shown that a recombinant PesL can activate L-alanine to catalyse fumiquinazoline F biosynthesis *in vitro* (Ames *et al.*, 2010). This suggests that PesL might exhibit relaxed substrate specificity, with the ability to activate alanine for fumiquinazoline biosynthesis (Ames *et al.*, 2010), and the apparent tethering of fumigaclavine A by an unknown mechanism. Also, it suggests that PesL may be active in more than one biosynthetic pathway in *A. fumigatus*. The findings also actually indicate that fumiquinazoline A may have more than one biosynthetic route in *A. fumigatus*. Returning to an earlier point; secondary metabolite gene cluster rearrangements mediated by transposable elements might be a phenomenon not restricted to the EA clusters. This could allow for evolution of secondary metabolite gene clusters, and might allow NRP synthetases to be used by more than one biosynthetic pathway, thereby increasing the diversity of secondary metabolites that can be produced by an organism. This hypothesis could aid in explaining how such a large repertoire of secondary metabolites can arise from 14 NRP synthetases in *A. fumigatus*.

Current understanding of NRP synthetases and secondary metabolite gene clusters might need to be reconsidered in light of the findings and ideas presented here, and the

current paradigm may not be as straightforward as one NRP synthetase – one peptide as has previously been found for NRPS in other pathways, (e.g. gliotoxin biosynthesis) (Balibar & Walsh, 2006; Cramer *et al.*, 2006a). The notion of cluster cross-talk is beginning to emerge with the confirmation of cross-talk between two separate NRP synthetases involved in siderophore biosynthesis in a bacterial species (Lazos *et al.*, 2010). More recently, cross-talk was identified between two SM clusters on different chromosomes in *A. nidulans* (Bergmann *et al.*, 2010). Importantly, the study presented here highlights that gene knockout is the most appropriate means to unambiguously show an essential biosynthetic function for any given gene. The role of non-cluster encoded NRP synthetases (e.g. PesL) in *A. fumigatus* EA biosynthesis suggests that secondary metabolite pathways in general might involve clustered genes as well as non-clustered genes in biosynthesis. This may have implications for partially characterised SM gene clusters to date, or in situations where it has been difficult to conceptualise a biosynthetic pathway based on the genes proposed to be in the biosynthetic cluster.

Furthermore, despite advances in the field of secondary metabolite biosynthesis, there still remains a large deficit relating NRP synthetases to peptide products in the important human pathogen *A. fumigatus*, an observation previously noted by others (Cramer *et al.*, 2006b; Stack *et al.*, 2007). This work has contributed to the list of characterised NRP synthetase genes in *A. fumigatus*, and brings the number to 7 out of a total of 14. Evidence for NRP synthetase redundancy (PesL) and a possible structural NRP (Pes3) implies that the biosynthetic and functional potential for NRP synthetases is greater than previously thought. As more NRP synthetases are functionally characterised one can predict that this potential will become even more apparent.

- Adams, T. H., Boylan, M. T. & Timberlake, W. E. (1988).** BrIA Is Necessary And Sufficient To Direct Conidiophore Development In *Aspergillus nidulans*. *Cell* **54**, 353-362.
- Aguirre, J. (1993).** Spatial And Temporal Controls Of The *Aspergillus* BrIA Developmental Regulatory Gene. *Molecular Microbiology* **8**, 211-218.
- Aimanianda, V., J. Bayry, S. Bozza, O. Kniemeyer, K. Perruccio, S. R. Elluru, C. Clavaud, S. Paris, A. A. Brakhage, S. V. Kaveri, L. Romani, and J. P. Latge. (2009).** Surface Hydrophobin Prevents Immune Recognition Of Airborne Fungal Spores. *Nature* **460**, 1117-U1179.
- Aimanianda, V. & Latge, J. P. (2010).** Problems And Hopes In The Development Of Drugs Targeting The Fungal Cell Wall. *Expert Review Of Anti-Infective Therapy* **8**, 359-364.
- Akira, S. & Takeda, K. (2004).** Toll-Like Receptor Signalling. *Nature Reviews Immunology* **4**, 499-511.
- Al-Bader, N., G. Vanier, H. Liu, F. N. Gravelat, M. Urb, C. M. Q. Hoareau, P. Campoli, J. Chabot, S. G. Filler, and D. C. Sheppard. (2010).** Role Of Trehalose Biosynthesis In *Aspergillus fumigatus* Development, Stress Response, And Virulence. *Infection And Immunity* **78**, 3007-3018.
- Albrecht, D., Guthke, R., Brakhage, A. A. & Kniemeyer, O. (2010).** Integrative Analysis Of The Heat Shock Response In *Aspergillus fumigatus*. *Bmc Genomics* **11**, 17.
- Allen, M. J., Voelker, D. R. & Mason, R. J. (2001).** Interactions Of Surfactant Proteins A And D With *Saccharomyces cerevisiae* and *Aspergillus fumigatus*. *Infection And Immunity* **69**, 2037-2044.
- Almyroudis, N. G., Holland, S. M. & Segal, B. H. (2005).** Invasive Aspergillosis In Primary Immunodeficiencies. *Medical Mycology* **43**, S247-S259.
- Altschul, S. F., Madden, T. L., Schaffer, A. A., Zhang, J. H., Zhang, Z., Miller, W. & Lipman, D. J. (1997).** Gapped Blast And Psi-Blast: A New Generation Of Protein Database Search Programs. *Nucleic Acids Research* **25**, 3389-3402.
- Ames, B. D., Liu, X. & Walsh, C. T. (2010).** Enzymatic Processing Of Fumiquinazoline F: A Tandem Oxidative-Acylation Strategy For The Generation Of Multicyclic Scaffolds In Fungal Indole Alkaloid Biosynthesis. *Biochemistry*.
- Ames, B. D. & Walsh, C. T. (2010).** Anthranilate-Activating Modules From Fungal Nonribosomal Peptide Assembly Lines. *Biochemistry* **49**, 3351-3365.
- Amitani, R., Taylor, G., Elezis, E. N., Llewellynjones, C., Mitchell, J., Kuze, F., Cole, P. J. & Wilson, R. (1995).** Purification And Characterization Of Factors Produced By

Aspergillus fumigatus Which Affect Human Ciliated Respiratory Epithelium. *Infection And Immunity* **63**, 3266-3271.

Anderson, K. V., Bokla, L. & Nussleinvolhard, C. (1985a). Establishment Of Dorsal-Ventral Polarity In The *Drosophila* Embryo - The Induction Of Polarity By The Toll Gene-Product. *Cell* **42**, 791-798.

Anderson, K. V., Jurgens, G. & Nussleinvolhard, C. (1985b). Establishment Of Dorsal-Ventral Polarity In The *Drosophila* Embryo - Genetic-Studies On The Role Of The Toll Gene-Product. *Cell* **42**, 779-789.

Aratani, Y., Kura, F., Watanabe, H., Akagawa, H., Takano, Y., Suzuki, K., Dinauer, M. C., Maeda, N. & Koyama, H. (2002). Relative Contributions Of Myeloperoxidase And NADPH-Oxidase To The Early Host Defense Against Pulmonary Infections With *Candida albicans* And *Aspergillus fumigatus*. *Medical Mycology* **40**, 557-563.

Araujo, R. & Rodrigues, A. G. (2004). Variability Of Germinative Potential Among Pathogenic Species Of *Aspergillus*. *Journal Of Clinical Microbiology* **42**, 4335-4337.

Ariizumi, K., G. L. Shen, S. Shikano, S. Xu, R. Ritter, T. Kumamoto, D. Edelbaum, A. Morita, P. R. Bergstresser, and A. Takashima. (2000). Identification Of A Novel, Dendritic Cell-Associated Molecule, Dectin-1, By Subtractive cDNA Cloning. *Journal Of Biological Chemistry* **275**, 20157-20167.

Arruda, L. K., Mann, B. J. & Chapman, M. D. (1992). Selective Expression Of A Major Allergen And Cytotoxin, Asp F-I, In *Aspergillus fumigatus* - Implications For The Immunopathogenesis Of *Aspergillus*-Related Diseases. *Journal Of Immunology* **149**, 3354-3359.

Baginski, M. & Czub, J. (2009). Amphotericin B And Its New Derivatives - Mode Of Action. *Current Drug Metabolism* **10**, 459-469.

Baker, L. J., Dorocke, J. A., Harris, R. A. & Timm, D. E. (2001). The Crystal Structure Of Yeast Thiamin Pyrophosphokinase. *Structure* **9**, 539-546.

Baker, S. M., Margison, G. P. & Strike, P. (1992). Inducible Alkyltransferase DNA-Repair Proteins In The Filamentous Fungus *Aspergillus nidulans*. *Nucleic Acids Research* **20**, 645-651.

Balibar, C. J. & Walsh, C. T. (2006). GliP, A Multimodular Nonribosomal Peptide Synthetase In *Aspergillus fumigatus*, Makes The Diketopiperazine Scaffold Of Gliotoxin. *Biochemistry* **45**, 15029-15038.

Balloy, V., Huerre, M., Latge, J. P. & Chignard, M. (2005). Differences In Patterns Of Infection And Inflammation For Corticosteroid Treatment And Chemotherapy In Experimental Invasive Pulmonary Aspergillosis. *Infection And Immunity* **73**, 494-503.

Balloy, V. & Chignard, M. (2009). The Innate Immune Response To *Aspergillus fumigatus*. *Microbes And Infection* **11**, 919-927.

- Banerjee, B., Kurup, V. P., Greenberger, P. A., Hoffman, D. R., Nair, D. S. & Fink, J. N. (1997).** Purification Of A Major Allergen, Asp F 2 Binding To Ige In Allergic Bronchopulmonary Aspergillosis, From Culture Filtrate Of *Aspergillus fumigatus*. *Journal Of Allergy And Clinical Immunology* **99**, 821-827.
- Bayram, O., S. Krappmann, M. Ni, J. W. Bok, K. Helmstaedt, O. Valerius, S. Braus-Stromeyer, N. J. Kwon, N. P. Keller, J. H. Yu, and G. H. Braus. (2008).** VelB/VeA/LaeA Complex Coordinates Light Signal With Fungal Development And Secondary Metabolism. *Science* **320**, 1504-1506.
- Beauvais, A., Drake, R., Ng, K., Diaquin, M. & Latge, J. P. (1993).** Characterization Of The 1,3-Beta-Glucan Synthase Of *Aspergillus fumigatus*. *Journal Of General Microbiology* **139**, 3071-3078.
- Beauvais, A., Monod, M., Debeaupuis, J. P., Diaquin, M., Kobayashi, H. & Latge, J. P. (1997).** Biochemical And Antigenic Characterization Of A New Dipeptidyl-Peptidase Isolated From *Aspergillus fumigatus*. *Journal Of Biological Chemistry* **272**, 6238-6244.
- Beauvais, A. & Latge, J. P. (2001).** Membrane And Cell Wall Targets In *Aspergillus fumigatus*. *Drug Resistance Updates* **4**, 38-49.
- Beauvais, A., Maubon, D., Park, S., Morelle, W., Tanguy, A., Huerre, M., Perlin, D. S. & Latge, J. P. (2005).** Two Alpha(1-3) Glucan Synthases With Different Functions In *Aspergillus fumigatus*. *Applied And Environmental Microbiology* **71**, 1531-1538.
- Beever, R. E. & Dempsey, G. P. (1978).** Function Of Rodlets On Surface Of Fungal Spores. *Nature* **272**, 608-610.
- Behnsen, J., Lessing, F., Schindler, S., Wartenberg, D., Jacobsen, I. D., Thoen, M., Zipfel, P. F. & Brakhage, A. A. (2010).** Secreted *Aspergillus fumigatus* Protease Alp1 Degrades Human Complement Proteins C3, C4, And C5. *Infection And Immunity* **78**, 3585-3594.
- Ben-Ami, R., Lewis, R. E. & Kontoyiannis, D. P. (2010).** Enemy Of The (Immunosuppressed) State: An Update On The Pathogenesis Of *Aspergillus fumigatus* Infection. *British Journal Of Haematology* **150**, 406-417.
- Berdal, K. G., Bjoras, M., Bjelland, S. & Seeberg, E. (1990).** Cloning And Expression In *Escherichia coli* Of A Gene For An Alkylbase DNA Glycosylase From *Saccharomyces cerevisiae* - A Homolog To The Bacterial *AlkA* Gene. *Embo Journal* **9**, 4563-4568.
- Bergin, D., Reeves, E. P., Renwick, J., Wientjes, F. B. & Kavanagh, K. (2005).** Superoxide Production In *Galleria mellonella* Hemocytes: Identification Of Proteins Homologous To The NADPH Oxidase Complex Of Human Neutrophils. *Infection And Immunity* **73**, 4161-4170.

- Bergmann, A., Hartmann, T., Cairns, T., Bignell, E. M. & Krappmann, S. (2009).** A Regulator Of *Aspergillus fumigatus* Extracellular Proteolytic Activity Is Dispensable For Virulence. *Infection And Immunity* **77**, 4041-4050.
- Bergmann, S., Funk, A. N., Scherlach, K., Schroeckh, V., Shelest, E., Horn, U., Hertweck, C. & Brakhage, A. A. (2010).** Activation Of A Silent Fungal Polyketide Biosynthesis Pathway Through Regulatory Cross Talk With A Cryptic Nonribosomal Peptide Synthetase Gene Cluster. *Appl Environ Microbiol.*
- Bernard, M. & Latge, J. P. (2001).** *Aspergillus fumigatus* Cell Wall: Composition And Biosynthesis. *Medical Mycology* **39**, 9-17.
- Berth-Jones, J. (2005).** The Use Of Ciclosporin In Psoriasis. *Journal Of Dermatological Treatment* **16**, 258-277.
- Bettelli, E., Das, M. P., Howard, E. D., Weiner, H. L., Sobel, R. A. & Kuchroo, V. K. (1998).** IL-10 Is Critical In The Regulation Of Autoimmune Encephalomyelitis As Demonstrated By Studies Of IL-10- And IL-4-Deficient And Transgenic Mice. *Journal Of Immunology* **161**, 3299-3306.
- Bianchi, M., Hakkim, A., Brinkmann, V., Siler, U., Seger, R. A., Zychlinsky, A. & Reichenbach, J. (2009).** Restoration Of NET Formation By Gene Therapy In CGD Controls Aspergillosis. *Blood* **114**, 2619-2622.
- Birch, M., Robson, G., Law, D. & Denning, D. W. (1996).** Evidence Of Multiple Extracellular Phospholipase Activities Of *Aspergillus fumigatus*. *Infection And Immunity* **64**, 751-755.
- Birch, M., Denning, D. W. & Robson, G. D. (2004).** Comparison Of Extracellular Phospholipase Activities In Clinical And Environmental *Aspergillus fumigatus* Isolates. *Medical Mycology* **42**, 81-86.
- Bird, D. & Bradshaw, R. (1997).** Gene Targeting Is Locus Dependent In The Filamentous Fungus *Aspergillus nidulans*. *Molecular & General Genetics* **255**, 219-225.
- Bittencourt, V. C. B., Figueiredo, R. T., Da Silva, R. B., Mourao-Sa, D. S., Fernandez, P. L., Sasaki, G. L., Mulloy, B., Bozza, M. T. & Barreto-Bergter, E. (2006).** An Alpha-Glucan Of *Pseudallescheria boydii* Is Involved In Fungal Phagocytosis And Toll-Like Receptor Activation. *Journal Of Biological Chemistry* **281**, 22614-22623.
- Boeke, J. D., Lacroute, F. & Fink, G. R. (1984).** A Positive Selection For Mutants Lacking Orotidine-5'-Phosphate Decarboxylase Activity In Yeast - 5-Fluoro-Orotic Acid Resistance. *Molecular & General Genetics* **197**, 345-346.
- Boeke, J. D., Trueheart, J., Natsoulis, G. & Fink, G. R. (1987).** 5-Fluoroorotic Acid As A Selective Agent In Yeast Molecular-Genetics. *Methods In Enzymology* **154**, 164-175.
- Bok, J. W. & Keller, N. P. (2004).** LaeA, A Regulator Of Secondary Metabolism In *Aspergillus spp.* *Eukaryotic Cell* **3**, 527-535.

- Bok, J. W., Balajee, S. A., Marr, K. A., Andes, D., Nielsen, K. F., Frisvad, J. C. & Keller, N. P. (2005).** LaeA, A Regulator Of Morphogenetic Fungal Virulence Factors. *Eukaryotic Cell* **4**, 1574-1582.
- Bok, J. W., Chung, D., Balajee, S. A., Marr, K. A., Andes, D., Nielsen, K. F., Frisvad, J. C., Kirby, K. A. & Keller, N. P. (2006).** GliZ, A Transcriptional Regulator Of Gliotoxin Biosynthesis, Contributes To *Aspergillus fumigatus* Virulence. *Infection And Immunity* **74**, 6761-6768.
- Bonassi, S., A. Znaor, M. Ceppi, C. Lando, W. P. Chang, N. Holland, M. Kirsch-Volders, E. Zeiger, S. Ban, R. Barale, M. P. Bigatti, C. Bolognesi, A. Cebulska-Wasilewska, E. Fabianova, A. Fucic, L. Hagmar, G. Joksic, A. Martelli, L. Migliore, E. Mirkova, M. R. Scarfi, A. Zijno, H. Norppa, and M. Fenech. (2007).** An Increased Micronucleus Frequency In Peripheral Blood Lymphocytes Predicts The Risk Of Cancer In Humans. *Carcinogenesis* **28**, 625-631.
- Bonnett, C. R., Cornish, E. J., Harmsen, A. G. & Burritt, J. B. (2006).** Early Neutrophil Recruitment And Aggregation In The Murine Lung Inhibit Germination Of *Aspergillus fumigatus* Conidia. *Infection And Immunity* **74**, 6528-6539.
- Botterel, F., Gross, K., Ibrahim-Granet, O., Khoufache, K., Escabasse, V., Coste, A., Cordonnier, C., Escudier, E. & Bretagne, S. (2008).** Phagocytosis Of *Aspergillus fumigatus* Conidia By Primary Nasal Epithelial Cells In Vitro. *Bmc Microbiology* **8**, 9.
- Boylan, M. T., Mirabito, P. M., Willett, C. E., Zimmerman, C. R. & Timberlake, W. E. (1987).** Isolation And Physical Characterization Of 3 Essential Conidiation Genes From *Aspergillus nidulans*. *Molecular And Cellular Biology* **7**, 3113-3118.
- Brajtburg, J. & Bolard, J. (1996).** Carrier Effects On Biological Activity Of Amphotericin B. *Clinical Microbiology Reviews* **9**, 512-&.
- Brakhage, A. A. & Langfelder, K. (2002).** Menacing Mold: The Molecular Biology Of *Aspergillus fumigatus*. *Annual Review Of Microbiology* **56**, 433-455.
- Brakhage, A. A. & Liebmann, B. (2005).** *Aspergillus fumigatus* Conidial Pigment And Camp Signal Transduction: Significance For Virulence. *Medical Mycology* **43**, S75-S82.
- Brakhage, A. A., Bruns, S., Thywissen, A., Zipfel, P. F. & Behnsen, J. (2010).** Interaction Of Phagocytes With Filamentous Fungi. *Current Opinion In Microbiology* **13**, 409-415.
- Brennan, M., Thomas, D. Y., Whiteway, M. & Kavanagh, K. (2002).** Correlation Between Virulence Of *Candida albicans* Mutants In Mice And *Galleria mellonella* Larvae. *Fems Immunology And Medical Microbiology* **34**, 153-157.
- Brikos, C. & O'Neill, L. A. (2008).** Signalling Of Toll-Like Receptors. *Handb Exp Pharmacol*, 21-50.

- Brinkmann, V., Reichard, U., Goosmann, C., Fauler, B., Uhlemann, Y., Weiss, D. S., Weinrauch, Y. & Zychlinsky, A. (2004).** Neutrophil Extracellular Traps Kill Bacteria. *Science* **303**, 1532-1535.
- Brinkmann, V. & Zychlinsky, A. (2007).** Beneficial Suicide: Why Neutrophils Die To Make Nets. *Nature Reviews Microbiology* **5**, 577-582.
- Brookman, J. L. & Denning, D. W. (2000).** Molecular Genetics In *Aspergillus fumigatus*. *Current Opinion In Microbiology* **3**, 468-474.
- Brown, D. W., Yu, J. H., Kelkar, H. S., Fernandes, M., Nesbitt, T. C., Keller, N. P., Adams, T. H. & Leonard, T. J. (1996).** Twenty-Five Coregulated Transcripts Define A Sterigmatocystin Gene Cluster In *Aspergillus nidulans*. *Proceedings Of The National Academy Of Sciences Of The United States Of America* **93**, 1418-1422.
- Brown, G. D., Taylor, P. R., Reid, D. M., Willment, J. A., Williams, D. L., Martinez-Pomares, L., Wong, S. Y. C. & Gordon, S. (2002).** Dectin-1 Is A Major Beta-Glucan Receptor On Macrophages. *Journal Of Experimental Medicine* **196**, 407-412.
- Brown, G. D. (2006).** Dectin-1: A Signalling Non-Tlr Pattern-Recognition Receptor. *Nature Reviews Immunology* **6**, 33-43.
- Brown, J. S., Aufauvre-Brown, A., Brown, J., Jennings, J. M., Arst, H. & Holden, D. W. (2000).** Signature-Tagged And Directed Mutagenesis Identify Paba Synthetase As Essential For *Aspergillus fumigatus* Pathogenicity. *Molecular Microbiology* **36**, 1371-1380.
- Brunner, R., Stutz, P. L., Tschertter, H. & Stadler, P. A. (1979).** Isolation Of Ergovaline, Ergoptine, And Ergonine, New Alkaloids Of The Peptide Type, From Ergot Sclerotia. *Canadian Journal Of Chemistry-Revue Canadienne De Chimie* **57**, 1638-1641.
- Bruns, S., O. Kniemeyer, M. Hasenberg, V. Amanianda, S. Nietzsche, A. Thywissen, A. Jeron, J. P. Latge, A. A. Brakhage, and M. Gunzer. (2010).** Production Of Extracellular Traps Against *Aspergillus fumigatus* In Vitro And In Infected Lung Tissue Is Dependent On Invading Neutrophils And Influenced By Hydrophobin RodA. *Plos Pathogens* **6**, 18.
- Bulet, P., Hetru, C., Dimarcq, J. L. & Hoffmann, D. (1999).** Antimicrobial Peptides In Insects; Structure And Function. *Developmental And Comparative Immunology* **23**, 329-344.
- Burns, C., Geraghty, R., Neville, C., Murphy, A., Kavanagh, K. & Doyle, S. (2005).** Identification, Cloning, And Functional Expression Of Three Glutathione Transferase Genes From *Aspergillus fumigatus*. *Fungal Genetics And Biology* **42**, 319-327.
- Busby, T. M., Miller, K. Y. & Miller, B. L. (1996).** Suppression And Enhancement Of The *Aspergillus nidulans* Medusa Mutation By Altered Dosage Of The Bristle And Stunted Genes. *Genetics* **143**, 155-163.

Busch, S., Eckert, S. E., Krappmann, S. & Braus, G. H. (2003). The Cop9 Signalosome Is An Essential Regulator Of Development In The Filamentous Fungus *Aspergillus nidulans*. *Molecular Microbiology* **49**, 717-730.

Bushley, K. E., Ripoll, D. R. & Turgeon, B. G. (2008). Module Evolution And Substrate Specificity Of Fungal Nonribosomal Peptide Synthetases Involved In Siderophore Biosynthesis. *Bmc Evolutionary Biology* **8**.

Butchko, R. A. E., Adams, T. H. & Keller, N. P. (1999). *Aspergillus nidulans* Mutants Defective In STC Gene Cluster Regulation. *Genetics* **153**, 715-720.

Calera, J. A., Paris, S., Monod, M., Hamilton, A. J., Debeaupuis, J. P., Diaquin, M., Lopezmedrano, R., Leal, F. & Latge, J. P. (1997). Cloning And Disruption Of The Antigenic Catalase Gene Of *Aspergillus fumigatus*. *Infection And Immunity* **65**, 4718-4724.

Calvo, A. M., Wilson, R. A., Bok, J. W. & Keller, N. P. (2002). Relationship Between Secondary Metabolism And Fungal Development. *Microbiology And Molecular Biology Reviews* **66**, 447-+.

Cannon, R. D., E. Lamping, A. R. Holmes, K. Niimi, P. V. Baret, M. V. Keniya, K. Tanabe, M. Niimi, A. Goffeau, and B. C. Monk. (2009). Efflux-Mediated Antifungal Drug Resistance. *Clinical Microbiology Reviews* **22**, 291-+.

Carvalho, N., Arentshorst, M., Kwon, M. J., Meyer, V. & Ram, A. F. J. (2010). Expanding The Ku70 Toolbox For Filamentous Fungi: Establishment Of Complementation Vectors And Recipient Strains For Advanced Gene Analyses. *Applied Microbiology And Biotechnology* **87**, 1463-1473.

Catlett, N. L., Lee, B.-N., Yoder, O. C. & Turgeon, B. G. (2002). Split-Marker Recombination For Efficient Targeted Deletion Of Fungal Genes. *Fungal Genetics Newsletter* **50**.

Cerenius, L. & Soderhall, K. (2004). The Prophenoloxidase-Activating System In Invertebrates. *Immunological Reviews* **198**, 116-126.

Chabane, S., Sarfati, J., Ibrahim-Granet, O., Du, C., Schmidt, C., Mouyna, I., Prevost, M. C., Calderone, R. & Latge, J. P. (2006). Glycosylphosphatidylinositol-Anchored Ecm33p Influences Conidial Cell Wall Biosynthesis In *Aspergillus fumigatus*. *Applied And Environmental Microbiology* **72**, 3259-3267.

Chakravarti, D., Ibeanu, G. C., Tano, K. & Mitra, S. (1991). Cloning And Expression In *Escherichia coli* Of A Human cDNA-Encoding The DNA-Repair Protein N-Methylpurine-DNA Glycosylase. *Journal Of Biological Chemistry* **266**, 15710-15715.

Chamilos, G. & Kontoyiannis, D. P. (2005). Update On Antifungal Drug Resistance Mechanisms Of *Aspergillus fumigatus*. *Drug Resistance Updates* **8**, 344-358.

Chang, P. K., Scharfenstein, L. L., Wei, Q. J. & Bhatnagar, D. (2010). Development And Refinement Of A High-Efficiency Gene-Targeting System For *Aspergillus flavus*. *Journal Of Microbiological Methods* **81**, 240-246.

Chang, R. S. L., V. J. Lotti, R. L. Monaghan, J. Birnbaum, E. O. Stapley, M. A. Goetz, G. Albersschonberg, A. A. Patchett, J. M. Liesch, O. D. Hensens, and J. P. Springer. (1985). A Potent Nonpeptide Cholecystokinin Antagonist Selective For Peripheral-Tissues Isolated From *Aspergillus alliaceus*. *Science* **230**, 177-179.

Chauhan, N., Latge, J. P. & Calderone, R. (2006). Signalling And Oxidant Adaptation In *Candida albicans* And *Aspergillus fumigatus*. *Nature Reviews Microbiology* **4**, 435-444.

Chen, J., Derfler, B. & Samson, L. (1990). *Saccharomyces cerevisiae* 3-Methyladenine DNA Glycosylase Has Homology To The AlkA Glycosylase Of *Escherichia coli* And Is Induced In Response To DNA Alkylation Damage. *Embo Journal* **9**, 4569-4575.

Chen, L., Shen, Z. & Wu, J. (2009). Expression, Purification And *In Vitro* Antifungal Activity Of Acidic Mammalian Chitinase Against *Candida albicans*, *Aspergillus fumigatus* And *Trichophyton rubrum* Strains. *Clinical And Experimental Dermatology* **34**, 55-60.

Chiang, L. Y., Sheppard, D. C., Gravelat, F. N., Patterson, T. F. & Filler, S. G. (2008). *Aspergillus fumigatus* Stimulates Leukocyte Adhesion Molecules And Cytokine Production By Endothelial Cells *In Vitro* And During Invasive Pulmonary Disease. *Infection And Immunity* **76**, 3429-3438.

Chignard, M., Balloy, V., Sallenave, J. M. & Si-Tahar, M. (2007). Role Of Toll-Like Receptors In Lung Innate Defense Against Invasive Aspergillosis. Distinct Impact In Immunocompetent And Immunocompromized Hosts. *Clinical Immunology* **124**, 238-243.

Chuang, T. H. & Ulevitch, R. J. (2000). Cloning And Characterization Of A Sub-Family Of Human Toll-Like Receptors: hTLR7, hTLR8 And hTLR9. *European Cytokine Network* **11**, 372-378.

Chuang, T. H. & Ulevitch, R. J. (2001). Identification Of hTLR10: A Novel Human Toll-Like Receptor Preferentially Expressed In Immune Cells. *Biochimica Et Biophysica Acta-Gene Structure And Expression* **1518**, 157-161.

Cisar, J. S. & Tan, D. S. (2008). Small Molecule Inhibition Of Microbial Natural Product Biosynthesis - An Emerging Antibiotic Strategy. *Chemical Society Reviews* **37**, 1320-1329.

Clay, K. & Schardl, C. (2002). Evolutionary Origins And Ecological Consequences Of Endophyte Symbiosis With Grasses. *American Naturalist* **160**, S99-S127.

Clemons, K. V., Grunig, G., Sobel, R. A., Mirels, L. F., Rennick, D. M. & Stevens, D. A. (2000). Role Of IL-10 In Invasive Aspergillosis: Increased Resistance Of IL-10 Gene Knockout Mice To Lethal Systemic Aspergillosis. *Clinical And Experimental Immunology* **122**, 186-191.

Clemons, K. V. & Stevens, D. A. (2005). The Contribution Of Animal Models Of Aspergillosis To Understanding Pathogenesis, Therapy And Virulence. *Medical Mycology* **43**, S101-S110.

Clutterbuck, A. J. (1969). A Mutational Analysis Of Conidial Development In *Aspergillus nidulans*. *Genetics* **63**, 317-&.

Cole, R. J., J. W. Kirksey, J. W. Dorner, D. M. Wilson, J. C. Johnson, A. N. Johnson, D. M. Bedell, J. P. Springer, K. K. Chexal, J. C. Clardy, and R. H. Cox. (1977). Mycotoxins Produced By *Aspergillus fumigatus* Species Isolated From Molded Silage. *Journal Of Agricultural And Food Chemistry* **25**, 826-830.

Conti, E., Stachelhaus, T., Marahiel, M. A. & Brick, P. (1997). Structural Basis For The Activation Of Phenylalanine In The Non-Ribosomal Biosynthesis Of Gramicidin S. *Embo Journal* **16**, 4174-4183.

Correia, T., Grammel, N., Ortel, I., Keller, U. & Tudzynski, P. (2003). Molecular Cloning And Analysis Of The Ergopeptine Assembly System In The Ergot Fungus *Claviceps purpurea*. *Chemistry & Biology* **10**, 1281-1292.

Cotter, G., Doyle, S. & Kavanagh, K. (2000). Development Of An Insect Model For The In Vivo Pathogenicity Testing Of Yeasts. *Fems Immunology And Medical Microbiology* **27**, 163-169.

Coulondre, C. & Miller, J. H. (1977). Genetic Studies Of Lac Repressor .4. Mutagenic Specificity In LacI Gene Of *Escherichia coli*. *Journal Of Molecular Biology* **117**, 577-606.

Cowen, L. E. & Lindquist, S. (2005). Hsp90 Potentiates The Rapid Evolution Of New Traits: Drug Resistance In Diverse Fungi. *Science* **309**, 2185-2189.

Cowen, L. E., Carpenter, A. E., Matangkasombut, O., Fink, G. R. & Lindquist, S. (2006). Genetic Architecture Of Hsp90-Dependent Drug Resistance. *Eukaryotic Cell* **5**, 2184-2188.

Cowen, L. E., S. D. Singh, J. R. Kohler, C. Collins, A. K. Zaas, W. A. Schell, H. Aziz, E. Mylonakis, J. R. Perfect, L. Whitesell, and S. Lindquist. (2009). Harnessing Hsp90 Function As A Powerful, Broadly Effective Therapeutic Strategy For Fungal Infectious Disease. *Proceedings Of The National Academy Of Sciences Of The United States Of America* **106**, 2818-2823.

Coyle, C. M. & Panaccione, D. G. (2005). An Ergot Alkaloid Biosynthesis Gene And Clustered Hypothetical Genes From *Aspergillus fumigatus*. *Applied And Environmental Microbiology* **71**, 3112-3118.

Coyle, C. M., Kenaley, S. C., Rittenour, W. R. & Panaccione, D. G. (2007). Association Of Ergot Alkaloids With Conidiation In *Aspergillus fumigatus*. *Mycologia* **99**, 804-811.

Coyle, C. M., Cheng, J. Z., O'connor, S. E. & Panaccione, D. G. (2010). An Old Yellow Enzyme Gene Controls The Branch Point Between *Aspergillus fumigatus* And *Claviceps*

purpurea Ergot Alkaloid Pathways. *Applied And Environmental Microbiology* **76**, 3898-3903.

Cramer, R. A., M. P. Gamcsik, R. M. Brooking, L. K. Najvar, W. R. Kirkpatrick, T. F. Patterson, C. J. Balibar, J. R. Graybill, J. R. Perfect, S. N. Abraham, and W. J. Steinbach. (2006a). Disruption Of A Nonribosomal Peptide Synthetase In *Aspergillus fumigatus* Eliminates Gliotoxin Production. *Eukaryotic Cell* **5**, 972-980.

Cramer, R. A., Stajich, J. E., Yamanaka, Y., Dietrich, F. S., Steinbach, W. J. & Perfect, J. R. (2006b). Phylogenomic Analysis Of Non-Ribosomal Peptide Synthetases In The Genus *Aspergillus*. *Gene* **383**, 24-32.

Cramer, R. (2002). Molecular Cloning Of *Aspergillus fumigatus* Allergens And Their Role In Allergic Bronchopulmonary Aspergillosis. In *Fungal Allergy And Pathogenicity*, Pp. 73-93. Basel: Karger.

Cress, W. A., Chayet, L. T. & Rilling, H. C. (1981). Crystallization And Partial Characterization Of Dimethylallyl Pyrophosphate - L-Tryptophan Dimethylallyltransferase From *Claviceps sp* Sd58. *Journal Of Biological Chemistry* **256**, 917-923.

Critchlow, S. E. & Jackson, S. P. (1998). DNA-End-Joining: From Yeast To Man. *Trends In Biochemical Sciences* **23**, 394-398.

Cui, C. B., Kakeya, H., Okada, G., Onose, R. & Osada, H. (1996a). Novel Mammalian Cell Cycle Inhibitors, Tryprostatins A, B And Other Diketopiperazines Produced By *Aspergillus fumigatus* .1. Taxonomy, Fermentation, Isolation And Biological Properties. *Journal Of Antibiotics* **49**, 527-533.

Cui, C. B., Kakeya, H. & Osada, H. (1996b). Spirotryprostatin B, A Novel Mammalian Cell Cycle Inhibitor Produced By *Aspergillus fumigatus*. *Journal Of Antibiotics* **49**, 832-835.

Dagenais, T. R. T. & Keller, N. P. (2009). Pathogenesis Of *Aspergillus fumigatus* In Invasive Aspergillosis. *Clinical Microbiology Reviews* **22**, 447-465.

Dagenais, T. R. T., Giles, S. S., Aimaniananda, V., Latge, J. P., Hull, C. M. & Keller, N. P. (2010). *Aspergillus fumigatus* LaeA-Mediated Phagocytosis Is Associated With A Decreased Hydrophobin Layer. *Infection And Immunity* **78**, 823-829.

Daly, P. & Kavanagh, K. (2001). Pulmonary Aspergillosis: Clinical Presentation, Diagnosis And Therapy. *British Journal Of Biomedical Science* **58**, 197-205.

Damrongkool, P., Sedlock, A. B., Young, C. A., Johnson, R. D., Goetz, K. E., Scott, B., Schardl, C. L. & Panaccione, D. G. (2005). Structural Analysis Of A Peptide Synthetase Gene Required For Ergopeptide Production In The Endophytic Fungus *Neotyphodium lolii*. *DNA Sequence* **16**, 379-385.

Damveld, R. A., Arentshorst, M., Franken, A., Vankuyk, P. A., Klis, F. M., Van Den Hondel, C. & Ram, A. F. J. (2005). The *Aspergillus niger* Mads-Box Transcription Factor

RlmA Is Required For Cell Wall Reinforcement In Response To Cell Wall Stress. *Molecular Microbiology* **58**, 305-319.

Daniels, D. S. & Tainer, J. A. (2000). Conserved Structural Motifs Governing The Stoichiometric Repair Of Alkylated DNA By O-6-Alkylguanine-DNA Alkyltransferase. *Mutation Research-DNA Repair* **460**, 151-163.

Das, S., Svaprakash, M. R. & Chakrabarti, A. (2009). New Antifungal Agents In Pediatric Practice. *Indian Pediatrics* **46**, 225-231.

De Groot, M. J. A., Bundock, P., Hooykaas, P. J. J. & Beijersbergen, A. G. M. (1998). *Agrobacterium tumefaciens*-Mediated Transformation Of Filamentous Fungi. *Nature Biotechnology* **16**, 839-842.

De Groot, P. W. J., Hellingwerf, K. J. & Klis, F. M. (2003). Genome-Wide Identification Of Fungal GPI Proteins. *Yeast* **20**, 781-796.

De Vries, J. E. (1995). Immunosuppressive And Anti-Inflammatory Properties Of Interleukin 10. *Ann Med* **27**, 537-541.

Demain, A. L. & Elander, R. P. (1999). The Beta-Lactam Antibiotics: Past, Present, And Future. *Antonie Van Leeuwenhoek International Journal Of General And Molecular Microbiology* **75**, 5-19.

Demple, B., Sedgwick, B., Robins, P., Totty, N., Waterfield, M. D. & Lindahl, T. (1985). Active-Site And Complete Sequence Of The Suicidal Methyltransferase That Counters Alkylation Mutagenesis. *Proceedings Of The National Academy Of Sciences Of The United States Of America* **82**, 2688-2692.

Denfert, C. (1996). Selection Of Multiple Disruption Events In *Aspergillus fumigatus* Using The Orotidine-5'-Decarboxylase Gene, PyrG, As A Unique Transformation Marker. *Current Genetics* **30**, 76-82.

Denning, D. W., Riniotis, K., Dobrashian, R. & Sambatakou, H. (2003). Chronic Cavitory And Fibrosing Pulmonary And Pleural Aspergillosis: Case Series, Proposed Nomenclature Change, And Review. *Clinical Infectious Diseases* **37**, S265-S280.

Denning, D. W. & Hope, W. W. (2010). Therapy For Fungal Diseases: Opportunities And Priorities. *Trends In Microbiology* **18**, 195-204.

Dinglay, S., Trewick, S. C., Lindahl, T. & Sedgwick, B. (2000). Defective Processing Of Methylated Single-Stranded DNA By *E. coli* AlkB Mutants. *Genes & Development* **14**, 2097-2105.

Do, J. H., Yamaguchi, R. & Miyano, S. (2009). Exploring Temporal Transcription Regulation Structure Of *Aspergillus fumigatus* In Heat Shock By State Space Model. *Bmc Genomics* **10**, 16.

- Donnelly, J. P. & De Pauw, B. E. (2004).** Voriconazole - A New Therapeutic Agent With An Extended Spectrum Of Antifungal Activity. *Clinical Microbiology And Infection* **10**, 107-117.
- Donzelli, B. G. G., Krasnoff, S. B., Churchill, A. C. L., Vandenberg, J. D. & Gibson, D. M. (2010).** Identification Of A Hybrid Pks-Nrps Required For The Biosynthesis Of NG-391 In *Metarhizium robertsii*. *Current Genetics* **56**, 151-162.
- Dosanjh, M. K., Chenna, A., Kim, E., Fraenkelconrat, H., Samson, L. & Singer, B. (1994a).** All 4 Known Cyclic Adducts Formed In DNA By The Vinyl-Chloride Metabolite Chloroacetaldehyde Are Released By A Human DNA Glycosylase. *Proceedings Of The National Academy Of Sciences Of The United States Of America* **91**, 1024-1028.
- Dosanjh, M. K., Roy, R., Mitra, S. & Singer, B. (1994b).** 1,N-6-Ethenoadenine Is Preferred Over 3-Methyladenine As Substrate By A Cloned Human N-Methylpurine DNA Glycosylase (3-Methyladenine DNA Glycosylase). *Biochemistry* **33**, 1624-1628.
- Dowling, D. K. & Simmons, L. W. (2009).** Reactive Oxygen Species As Universal Constraints In Life-History Evolution. *Proceedings Of The Royal Society B-Biological Sciences* **276**, 1737-1745.
- Doyle, S. (2009).** Nonribosomal Peptide Synthesis. *Amino Acids, Peptides And Proteins In Organic Chemistry*, Weinheim: Wiley-Vch.
- Du, X., Poltorak, A., Wei, Y. G. & Beutler, B. (2000).** Three Novel Mammalian Toll-Like Receptors: Gene Structure, Expression, And Evolution. *European Cytokine Network* **11**, 362-371.
- Dudasova, Z., Dudas, A. & Chovanec, M. (2004).** Non-Homologous End-Joining Factors Of *Saccharomyces cerevisiae*. *Fems Microbiology Reviews* **28**, 581-601.
- Dunphy, G. B. & Thurston, G. S. (1990).** Insect Immunity. In *Entomopathogenic Nematodes In Biological Control*, Pp. 301-323. Edited By R. Gaugler & H. K. Kaya. New York: Crc Press.
- Duong, M., Ouellet, N., Simard, M., Bergeron, Y., Olivier, M. & Bergeron, M. G. (1998).** Kinetic Study Of Host Defense And Inflammatory Response To *Aspergillus fumigatus* In Steroid-Induced Immunosuppressed Mice. *Journal Of Infectious Diseases* **178**, 1472-1482.
- Dupont, B. (2002).** Overview Of The Lipid Formulations Of Amphotericin B. *Journal Of Antimicrobial Chemotherapy* **49**, 31-36.
- Dyakonov, A. L. & Telezhenetskaya, M. V. (1997).** Natural Quinazoline Alkaloids. *Khimiya Prirodnikh Soedinenii*, 297-351.
- Eisendle, M., Oberegger, H., Zadra, I. & Haas, H. (2003).** The Siderophore System Is Essential For Viability Of *Aspergillus nidulans*: Functional Analysis Of Two Genes

Encoding L-Ornithine N-5-Monooxygenase (Sida) And A Non-Ribosomal Peptide Synthetase (Sidc). *Molecular Microbiology* **49**, 359-375.

Eisendle, M., Schrettl, M., Kragl, C., Muller, D., Illmer, P. & Haas, H. (2006). The Intracellular Siderophore Ferricrocin Is Involved In Iron Storage, Oxidative-Stress Resistance, Germination, And Sexual Development In *Aspergillus nidulans*. *Eukaryotic Cell* **5**, 1596-1603.

Eisenhaber, B., Schneider, G., Wildpaner, M. & Eisenhaber, F. (2004). A Sensitive Predictor For Potential GPI Lipid Modification Sites In Fungal Protein Sequences And Its Application To Genome-Wide Studies For *Aspergillus nidulans*, *Candida albicans*, *Neurospora crassa*, *Saccharomyces cerevisiae* And *Schizosaccharomyces pombe*. *Journal Of Molecular Biology* **337**, 243-253.

Ejzykowicz, D. E., Cunha, M. M., Rozental, S., Solis, N. V., Gravelat, F. N., Sheppard, D. C. & Filler, S. G. (2009). The *Aspergillus fumigatus* Transcription Factor Ace2 Governs Pigment Production, Conidiation And Virulence. *Molecular Microbiology* **72**, 155-169.

Ejzykowicz, D. E., Solis, N. V., Gravelat, F. N., Chabot, J., Li, X., Sheppard, D. C. & Filler, S. G. (2010). Role Of *Aspergillus fumigatus* DvrA In Host Cell Interactions And Virulence. *Eukaryot Cell* **9**, 1432-1440.

Eley, K. L., Halo, L. M., Song, Z. S., Powles, H., Cox, R. J., Bailey, A. M., Lazarus, C. M. & Simpson, T. J. (2007). Biosynthesis of the 2-pyridone tenellin in the insect pathogenic fungus *Beauveria bassiana*. *Chembiochem* **8**, 289-297.

Elliott, M. W. & Taylor, A. J. N. (1997). Allergic Bronchopulmonary Aspergillosis. *Clinical And Experimental Allergy* **27**, 55-59.

Erdeniz, N., Mortensen, U. H. & Rothstein, R. (1997). Cloning-Free PCR-Based Allele Replacement Methods. *Genome Research* **7**, 1174-1183.

Evensen, G. & Seeberg, E. (1982). Adaptation To Alkylation Resistance Involves The Induction Of A DNA Glycosylase. *Nature* **296**, 773-775.

Fallon, J. P., Reeves, E. P. & Kavanagh, K. (2010). Inhibition Of Neutrophil Function Following Exposure To The *Aspergillus fumigatus* Toxin Fumagillin. *Journal Of Medical Microbiology* **59**, 625-633.

Fanelli, C., Ricelli, A., Reverberi, M. & Fabbri, A. A. (2004). Aflatoxins And Ochratoxins In Cereal Grains: An Open Challenge. *Recent Res Devel Crop Sci* **1**, 295-317.

Fedorova, N. D., N. Khaldi, V. S. Joardar, R. Maiti, P. Amedeo, M. J. Anderson, J. Crabtree, J. C. Silva, J. H. Badger, A. Albarraq, S. Angiuoli, H. Bussey, P. Bowyer, P. J. Cotty, P. S. Dyer, A. Egan, K. Galens, C. M. Fraser-Liggett, B. J. Haas, J. M. Inman, R. Kent, S. Lemieux, I. Malavazi, J. Orvis, T. Roemer, C. M. Ronning, J. P. Sundaram, G. Sutton, G. Turner, J. C. Venter, O. R. White, B. R. Whitty, P. Youngman, K. H. Wolfe, G. H. Goldman, J. R. Wortman, B. Jiang, D. W. Denning,

and W. C. Nierman. (2008). Genomic Islands In The Pathogenic Filamentous Fungus *Aspergillus fumigatus*. *Plos Genetics* **4**, 13.

Ferreira, M. E. D., Kress, M., Savoldi, M., Goldman, M. H. S., Hartl, A., Heinekamp, T., Brakhage, A. A. & Goldman, G. H. (2006a). The *AkuB(Ku80)* Mutant Deficient For Nonhomologous End Joining Is A Powerful Tool For Analyzing Pathogenicity In *Aspergillus fumigatus*. *Eukaryotic Cell* **5**, 207-211.

Ferreira, M. E. D., Malavazi, I., Savoldi, M., Brakhage, A. A., Goldman, M. H. S., Kim, H. S., Nierman, W. C. & Goldman, G. H. (2006b). Transcriptome Analysis Of *Aspergillus fumigatus* Exposed To Voriconazole. *Current Genetics* **50**, 32-44.

Fisch, K. M., Gillaspay, A. F., Gipson, M., Henrikson, J. C., Hoover, A. R., Jackson, L., Najar, F. Z., Wagele, H. & Cichewicz, R. H. (2009). Chemical Induction Of Silent Biosynthetic Pathway Transcription In *Aspergillus niger*. *Journal Of Industrial Microbiology & Biotechnology* **36**, 1199-1213.

Fleck, C. B. & Brock, M. (2010). *Aspergillus fumigatus* Catalytic Glucokinase And Hexokinase: Expression Analysis And Importance For Germination, Growth, And Conidiation. *Eukaryotic Cell* **9**, 1120-1135.

Fleetwood, D. J., Scott, B., Lane, G. A., Tanaka, A. & Johnson, R. D. (2007). A Complex Ergovaline Gene Cluster In *Epichloe* Endophytes Of Grasses. *Applied And Environmental Microbiology* **73**, 2571-2579.

Flieger, M., Wurst, M. & Shelby, R. (1997). Ergot Alkaloids - Sources, Structures And Analytical Methods. *Folia Microbiologica* **42**, 3-29.

Floss, H. G. (1976). Biosynthesis Of Ergot Alkaloids And Related Compounds. *Tetrahedron* **32**, 873-912.

Folch-Mallol, J. L., Martinez, L. M., Casas, S. J., Yang, R. Y., Martinez-Anaya, C., Lopez, L., Hernandez, A. & Nieto-Sotelo, J. (2004). New Roles For Cdc25 In Growth Control, Galactose Regulation And Cellular Differentiation In *Saccharomyces cerevisiae*. *Microbiology-Sgm* **150**, 2865-2879.

Fontaine, T., Simenel, C., Dubreucq, G., Adam, O., Delepierre, M., Lemoine, J., Vorgias, C. E., Diaquin, M. & Latge, J. P. (2000a). Molecular Organization Of The Alkali-Insoluble Fraction Of *Aspergillus fumigatus* Cell Wall. *Journal Of Biological Chemistry* **275**, 27594-27607.

Fontaine, T., Sinenel, C., Dubreucq, G., Adam, O., Delepierre, M., Lemoine, J., Vorgias, C. E., Diaquin, M. & Latge, J. P. (2000b). Molecular Organization Of The Alkali-Insoluble Fraction Of *Aspergillus fumigatus* Cell Wall. (Vol 275, Pg 27603, 2000). *Journal Of Biological Chemistry* **275**, 41528-41529.

Fox, E. M. & Howlett, B. J. (2008). Secondary Metabolism: Regulation And Role In Fungal Biology. *Current Opinion In Microbiology* **11**, 481-487.

- Friedberg, E., Walker, G. & Siede, W. (1995).** *DNA Repair And Mutagenesis*. Washington D.C.: Asm Press.
- Frisvad, J. C., Larsen, T. O., De Vries, R., Meijer, M., Houbraken, J., Cabanes, F. J., Ehrlich, K. & Samson, R. A. (2007).** Secondary Metabolite Profiling, Growth Profiles And Other Tools For Species Recognition And Important *Aspergillus* Mycotoxins. *Studies In Mycology*, 31-37.
- Frisvad, J. C., Rank, C., Nielsen, K. F. & Larsen, T. O. (2009).** Metabolomics Of *Aspergillus fumigatus*. *Medical Mycology* 47, S53-S71.
- Fuchs, T. A., Abed, U., Goosmann, C., Hurwitz, R., Schulze, I., Wahn, V., Weinrauch, Y., Brinkmann, V. & Zychlinsky, A. (2007).** Novel Cell Death Program Leads To Neutrophil Extracellular Traps. *Journal Of Cell Biology* 176, 231-241.
- Furtado, N., Said, S., Ito, I. Y. & Bastos, J. K. (2002).** The Antimicrobial Activity Of *Aspergillus fumigatus* Is Enhanced By A Pool Of Bacteria. *Microbiological Research* 157, 207-211.
- Furtado, N., Fonseca, M. J. V. & Bastos, J. K. (2005).** The Potential Of An *Aspergillus fumigatus* Brazilian Strain To Produce Antimicrobial Secondary Metabolites. *Brazilian Journal Of Microbiology* 36, 357-362.
- Galagan, J. E., S. E. Calvo, C. Cuomo, L. J. Ma, J. R. Wortman, S. Batzoglou, S. I. Lee, M. Basturkmen, C. C. Spevak, J. Clutterbuck, V. Kapitonov, J. Jurka, C. Scaccocchio, M. Farman, J. Butler, S. Purcell, S. Harris, G. H. Braus, O. Draht, S. Busch, C. D'Enfert, C. Bouchier, G. H. Goldman, D. Bell-Pedersen, S. Griffiths-Jones, J. H. Doonan, J. Yu, K. Vienken, A. Pain, M. Freitag, E. U. Selker, D. B. Archer, M. A. Penalva, B. R. Oakley, M. Momany, T. Tanaka, T. Kumagai, K. Asai, M. Machida, W. C. Nierman, D. W. Denning, M. Caddick, M. Hynes, M. Paoletti, R. Fischer, B. Miller, P. Dyer, M. S. Sachs, S. A. Osmani, and B. W. Birren. (2005).** Sequencing Of *Aspergillus nidulans* And Comparative Analysis With *A. fumigatus* And *A. oryzae*. *Nature* 438, 1105-1115.
- Gamble, J. R., Harlan, J. M., Klebanoff, S. J. & Vadas, M. A. (1985).** Stimulation Of The Adherence Of Neutrophils To Umbilical Vein Endothelium By Human Recombinant Tumor-Necrosis-Factor. *Proceedings Of The National Academy Of Sciences Of The United States Of America* 82, 8667-8671.
- Gao, J. L., T. A. Wynn, Y. Chang, E. J. Lee, H. E. Broxmeyer, S. Cooper, H. L. Tiffany, H. Westphal, J. KwonChung, and P. M. Murphy. (1997).** Impaired Host Defense, Hematopoiesis, Granulomatous Inflammation And Type 1-Type 2 Cytokine Balance In Mice Lacking Cc Chemokine Receptor 1. *Journal Of Experimental Medicine* 185, 1959-1968.
- Gardiner, D. M., Cozijnsen, A. J., Wilson, L. M., Pedras, M. S. C. & Howlett, B. J. (2004).** The Sirodesmin Biosynthetic Gene Cluster Of The Plant Pathogenic Fungus *Leptosphaeria maculans*. *Molecular Microbiology* 53, 1307-1318.

Gardiner, D. M. & Howlett, B. J. (2005). Bioinformatic And Expression Analysis Of The Putative Gliotoxin Biosynthetic Gene Cluster Of *Aspergillus fumigatus*. *Fems Microbiology Letters* **248**, 241-248.

Gardiner, D. M., Waring, P. & Howlett, B. J. (2005). The Epipolythiodioxopiperazine (Etp) Class Of Fungal Toxins: Distribution, Mode Of Action, Functions And Biosynthesis. *Microbiology-Sgm* **151**, 1021-1032.

Gebler, J. C. & Poulter, C. D. (1992). Purification And Characterization Of Dimethylallyl Tryptophan Synthase From *Claviceps purpurea*. *Archives Of Biochemistry And Biophysics* **296**, 308-313.

Gerik, K. J., Donlin, M. J., Soto, C. E., Banks, A. M., Banks, I. R., Maligie, M. A., Selitrennikoff, C. P. & Lodge, J. K. (2005). Cell Wall Integrity Is Dependent On The Pkc1 Signal Transduction Pathway In *Cryptococcus neoformans*. *Molecular Microbiology* **58**, 393-408.

Glaser, A. G., Kirsch, A. I., Zeller, S., Menz, G., Rhyner, C. & Cramer, R. (2009). Molecular And Immunological Characterization Of Asp F 34, A Novel Major Cell Wall Allergen Of *Aspergillus fumigatus*. *Allergy* **64**, 1144-1151.

Gocke, E., Burgin, H., Muller, L. & Pfister, T. (2009). Literature Review On The Genotoxicity, Reproductive Toxicity, And Carcinogenicity Of Ethyl Methanesulfonate. *Toxicology Letters* **190**, 254-265.

Goldman, M., Velu, T. & Pretolani, M. (1997). Interleukin-10 - Actions And Therapeutic Potential. *Biodrugs* **7**, 6-14.

Gosselin, D., Desanctis, J., Boule, M., Skamene, E., Matouk, C. & Radzioch, D. (1995). Role Of Tumor-Necrosis-Factor-Alpha In Innate Resistance To Mouse Pulmonary Infection With *Pseudomonas aeruginosa*. *Infection And Immunity* **63**, 3272-3278.

Gravelat, F. N., Doedt, T., Chiang, L. Y., Liu, H., Filler, S. G., Patterson, T. F. & Sheppard, D. C. (2008). *In Vivo* Analysis Of *Aspergillus fumigatus* Developmental Gene Expression Determined By Real-Time Reverse Transcription-PCR. *Infection And Immunity* **76**, 3632-3639.

Grundmann, A. & Li, S. M. (2005). Overproduction, Purification And Characterization Of Ftmpt1, A Brevianamide F Prenyltransferase From *Aspergillus fumigatus*. *Microbiology-Sgm* **151**, 2199-2207.

Grundmann, A., Kuznetsova, T., Afiyatullo, S. S. & Li, S. M. (2008). Ftmpt2, An N-Prenyltransferase From *Aspergillus fumigatus*, Catalyses The Last Step In The Biosynthesis Of Fumitremorgin B. *Chembiochem* **9**, 2059-2063.

Grunewald, J. & Marahiel, M. A. (2006). Chemoenzymatic And Template-Directed Synthesis Of Bioactive Macrocyclic Peptides. *Microbiology And Molecular Biology Reviews* **70**, 121-+.

Grunig, G., Corry, D. B., Leach, M. W., Seymour, B. W. P., Kurup, V. P. & Rennick, D. M. (1997). Interleukin-10 Is A Natural Suppressor Of Cytokine Production And Inflammation In A Murine Model Of Allergic Bronchopulmonary Aspergillosis. *Journal Of Experimental Medicine* **185**, 1089-1099.

Gutteridge, J. M. C. & Halliwell, B. (2000). Free Radicals And Antioxidants In The Year 2000 - A Historical Look To The Future. In *Reactive Oxygen Species: From Radiation To Molecular Biology - A Festschrift In Honor Of Daniel L Gilbert*, Pp. 136-147. Edited By C. C. Chiueh.

Haarmann, T., Machado, C., Lubbe, Y., Correia, T., Schardl, C. L., Panaccione, D. G. & Tudzynski, P. (2005). The Ergot Alkaloid Gene Cluster In *Claviceps purpurea*: Extension Of The Cluster Sequence And Intra Species Evolution. *Phytochemistry* **66**, 1312-1320.

Haarmann, T., Ortel, I., Tudzynski, P. & Keller, U. (2006). Identification Of The Cytochrome P450 Monooxygenase That Bridges The Clavine And Ergoline Alkaloid Pathways. *Chembiochem* **7**, 645-652.

Haarmann, T., Lorenz, N. & Tudzynski, P. (2008). Use Of A Nonhomologous End Joining Deficient Strain (Delta Ku70) Of The Ergot Fungus *Claviceps purpurea* For Identification Of A Nonribosomal Peptide Synthetase Gene Involved In Ergotamine Biosynthesis. *Fungal Genetics And Biology* **45**, 35-44.

Haas, H. (2003). Molecular genetics of fungal siderophore biosynthesis and uptake: the role of siderophores in iron uptake and storage. *Applied Microbiology and Biotechnology* **62**, 316-330.

Hall, J. A. & Saffhill, R. (1983). The Incorporation Of O-6-Methyldeoxyguanosine And O-4-Methyldeoxythymidine Monophosphates Into DNA By DNA-Polymerase-I And Polymerase-Alpha. *Nucleic Acids Research* **11**, 4185-4193.

Hang, B., Singer, B., Margison, G. P. & Elder, R. H. (1997). Targeted Deletion Of Alkylpurine-DNA-N-Glycosylase In Mice Eliminates Repair Of 1,N-6-Ethenoadenine And Hypoxanthine But Not Of 3,N-4-Ethenocytosine Or 8-Oxoguanine. *Proceedings Of The National Academy Of Sciences Of The United States Of America* **94**, 12869-12874.

Hanin, A., Sava, I., Bao, Y., Huebner, J., Hartke, A., Auffray, Y. & Sauvageot, N. (2010). Screening Of *In Vivo* Activated Genes In *Enterococcus faecalis* During Insect And Mouse Infections And Growth In Urine. *Plos One* **5**, E11879.

He, C., Wei, H. & Verdine, G. L. (2003). Converting The Sacrificial DNA Repair Protein N-Ada Into A Catalytic Methyl Phosphotriester Repair Enzyme. *Journal Of The American Chemical Society* **125**, 1450-1451.

Heinsbroek, S. E. M., Taylor, P. R., Rosas, M., Willment, J. A., Williams, D. L., Gordon, S. & Brown, G. D. (2006). Expression Of Functionally Different Dectin-1 Isoforms By Murine Macrophages. *Journal Of Immunology* **176**, 5513-5518.

Herbrecht, R., D. W. Denning, T. F. Patterson, J. E. Bennett, R. E. Greene, J. W. Oestmann, W. V. Kern, K. A. Marr, P. Ribaud, O. Lortholary, R. Sylvester, R. H. Rubin, J. R. Wingard, P. Stark, C. Durand, D. Caillot, E. Thiel, P. H. Chandrasekar, M. R. Hodges, H. T. Schlamm, P. F. Troke, B. de Pauw, and E. Invasive Fungal Infect Grp. (2002). Voriconazole Versus Amphotericin B For Primary Therapy Of Invasive Aspergillosis. *New England Journal Of Medicine* **347**, 408-415.

Herranz, R. (2003). Cholecystokinin Antagonists: Pharmacological And Therapeutic Potential. *Medicinal Research Reviews* **23**, 559-605.

Herth, W. (1980). Calcofluor White And Congo Red Inhibit Chitin Microfibril Assembly Of *Poterioochromonas* - Evidence For A Gap Between Polymerization And Microfibril Formation. *Journal Of Cell Biology* **87**, 442-450.

Hissen, A. H. T., Wan, A. N. C., Warwas, M. L., Pinto, L. J. & Moore, M. M. (2005). The *Aspergillus fumigatus* Siderophore Biosynthetic Gene *SidA*, Encoding L-Ornithine N-5-Oxygenase, Is Required For Virulence. *Infection And Immunity* **73**, 5493-5503.

Ho, A. S. Y., Wei, S. H. Y. & Moore, K. W. (1994). Structural And Functional-Studies Of Interleukin-10 Receptors. *Faseb Journal* **8**, A744-A744.

Hohl, T. M., Van Epps, H. L., Rivera, A., Morgan, L. A., Chen, P. L., Feldmesser, M. & Pamer, E. G. (2005). *Aspergillus fumigatus* Triggers Inflammatory Responses By Stage-Specific Beta-Glucan Display. *Plos Pathogens* **1**, 232-240.

Holdom, M. D., Hay, R. J. & Hamilton, A. J. (1996). The Cu,Zn Superoxide Dismutases of *Aspergillus flavus*, *Aspergillus niger*, *Aspergillus terreus*: Purification And Biochemical Comparison With The *Aspergillus fumigatus* Cu,Zn Superoxide Dismutase. *Infection And Immunity* **64**, 3326-3332.

Holdom, M. D., Lechenne, B., Hay, R. J., Hamilton, A. J. & Monod, M. (2000). Production And Characterization Of Recombinant *Aspergillus fumigatus* Cu,Zn Superoxide Dismutase And Its Recognition By Immune Human Sera. *Journal Of Clinical Microbiology* **38**, 558-562.

Hooley, P., Shawcross, S. G. & Strike, P. (1988). An Adaptive Response To Alkylating-Agents In *Aspergillus nidulans*. *Current Genetics* **14**, 445-449.

Horie, Y. & Yamazaki, M. (1981). Productivity Of Tremorgenic Myco-Toxins, Fumitremorgin-A And Fumitremorgin-B In *Aspergillus fumigatus* And Allied Species. *Transactions Of The Mycological Society Of Japan* **22**, 113-119.

Ingber, D., Fujita, T., Kishimoto, S., Sudo, K., Kanamaru, T., Brem, H. & Folkman, J. (1990). Synthetic Analogs Of Fumagillin That Inhibit Angiogenesis And Suppress Tumor-Growth. *Nature* **348**, 555-557.

Jacobsen, I. D., Grosse, K., Slesiona, S., Hube, B., Berndt, A. & Brock, M. (2010). Embryonated Eggs As An Alternative Infection Model To Investigate *Aspergillus fumigatus* Virulence. *Infection And Immunity* **78**, 2995-3006.

- Jahn, B., Koch, A., Schmidt, A., Wanner, G., Gehringer, H., Bhakdi, S. & Brakhage, A. A. (1997).** Isolation And Characterization Of A Pigmentless-Conidium Mutant Of *Aspergillus fumigatus* With Altered Conidial Surface And Reduced Virulence. *Infection And Immunity* **65**, 5110-5117.
- Jahn, B., Langfelder, K., Schneider, U., Schindel, C. & Brakhage, A. A. (2002).** Pksp-Dependent Reduction Of Phagolysosome Fusion And Intracellular Kill Of *Aspergillus fumigatus* Conidia By Human Monocyte-Derived Macrophages. *Cellular Microbiology* **4**, 793-803.
- Jaillon, S., G. Peri, Y. Delneste, I. Fremaux, A. Doni, F. Moalli, C. Garlanda, L. Romani, H. Gascan, S. Bellocchio, S. Bozza, M. A. Cassatella, P. Jeannin, and A. Mantovani. (2007).** The Humoral Pattern Recognition Receptor Ptx3 Is Stored In Neutrophil Granules And Localizes In Extracellular Traps. *Journal Of Experimental Medicine* **204**, 793-804.
- Janeway, C. A. (1992).** The Immune-System Evolved To Discriminate Infectious Nonself From Noninfectious Self. *Immunology Today* **13**, 11-16.
- Janeway, C. A. (1998).** Presidential Address To The American Association Of Immunologists - The Road Less Traveled By: The Role Of Innate Immunity In The Adaptive Immune Response. *Journal Of Immunology* **161**, 539-544.
- Jimenez-A, M. D., Viriyakosol, S., Walls, L., Datta, S. K., Kirkland, T., Heinsbroek, S. E. M., Brown, G. & Fierer, J. (2008).** Susceptibility To *Coccidioides* Species In C57bl/6 Mice Is Associated With Expression Of A Truncated Splice Variant Of Dectin-1 (Clec7a). *Genes And Immunity* **9**, 338-348.
- Joyce, S. A. & Gahan, C. G. (2010).** The Molecular Pathogenesis Of *Listeria monocytogenes* In The Alternative Model Host *Galleria mellonella*. *Microbiology*.
- Jung, W. H., Wam, P., Ragni, E., Popolo, L., Nunn, C. D., Turner, M. P. & Stateva, L. (2005).** Deletion Of Pde2, The Gene Encoding The High-Affinity cAMP Phosphodiesterase, Results In Changes Of The Cell Wall And Membrane In *Candida zblicans*. *Yeast* **22**, 285-294.
- Kaestel, M., Meyer, W., Mittelmeier, H. O. & Gebhardt, C. (1999).** Pulmonary Aspergilloma - Clinical Findings And Surgical Treatment. *Thoracic And Cardiovascular Surgeon* **47**, 340-345.
- Kaina, B. (2004).** Mechanisms And Consequences Of Methylating Agent-Induced Sces And Chromosomal Aberrations: A Long Road Traveled And Still A Far Way To Go. *Cytogenetic And Genome Research* **104**, 77-86.
- Kamei, K. & Watanabe, A. (2005).** *Aspergillus* Mycotoxins And Their Effect On The Host. *Medical Mycology* **43**, S95-S99.

- Kao, R. & Davies, J. (1995).** Fungal Ribotoxins: A Family Of Naturally Engineered Targeted Toxins? *Biochemistry And Cell Biology-Biochimie Et Biologie Cellulaire* **73**, 1151-1159.
- Kao, R. & Davies, J. (1999).** Molecular Dissection Of Mitogillin Reveals That The Fungal Ribotoxins Are A Family Of Natural Genetically Engineered Ribonucleases. *Journal Of Biological Chemistry* **274**, 12576-12582.
- Karran, P., Hjelmgren, T. & Lindahl, T. (1982).** Induction Of A DNA Glycosylase For N-Methylated Purines Is Part Of The Adaptive Response To Alkylating-Agents. *Nature* **296**, 770-773.
- Kataoka, H. & Sekiguchi, M. (1985).** Molecular-Cloning And Characterization Of The AlkB Gene Of *Escherichia coli*. *Molecular & General Genetics* **198**, 263-269.
- Kataoka, H., Hall, J. & Karran, P. (1986).** Complementation Of Sensitivity To Alkylating-Agents In *Escherichia coli* And Chinese-Hamster Ovary Cells By Expression Of A Cloned Bacterial-DNA Repair Gene. *Embo Journal* **5**, 3195-3200.
- Kato, N., Brooks, W. & Calvo, A. M. (2003).** The Expression Of Sterigmatocystin And Penicillin Genes In *Aspergillus nidulans* Is Controlled By *Vea*, A Gene Required For Sexual Development. *Eukaryotic Cell* **2**, 1178-1186.
- Kato, N., H. Suzuki, H. Takagi, Y. Asami, H. Kakeya, M. Uramoto, T. Usui, S. Takahashi, Y. Sugimoto, and H. Osada. (2009).** Identification Of Cytochrome P450s Required For Fumitremorgin Biosynthesis In *Aspergillus fumigatus*. *Chembiochem* **10**, 920-928.
- Kavanagh, K. & Reeves, E. P. (2004).** Exploiting The Potential Of Insects For *In Vivo* Pathogenicity Testing Of Microbial Pathogens. *Fems Microbiology Reviews* **28**, 101-112.
- Kavanagh, K. & Fallon, J. P. (2010).** *Galleria mellonella* Larvae As Models For Studying Fungal Virulence. *Fungal Biology Reviews*, 1-5.
- Keating, G. M. & Jarvis, B. (2001).** Caspofungin. *Drugs* **61**, 1121-1129.
- Keating, T. A., Ehmann, D. E., Kohli, R. M., Marshall, C. G., Trauger, J. W. & Walsh, C. T. (2001).** Chain Termination Steps In Nonribosomal Peptide Synthetase Assembly Lines: Directed Acyl-S-Enzyme Breakdown In Antibiotic And Siderophore Biosynthesis. *Chembiochem* **2**, 99-107.
- Keller, N. P. & Hohn, T. M. (1997).** Metabolic Pathway Gene Clusters In Filamentous Fungi. *Fungal Genetics And Biology* **21**, 17-29.
- Keszenman-Pereyra, D., Lawrence, S., Twfieg, M. E., Price, J. & Turner, G. (2003).** The *Npga/Cfwa* Gene Encodes A Putative 4'-Phosphopantetheinyl Transferase Which Is Essential For Penicillin Biosynthesis In *Aspergillus nidulans*. *Current Genetics* **43**, 186-190.

Khalidi, N., Seifuddin, F. T., Turner, G., Haft, D., Nierman, W. C., Wolfe, K. H. & Fedorova, N. D. (2010). Smurf: Genomic Mapping Of Fungal Secondary Metabolite Clusters. *Fungal Genetics And Biology* **47**, 736-741.

Kim, H. S., Han, K. Y., Kim, K. J., Han, D. M., Jahng, K. Y. & Chae, K. S. (2002). The *Vea* Gene Activates Sexual Development In *Aspergillus nidulans*. *Fungal Genetics And Biology* **37**, 72-80.

Kim, K. H., Cho, Y., La Rota, M., Cramer, R. A. & Lawrence, C. B. (2007). Functional Analysis Of The *Alternaria brassicicola* Non-Ribosomal Peptide Synthetase Gene *Abnps2* Reveals A Role In Conidial Cell Wall Construction. *Molecular Plant Pathology* **8**, 23-39.

Kim, K. H., Willger, S. D., Park, S. W., Puttikamonkul, S., Grahl, N., Cho, Y., Mukhopadhyay, B., Cramer, R. A. & Lawrence, C. B. (2009). TmpL, A Transmembrane Protein Required For Intracellular Redox Homeostasis And Virulence In A Plant And An Animal Fungal Pathogen. *Plos Pathogens* **5**, 25.

Kishore, U., Madan, T., Sarma, P. U., Singh, M., Urban, B. C. & Reid, K. B. M. (2002). Protective Roles Of Pulmonary Surfactant Proteins, Sp-A And Sp-D, Against Lung Allergy And Infection Caused By *Aspergillus fumigatus*. *Immunobiology* **205**, 610-618.

Klaunig, J. E., Kamendulis, L. M. & Hocevar, B. A. (2010). Oxidative Stress And Oxidative Damage In Carcinogenesis. *Toxicologic Pathology* **38**, 96-109.

Knox, J. P. (2008). Mapping The Walls Of The Kingdom: The View From The Horsetails. *New Phytologist* **179**, 1-3.

Kohchi, C., Inagawa, H., Nishizawa, T. & Soma, G. I. (2009). ROS And Innate Immunity. *Anticancer Research* **29**, 817-821.

Kohli, R. M. & Walsh, C. T. (2003). Enzymology Of Acyl Chain Macrocyclization In Natural Product Biosynthesis. *Chemical Communications*, 297-307.

Kollar, R., Petrakova, E., Ashwell, G., Robbins, P. W. & Cabib, E. (1995). Architecture Of The Yeast-Cell Wall - The Linkage Between Chitin And Beta(1- 3)-Glucan. *Journal Of Biological Chemistry* **270**, 1170-1178.

Kozlovsky, A. G. (1999). Nontraditional Producers Of Ergot Alkaloids (Review). *Applied Biochemistry And Microbiology* **35**, 477-485.

Krappmann, S., Bignell, E. M., Reichard, U., Rogers, T., Haynes, K. & Braus, G. H. (2004). The *Aspergillus fumigatus* Transcriptional Activator CpcA Contributes Significantly To The Virulence Of This Fungal Pathogen. *Molecular Microbiology* **52**, 785-799.

Krappmann, S., Sasse, C. & Braus, G. H. (2006). Gene Targeting In *Aspergillus fumigatus* By Homologous Recombination Is Facilitated In A Nonhomologous End-Joining-Deficient Genetic Background. *Eukaryotic Cell* **5**, 212-215.

Krasnoff, S. B., Keresztes, I., Gillilan, R. E., Szebenyi, D. M. E., Donzelli, B. G. G., Churchill, A. C. L. & Gibson, D. M. (2007). Serinocyclins A And B, Cyclic Heptapeptides From *Metarhizium anisopliae*. *Journal Of Natural Products* **70**, 1919-1924.

Krogh, B. O. & Symington, L. S. (2004). Recombination Proteins In Yeast. *Annual Review Of Genetics* **38**, 233-271.

Kubodera, T., Yamashita, N. & Nishimura, A. (2000). Pyrithiamine Resistance Gene (*ptrA*) Of *Aspergillus oryzae*: Cloning, Characterization And Application As A Dominant Selectable Marker For Transformation. *Bioscience Biotechnology And Biochemistry* **64**, 1416-1421.

Kubodera, T., Yamashita, N. & Nishimura, A. (2002). Transformation Of *Aspergillus sp* And *Trichoderma reesei* Using The Pyrithiamine Resistance Gene (*ptrA*) Of *Aspergillus oryzae*. *Bioscience Biotechnology And Biochemistry* **66**, 404-406.

Kuroki, Y., Takahashi, M. & Nishitani, C. (2007). Pulmonary Collectins In Innate Immunity Of The Lung. *Cellular Microbiology* **9**, 1871-1879.

Kuwayama, H., Obara, S., Morio, T., Katoh, M., Urushihara, H. & Tanaka, Y. (2002). PCR-Mediated Generation Of A Gene Disruption Construct Without The Use Of DNA Ligase And Plasmid Vectors. *Nucleic Acids Research* **30**.

Kwon-Chung, K. J. & Sugui, J. A. (2009). What Do We Know About The Role Of Gliotoxin In The Pathobiology Of *Aspergillus fumigatus*? *Medical Mycology* **47**, S97-S103.

Laichalk, L. L., Kunkel, S. L., Strieter, R. M., Danforth, J. M., Bailie, M. B. & Standiford, T. J. (1996). Tumor Necrosis Factor Mediates Lung Antibacterial Host Defense In Murine *Klebsiella* Pneumonia. *Infection And Immunity* **64**, 5211-5218.

Lamaris, G. A., Lewis, R. E., Chamilos, G., May, G. S., Safdar, A., Walsh, T. J., Raad, Ii & Kontoyiannis, D. P. (2008). Caspofungin-Mediated Beta-Glucan Unmasking And Enhancement Of Human Polymorphonuclear Neutrophil Activity Against *Aspergillus* And Non-*Aspergillus* Hyphae. *Journal Of Infectious Diseases* **198**, 186-192.

Lamarre, C., Ibrahim-Granet, O., Du, C., Calderone, R. & Latge, J. P. (2007). Characterization Of The Skn7 Ortholog Of *Aspergillus fumigatus*. *Fungal Genetics And Biology* **44**, 682-690.

Lamarre, C., Sokol, S., Debeaupuis, J. P., Henry, C., Lacroix, C., Glaser, P., Coppee, J. Y., Francois, J. M. & Latge, J. P. (2008). Transcriptomic Analysis Of The Exit From Dormancy Of *Aspergillus fumigatus* Conidia. *Bmc Genomics* **9**, 15.

Lambalot, R. H., Gehring, A. M., Flugel, R. S., Zuber, P., Lacelle, M., Marahiel, M. A., Reid, R., Khosla, C. & Walsh, C. T. (1996). A New Enzyme Superfamily - The Phosphopantetheinyl Transferases. *Chemistry & Biology* **3**, 923-936.

Landini, P., Hajec, L. I. & Volkert, M. R. (1994). Structure And Transcriptional Regulation Of The *Escherichia coli* Adaptive Response Gene AidB. *Journal Of Bacteriology* **176**, 6583-6589.

Langfelder, K., Jahn, B., Gehringer, H., Schmidt, A., Wanner, G. & Brakhage, A. A. (1998). Identification Of A Polyketide Synthase Gene (PksP) Of *Aspergillus fumigatus* Involved In Conidial Pigment Biosynthesis And Virulence. *Medical Microbiology And Immunology* **187**, 79-89.

Larsen, R. A., Pappas, P. G., Perfect, J., Aberg, J. A., Casadevall, A., Cloud, G. A., James, R., Filler, S. & Dismukes, W. E. (2005). Phase I Evaluation Of The Safety And Pharmacokinetics Of Murine-Derived Anticryptococcal Antibody 18b7 In Subjects With Treated *Cryptococcal* Meningitis. *Antimicrobial Agents And Chemotherapy* **49**, 952-958.

Larsen, T. O., Smedsgaard, J., Nielsen, K. F., Hansen, M. A. E., Samson, R. A. & Frisvad, J. C. (2007). Production Of Mycotoxins By *Aspergillus lentulus* And Other Medically Important And Closely Related Species In Section *Fumigati*. *Medical Mycology* **45**, 225-232.

Latge, J. P. (1999). *Aspergillus fumigatus* And Aspergillosis. *Clinical Microbiology Reviews* **12**, 310-350.

Latge, J. P. (2001). The Pathobiology Of *Aspergillus fumigatus*. *Trends In Microbiology* **9**, 382-389.

Latge, J. P. & Calderone, R. (2002). Host-Microbe Interactions: Fungi Invasive Human Fungal Opportunistic Infections - Editorial Overview. *Current Opinion In Microbiology* **5**, 355-358.

Latge, J. P. (2007). The Cell Wall: A Carbohydrate Armour For The Fungal Cell. *Molecular Microbiology* **66**, 279-290.

Latge, J. P. (2010). Tasting The Fungal Cell Wall. *Cellular Microbiology* **12**, 863-872.

Lautru, S. & Challis, G. L. (2004). Substrate Recognition By Nonribosomal Peptide Synthetase Multi-Enzymes. *Microbiology-Sgm* **150**, 1629-1636.

Lazos, O., Tosin, M., Slusarczyk, A. L., Boakes, S., Cortes, J., Sidebottom, P. J. & Leadlay, P. F. (2010). Biosynthesis Of The Putative Siderophore Erythrochelin Requires Unprecedented Crosstalk Between Separate Nonribosomal Peptide Gene Clusters. *Chemistry & Biology* **17**, 160-173.

Leclerc, V. & Reichhart, J. M. (2004). The Immune Response Of *Drosophila melanogaster*. *Immunological Reviews* **198**, 59-71.

Lee, B. N., Kroken, S., Chou, D. Y. T., Robbertse, B., Yoder, O. C. & Turgeon, B. G. (2005). Functional Analysis Of All Nonribosomal Peptide Synthetases In *Cochliobolus heterostrophus* Reveals A Factor, NPS6, Involved In Virulence And Resistance To Oxidative Stress. *Eukaryotic Cell* **4**, 545-555.

- Lee, C. G., Da Silva, C. A., Lee, J. Y., Hartl, D. & Elias, J. A. (2008).** Chitin Regulation Of Immune Responses: An Old Molecule With New Roles. *Current Opinion In Immunology* **20**, 684-689.
- Lee, S. L., Floss, H. G. & Heinstein, P. (1976).** Purification And Properties Of Dimethylallylpyrophosphate - Tryptophan Dimethylallyl Transferase, First Enzyme Of Ergot Alkaloid Biosynthesis In *Claviceps-sp* Sd-58. *Archives Of Biochemistry And Biophysics* **177**, 84-94.
- Leitao, E. A., Bittencourt, V. C. B., Haido, R. M. T., Valente, A. P., Peter-Katalinic, J., Letzel, M., De Souza, L. M. & Barreto-Bergter, E. (2003).** Beta-Galactofuranose-Containing O-Linked Oligosaccharides Present In The Cell Wall Peptidogalactomannan Of *Aspergillus fumigatus* Contain Immunodominant Epitopes. *Glycobiology* **13**, 681-692.
- Lemaitre, B., Nicolas, E., Michaut, L., Reichhart, J. M. & Hoffmann, J. A. (1996).** The Dorsoventral Regulatory Gene Cassette Spatzle/Toll/Cactus Controls The Potent Antifungal Response In *Drosophila* Adults. *Cell* **86**, 973-983.
- Lemaitre, B., Reichhart, J. M. & Hoffmann, J. A. (1997).** *Drosophila* Host Defense: Differential Induction Of Antimicrobial Peptide Genes After Infection By Various Classes Of Microorganisms. *Proceedings Of The National Academy Of Sciences Of The United States Of America* **94**, 14614-14619.
- Leong, S. A. & Winkelmann, G. (1998).** Molecular biology of iron transport in fungi. In *Metal Ions in Biological Systems, Vol 35*, pp. 147-186.
- Lesage, G. & Bussey, H. (2006).** Cell Wall Assembly In *Saccharomyces cerevisiae*. *Microbiology And Molecular Biology Reviews* **70**, 317-+.
- Lessing, F., Kniemeyer, O., Wozniok, W., Loeffler, J., Kurzai, O., Haertl, A. & Brakhage, A. A. (2007).** The *Aspergillus fumigatus* Transcriptional Regulator AfYAP1 Represents The Major Regulator For Defense Against Reactive Oxygen Intermediates But Is Dispensable For Pathogenicity In An Intranasal Mouse Infection Model. *Eukaryotic Cell* **6**, 2290-2302.
- Levdansky, E., Kashi, O., Sharon, H., Shadkchan, Y. & Oshero, N. (2010).** The *Aspergillus fumigatus* Cspa Gene Encoding A Repeat-Rich Cell Wall Protein Is Important For Normal Conidial Cell Wall Architecture And Interaction With Host Cells. *Eukaryotic Cell* **9**, 1403-1415.
- Levin, D. E. (2005).** Cell Wall Integrity Signaling In *Saccharomyces cerevisiae*. *Microbiology And Molecular Biology Reviews* **69**, 262-+.
- Levitz, S. A. (2004).** Interactions Of Toll-Like Receptors With Fungi. *Microbes And Infection* **6**, 1351-1355.

- Levitz, S. M. & Diamond, R. D. (1985).** Mechanisms Of Resistance Of *Aspergillus fumigatus* Conidia To Killing By Neutrophils In Vitro. *Journal Of Infectious Diseases* **152**, 33-42.
- Levitz, S. M., Selsted, M. E., Ganz, T., Lehrer, R. I. & Diamond, R. D. (1986).** In Vitro Killing Of Spores And Hyphae Of *Aspergillus fumigatus* And *Rhizopus oryzae* By Rabbit Neutrophil Cationic Peptides And Bronchoalveolar Macrophages. *Journal Of Infectious Diseases* **154**, 483-489.
- Levitz, S. M. & Farrell, T. P. (1990).** Human Neutrophil Degranulation Stimulated By *Aspergillus fumigatus*. *Journal Of Leukocyte Biology* **47**, 170-175.
- Levitz, S. M. & Specht, C. A. (2006).** The Molecular Basis For The Immunogenicity Of *Cryptococcus neoformans* Mannoproteins. *Fems Yeast Research* **6**, 513-524.
- Levitz, S. M. (2010).** Innate Recognition Of Fungal Cell Walls. *Plos Pathogens* **6**.
- Lin, S. J., Schranz, J. & Teutsch, S. M. (2001).** Aspergillosis Case - Fatality Rate: Systematic Review Of The Literature. *Clinical Infectious Diseases* **32**, 358-366.
- Lionakis, M. S. & Kontoyiannis, D. P. (2005).** Fruit Flies As A Minihost Model For Studying Drug Activity And Virulence In *Aspergillus*. *Medical Mycology* **43**, S111-S114.
- Lipmann, F. (1971).** Attempts To Map A Process Evolution Of Peptide Biosynthesis. *Science* **173**, 875-&.
- Lipmann, F., Gevers, W., Kleinkau, H. & Roskoski, R. (1971).** Polypeptide Synthesis On Protein Templates - Enzymatic Synthesis Of Gramicidin-S And Tyrocidine. *Advances In Enzymology And Related Areas Of Molecular Biology* **35**, 1-&.
- Liu, M., Panaccione, D. G. & Schardl, C. L. (2009a).** Phylogenetic Analyses Reveal Monophyletic Origin Of The Ergot Alkaloid Gene *DmaW* In Fungi. *Evolutionary Bioinformatics* **5**, 15-30.
- Liu, X. Q., Wang, L., Steffan, N., Yin, W. B. & Li, S. M. (2009b).** Ergot Alkaloid Biosynthesis In *Aspergillus fumigatus*: Fgaat Catalyses The Acetylation Of Fumigaclavine B. *Chembiochem* **10**, 2325-2328.
- Livak, K. J. & Schmittgen, T. D. (2001).** Analysis Of Relative Gene Expression Data Using Real-Time Quantitative PCR And The 2^(-Delta Delta C) Method. *Methods* **25**, 402-408.
- Loechler, E. L., Green, C. L. & Essigmann, J. M. (1984).** In Vivo Mutagenesis By O⁶ Methylguanine Built Into A Unique Site In A Viral Genome. *Proceedings Of The National Academy Of Sciences Of The United States Of America-Biological Sciences* **81**, 6271-6275.
- Loeffler, J. & Stevens, D. A. (2003).** Antifungal Drug Resistance. *Clinical Infectious Diseases* **36**, S31-S41.

Lorenz, N., Wilson, E. V., Machado, C., Schardl, C. L. & Tudzynski, P. (2007). Comparison Of Ergot Alkaloid Biosynthesis Gene Clusters In *Claviceps* Species Indicates Loss Of Late Pathway Steps In Evolution Of C-Fusiformis. *Applied And Environmental Microbiology* **73**, 7185-7191.

Lorenz, N., Olsovska, J., Sulc, M. & Tudzynski, P. (2010). Alkaloid Cluster Gene *ccsa* Of The Ergot Fungus *Claviceps purpurea* Encodes Chanoclavine I Synthase, A Flavin Adenine Dinucleotide-Containing Oxidoreductase Mediating The Transformation Of N-Methyl-Dimethylallyltryptophan To Chanoclavine I. *Applied And Environmental Microbiology* **76**, 1822-1830.

Mabey, J. E., M. J. Anderson, P. F. Giles, C. J. Miller, T. K. Attwood, N. W. Paton, E. Bornberg-Bauer, G. D. Robson, S. G. Oliver, and D. W. Denning. (2004). CADRE: The Central *Aspergillus* Data Repository. *Nucleic Acids Research* **32**, D401-D405.

Machida, M., K. Asai, M. Sano, T. Tanaka, T. Kumagai, G. Terai, K. I. Kusumoto, T. Arima, O. Akita, Y. Kashiwagi, K. Abe, K. Gomi, H. Horiuchi, K. Kitamoto, T. Kobayashi, M. Takeuchi, D. W. Denning, J. E. Galagan, W. C. Nierman, J. J. Yu, D. B. Archer, J. W. Bennett, D. Bhatnagar, T. E. Cleveland, N. D. Fedorova, O. Gotoh, H. Horikawa, A. Hosoyama, M. Ichinomiya, R. Igarashi, K. Iwashita, P. R. Juvvadi, M. Kato, Y. Kato, T. Kin, A. Kokubun, H. Maeda, N. Maeyama, J. Maruyama, H. Nagasaki, T. Nakajima, K. Oda, K. Okada, I. Paulsen, K. Sakamoto, T. Sawano, M. Takahashi, K. Takase, Y. Terabayashi, J. R. Wortman, O. Yamada, Y. Yamagata, H. Anazawa, Y. Hata, Y. Koide, T. Komori, Y. Koyama, T. Minetoki, S. Suharnan, A. Tanaka, K. Isono, S. Kuhara, N. Ogasawara, and H. Kikuchi. (2005). Genome sequencing and analysis of *Aspergillus oryzae*. *Nature* **438**, 1157-1161.

Madan, T., Kishore, U., Shah, A., Eggleton, P., Strong, P., Wang, J. Y., Aggrawal, S. S., Sarma, P. U. & Reid, K. B. M. (1997). Lung Surfactant Proteins A And D Can Inhibit Specific IgE Binding To The Allergens Of *Aspergillus fumigatus* And Block Allergen-Induced Histamine Release From Human Basophils. *Clinical And Experimental Immunology* **110**, 241-249.

Madan, T., Priyadarsiny, P., Vaid, M., Kamal, N., Shah, A., Haq, W., Katti, S. B. & Sarma, P. U. (2004). Use Of A Synthetic Peptide Epitope Of Asp F 1, A Major Allergen Or Antigen Of *Aspergillus fumigatus*, For Improved Immunodiagnosis Of Allergic Bronchopulmonary Aspergillosis. *Clinical And Diagnostic Laboratory Immunology* **11**, 552-558.

Madan, T., Reid, K. B. M., Clark, H., Singh, M., Nayak, A., Sarma, P. U., Hawgood, S. & Kishore, U. (2010). Susceptibility Of Mice Genetically Deficient In Sp-A Or Sp-D Gene To Invasive Pulmonary Aspergillosis. *Molecular Immunology* **47**, 1923-1930.

Maga, J. A. & Mcentee, K. (1985). Response Of S-Cerevisiae To N-Methyl-N'-Nitro-N-Nitrosoguanidine - Mutagenesis, Survival And Ddr Gene-Expression. *Molecular & General Genetics* **200**, 313-321.

Mahoney, N., Molyneux, R. J., Kim, J. H., Campbell, B. C., Waiss, A. C. & Hagerman, A. E. (2010). Aflatoxigenesis Induced In *Aspergillus flavus* By Oxidative

Stress And Reduction By Phenolic Antioxidants From Tree Nuts. *World Mycotox J* **3**, 45-48.

Maiya, S., Grundmann, A., Li, S. M. & Turner, G. (2006). The Fumitremorgin Gene Cluster Of *Aspergillus fumigatus*: Identification Of A Gene Encoding Brevianamide F Synthetase. *Chembiochem* **7**, 1062-1069.

Maiya, S., Grundmann, A., Li, X., Li, S. M. & Turner, G. (2007). Identification of a hybrid PKS/NRPS required for pseurotin A biosynthesis in the human pathogen *Aspergillus fumigatus*. *Chembiochem* **8**, 1736-1743.

Mambula, S. S., Sau, K., Henneke, P., Golenbock, D. T. & Levitz, S. M. (2002). Toll-Like Receptor (TLR) Signaling In Response To *Aspergillus fumigatus*. *Journal Of Biological Chemistry* **277**, 39320-39326.

Marahiel, M. A., Stachelhaus, T. & Mootz, H. D. (1997). Modular Peptide Synthetases Involved In Nonribosomal Peptide Synthesis. *Chemical Reviews* **97**, 2651-2673.

Marr, K. A., Carter, R. A., Boeckh, M., Martin, P. & Corey, L. (2002). Invasive Aspergillosis In Allogeneic Stem Cell Transplant Recipients: Changes In Epidemiology And Risk Factors. *Blood* **100**, 4358-4366.

Martin, H., Arroyo, J., Sanchez, M., Molina, M. & Nombela, C. (1993). Activity Of The Yeast Map Kinase Homolog Slt2 Is Critically Required For Cell Integrity At 37-Degrees-C. *Molecular & General Genetics* **241**, 177-184.

Martin, J. F. (2000). Alpha-Aminoadipyl-Cysteinyl-Valine Synthetases In Beta-Lactam Producing Organisms - From Abraham's Discoveries To Novel Concepts Of Non-Ribosomal Peptide Synthesis. *Journal Of Antibiotics* **53**, 1008-1021

Martinez-Lopez, R., Monteoliva, L., Diez-Orejas, R., Nombela, C. & Gil, C. (2004). The GPI-Anchored Protein Caecm33p Is Required For Cell Wall Integrity, Morphogenesis And Virulence In *Candida albicans*. *Microbiology-Sgm* **150**, 3341-3354.

Martinez-Lopez, R., Park, H., Myers, C. L., Gil, C. & Filler, S. G. (2006). *Candida albicans* Ecm33p Is Important For Normal Cell Wall Architecture And Interactions With Host Cells. *Eukaryotic Cell* **5**, 140-147.

Matha, V. & Mracek, Z. (1984). Changes In Hemocyte Counts In *Galleria mellonella* (L) (*Lepidoptera, Galleriidae*) Larvae Infected With *Steinernema-sp* (Nematoda, Steinernematidae). *Nematologica* **30**, 86-89.

Matzinger, P. (1994). Tolerance, Danger, And The Extended Family. *Annual Review Of Immunology* **12**, 991-1045.

Maubon, D., Park, S., Tanguy, M., Huerre, M., Schmitt, C., Prevost, M. C., Perlin, D. S., Latge, J. P. & Beauvais, A. (2006). Ags3, An Alpha(1-3)Glucan Synthase Gene Family Member Of *Aspergillus fumigatus*, Modulates Mycelium Growth In The Lung Of Experimentally Infected Mice. *Fungal Genetics And Biology* **43**, 366-375.

McCarthy, T. V. & Lindahl, T. (1985). Methyl Phosphotriesters In Alkylated DNA Are Repaired By The Ada Regulatory Protein Of *Escherichia coli*. *Nucleic Acids Research* **13**, 2683-2698.

McCormick, A., Heesemann, L., Wagener, J., Marcos, V., Hartl, D., Loeffler, J., Heesemann, J. & Ebel, F. (2010). NETs formed by human neutrophils inhibit growth of the pathogenic mold *Aspergillus fumigatus*. *Microbes Infect.*

Medzhitov, R., Prestonhurlburt, P. & Janeway, C. A. (1997). A Human Homologue Of The *Drosophila* Toll Protein Signals Activation Of Adaptive Immunity. *Nature* **388**, 394-397.

Medzhitov, R. & Janeway, C. A. (2000). How Does The Immune System Distinguish Self From Nonself? *Seminars In Immunology* **12**, 185-188.

Mehrad, B., Strieter, R. M. & Standiford, T. J. (1999). Role Of TNF-Alpha In Pulmonary Host Defense In Murine Invasive Aspergillosis. *Journal Of Immunology* **162**, 1633-1640.

Meier, A., Kirschning, C. J., Nikolaus, T., Wagner, H., Heesemann, J. & Ebel, F. (2003). Toll-Like Receptor (TLR) 2 And TLR4 Are Essential For *Aspergillus*-Induced Activation Of Murine Macrophages. *Cellular Microbiology* **5**, 561-570.

Meier, J. L. & Burkart, M. D. (2009). The Chemical Biology Of Modular Biosynthetic Enzymes. *Chemical Society Reviews* **38**, 2012-2045.

Meyer, V. (2008). Genetic Engineering Of Filamentous Fungi - Progress, Obstacles And Future Trends. *Biotechnology Advances* **26**, 177-185.

Michielse, C. B., Arentshorst, M., Ram, A. F. J. & Van Den Hondel, C. (2005a). *Agrobacterium*-Mediated Transformation Leads To Improved Gene Replacement Efficiency In *Aspergillus awamori*. *Fungal Genetics And Biology* **42**, 9-19.

Michielse, C. B., Hooykaas, P. J. J., Van Den Hondel, C. & Ram, A. F. J. (2005b). *Agrobacterium*-Mediated Transformation As A Tool For Functional Genomics In Fungi. *Current Genetics* **48**, 1-17.

Mikulska, M., A. M. Raiola, B. Bruno, E. Furfaro, M. T. Van Lint, S. Bregante, A. Ibatici, V. Del Bono, A. Bacigalupo, and C. Viscoli. (2009). Risk Factors For Invasive Aspergillosis And Related Mortality In Recipients Of Allogeneic SCT From Alternative Donors: An Analysis Of 306 Patients. *Bone Marrow Transplantation* **44**, 361-370.

Miller, K. Y., Toennis, T. M., Adams, T. H. & Miller, B. L. (1991). Isolation And Transcriptional Characterization Of A Morphological Modifier - The *Aspergillus nidulans* Stunted (StuA) Gene. *Molecular & General Genetics* **227**, 285-292.

Miller, K. Y., Wu, J. G. & Miller, B. L. (1992). StuA Is Required For Cell Pattern-Formation In *Aspergillus*. *Genes & Development* **6**, 1770-1782.

- Mirabito, P. M., Adams, T. H. & Timberlake, W. E. (1989).** Interactions Of 3 Sequentially Expressed Genes Control Temporal And Spatial Specificity In *Aspergillus* Development. *Cell* **57**, 859-868.
- Mircescu, M. M., Lipuma, L., Van Rooijen, N., Pamer, E. G. & Hohl, T. M. (2009).** Essential Role For Neutrophils But Not Alveolar Macrophages At Early Time Points Following *Aspergillus fumigatus* Infection. *Journal Of Infectious Diseases* **200**, 647-656.
- Misiek, M. & Hoffmeister, D. (2007).** Fungal Genetics, Genomics, And Secondary Metabolites In Pharmaceutical Sciences. *Planta Medica* **73**, 103-115.
- Missall, T. A., Lodge, J. K. & Mcewen, J. E. (2004).** Mechanisms Of Resistance To Oxidative And Nitrosative Stress: Implications For Fungal Survival In Mammalian Hosts. *Eukaryotic Cell* **3**, 835-846.
- Mitchell, C. G., Slight, J. & Donaldson, K. (1997).** Diffusible Component From The Spore Surface Of The Fungus *Aspergillus fumigatus* Which Inhibits The Macrophage Oxidative Burst Is Distinct From Gliotoxin And Other Hyphal Toxins. *Thorax* **52**, 796-801.
- Moen, M. D., Lyseng-Williamson, K. A. & Scott, L. J. (2009).** Liposomal Amphotericin B A Review Of Its Use As Empirical Therapy In Febrile Neutropenia And In The Treatment Of Invasive Fungal Infections. *Drugs* **69**, 361-392.
- Monari, C., Retini, C., Palazzetti, B., Bistoni, F. & Vecchiarelli, A. (1997).** Regulatory Role Of Exogenous Il-10 In The Development Of Immune Response Versus *Cryptococcus neoformans*. *Clinical And Experimental Immunology* **109**, 242-247.
- Monfeli, R. R. & Beeson, C. (2007).** Targeting Iron Acquisition By *Mycobacterium tuberculosis*. *Infect Disord Drug Targets* **7**, 213-220.
- Monk, B. C. & Goffeau, A. (2008).** Outwitting Multidrug Resistance To Antifungals. *Science* **321**, 367-369.
- Monod, M., Paris, S., Sanglard, D., Jattonogay, K., Bille, J. & Latge, J. P. (1993).** Isolation And Characterization Of A Secreted Metalloprotease Of *Aspergillus fumigatus*. *Infection And Immunity* **61**, 4099-4104.
- Moon, Y. S., Donzelli, B. G. G., Krasnoff, S. B., Mclane, H., Griggs, M. H., Cooke, P., Vandenberg, J. D., Gibson, D. M. & Churchill, A. C. L. (2008).** *Agrobacterium*-Mediated Disruption Of A Nonribosomal Peptide Synthetase Gene In The Invertebrate Pathogen *Metarhizium anisopliae* Reveals A Peptide Spore Factor. *Applied And Environmental Microbiology* **74**, 4366-4380.
- Mooney, J. L. & Yager, L. N. (1990).** Light Is Required For Conidiation In *Aspergillus nidulans*. *Genes & Development* **4**, 1473-1482.
- Moore, K. W., Ogarra, A., Malefyt, R. D., Vieira, P. & Mosmann, T. R. (1993).** Interleukin-10. *Annual Review Of Immunology* **11**, 165-190.

- Mootz, H. D., Schorgendorfer, K. & Marahiel, M. A. (2002a).** Functional Characterization Of 4'-Phosphopantetheinyl Transferase Genes Of Bacterial And Fungal Origin By Complementation Of *Saccharomyces cerevisiae* Lys5. *Fems Microbiology Letters* **213**, 51-57.
- Mootz, H. D., Schwarzer, D. & Marahiel, M. A. (2002b).** Ways Of Assembling Complex Natural Products On Modular Nonribosomal Peptide Synthetases. *ChemBiochem* **3**, 491-504.
- Morelle, W., Bernard, M., Debeaupuis, J. P., Buitrago, M., Tabouret, M. & Latge, J. P. (2005).** Galactomannoproteins Of *Aspergillus fumigatus*. *Eukaryotic Cell* **4**, 1308-1316.
- Morohoshi, F. & Munakata, N. (1987).** Multiple Species Of *Bacillus subtilis* DNA Alkyltransferase Involved In The Adaptive Response To Simple Alkylating-Agents. *Journal Of Bacteriology* **169**, 587-592.
- Morohoshi, F., Hayashi, K. & Munakata, N. (1990).** *Bacillus subtilis* Ada Operon Encodes 2 Dna Alkyltransferases. *Nucleic Acids Research* **18**, 5473-5480.
- Morschhauser, J. (2010).** Regulation Of Multidrug Resistance In Pathogenic Fungi. *Fungal Genetics And Biology* **47**, 94-106.
- Moss, R. B. (2002).** Allergic Bronchopulmonary Aspergillosis. *Clinical Reviews In Allergy & Immunology* **23**, 87-104.
- Moussa, K., Michie, H. J., Cree, I. A., Mccafferty, A. C., Winter, J. H., Dhillon, D. P., Stephens, S. & Brown, R. A. (1994).** Phagocyte Function And Cytokine Production In Community-Acquired Pneumonia. *Thorax* **49**, 107-111.
- Muller, U., Vogel, P., Alber, G. & Schaub, G. A. (2008).** The Innate Immune System Of Mammals And Insects. *Contrib Microbiol* **15**, 21-44.
- Mullins, J., Hutcheson, P. S. & Slavin, R. G. (1984).** *Aspergillus fumigatus* Spore Concentration In Outside Air - Cardiff And St-Louis Compared. *Clinical Allergy* **14**, 351-354.
- Munday, R. (1982).** Studies On The Mechanism Of Toxicity Of The Myco-Toxin, Sporidesmin .1. Generation Of Superoxide Radical By Sporidesmin. *Chemico-Biological Interactions* **41**, 361-374.
- Nakabeppu, Y. & Sekiguchi, M. (1986).** Regulatory Mechanisms For Induction Of Synthesis Of Repair Enzymes In Response To Alkylating-Agents - Ada Protein Acts As A Transcriptional Regulator. *Proceedings Of The National Academy Of Sciences Of The United States Of America* **83**, 6297-6301.
- Nakamura, T., Tokumoto, Y., Sakumi, K., Koike, G., Nakabeppu, Y. & Sekiguchi, M. (1988).** Expression Of The Ada Gene Of *Escherichia coli* In Response To Alkylating-

Agents - Identification Of Transcriptional Regulatory Elements. *Journal Of Molecular Biology* **202**, 483-494.

Netea, M. G., T. Azam, G. Ferwerda, S. E. Girardin, M. Walsh, J. S. Park, E. Abraham, J. M. Kim, D. Y. Yoon, C. A. Dinarello, and S. H. Kim. (2005). Il-32 Synergizes With Nucleotide Oligomerization Domain (Nod) 1 And Nod2 Ligands For IL-1 Beta And IL-6 Production Through A Caspase 1-Dependent Mechanism. *Proceedings Of The National Academy Of Sciences Of The United States Of America* **102**, 16309-16314.

Netea, M. G., Ferwerda, G., Van Der Graaf, C. A. A., Van Der Meer, J. W. M. & Kullberg, B. J. (2006). Recognition Of Fungal Pathogens By Toll-Like Receptors. *Current Pharmaceutical Design* **12**, 4195-4201.

Neville, C., Murphy, A., Kavanagh, K. & Doyle, S. (2005). A 4'-Phosphopantetheinyl Transferase Mediates Non-Ribosomal Peptide Synthetase Activation In *Aspergillus fumigatus*. *Chembiochem* **6**, 679-685.

Nguyen, T. H., Fleet, G. H. & Rogers, P. L. (1998). Composition Of The Cell Walls Of Several Yeast Species. *Applied Microbiology And Biotechnology* **50**, 206-212.

Nielsen, J. B., Nielsen, M. L. & Mortensen, U. H. (2008). Transient Disruption Of Non-Homologous End-Joining Facilitates Targeted Genome Manipulations In The Filamentous Fungus *Aspergillus nidulans*. *Fungal Genetics And Biology* **45**, 165-170.

Nielsen, M. L., Albertsen, L., Lettier, G., Nielsen, J. B. & Mortensen, U. H. (2006). Efficient Pcr-Based Gene Targeting With A Recyclable Marker For *Aspergillus nidulans*. *Fungal Genetics And Biology* **43**, 54-64.

Nierman, W. C., A. Pain, M. J. Anderson, J. R. Wortman, H. S. Kim, J. Arroyo, M. Berriman, K. Abe, D. B. Archer, C. Bermejo, J. Bennett, P. Bowyer, D. Chen, M. Collins, R. Coulsen, R. Davies, P. S. Dyer, M. Farman, N. Fedorova, T. V. Feldblyum, R. Fischer, N. Fosker, A. Fraser, J. L. Garcia, M. J. Garcia, A. Goble, G. H. Goldman, K. Gomi, S. Griffith-Jones, R. Gwilliam, B. Haas, H. Haas, D. Harris, H. Horiuchi, J. Huang, S. Humphray, J. Jimenez, N. Keller, H. Khouri, K. Kitamoto, T. Kobayashi, S. Konzack, R. Kulkarni, T. Kumagai, A. Lafton, J. P. Latge, W. X. Li, A. Lord, W. H. Majoros, G. S. May, B. L. Miller, Y. Mohamoud, M. Molina, M. Monod, I. Mouyna, S. Mulligan, L. Murphy, S. O'Neil, I. Paulsen, M. A. Penalva, M. Peretea, C. Price, B. L. Pritchard, M. A. Quail, E. Rabinowitsch, N. Rawlins, M. A. Rajandream, U. Reichard, H. Renault, G. D. Robson, S. R. de Cordoba, J. M. Rodriguez-Pena, C. M. Ronning, S. Rutter, S. L. Salzberg, M. Sanchez, J. C. Sanchez-Ferrero, D. Saunders, K. Seeger, R. Squares, S. Squares, M. Takeuchi, F. Tekaia, G. Turner, C. R. V. de Aldana, J. Weidman, O. White, J. Woodward, J. H. Yu, C. Fraser, J. E. Galagan, K. Asai, M. Machida, N. Hall, B. Barrell, and D. W. Denning. (2006). Genomic Sequence Of The Pathogenic And Allergenic Filamentous Fungus *Aspergillus fumigatus* (Vol 438, Pg 1151, 2005). *Nature* **439**, 502-502.

Ninomiya, Y., Suzuki, K., Ishii, C. & Inoue, H. (2004b). Highly Efficient Gene Replacements In *Neurospora* Strains Deficient For Nonhomologous End-Joining (Vol 101,

Pg 12248, 2004). *Proceedings Of The National Academy Of Sciences Of The United States Of America* **101**, 16391-16391.

O'Gorman, C. M., Fuller, H. T. & Dyer, P. S. (2009). Discovery Of A Sexual Cycle In The Opportunistic Fungal Pathogen *Aspergillus fumigatus*. *Nature* **457**, 471-U475.

O'Neill, L. A. J. & Bowie, A. G. (2007). The Family Of Five: Tir-Domain-Containing Adaptors In Toll-Like Receptor Signalling. *Nature Reviews Immunology* **7**, 353-364.

Oakley, B. R., Rinehart, J. E., Mitchell, B. L., Oakley, C. E., Carmona, C., Gray, G. L. & May, G. S. (1987). Cloning, Mapping And Molecular Analysis Of The PyrG (Orotidine-5'-Phosphate Decarboxylase) Gene Of *Aspergillus nidulans*. *Gene* **61**, 385-399.

O'Connor, T. R. & Laval, F. (1990). Isolation And Structure Of A cDNA Expressing A Mammalian 3-Methyladenine-DNA Glycosylase. *Embo Journal* **9**, 3337-3342.

Oide, S., Moeder, W., Krasnoff, S., Gibson, D., Haas, H., Yoshioka, K. & Turgeon, B. G. (2006). NPS6, Encoding A Nonribosomal Peptide Synthetase Involved In Siderophore-Mediated Iron Metabolism, Is A Conserved Virulence Determinant Of Plant Pathogenic Ascomycetes. *Plant Cell* **18**, 2836-2853.

Ok, M., J. P. Latge, C. Baeuerlein, F. Ebel, M. Mezger, M. Topp, O. Kurzai, D. Killian, M. Kapp, G. U. Grigoleit, H. Sennefelder, J. Arroyo, H. Einsele, and J. Loeffler. (2009). Immune Responses Of Human Immature Dendritic Cells Can Be Modulated By The Recombinant *Aspergillus fumigatus* Antigen Aspfl. *Clinical And Vaccine Immunology* **16**, 1485-1492.

Oka, T., Sameshima, Y., Koga, T., Kim, H., Goto, M. & Furukawa, K. (2005). Protein O-Mannosyltransferase A Of *Aspergillus awamori* Is Involved In O-Mannosylation Of Glucoamylase I. *Microbiology-Sgm* **151**, 3657-3667.

Olsson, M. & Lindahl, T. (1980). Repair Of Alkylated DNA In *Escherichia coli* - Methyl-Group Transfer From O⁶ Methylguanine To A Protein Cysteine Residue. *Journal Of Biological Chemistry* **255**, 569-571.

Ortel, I. & Keller, U. (2009). Combinatorial Assembly Of Simple And Complex D-Lysergic Acid Alkaloid Peptide Classes In The Ergot Fungus *Claviceps purpurea*. *Journal Of Biological Chemistry* **284**, 6650-6660.

Ozeki, K., Kyoya, F., Hizume, K., Kanda, A., Hamachi, M. & Nunokawa, Y. (1994). Transformation Of Intact *Aspergillus niger* By Electroporation. *Bioscience Biotechnology And Biochemistry* **58**, 2224-2227.

Pagano, L., C. Girmenia, L. Mele, P. Ricci, M. E. Tosti, A. Nosari, M. Buelli, M. Picardi, B. Allione, L. Corvatta, D. D'Antonio, M. Montillo, L. Melillo, A. Chierichini, A. Cenacchi, A. Tonso, L. Cudillo, A. Candoni, C. Savignano, A. Bonini, P. Martino, and A. Del Favero. (2001). Infections Caused By Filamentous Fungi In Patients With Hematologic Malignancies. A Report Of 391 Cases By Gimema Infection Program. *Haematologica* **86**, 862-870.

- Palotai, R., Szalay, M. S. & Csermely, P. (2008).** Chaperones As Integrators Of Cellular Networks: Changes Of Cellular Integrity In Stress And Diseases. *Iubmb Life* **60**, 10-18.
- Panaccione, D. G., Johnson, R. D., Wang, J. H., Young, C. A., Damrongkool, P., Scott, B. & Schardl, C. L. (2001).** Elimination Of Ergovaline From A Grass-*Neotyphodium* Endophyte Symbiosis By Genetic Modification Of The Endophyte. *Proceedings Of The National Academy Of Sciences Of The United States Of America* **98**, 12820-12825.
- Panaccione, D. G., Tapper, B. A., Lane, G. A., Davies, E. & Fraser, K. (2003).** Biochemical Outcome Of Blocking The Ergot Alkaloid Pathway Of A Grass Endophyte. *Journal Of Agricultural And Food Chemistry* **51**, 6429-6437.
- Panaccione, D. G. (2005).** Origins And Significance Of Ergot Alkaloid Diversity In Fungi. *Fems Microbiology Letters* **251**, 9-17.
- Panaccione, D. G. & Coyle, C. M. (2005).** Abundant Respirable Ergot Alkaloids From The Common Airborne Fungus *Aspergillus fumigatus*. *Applied And Environmental Microbiology* **71**, 3106-3111.
- Pancaldi, S., Poli, F., Dallolio, G. & Vannini, G. L. (1984).** Morphological Anomalies Induced By Congo Red In *Aspergillus niger*. *Archives Of Microbiology* **137**, 185-187.
- Paques, F. & Haber, J. E. (1999).** Multiple Pathways Of Recombination Induced By Double-Strand Breaks In *Saccharomyces cerevisiae*. *Microbiology And Molecular Biology Reviews* **63**, 349-+.
- Pardo, M., Monteoliva, L., Vazquez, P., Martinez, R., Molero, G., Nombela, C. & Gil, C. (2004).** Pst1 And Ecm33 Encode Two Yeast Cell Surface GPI Proteins Important For Cell Wall Integrity. *Microbiology-Sgm* **150**, 4157-4170.
- Paris, S., Boisvieuxulrich, E., Crestani, B., Houcine, O., Taramelli, D., Lombardi, L. & Latge, J. P. (1997).** Internalization Of *Aspergillus fumigatus* Conidia By Epithelial And Endothelial Cells. *Infection And Immunity* **65**, 1510-1514.
- Paris, S., Debeaupuis, J. P., Cramer, R., Carey, M., Charles, F., Prevost, M. C., Schmitt, C., Philippe, B. & Latge, J. P. (2003a).** Conidial Hydrophobins Of *Aspergillus fumigatus*. *Applied And Environmental Microbiology* **69**, 1581-1588.
- Paris, S., Wysong, D., Debeaupuis, J. P., Shibuya, K., Philippe, B., Diamond, R. D. & Latge, J. P. (2003b).** Catalases Of *Aspergillus fumigatus*. *Infection And Immunity* **71**, 3551-3562.
- Parsons, W. J., Ramkumar, V. & Stiles, G. L. (1988).** Isobutylmethylxanthine Stimulates Adenylate-Cyclase By Blocking The Inhibitory Regulatory Protein, Gi. *Molecular Pharmacology* **34**, 37-41.
- Pel, H. J., J. H. de Winde, D. B. Archer, P. S. Dyer, G. Hofmann, P. J. Schaap, G. Turner, R. P. de Vries, R. Albang, K. Albermann, M. R. Andersen, J. D. Bendtsen, J.**

A. E. Benen, M. van den Berg, S. Breestraat, M. X. Caddick, R. Contreras, M. Cornell, P. M. Coutinho, E. G. J. Danchin, A. J. M. Debets, P. Dekker, P. W. M. van Dijk, A. van Dijk, L. Dijkhuizen, A. J. M. Driessen, C. d'Enfert, S. Geysens, C. Goosen, G. S. P. Groot, P. W. J. de Groot, T. Guillemette, B. Henrissat, M. Herweijer, J. van den Hombergh, C. van den Hondel, R. van der Heijden, R. M. van der Kaaij, F. M. Klis, H. J. Kools, C. P. Kubicek, P. A. van Kuyk, J. Lauber, X. Lu, M. van der Maarel, R. Meulenberg, H. Menke, M. A. Mortimer, J. Nielsen, S. G. Oliver, M. Olsthoorn, K. Pal, N. van Peij, A. F. J. Ram, U. Rinas, J. A. Roubos, C. M. J. Sagt, M. Schmoll, J. B. Sun, D. Ussery, J. Varga, W. Vervecken, P. de Vondervoort, H. Wedler, H. A. B. Wosten, A. P. Zeng, A. J. J. van Ooyen, J. Visser, and H. Stam. (2007). Genome sequencing and analysis of the versatile cell factory *Aspergillus niger* CBS 513.88. *Nature Biotechnology* **25**, 221-231.

Perera, K., Day, J. B., Mantle, P. G. & Rodrigues, L. (1982). Metabolism Of Verruculogen In Rats. *Applied And Environmental Microbiology* **43**, 503-508.

Perez, P. & Ribas, J. C. (2004). Cell Wall Analysis. *Methods* **33**, 245-251.

Perkhofer, S., Kehrel, B. E., Dierich, M. P., Donnelly, J. P., Nussbaumer, W., Hofmann, J., Von Eiff, C. & Lass-Flörl, C. (2008a). Human Platelets Attenuate *Aspergillus* Species Via Granule-Dependent Mechanisms. *Journal Of Infectious Diseases* **198**, 1243-1246.

Perkhofer, S., Salvenmoser, W., Dierich, M. P. & Lass-Flörl, C. (2008b). Human Platelets Impair Mitochondrial Activity Of *Aspergillus fumigatus* In Vitro. *Mycoses* **51**, 367-367.

Perrin, R. M., Fedorova, N. D., Bok, J. W., Cramer, R. A., Wortman, J. R., Kim, H. S., Nierman, W. C. & Keller, N. P. (2007). Transcriptional Regulation Of Chemical Diversity In *Aspergillus fumigatus* By Laea. *Plos Pathogens* **3**, 508-517.

Philippe, B., Ibrahim-Granet, O., Prevost, M. C., Gougerot-Pocidallo, M. A., Perez, A. S., Van Der Meeren, A. & Latge, J. P. (2003). Killing Of *Aspergillus fumigatus* By Alveolar Macrophages Is Mediated By Reactive Oxidant Intermediates. *Infection And Immunity* **71**, 3034-3042.

Pihet, M., P. Vandeputte, G. Tronchin, G. Renier, P. Saulnier, S. Georgeault, R. Mallet, D. Chabasse, F. Symoens, and J. P. Bouchara. (2009). Melanin Is An Essential Component For The Integrity Of The Cell Wall Of *Aspergillus fumigatus* Conidia. *Bmc Microbiology* **9**, 11.

Pinto, L. J. & Moore, M. M. (2009). Screening Method To Identify Inhibitors Of Siderophore Biosynthesis In The Opportunistic Fungal Pathogen, *Aspergillus fumigatus*. *Letters In Applied Microbiology* **49**, 8-13.

Plaine, A., Walker, L., Da Costa, G., Mora-Montes, H. M., Mckinnon, A., Gow, N. A. R., Gaillardin, C., Munro, C. A. & Richard, M. L. (2008). Functional Analysis Of *Candida albicans* GPI-Anchored Proteins: Roles In Cell Wall Integrity And Caspofungin Sensitivity. *Fungal Genetics And Biology* **45**, 1404-1414.

Pocsi, I., Prade, R. A. & Penninckx, M. J. (2004). Glutathione, Altruistic Metabolite In Fungi. In *Advances In Microbial Physiology, Vol 49*, Pp. 1-76.

Pocsi, I., Miskei, M., Karanyi, Z., Emri, T., Ayoubi, P., Pusztahelyi, T., Balla, G. & Prade, R. A. (2005). Comparison Of Gene Expression Signatures Of Diamide, H₂O₂ And Menadione Exposed *Aspergillus nidulans* Cultures - Linking Genome-Wide Transcriptional Changes To Cellular Physiology. *Bmc Genomics* **6**.

Polakowska, R., Perozzi, G. & Prakash, L. (1986). Alkylation Mutagenesis In *Saccharomyces cerevisiae* - Lack Of Evidence For An Adaptive Response. *Current Genetics* **10**, 647-655.

Ponts, N., Pinson-Gadais, L., Verdal-Bonnin, M. N., Barreau, C. & Richard-Forget, F. (2006). Accumulation Of Deoxynivalenol And Its 15-Acetylated Form Is Significantly Modulated By Oxidative Stress In Liquid Cultures Of *Fusarium graminearum*. *Fems Microbiology Letters* **258**, 102-107.

Ponts, N., Pinson-Gadais, L., Barreau, C., Richard-Forget, F. & Ouellet, T. (2007). Exogenous H₂O₂ And Catalase Treatments Interfere With Tri Genes Expression In Liquid Cultures Of *Fusarium graminearum*. *Febs Letters* **581**, 443-447.

Popolo, L. & Vai, M. (1998). Defects In Assembly Of The Extracellular Matrix Are Responsible For Altered Morphogenesis Of A *Candida albicans* Phr1 Mutant. *Journal Of Bacteriology* **180**, 163-166.

Porter, J. K., Bacon, C. W., Robbins, J. D. & Betowski, D. (1981). Ergot Alkaloid Identification In *Clavicipitaceae* Systemic Fungi Of Pasture Grasses. *Journal Of Agricultural And Food Chemistry* **29**, 653-657.

Post, M. J., Lass-Floerl, C., Gastl, G. & Nachbaur, D. (2007). Invasive Fungal Infections In Allogeneic And Autologous Stem Cell Transplant Recipients: A Single-Center Study Of 166 Transplanted Patients. *Transplant Infectious Disease* **9**, 189-195.

Pugin, J., Heumann, D., Tomasz, A., Kravchenko, V. V., Akamatsu, Y., Nishijima, M., Glauser, M. P., Tobias, P. S. & Ulevitch, R. J. (1994). CD14 Is A Pattern-Recognition Receptor. *Immunity* **1**, 509-516.

Ram, A. F. J. & Klis, F. M. (2006). Identification Of Fungal Cell Wall Mutants Using Susceptibility Assays Based On Calcofluor White And Congo Red. *Nature Protocols* **1**, 2253-2256.

Ratcliffe, N. A. (1985). Invertebrate Immunity - A Primer For The Non-Specialist. *Immunology Letters* **10**, 253-270.

Recio, L., Hobbs, C., Caspary, W. & Witt, K. L. (2010). Dose-Response Assessment Of Four Genotoxic Chemicals In A Combined Mouse And Rat Micronucleus (Mn) And Comet Assay Protocol. *Journal Of Toxicological Sciences* **35**, 149-162.

- Rees, D. O., Bushby, N., Cox, R. J., Harding, J. R., Simpson, T. J. & Willis, C. L. (2007).** Synthesis of 1,2-C-13(2), N-15 -L-homoserine and its incorporation by the PKS-NRPS system of *Fusarium moniliforme* into the mycotoxin fusarin C. *Chembiochem* **8**, 46-50.
- Reeves, E. P., H. Lu, H. Lortat-Jacob, C. G. M. Messina, S. Bolsover, G. Gabella, E. O. Potma, A. Warley, J. Roes, and A. W. Segal. (2002).** Killing Activity Of Neutrophils Is Mediated Through Activation Of Proteases By K⁺ Flux. *Nature* **416**, 291-297.
- Reeves, E. P., Messina, C. G. M., Doyle, S. & Kavanagh, K. (2004).** Correlation Between Gliotoxin Production And Virulence Of *Aspergillus fumigatus* In *Galleria mellonella*. *Mycopathologia* **158**, 73-79.
- Reeves, E. P., Reiber, K., Neville, C., Scheibner, O., Kavanagh, K. & Doyle, S. (2006).** A Nonribosomal Peptide Synthetase (Pes1) Confers Protection Against Oxidative Stress In *Aspergillus fumigatus*. *Febs Journal* **273**, 3038-3053.
- Reiber, K., Reeves, E. P., Neville, C. M., Winkler, R., Gebhardt, P., Kavanagh, K. & Doyle, S. (2005).** The Expression Of Selected Non-Ribosomal Peptide Synthetases In *Aspergillus fumigatus* Is Controlled By The Availability Of Free Iron. *Fems Microbiology Letters* **248**, 83-91.
- Reichard, U. (1998).** The Role Of Secretory And Structure-Associated Proteinases Of *Aspergillus fumigatus* In The Pathogenesis Of Invasive Aspergillosis. *Mycoses* **41**, 78-82.
- Reid, D. M., Montoya, M., Taylor, P. R., Borrow, P., Gordon, S., Brown, G. D. & Wong, S. Y. C. (2004).** Expression Of The Beta-Glucan Receptor, Dectin-1, On Murine Leukocytes In Situ Correlates With Its Function In Pathogen Recognition And Reveals Potential Roles In Leukocyte Interactions. *Journal Of Leukocyte Biology* **76**, 86-94.
- Reid, D. M., Gow, N. A. R. & Brown, G. D. (2009).** Pattern Recognition: Recent Insights From Dectin-1. *Current Opinion In Immunology* **21**, 30-37.
- Rementeria, A., Lopez-Molina, N., Ludwig, A., Vivanco, A. B., Bikandi, J., Ponton, J. & Garaizar, J. (2005).** Genes And Molecules Involved In *Aspergillus fumigatus* Virulence. *Rev Iberoam Micol* **22**, 1-23.
- Reverberi, M., Ricelli, A., Zjalic, S., Fabbri, A. A. & Fanelli, C. (2010).** Natural Functions Of Mycotoxins And Control Of Their Biosynthesis In Fungi. *Applied Microbiology And Biotechnology* **87**, 899-911.
- Reverchon, S., Rouanet, C., Expert, D. & Nasser, W. (2002).** Characterization Of Indigoidine Biosynthetic Genes In *Erwinia chrysanthemi* And Role Of This Blue Pigment In Pathogenicity. *Journal Of Bacteriology* **184**, 654-665.
- Rex, J. H., Bennett, J. E., Gallin, J. I., Malech, H. L. & Melnick, D. A. (1990).** Normal And Deficient Neutrophils Can Cooperate To Damage *Aspergillus fumigatus* Hyphae. *Journal Of Infectious Diseases* **162**, 523-528.

- Riederer, B., Han, M. & Keller, U. (1996).** D-Lysergyl Peptide Synthetase From The Ergot Fungus *Claviceps purpurea*. *Journal Of Biological Chemistry* **271**, 27524-27530.
- Rigbers, O. & Li, S. M. (2008).** Ergot Alkaloid Biosynthesis In *Aspergillus fumigatus* - Overproduction And Biochemical Characterization Of A 4-Dimethylallyltryptophan N-Methyltransferase. *Journal Of Biological Chemistry* **283**, 26859-26868.
- Robles, S. J., Buehler, P. W., Negrusz, A. & Adami, G. R. (1999).** Permanent Cell Cycle Arrest In Asynchronously Proliferating Normal Human Fibroblasts Treated With Doxorubicin Or Etoposide But Not Camptothecin. *Biochemical Pharmacology* **58**, 675-685.
- Rock, F. L., Hardiman, G., Timans, J. C., Kastelein, R. A. & Bazan, J. F. (1998).** A Family Of Human Receptors Structurally Related To *Drosophila* Toll. *Proceedings Of The National Academy Of Sciences Of The United States Of America* **95**, 588-593.
- Rohankhedkar, M. S., Mulrooney, S. B., Wedemeyer, W. J. & Hausinger, R. P. (2006).** The AidB Component Of The *Escherichia coli* Adaptive Response To Alkylating Agents Is A Flavin-Containing, DNA-Binding Protein. *Journal Of Bacteriology* **188**, 223-230.
- Roilides, E., Dimitriadou, A., Kadiltsoglou, I., Sein, T., Karpouzas, J., Pizzo, P. A. & Walsh, T. J. (1997).** IL-10 Exerts Suppressive And Enhancing Effects On Antifungal Activity Of Mononuclear Phagocytes Against *Aspergillus fumigatus*. *Journal Of Immunology* **158**, 322-329.
- Romani, L., Puccetti, P., Mencacci, A., Cenci, E., Spaccapelo, R., Tonnetti, L., Grohmann, U. & Bistoni, F. (1994).** Neutralization Of IL-10 Up-Regulates Nitric-Oxide Production And Protects Susceptible Mice From Challenge With *Candida albicans*. *Journal Of Immunology* **152**, 3514-3521.
- Romani, L. (2004).** Immunity To Fungal Infections. *Nature Reviews Immunology* **4**, 11-23.
- Romano, J., Nimrod, G., Ben-Tal, N., Shadkchan, Y., Baruch, K., Sharon, H. & Osherov, N. (2006).** Disruption Of The *Aspergillus fumigatus* Ecm33 Homologue Results In Rapid Conidial Germination, Antifungal Resistance And Hypervirulence. *Microbiology-Sgm* **152**, 1919-1928.
- Roncero, C. & Duran, A. (1985).** Effect Of Calcofluor White And Congo Red On Fungal Cell-Wall Morphogenesis - In vivo Activation Of Chitin Polymerization. *Journal Of Bacteriology* **163**, 1180-1185.
- Ruiz-Diez, B. (2002).** Strategies For The Transformation Of Filamentous Fungi. *Journal Of Applied Microbiology* **92**, 189-195.
- Samson, L. & Cairns, J. (1977).** New Pathway For DNA-Repair In *Escherichia-coli*. *Nature* **267**, 281-283.

Sassanfar, M. & Samson, L. (1990). Identification And Preliminary Characterization Of An O-6-Methylguanine DNA-Repair Methyltransferase In The Yeast *Saccharomyces-cerevisiae*. *Journal Of Biological Chemistry* **265**, 20-25.

Schaffner, A., Douglas, H. & Braude, A. (1982). Selective Protection Against Conidia By Mononuclear And Against Mycelia By Polymorphonuclear Phagocytes In Resistance To *Aspergillus* - Observations On These 2 Lines Of Defense *In vivo* And *In vitro* With Human And Mouse Phagocytes. *Journal Of Clinical Investigation* **69**, 617-631.

Schaffner, A., Douglas, H., Braude, A. I. & Davis, C. E. (1983). Killing Of *Aspergillus* Spores Depends On The Anatomical Source Of The Macrophage. *Infection And Immunity* **42**, 1109-1115.

Schardl, C. L., Leuchtman, A., Tsai, H. F., Collett, M. A., Watt, D. M. & Scott, D. B. (1994). Origin Of A Fungal Symbiont Of Perennial Ryegrass By Interspecific Hybridization Of A Mutualist With The Ryegrass Choke Pathogen, *Epichloe typhina*. *Genetics* **136**, 1307-1317.

Schrettl, M., Bignell, E., Kragl, C., Joechl, C., Rogers, T., Arst, H. N., Haynes, K. & Haas, H. (2004). Siderophore Biosynthesis But Not Reductive Iron Assimilation Is Essential For *Aspergillus fumigatus* Virulence. *Journal Of Experimental Medicine* **200**, 1213-1219.

Schrettl, M., E. Bignell, C. Kragl, Y. Sabiha, O. Loss, M. Eisendle, A. Wallner, H. N. Arst, K. Haynes, and H. Haas. (2007). Distinct Roles For Intra- And Extracellular Siderophores During *Aspergillus fumigatus* Infection. *Plos Pathogens* **3**, 1195-1207.

Schrettl, M., S. Carberry, K. Kavanagh, H. Haas, G. W. Jones, J. O'Brien, A. Nolan, J. Stephens, O. Fenelon, and S. Doyle. (2010). Self-Protection Against Gliotoxin-A Component Of The Gliotoxin Biosynthetic Cluster, GliT, Completely Protects *Aspergillus fumigatus* Against Exogenous Gliotoxin. *Plos Pathogens* **6**, 15.

Schroeckh, V., Scherlach, K., Nutzmann, H. W., Shelest, E., Schmidt-Heck, W., Schuemann, J., Martin, K., Hertweck, C. & Brakhage, A. A. (2009). Intimate Bacterial-Fungal Interaction Triggers Biosynthesis Of Archetypal Polyketides In *Aspergillus nidulans*. *Proceedings Of The National Academy Of Sciences Of The United States Of America* **106**, 14558-14563.

Schumann, J. & Hertweck, C. (2007). Molecular basis of cytochalasan biosynthesis in fungi: Gene cluster analysis and evidence for the involvement of a PKS-NRPS hybrid synthase by RNA silencing. *Journal of the American Chemical Society* **129**, 9564-+.

Schwarzer, D. & Marahiel, M. A. (2001). Multimodular Biocatalysts For Natural Product Assembly. *Naturwissenschaften* **88**, 93-101.

Schwarzer, D., Finking, R. & Marahiel, M. A. (2003). Nonribosomal Peptides: From Genes To Products. *Natural Product Reports* **20**, 275-287.

Schwimmer, C. & Masison, D. C. (2002). Antagonistic Interactions Between Yeast PSI+ And URE3 Prions And Curing Of URE3 By Hsp70 Protein Chaperone Ssa1p But Not By Ssa2p. *Molecular And Cellular Biology* **22**, 3590-3598.

Scott, L. J. & Simpson, D. (2007). Voriconazole - A Review Of Its Use In The Management Of Invasive Fungal Infections. *Drugs* **67**, 269-298.

Sedgwick, B. & Vaughan, P. (1991). Widespread Adaptive Response Against Environmental Methylating Agents In Microorganisms. *Mutation Research* **250**, 211-221.

Sedgwick, B. & Lindahl, T. (2002). Recent Progress On The Ada Response For Inducible Repair Of DNA Alkylation Damage. *Oncogene* **21**, 8886-8894.

Segal, A. W. (2005). How Neutrophils Kill Microbes. *Annual Review Of Immunology* **23**, 197-223.

Shahan, T. A., Sorenson, W. G., Paulauskis, J. D., Morey, R. & Lewis, D. M. (1998). Concentration- And Time-Dependent Upregulation And Release Of The Cytokines MIP-2, KC, TNF, And MIP-1 Alpha In Rat Alveolar Macrophages By Fungal Spores Implicated In Airway Inflammation. *American Journal Of Respiratory Cell And Molecular Biology* **18**, 435-440.

Shaw, B. D. & Momany, M. (2002). *Aspergillus nidulans* Polarity Mutant SwoA Is Complemented By Protein O-Mannosyltransferase PmtA. *Fungal Genetics And Biology* **37**, 263-270.

Sheppard, D. C., Rieg, G., Chiang, L. Y., Filler, S. G., Edwards, J. E. & Ibrahim, A. S. (2004). Novel Inhalational Murine Model Of Invasive Pulmonary Aspergillosis. *Antimicrobial Agents And Chemotherapy* **48**, 1908-1911.

Sheppard, D. C., Doedt, T., Chiang, L. Y., Kim, H. S., Chen, D., Nierman, W. C. & Filler, S. G. (2005). The *Aspergillus fumigatus* StuA Protein Governs The Up-Regulation Of A Discrete Transcriptional Program During The Acquisition Of Developmental Competence. *Molecular Biology Of The Cell* **16**, 5866-5879.

Shibuya, K., Takaoka, M., Uchida, K., Wakayama, M., Yamaguchi, H., Takahashi, K., Paris, S., Latge, J. P. & Naoe, S. (1999). Histopathology Of Experimental Invasive Pulmonary Aspergillosis In Rats: Pathological Comparison Of Pulmonary Lesions Induced By Specific Virulent Factor Deficient Mutants. *Microbial Pathogenesis* **27**, 123-131.

Shrivastav, M., De Haro, L. P. & Nickoloff, J. A. (2008). Regulation Of DNA Double-Strand Break Repair Pathway Choice. *Cell Research* **18**, 134-147.

Sies, H. (1991). Role Of Reactive Oxygen Species In Biological Processes. *Klinische Wochenschrift* **69**, 965-968.

Simitsopoulou, M., Roilides, E., Paliogianni, F., Likartsis, C., Ioannidis, J., Kanellou, K. & Walsh, T. J. (2008). Immunomodulatory Effects Of Voriconazole On Monocytes

Challenged With *Aspergillus fumigatus*: Differential Role Of Toll-Like Receptors. *Antimicrobial Agents And Chemotherapy* **52**, 3301-3306.

Singer, M. A. & Lindquist, S. (1998). Multiple Effects Of Trehalose On Protein Folding In Vitro And In Vivo. *Molecular Cell* **1**, 639-648.

Singh, B., Oellerich, M., Kumar, R., Kumar, M., Bhadoria, D. P., Reichard, U., Gupta, V. K., Sharma, G. L. & Asif, A. R. (2010a). Immuno-Reactive Molecules Identified From The Secreted Proteome Of *Aspergillus fumigatus*. *J Proteome Res.*

Singh, B., Sharma, G. L., Oellerich, M., Kumar, R., Singh, S., Bhadoria, D. P., Katyal, A., Reichard, U. & Asif, A. R. (2010b). Novel Cytosolic Allergens Of *Aspergillus fumigatus* Identified From Germinating Conidia. *J Proteome Res.*

Slater, J. L., Gregson, L., Denning, D. W. & Warn, P. A. (2010). Pathogenicity Of *Aspergillus fumigatus* Mutants Assessed In *Galleria mellonella* Matches That In Mice. *Med Mycol.*

Sleigh, M. J. (1976). Mechanism Of DNA Breakage By Phleomycin In Vitro. *Nucleic Acids Research* **3**, 891-901.

Sleigh, M. J. & Grigg, G. W. (1976). Mechanism Of Sensitivity To Phleomycin In Growing *Escherichia coli* cells. *Biochemical Journal* **155**, 87-99.

Smedsgaard, J. (1997). Micro-Scale Extraction Procedure For Standardized Screening Of Fungal Metabolite Production In Cultures. *Journal Of Chromatography A* **760**, 264-270.

Sorenson, W. G., Frazer, D. G., Jarvis, B. B., Simpson, J. & Robinson, V. A. (1987). Trichothecene Mycotoxins In Aerosolized Conidia Of *Stachybotrys-atra*. *Applied And Environmental Microbiology* **53**, 1370-1375.

Spagnolo, L., Rivera-Calzada, A., Pearl, L. H. & Llorca, O. (2006). Three-Dimensional Structure Of The Human Dna-Pkcs/Ku70/Ku80 Complex Assembled On DNA And Its Implications For DNA DSB Repair. *Molecular Cell* **22**, 511-519.

Spilsbury, J. & Wilkinson, S. (1961). Isolation Of Festuclavine And 2 New Clavine Alkaloids From *Aspergillus fumigatus* fres. *Journal Of The Chemical Society*, 2085-&.

Sprote, P. & Brakhage, A. A. (2007). The Light-Dependent Regulator Velvet A Of *Aspergillus nidulans* Acts As A Repressor Of The Penicillin Biosynthesis. *Archives Of Microbiology* **188**, 69-79.

Srivastava, R., Bhargava, A. & Singh, R. K. (2007). Synthesis And Antimicrobial Activity Of Some Novel Nucleoside Analogues Of Adenosine And 1,3-Dideazaadenosine. *Bioorganic & Medicinal Chemistry Letters* **17**, 6239-6244.

Stachelhaus, T. & Marahiel, M. A. (1995). Modular Structure Of Genes Encoding Multifunctional Peptide Synthetases Required For Nonribosomal Peptide-Synthesis. *Fems Microbiology Letters* **125**, 3-14.

Stachelhaus, T., Mootz, H. D. & Marahiel, M. A. (1999). The Specificity-Confering Code Of Adenylation Domains In Nonribosomal Peptide Synthetases. *Chemistry & Biology* **6**, 493-505.

Stack, D., Neville, C. & Doyle, S. (2007). Nonribosomal Peptide Synthesis In *Aspergillus fumigatus* And Other Fungi. *Microbiology-Sgm* **153**, 1297-1306.

Stack, D., Frizzell, A., Tomkins, K. & Doyle, S. (2009). Solid Phase 4'-Phosphopantetheinylation: Fungal Thiolation Domains Are Targets For Chemoenzymatic Modification. *Bioconjugate Chemistry* **20**, 1514-1522.

Steele, C., Rapaka, R. R., Metz, A., Pop, S. M., Williams, D. L., Gordon, S., Kolls, J. K. & Brown, G. D. (2005). The Beta-Glucan Receptor Dectin-1 Recognizes Specific Morphologies Of *Aspergillus fumigatus*. *Plos Pathogens* **1**, 323-334.

Steinbach, W. J., Benjamin, D. K., Trasi, S. A., Miller, J. L., Schell, W. A., Zaas, A. K., Foster, W. M. & Perfect, J. R. (2004). Value Of An Inhalational Model Of Invasive Aspergillosis. *Medical Mycology* **42**, 417-425.

Stephens-Romero, S. D., Mednick, A. J. & Feldmesser, M. (2005). The Pathogenesis Of Fatal Outcome In Murine Pulmonary Aspergillosis Depends On The Neutrophil Depletion Strategy. *Infection And Immunity* **73**, 114-125.

Stergiopoulou, T., J. Meletiadis, E. Roilides, D. E. Kleiner, R. Schaufele, M. Roden, S. Harrington, L. Dad, B. Segal, and T. J. Walsh. (2007). Host-Dependent Patterns Of Tissue Injury In Invasive Pulmonary Aspergillosis. *American Journal Of Clinical Pathology* **127**, 349-355.

Stevens, D. A., V. L. Kan, M. A. Judson, V. A. Morrison, S. Dummer, D. W. Denning, J. E. Bennett, T. J. Walsh, T. F. Patterson, and G. A. Pankey. (2000). Practice Guidelines For Diseases Caused By *Aspergillus*. *Clinical Infectious Diseases* **30**, 696-709.

Stinnett, S. M., Espeso, E. A., Cobeno, L., Araujo-Bazan, L. & Calvo, A. M. (2007). *Aspergillus nidulans* VeA Subcellular Localization Is Dependent On The Importin Alpha Carrier And On Light. *Molecular Microbiology* **63**, 242-255.

Strieker, M., Tanovic, A. & Marahiel, M. A. (2010). Nonribosomal Peptide Synthetases: Structures And Dynamics. *Current Opinion In Structural Biology* **20**, 234-240.

Sturtevant, J. E. & Latge, J. P. (1992). Interactions Between Conidia Of *Aspergillus fumigatus* And Human-Complement Component-C3. *Infection And Immunity* **60**, 1913-1918.

Sucher, A. J., Chahine, E. B. & Balcer, H. E. (2009). Echinocandins: The Newest Class of Antifungals. *Annals Of Pharmacotherapy* **43**, 1647-1657.

Sugui, J. A., Chang, Y. C. & Kwon-Chung, K. J. (2005). *Agrobacterium tumefaciens*-Mediated Transformation Of *Aspergillus fumigatus*: An Efficient Tool For Insertional

Mutagenesis And Targeted Gene Disruption. *Applied And Environmental Microbiology* **71**, 1798-1802.

Sugui, J. A., Kim, H. S., Zarembek, K. A., Chang, Y. C., Gallin, J. I., Nierman, W. C. & Kwon-Chung, K. J. (2008). Genes Differentially Expressed In Conidia And Hyphae Of *Aspergillus fumigatus* Upon Exposure To Human Neutrophils. *Plos One* **3**, 15.

Swirski, R. A., Shawcross, S. G., Faulkner, B. M. & Strike, P. (1988). Repair Of Alkylation Damage in the fungus *Aspergillus nidulans*. *Mutation Research* **193**, 255-268.

Tada, H., E. Nemoto, H. Shimauchi, T. Watanabe, T. Mikami, T. Matsumoto, N. Ohno, H. Tamura, K. Shibata, S. Akashi, K. Miyake, S. Sugawara, and H. Takada. (2002). *Saccharomyces cerevisiae* and *Candida albicans*-Derived Mannan Induced Production Of Tumor Necrosis Factor Alpha By Human Monocytes In A CD14-And Toll-Like Receptor 4-Dependent Manner. *Microbiology And Immunology* **46**, 503-512.

Takahashi, C., Matsushita, T., Doi, M., Minoura, K., Shingu, T., Kumeda, Y. & Numata, A. (1995). Fumiquinazolines A-G, Novel Metabolites Of A Fungus Separated From A *Pseudolabrus* Marine Fish. *Journal Of The Chemical Society-Perkin Transactions I*, 2345-2353.

Takeda, K., Kaisho, T. & Akira, S. (2003). Toll-Like Receptors. *Annual Review Of Immunology* **21**, 335-376.

Takeuchi, O., Kawai, T., Sanjo, H., Copeland, N. G., Gilbert, D. J., Jenkins, N. A., Takeda, K. & Akira, S. (1999). TLR6: A Novel Member Of An Expanding Toll-Like Receptor Family. *Gene* **231**, 59-65.

Takinowaki, H., Matsuda, Y., Yoshida, T., Kobayashi, Y. & Ohkubo, T. (2004). 1h, 13c And 15n Resonance Assignments Of The N-Terminal 16 kDA Domain Of *Escherichia coli* Ada Protein. *J Biomol Nmr* **29**, 447-448.

Tamano, K., M. Sano, N. Yamane, Y. Terabayashi, T. Toda, M. Sunagawa, H. Koike, O. Hatamoto, G. Umitsuki, T. Takahashi, Y. Koyama, R. Asai, K. Abe, and M. Machida. (2008). Transcriptional Regulation Of Genes On The Non-Syntenic Blocks Of *Aspergillus oryzae* And Its Functional Relationship To Solid-State Cultivation. *Fungal Genetics And Biology* **45**, 139-151.

Taylor, P. R., Brown, G. D., Reid, D. M., Willment, J. A., Martinez-Pomares, L., Gordon, S. & Wong, S. Y. C. (2002). The Beta-Glucan Receptor, Dectin-1, Is Predominantly Expressed On The, Surface Of Cells Of The Monocyte/Macrophage And Neutrophil Lineages. *Journal Of Immunology* **169**, 3876-3882.

Taylor, P. R., S. V. Tsoni, J. A. Willment, K. M. Dennehy, M. Rosas, H. Findon, K. Haynes, C. Steele, M. Botto, S. Gordon, and G. D. Brown. (2007). Dectin-1 Is Required For Beta-Glucan Recognition And Control Of Fungal Infection. *Nature Immunology* **8**, 31-38.

Temple, M. D., Perrone, G. G. & Dawes, I. W. (2005). Complex Cellular Responses To Reactive Oxygen Species. *Trends In Cell Biology* **15**, 319-326.

Teo, I., Sedgwick, B., Demple, B., Li, B. & Lindahl, T. (1984). Induction Of Resistance To Alkylating-Agents In *Escherichia coli* - The Ada+ Gene-Product Serves Both As A Regulatory Protein And As An Enzyme For Repair Of Mutagenic Damage. *Embo Journal* **3**, 2151-2157.

Thau, N., Monod, M., Crestani, B., Rolland, C., Tronchin, G., Latge, J. P. & Paris, S. (1994). Rodletless Mutants Of *Aspergillus fumigatus* (Vol 62, Pg 4380, 1994). *Infection And Immunity* **62**, 5706-5706.

Thompson, G. R. & Patterson, T. F. (2008). Pulmonary Aspergillosis. *Seminars In Respiratory And Critical Care Medicine* **29**, 103-110.

Thon, M. R., Pan, H. Q., Diener, S., Papalas, J., Taro, A., Mitchell, T. K. & Dean, R. A. (2006). The Role Of Transposable Element Clusters In Genome Evolution And Loss Of Synteny In The Rice Blast Fungus *Magnaporthe oryzae*. *Genome Biology* **7**.

Thornton, C. R. (2010). Detection Of Invasive Aspergillosis. In *Advances In Applied Microbiology, Vol 70*, Pp. 187-216. San Diego: Elsevier Academic Press Inc.

Thorpe, G. W., Fong, C. S., Alic, N., Higgins, V. J. & Dawes, I. W. (2004). Cells Have Distinct Mechanisms To Maintain Protection Against Different Reactive Oxygen Species: Oxidative-Stress-Response Genes. *Proceedings Of The National Academy Of Sciences Of The United States Of America* **101**, 6564-6569.

Tiburzi, F., Visca, P. & Imperi, F. (2007). Do Nonribosomal Peptide Synthetases Occur In Higher Eukaryotes? *Iubmb Life* **59**, 730-733.

Tkalcevic, J., Novelli, M., Phylactides, M., Iredale, J. P., Segal, A. W. & Roes, J. (2000). Impaired Immunity And Enhanced Resistance To Endotoxin In The Absence Of Neutrophil Elastase And Cathepsin G. *Immunity* **12**, 201-210.

Tomee, J. F. C. & Kauffman, H. F. (2000). Putative Virulence Factors Of *Aspergillus fumigatus*. *Clinical And Experimental Allergy* **30**, 476-484.

Tomee, J. F. C. & Van Der Werf, T. S. (2001). Pulmonary Aspergillosis. *Netherlands Journal Of Medicine* **59**, 244-258.

Tonnetti, L., Spaccapelo, R., Cenci, E., Mencacci, A., Puccetti, P., Coffman, R. L., Bistoni, F. & Romani, L. (1995). Interleukin-4 And Interleukin-10 Exacerbate Candidiasis In Mice. *European Journal Of Immunology* **25**, 1559-1565.

Travis, S. M., Conway, B. A. D., Zabner, J., Smith, J. J., Anderson, N. N., Singh, P. K., Greenberg, E. P. & Welsh, M. J. (1999). Activity Of Abundant Anti-microbials Of The Human Airway. *American Journal Of Respiratory Cell And Molecular Biology* **20**, 872-879.

- Trewick, S. C., Henshaw, T. F., Hausinger, R. P., Lindahl, T. & Sedgwick, B. (2002).** Oxidative Demethylation By *Escherichia coli* AlkB Directly Reverts DNA Base Damage. *Nature* **419**, 174-178.
- Tronchin, G., Esnault, K., Sanchez, M., Larcher, G., Marot-Leblond, A. & Bouchara, J. P. (2002).** Purification And Partial Characterization Of A 32-Kilodalton Sialic Acid-Specific Lectin From *Aspergillus fumigatus*. *Infection And Immunity* **70**, 6891-6895.
- Tsai, H. F., Wang, H., Gebler, J. C., Poulter, C. D. & Schardl, C. L. (1995).** The *Claviceps purpurea* Gene Encoding Dimethylallyltryptophan Synthase, The Committed Step For Ergot Alkaloid Biosynthesis. *Biochemical And Biophysical Research Communications* **216**, 119-125.
- Tsai, H. F., Chang, Y. C., Washburn, R. G., Wheeler, M. H. & Kwon-Chung, K. J. (1998).** The Developmentally Regulated Alb1 Gene Of *Aspergillus fumigatus*: Its Role In Modulation Of Conidial Morphology And Virulence. *Journal Of Bacteriology* **180**, 3031-3038.
- Tsai, H. F., Wheeler, M. H., Chang, Y. C. & Kwon-Chung, K. J. (1999).** A Developmentally Regulated Gene Cluster Involved In Conidial Pigment Biosynthesis In *Aspergillus fumigatus*. *Journal Of Bacteriology* **181**, 6469-6477.
- Tsitsigiannis, D. I., Bok, J. W., Andes, D., Nielsen, K. F., Frisvad, J. C. & Keller, N. P. (2005).** *Aspergillus* Cyclooxygenase-Like Enzymes Are Associated With Prostaglandin Production And Virulence. *Infection And Immunity* **73**, 4548-4559.
- Tsoni, S. V. & Brown, G. D. (2008).** Beta-Glucans And Dectin-1. In *Year In Immunology 2008*, Pp. 45-60. Oxford: Blackwell Publishing.
- Tsunawaki, S., Yoshida, L. S., Nishida, S., Kobayashi, T. & Shimoyama, T. (2004).** Fungal Metabolite Gliotoxin Inhibits Assembly Of The Human Respiratory Burst NADPH Oxidase. *Infection And Immunity* **72**, 3373-3382.
- Tudzynski, P., Holter, K., Correia, T., Arntz, C., Grammel, N. & Keller, U. (1999).** Evidence For An Ergot Alkaloid Gene Cluster In *Claviceps purpurea*. *Molecular And General Genetics* **261**, 133-141.
- Turgeon, B. G., Oide, S. & Bushley, K. (2008).** Creating And Screening *Cochliobolus heterostrophus* Non-Ribosomal Peptide Synthetase Mutants. *Mycological Research* **112**, 200-206.
- Twumasi-Boateng, K., Yu, Y., Chen, D., Gravelat, F. N., Nierman, W. C. & Sheppard, D. C. (2009).** Transcriptional Profiling Identifies A Role For BrlA In The Response To Nitrogen Depletion And For StuA In The Regulation Of Secondary Metabolite Clusters In *Aspergillus fumigatus*. *Eukaryotic Cell* **8**, 104-115.
- Unsold, I. A. & Li, S. M. (2005).** Overproduction, Purification And Characterization Of FgaPT2, A Dimethylallyltryptophan Synthase From *Aspergillus fumigatus*. *Microbiology-Sgm* **151**, 1499-1505.

- Unsold, I. A. & Li, S. M. (2006).** Reverse Prenyltransferase In The Biosynthesis Of Fumigaclavine C In *Aspergillus fumigatus*: Gene Expression, Purification, And Characterization Of Fumigaclavine C Synthase FgaPT1. *Chembiochem* **7**, 158-164.
- Valiante, V., Jain, R., Heinekamp, T. & Brakhage, A. A. (2009).** The MpkA Map Kinase Module Regulates Cell Wall Integrity Signaling And Pyomelanin Formation In *Aspergillus fumigatus*. *Fungal Genetics And Biology* **46**, 909-918.
- Vannini, G. L., Poli, F., Donini, A. & Pancaldi, S. (1983).** Effects Of Congo Red On Wall Synthesis And Morphogenesis In *Saccharomyces cerevisiae*. *Plant Science Letters* **31**, 9-17.
- Vazquez, M. J., Roa, A. M., Reyes, F., Vega, A., Rivera-Sagredo, A., Thomas, D. R., Diez, E. & Hueso-Rodriguez, J. A. (2003).** A Novel Ergot Alkaloid As A 5-Ht1a Inhibitor Produced By *Dicyma Sp.* *Journal Of Medicinal Chemistry* **46**, 5117-5120.
- Vega, M. T. M. & Martin, A. D. (2008).** Toll-Like Receptors: A Family Of Innate Sensors Of Danger That Alert And Drive Immunity. *Allergologia Et Immunopathologia* **36**, 347-357.
- Vickers, I., Reeves, E. P., Kavanagh, K. A. & Doyle, S. (2007).** Isolation, Activity And Immunological Characterisation Of A Secreted Aspartic Protease, CtsD, From *Aspergillus fumigatus*. *Protein Expression And Purification* **53**, 216-224.
- Vilmos, P. & Kurucz, E. (1998).** Insect Immunity: Evolutionary Roots Of The Mammalian Innate Immune System. *Immunology Letters* **62**, 59-66.
- Volkert, M. R. & Landini, P. (2001).** Transcriptional Responses To DNA Damage. *Current Opinion In Microbiology* **4**, 178-185.
- Vondohren, H., Keller, U., Vater, J. & Zocher, R. (1997).** Multifunctional Peptide Synthetases. *Chemical Reviews* **97**, 2675-2705.
- Vora, S., Chauhan, S., Brummer, E. & Stevens, D. A. (1998).** Activity Of Voriconazole Combined With Neutrophils or Monocytes Against *Aspergillus fumigatus*: Effects Of Granulocyte Colony-Stimulating Factor And Granulocyte-Macrophage Colony-Stimulating Factor. *Antimicrobial Agents And Chemotherapy* **42**, 2299-2303.
- Wagner, J. G. & Roth, R. A. (2000).** Neutrophil Migration Mechanisms, With An Emphasis On The Pulmonary Vasculature. *Pharmacological Reviews* **52**, 349-374.
- Wallwey, C., Matuschek, M. & Li, S. M. (2010a).** Ergot Alkaloid Biosynthesis In *Aspergillus fumigatus*: Conversion Of Chanoclavine-I To Chanoclavine-I Aldehyde Catalyzed By A Short-Chain Alcohol Dehydrogenase FgaDH. *Archives Of Microbiology* **192**, 127-134.
- Wallwey, C., Matuschek, M., Xie, X. L. & Li, S. M. (2010b).** Ergot Alkaloid Biosynthesis In *Aspergillus fumigatus*: Conversion Of Chanoclavine-I Aldehyde To

Festuclovine By The Festuclovine Synthase FgaFS In The Presence Of The Old Yellow Enzyme FgaOX3. *Organic & Biomolecular Chemistry* **8**, 3500-3508.

Walsh, C. T., Gehring, A. M., Weinreb, P. H., Quadri, L. E. N. & Flugel, R. S. (1997). Post-Translational Modification Of Polyketide And Nonribosomal Peptide Synthases. *Current Opinion In Chemical Biology* **1**, 309-315.

Walter, J. (1990). Poisons Of The Past - Molds, Epidemics, And History - Matossian, Mk. *Nature* **343**, 708-708.

Walters, J. B. & Ratcliffe, N. A. (1983). Studies On The *in-vivo* Cellular Reactions Of Insects - Fate Of Pathogenic And Non-Pathogenic Bacteria In *Galleria mellonella* Nodules. *Journal Of Insect Physiology* **29**, 417-424.

Walzel, B., Riederer, B. & Keller, U. (1997). Mechanism Of Alkaloid Cyclopeptide Synthesis In The Ergot Fungus *Claviceps purpurea*. *Chemistry & Biology* **4**, 223-230.

Wang, J. E., Warris, A., Ellingsen, E. A., Jorgensen, P. F., Flo, T. H., Espevik, T., Solberg, R., Verweij, P. E. & Aasen, A. O. (2001). Involvement Of CD14 And Toll-Like Receptors In Activation Of Human Monocytes By *Aspergillus fumigatus* Hyphae. *Infection And Immunity* **69**, 2402-2406.

Wang, J. H., Machado, C., Panaccione, D. G., Tsai, H. F. & Schardl, C. L. (2004). The Determinant Step In Ergot Alkaloid Biosynthesis By An Endophyte Of Perennial Ryegrass. *Fungal Genetics And Biology* **41**, 189-198.

Wasylnka, J. A. & Moore, M. M. (2002). Uptake Of *Aspergillus fumigatus* Conidia By Phagocytic And Nonphagocytic Cells In Vitro: Quantitation Using Strains Expressing Green Fluorescent Protein. *Infection And Immunity* **70**, 3156-3163.

Wasylnka, J. A. & Moore, M. M. (2003). *Aspergillus fumigatus* Conidia Survive And Germinate In Acidic Organelles Of A549 Epithelial Cells. *Journal Of Cell Science* **116**, 1579-1587.

Weig, M., Frosch, M., Tintelnot, K., Haas, A., Gross, U., Linsmeier, B. & Heesemann, J. (2001). Use Of Recombinant Mitogillin For Improved Serodiagnosis Of *Aspergillus fumigatus*-Associated Diseases. *Journal Of Clinical Microbiology* **39**, 1721-1730.

Werner, J. L., Metz, A. E., Horn, D., Schoeb, T. R., Hewitt, M. M., Schwiebert, L. M., Faro-Trindade, I., Brown, G. D. & Steele, C. (2009). Requisite Role For The Dectin-1 Beta-Glucan Receptor In Pulmonary Defense Against *Aspergillus fumigatus*. *Journal Of Immunology* **182**, 4938-4946.

Wessels, J. G. H. (1997). Hydrophobins: Proteins That Change The Nature Of The Fungal Surface. In *Advances In Microbial Physiology, Vol 38*, Pp. 1-45.

Wiederhold, N. P. & Lewis, R. E. (2003). Invasive Aspergillosis In Patients With Hematologic Malignancies. *Pharmacotherapy* **23**, 1592-1610.

- Williams, R. M., Stocking, E. M. & Sanz-Cervera, J. F. (2000).** Biosynthesis Of Prenylated Alkaloids Derived From Tryptophan. In *Biosynthesis: Aromatic Polyketides, Isoprenoids, Alkaloids*, Pp. 97-173. Berlin: Springer-Verlag Berlin.
- Willment, J. A., Gordon, S. & Brown, G. D. (2001).** Characterization Of The Human Beta-Glucan Receptor And Its Alternatively Spliced Isoforms. *Journal Of Biological Chemistry* **276**, 43818-43823.
- Wilson, L. J., Carmona, C. L. & Ward, M. (1988).** Sequence Of The *Aspergillus-niger* PyrG Gene. *Nucleic Acids Research* **16**, 2339-2339.
- Woo, P. C. Y., Leung, A. S. P., Lau, S. K. P., Chong, K. T. K. & Yuen, K. Y. (2001).** Use Of Recombinant Mitogillin For Serodiagnosis Of *Aspergillus fumigatus*-Associated Diseases. *Journal Of Clinical Microbiology* **39**, 4598-4599.
- Wood, P. J. (1980).** Specificity In The Interaction Of Direct Dyes With Polysaccharides. *Carbohydrate Research* **85**, 271-287.
- Wosten, H. A. B. & De Vocht, M. L. (2000).** Hydrophobins, The Fungal Coat Unravelling. *Biochimica Et Biophysica Acta-Reviews On Biomembranes* **1469**, 79-86.
- Wright, J. R. (2005).** Immunoregulatory Functions Of Surfactant Proteins. *Nature Reviews Immunology* **5**, 58-68.
- Wyatt, M. D. & Pittman, D. L. (2006).** Methylating Agents And DNA Repair Responses: Methylated Bases And Sources Of Strand Breaks. *Chemical Research In Toxicology* **19**, 1580-1594.
- Xiao, W., Derfler, B., Chen, J. & Samson, L. (1991).** Primary Sequence And Biological Functions Of A *Saccharomyces-cerevisiae*-O⁶-Methylguanine O4-Methylthymine DNA-Repair Methyltransferase Gene. *Embo Journal* **10**, 2179-2186.
- Xu, Y. Q., Rozco, R., Wijeratne, E. M. K., Espinosa-Artiles, P., Gunatilaka, A. A. L., Stock, S. P. & Molnar, I. (2009).** Biosynthesis Of The Cyclooligomer Depsipeptide Bassianolide, An Insecticidal Virulence Factor Of *Beauveria bassiana*. *Fungal Genetics And Biology* **46**, 353-364.
- Xue, T., Nguyen, C. K., Romans, A., Kontoyiannis, D. P. & May, G. S. (2004).** Isogenic Auxotrophic Mutant Strains In The *Aspergillus fumigatus* Genome Reference Strain Af293. *Archives Of Microbiology* **182**, 346-353.
- Yamazaki, M., Suzuki, S. & Miyaki, K. (1971).** Tremorgenic Goxins From *Aspergillus-fumigatus* fres. *Chemical & Pharmaceutical Bulletin* **19**, 1739-&.
- Yang, L., Ukil, L., Osmani, A., Nahm, F., Davies, J., De Souza, C. P. C., Dou, X. W., Perez-Balaguer, A. & Osmani, S. A. (2004).** Rapid Production Of Gene Replacement Constructs And Generation Of A Green Fluorescent Protein-Tagged Centromeric Marker In *Aspergillus nidulans*. *Eukaryotic Cell* **3**, 1359-1362.

Yin, W. B., Grundmann, A., Cheng, J. & Li, S. M. (2009). Acetylaszonalenin Biosynthesis In *Neosartorya fischeri* Identification Of The Biosynthetic Gene Cluster By Genomic Mining And Functional Proof Of The Genes By Biochemical Investigation. *Journal Of Biological Chemistry* **284**, 100-109.

Young, C. A., Bryant, M. K., Christensen, M. J., Tapper, B. A., Bryan, G. T. & Scott, B. (2005). Molecular Cloning And Genetic Analysis Of A Symbiosis-Expressed Gene Cluster For Lolitrem Biosynthesis From A Mutualistic Endophyte Of Perennial Ryegrass. *Molecular Genetics And Genomics* **274**, 13-29.

Young, C. A., Felitti, S., Shields, K., Spangenberg, G., Johnson, R. D., Bryan, G. T., Saikia, S. & Scott, B. (2006). A Complex Gene Cluster For Indole-Diterpene Biosynthesis In The Grass Endophyte *Neotyphodium lolii*. *Fungal Genetics And Biology* **43**, 679-693.

Yu, J. H., Hamari, Z., Han, K. H., Seo, J. A., Reyes-Dominguez, Y. & Scazzocchio, C. (2004). Double-Joint PCR: A PCR-Based Molecular Tool For Gene Manipulations In Filamentous Fungi. *Fungal Genetics And Biology* **41**, 973-981.

Zarembek, K. A., Sugui, J. A., Chang, Y. C., Kwon-Chung, K. J. & Gallin, J. I. (2007). Human Polymorphonuclear Leukocytes Inhibit *Aspergillus fumigatus* Conidial Growth By Lactoferrin-Mediated Iron Depletion. *Journal Of Immunology* **178**, 6367-6373.

Zhao, J. & Wu, X. Y. (2008). Triggering Of Toll-Like Receptors 2 And 4 By *Aspergillus fumigatus* Conidia In Immortalized Human Corneal Epithelial Cells To Induce Inflammatory Cytokines. *Chinese Medical Journal* **121**, 450-454.

Zhao, S., Smith, K. S., Deveau, A. M., Dieckhaus, C. M., Johnson, M. A., Macdonald, T. L. & Cook, J. M. (2002). Biological Activity Of The Tryprostatins And Their Diastereomers On Human Carcinoma Cell Lines. *Journal Of Medicinal Chemistry* **45**, 1559-1562.

Zhao, W., Panepinto, J. C., Fortwendel, J. R., Fox, L., Oliver, B. G., Askew, D. S. & Rhodes, J. C. (2006). Deletion Of The Regulatory Subunit Of Protein Kinase A In *Aspergillus fumigatus* Alters Morphology, Sensitivity To Oxidative Damage, And Virulence. *Infection And Immunity* **74**, 4865-4874.